CRC Press
Taylor & Francis Group

WITH VITALSOURCE®
EBOOK

Clinical Head and Neck Anatomy for Surgeons

EDITED BY

Peter A. Brennan
Vishy Mahadevan
Barrie T. Evans

Foreword by **Jatin P. Shah**

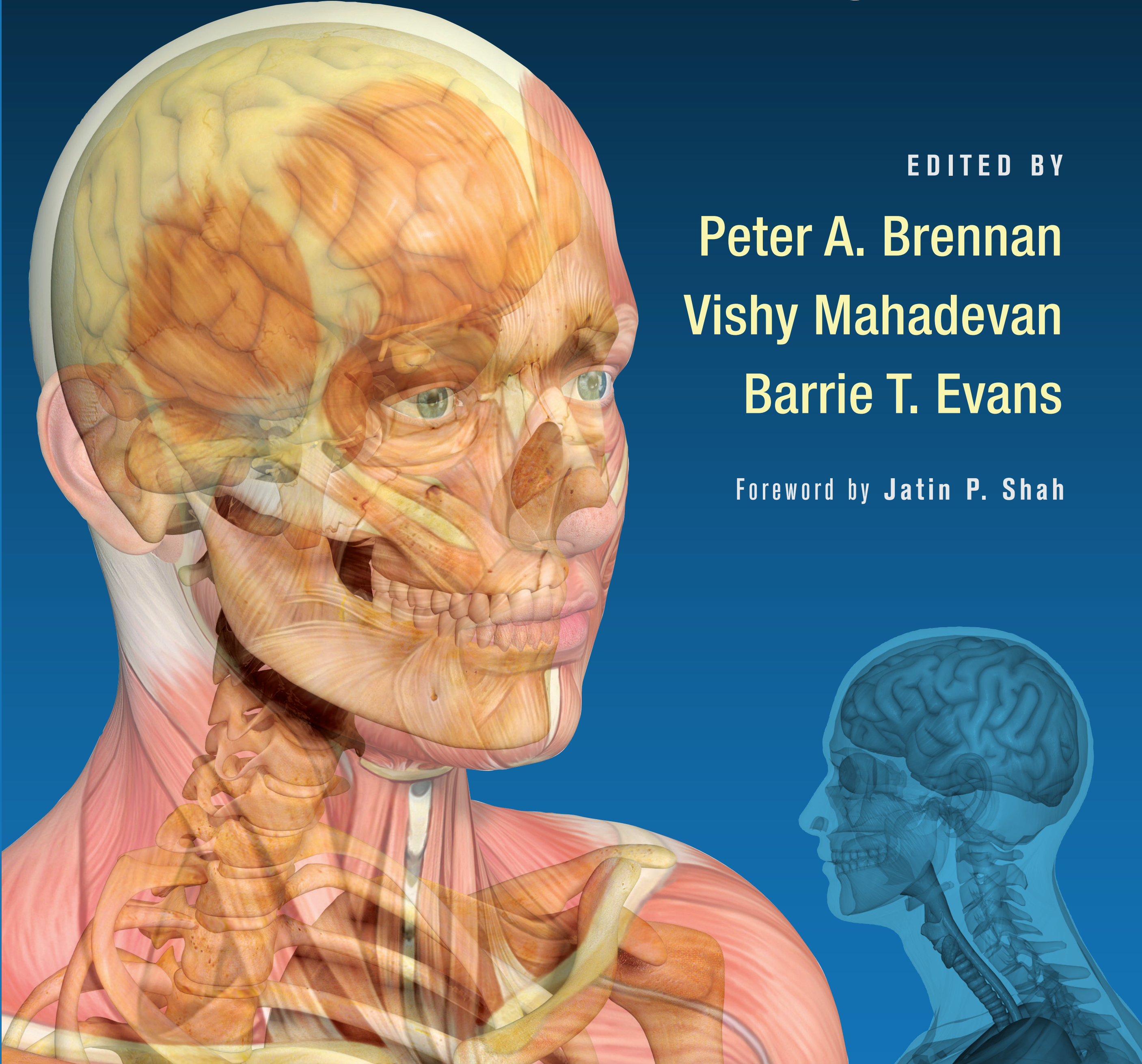

Clinical Head and Neck Anatomy for Surgeons

Clinical Head and Neck Anatomy for Surgeons

EDITED BY

Peter A. Brennan
Chairman, Intercollegiate Committee
for Basic Surgical Examinations (MRCS and DOHNS);
2016 President,
British Association of Oral and Maxillofacial Surgeons;
Consultant Oral and Maxillofacial Surgeon,
Honorary Professor of Surgery,
Queen Alexandra Hospital,
Portsmouth, UK

Vishy Mahadevan
Barbers' Company Professor of Anatomy,
Royal College of Surgeons of England,
London, UK

Barrie T. Evans
Past President,
British Association of Oral and Maxillofacial Surgeons;
Formerly Consultant Oral and Maxillofacial Surgeon,
Southampton University Hospitals,
Southampton, UK

Foreword by **Jatin P. Shah**

CRC Press
Taylor & Francis Group
Boca Raton London New York

CRC Press is an imprint of the
Taylor & Francis Group, an **informa** business

CRC Press
Taylor & Francis Group
6000 Broken Sound Parkway NW, Suite 300
Boca Raton, FL 33487-2742

© 2016 by Taylor & Francis Group, LLC
CRC Press is an imprint of Taylor & Francis Group, an Informa business

No claim to original U.S. Government works
Version Date: 20150820

International Standard Book Number-13: 978-1-4441-5738-3 (eBook - PDF)

This book contains information obtained from authentic and highly regarded sources. While all reasonable efforts have been made to publish reliable data and information, neither the author[s] nor the publisher can accept any legal responsibility or liability for any errors or omissions that may be made. The publishers wish to make clear that any views or opinions expressed in this book by individual editors, authors or contributors are personal to them and do not necessarily reflect the views/opinions of the publishers. The information or guidance contained in this book is intended for use by medical, scientific or health-care professionals and is provided strictly as a supplement to the medical or other professional's own judgement, their knowledge of the patient's medical history, relevant manufacturer's instructions and the appropriate best practice guidelines. Because of the rapid advances in medical science, any information or advice on dosages, procedures or diagnoses should be independently verified. The reader is strongly urged to consult the relevant national drug formulary and the drug companies' and device or material manufacturers' printed instructions, and their websites, before administering or utilizing any of the drugs, devices or materials mentioned in this book. This book does not indicate whether a particular treatment is appropriate or suitable for a particular individual. Ultimately it is the sole responsibility of the medical professional to make his or her own professional judgements, so as to advise and treat patients appropriately. The authors and publishers have also attempted to trace the copyright holders of all material reproduced in this publication and apologize to copyright holders if permission to publish in this form has not been obtained. If any copyright material has not been acknowledged please write and let us know so we may rectify in any future reprint.

Except as permitted under U.S. Copyright Law, no part of this book may be reprinted, reproduced, transmitted, or utilized in any form by any electronic, mechanical, or other means, now known or hereafter invented, including photocopying, microfilming, and recording, or in any information storage or retrieval system, without written permission from the publishers.

For permission to photocopy or use material electronically from this work, please access www.copyright.com (http://www.copyright.com/) or contact the Copyright Clearance Center, Inc. (CCC), 222 Rosewood Drive, Danvers, MA 01923, 978-750-8400. CCC is a not-for-profit organization that provides licenses and registration for a variety of users. For organizations that have been granted a photocopy license by the CCC, a separate system of payment has been arranged.

Trademark Notice: Product or corporate names may be trademarks or registered trademarks, and are used only for identification and explanation without intent to infringe.

Visit the Taylor & Francis Web site at
http://www.taylorandfrancis.com

and the CRC Press Web site at
http://www.crcpress.com

For Rachel, Ellie, Katie and Rosalind.

(PAB)

For Neila, Janaki, Tom, Arjun and Olivia.

(VM)

Contents

Foreword **xi**

Introduction **xiii**

In memoriam **xv**

Contributors **xvii**

PART 1 **1**

1 The scalp 3
Siavash Siv Eftekhari and R. Bryan Bell

2 Anatomy of the ageing face 11
Parkash L. Ramchandani

PART 2 **25**

3 External nose 27
Shan R. Baker and Parkash L. Ramchandani

4 Internal nose and paranasal sinuses 37
Tawakir Kamani and Anshul Sama

5 External ear 45
David Richardson

6 Temporal bone, middle ear and mastoid 53
Michael Gleeson

PART 3 **59**

7 Parotid gland 61
Luke Cascarini and Zaid Sadiq

8 Submandibular triangle 69
Daryl Godden and Barrie T. Evans

9 Oral cavity 77
Madan G. Ethunandan

10 Alveolar process 89
Niall McLeod

11 Anatomy of cleft lip and palate 99
Serryth Colbert and Chris Penfold

PART 4 **109**

12 Orbital skeleton 111
Barrie T. Evans and Simon Holmes
13 Orbital contents and periorbita 119
Antony Tyers
14 Mandible 133
Barrie T. Evans, Darryl Coombes, Peter A. Brennan and Vishy Mahadevan
15 Maxilla and zygoma 141
Barrie T. Evans, Darryl Coombes, Vishy Mahadevan and Peter A. Brennan
16 Infratemporal fossa, pterygopalatine fossa and muscles of mastication 151
Barrie T. Evans
17 Temporomandibular joint 167
Andrew J. Sidebottom

PART 5 **179**

18 Pharynx 181
Anthony D. Cheesman
19 Superior and posterior mediastinum 195
Vishy Mahadevan
20 Tissue spaces of the head and neck 201
Daren Gibson and Curtis Offiah
21 Larynx, trachea and tracheobronchial tree 209
Emma V. King and Vishy Mahadevan
22 Thyroid gland 221
Vishy Mahadevan and James N. Crinnion
23 Parathyroid glands 233
James N. Crinnion and Tom Wiggins

PART 6 **241**

24 The neck 243
Peter A. Brennan, Vishy Mahadevan and Barrie T. Evans
25 Posterior triangle and its contents 253
Rolfe Birch
26 Thoracic outlet 261
Vishy Mahadevan
27 Cervical spine 267
Hitesh Dabasia and Jason Harvey

PART 7 **277**

28 Neuroanatomy for the head and neck surgeon 279
Peter C. Whitfield
29 Skull base 287
Peter C. Whitfield

30 Osteology of the skull 295
Susan Standring
31 Overview of the cranial nerves 309
Susan Standring
32 Autonomic system in the head and neck 317
Susan Standring

Foreword

Mastery of the complex anatomy of the head and neck region is an essential requirement for all surgeons involved in surgical procedures in this area, regardless of their specialty. Navigating with ease through this complex maze of vital structures requires familiarity with anatomic relationships, to anticipate the presence and proximity of vital structures for smooth and safe conduct of surgical procedures. Lack of the knowledge of relevant surgical anatomy can lead to inadvertent injuries during operations, and disastrous functional and esthetic sequelae. Professor Peter Brennan, Professor Vishy Mahadevan, and Mr Barrie Evans are to be complimented for taking the challenge of compiling an authentic text book of surgical anatomy of the head and neck to aid students, trainees and practitioners of surgery in the head and neck region. This book is a much needed resource in this specialty.

The Editors have done an outstanding job in attracting leading surgeons and teachers of anatomy to contribute to this book and share their knowledge, expertise, experience and wisdom in making this a user-friendly and valuable reference volume. Accurate details of clinically relevant anatomic features and relationships at each site with emphasis on surgical anatomy, complemented by line drawings and actual intraoperative photographs, make this a unique compilation of topics regularly encountered in day-to-day practice of head and neck surgery. Tips recommended by experienced surgeons to avoid injury to vital structures are valuable features. The surgeon's perspective of operative regional anatomy is evident throughout, which is the very focus of this book.

In summary, the publishers and editors have produced a unique text book, which would be of tremendous value to students, trainees and practitioners in the fields of head and neck surgery, maxillofacial surgery, otolaryngology, facial plastic and reconstructive surgery, oral surgery, dentistry and allied surgical specialties. This would be a ready reference for surgeons not familiar with the field to brush up on anatomy, prior to embarking upon a surgical procedure. To that end, this book will have a definite place, in the libraries, of medical schools, training programs, and operating rooms, as well as the book shelves of students, trainees and practicing surgeons.

Jatin P Shah, MD, MS(Surg), PhD(Hon),
DSc (Hon), FACS, FRCS(Hon), FDSRCS(Hon),
FRCSDS(Hon), FRACS(Hon)
Professor of Surgery
EW Strong Chair in Head and Neck Oncology
Memorial Sloan Kettering Cancer Center
New York, NY

Introduction

PETER A. BRENNAN

The head and neck is one of the most complex parts of the body, with so many structures found in a relatively small area. It contains specialized sensory organs that allow us to see, hear, smell and taste, and is the start of both the respiratory and alimentary tracts. The thyroid and parathyroid glands are also located in the neck and form part of the endocrine system. Approximately 300 of the 800 or so lymph nodes that form part of the lymphoreticular system are found in the head and neck region, together with extra-nodal lymphoid tissue such as the palatine tonsils and adenoids. It is therefore not surprising that many lymphoid-related diseases present to head and neck specialists.

The face itself – with its large number of muscles of expression arising from the many bones that form the facial skeleton – conveys emotion, and in most societies is not hidden by clothing (and therefore always in view), so problems whether caused by disease, trauma or surgery are difficult to conceal.

The embryology of the head and neck is fascinating and explains many of the particularly interesting anatomical findings. An appreciation of the embryology is also important for understanding disease processes such as branchial cleft and thyroglossal cysts, and cleft lip and palate.

The diverse group of structures that make up the head and neck region are intimately related. Many nerves and blood vessels pass through other anatomical structures and have complicated relations. The area is richly innervated with sensory and motor nerves. All of the 12 cranial nerves have at least one or more functions in the head and neck, with two of them (vagus and accessory) passing through the neck to additionally innervate remote structures. Other important nerves arising from the cervical part of the spinal cord, including the phrenic nerve and brachial plexus, pass through the neck.

With all these structures found in such a small area, a detailed knowledge of the relevant surgical anatomy is essential for surgeons operating in this region. Unlike body cavity surgery where most of the important anatomy is located much deeper to the skin and protected by, for example, the ribs or anterior abdominal wall musculature, in the head and neck many structures are superficial. For example, it is relatively easy to permanently damage one or more branches of the facial nerve or the parotid duct with a knife or even a broken glass assault to the face, with potentially serious consequences for the patient's future quality of life (Figures 1 and 2). Major blood vessels are also quite superficial when compared to other anatomical areas. Sensory nerves pass through the facial bones en route to supplying the facial skin – in most other regions of the human body, sensory nerves do not enter bony canals. Finally, the teeth are attached to the mandible and maxilla in a unique way.

Head and neck anatomy is a difficult subject to learn, and just when junior doctors think that they may have mastered it, they often become confused and frustrated when trying to apply the knowledge gained from a textbook and cadaveric dissections to the operating room. Given the complexity of the head and neck, this is not surprising. Furthermore, some parts of the head and neck (such as the complex infratemporal fossa area) are not readily familiar to even the most experienced of surgeons, who may have to refer to anatomy texts and a dried skull before operating in this region.

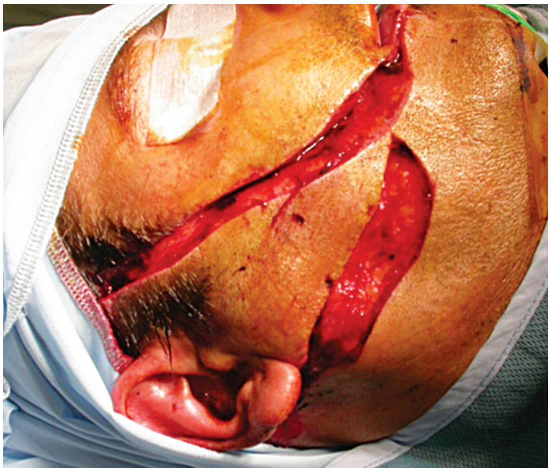

Figure 1 Many anatomical structures of the head and neck are located superficially. This shows a gross example of an assault by an assailant with broken glass resulting in transection of the parotid duct and three peripheral branches of the facial nerve.

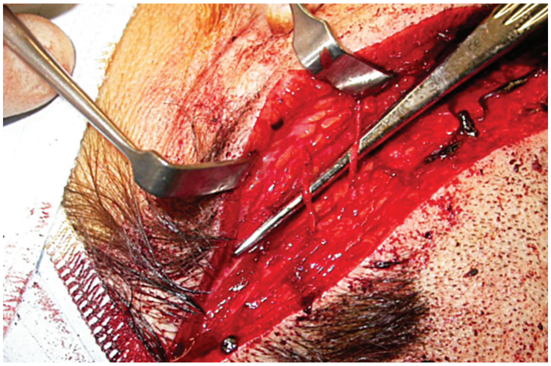

Figure 2 The same injury seen in Figure 1 clearly showing two facial nerve branches repaired with cable nerve graft. A branch at the end of the forceps was repaired directly. The patient went on to make an almost complete recovery with good facial nerve function.

While there are many head and neck anatomy and operative surgery textbooks available, few anatomy books are written *by* surgeons *for* surgeons, detailing, explaining and illustrating with operative pictures the relevant surgical anatomy that one needs to appreciate before operating in this fascinating area.

In the following chapters we have brought together expert surgeons from specialties including ear, nose and throat; oral and maxillofacial surgery; plastic surgery; general surgery; orthopaedics and neurosurgery, as well as internationally respected anatomy teachers. While the book covers the orbit and orbital contents, the eye itself has deliberately not been included. Similarly, only the neuroanatomy relevant to surgeons operating in the head and neck region has been included rather than a detailed account for neurosurgery. For completeness we have included chapters on skull osteology and the autonomic ganglia.

Where appropriate, anatomical variants, basic embryology, and potential hazards are discussed. The book has been illustrated throughout with clear photographs taken during surgery to demonstrate the essential anatomy seen at operation. Line diagrams have also been included either when needed or when a surgical photograph does not succinctly illustrate the points being made. A few radiological images have also been included to complement the surgical anatomy. Each chapter includes a list of references for further reading.

In memoriam

Barrie T. Evans

It is with great sadness that we inform you of the sudden, unexpected and untimely death of our co-editor, Barrie Evans, on 3rd July 2015.

Barrie was a well-respected surgeon and trainer, renowned in the UK and abroad. He had a great sense of humour, was passionate about head and neck anatomy, and inspired generations of both junior and senior colleagues at all stages of their careers.

While he was not part of the original conception and planning of this book, he gave a wealth of advice in its early stages. As a result, and while sitting in a well-known coffee outlet in his hospital - one of Barrie's favourite places to talk – we invited him to join us. It was a joy to see him looking excited and enthusiastic with the project; he worked tirelessly on it, inviting many respected authors and contributing to the editorial process.

He was pleased to see the first batch of chapter proofs which arrived in June 2015 and was particularly proud of his own chapter on the infra-temporal fossa, an anatomical area for which he was respected internationally.

Literally 36 hours before his death, Barrie sent an email to Peter, writing that he was counting down the days until publication. It is of course tragic that he didn't get to see the book that you are now holding in your hand, but we are certain that he would have been delighted with it.

We offer our sincere condolences to his wife, Christine.

Peter A. Brennan
Vishy Mahadevan

Contributors

Peter A. Brennan MD, FRCS, FRCSI, FDRCS
Barrie T. Evans FRCS (Eng & Edin), FDSRCS (Eng), FFDRCS (Ire)
Vishy Mahadevan MBBS, PhD, FRCS

Shan R. Baker MD (3)
Section of Facial Plastic and Reconstructive Surgery
Department of Otolaryngology – Head and Neck Surgery
University of Michigan
Center for Specialty Care
Livonia, Michigan, USA

R. Bryan Bell MD, DDS, FACS (1)
Medical Director
Providence Oral, Head and Neck Cancer Program and Clinic
Providence Cancer Center
Providence Portland Medical Center
Attending Surgeon, Trauma Service
Legacy Emanuel Medical Center
Affiliate Professor
Oregon Health and Science University
Head and Neck Surgical Associates
Portland, Oregon, USA

Rolfe Birch MChir, FRCPS (Glas), FRCS (Edin), FRCS (Eng) (25)
Professor in Neurological Orthopedic Surgery
University College London
Visiting Professor
Department of Academic Neurology
Imperial College London
Honorary Orthopaedic Consultant
Great Ormond Street Hospital for Sick Children
London, UK

Peter A. Brennan MD, FRCS, FRCSI, FDSRCS (Introduction, 14, 15, 24)
Chairman
Intercollegiate Committee for Basic Surgical Examinations (MRCS and DOHNS)
2016 President
British Association of Oral and Maxillofacial Surgeons
Consultant Oral and Maxillofacial Surgeon
Honorary Professor of Surgery
Queen Alexandra Hospital
Portsmouth, UK

Luke Cascarini FDSRCS, FRCS (OMFS) (7)
Head and Neck Surgeon
Guy's Hospital
London, UK

Anthony D. Cheesman FRCS, FRCSLT, BSc (Hons) (18)
Former Professor of Otolaryngology and Skull Base Surgery
Barts and the London NHS Trust
Charing Cross Hospital
Royal National Throat Nose and Ear Hospital
London, UK

Serryth Colbert MB BCh, BAO, BDS, MFDS (Eng), MRCS (Edin), MRCS (Irl), MSc (Oxon), FRCS (OMFS), FFD (Irl) (11)
Interface Fellow in Cleft Lip and Palate Surgery
South Wales and the South West (Morriston Hospital, Swansea, and Frenchay Hospital, Bristol)
UK

Darryl Coombes FDSRCS, FRCS (14, 15)
Consultant Oral and Maxillofacial Surgeon
Queen Victoria Hospital
East Grinstead, UK

James N. Crinnion MD, FRCS (22, 23)
Consultant Vascular and General Surgeon
Whipps Cross and the Royal London Hospitals
London, UK

Hitesh Dabasia FRCS (Tr & Orth), BSc (Hons) (27)
Specialist Registrar
Wessex Deanery
Queen Alexandra Hospital
Portsmouth, UK

Siavash Siv Eftekhari MD, DDS (1)
Resident
Department of Oral and Maxillofacial Surgery
Oregon Health and Science University
Portland, Oregon, USA

Madan G. Ethunandan MDS, FRCS (OMFS), FDSRCS, FFDRCS (9)
Consultant, Oral and Maxillofacial Surgery
Honorary Senior Clinical Lecturer
University Hospital Southampton NHS Foundation Trust
Southampton, UK

Barrie T. Evans FRCS (Eng & Edin), FDSRCS (Eng), FFDRCS (Ire) (8, 12, 14, 15, 16, 24)
Past President
British Association of Oral and Maxillofacial Surgeons
Formerly Consultant Oral and Maxillofacial Surgeon
Southampton University Hospitals
Southampton, UK

Daren Gibson BSc, MBBS, MRCS, DLO, FRCR ESHNR Fellow (20)
Consultant Radiologist
Fiona Stanley Hospital
Perth, Western Australia

Michael Gleeson MD, FRCS, FRACS, FDS (6)
Professor
Otolaryngology and Skull Base Surgery
National Hospital for Neurology and Neurosurgery
Queen Square
Honorary Consultant Skull Base Surgeon
Great Ormomd Street Hospital for Sick Children
Emeritus Professor
Otolaryngology
Consultant Surgeon
King's College London, Guy's, King's and St. Thomas' Hospitals
London, UK

Daryl Godden FRCS (OMFS) (8)
Consultant Maxillofacial Surgeon
Department of Maxillofacial Surgery
Gloucestershire Royal Hospital
Gloucester, UK

Jason Harvey MBBS, FRCSEd (Tr & Orth) (27)
Orthopaedic Spinal Consultant
Queen Alexandra Hospital
Portsmouth, UK

Simon Holmes FDSRCS, FRCS (12)
Consultant Oral and Maxillofacial Surgeon
The Royal London Hospital
Honorary Professor
Barts and the London School of Medicine and Dentistry
London, UK

Tawakir Kamani MD, MSc, FRCS, FRCS (Otol) (4)
Clinical Fellow in Paediatric Otoloaryngology
Royal Children's Hospital
Melbourne, Australia

Emma V. King PhD, FRCS-ORL(HNS) (21)
Consultant Surgeon and Associate Professor of Head and Neck Surgery
Poole Hospital NHS Foundation Trust
Poole, Dorset, UK

Vishy Mahadevan MBBS, PhD, FRCS (14, 15, 19, 21, 22, 24, 26)
Barbers' Company Professor of Anatomy
Royal College of Surgeons of England
London, UK

Niall McLeod FRCS(OMFS), FDS, MRCS (10)
Consultant Oral and Maxillofacial Surgeon
Oxford University Hospitals NHS Trust
Oxford, UK

Curtis Offiah BSc, MB ChB, FRCS, FRCR (20)
Consultant Neuroradiologist
Department of Radiology and Imaging
Royal London Hospital
Barts Health NHS Trust
London, UK

Chris Penfold MB BS, BDS, FRCS (Ed), FDRCS (Ed), FDRCS (Eng) (11)
Consultant Oral and Maxillofacial Surgeon
Glan Clwyd Hospital Rhyl
North East Wales NHS Trust
Wrexham Maelor Hospital
North Wales NHS Trust, Maelor Hospital,
Wrexham & Glan Clwyd Hospital, Bodelwyddan
Alder Hey Children's Hospital
Liverpool, UK

Parkash L. Ramchandani MB ChB (Hons), BDS, FDSRCS, FRCS, FRCS (OMFS) (2, 3)
Consultant
Oral and Maxillofacial Surgery
Head and Neck Surgery
Poole Hospital NHS Foundation Trust
Poole, Dorset, UK

David Richardson FRCS (Eng), FDSRCS (Eng) (5)
Consultant Maxillofacial Surgeon
Maxillofacial Unit
University Hospital Aintree
Paediatric Craniofacial Unit
Alder Hey Children's Hospital
Liverpool, UK

Zaid Sadiq FRCS (OMFS), MFDSRCS (7)
Consultant Oral and Maxillofacial/Head and Neck Surgeon
University College London Hospitals
London, UK

Anshul Sama BM, BSc, FRCS, FRCS (Orl) (4)
Consultant Otorhinolaryngologist
Queens' Medical Centre
Nottingham University Hospital
Nottingham, UK

Andrew J. Sidebottom BDS, FDSRCS, MB ChB, FRCS, FRCS (OMFS) (17)
Consultant Oral and Maxillofacial Surgeon
Queens Medical Centre
Nottingham University Hospitals
BMI Park Hospital
Circle Nottingham Treatment Centre
Trent Bridge Oral Surgery
Nottingham, UK

Susan Standring PhD, DSc, FKC, Hon FRCS (30, 31, 32)
Emeritus Professor Anatomy
King's College London
Anatomy Development Tutor
Royal College of Surgeons of England
London, UK

Antony Tyers FRCS, FRCSEd, FRCOphth (13)
Consultant Ophthalmologist and Ophthalmic Plastic Surgeon
Salisbury Health Care NHS Foundation Trust
Salisbury, UK

Peter C. Whitfield BM (Dist.) PhD, FRCS (Eng), FRCS (Surg Neurol) (28, 29)
Consultant and Associate Professor
Neurosurgery
South West Neurosurgery Centre
Plymouth Hospitals NHS Trust
Plymouth, UK

Tom Wiggins MB ChB, MRCS (23)
Specialist Registrar
General Surgery
Department of Endocrine Surgery
Barts Health NHS Trust
London, UK

PART 1

1 The scalp 3
Siavash Siv Eftekhari and R. Bryan Bell
2 Anatomy of the ageing face 11
Parkash L. Ramchandani

1

The scalp

SIAVASH SIV EFTEKHARI AND R. BRYAN BELL

INTRODUCTION

The scalp is subject to a multiplicity of conditions amenable to surgical treatment, including benign lesions (sebaceous cysts, naevi, keratoses, hemangiomas and others), malignant lesions (basal cell and squamous cell carcinoma, melanoma), burns, congenital malformations, neurofibromas, aneurysms and others. The scalp also serves as an important conduit to the facial skeleton and intracranial contents by virtue of the coronal incision. Therefore, a thorough and precise understanding of its anatomy is crucial for surgeons.

The scalp is a five-layered tissue that comprises collagen, elastin, blood vessels, nerve fibres and lymphatics, which contains mucopolysaccharide ground substance, hair follicles and sebaceous and sweat glands. It extends from the top of the forehead anteriorly to the superior nuchal line posteriorly. Laterally it projects down to the zygomatic arch and external acoustic meatus. The anatomic layers are well described by the convenient acronym SCALP: Skin, subcutaneous Connective tissue, galea Aponeurosis, Loose areolar tissue and Pericranium (Figure 1.1).

The first superficial three layers are united as one and difficult to separate. These three layers can easily slide over the loose areolar connective tissue layer, which is the ideal dissection plane for the surgeon. There is no good plane of dissection between the subcutaneous fat and the musculoaponeurotic layer. Epicranial muscles, where present, lie between the galea and the loose areolar tissue.

SKIN AND SUBCUTANEOUS TISSUE

The skin of the entire scalp is thick especially over the occipital area, ranging from 3 mm (vertex) to 8 mm (occiput). The subcutaneous fat just beneath the dermis contains many hair follicles and sebaceous and sweat glands, and thus is the most common site for sebaceous cyst. The thickness of the subcutaneous fat layer decreases with age but does not change significantly with obesity or weight loss. When developing skin flaps, the surgeon should include the fat layer in order to protect these important structures.

The skin and subcutaneous tissue are considered together because they are difficult to separate during surgery. A network of connective tissue fibres in the subcutaneous layer joins the skin to the musculoaponeurotic layer in a fashion similar to that in the palm and sole. The subcutaneous tissue contains many anastomosing arteries, veins and lymphatics. Subcutaneous fat is divided into multiple small compartments by fibrous septa. The arteries are attached to the deep layers

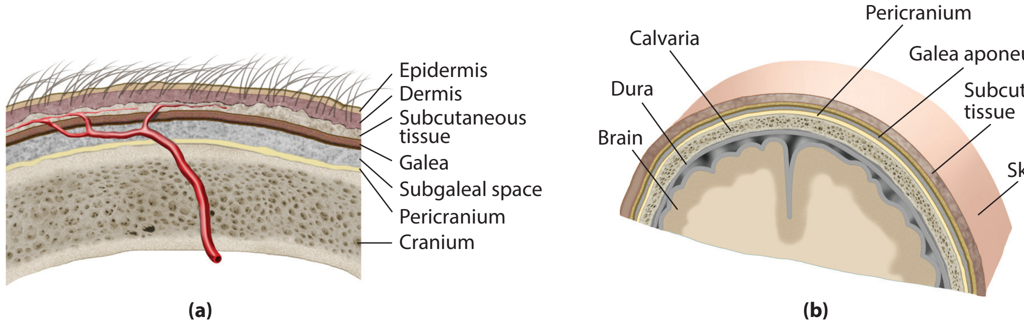

Figure 1.1**(a, b)** Tissue layers of the scalp.

of the dermis, and profuse bleeding that is commonly seen in scalp wounds is attributed to a relative inability of the arteries to retract due to their attachment to the dermis and fibrous septa. In practical application, the most expedient method of controlling haemorrhage during surgery or following trauma is by manual compression and immediate suturing of the subcutaneous and aponeurotic layer. Intraoperatively, hemostatic appliances, such as Raney clips may be used for the same purpose. Attempts to grasp bleeding points with haemostats or cauterize bleeding vessels should be avoided, as this will only damage hair follicles and lead to alopecia postoperatively.

Galea aponeurotica

The third layer composing the scalp is a dense connective tissue layer called galea aponeurotica. Strictly speaking, the galea only refers to the aponeurotic portion of the layer, which is manifested by a glistening sheet of fibrous tissue approximately 0.5 mm thick immediately below the subcutaneous tissue. The musculoaponeurotic layer consists of a series of paired muscles that include the frontalis, the occipitalis as well as the auricular muscles connected to a broad aponeurosis.

The lateral extension of the galea aponeurosis is into the temporoparietal region and is called the temporoparietal fascia (also known as superficial temporal fascia), which is continuous with the superficial musculoaponeurotic system (SMAS) of the face and the superficial cervical fascia (encasing the platysma) of the neck. The superficial temporal vessels travel just superior to the temporoparietal fascia, whereas the temporal branch of the facial nerve travels just deep to this layer. The paired frontalis muscles originate from the galeal aponeurosis and insert on the dermis at the level of the eyebrows. An extension of the galea aponeurosis splits the two quadrilateral frontalis muscles at the midline of the forehead. The paired occipitalis muscles originate from the lateral two-thirds of the superior nuchal line and external occipital protuberance and insert onto the galea aponeurosis overlying the occipital bone.

An important point for surgeons is that the galea is the strongest layer in the scalp. Care should be taken to include the aponeurosis in layered wound closure using resorbable sutures. Skin-only closures should be avoided whenever possible to prevent wound dehiscence. This is particularly important when repairing transverse lacerations of the scalp, as the opposing actions of the frontalis and occipitalis muscles tend to contribute to wound dehiscence.

Loose areolar tissue layer

The loose areolar tissue layer, also known as subgaleal layer, is the danger space of the scalp. It is a space which is largely avascular, containing only a filmy layer of loose fibroareolar tissue traversed by small arteries and emissary veins connecting the superficial scalp veins to the intracranial venous system. It is of great surgical importance and is a space that readily lends itself to surgical dissection. It is in this facial plane that cleavage occurs during traumatic avulsion of the scalp (Figure 1.2). Infections of this space may result in septic emboli in the intracranial sinuses and other complications

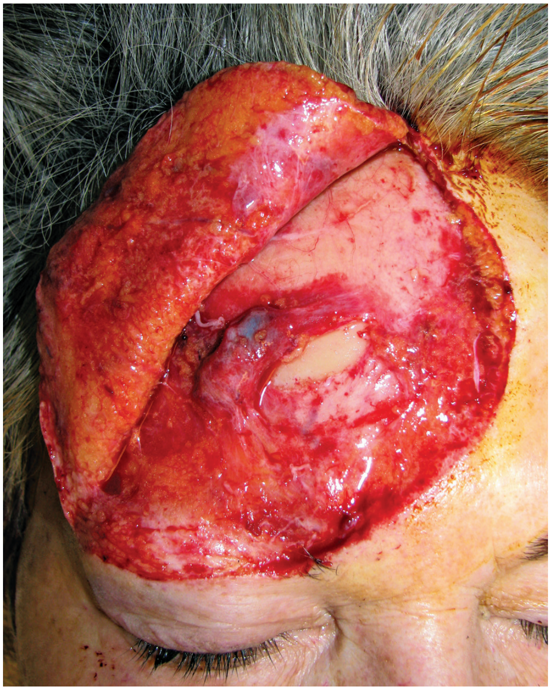

Figure 1.2 Partial scalp avulsion.

such as meningitis. Also, haemorrhage or infection in this layer can spread quickly, even as anteriorly as the level of periorbital region. This subgaleal fascia continues anteriorly deep to the orbicularis oris muscles and attaches laterally to the frontal process and superior surface of the zygomatic arch. Posteriorly, the loose areolar layer extends to just above the external auditory meatus and mastoid processes, eventually attaching again to the periosteum at the superior nuchal line.

A coronal flap for approaching the facial skeleton or calvarium is developed in the subgaleal plane, which is easily separated from the skin, subcutaneous tissue and galea aponeurosis. It is a versatile surgical approach to the upper and middle regions of the facial skeleton, including the nasal bones and zygomatic arch with the scar well hidden in the hairline (Figure 1.3). The location of the incision is influenced by the hairline and the extent of inferior access required. It is usually designed in sinusoidal (or s-like) fashion, extending if necessary on both sides to the preauricular skin fold. The incision does not need to be carried inferior to the helix, unless the zygoma is to be approached. Initially the incision is carried down to subgaleal plane from the level of one superior temporal line to the other. This prevents incising through the

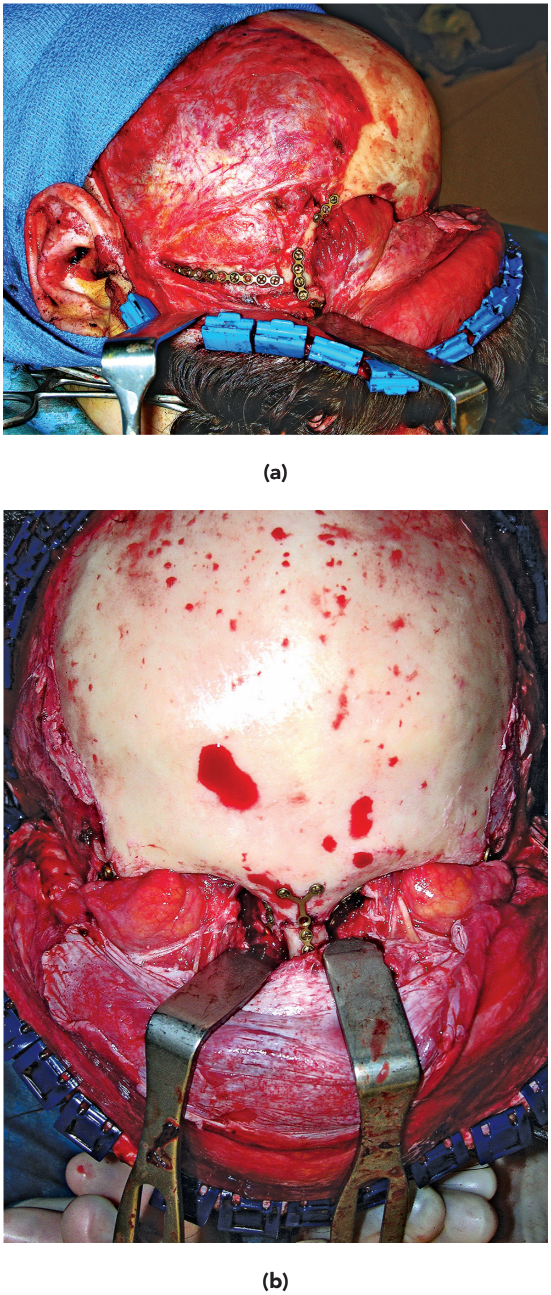

(a)

(b)

Figure 1.3 Coronal approach. **(a)** Showing access to zygomatic arch, zygomaticofrontal suture and infraorbital rim with tissue dissection over the temporalis muscle. **(b)** Showing access to nasal bone.

temporalis fascia into the temporalis musculature, which bleeds freely. Below the temporal line the skin incision should extend to the depth of the glistening superficial layer of the temporalis fascia, which is continuous with the subgaleal dissection plane. The scalp may be elevated anteriorly atop the pericranium and laterally just above the superficial layer of the temporalis facia. Laterally, care must be taken not to damage the superficial temporal artery and the temporal branch of facial nerve, the outer limits of the latter being 0.5 cm from the tragus, 1 cm from the junction of the pinna and temporal region, joined to a line 2 cm above and lateral to the frontozygomatic suture region. The upper trunk of the facial nerve itself crosses the zygomatic arch between 0.5 cm and 3.5 cm from its root in the classic study by Al Kayat and Bramley. The pericranium is then incised anteriorly to expose the facial skeleton at the level about 3–4 cm above the supraorbital rim. The design may vary if it is necessary to create a vascularized pericranial flap.

Pericranium

The pericranium, or the periosteum of the skull, is a dense membranous or fibrous sheet loosely fused on its outer aspect to the galea aponeurotica, from which it is readily separable via the subgaleal space. It is firmly attached to the calvarium, particularly along the suture lines, and it readily retracts when released owing to its elasticity. Its properties are not unlike periosteum elsewhere in the body: It provides minimal blood supply to the underlying cranial bone, and therefore, detachment of the periosteum in the scalp does not cause underlying bone necrosis but may produce some demineralization. Pericranial thickness varies from one individual to another and from one skull location to another in the same individual, but in general the pericranium in the frontal areas is slightly thinner than that on the crown.

Clinically, the pericranium is important in that it can be raised as a robust and versatile pedicled flap, which has utility in skull base surgery and frontobasilar trauma repair (Figure 1.4). Frontal sinus obliteration for traumatic injuries to the frontal sinus and reconstruction after frontal sinus cranialization are common applications of the pericranial flap and have been shown to be reliable in long-term series with relatively few complications. It is usually reflected from posterior border of our coronal flap edge anteriorly, keeping a wide base. This flap, when elevated as a pedicle flap, is in fact vascularized. The blood supply to the nondetached pericranium arises from terminal branches of the internal and external carotid arteries, namely the supraorbital and supratrochlear vessels and branches of the superficial temporal vessels. In raising the narrow base pericranial pedicle flap, care must be taken to include the supratrochlear branch as studies show that this branch is crucial in providing the blood supply to this flap. Doppler studies have also demonstrated good blood supply to the elevated pericranium, which may explain why reconstructive procedures involving this flap have been extremely successful.

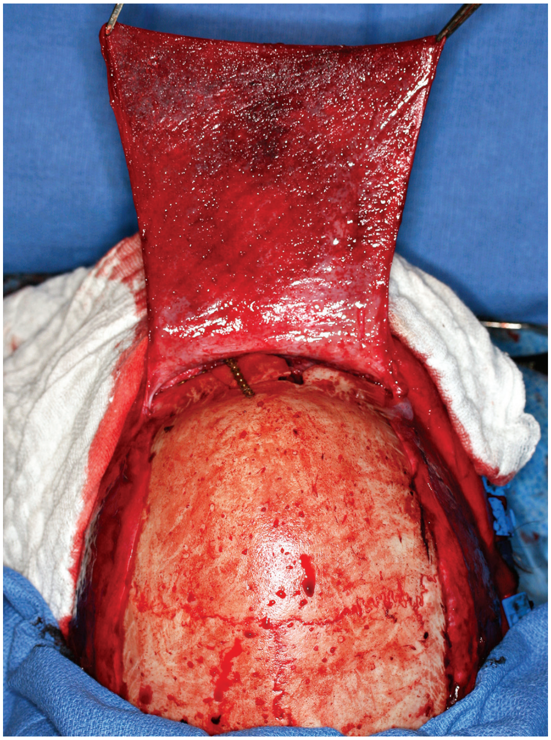

Figure 1.4 Pericranial flap reflected anteriorly. The wide base will ensure inclusion of supraorbital and supratrochlear vessels.

In addition, preservation of the pericranium can be useful to serve as a foundation for skin grafting and other reconstructive procedures of the scalp.

Temporoparietal region of the scalp

In the temporoparietal region, beneath the temporoparietal fascia, lies the extension of the subgaleal fascia, which can be dissected as a separate layer in this area but is usually used only as a continuance of the subgaleal plane in the coronal flap approach to the facial skeleton. Beneath subgaleal fascia in the temporoparietal region lies the temporalis fascia (deep temporal fascia), which arises superiorly from the superior temporal line where it fuses with the pericranium (Figure 1.5). The temporalis fascia is continuous with the pericranium above the superior temporal lines, the parotidomasseteric fascia below the level of the zygomatic arch, and the cervical fascia incasing the muscles of the neck. At the level of the superior orbital rim, the temporalis fascia divides into a superficial layer, which attaches to the lateral border of the zygomatic arch, and a deep layer, which attaches to the medial border of the zygomatic arch. The middle temporal artery, a branch of the superficial temporal artery, is the primary blood supply to the temporalis fascia. Intervening between the superficial and deep layers is the superficial temporal fat pad. The blood supply to the temporal fat pad is the middle temporal artery, a branch of the superficial temporal artery. Deep to the deep temporalis fascia

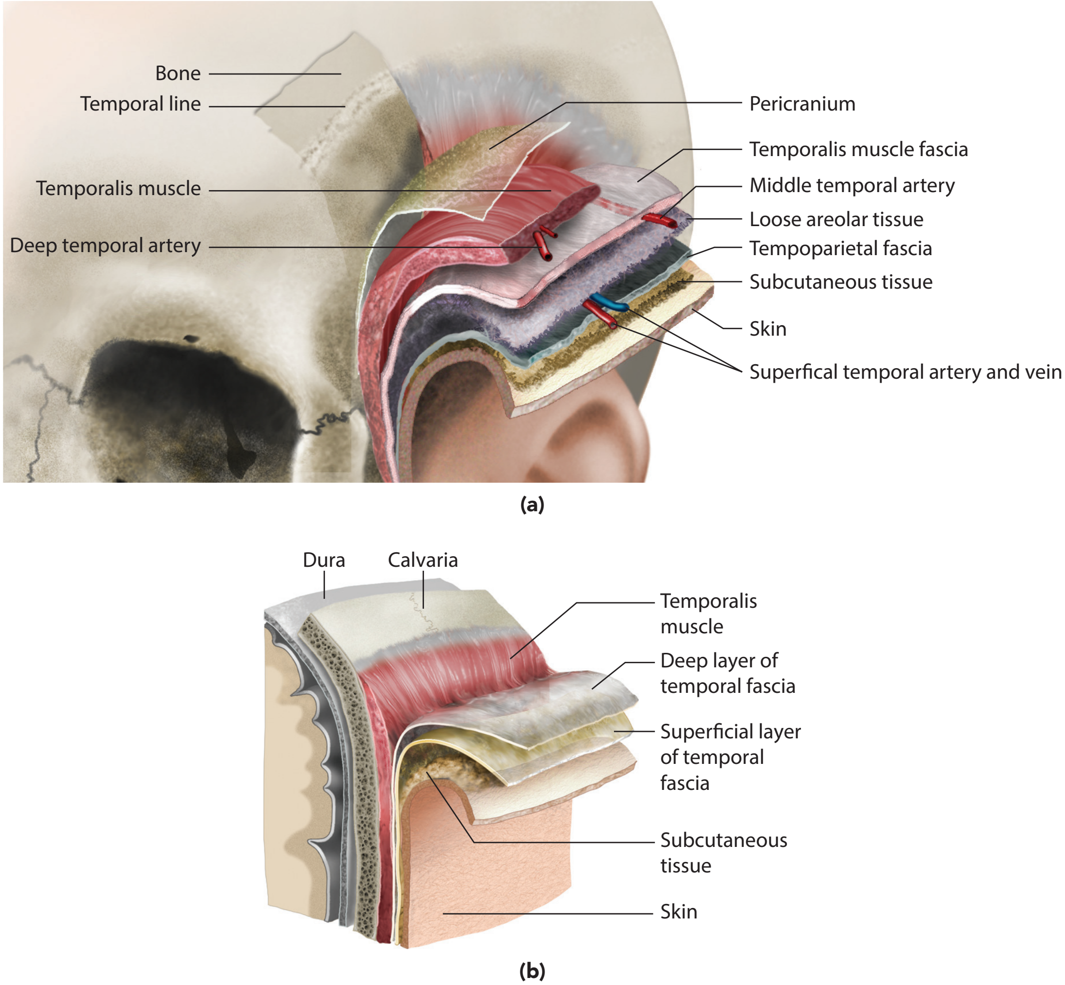
Bone
Temporal line
Temporalis muscle
Deep temporal artery
Pericranium
Temporalis muscle fascia
Middle temporal artery
Loose areolar tissue
Tempoparietal fascia
Subcutaneous tissue
Skin
Superfical temporal artery and vein
(a)
Dura
Calvaria
Temporalis muscle
Deep layer of temporal fascia
Superficial layer of temporal fascia
Subcutaneous tissue
Skin
(b)

Figure 1.5**(a, b)** Tissue layers of the temporoparietal region of scalp. The facial nerve crosses the zygomatic arch passing between the under surface of the temporoparietal fascia and the fusion of the zygomatic arch, the superficial layer of temporalis fascia, and subgaleal fascia.

is the buccal fat pad. The temporalis muscle arises from the deep layers of the temporalis fascia at the temporal fossa, passing medial to the zygomatic arch and inserting onto the coronoid process of the mandible. The blood supply to the temporalis muscle is primarily from the anterior and posterior deep temporal arteries (branches of internal maxillary artery), and secondarily from the superficial temporal artery.

The temporoparietal fascia can be harvested as a pedicled or free flap and has numerous applications in craniomaxillofacial surgery. It is a thin and pliable flap with an axial blood supply and a good arc of rotation for head and neck reconstruction. The flap can be used as a fascial flap, a fasciocutaneous flap or an osteofascial flap with good, predictable results. It is the only single-layered fascial flap that can be transposed into the craniofacial and head and neck region on its vascular pedicle. It is pedicled on the superficial temporal vessels and is a component of the SMAS layer. It can be made as wide as 14 cm on a 17- to 18-cm superficial temporal vascular pedicle. When necessary, the flap can be transferred to more distal locations using microvascular techniques.

BLOOD SUPPLY OF THE SCALP

The arterial blood supply to the scalp is via the internal and external carotid artery system. The internal carotid artery contributes to blood supply of the scalp through the supraorbital and supratrochlear arteries, both of which are small branches of the ophthalmic artery entering the scalp anteriorly. The external carotid artery contributes to the blood supply of the scalp via the superficial temporal artery and its lateral branches, the frontalis and parietal arteries. Additionally, the posterior auricular artery and occipital arteries supply the posterior portion of the scalp. The mastoid branch of the occipital artery contributes to the scalp overlying the mastoid air cells.

The blood supply is centripetal, meaning that the larger trunks run medially and centrally from the periphery, becoming smaller as they enter a system of free anastomoses running within the subcutaneous tissues towards the midline. It is important to understand that when the internal carotid artery is thrombosed, the external carotid artery supplies blood to the anterior part of the scalp via the angular and the ophthalmic arteries. In all likelihood, the scalp also derives at least some minimal blood supply from bone perforators deriving from meningeal vessels. This would explain the survival of areas of the surgically circumscribed scalp. The fact that the scalp is not supplied by musculocutaneous perforators, however, is of enormous practical importance for surgeons, as surgical transection of subcutaneous vasculature, and particularly of larger trunks in the periphery of the scalp, has dire consequences for the blood supply of tissues both adjacent to and distant from the transection site.

NERVES OF THE SCALP

The sensory nerve supply of the scalp is similar to the vascular anatomy in that it is centripetal, subcutaneous and of a similar distribution. Incisions in the peripheral scalp that transect vital larger vascular and nerve trunks result in extensive, hypesthetic, poorly vascularized tissues and should be avoided. Where avoidance is not possible because of the specific goals of the surgery, a knowledge of the exact anatomic location of the major neurovascular trunks is imperative if these structures are to be spared during surgery.

The scalp is innervated by branches of the three divisions of the trigeminal nerve, cervical spinal nerves and branches from the cervical plexus. The superficial division of the supraorbital nerve pierces the frontalis muscle on the forehead and supplies the skin of the forehead and anterior hairline region. The deep division of the supraorbital nerve runs just superficial to the periosteum up until the level of the coronal suture, where it pierces the galea aponeurosis approximately 0.5 to 1.5 cm medial to the superior temporal line to innervate the frontoparietal scalp.

Consideration can be given to preservation of this nerve in scalp reconstruction. A branch from the maxillary division of the trigeminal nerve, the zygomaticotemporal nerve, supplies a small region lateral to the brow up to the superficial temporal crest. The auriculotemporal nerve, a branch from the mandibular division of the trigeminal nerve, supplies the lateral scalp territory. The greater occipital nerve, from the dorsal rami of the cervical spinal nerves, and the lesser occipital nerve, from the cervical plexus, both innervate the occipital territory. The greater occipital nerve has been shown to emerge from the semispinalis muscle approximately 3 cm below the occipital protuberance and 1.5 cm lateral to the midline.

Knowledge of scalp anatomy is critically important for the surgeon managing acquired, congenital and developmental craniomaxillofacial deformity and conditions. It is hoped that the reader will be able to apply this basic anatomic knowledge to the operating room, ultimately to improve patient care and outcomes.

FURTHER READING

Abdul-Hassan HS, von Drasek Ascher G, Acland RD. Surgical anatomy and blood supply of the fascial layers of the temporal region. *Plastic Reconstructive Surgery*. 1986; 77: 17.

Abubaker AO, Sotereanos G, Patterson GT. Use of the coronal surgical incision for reconstruction of severe craniomaxillofacial injuries. *Journal of Oral and Maxillofacial Surgery.* 1990; 48(6): 579–86.

Al-Kayat A, Bramley P. A modified pre-auricular approach to the temporomandibular joint and malar arch. *British Journal of Oral Surgery*. 1979; 17: 91–103.

Argenta LC, Friedman RJ, Dingman RO, et al. The versatility of pericranial flaps. *Plastic Reconstructive Surgery.* 1985; 76: 695–702.

Bell RB, Dierks EJ, Brar P, et al. A protocol for the management of frontal sinus fractures emphasizing sinus preservation. *Journal of Oral and Maxillofacial Surgery.* 2007; 65: 825.

Bell BR, Markiewicz MR. Traditional and contemporary surgical approaches to the orbit. *Oral and Maxillofacial Surgery Clinics of North America.* 2012; 24: 573–607.

Cesteleyn L. The temporoparietal galea flap. *Oral Maxillofacial and Surgery Clinics of North America*. 2003; 15: 537–50.

Ellis E, Zide MF. *Surgical Approaches to the Facial Skeleton.* 2nd ed. Philadelphia: Lippincott Williams & Wilkins, 2006.

Fallah DM, Baur DA, Ferguson HW, Helman JI. Clinical application of the temporoparietal-galeal flap in closure of a chronic oronasal fistula: Review of the anatomy, surgical technique, and report of a case. *Journal of Oral and Maxillofacial Surgery.* 2003; 61: 1228–30.

Helman JI, Cesteleyn L. Local flaps in facial reconstruction. A comprehensive approach for the oral and maxillofacial surgeon. In: *Dissection Manual*. Ann Arbor, MI: The University of Michigan Section of Oral and Maxillofacial Surgery, 1998.

Luo W, Wang L, Jing W, et al. A new coronal scalp technique to treat craniofacial fracture: The supra temporalis approach. *Oral Surgery, Oral Medicine, Oral Pathology and Oral Radiology*; 2012; 113(2): 177–82.

Matloub H, Molnar J. Anatomy of the scalp. In: Stough D, Haber R. (Eds.). *Hair Replacement.* St. Louis: Mosby, 1996.

Miles B, Davis S, Candall C, Ellis E. Laser-Doppler examination of the blood supply in pericranial flaps. *Journal of Oral and Maxillofacial Surgery.* 2010; 68: 1740–45.

Munro IR, Fearon JA. The coronal incision revisited. *Plastic and Reconstructive Surgery.* 1994; 93(1): 185–7.

Nameki H, Kato T, Nameki I, et al. Selective reconstructive options for the anterior skull base. *International Journal of Clinical Oncology.* 2005; 10: 223.

Newman J, Costantino P, Moche J. The use of unilateral pericranial flaps for the closure of difficult medial orbital and upper lateral nasal defects. *Skull Base*. 2003; 13: 205.

Raposio R, Santi L, Nordstrom REA. Serial scalp reductions: A biomedical approach. *Dermatological Surgery.* 1999; 25: 210–4.

Rose EH, Norris MS. The versatile temporoparietal fascial flap: Adaptability to a variety of composite defects. *Plastic Reconstructive Surgery.* 1990; 85: 224.

Seery GE. Surgical anatomy of the scalp. *Dermatological Surgery*. 2002 July; 28(7): 581–7.

Seery GE. Scalp surgery: Anatomic and biomechanical considerations. *Dermatological Surgery.* 2001 September; 27(9): 827–34.

Tolhurst ED, Carstens MH, Greco RJ, Hurwitz DJ. The surgical anatomy of the scalp. *Plastic and Reconstructive Surgery*. 1991 Apr; 87(4): 603–12.

Williams PH, Warwick R. (Eds.). *Gray's Anatomy.* 36th ed. Philadelphia: Saunders, 1985.

Yano H, Sakihama N, Matsuo T, et al. The composite galeal frontalis pericranial flap designed for anterior skull base surgery. *Plastic and Reconstructive Surgery.* 2008; 122: 79e.

2

Anatomy of the ageing face

PARKASH L. RAMCHANDANI

Introduction 11
Skin 11
Fat 13
SMAS 15
Ligaments 16
Facial nerve 17
Muscles of facial expression 18
Periocular muscles *18*
Perioral muscles *20*
Platysma *20*
Effect of ageing on muscles 21
Chin and cervicomental angle 21
Blood supply 21
Sensory nerve supply 21
Effect of ageing on bone 22
Further reading 23

INTRODUCTION

Knowledge of the surgical anatomy of the face and the changes that occur with ageing is paramount for safe operating and helps to achieve an enduring result. The face does not age as one confluent mass; rather, there is a complex interaction between the hard and soft tissues and between independent soft tissue compartments. The genetic variability of facial morphology and the differing pace of ageing between patients make it difficult to generalize, but some common themes emerge, which will be discussed in this chapter.

SKIN

Facial skin is composed of the epidermis and more fibrous dermis. It is thickest in the scalp and thinnest over the eyelid, where it can be as thin as 0.04 mm in depth. The dermis is divided into the superficial papillary layer and the deeper and thicker reticular layer. The papillary dermis has a rich microcirculation, the subpapillary plexus, which runs just beneath the epidermis, from where it sends an arcade of capillary loops into each dermal papilla. It also has collagen bundles, elastic fibres and ground substance produced by fibroblasts. Ground substance 'plumps' the skin, giving it a youthful appearance. The reticular dermis has a deeper dermal plexus, which surrounds the skin appendages and is composed of larger vessels. It also contains thick bundles of coarse collagen and elastic fibres.

Skin ageing is influenced by genetically determined intrinsic factors and modified by extrinsic insults. Over time there is atrophy of the epidermis with a decrease in Langerhans cells and melanocytes; variability in the size and shape of epidermal cells; the appearance of atypical nuclei; a reduced number of fibroblasts, mast cells and blood vessels; shortening of capillary loops and abnormal morphology of nerve endings. There is also fragmentation of the dermal collagen and decrease in elastin and ground substance, which become replaced by fibrous tissue. This results from the action of matrix metalloproteinases and leads to a loss in structural integrity and impairment of fibroblast function because they cannot attach to fragmented collagen. Treatments that stimulate the production of new non-fragmented collagen should improve the facial appearance; this is seen with topical agents such as retinoic acid and with carbon dioxide laser. The rate of skin renewal also decreases, which causes the epidermis to become loose and skin creases to become evident in a direction perpendicular to the direction of muscle action. In women oestrogen levels decrease at menopause, which causes further thinning of the dermis, irregularity of the epidermis and atrophy of the fat; decreased blood supply to the skin, loosening of the epidermis and rough texture of the skin; and hyperpigmentation because of increased melanin.

These changes are modified by long-term exposure to external insults, including dehydration, inadequate nutrition, extremes of temperature, trauma, toxins such as cigarette smoke, and ultraviolet radiation. Photodamage causes thickening of the epidermis, flattening of the dermoepidermal junction and an increase in hyperplastic fibroblasts and inflammatory infiltrates.

Both intrinsic and extrinsic ageing affect the ability of the outer skin envelope to adjust to underlying volume loss. A very elastic outer skin envelope in unlikely to ‘lift’ significantly with fillers alone and may require treatment with multiple modalities such as surgical lifting, lasers and deep chemical peels.

A formal assessment of skin helps to achieve a satisfactory outcome and avoid complications in procedures such as dermabrasion. The Fitzpatrick classification of skin colour type measures genetic disposition, reaction to sun and tanning habits (Table 2.1).

The earliest textural changes in skin are fine superficial lines or wrinkles, which with time increase and become organized. Mimetic lines due to facial muscle contraction get added. With repeated muscular contractions these mimetic lines extend into the dermis causing skin furrows and folds. Worry lines are transverse lines on the forehead perpendicular to frontalis; frown lines in the glabellar region are oblique and perpendicular to corrugator. Crow’s feet are lateral periorbital lines perpendicular to orbicularis oculi. Smile lines are perpendicular to zygomaticus. Lines from the corner of the mouth to the jowls are marionette lines. Clinically, mimetic lines and furrows respond to multimodality therapy such as injectable fillers, Botox or laser resurfacing. Skin folds, however, require surgical tightening procedures like brow lift, blepharoplasty and facelift.

The Glogau classification was developed to objectively measure the severity of photoageing and especially wrinkles (Table 2.2). It helps the surgeon to pick the best procedures to treat photoageing.

Table 2.1 Fitzpatrick classification of skin colour types

Skin type	Skin colour	Reaction to sun and tanning habit
Type I	Light, pale white	Always burns, never tans
Type II	White, fair	Usually burns, tans with difficulty
Type III	Medium, white to light brown	Sometimes burns mildly, gradually tans to a light brown
Type IV	Olive, moderate brown	Rarely burns, tans with ease to a moderate brown
Type V	Brown, dark black	Very rarely burns, tans very easily
Type VI	Black, very dark brown to black	Never burns, tans very easily, deeply pigmented

Table 2.2 Glogau classification of skin photoageing

Group	Classification	Typical age	Description	Skin characteristics
I	Mild	28–35	No wrinkles	Early photoageing: mild pigment changes, no keratosis, minimal wrinkles, minimal or no makeup
II	Moderate	35–50	Wrinkles in motion	Early to moderate photoageing: Early brown spots visible, keratosis palpable but not visible, parallel smile lines begin to appear, wears some foundation
III	Advanced	50–65	Wrinkles at rest	Advanced photoageing: Obvious discolorations, telangiectasis, visible keratosis, always wears heavier foundation
IV	Severe	60–75	Only wrinkles	Severe photoageing: Yellow-grey skin colour, prior skin malignancies, wrinkles throughout – no normal skin, cannot wear makeup because it cakes and cracks

FAT

Subcutaneous fat varies greatly in thickness and texture among individuals and in different regions of the face, and forms the basis of facial volume and contour. Eighty per cent is located in the face and 20 per cent in the neck. The fat is divided into superficial and deep layers by the superficial musculoaponeurotic system (SMAS), with 57 per cent above it and 43 per cent below it, and in both layers it is present as multiple compartments that are thought to age independently.

In the superficial layer, fat is arranged as small yellow lobules interwoven with fibrous septa that connect the SMAS to the dermis. It has a protective role. The named superficial fat compartments are the nasolabial, cheek (medial, middle and lateral-temporal), infraorbital, forehead-temporal (central, middle temporal, temporal-cheek) and jowl (Figure 2.1).

Fat in the deep layer is found in or around muscles, where it is thought to improve the gliding of tissue planes during muscle movement (Figure 2.1). It is present as large white lobules with a sparse network of thin fibrous septa. The buccal fat pad (Bichat's fat pad) consists of a main body and four extensions: buccal, pterygoid, pterygopalatine and temporal (Figure 2.2). The main body lies on the anterior border of the masseter and extends deeply to lie on the posterior maxilla and forward along the buccal vestibule. The parotid duct and zygomatic and buccal branches of the facial nerve cross the lateral surface of the fat pad. The buccal extension, which together with the body accounts for about half the total weight, lies superficially within the cheek and is partially responsible for the cheek contour. The pterygopalatine extension extends to the pterygopalatine fossa and inferior orbital fissure. The pterygoid extension is a posterior extension in the pterygomandibular space. The temporal extension is divided into the superficial and deep components. The superficial part is between the deep temporal fascia and temporalis muscle and tendon. The deep part lies behind the lateral orbital wall and frontal process of the zygoma and turns backwards into the infratemporal space. The mean weight is about 9.3 g and the mean volume 9.6 mL. It has a rich plexus of blood vessels from branches of the maxillary, superficial temporal and facial arteries, which allow it to be used as an axial pattern pedicled flap. It also contains lymphatics and myelinated nerves, and the veins are tributaries of the pterygoid venous plexus.

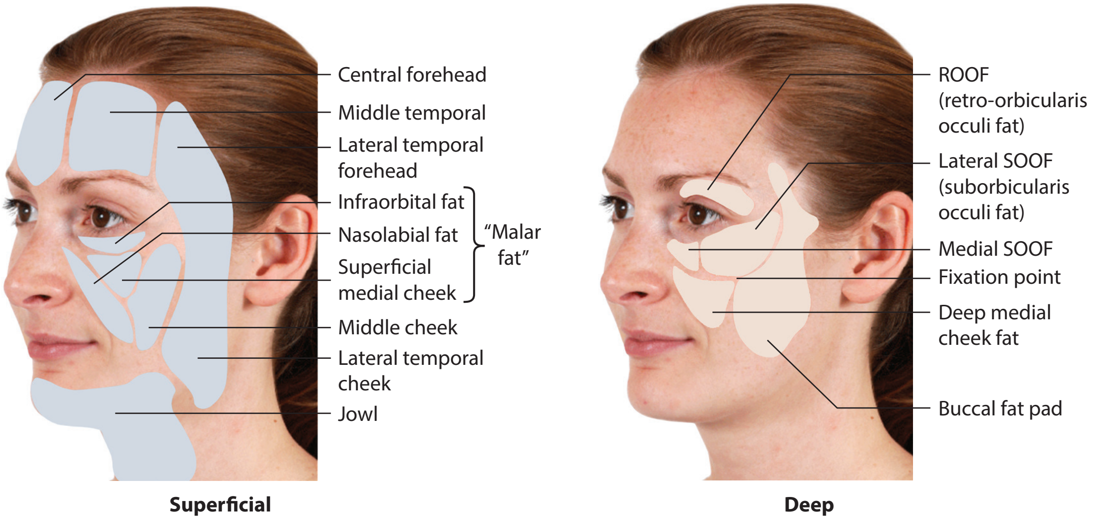
Central forehead
Middle temporal
Lateral temporal forehead
Infraorbital fat
Nasolabial fat
Superficial medial cheek
"Malar fat"
Middle cheek
Lateral temporal cheek
Jowl
Superficial
ROOF (retro-orbicularis occuli fat)
Lateral SOOF (suborbicularis occuli fat)
Medial SOOF
Fixation point
Deep medial cheek fat
Buccal fat pad
Deep

Figure 2.1 Fat compartments of the face.

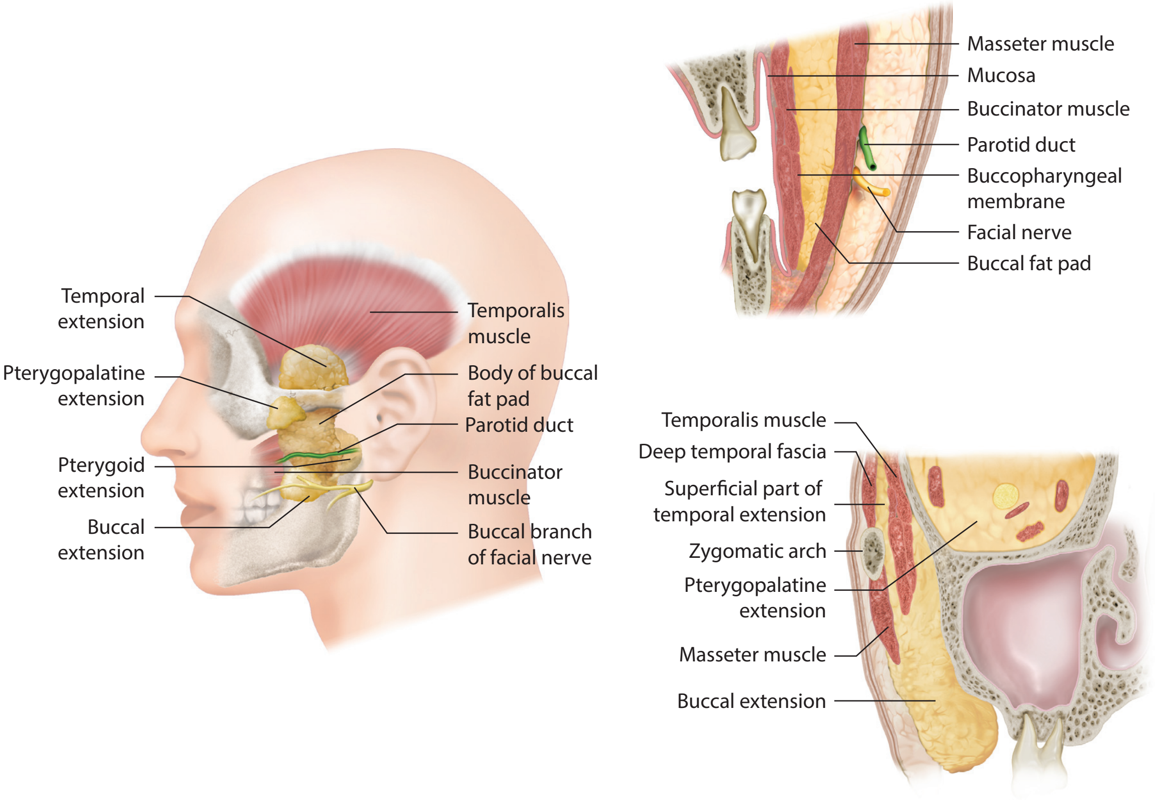
Masseter muscle
Mucosa
Buccinator muscle
Parotid duct
Buccopharyngeal membrane
Facial nerve
Buccal fat pad
Temporal extension
Pterygopalatine extension
Pterygoid extension
Buccal extension
Temporalis muscle
Body of buccal fat pad
Parotid duct
Buccinator muscle
Buccal branch of facial nerve
Temporalis muscle
Deep temporal fascia
Superficial part of temporal extension
Zygomatic arch
Pterygopalatine extension
Masseter muscle
Buccal extension

Figure 2.2 Extensions of the buccal fat pad.

In the periocular region the fat pad deep to the orbital septum is called periorbital fat, and that deep to the orbicularis oculi is the suborbicularis oculi fat pad (SOOF). The SOOF facilitates sliding of the muscle over the periosteum. It is contiguous with the subcutaneous malar fat pad so that elevation of the SOOF also lifts the malar pad reducing the melolabial fold. It is composed of two compartments – medial SOOF lying between medial limbus and lateral canthus; and lateral SOOF, extending from the lateral canthus to the lateral orbital thickening (Figure 2.1). The cephalic attachment is at the arcus marginalis. The SOOF wraps around the attachment of the levator anguli oris, just inferior to the medial third of the inferior orbital rim. The aged face is associated with descent of the SOOF over the orbital rim producing malar bags that are lateral to the lower eyelid bags. These can be resuspended superiorly and laterally during a lower lid blepharoplasty, correcting the 'tear trough deformity'. Deep to orbicularis and adjacent to the periosteum of the supraorbital rim lies the eyebrow fat pad, the retro-orbicularis oculi fat (ROOF) (Figure 2.1). This becomes more diffuse and extends into the plane between the septum and the orbicularis muscle as flimsy areolar tissue. The upper eyelid usually contains two fat pads, nasal and central, while the lower eyelid contains three, temporal, central and nasal (Figure 2.3). The lacrimal gland is located laterally in the same plane as the upper eyelid fat pad. Its pink colour is distinctive and great care should be taken to avoid injuring it during surgery. The central fat pad of the upper eyelid is less vascular than the nasal. The inferior oblique muscle separates the nasal and central fat pads of the lower eyelid. Injury to this muscle during dissection may result in postoperative diplopia.

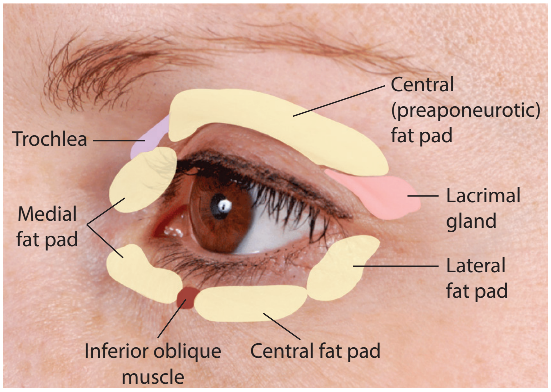

Figure 2.3 Eyelid fat pads.

With age there is loss of superficial subcutaneous fat due to decreased vascularity. However, there is increased accumulation of fat in the deep fat layer, due to slowing of metabolism after the fourth decade. These changes are accentuated in women due to decreasing oestrogen levels after the age of 50. Differential fat loss and/or ptosis lead to changes in shape and contour. Folds occur at transition points between thick and thinner superficial fat compartments (pseudoptosis), and these can be seen in the nasolabial fold, submental crease and preauricular fold.

SMAS

The SMAS is a fibromuscular layer investing and interlinking the muscles of facial expression. It is strongest in the scalp, where it is called galea aponeurotica, and it continues caudally as the temporoparietal fascia. It is discontinuous at the zygoma, becoming thin and tenuous in the midcheek, continuing into the neck to invest platysma. SMAS is thick and uniform over the parotid gland and masseter. It is closely applied to the capsule of the parotid gland but thins out in the anterior cheek region where it splits to invest the facial mimetic and platysma musculature.

In the lower face, the facial nerve branches are always deep to the SMAS innervating the facial muscles on their undersurface. The vessels and sensory nerves similarly arise deep to the SMAS and remain at that level, except for their terminal branches. These structures are protected if dissection is superficial to the muscles of facial expression. In the temporal area, the temporal branch of the facial nerve runs on the deep surface of the temporoparietal fascia. In the upper face the supraorbital and supratrochlear neurovascular bundles arise from their respective bony foramina and notches and penetrate the SMAS to run on its surface superficial to the frontalis muscle. The more medial branches of the nerves emerge from the submuscular to the subcutaneous plane almost immediately after leaving the orbit; the more lateral branches traverse superiorly before making this change to the subcutaneous plane. Similarly, the superficial temporal vessels run with the auriculotemporal nerve along the temporoparietal fascia for a few centimetres before entering the subcutaneous fat.

Deep to the SMAS is the deep fascia. In the temporal region it is called the deep temporal fascia and is made of superficial and deep layers separated by the temporal fat pad. Deep to the deep layer is the temporalis muscle, and in the same plane just above the zygomatic arch is the temporal component of the fat pad of Bichat, also known as the deep temporal fat pad. Below the zygomatic arch the deep fascia is a thin translucent layer covering the masseter muscle, facial nerve, facial artery, vein and parotid duct. This is the parotidomasseteric fascia. Deep to this fascia more anteriorly are the buccal fat pad and the deep facial mimetic muscles (levator anguli oris, buccinators and mentalis). The facial nerve branches lie superficial to branches of the facial artery and vein, parotid duct and buccal fat pad, and they innervate the deep facial mimetic muscles from their superficial surface. The parotidomasseteric fascia is thin and fragile. Great care must be taken while dissecting the SMAS off this thin layer, particularly anteriorly, as the facial nerve branches pierce this fascia to innervate the superficial mimetic facial muscles.

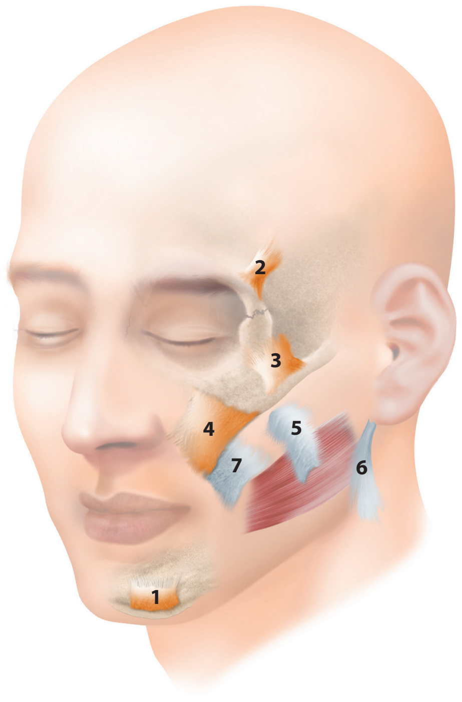

True retaining ligaments

1. Mandibular ligaments
2. Orbital ligaments
3. Zygomatic ligaments
4. Buccal maxillary ligaments (maxillary part)

False retaining ligaments

5. Masseteric ligaments
6. Platysma auricular ligaments
7. Buccal maxillary ligaments (buccal part)

Figure 2.4 Ligaments of the face.

LIGAMENTS

The retaining ligaments are aponeurotic condensations of fibrous tissue that run from deeper structures to overlying dermis and help to anchor the skin and mobile soft tissues to the underlying skeleton. There are two types, true and false (Figure 2.4).

True ligaments are short and stout fibrous bands that run from periosteum to dermis. They are found in four locations: orbital, zygomatic, mandibular and buccal maxillary. The orbital ligaments are located over the zygomaticofrontal sutures. The zygomatic ligaments (McGregor's patch) attach the fat to the underlying zygomatic eminence. The mandibular ligaments attach the parasymphyseal dermis to the underlying bone and help support the chin to the underlying bone. The buccal maxillary ligaments have both true and false components with the true components attaching the skin to zygomaticomaxillary suture. These ligaments are obstacles to surgical manoeuvres to advance the overlying skin and must be interrupted if maximum upward movement of the facial skin is desired.

The false retaining ligaments fix the SMAS to the deep fascia preventing gravitational descent. They are located in three regions and are accordingly named platysma-auricular ligament, masseteric ligaments and buccal maxillary ligaments. The platysma-auricular ligament is a thick fascial aponeurosis that attaches the postero-superior border of platysma to the lobule of the ear. It provides a dissection plane in the subcutaneous preauricular region that leads directly to the external surface of the platysma. Masseteric ligaments are a series of fibrous bands extending between the skin and anterior border of the masseter, which help to support the medial cheek. Dissection of the SMAS anterior to the parotidomasseteric fascia leads to a loose areolar tissue plane and the masseteric ligaments. Laxity of these ligaments results in the characteristic submalar hollow seen in the ageing face. The soft tissues of the anterior cheek are supported by buccal maxillary ligaments situated adjacent to the nasolabial folds. They are the weakest of the retaining ligaments, making the anterior cheek more susceptible to sagging with ageing.

The retaining ligaments are taut in youth, but years of muscular activity and gravity cause facial and ligamentous laxity, which in combination with dermal elastosis and increased fat in the deep compartment results in descent of all elements of soft tissues. The malar soft tissues are suspended form the zygomatic eminence and maxilla by the zygomatic ligaments laterally and buccal maxillary ligaments medially. As these ligaments become lax with ageing, there is inferior migration of malar tissues. This soft tissue ptosis occurs adjacent to line of fixation along the nasolabial fold, leading to the prominence of the nasolabial fold. The attenuation of masseteric ligaments leads to descent of cheek soft tissues below the mandibular border and formation of jowls. The anterior border of jowls is formed by mandibular ligaments and posterior border by masseteric ligaments.

The surgical correction of the retaining ligaments of the face, plication of the SMAS and repositioning of the soft tissues of the face are common techniques in rejuvenation of the face.

FACIAL NERVE

The main trunk of the nerve exits the stylomastoid foramen and immediately enters the parotid gland where it divides into the temporofacial and cervicofacial divisions, but the branching pattern then becomes quite variable (Figure 2.5). The temporal (or frontal), zygomatic, buccal, marginal mandibular, and cervical rami exit the parotid gland to lie on the superficial surface of the masseter before piercing the deep layer of the SMAS to innervate the facial muscles.

The temporofacial division divides into five to seven branches to supply the muscles in frontal, orbital, zygomatic and buccal regions. All branches except the frontal have many interconnections

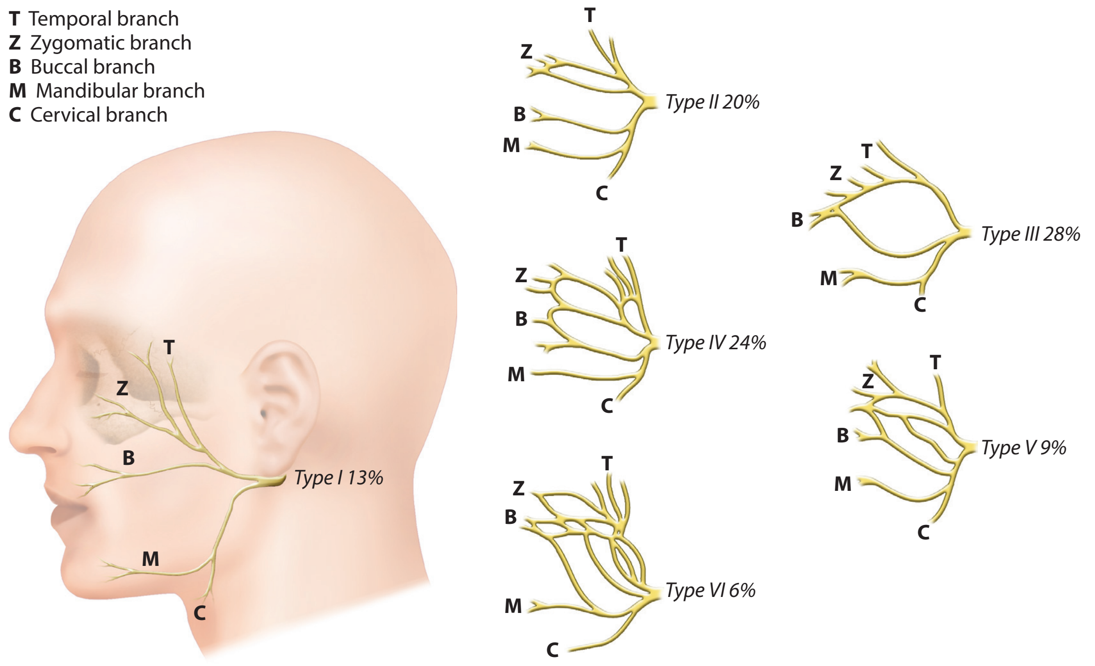

Figure 2.5 Variable branching of the facial nerve.

among themselves. The frontal branch is also the smallest, and being a terminal branch, its injury causes significant motor deficit in the frontal region. It emerges from deep within the parotid gland to just caudal to the zygomatic arch and then becomes more superficial, crossing the zygomatic arch at its midpoint and running on the deep surface of the temporoparietal fascia before entering the undersurface of frontalis. The nerve branches are superficial to both layers of the deep temporalis fascia. Thus to avoid injury to the temporal branch of the nerve when elevating flaps, one should dissect either in the immediate subcutaneous plane or deep to the temporoparietal fascia immediately adjacent to the superficial layer of the deep temporal fascia. Particular care is required over the zygomatic arch where there is fusion of the fascial layers. Practically, the nerve is protected by dissection deep to the temporoparietal fascia in the temporal region above the zygomatic arch and superficial to the parotidomasseteric fascia below the zygomatic arch, creating a mesentery in the zygomatic arch area called the mesotemporalis.

The cervicofacial division is the smaller of the two branches and divides into three to five branches to buccal, mandibular and cervical regions. Like the frontal branch of the upper division, the marginal mandibular branch of the lower division is a terminal branch and is most liable to injury, which causes obvious clinical deficit due to paralysis of the depressor labii inferioris muscle. It enters the platysma along its deep surface and is liable to injury in operations requiring elevation and division of the platysma in the upper neck. Dingman and Grabb noted in a large cadaver study that posterior to the facial artery the marginal mandibular nerve passed above the inferior border of the mandible in 81 per cent of dissections. In 19 per cent it descends inferior to the mandible lying 1–2 cm inferior to its lower border and even lower in older individuals with extension of the neck. Anterior to the facial artery, all of the marginal mandibular nerve branches innervating the mouth depressors pass above the lower border of the mandible, with only the cervical branches to the platysma passing below the mandible. The nerve was superficial to the posterior facial vein in 98 per cent of the cases and superficial to the anterior facial vein in 100 per cent of the cases. In 10 per cent to 15 per cent of patients there are connections between this nerve and the buccal branches, and in these patients considerable recovery of function will take place even if the nerve is transected. The cervical branches are somewhat at risk with subplatysmal dissection. In 4 per cent to 5 per cent of the population the cervical branch innervated the depressors of the lip; in these patients damage to the cervical branch can give a pseudomarginal paralysis. The buccal branches are at risk during surgery where they cross over the masseter muscle and the buccal fat pad.

MUSCLES OF FACIAL EXPRESSION

The facial muscles are sandwiched between the two layers of the SMAS, which itself has connections with the dermis through fibrous strands. Working in groups through these fibrous strands, they cause multiple and complex facial movements, resulting in a variety of facial expressions. The facial muscles are divided into the periocular, perioral and platysma muscles (Figure 2.6).

Periocular muscles

Frontalis and corrugator supercilii are the primary muscles of the forehead. Frontalis, the primary brow elevator, runs vertically and inserts into the galea aponeurotica; inferiorly it merges with the procerus, corrugator, orbicularis oculi and depressor supercilii muscles – the brow depressors. Frontalis raises the eyebrows to express surprise and produces transverse forehead wrinkles. The corrugators originate from the medial supraorbital ridge on the frontal bone deep to the orbicularis oculi; they pass upwards and outwards through the orbicularis to insert into the frontalis and skin of the middle of the eyebrows. They are the principal muscles in the expression of suffering, producing vertical ridges above the bridge of the nose when frowning by drawing the eyebrows downwards and inwards. Procerus arises from the nasal bone and the lateral nasal cartilage. It produces horizontal rhytides because its fibres pass vertically to insert into the skin overlying the bridge of the nose.

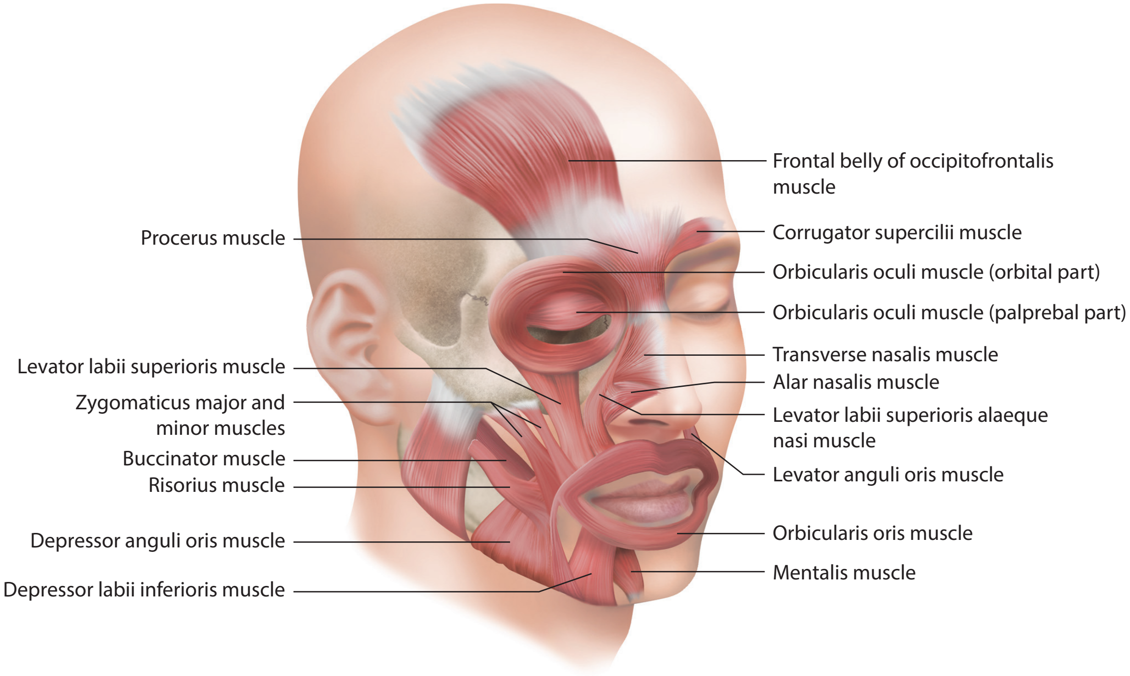
Frontal belly of occipitofrontalis muscle
Procerus muscle
Corrugator supercilii muscle
Orbicularis oculi muscle (orbital part)
Orbicularis oculi muscle (palprebal part)
Levator labii superioris muscle
Transverse nasalis muscle
Alar nasalis muscle
Zygomaticus major and minor muscles
Levator labii superioris alaeque nasi muscle
Buccinator muscle
Levator anguli oris muscle
Risorius muscle
Depressor anguli oris muscle
Orbicularis oris muscle
Mentalis muscle
Depressor labii inferioris muscle

Figure 2.6 Muscles of facial expression.

The orbicularis oculi muscle is composed of three parts. The largest orbital part extends onto the face beyond the orbital rim. It arises from the nasal part of the frontal bone, frontal process of the maxilla, and from the medial palpebral ligament with its fibres passing around the orbit in concentric loops. It is confluent with frontalis superiorly and is superficial to the zygomatic major and other lip elevators inferiorly, and is responsible for forced closure ('screwing up' the eye). The palpebral part is confined to the eyelids. It is involved in closure during involuntary blinking. The lacrimal part arises from the lacrimal bone and passes behind the lacrimal sac where some fibres insert into the lacrimal fascia with the rest inserting into the tarsi and lateral palpebral raphe. It is thought to dilate the lacrimal sac and so aid the flow of tears into the sac. Some fibres from the upper part of the orbicularis oculi are inserted into the eyebrow and are called the depressor supercilii muscle, which acts to depress the eyebrow.

The deeper layer of the frontalis muscle fascia attaches to the supraorbital rim periosteum over the medial one-half to two-thirds of the orbit. Laterally, these attachments have less dense connections and they may become quite attenuated in older individuals. Laterally, there is no supraorbital ridge and no firm attachments between the brow fat and the bone. In this lateral area brow ptosis is more rapid in patients with involutional ptosis or paralysis of the seventh nerve. When performing a brow lift it is important to transect the orbital ligament, which otherwise tethers the eyebrow, restricting superior mobility. There vertical orbicularis fibres laterally are responsible for rhytides in the lateral canthal area.

Deep to orbicularis oculi, the orbital septum is a fibrous structure that originates from the periosteum of the orbital margins, including the tough arcus marginalis of the superior orbital rim. In the upper lid it fuses with the levator aponeurosis 2–3 mm above the tarsus. In the lower lid it becomes contiguous with the capsulopalpebral fascia 5 mm beneath the tarsus. Medially, the septum attaches to the posterior lacrimal crest, and in the lower lid it also has an attachment to the anterior lacrimal crest. In the lateral canthal area, it fuses with the lateral canthal tendon. The septum is thinner medially, and the entire septum weakens with age, allowing pseudoherniation of the underlying fat with the formation of eyebags.

Perioral muscles

The perioral muscles are responsible for the movement of the upper and lower lips and the angles of mouth. They are situated in superficial and deep planes. The SMAS splits to invest the superficial muscles (zygomaticus major, minor, platysma, risorius, depressor anguli oris and superficial head of orbicularis oris). The facial nerve branches innervate them along their deep surface. The zygomaticus major and minor, which are the predominant muscles of smile, can be injured during facelift surgery. The deep perioral muscles (levator labii superioris, levator anguli oris, buccinators, mentalis, depressor labii inferioris and deep portion of orbicularis oris) are innervated by branches of facial nerve along their superficial surface. The buccal fat pad is situated deep to the buccinators. This accounts for the safety of facial muscles and nerves during excision of the buccal fat pad through the buccal mucosa. The lip elevators are responsible for the nasolabial crease, and lip depressors (depressor anguli oris) for the labiomandibular crease.

Platysma

The platysma muscle arises from the superficial fascia of the upper part of the thorax. It then runs across the clavicle and up the neck to insert into the lower border of the mandible, the skin of the lower part of the face and musculature around the angle and lower part of the mouth. Posteriorly and superiorly, the muscular fascicles form a lazy 'S' always passing posterior to the angle of the mandible. The medial platysmal fibres possess the highest degree of variability. Medially at the level of the thyroid cartilage, the platysma fibres interdigitate forming an inverted 'V'. The apex can be at the level of the chin or slightly below at the level of the thyroid cartilage. Because of this the submental area may or may not be covered by the muscle fibres. Flaccidity of the superolateral fibres of the platysma muscle may contribute to chin droop and jowling. Three patterns have been described (Figure 2.7). The most common type is Type I (seen in 75 per cent of cadavers) where the medial fibres interlace with those on the opposite side, 1–2 cm below the chin, the fibres remaining separate in the suprahyoid region. In Type II (15 per cent to 17 per cent), muscular fibres begin to interdigitate at a lower level so that a continuous muscular sheet covers the area from the thyroid to the submental region. In Type III (10 per cent), the fibres remain entirely separate and do not interlace with the contralateral platysmal fibres, inserting instead directly into the chin's cutaneous muscles.

Posteriorly, the platysma forms fascial condensations that attach to the overlying skin. The fibrous condensation is the posterior auricular ligament and acts to anchor the platysma to the dermis of the infra-auricular region. Cutaneous branches of the greater auricular nerve can be seen coursing on or within this fascial condensation. Great auricular branches pierce the ligament to

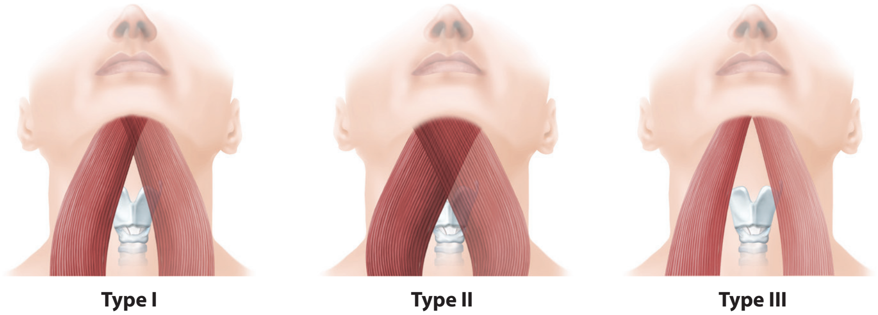

Figure 2.7 Variability of platysmal interdigitation.

provide sensation to the area of the parotid. This fascial condensation may alert the surgeon that the greater auricular nerve is in the vicinity.

EFFECT OF AGEING ON MUSCLES

The traditional concept that facial muscle laxity and weakness caused a downward displacement of the soft tissue has been challenged. It is thought that muscle tone actually increases with age. This may be due to a reactional adaptation to bone resorption or to the lengthening of the bone bases. There is also a marked decrease in muscle mass, which might further increase the tone of the remaining muscle. Whatever the cause, the permanent contracture results in shifting of the underlying fat, accentuation of the skin creases, and permanent skin wrinkling. This is well observed in facial palsy in which the absence of movement results in the disappearance of the wrinkles and the nasolabial fold.

CHIN AND CERVICOMENTAL ANGLE

Attributes of a youthful and attractive neck include an acute cervicomental angle, a distinct jawline, a slightly visible thyroid cartilage, and a visible anterior sternocleidomastoid border. An undesirable appearance may be due to excess skin, excess or ptotic submental fat, platysmal fat, platysmal bands, larger submandibular glands, microgenia or retrognathia.

The chin is the keystone structure linking the face and neck. A desirable relationship of the chin and cervicomental angle is one in which the vertical tangent from the glabella to the pogonion intersects with a second horizontal tangent drawn from the cervical point through the menton. Called the cervicomental angle, ideally it measures 75–90 degrees. The chin should lie on an imaginary line dropped from the lower lip.

Three muscles are primarily responsible for the cervicomental region. These are the geniohyoid, mylohyoid and anterior belly of digastric. Along the medial mandibular arch, the geniohyoid muscle inserts into the genial tubercle. It runs from the mandible to the body of the hyoid. The mylohyoid is a fan-shaped muscle that forms the muscular floor of the mouth. Directly superficial to it is the anterior belly of the digastric muscle. The submental artery, along with the nerve, artery and vein of the mylohyoid muscle, provide the neurovascular supply to the deep structures of this area.

The hyoid is usually located at the third or fourth cervical vertebra (C3 or C4). A more superiorly positioned hyoid (C2 or C3) favours a more acute cervicomental angle improving the jawline. A lower hyoid (C4 or C5) renders a more obtuse cervicomental angle and gives the appearance of a sloping neck and poorly defined jawline.

BLOOD SUPPLY

The skin of the face has a rich arterial blood supply through a rich arterial network of fasciocutaneous perforating arteries (Figure 2.8). The peripheral zone of the face is supplied predominantly by branches of the superficial temporal artery (transverse facial, zygomatico-orbital and frontal). The central zone is supplied by branches of facial artery, along with supraorbital and infraorbital arteries and submental artery. The lifting of the preauricular and neck skin flap for cervicofacial access results in division of contributions from the branches of the superficial temporal artery. The flap thus raised is supplied by branches of facial artery, which ensures the flap survival provided it is not too thin. The facial artery is situated under the deep fascia and should not be ligated. In patients who are smokers or have had facial artery ligation in a previous surgery, the flap undermining should be conservative.

SENSORY NERVE SUPPLY

The sensory nerve supply of the face is by branches of the three divisions of the trigeminal nerve and the cervical plexus (Figure 2.9). Raising of the facelift flap results in its denervation. However, the rich networks of sensory nerves regenerate to a completely new network within a few months. The delay in sensory recovery is most commonly seen in the lateral cheek, which is a watershed zone between the trigeminal nerve and cervical plexus nerve territories. The greater auricular crosses the sternocleidomastoid deep to the superficial fascia, 6.5 cm inferior to the external auditory meatus.

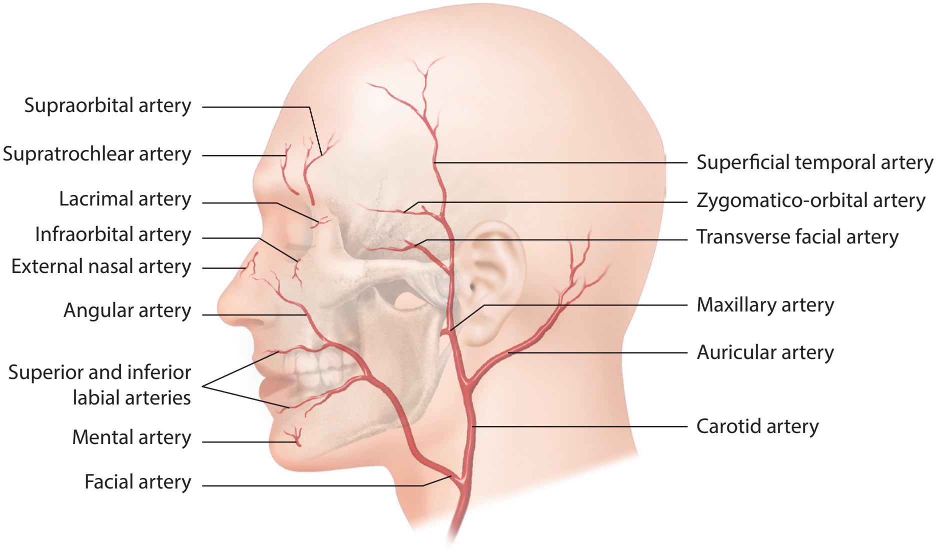
Supraorbital artery
Supratrochlear artery
Lacrimal artery
Infraorbital artery
External nasal artery
Angular artery
Superior and inferior labial arteries
Mental artery
Facial artery
Superficial temporal artery
Zygomatico-orbital artery
Transverse facial artery
Maxillary artery
Auricular artery
Carotid artery

Figure 2.8 Arteries of the face.

EFFECT OF AGEING ON BONE

Craniofacial bones, being of dermal origin, show continuous growth throughout life. They present with permanent zones of bone deposition and resorption induced by forces applied to the periosteum, which modify their shape, as can be seen with transverse enlargement at the malar and zygomatic arch levels.

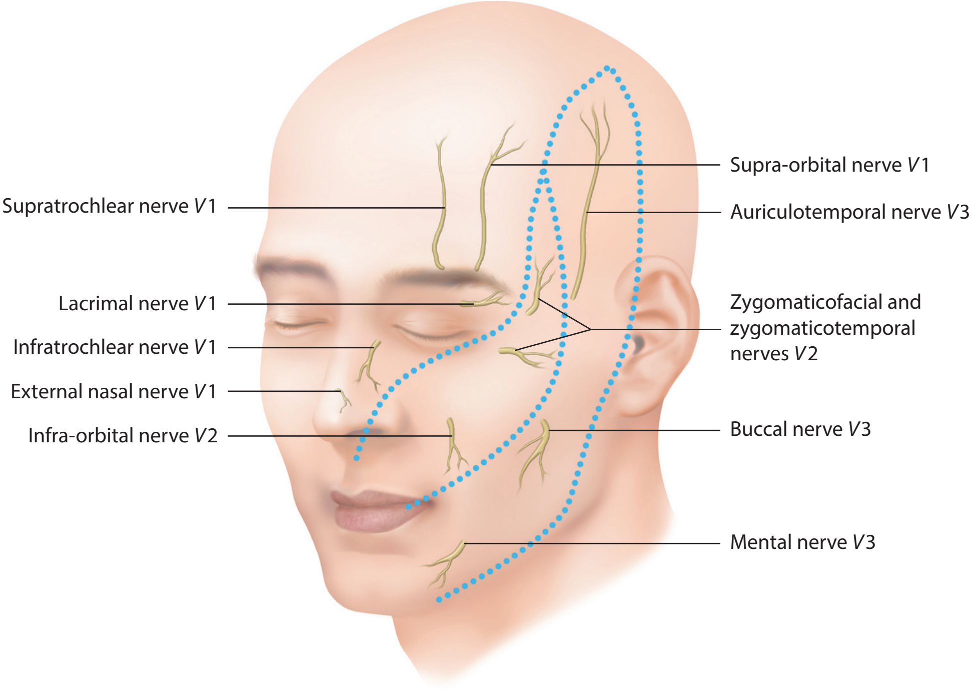
Supratrochlear nerve V1
Lacrimal nerve V1
Infratrochlear nerve V1
External nasal nerve V1
Infra-orbital nerve V2
Supra-orbital nerve V1
Auriculotemporal nerve V3
Zygomaticofacial and zygomaticotemporal nerves V2
Buccal nerve V3
Mental nerve V3

Figure 2.9 Cutaneous innervation of the face.

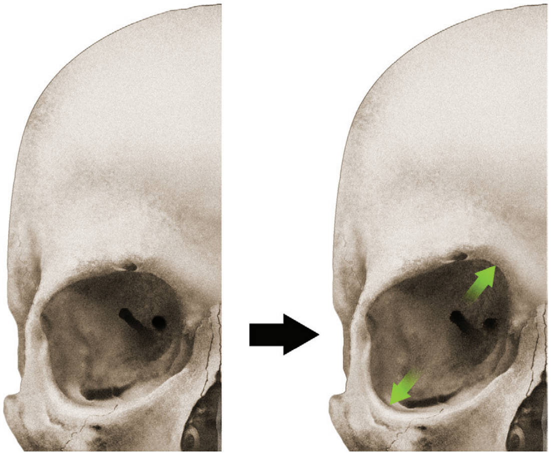

Figure 2.10 Change in contour of orbit with aging.

The most extensive age-related skeletal changes occur at about 50 years of age in both sexes. The most consistent findings include a change in contour of the orbit (with superior, medial and inferolateral remodelling) (Figure 2.10), decreased midface vertical height in edentulous patients, and a decrease in glabellar, pyriform and maxillary angle. There is a clockwise rotation of the maxilla and mandible when viewed in profile. Men show a trend towards more acute measurements in the upper face (glabellar and orbital angles) compared with women, whereas women show a trend towards more acute angular measurements in the lower face – the maxillary and pyriform angles. This might be expected when one considers that men are known to have more prominent foreheads and superior orbital rims than women, whereas women are known to have more diminutive midface than men. Finally, age-related bony remodelling causes a decrease in the space available for the soft tissue in the midface, resulting in a folding in of the soft tissue in what has been called the 'concertina effect'. An inadequate underlying bony structure may be augmented by solid implants, resulting in the restoration of soft tissue support and therefore a reversal of the concertina effect.

Acknowledgements: Mrs Becky Ward, Senior Medical Photographer, Poole Hospital NHS Foundation Trust, Poole, Dorset, UK. Miss Victoria Knapp, Senior House Officer in Oral and Maxillofacial Surgery, Poole Hospital NHS Foundation Trust, Poole, Dorset, UK.

FURTHER READING

Anastassov GE, St Hilaire H. Periorbital and midfacial rejuvenation via blepharoplasty and subperiosteal midface rhytidectomy. *International Journal of Oral and Maxillofacial Surgery*. 2006; 35: 301–11.

Aszmann OC, Ebmer JM, Dellon AL. The anatomic basis for the innervated mylohyoid/digastric flap in facial reanimation. *Plastic and Reconstructive Surgery*. 1998; 102: 369–72.

Danahey DG, Dayan SH, Benson AG, Ness JA. Importance of chin evaluation and treatment to optimizing neck rejuvenation surgery. *Facial Plastic Surgery*. 2001; 17: 91–97.

de Castro CC. The anatomy of the platysma muscle. *Plastic and Reconstructive Surgery*. 1980; 66: 680–83.

Doual JM, Ferri J, Laude M. The influence of senescence on craniofacial and cervical morphology in humans. *Surgical and Radiologic Anatomy*. 1997; 19: 175–83.

Dumont T, Simon E, Stricker M, et al. Analysis of the implications of the adipose tissue in facial morphology, from a review of the literature and dissection of 10 half faces. *Annales de Chirurgie Plastique Esthétique*. 2007; 119: 2219–27.

Dingman RO, Grabb WC. Surgical anatomy of the mandibular ramus of the facial nerve based on the dissection of 100 facial halves. *Plastic and Reconstructive Surgery and the Transplantation Bulletin*. 1962; 29: 266–72.

Fisher GJ, Varani V, Voorhees JJ. Looking older: Fibroblast collapse and therapeutic implications. *Archives of Dermatology*. 2008; 144: 666–72.

Furnas DW. The retaining ligaments of the cheek. *Plastic and Reconstructive Surgery*. 1989; 83: 11–16.

Khazanchi R, Aggarwal A, Johar M. Anatomy of aging face. *Indian Journal of Plastic Surgery*. 2007; 40: 223–29.

Le Louran C. Botulinum toxin and the Face Recurve concept: Decreasing resting tone and muscular regeneration. *Annales de Chirurgie Plastique Esthétique*. 2007; 52: 165–76.

Larrabee WF, Makielski KH, Henderson JL. *Surgical Anatomy of the Face*. 2nd ed. Philadelphia: Lippincott Williams and Wilkins, 2004.

Pessa JE, Chen Y. Curve analysis of the aging orbital aperture. *Plastic and Reconstructive Surgery*. 2002; 109: 751–55; discussion 756–60.

Pessa JE, Zadoo VP, Yuan C, et al. Concertina effect and facial aging: Nonlinear aspects of youthfulness and skeletal remodelling, and why, perhaps, infants have jowls. *Plastic and Reconstructive Surgery*. 1999; 103: 635–44.

Rabe JH, Mamelak AJ, McElgunn PJ, Morison WL, Sauder DN. Photoaging: Mechanisms and repair. *Journal of the American Academy of Dermatology.* 2006; 55: 1–19.

Raskin E, LaTrenta GS. Why do we age in our cheeks? *Aesthetic Surgery Journal*. 2007; 27: 19–28.

Richard MJ, Morris C, Deen B, et al. Analysis of the anatomic changes of the aging facial skeleton using computer-assisted tomography. *Ophthalmic Plastic and Reconstructive Surgery*. 2009; 25: 382–86.

Rohrich RJ, Pessa JE. The fat compartments of the face: Anatomy and clinical implications for cosmetic surgery. *Plastic and Reconstructive Surgery*. 2007; 119: 2219–27; discussion 2228–31.

Salmon M. *Arteries of the Skin.* New York: Churchill Livingstone, 1988.

Singh J, Prasad K, Lalitha RM, Ranganath K. Buccal pad of fat and its applications in oral and maxillofacial surgery: A review of published literature (February) 2004 to (July) 2009. *Oral Surgery, Oral Medicine, Oral Pathology, Oral Radiology, and Endodontology.* 2010; 110: 698–705.

Zoumalan RA, Larrabee WF. Anatomic considerations in the aging face. *Facial Plastic Surgery*. 2011; 27: 16–22.

PART 2

3 External nose 27
Shan R. Baker and Parkash L. Ramchandani
4 Internal nose and paranasal sinuses 37
Tawakir Kamani and Anshul Sama
5 External ear 45
David Richardson
6 Temporal bone, middle ear and mastoid 53
Michael Gleeson

3

External nose

SHAN R. BAKER AND PARKASH L. RAMCHANDANI

Topographic and cephalometric assessment 27
Aesthetic subunits 28
External nasal anatomy 28
Skin *29*
Subcutaneous layer *29*
Muscles *30*
External blood supply *31*
External sensory nerve supply *32*
Nasal skeletal anatomy 33
Nasal tip *33*
Cartilaginous dorsum *35*
Bony dorsum *35*
Further reading 35

The nose is a central feature of the face. It characterizes the individual; warms, humidifies and filters the air; and enables olfaction. It has a complex three-dimensional shape that poses a formidable challenge for the reconstructive surgeon. The aesthetically pleasing nose provides a smooth and natural transition from the eyes to the lips. A deformed nose draws attention away from the eyes and lips, disturbing the aesthetic balance of the face. The external nose is composed of skin, mucosa, bone, cartilage and intervening supportive tissues, including fat, muscle and connective tissue. A thorough knowledge of nasal anatomy underpins successful restoration of form and function. The stakes are high with no margin for error. If the surgeon gets it wrong, the aesthetic, physiological, social and psychological disability can be devastating.

TOPOGRAPHIC AND CEPHALOMETRIC ASSESSMENT

In the frontal view the face is divided into horizontal thirds (Figure 3.1).

- The upper third begins at the trichion and ends at the glabella.
- The middle third extends from the glabella to the subnasale.
- The lower third extends from the subnasale to the menton.

Nasal height is measured from the radix – sometimes termed the nasal root and defines where the nose has its origin from the glabella – to the subnasale and should be 50 per cent of the lower face height. Similarly, in the vertical plane the face is divided into fifths. Each division equals the horizontal width of

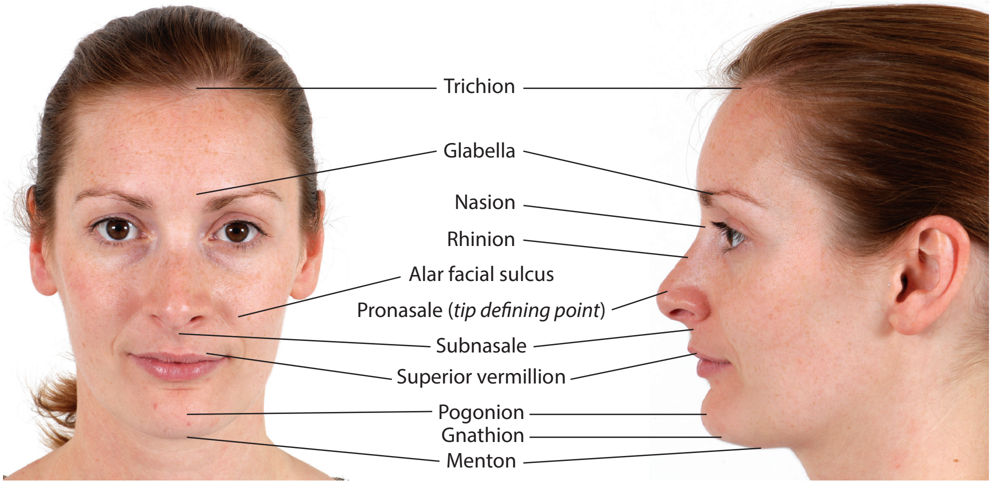

Figure 3.1 Anatomic landmarks on frontal and lateral views.

a single palpebral aperture. The nasal base, the distance between the alar creases, is ideally equal to the intercanthal distance and represents one-fifth of the facial width. The nose occupies the central third of the face in the horizontal axis and the central fifth in the vertical axis, and thus should lie precisely in the midline of the face. On the frontal view a gentle, curved broken line, called the dorsal aesthetic line, can be drawn from the eyebrow along the lateral border of the dorsum to the tip defining point.

The nasofrontal angle (115–130 degrees) is the obtuse angle at the nasion between a line tangent to the glabella and a line tangent to the tip defining point, or pronasale. The nasofacial angle (30–40 degrees) is the acute angle formed between a line drawn from the nasion to the pronasale and another line drawn from the nasion to the pogonion. The nasomental angle (120–132 degrees) is the angle between a line extending from the nasion to the pronasalae and a line extending from the pronasalae to the menton. The nasolabial angle is the angle between the columella and upper lip; it determines the cephalic rotation of the tip and ideally measures between 105 and 115 degrees in females and 90 and 105 degrees in males.

The aesthetic proportions of the ideal nasal shape have been established (Figure 3.1). On the lateral view the distance from the vermillion border of the upper lip to the subnasale is equal to the distance from the subnasale to the pronasalae. The distance from the alar facial sulcus to the midpoint of the nares ideally equals that from the midpoint to the caudal border of the nasal tip. On the lateral view a right-angle triangle with the ratio of its sides being 3:4:5 and the vertices being at the nasion, alar-facial sulcus and tip has been described to illustrate the ideal nasal proportions and size.

AESTHETIC SUBUNITS

The nose can be divided into aesthetic subunits by the contour lines that mark boundaries between nasal skin of differing textures and thicknesses. These include the nasal dorsum, sidewalls, tip lobule, soft triangles, alae and columella (Figure 3.2). They are highlighted when incident light is cast on the nasal surface, creating shadows along the borders of each unit. The framework underlying the nasal skin is primarily responsible for these variations in light reflections. Therefore, precise restoration of the framework is important in the reconstruction of the nose so as to avoid contour irregularities and asymmetries. In addition, repair of nasal skin defects with a thin covering flap will help to maintain the definition of aesthetic units and anatomic landmarks.

EXTERNAL NASAL ANATOMY

The external nose consists of overlying skin, soft tissue, blood vessels and nerves with cartilage and bone support. Understanding the variations in skin thickness among the various regions of the nose is

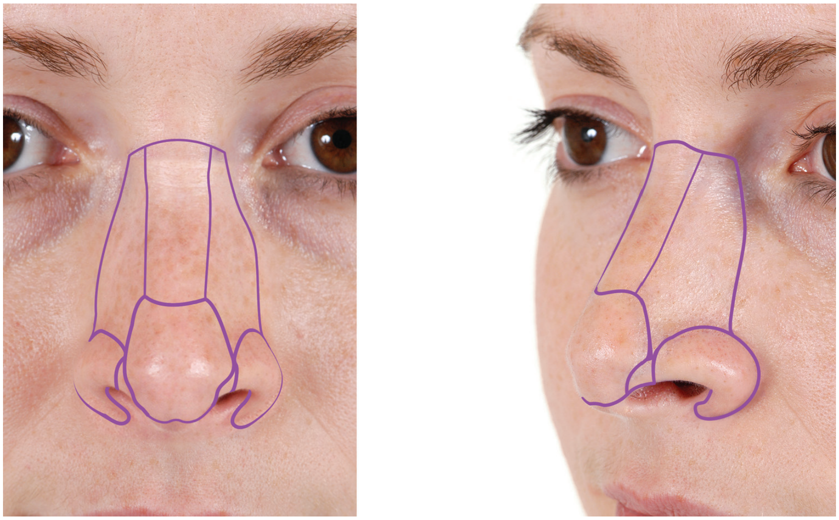

Figure 3.2 Aesthetic subunits of the nose, frontal and oblique views.

an essential aspect of reconstructive nasal surgery. Familiarity with the blood supply is a prerequisite to using local flaps for soft tissue restoration of nasal defects.

Skin

Skin thickness varies widely among individuals and among the aesthetic units in any given individual. Lessard and Daniel analysed 60 cadaver dissections and 25 patients undergoing septorhinoplasty and found the average skin thickness to be greatest at the radix (1.25 mm) and least at the rhinion (0.6 mm). Skin is thinner and more mobile over the dorsum, whereas it is thicker and more adherent to the underlying nasal framework at the nasal tip and alae. At the cephalic portion of the nasal sidewalls, the skin is thin; however, caudally it becomes thicker in the vicinity of the alar groove. Despite being thicker at the nasal tip, the skin rapidly transitions to being very thin where it covers the nostril margin and columella. The close approximation of the dermis of the skin lining and covering the nasal facets and nostril margins makes these areas especially vulnerable to notching and contour irregularities after reconstruction. Sebaceous glands are more numerous in the caudal half of the nasal skin. This is especially true in the non-Caucasian nose, which commonly displays a greater amount of subcutaneous fibrous fatty tissue. This dense layer of tissue, often measuring as much as 6 mm thick, obscures the contour of the underlying alar cartilages in the non-Caucasian nose.

Subcutaneous layer

The soft tissue between the skin and the bony cartilaginous skeleton is made up of four layers. Immediately beneath the skin is the *superficial fatty panniculus*, which consists of adipose tissue interlacing with vertical fibrous septi running from the deep dermis to the underlying *fibromuscular layer*. This layer is thicker in the glabella and supratip areas. The fibromuscular layer contains the nasal musculature and the nasal subcutaneous muscular aponeurotic system (SMAS), which is a continuation of the facial SMAS. Histologically, the nasal SMAS is a distinct sheet of collagenous bundles that envelops the nasal musculature. The *deep fatty layer* located between the SMAS and the thin covering of the nasal skeleton contains the major superficial blood vessels and nerves. This layer of loose areolar fat has no fibrous septae; as a result, immediately below it is the preferred plane for undermining nasal skin. The nasal bones and cartilages are covered with *periosteum* and *perichondrium*, respectively. The periosteum of the nasal bones extends over the upper lateral cartilages and fuses with the periosteum of the piriform process laterally. Perichondrium covers the nasal cartilages, and dense interwoven fibrous interconnections can be found between the tip cartilages.

Muscles

The nasal musculature has been described and classified by Griesman and Letourneau (Figure 3.3). The greatest concentration of muscle is located at the junction of the upper lateral and alar cartilages. This allows for muscular dilation and stenting of the nasal valve area. All nasal musculature is innervated by the zygomaticotemporal division of the facial nerve.

The elevator muscles include the procerus, the levator labii superioris alaeque nasi and the anomalous nasi. These muscles rotate the nasal tip in a cephalic direction and dilate the nostrils. The procerus muscle has a dual origin. The medial fibres originate from the aponeurosis of the transverse nasalis and the periosteum of the nasal bones. The lateral fibres originate from the perichondrium of the upper lateral cartilages and the musculature of the upper lip. The procerus inserts into the glabellar skin. The levator labii superioris alaeque nasi originates from the medial part of the orbicularis oculi and frontal process of the maxilla and inserts into the melolabial fold, ala nasi, and the skin and muscle of the upper lip. The anomalous nasi originates from the frontal process of the maxilla and inserts into the nasal bone, upper lateral cartilage, procerus and transverse part of the nasalis.

The depressor muscles of the nose include the alar nasalis and the depressor septi. These muscles lengthen the nose and dilate the nostrils. The alar nasalis originates from the maxilla above the lateral incisor tooth and inserts into the skin along the posterior circumference of the lateral crura. The depressor septi nasi originates from the maxillary periosteum above the central and lateral incisors and inserts into the membranous septum and the footplate of the medial crura. A minor dilator muscle is the dilator naris anterior, a fanlike muscle originating from the upper lateral cartilage and alar portion

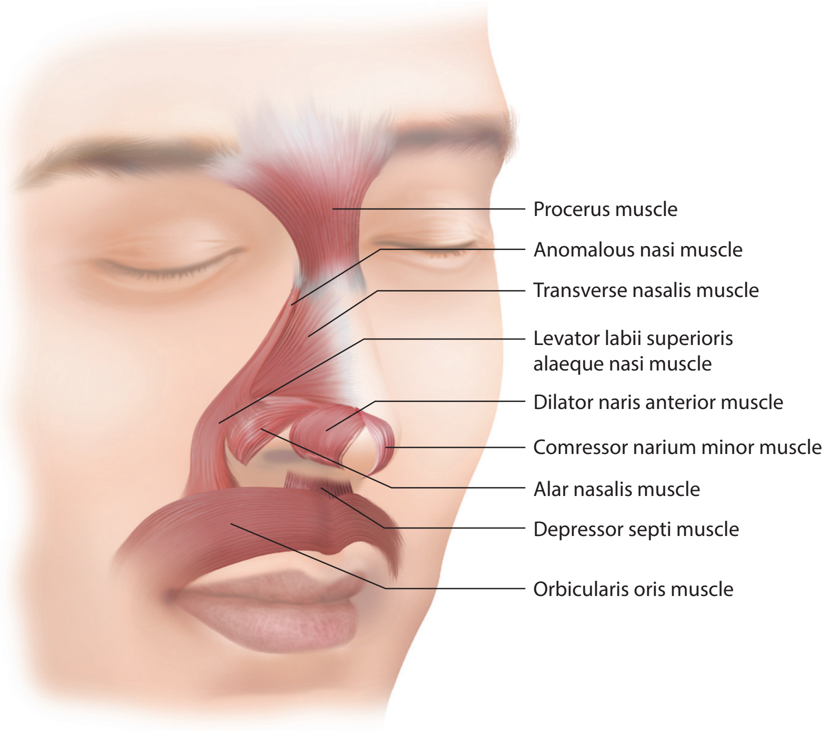
Procerus muscle
Anomalous nasi muscle
Transverse nasalis muscle
Levator labii superioris alaeque nasi muscle
Dilator naris anterior muscle
Comressor narium minor muscle
Alar nasalis muscle
Depressor septi muscle
Orbicularis oris muscle

Figure 3.3 Nasal musculature.

of the nasalis before inserting into the caudal margin of the lateral crura and the lateral alar skin.

The compressor muscles lengthen the nose by rotating the nasal tip in a caudal direction and narrowing the nostrils. These muscles include the transverse portion of the nasalis and the compressor narium minor. The transverse portion of the nasalis muscle originates from the maxilla above and lateral to the incisor fossa. Fibres from the transverse portion insert into the skin and procerus, and some fibres join the alar portion of the nasalis muscle. The compressor narium minor arises from the anterior part of the lower lateral cartilage and inserts into the skin near the margin of the nostrils.

External blood supply

Both the internal and external carotid arteries contribute to the superficial arterial supply of the nose and adjacent area (Figure 3.4). The angular artery arises from the facial artery and provides a rich blood supply for the melolabial and subcutaneous hinge flaps used for alar reconstruction. A branch of the angular artery, the lateral nasal artery, supplies the lateral surface of the caudal nose. The lateral nasal artery passes deep to the nose in the sulcus between the ala and cheek and is covered by the levator labii superioris alaeque nasi. It follows closely the margin of the pyriform aperture. The artery branches multiple times to enter the subdermal plexus of the skin covering the nostril and cheek.

The dorsal nasal artery, a branch of the ophthalmic artery, pierces the orbital septum above the medial palpebral ligament and travels along the side of the nose to anastomose with the lateral nasal branch of the angular artery. The dorsal nasal artery provides a rich axial blood supply to

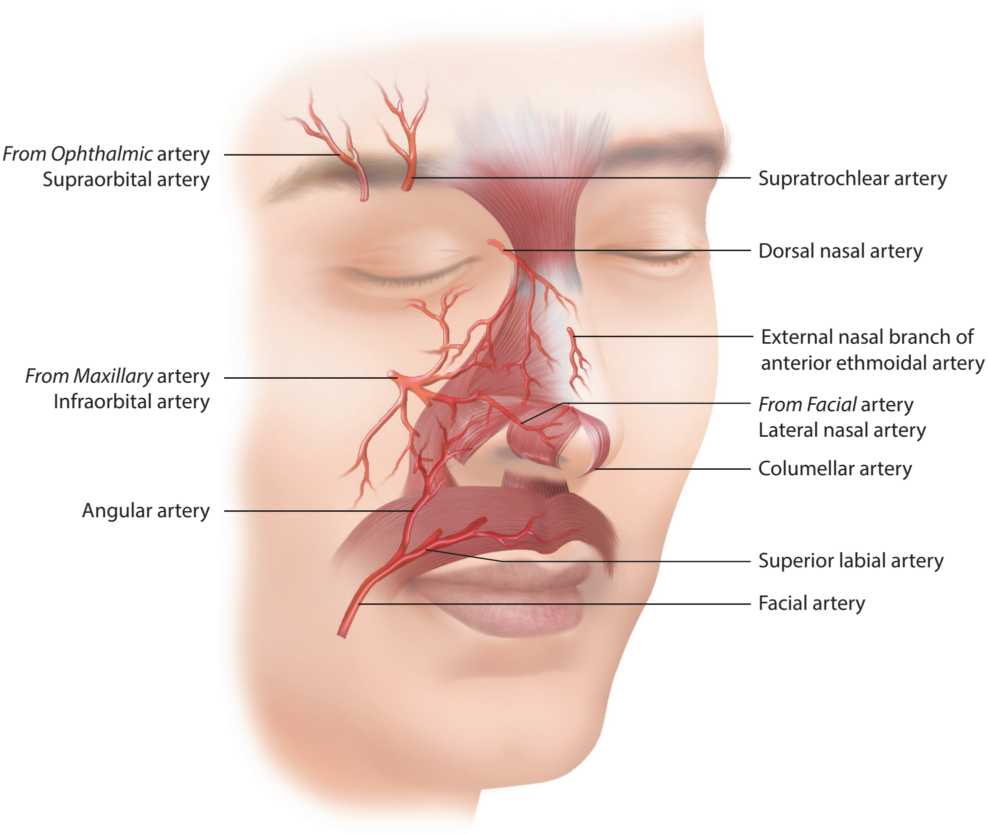
From Ophthalmic artery
Supraorbital artery
Supratrochlear artery
Dorsal nasal artery
External nasal branch of anterior ethmoidal artery
From Maxillary artery
Infraorbital artery
From Facial artery
Lateral nasal artery
Columellar artery
Angular artery
Superior labial artery
Facial artery

Figure 3.4 Arterial supply of external nose.

the dorsal nasal skin and serves as the main arterial contributor to the dorsal nasal flap.

The nostril sill and columellar base are supplied by branches of the superior labial artery. A branch of the superior labial artery, the columellar artery, ascends superficial to the medial crura and is transected by a transcolumellar incision during an external rhinoplasty approach.

The nasal tip is supplied by the external nasal branch of the anterior ethmoidal artery as well as by the columellar artery. The anterior ethmoidal artery, a branch of the ophthalmic artery, pierces bone on the medial wall of the orbit at the point where the lamina papyracea of the ethmoid bone articulates with the orbital portion of the frontal bone (the frontoethmoid suture). The vessel enters the ethmoid sinuses to supply the mucosa and sends branches to the superior aspect of the nasal cavity. The external nasal branch of the anterior ethmoidal artery emerges between the nasal bone and the upper lateral cartilage to supply the skin covering the nasal tip. The blood supply of the nasal tip also receives contributions from the lateral nasal artery, a branch of the angular artery.

The venous drainage consists of veins with names that correspond to the associated arteries. These veins drain via the facial vein, the pterygoid plexus and ophthalmic veins into the cavernous sinus.

External sensory nerve supply

Sensation to the nasal skin is supplied by the ophthalmic and maxillary of the trigeminal nerve (5th cranial nerve) (Figure 3.5). Branches of the

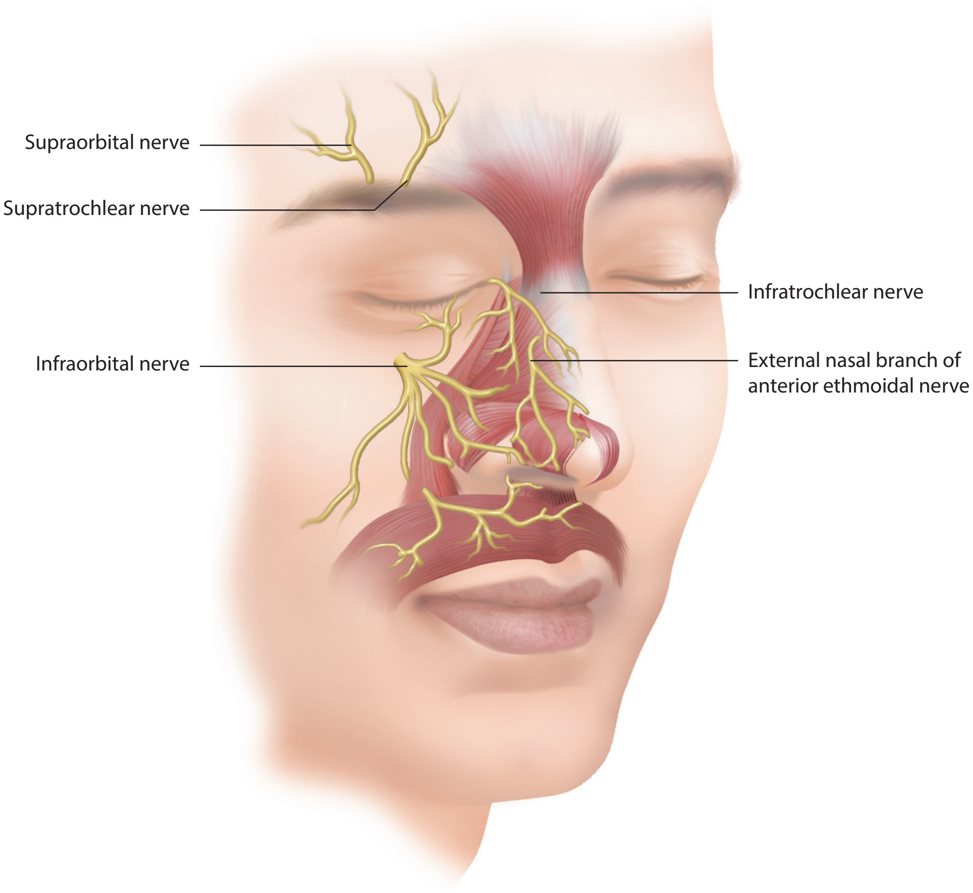

Figure 3.5 Sensory nerve supply of external nose.

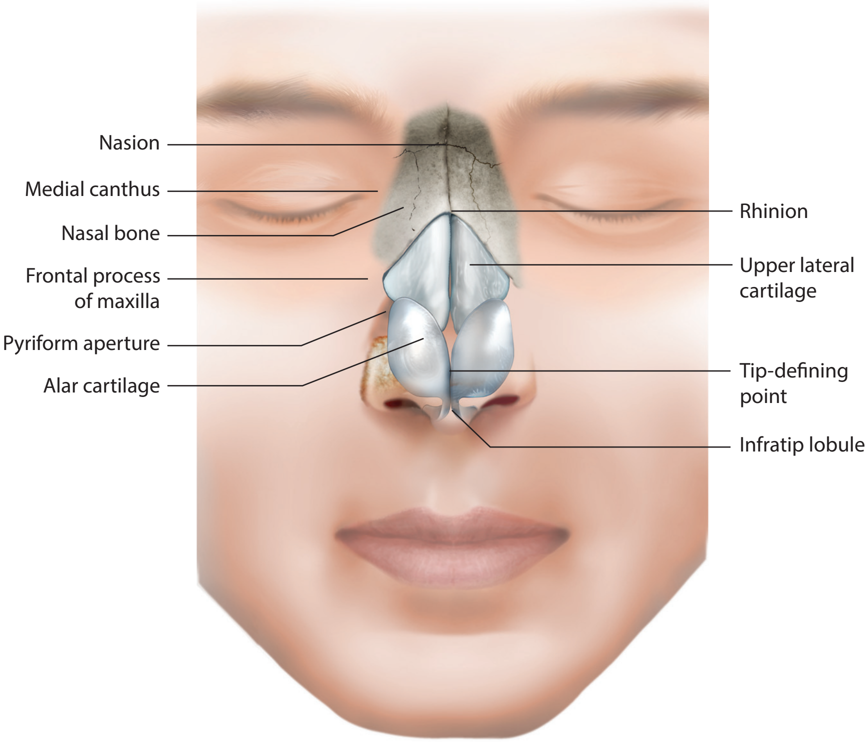

Figure 3.6 Frontal view of bony and cartilaginous nose.

supratrochlear and infratrochlear nerves supply the skin covering the radix, the rhinion and the cephalic portion of the nasal sidewalls. The external nasal branch of the anterior ethmoidal nerve emerges between the nasal bone and the upper lateral cartilage to supply the skin over the caudal half of the nose down to and including the tip. This nerve is vulnerable during intercartilage and cartilage-splitting incisions and is usually transected by soft tissue elevation during rhinoplasty. To minimize the risk it is best to avoid deep endonasal incisions and maintain dissection directly on the surface of the cartilage. The infraorbital nerve provides sensory branches to the skin of the lateral half of the nose and parts of the columella and lateral vestibule.

NASAL SKELETAL ANATOMY

A thorough understanding of the nasal skeleton is essential for proper reconstruction of the nose. When constructing framework grafts, errors in duplicating normal contour may compromise the repair, leading to contour irregularities and functional limitations. The nasal framework consists of bony and cartilaginous components (Figure 3.6).

Nasal tip

The caudal third of the nose consists of the lobule (tip), columella, vestibules and alae. It is structurally supported by paired alar (lower lateral) cartilages, the caudal septum, accessory cartilages and fibrous fatty connective tissue (Figure 3.7). The variable configuration of the nasal tip depends on the size, shape, orientation and strength of the alar and septal cartilages and on the quality and thickness of the overlying soft tissue and skin. The alar cartilages are attached to the upper lateral cartilages and the septum, and they provide the majority of the support for the tip. The vestibule is bounded medially by the septum and columella and laterally by the alar base. It contains a

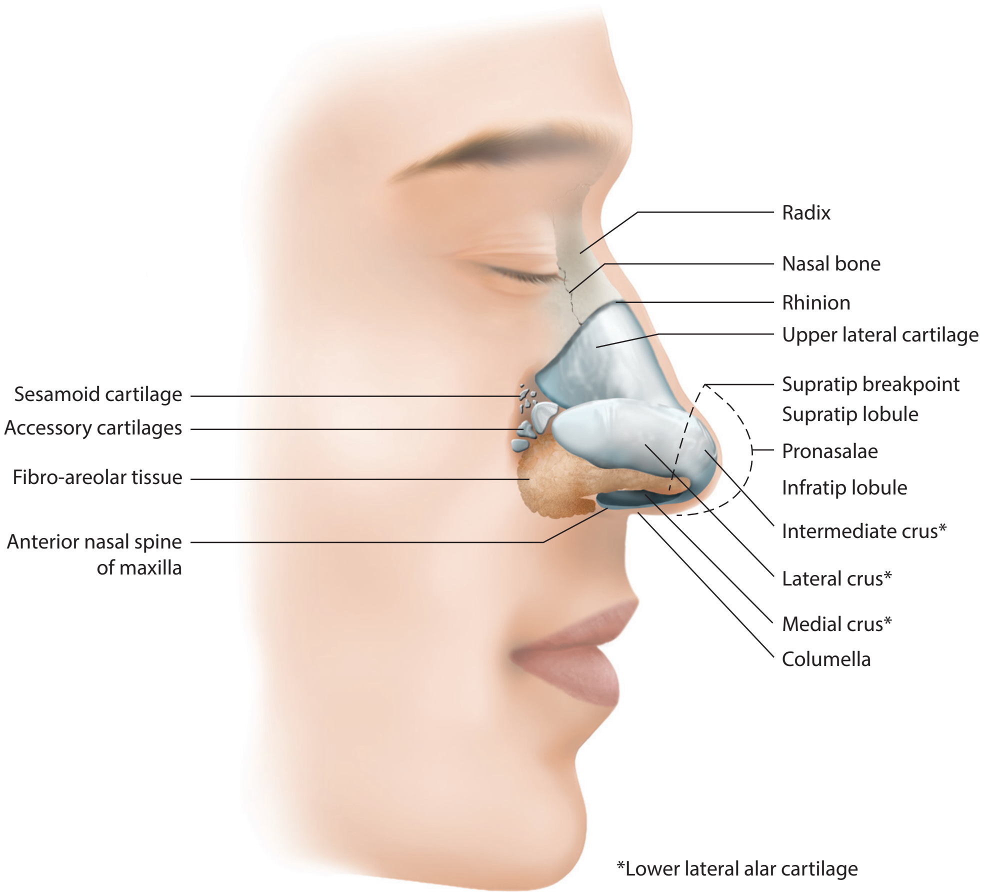
Radix
Nasal bone
Rhinion
Upper lateral cartilage
Sesamoid cartilage
Accessory cartilages
Fibro-areolar tissue
Anterior nasal spine of maxilla
Supratip breakpoint
Supratip lobule
Pronasalae
Infratip lobule
Intermediate crus*
Lateral crus*
Medial crus*
Columella
*Lower lateral alar cartilage

Figure 3.7 Right lateral view of bony and cartilaginous nose.

protruding fold of skin with vibrissae and terminates at the caudal edge of the lateral crus.

The alar cartilage is subdivided into medial, intermediate and lateral crura (Figure 3.8). The medial crus consist of the footplate and columellar segments. The footplate is more posterior and accounts for the flared portion of the columellar base. The columellar segment begins at the upper limit of the footplate and joins the intermediate crus at the columellar breakpoint. The breakpoint represents the junction of the tip and the columella. The appearance and projection of the columella are influenced by the configuration of the medial crura as well as that of the caudal septum. Intervening soft tissue between the columellar segments of the medial crura may fill this space; however, in patients with thin skin, the columella may have a bifid appearance. Columellar asymmetries may be secondary to deflections of the caudal septum or intrinsic asymmetries of the alar cartilages. In the aesthetically pleasing nose, the columella is

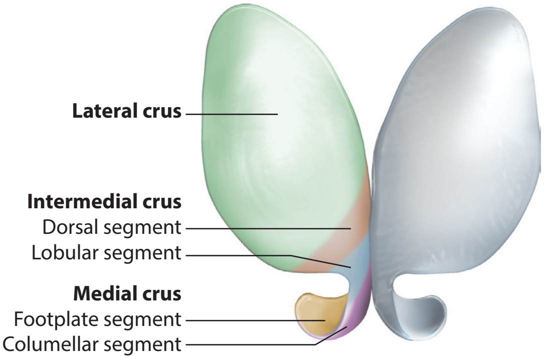
Lateral crus
Intermedial crus
Dorsal segment
Lobular segment
Medial crus
Footplate segment
Columellar segment

Figure 3.8 Frontal view of the paired alar cartilages.

positioned 2 to 4 mm caudal to the nostril margins, and the shape of the nasal base resembles an equilateral triangle. Attractive nostrils are teardrop-shaped in the opinion of many.

The intermediate crus consists of a lobular and a domal segment (Figure 3.8). In the majority of noses, the cephalic borders of the lobular segment are in close approximation and the caudal margins diverge. The intermediate crura are bound together by the intermodal ligament, and lack of intervening soft tissue may give the tip a bifid appearance. On a lateral view the internal structure responsible for the prominence of the tip-defining point, or pronasalae, is the cephalic border of the domal segment of the intermediate crus (Figure 3.7). Thus the shape, length and angulation of the intermediate crura determine the configuration of the infratip lobule and the position of the tip-defining point. The supratip breakpoint is the junction between the intermediate crus and the lateral crus.

The lateral crus is the largest component of the alar cartilage; it provides the support to the anterior half of the nostril rim. Resection or weakening of the lateral crus causes a predisposition to nostril retraction and notching, an important consideration during nasal reconstruction. Laterally, small sesamoid cartilages are interconnected by a dense, fibrous connective tissue that is contiguous with the superficial and deep perichondrium of the upper lateral cartilage and lateral crus. Inferolaterally, the ala contains fat and fibrous connective tissue but no cartilage (Figure 3.7). The shape and resiliency of the nostril depend on the dense, fibrous fatty connective tissue located within the confines of the ala, and the integrity of this area should be restored with cartilage grafting when necessary.

Cartilaginous dorsum

The cartilaginous dorsum consists of paired upper lateral cartilages and the cartilaginous septum. The upper lateral cartilages are overlapped superiorly by the bony framework for a variable distance (Figure 3.6). The free caudal border of the nasal bones has fibrous connections to the cephalic margin of the upper lateral cartilages. The cephalic two-thirds of the cartilaginous dorsum is a single cartilaginous unit. However, caudally there is gradual separation of the upper lateral cartilages from the septum. The lateral borders of the upper lateral cartilages are rectangular in shape and are connected to the piriform aperture by an aponeurosis. The lateral border of the upper lateral cartilage creates a space known as the external lateral triangle. This space is defined by the lateral border of the upper lateral cartilage, the extreme lateral portion of the lateral crus and the border of the piriform fossa. The space is lined by mucosa and covered by the transverse portion of the nasalis muscle. It may contain accessory cartilages and fibrous fatty tissue that contribute to the lateral aspect of the internal nasal valve (Figure 3.7). Nasal obstruction may occur as a result of medialization of this space by scar tissue or cartilage grafts used in nasal reconstruction.

Bony dorsum

The bony dorsum consists of the paired nasal bones and paired frontal processes of the maxillae (Figure 3.6). The bony vault is pyramidal in shape, and the narrowest part is at the level of the intercanthal line. The bony dorsum is divided approximately in half by the intercanthal line, and the nasal bones are much thicker and denser above this level. The sellion is the deepest portion of the curve of soft tissue between the glabella and nasal dorsum, and it marks the level of the nasofrontal suture line. The nasion is approximately at the level of the supratarsal fold of the upper eyelid. Laterally, the nasal bones articulate with the frontal processes of the maxillae.

FURTHER READING

Burget GC, Menick FJ. The subunit principle in nasal reconstruction. *Plastic and Reconstructive Surgery*. 1985; 76: 239.

Crumley RL, Lancer R. Quantitative analysis of nasal tip projection. *Laryngoscope*. 1988; 2: 202.

Daniel RK, Letourneau A. Rhinoplasty: Nasal anatomy. *Annals of Plastic Surgery*. 1988; 20: 5.

Firmin F. Discussion on Letourneau A, Daniel RK. The superficial musculoaponeurotic system of the nose. *Plastic and Reconstructive Surgery*. 1988; 82: 56.

Griesman BL. Muscles and cartilages of the nose from the standpoint of typical rhinoplasty. *Archives of Otolaryngology – Head and Neck Surgery*. 1994; 39: 334.

Letourneau A, Daniel RK. The superficial musculo-aponeurotic system of the nose. *Plastic and Reconstructive Surgery*. 1988; 82: 4.

Lessard ML, Daniel RK. Surgical anatomy of septorhinoplasty. *Archives of Otolaryngology – Head and Neck Surgery*. 1985; 111:25.

Oneal RM, Beil RJ, Schlesinger J. Surgical anatomy of the nose. *Clinics in Plastic Surgery*. 1996; 23: 1985.

Simons RL. Adjunctive measures in rhinoplasty. *Otolaryngologic Clinics of North America*. 1975; 8: 717–42.

Wright WK. Surgery of the bony and cartilaginous dorsum. *Otolaryngologic Clinics of North America*. 1975; 8: 575.

Zingaro EA, Falces E. Aesthetic anatomy of the non-Caucasian nose. *Clinics in Plastic Surgery*. 1987; 14: 749.

4

Internal nose and paranasal sinuses

TAWAKIR KAMANI AND ANSHUL SAMA

Introduction 37
Anatomy of the nasal cavity 37
Nasal septum 37
The lateral nasal wall and paranasal sinuses 39
Further reading 43

INTRODUCTION

The function of the nose is filtration and conditioning of inspired air and olfaction. This chapter outlines the anatomy of the nasal cavity, nasal septum, lateral nasal wall and paranasal sinuses. The external nose is discussed in Chapter 3. The close proximity of the orbit and cranial cavity means that catastrophic complications can occur if there is a lack of clear and detailed knowledge the anatomy. A thorough knowledge of the anatomy of the internal nose and paranasal sinuses and an appreciation of the possible variations in these structures is paramount for effective and safe endoscopic sinus surgery.

ANATOMY OF THE NASAL CAVITY

The nasal cavity extends from the nares anteriorly to the choanae posteriorly, where it becomes continuous with the nasopharynx. The nasal floor is made up of the palatine process of the maxillary bone anteriorly, fused with the horizontal process of the palatal bones posteriorly (Figure 4.1a). The roof is supported by the lateral cartilages (upper and lower) and nasal bones anteriorly, and the cribriform plate posteriorly. The nasal septum divides the nasal cavity into two nasal passages. The majority of the nasal cavity is lined by respiratory epithelium except at the superior septum and supero-medial part of the middle turbinate, which house the olfactory epithelium.

The blood supply to the nasal cavity is mainly provided by branches of the sphenopalatine artery with contribution from the anterior and posterior ethmoid artery, the greater palatine artery and the facial artery. The venous drainage of the posterior nasal cavity drains to the pharyngeal plexus, the central follows the arteries to the pterygoid plexus and the anterior to the facial vein. The lymphatics follow the veins rather than the arteries. Lymphatic drainage is to the submandibular nodes anteriorly and to the retropharyngeal and upper deep cervical nodes posteriorly. The nasociliary nerve, branches of the pterygopalatine ganglion and anterior palatine nerves provide innervation.

Nasal septum

The nasal septum is composed of a small anterior membranous portion, the quadrilateral cartilage, the perpendicular plate of the ethmoid, vomer and the nasal crests of the maxilla and palatine bones (Figure 4.2). The upper lateral cartilages are fused to the quadrilateral cartilage at its dorsal margin and contribute toward the projection and height of the mid-third of the nose. The attachment of the

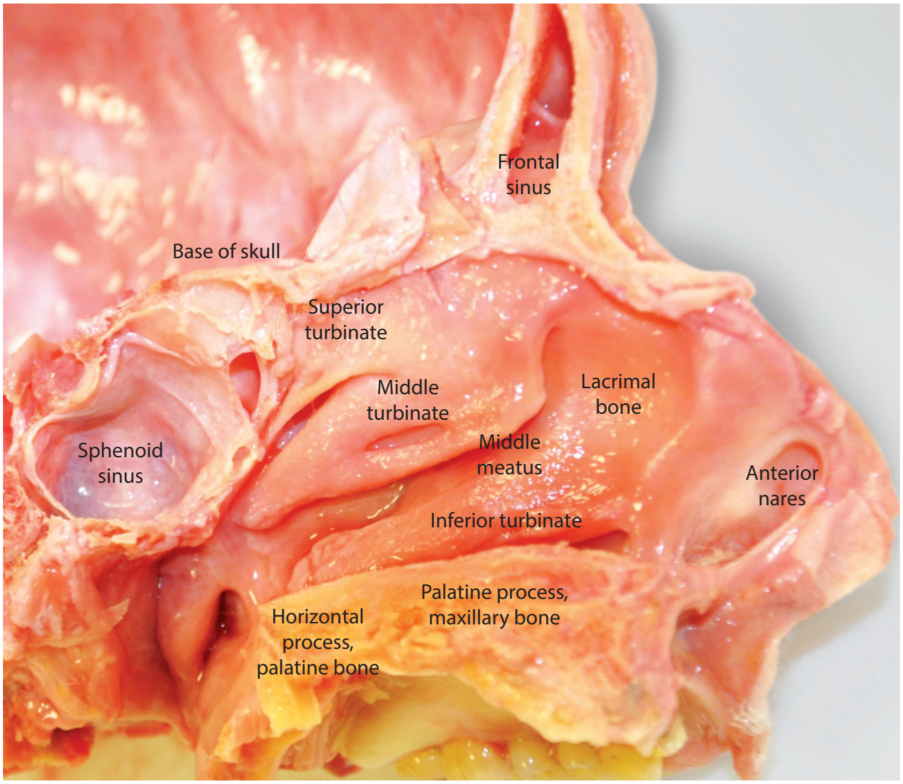
Frontal sinus
Base of skull
Superior turbinate
Middle turbinate
Lacrimal bone
Sphenoid sinus
Middle meatus
Anterior nares
Inferior turbinate
Palatine process, maxillary bone
Horizontal process, palatine bone

Figure 4.1**a** Lateral nasal wall.

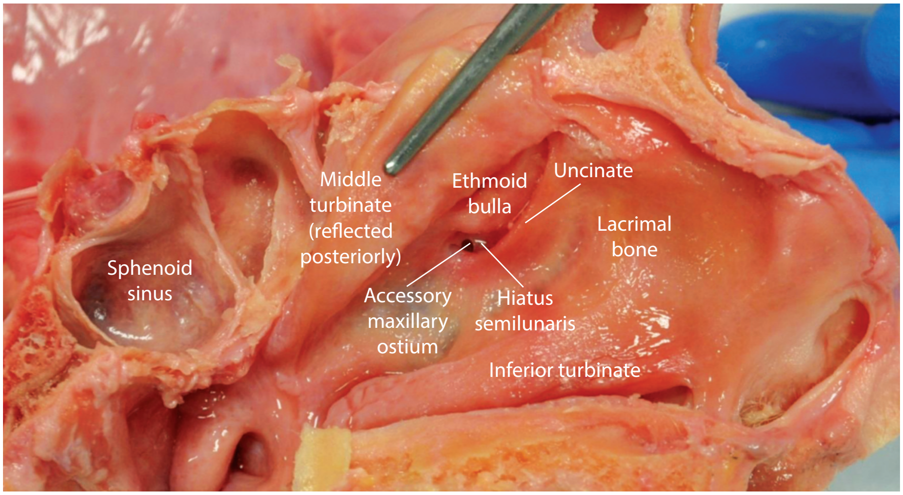
Middle turbinate (reflected posteriorly)
Ethmoid bulla
Uncinate
Lacrimal bone
Sphenoid sinus
Accessory maxillary ostium
Hiatus semilunaris
Inferior turbinate

Figure 4.1**b** Lateral nasal wall with middle turbinate reflected posteriorly exposing the middle meatal complex.

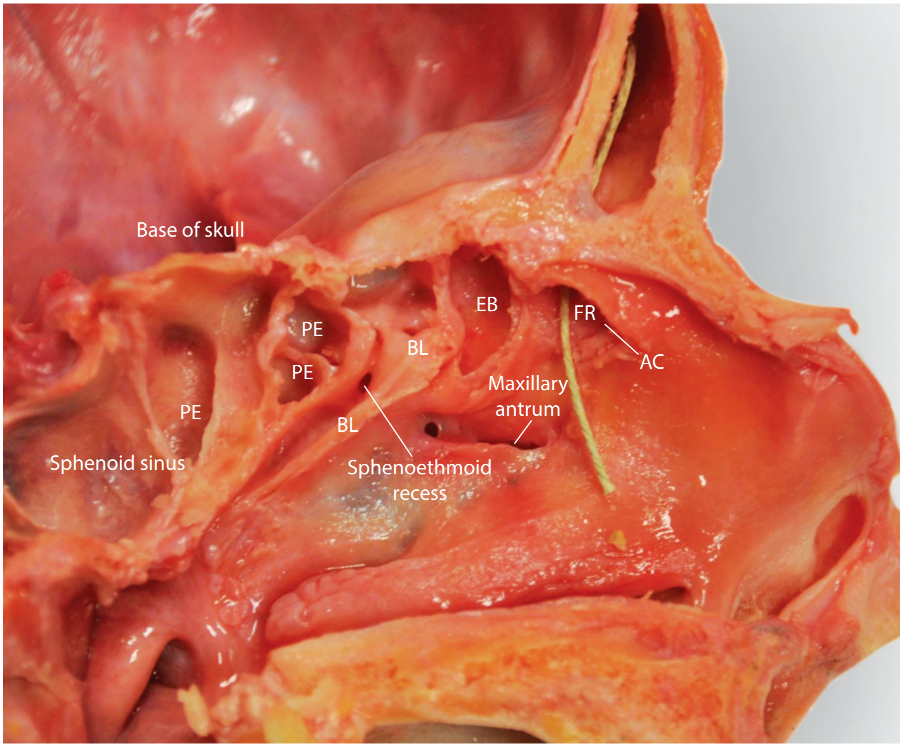

Figure 4.1c Lateral nasal wall with middle turbinate removed illustrating the basal lamella (BL) separating the ethmoid bulla (EB) from the posterior ethmoid cells (PE). FR – to frontal recess. AC – Agger nasi cell.

quadrilateral cartilage to the bony septum and nasal bones at the rhinion represents the keystone area. Continuity and fixation at this point is important both aesthetically and functionally as it supports the projection of the nose at the level of the rhinion.

The internal nasal valve is the narrowest part of the nasal airway and present at the anterior nasal cavity. It is a right angled triangular space in a coronal plane, bordered by the septum, the caudal edge of the upper lateral cartilage and the floor of the nasal cavity with variable intrusion from the anterior end of the inferior turbinate.

The lateral nasal wall and paranasal sinuses

THE NASAL TURBINATES AND MEATI

The lateral wall of the nasal cavity has three prominent projections called turbinates: inferior, middle and superior (Figure 4.1a). A fourth turbinate, the supreme turbinate, may occasionally be found. The turbinates provide an increase in surface area for the conditioning (warming and humidification) of the inspired air. The inferior turbinate is an independent bone articulating to the medial wall of the maxilla. The middle and superior turbinates (and supreme if present) are part of the ethmoid bone.

The ethmoturbinates are attached to the ethmoid complex via 'lamella'. The middle turbinate lamella has the most complex and important anatomical configuration. It has an *S*-shaped attachment that can be divided into thirds (Figure 4.1b). The anterior third of the middle turbinate lies in an axial plane and attaches to the lateral nasal cavity, and continues in its attachment to the skull base as the level of the lateral lamella of the cribriform plate. The mid-third is specifically termed 'basal lamella', which lies more in a coronal plane. The posterior third lies once again in an axial plane and is attached to the lamina papyracea as far as the perpendicular plate of the palatine bone. The ethmoid cells anterior to the basal lamella are

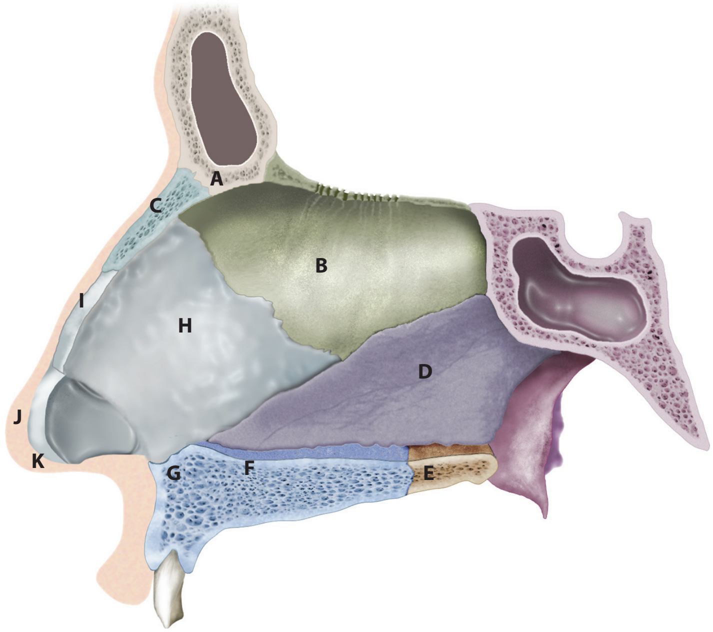

Figure 4.2 Nasal septum. A – Nasal process of frontal bone. B – Perpendicular plate of ethmoid. C – Nasal bones. D – Vomer. E – Horizontal plate of palatine bone. F – Palatine process of maxillary bone. G – Anterior nasal spine. H – Quadrangular cartilage. I – Upper lateral cartilage. J – membranous part of septum. K – Alar cartilage.

categorized as 'anterior ethmoid cells' and those posterior as 'posterior ethmoid cells'. An aerated middle turbinate is termed as concha bullosa.

Spaces lateral to the turbinates are termed meati (inferior, middle and superior, respectively) with different structures or cavities draining into these recesses. The inferior meatus drains the lacrimal sac via the nasolacrimal duct. The superior and supreme drain the posterior ethmoid cells. The middle meatus drains the frontal, maxillary and anterior ethmoid sinuses, and this common drainage space is called the 'osteomeatal complex'.

The osteomeatal complex and the middle meatus is an important anatomical complex and merits more detailed description. It is a complex of communicating recesses that drain into a common mucociliary drainage pathway for the frontal, anterior ethmoidal and maxillary sinuses. The main structures in this area are the uncinate process, ethmoid bulla and the ethmoidal infundibulum. The uncinate process is a thin, sagitally oriented boomerang-shaped bone which attaches to the lacrimal bone anteriorly and to the inferior turbinate inferiorly (Figure 4.1a). Superiorly, its attachment can be variable depending on the degree of pneumatization of the anterior ethmoidal cells. The posterior unattached margin forms the hiatus semilunaris allowing communication between the ethmoidal infundibulum and middle meatus. The ethmoidal infundibulum is a three-dimensional space into which the frontal sinus, anterior ethmoid cells and the maxillary sinuses drain. It is bound anteriorly by the aggar nasi and frontoethmoidal cells, medially by the uncinate process, posteriorly by the bulla ethmoidalis and laterally by the lamina papyracea (Figure 4.1b).

THE ETHMOID SINUS

The ethmoid sinuses are the most variable of the sinuses and develop from pneumatization of the ethmoid bone. Pneumatization can occasionally extend beyond the ethmoid bone and these cells are often allocated specific terms: orbit bone (supraorbital cell), roof of the maxillary sinus (Haller cell), into the floor of the frontal sinus (frontoethmoidal cell) and superolateral to the sphenoid sinus (Onodi cell).

The ethmoid sinuses are bound laterally by the lamella papyracia, superiorly by the anterior skull base and medially by the vertical lamella of the turbinates (middle for anterior and superior or supreme for the posterior). The ethmoid roof slopes medially and posteriorly. Medially it forms the fovea ethmoidalis and the cribriform plate and posteriorly it fuses with the sphenoid bone. The sphenoid sinus forms the posterior boundary of the ethmoid sinuses.

Bony septae divide the ethmoidal sinus into up to 18 air cells. These are divided to form the anterior and posterior ethmoid systems depending on their relationship to the basal lamella of the middle turbinate as described previously.

There are certain named ethmoidal cells that merit mention. The agger nasi cell is the most anterior and consistent of all ethmoid cells and is pneumatized in 98 per cent of patients. It is located anterosuperior to the anterior insertion of the middle turbinate (Figure 4.1c). It forms the anterior boundary of the infundibulum and frontal recess and is an important landmark for identification of the frontal recess.

The ethmoid bulla, the most prominent anterior ethmoid air cell, is easily identified posterior to the uncinate process (Figure 4.1b, c). Laterally, it is attached to the lamina papyracea. Between the posterior wall of ethmoid bulla and the basal lamella lies a potential space: suprabullar and retrobullar recesses (collectively called the lateral sinus) (Figure 4.1c).

The ethmoidal arteries transverse the roof of the ethmoid complex and are at potential risk of damage during sinus surgery. The anterior ethmoid artery most commonly lies between the superior attachments of the face of the bulla and the basal lamella, while the posterior lies between the basal lamella and the sphenoid face. Although the posterior lies in a coronal plane, the anterior ethmoidal artery has a diagonal course going latero-superior to antero-medial. Dehiscences have been reported in up to 40 per cent of patients and care should be taken during surgery to avoid damage that could lead to retraction into the orbit and intraorbital haemorrhage.

The posterior ethmoid cells are much larger and vary between one and five in number. All drain into the superior and supreme meatia. In approximately 10 per cent of cases, the most posterior ethmoidal air cells can extend laterally and superiorly beyond the anterior wall of the sphenoid sinus and are called Onodi cells. These sphenoethmoidal cells are important as they can contain the optic nerve and internal carotid artery in their lateral or posterior walls.

The blood supply to the ethmoid sinus is from branches of the anterior and posterior ethmoidal and sphenopalatine arteries. Venous drainage follows the arterial supply. Lymph drainage is to submandibular and retropharyngeal nodes. The innervation is from the supraorbital, anterior ethmoidal and by orbital branches from the pterygopalatine ganglion.

THE MAXILLARY SINUS

This is pyramidal in shape with its base forming part of the lateral nasal wall and its apex pointing towards the zygomatic process. The orbital floor forms its roof and contains the infraorbital nerve (dehiscent in 14 per cent). The alveolar process of the maxilla and the hard palate form the floor. The thinnest part of the anterior wall corresponds with the canine fossa. The pterygomaxillary fossa and its contents (internal maxillary artery, sphenopalatine ganglion and greater palatine nerve) lie behind the posterior wall of the maxillary sinus.

The maxillary sinus ostium opens into the inferior aspect of the infundibulum and is normally hidden from view by the uncinate process (Figure 4.3). The maxillary sinus medial wall has areas of bony dehiscence usually covered by mucosa called the anterior and posterior fontanelles. These may be patent (in 30 per cent) to form an accessory ostium, which is usually nonfunctional.

Branches of the internal maxillary artery, i.e. the infraorbital and greater palatine arteries, provide the blood supply and venous drainage is through the pterygoid plexus and facial vein. Lymphatic drainage is to the submandibular lymph nodes. The infraorbital, greater palatine and superior alveolar nerves provide the nerve supply to the maxillary sinus mucosa.

FRONTAL SINUS

The pneumatization of the frontal sinus is variable and is underdeveloped in approximately 5 to 10 per cent of cases. The anterior and posterior walls of

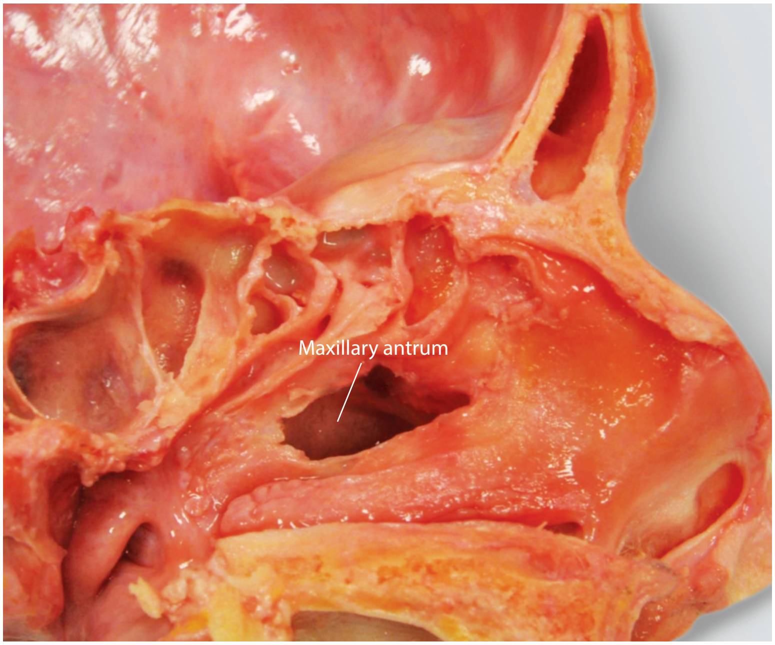

Figure 4.3 Maxillary antrum. Uncinectomy has been performed after removal of the middle turbinate. Note the basal lamella.

the frontal sinus are composed of diploeic bone. The posterior wall separates the frontal sinus from the anterior cranial fossa and is much thinner. An intersinus septum divides the two sides and each drain independently at the lowest medial portion of the cavity into the superior aspect of the ethmoid infundibulum via the frontal recess. The frontal sinus does not have a defined ostium but instead a drainage pathway that connects the frontal sinus cavity to the frontal recess. The frontal recess in turn drains into the superior aspect of the infundibulum. This drainage pathway can be notably variable and affected by the presence and the degree of pneumatization of anterior ethmoidal cells called the 'frontoethmoidal cells'.

The supraorbital and supratroclear branches of the ophthalmic artery provide its blood supply but venous drainage is to the cavernous sinus via the superior ophthalmic veins and to the dural sinuses through the posterior wall venules (veins of Breschet). The supraorbital and supratrochlear nerves provide its innervation.

SPHENOID SINUS

The sphenoid sinuses show variable pneumatization and can be absent in about 1 per cent of the population. They are often asymmetrically divided by a septum. Antero-inferiorly, the sphenoid rostrum articulates with the perpendicular plate and vomer of the nasal septum (Figure 4.2a). The sphenoid ostia are located in the anterior medial wall of the sinus and drain into the sphenoethmoidal recess medial to the superior turbinate (Figure 4.1b).

Depending on the degree of pneumatization, the posterior wall is formed by the sella turcica superiorly and clival bone inferiorly. The clival carotid artery transverses vertically in the clival portion of the posterior wall and loops forward in the cavernous portion. Together with the optic nerve, these are prominences evident in the superolateral wall of the sphenoid sinus with an indentation separating the two called the lateral optic-carotid recess. Bony dehiscence over the optic nerve (6 per cent) and carotid arteries (8 per cent) are not infrequent. Inter-sinus septa can often be in continuity with the carotid and optic canal, and uncontrolled avulsion can result in a catastrophic bleed or blindness. The maxillary part of the trigeminal nerve (V2) traverses the lateral wall and vidian nerve of the floor of the sphenoid sinus.

The sphenoid sinus receives most of its blood supply from the sphenopalatine artery. Its roof is supplied by the posterior ethmoid artery. Venous drainage is via the maxillary veins to the jugular and pterygoid plexus systems. The nasociliary nerve supplies the roof while the floor receives its innervations from branches of the sphenopalatine nerve.

FURTHER READING

Dharmbir S. *Applied Surgical Anatomy of the Nasal Cavity and Paranasal Sinuses.* In: Jones N. (Ed.). *Practical Rhinology*. London: Hodder Arnold, 2010: 1–14.

Lund V, Stammberger H. *Anatomy of the Nose and Paranasal Sinuses.* In: Gleeson M, Browning G, Burton MJ, et al. (Eds.). *Scott-Brown's Otorhinolaryngology, Head and Neck Surgery*. London: Hodder Arnold, 2008: 1313–43.

Stammberger H. *The Messerklinger Technique.* In: Stammberger H. (Ed.). *Functional Endoscopic Sinus Surgery*. Philadelphia: B.C. Dekker, 1991: 17–46.

Wormald PJ. *Endoscopic Sinus Surgery: Anatomy, Three-Dimensional Reconstruction, and Surgical Technique*. New York: Thieme, 2012.

5

External ear

DAVID RICHARDSON

Embryology 45
Topography 46
Ridges and fossae 46
Vertical planes of the ear 46
Ear position 47
Vertical 47
Anteroposterior 47
Angulation 47
Projection 47
Surgical anatomy 47
Skin 48
Blood supply 48
Cartilage 49
Lymphatic drainage 50
Nerve supply 50
Muscles 50
Further reading 52

EMBRYOLOGY

The embryology of the external ear is of direct relevance to surgical anatomy and pathology. Development of the external ear begins during the sixth week in utero as swellings of the first and second branchial arches, coincident with the period of organogenesis (4 to 8 weeks). It is not surprising that there is an association between ear anomalies and other anomalies, particularly cardiac and renal, and the possibility that these may be present in association with congenital ear anomalies should always be investigated.

The external ear commences its development caudal to the developing face, the ear migrating superiorly as development progresses. Many external ear deformities are also associated with a ‘low set’ position – a condition that is extremely difficult to alter surgically, but which is very important to the aesthetic outcome of corrective surgery.

The external ear develops from the first and second branchial arches, which also give rise to development of the face, mouth and jaws, so it is not surprising that there is an association between ear and facial anomalies in 50 per cent of cases, usually oculo-auriculo-vertebral syndrome (OAVS)/hemifacial microsomia (usually unilateral) or Treacher Collins syndrome (bilateral).

The first branchial cleft and pouch contribute to development of the external auditory meatus, tympanic membrane, middle ear and Eustachian tube. Congenital anomalies of the external ear are often associated with conductive deafness due to external auditory meatus atresia and/or anomalies of the middle ear. Assessment for and treatment of deafness is particularly important in bilateral cases, and in the presence of a normal inner ear, bone-conducting hearing aids are the technique of choice to restore useful hearing.

The external ear is derived from six auricular hillocks, three from the first and three from the second branchial arches. These migrate and fuse in a complex topographical pattern to produce the three-dimensional structure recognizable as

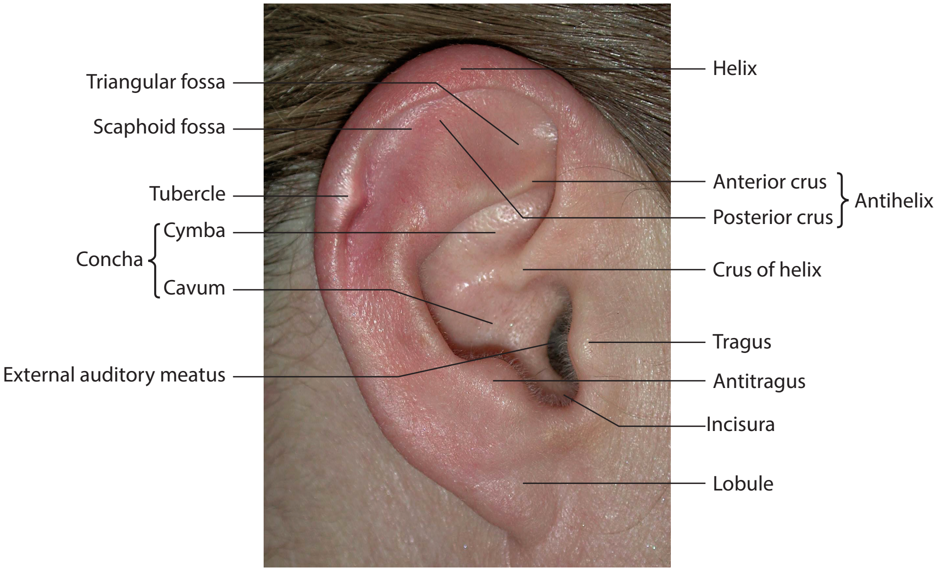

Figure 5.1 Lateral view of the ear. Topographical features of the ear.

a normal ear. The majority of the external ear is derived from the second arch, the first arch contributing to the anterior helix, tragus, incisura and lobule only. The vascular, lymphatic and neural connections of different areas of the ear are related to embryological origin. In cases of microtia, there is often an absence of second arch-derived tissue, with hypoplastic and distorted remnants derived from the first arch.

Abnormalities of development and fusion of the auricular hillocks gives rise to a wide variety of deformities of varying severity, including auricular pits, accessory auricles, malposition ('low set'), lop ear, cup ear, question mark ear, bat ear, cryptotia, microtia and anotia.

TOPOGRAPHY

To obtain good aesthetic results in corrective or reconstructive surgery of the external ear, a thorough understanding of the topographical anatomy is of paramount importance, and every effort is required to reproduce as accurately as possible the complex three-dimensional shape of the ear. The characteristic ear shape is formed by a number of depressions or recesses (fossae), situated in different spatial planes, defined and separated by a number of ridges.

Ridges and fossae

The ridges comprise the helix, antihelix with its anterior and posterior crura, antitragus, incisura and tragus. These ridges define the concha (cymba and cavum), triangular fossa, and scaphoid fossa. Figure 5.1 illustrates these features.

VERTICAL PLANES OF THE EAR

Two-dimensional views fail to demonstrate the vertical relief of the ear, which is crucial to successful reconstructive surgery. The ear is not a flat structure on one plane, but has fossae on a number of planes at different heights and depths, separated by ridges which themselves are not planar structures, but curve and adapt to the different levels of the fossae and other ridges to which they relate.

The cavum concha is on the deepest plane, with the cymba concha slightly superficial to this. The scaphoid and triangular fossae are on the superficial plane (Figure 5.2).

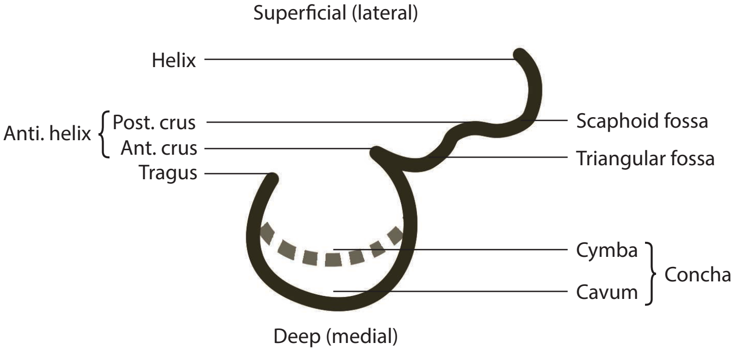

Figure 5.2 Vertical planes of the ear.

EAR POSITION

There is a normal range for ear position, which will not be identical in all subjects. There are, however, some approximate guides to normal ear position that can be useful clinically.

Vertical

When viewed from the front with the head in the natural head position, the upper pole is usually between the lower margin of the eyebrow and the interpupillary line; the point at which the helix merges with the side of the head level with the lateral canthus; and the lower pole at the level of junction of the alum of the nose with the upper lip (Figure 5.3a). The vertical position of the ear is crucial to its aesthetic appearance as the ear is viewed from the front during normal social contact and even small degrees of vertical asymmetry are obvious. Vertical asymmetry may result from conditions that affect skull base symmetry (e.g. torticollis, unilateral lambdoid synostosis), whilst symmetrically low set ears are associated with a number of congenital abnormalities.

Anteroposterior

The point at which the helix merges with the side of the head is situated at a distance behind the lateral orbital margin equal to the length of the long axis of the ear. The antero-posterior position, although important, is slightly less critical than the vertical position as small degrees of asymmetry are only apparent when viewed from above. Deformational (positional) plagiocephaly as well as unicoronal and unilambdoid synostosis may result in antero-posterior asymmetry of the skull base, and affect horizontal ear position.

Angulation

The long axis of the ear is orientated at approximately 25 degrees to the vertical, the upper pole being posterior to the lower pole, and equates to (or slightly less than) the angulation of the (normal) nasal dorsum (Figure 5.3b).

Projection

The projection of the ear is dependent on underlying skull morphology, conchal depth, antihelical height, and the degree of folding of the posterior crus of the antihelix (which is deficient in 'bat ears'). The normal auriculo-cephalic angle is approximately 30 degrees

SURGICAL ANATOMY

The surgical anatomy is relatively simple, with skin on the anterior and posterior surfaces, and in the majority of the ear, elastic cartilage between the two layers of skin. The lobule is devoid of cartilage, and there is a layer of subcutaneous adipose tissue between the anterior and posterior skin in the lobule.

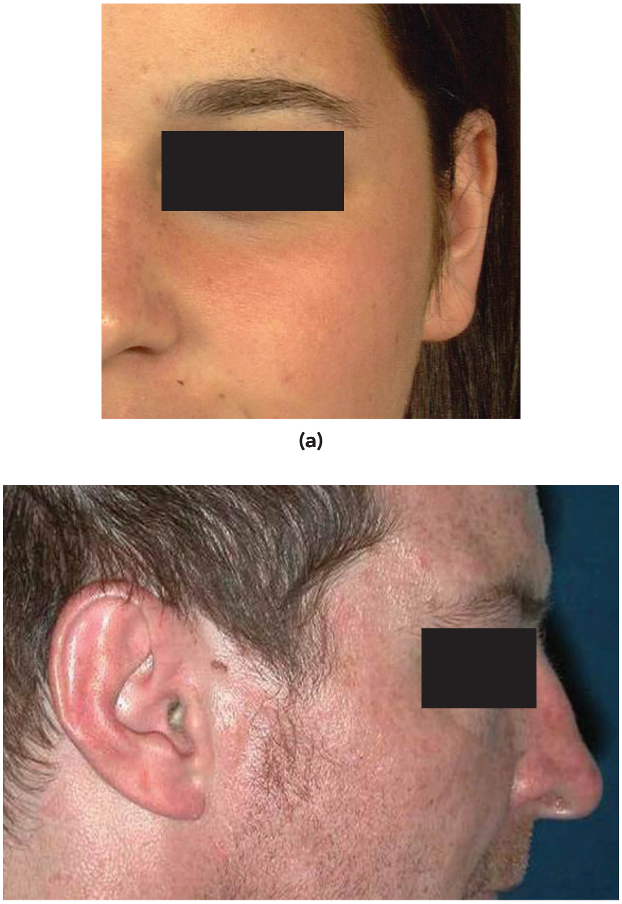

(a)

(b)

Figure 5.3 Ear position: **(a)** vertical position, **(b)** horizontal position depicting ear angulation.

Skin

The skin overlies a layer of subcutaneous fat, beneath which is perichondrium covering ear cartilage. The skin receives its blood supply via the subdermal plexus, enabling a variety of different thin random and axial pattern flaps to be raised with excellent blood supply.

Blood supply

Arterial supply to the ear is from the superficial temporal (STA) and posterior auricular arteries (PAA), with the occipital artery (OA) contributing the posterior supply where the auricular branches of the PAA are absent (in 20 per cent of cases).

Two or three posterior branches of the STA supply the anterior surface of the ear. A branch arising in the region of the helical root (the superior auricular artery) continues into the helix as the helical artery and gives rise to the helical arcade, which forms anastamotic connections between the anterior and posterior blood supplies. A branch is also given off below the tragus towards the lobule (lobular branch), and each branch can be sufficient to maintain vascularity of the ear in near avulsive injuries where a small anterior skin pedicle is maintained. There is a third (median auricular) branch in some cases. All these vessels send shoots to the conchal bowl, and anastamose with branches of the PAA.

The PAA supplies the posterior surface of the ear in most cases, giving rise to three branches in the post-auricular sulcus — the upper, median and lower branches — which extend towards the helical rim. Perforating branches pass through the lobule and the cartilage of the conchal bowl, and circumflex branches pass over the helical rim to contribute to the helical plexus and provide an additional supply to the anterior surface. Where branches from the PAA do not provide the posterior supply, this function is taken by the OA

Anastomotic connections are numerous, and Doppler studies have shown reverse flow to occur when the orthograde flow is occluded. A wide variety of local flaps have been described based on an understanding of the vascularity of the ear.

The continuation of the superficial temporal artery and its posterior branch into the temporo-parietal area, and the posterior branches of the post-auricular artery allow use of the temporo-parietal and occipito-mastoid fascias for soft tissue cover in ear reconstruction (Figure 5.4a and b). Venous drainage follows the arterial supply.

Cartilage

The elastic cartilage of the external ear acts as a splint to the skin and produces the characteristic topographical features discussed above. It therefore closely mirrors the external shape of the ear (with the exception of the lobe). Surgical techniques to alter the shape of the ear must take into account the elastic memory inherent in the cartilage, and steps must be taken to weaken this (e.g. cartilage scoring) or to support surgical change (e.g. suturing techniques) to achieve stability. It must also be recognized that where full thickness defects are reconstructed, the native elastic cartilage is not strong enough to withstand post-surgical scar contracture, and in almost all cases of traumatic full thickness loss, using cartilage of the avulsed segment (or concha of the contra lateral ear) should not be attempted since it is likely to achieve a very poor result in all but the smallest defects.

The auricular cartilage and the cartilage of the external meatus are continuous. However, the cartilage does not extend into the lobe where there is adipose tissue; the only cartilaginous support is from the cauda of helix and the inferior border of the meatal cartilage (Figure 5.5a and b).

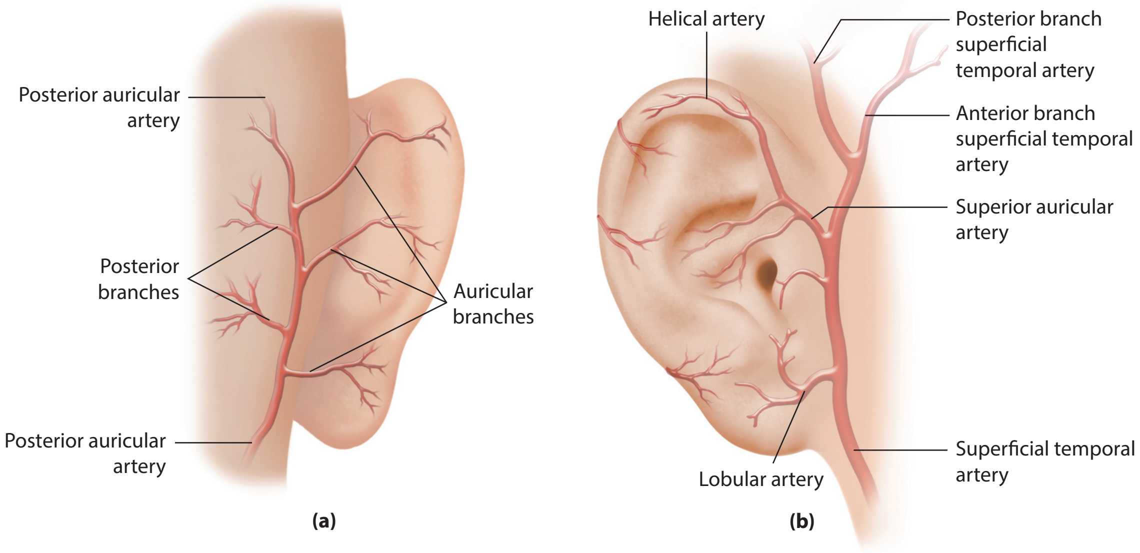
Posterior auricular artery
Posterior branches
Auricular branches
Posterior auricular artery
(a)
Helical artery
Posterior branch superficial temporal artery
Anterior branch superficial temporal artery
Superior auricular artery
Lobular artery
Superficial temporal artery
(b)

Figure 5.4 Arterial supply of the ear.

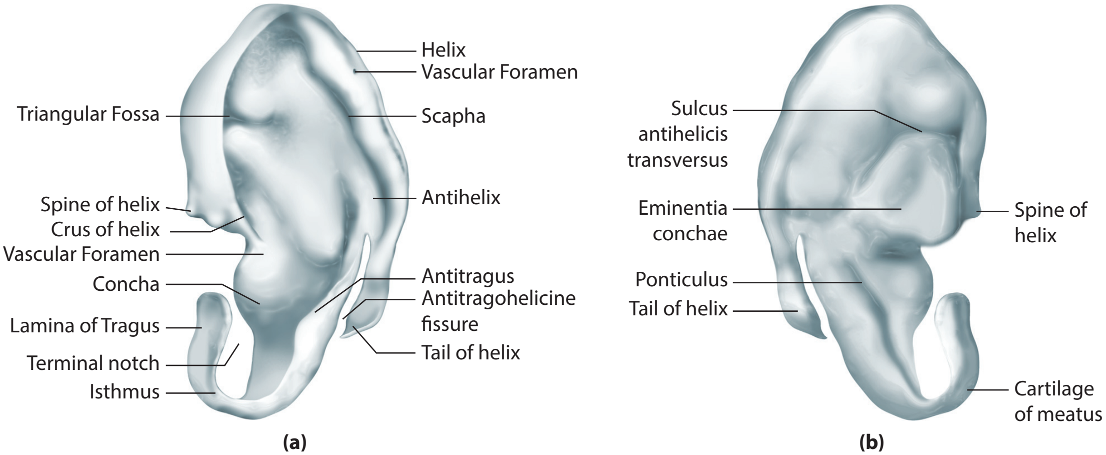
Helix
Vascular Foramen
Triangular Fossa
Scapha
Antihelix
Spine of helix
Crus of helix
Vascular Foramen
Concha
Antitragus
Antitragohelicine fissure
Lamina of Tragus
Tail of helix
Terminal notch
Isthmus
(a)
Sulcus antihelicis transversus
Eminentia conchae
Spine of helix
Ponticulus
Tail of helix
Cartilage of meatus
(b)

Figure 5.5 Auricular cartilage: **(a)** anterior view, **(b)** posterior view.[3]

Lymphatic drainage

Pan et al. demonstrated an anterior channel draining the anterior surface of the concha to the pre-auricular nodes; an inferior branch draining the lobule to infra-auricular or parotid nodes: and superior and middle branches draining the upper two thirds of the ear to the infra-auricular nodes (Figure 5.6). The pattern of drainage reflects embryologic origin, the anterior helix, helical root and tragus (first arch) draining to pre-auricular nodes, with the remainder of the ear (derived from the second arch) draining to the infra-auricular, parotid and mastoid nodes. However, in clinical practice, the pattern of lymph drainage is highly variable, with studies of sentinel node biopsy demonstrating a high incidence variability and bypass of first echelon nodes, as far distant as the submental area, and levels 4 and 5 in the neck.

Nerve supply

A number of descriptions of the sensory supply to the external ear vary in detail, and the sensory supply to the ear is complex and not fully understood (Figure 5.7).

The great auricular nerve (C2, 3), via its posterior branch, gives sensation to most of the posterior surface, part of the anterior surface from the antihelical fold to the helix, and the lobule. Some authors state the anterior sensation is confined to the lower half of the ear below the external auditory meatus. Preservation of the posterior branch during parotid surgery has been advocated.

The auriculotemporal branch of the trigeminal nerve gives two branches to the helix and tragus, and branches to the external auditory meatus, supplying the skin on the front of the ear above the level of the external auditory meatus, extending towards the antihelix and helical rim

The lesser occipital nerve (C2) gives sensation to the superior part of the helix at the upper pole of the ear, and a small amount of the adjacent posterior surface

The auricular branch of the vagus (Arnold's nerve) gives sensation to a small area of meatus, conchal bowl and mastoid skin, and auricular branches of the facial nerve contribute sensation to the meatus and inferior conchal bowl, explaining the vesicles present in geniculate herpes (Ramsay Hunt syndrome).

Muscles

There are a number of intrinsic ear muscles, which are vestigial and have no significant function. The extrinsic muscles (anterior, superior and posterior auricular muscles) are innervated by the facial nerve (temporal and posterior auricular branches). They originate from the epicranial aponeurosis, and insert into the anterior, superior and posterior

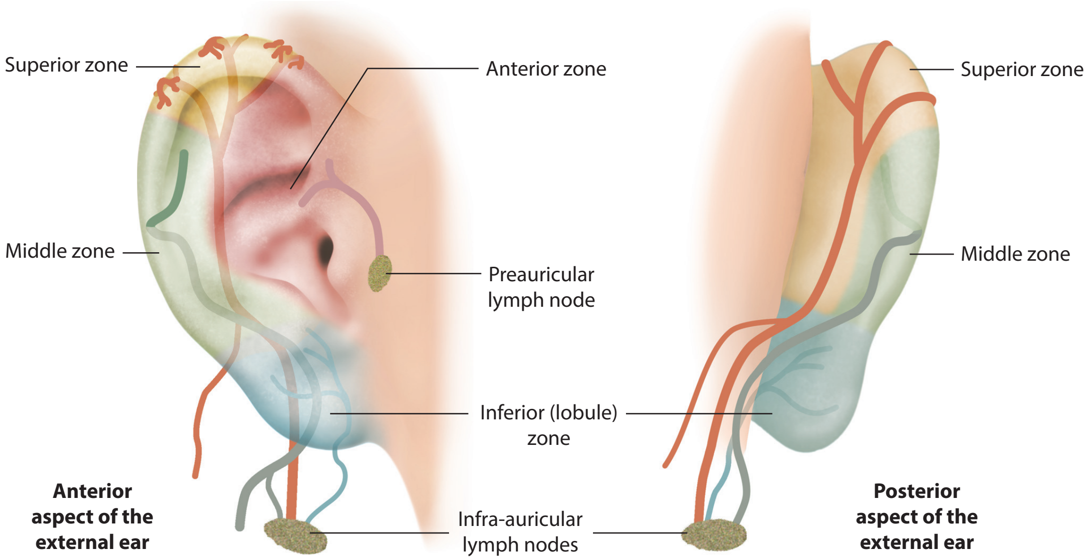
Superior zone
Anterior zone
Middle zone
Preauricular lymph node
Inferior (lobule) zone
Anterior aspect of the external ear
Infra-auricular lymph nodes
Superior zone
Middle zone
Posterior aspect of the external ear

Figure 5.6 Lymphatic channels of the ear. From Pan WR, le Roux CM, Levy SM, Briggs CA. Lymphatic drainage of the external ear. *Head & Neck*. 2011 Jan; 33(1): 60–4.

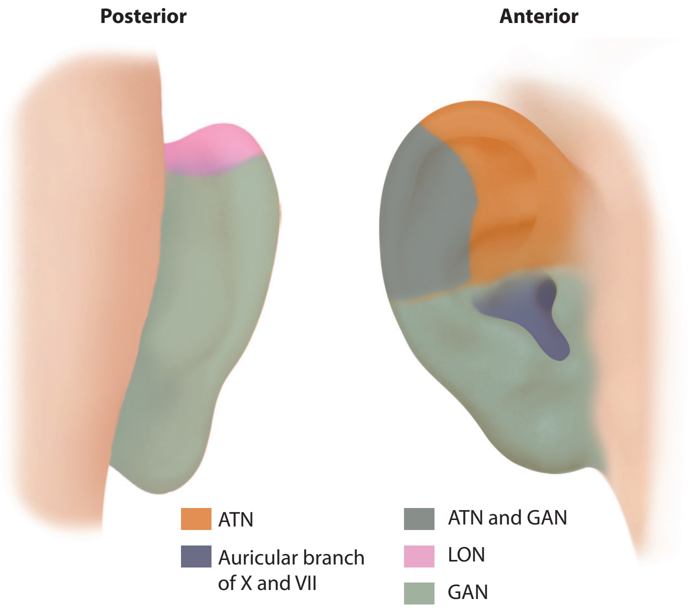
Posterior
Anterior
ATN
Auricular branch of X and VII
ATN and GAN
LON
GAN

Figure 5.7 Sensory supply of the ear, posterior and anterior.

aspects of the auricular cartilage on its posterior surface. They act together to produce upward and backward movement associated with smiling and yawning. Reflex contraction of the posterior and superior muscles has been observed in response to noise, and has been used as an objective neurophysiological test of deafness.

FURTHER READING

Grey P. The clinical significance of the communicating branches of the somatic sensory supply of the middle and external ear. *Journal of Laryngology and Otology*. 1995 Dec; (12): 1141–5.

Klockars T, Rautio J. Embryology and epidemiology of microtia. *Facial Plastic Surgery*. 2009 Aug; 25(3): 145–8.

Pan, WR, le Roux CM, Levy SM, Briggs CA. Lymphatic drainage of the external ear. *Head & Neck*. 2011 Jan; 33(1): 60–4.

Standring S. (Ed.). *Gray's Anatomy, 40th ed*. Edinburgh: Churchill Livingstone, 2008.

Tillota F, Lazaroo B, Laujac M-H, Gaudy J-F. A study of the vascularisation of the auricle by dissection and diaphinization. *Surgical and Radiologic Anatomy*. 2009; 31: 259–65.

6

Temporal bone, middle ear and mastoid

MICHAEL GLEESON

Introduction 53
Embryology 53
Anatomy 54
Anatomical hazards in mastoid and middle ear surgery 58
Further reading 58

INTRODUCTION

The temporal bone contains the organs of hearing and balance. The facial nerve, internal carotid artery, sigmoid sinus and jugular bulb passage through it or adjacent to it. These are all very important or vital structures and so a thorough knowledge of temporal bone anatomy is necessary for those who operate on or around it. Variants of the normal anatomy are not uncommon in the temporal bone and can take the surgeon by surprise even with seemingly good pre-operative scan data. This is particularly the case when chronic infection or tumours have destroyed much of the normal anatomy, particularly in regard to the path of the facial nerve within the Fallopian canal. In this chapter the surgical anatomy of the temporal bone, middle ear and mastoid are described together with those aspects that can present a hazard for the surgeon and his patient. The detailed anatomy of the inner ear is not included because of constraints on chapter length. References where this information can be obtained are listed at the end of this chapter.

EMBRYOLOGY

In the embryo, the brain is supported by a sheet of condensed mesenchyme that surrounds the notochord. It extends laterally to fuse with the chondrified otic capsule. Inferiorly, it is continuous with the mesenchyme of the branchial arches. Four distinct zones of ossification develop within the mesenchyme that will ultimately define the component parts of the temporal bone.

The squamous part begins to ossify from a single centre near the zygomatic root in the seventh or eighth week in utero. Several ossification centres develop in the cartilagenous otic capsule during the fifth month. These fuse so that the otic capsule is almost completely ossified by the sixth month and destined to be contained in the petromastoid part of the temporal bone. The tympanic part ossifies from a solitary centre around the third month and is an incomplete ring of bone at birth, deficient superiorly but already containing a groove to house the annulus of the tympanic membrane. The styloid process is derived from the cranial end of the second branchial arch cartilage and ossifies from two centres, one at each end of the process, around the time of birth. The tympanic ring unites with the squamous part shortly before birth, and the petromastoid fuses with it during the first year. The styloid process is not completely ossified until after puberty.

ANATOMY

By convention, the temporal bone is divided into four component parts. As mentioned above, these reflect its embryological development and primary ossification sites, namely squamous, petro-mastoid, tympanic and styloid process (Figures 6.1–6.3).

The **squamous part** overlies the lateral and part of the inferior aspect of the temporal lobe. It fuses with the petro-mastoid portion inferiorly and is separated from the parietal bone antero-superiorly by a suture. The antero-inferior border adjoins the greater wing of the sphenoid bone. Its internal surface is concave and contains depressions which correspond to the convolutions of the temporal gyri, and it is grooved by the middle meningeal vessels. The external squamous temporal surface is smooth, slightly convex and forms part of the temporal fossa to which the temporalis muscle is attached. A crest, the supra-mastoid crest, curves backwards and upwards across the posterior element to give attachment to the temporal fascia. The squamous part projects the zygomatic process anteriorly. The anterior part of the zygomatic process is thin and flat. It provides attachment for the temporal fascia on its superior border. Its inferior border gives origin to part of the masseter, while the rest of the masseter is attached to the concave medial surface. Anteriorly, the zygomatic arch articulates with the temporal process of the zygomatic bone to form the zygomatic arch. Immediately posterior to the zygomatic process is the mandibular fossa. The latter is limited in front by the articular tubercle or eminence of the zygomatic process. The articular surface of the mandibular fossa is smooth, oval and concave. It contains the articular disc of the temporo-mandibular joint. Posteriorly, the mandibular fossa is separated from the tympanic part of the temporal bone by the squamo-tympanic fissure.

The **petro-mastoid part** of the temporal bone contains the middle and inner ear structures together with the facial nerve, internal carotid artery and sigmoid sinus. The ***petrous element*** lies wedged between the sphenoid and occipital bones. It is pyramidal in shape with a base, apex and three surfaces – anterior, posterior and inferior. The base adjoins the squamous portion of the temporal bone and forms part of the skull base itself. The apex lies between the posterior border of the greater wing of the sphenoid and the basilar part of the occipital bone. It contains the anterior opening of the carotid canal.

The ***anterior surface*** forms part of the middle cranial fossa floor and is in continuity with the internal surface of the squamous part of the temporal bone. The trigeminal ganglion leaves an impression on this surface just behind the apex. Bone antero-lateral to the trigeminal impression provides the roof of the carotid canal, internal acoustic meatus, cochlea and labyrinth. The most conspicuous landmark is an eminence, the arcuate eminence, which is raised by, but not directly over, the superior semicircular canal. Laterally, the anterior surface roofs the vestibule of the inner ear and part of the facial nerve canal. A thin region of this surface, the tegmen tympani, roofs the mastoid antrum and middle ear, extending forwards to contribute to the bony part of the Eustachian tube and canal for the tensor tympani. A groove on the tegmen tympani houses the greater superficial petrosal nerve as it courses forwards towards the foramen lacerum.

The ***posterior surface*** of the petrous bone contributes to the anterior part of the posterior cranial fossa. The internal acoustic meatus opens onto this surface and contains the cochleovestibulaar and facial nerves and the labyrinthine artery. Posterior to the internal acoustic meatus is the opening of the vestibular aqueduct that contains the endolymphatic duct and sac.

The ***inferior surface*** of the petrous bone is part of the external surface of the skull base. Towards the apex on this surface is an area of bone that gives some attachment to the levator veli palatini and the cartilaginous part of the Eustachian tube. Behind this is the opening of the carotid canal and posterior to this, the jugular fossa. The stylomastoid foramen is postero-lateral to the jugular fossa and posterior to the base of the styloid process.

The ***mastoid element*** comprises the posterior aspect of the temporal bone. Its outer surface provides attachment for the occipitofrontalis and auricularis posterior. An emissary vein of very

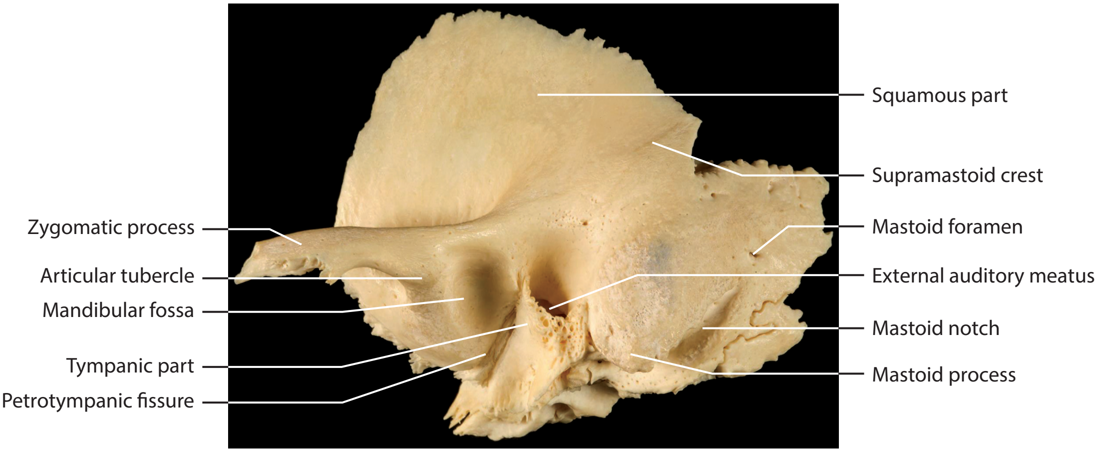
Squamous part
Supramastoid crest
Zygomatic process
Mastoid foramen
Articular tubercle
External auditory meatus
Mandibular fossa
Mastoid notch
Tympanic part
Mastoid process
Petrotympanic fissure

Figure 6.1 Lateral aspect.

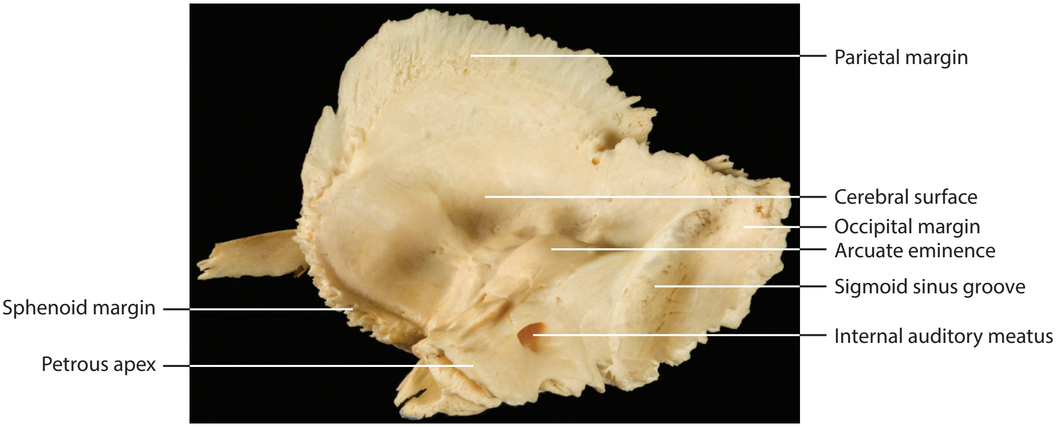
Parietal margin
Cerebral surface
Occipital margin
Arcuate eminence
Sigmoid sinus groove
Sphenoid margin
Internal auditory meatus
Petrous apex

Figure 6.2 Medial aspect.

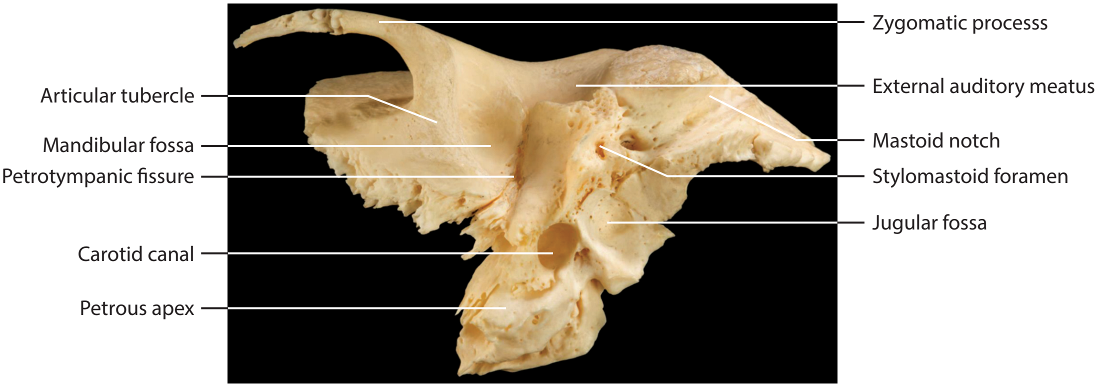
Zygomatic processs
Articular tubercle
External auditory meatus
Mandibular fossa
Mastoid notch
Petrotympanic fissure
Stylomastoid foramen
Jugular fossa
Carotid canal
Petrous apex

Figure 6.3 Inferior aspect.

variable size exits from a foramen near its posterior border. The mastoid part projects downwards to a tip that provides attachment for the sternocleidomastoid, splenius capitis and longissimus capitis, all of which are attached to its lateral surface. The posterior belly of the digastric is attached to its medial surface in a deep notch. A wide, curved groove on the internal surface of the mastoid indicates the site of the sigmoid sinus.

The **tympanic part** of the temporal bone is a curved plate of bone below the squamous part and anterior to the mastoid process. It fuses with the petrous and squamous parts, and its concave posterior surface forms the anterior wall, floor and part of the posterior wall of the external auditory meatus, while its concave anterior surface is the posterior wall of the mandibular fossa. The tympanic membrane lies in a narrow groove on its medial surface, the tympanic sulcus. The petrotympanic fissure is also found antero-medially and contains the anterior malleolar ligament, the anterior tympanic branch of the maxillary artery and the chorda tympani nerve.

The **styloid process** projects antero-inferiorly from the inferior aspect of the temporal bone. Its length is extremely variable. In some it can be 3–4 cm in length while in others it is very rudimentary. Its base is ensheathed by a split in the lateral aspect of the tympanic plate, the vaginal process. The styloid process provides attachment for the stylopharyngeus, stylohyoid and styloglossus muscles. The stylomastoid foramen lies between the styloid and mastoid processes and through this the facial nerve emerges from the skull into the parotid gland together with the stylomastoid artery.

The **external auditory canal** runs from the concha of the pinna to the tympanic membrane. It is about 2.5 cm in length. The lateral third is cartilaginous and is continuous with the auricular cartilage. The medial two-thirds of the canal is bony. Initially directed medially, anteriorly and slightly upwards, it then runs postero-medially and finally antero-medially again, but also slightly downwards. So, it has a sigmoid course which in some patients can be quite pronounced and obstruct a view of the entire tympanic membrane. Generally oval in cross section, it has two constrictions. One is at or near the junction of the cartilaginous and bony part, while the second is within the bony canal, closer to the tympanic membrane, and is called the isthmus. The floor of the canal and anterior wall is longer than the roof and posterior wall. This results in the tympanic membrane being obliquely positioned at the medial end of the canal. This obliquity is most marked in the neonate when the tympanic membrane is almost horizontally set across the medial end of the canal.

Just postero-superior to the external auditory canal is a surgical landmark, Macewen's triangle, that marks the lateral wall of the mastoid antrum. This triangle is defined as the area beneath the supramastoid crest, behind the postero-superior margin of the external acoustic meatus and a line tangential to the posterior margin of the external auditory meatus.

The posterior auricular artery, deep auricular branch of the maxillary artery and the auricular branches of the superficial temporal artery supply the external auditory canal. Veins drain into the external jugular, maxillary veins and pterygoid plexus. Lymphatics drain into pre- and post-auricular nodes. The auriculotemporal branch of the mandibular nerve provides sensation to the anterior and superior walls, while the auricular branch of the vagus and sensory component of the facial nerve supply the posterior and inferior walls.

The **tympanic membrane** is thin, semi-transparent and almost oval in shape. It forms part of the lateral wall of the tympanic cavity, otherwise called the middle ear. It is thickened peripherally to form a fibrocartilaginous ring, the annulus, which lies in the tympanic sulcus. This sulcus is incomplete and deficient superiorly in the attic leaving a notch. The anterior and posterior malleolar folds extend from the edges of this notch to the lateral process of the malleus, defining a visible border between the upper and thinner part of the tympanic membrane, the pars flaccida, and the thicker and more taut inferior part, the pars tensa. The handle of the malleus is firmly attached to the medial surface of the tympanic membrane as far as its centre, the umbo, which projects towards the tympanic cavity. The external surface of the tympanic membrane is therefore concave, centred on the umbo. The tympanic membrane has a trilaminar structure composed of an outer cuticular layer, an intermediate fibrous layer and an inner mucous layer. The fibrous element has an outer layer of radiating fibres that emerge from the handle of the malleus and a deeper but sparser layer of circular fibres. The tympanic membrane is mainly innervated by the auriculotemporal nerve with contributions from branches of the facial, glossopharyngeal and vagus nerves.

The **tympanic cavity** or middle ear has a roof, a floor, lateral, medial, posterior and anterior walls. It contains air, is lined by a mucous membrane and communicates with the nasopharynx through the pharyngotympanic tube, the Eustachian tube, and with the mastoid air cells posteriorly through the additus of the mastoid antrum. It measures approximately 15 mm both antero-posteriorly and vertically, while 6 mm wide superiorly and 4 mm inferiorly, narrowing to 2 mm at the level of the umbo. The middle ear contains three small bones or ossicles, the malleus, incus and stapes. These bones form a connecting chain, the ossicular chain, that conducts auditory vibration from the tympanic membrane to the inner ear. By convention, the tympanic cavity is divided into three zones. The zone above the tympanic segment of the facial nerve is called the epitympanum. That between the tympanic segment of the facial nerve and the inferior margin of the tympanic membrane is the mesotympanum. The zone beneath that is the hypotympanum.

The roof of the tympanic cavity is a very thin plate of compact bone, the tegmen tympani. It separates the cranial and tympanic cavities and through it veins pass that drain into the superior petrosal sinus. The floor is a thin, convex plate of bone raised by the jugular bulb. It is often deficient in places. The tympanic branch of the glossopharyngeal nerve exits through a foramen adjacent to the medial wall. The tympanic membrane, surrounded by a ring of bone, forms the lateral wall. The superior aspect of this is shaped like a shield, the scutum, and constitutes the lateral aspect of the attic of the middle ear.

The most conspicuous landmark in the anterior wall of the tympanic cavity is the opening of the pharyngotympanic tube. Below this the bone is relatively thin and covers the posterior aspect of the internal carotid artery. Tympanic branches of the artery perforate this wall along with caroticotympanic nerves. The internal carotid artery turns forwards at the entrance of the Eustachian tube and runs medial to it. In the roof of the pharyngotympanic tube is the canal for the tensor tympani. This canal ends in the cochleariform process that marks the geniculate ganglion at the first genu of the facial nerve. At this point, the tendon of the tensor tympani emerges to attach itself to the upper part of the malleus handle. Both the pharyngotympanic canal and the tensor tympani canal pass anteriorly pursuing a downwards and antero-medial course, eventually opening in the angle between the squamous and petrous parts of the temporal bone. Throughout this course they are separated by a thin partition of bone.

The medial wall of the tympanic cavity is dominated by the promontory, the dense bone that is the otic capsule overlying the basal turn of the cochlea. The tympanic plexus of nerves runs in small grooves on its surface. The fenestra vestibule, oval window, lies posterior to the promontory and is sealed by the stapes footplate sitting in an anular ligament. Below this lies the fenestra cochleae, round window, within a deep niche that often contains mucosal folds and is overhung by the promontory.

The tympanic part of the facial nerve canal, Fallopian canal, runs horizontally across the medial wall just above the promontory, from the cochleariform process (the first genu) to the oval window (the second genu), where it turns into the posterior wall of the tympanic cavity coursing inferiorly towards the stylomastoid foramen. Deep to the facial nerve canal in the posterior wall is the sinus tympani. Lateral to the facial nerve posterior to the oval window is a small projection of bone, the pyramidal process, through which the stapedial tendon passes towards the capitelum of the stapes. Above and behind the facial nerve at the second genu is a prominence, the otic capsule surrounding the lateral semi-circular canal. It is at this point that the middle ear communicates with the mastoid air cells, the additus of the mastoid antrum. The short process of the incus sits in a depression called the fossa incudis in the antero-inferior part of the additus and is attached to it by ligaments.

The mastoid air cell system is variable in its extent both between sides and individuals. It is rudimentary at birth and develops progressively until puberty. In some the air cells extend into the apex of the temporal bone and even the zygomatic process. Air cells that develop in the squamous part of the temporal bone become separated by a bony septum from those deeper in the petrous bone. At surgery, this septum, Körner's septum, can be mistaken for the posterior entrance to the mastoid antrum. In others the entire bone may be almost devoid of air cells. As stated previously, it opens into the middle ear through the additus. The descending part of the facial nerve canal lies in its anterior wall, and the posterior semicircular canal, within the otic capsule, is contained medially. The sigmoid sinus is situated posteriorly and traverses towards the jugular bulb. In well-pneumatized bones there are often numerous air cells posterior to the sigmoid. The roof of the mastoid air cell system is formed by a continuation of the tegmen tympani. The attachment of the posterior belly of the digastic is denoted by a conspicuous ridge of bone, the digastric ridge, in the mastoid tip. The anterior limit of this ridge is a landmark for the facial nerve at the styolomastoid foramen.

The chorda tympani is a branch of the facial nerve that emerges from the facial nerve about 6 mm above the stylomastoid foramen. It travels in its own canal just lateral to the main trunk of the facial nerve and enters the middle ear at a variable level but always 3–4 mm below the oval window. It is easily visible behind the tympanic membrane as it arcs across the middle ear cavity passing between the handle of the malleus and long process of the incus, and finally leaving the middle ear through the petrotympanic fissure.

ANATOMICAL HAZARDS IN MASTOID AND MIDDLE EAR SURGERY

The facial nerve is the one structure that every surgeon fears damaging. It is important to be aware that the Fallopian canal may not be complete throughout the temporal bone. Congenital or acquired dehiscences are not uncommon. Congenital dehiscences that result from incomplete closure of the encircling mesoderm in embryo are most common around the oval window and tympanic segment. It is here that the facial nerve is susceptible to heat injury during laser stapedectomy. Extensive dehiscences around the oval window may allow the facial nerve to prolapse over the oval window. An aberrant course of the entire Fallopian canal may be heralded by, or associated with, an abnormal pinna or craniofacial abnormality. In these patients the facial nerve may run across the promontory and be completely uncovered, appearing like a thickened and flattened area of mucosa. Bifurcation of the facial nerve may be found in the mastoid segment just above the stylomastoid foramen and be mistaken for the main trunk and chorda tympani. But, erosion of the canal by cholesteatoma or tumour is a more frequent cause of iatrogenic injury by the unwary surgeon. Facial nerve monitoring helps to avoid this but is no substitute for a sound anatomical knowledge.

The mastoid process is absent or underdeveloped in the neonate or young child. As a result, the facial nerve is very superficial as it exits the stylomastoid foramen. Surgeons operating on the parotid in children must be aware of this possibility.

The jugular bulb is of variable height and can fill the tympanic cavity rather than be restricted to the hypotympanum. Its bluish appearance through the tympanic membrane resembles the 'blue drum' of a cholesterol granuloma. Surgeons have been known to perform a myringotomy on the jugular bulb. Aberrations of the course of the internal carotid artery may partially obstruct the Eustachian tube and be visible through the tympanic membrane. A persistent stapedial artery, part of the developmental anatomy of the internal carotid artery, may also be encountered and appear as a vessel running across the promontory, through the stapes crura and across the facial nerve to replace the middle meningeal artery.

FURTHER READING

Anson BJ, Donaldson JA. *Surgical Anatomy of the Temporal Bone, 3rd ed.* Philadelphia: WB Saunders, 1981.

Gleeson M. External and middle ear. In: Standring, S. (Ed.). *Gray's Anatomy: The Anatomical Basis of Clinical Practice, 40th ed.* Edinburgh: Elsevier/Churchill Livingstone, 2008.

Schuknecht HF. (Ed.). Developmental defects. In: *Pathology of the Ear, 2nd ed.* Philadelphia: Lea & Febiger, 1993.

PART 3

7 Parotid glands 61
Luke Cascarini and Zaid Sadiq
8 Submandibular triangle 69
Daryl Godden and Barrie T. Evans
9 Oral cavity 77
Madan G. Ethunandan
10 Alveolar process 89
Niall McLeod
11 Anatomy of cleft lip and palate 99
Serryth Colbert and Chris Penfold

7

Parotid gland

LUKE CASCARINI AND ZAID SADIQ

Introduction 61
Development of the parotid gland 61
Surgical anatomy 61
Relations 62
Antero-lateral relations *62*
Structures within the parotid gland *64*
The blood supply of the parotid 65
Venous drainage 65
The lymphatics 65
Innervation of the parotid gland 65
Facial nerve 65
Frey's (auriculotemporal) syndrome *68*
Sialocele *68*
Further reading 68

INTRODUCTION

Parotid surgery presents special challenges to the surgeon. Most parotid tumours are benign, so patients expect to be left without deformity after surgery especially with regard to facial nerve function.

Parotid surgery may be further complicated by other factors including tumours involving the deep aspect, previous irradiation, infection and previous surgery. Tumour size and the special relationship of the tumour to the facial nerve may also increase the complexity of parotid surgery. The importance of understanding the surgical landmarks and safe approach to the facial nerve and major vascular structures cannot be overemphasized.

DEVELOPMENT OF THE PAROTID GLAND

At 6 weeks of intrauterine development, solid epithelial buds of ectodermal origin from the wall of the primitive mouth invaginate into the surrounding mesencheyme. This process forms a groove that later becomes a tunnel. The parotid gland is formed in the blind end of this tunnel by proliferation, budding and extensive branching. The mesenchyme is responsible for the genesis of the capsule and surrounding connective parotid tissue.

The facial nerve develops from a separate analagen to the gland. The primary bifurcation of the nerve grows forward and embraces the isthmus of the gland, which grows backwards from the stomadeum.

SURGICAL ANATOMY

The parotid gland is the largest of the paired major salivary glands. It is an irregular wedge or pyramidal shaped gland with the base outward. The bulk of the gland is interposed between the ramus of the mandible with its attached masseter and medial pterygoid muscles anteriorly, and the mastoid process with its attached sternocleidomastoid and digastric muscles posteriorly. Its position readily

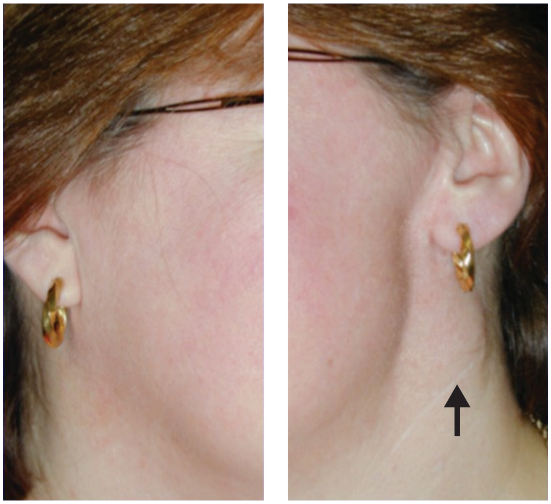

(a) (b)

Figure 7.1 Position of the parotid gland apparent on the left **(a)**, by comparison with the defect evident following excision of the superficial lobe **(b)**, Surgical scar is indicated by the black arrow.

appreciated following parotidectomy (Figure 7.1). The wedge shape of the gland is best appreciated in MRI scans.

The parotid gland is divided into a superficial and a deep lobe by the facial nerve and its branches; the superficial lobe as expected, being superficial to the nerve. This has clinical significance in two ways; firstly, tumours in the deep lobe may require a different surgical approach than those confined to the superficial lobe and secondly, the capsule of the gland is a less well defined structure in relation to the deep lobe. Pathology does not respect this division. The connection between the superficial and deep lobes is called the isthmus. So-called ‘dumbell’ tumours of the gland traverse the isthmus and involve both lobes. The deep lobe is smaller than the superficial lobe.

The gland is considered to have four surfaces: superficial, deep, anterior and posterior. It is not palpable as a discrete structure in the absence of pathology.

The parotid gland is surrounded by a fibrous capsule derived from the investing layer of the deep cervical fascia which divides to enclose the gland on its superficial and deep aspects. The superficial layer – well developed – attaches superiorly to the zygomatic arch, cartilaginous external meatus and the mastoid process. The capsule on the deep aspect of the gland (the deep lobe) is less well defined as the fascia thins appreciably the further medially it extends. It is attached to the styloid process, tympanic plate and the mastoid process. The stylomandibular ligament running from the styloid process to the angle of the mandible is derived from this layer and separates the parotid from the submandibular gland.

Anteriorly the capsule overlying the superficial lobe becomes thinner and continues as the so-called parotid-masseteric fascia, where it overlies the masseter. Whether the superficial capsule can be considered a component of the the superficial muscular aponeurotic system (SMAS) or is a separate layer is debated. If separate layers, they are nonetheless firmly adherent over the parotid.

RELATIONS

Antero-lateral relations

The superficial surface is covered by skin, superficial fascia, the branches of the great auricular nerve supplying the skin over the angle of the mandible, the posterior border of the platysma and the superficial parotid lymph nodes (preauricular nodes) – the latter superficial to the capsule of the gland. The ‘parotid nodes’ are deep to the capsule i.e. intraglandular – see below. The gland extends forwards over the masseter to a variable extent, below the parotid duct. Superiorly it reaches the zygomatic arch and may overlap the lateral capsule of the temporomandibular joint. Inferiorly it extends below the mandibular angle – the ‘lower pole’, and its posterior margin may either abut or overlap the sternocleidomastoid.

The great auricular nerve, emerging from the posterior border of the sternocleidomastoid at its midpoint (Erb’s point) is either immediately subcutaneous (or beneath platysma) over the muscle, and care is needed to avoid inadvertant injury to it when elevating the skin flap in parotid surgery. The external jugular vein runs in the same plane and parallel with the great auricular nerve in the upper half of the nerve. Again care is needed to avoid injury to this vein; its division early in parotid surgery may result in oedema and engorgement of the gland.

The great auricular nerve, 2-4 mms in diameter, divides into anterior and posterior branches close to its entry into the gland; the anterior branch enters the parotid gland supplying the skin over the angle of the mandible and the posterior branch supplies the skin over the mastoid process and the majority of the back of the ear and lobule and concha laterally.

Preservation of the posterior branch in some instances is possible with tumour surgery (Figure 7.2). The main trunk of the great auricular nerve may be used as a cable graft should sacrifice of the main trunk or a larger peripheral branch be required.

The auriculotemporal nerve in the immediate preauricular region follows the superficial temporal artery into the temple above the (superficial) temporoparietal fascia – immediately behind the artery. This can be at risk in parotid surgery. The resulting area of temporal anaesthesia is not usually of consequence to the patient.

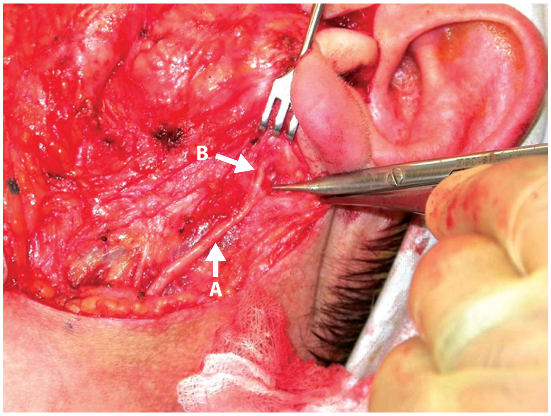

Figure 7.2 Great auricular nerve main trunk – A. Anterior branch – B. Posterior branch at the end of dissecting scissors. Photo courtesy of Professor P Brennan.

As noted, the main bulk of the gland is interposed between the mandibular ramus with its two attached muscles anteriorly and the mastoid process and its two attached muscles posteriorly.

Anteromedially the gland is grooved by the posterior mandibular ramus and further medially, abuts medial pterygoid (see Figure 7.1).

Posteromedially, at the junction of the mastoid process and the sternocleidomastoid, the gland lies directly on the posterior belly of the digastric, the styloid process with its attached muscles and ligaments – the styloid 'apparatus'. The styloid with its attachments separate the gland from the internal carotid artery and the internal jugular vein. The external carotid artery enters the gland on its posteromedial aspect. Superiorly the posteromedial surface lies behind the temporomandibular joint, in contact with both the cartilaginous and bony parts of the external meatus – this has been termed the glenoid lobe.

The anteromedial and posteromedial surfaces meet at the apex of the glandular pyramid, immediately lateral to the superior pharyngeal constrictor.

The parotid duct or Stensen's duct passes forwards from the antero-lateral edge of the deep aspect of the gland superficial to masseter. It runs parallel to the zygomatic arch along a line described as either, running from the lobe of the ear to the midpoint of the upper lip or, from the floor of the external meatus to just above the commissure of the lip. There is no appreciable difference between the two. The duct occupies the middle third of this imaginary line. An 'accessory' parotid gland is present in about 20% of individuals. It lies on the masseter related to the superior aspect of the duct i.e. between the duct and the zygomatic arch. This can also be the site of pathology and present as a mass anterior to the parotid. It measures 4–6 cm in length and 3–5 mms in diameter. The duct turns medially at the anterior border of the muscle and passes through buccinator in the third molar region, runs obliquely forward on the oral aspect of buccinator to open through the buccal mucosa at the parotid papilla, in the second molar region just above the occlusal surface of this tooth. This arrangement prevents prevents air being forced into the gland ('pneumoparotid') with raised intraoral pressures.

The position of the parotid duct is relatively constant and in view of its size provides a reliable soft tissue landmark in parotid surgery. The buccal branch(es) of the facial nerve is closely related to the duct and may be either above or below the duct. Anastomoses between the buccal branches or between the buccal and zygomatic branches occur in relation to the duct. Where anasotomes between the nerve branches occurs, in over 90% of cases the nerves are superficial to the duct. This makes it possible to retain the duct and residual gland function when resecting tumours superficial to the nerve in some instances. In retrograde (also termed 'centripetal') approaches to the gland in parotid surgery i.e. from peripheral branches moving to the main trunk, the parotid duct is identified initially and the buccal branch located using the duct as the landmark (Figure 7.3).

Deep lobe parotid tumours may extend into the parapharyngeal space and be visible in the mouth as pharyngeal bulging. Such tumours can be picked up as an incidental finding on magnetic resonance images (MRI). Dissection of deep-lobe tumours requires a balance of adequate retraction and evaluation of tumour margins. Accessing the deep lobe may be best achieved by elevation and preservation of the superficial lobe. Alternatively, an inferior deep tumour may be removed by approaching the mass through the neck. Removal of deep extensions requires cautious circumferential extracapsular dissection with attention to the deep structures including the terminal branches of the external carotid artery. Often, deep-lobe or dumbbell tumours can be manually dissected by light finger dissection. Malignant tumours of the deep lobe may require an osteotomy of the mandible for a safe oncological resection. More access is possible by dividing the digastric and by dislocating the mandible anteriorly.

Structures within the parotid gland

The structures within the gland are the external carotid artery and its branches, the retromandibular vein and its tributaries, the main trunk of the facial nerve and its peripheral branches and the (intra)parotid lymph nodes.

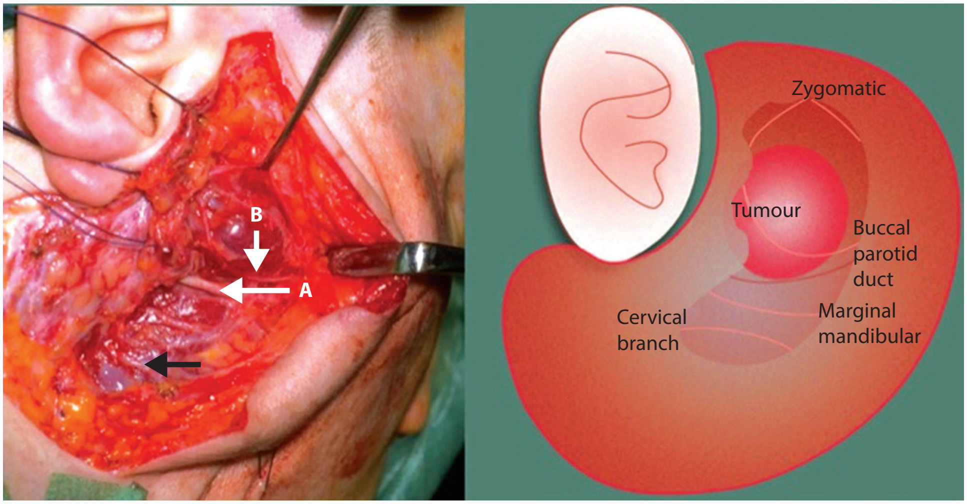

(a) (b)

Figure 7.3 Relationship of parotid duct and buccal branch of facial nerve. **(a)** Operative photograph: Black arrow - marginal mandibular branch of facial nerve. A – parotid duct. B – buccal branch facial nerve. **(b)** Schematic of operative image. Modified with permission from: O'Regan B, Bharadwaj B, Bhopal S and Cook V. Facial nerve morbidity after retrograde nerve dissection in parotid surgery for benign disease. A 10-year prospective observational study of 136 cases. *British Journal of Oral and Maxillofacial Surgery*. 2007; 45: 101–107.

THE BLOOD SUPPLY OF THE PAROTID

The external carotid enters the inferior surface of the gland on its posteromedial aspect and divides into the maxillary and superficial temporal arteries at the junction between the middle and upper thirds of the gland. The superficial temporal artery gives off the transverse facial artery to supply the face before continuing upward to emerge from the upper border of the gland. The maxillary artery passes forward and slightly upward behind the condylar neck in the part of the gland lying deep to it. The artery emerges from the gland and passes into the infratemporal fossa. The gland receives its arterial supply from the branches of the external carotid artery that run both within and in close proximity to it.

VENOUS DRAINAGE

The venous drainage of the area varies, but the superficial temporal vein typically enters the superior surface and receives the maxillary vein which runs in close proximity to the first part of the maxillary artery immediately deep to the neck of the mandibular condyle, to become the retromandibular vein (syn. posterior facial vein). Within the gland, it divides into a posterior branch, which joins the posterior auricular vein to form the external jugular. The anterior branch emerges from the gland to join the (anterior) facial vein to form the common facial vein which empties into the internal jugular vein. Venous drainage of the parotid is therefore into the internal and external jugular veins. The facial nerve branches are superficial to the retromandibular vein – the relationship of the marginal mandibular branch of the nerve to this vein is a further soft tissue landmark used in parotid dissection. The external carotid and its branches are deep to the retromandibular vein.

THE LYMPHATICS

The lymphatics of the parotid gland are important in evaluating skin cancers of the head. Preauricular lymph nodes in the superficial fascia drain the temporal scalp, upper face, and anterior pinna. The lateral aspects of the upper and lower eyelids drain to the preauricular nodes (see Chapter 13). Lymph nodes within the parotid substance drain the gland, nasopharynx, palate, middle ear and external meatus. These lymphatics drain into the internal jugular and spinal accessory nodes – (level 5 nodes in the posterior triangle).

INNERVATION OF THE PAROTID GLAND

The parotid gland receives sympathetic and parasympathetic innervation, and this mixed supply is responsible for vasoconstriction and secretory function.

The otic ganglion, well protected, is situated deep to the mandibular division of the trigeminal nerve below foramen ovale. Whilst related to the mandibular division in its position, it is functionally related to the glossopharyngeal nerve from which it receives the preganglionic parasympathetic fibres from the lesser petrosal nerve. These – and only these nerves – synapse in the ganglion; the postganglionic branches then pass into the auriculotemporal nerve for distribution to the parotid gland. they are responsible for salivary secretion. The sympathetic component is derived from the plexus on the middle meningeal artery, which is situated immediately posterior to the ganglion. The postganglionic sympathetic fibres come from the superior cervical sympathetic ganglion and are distributed to the vasculature of the gland via the auriculotemporal nerve. General sensory fibres from the gland run in the auriculotemporal nerve.

FACIAL NERVE

The facial nerve is a mixed nerve carrying motor, sensory and parasympathetic fibres intimately associated with the gland. It emerges from the stylomastoid foramen immediately posterior to the base of the styloid process and anterior to the attachment of the digastric. At birth, infants have no mastoid process, so the stylomastoid foramen is subcutaneous; relevant in the surgical management of paediatric parotid pathology.

The nerve enters the posterior surface of the gland approximately 1 cm after exiting the skull.

Before entering the gland, there are branches to the posterior belly of digastric, the stylohyoid and the posterior auricular nerve supplying the occipital belly of occipitofrontalis. It then turns anterolateral into the parotid gland, superficial to both the retromandibular vein and the external carotid artery. The main trunk of the nerve then branches into an upper temporofacial division, and a lower cervicofacial division. A variable number of communicating branches occur between these two principle divisions to form a nerve plexus – the pes anserinus (goose's foot). The five terminal branches – temporal, zygomatic, buccal, mandibular and cerivical, emerge from this plexus.

The temporal branch alone supplies the forehead musculature and the temporal and zygomatic branches share the motor supply of the orbicularis oculi. Zygomatic branches are usually the most abundant – a possible reflection of the importance of eyelid competence. Communication between the buccal branch(es) and zygomatic branches – usually superficial to the parotid duct – is common. The (marginal) mandibular branches supply the lower lip musculature – the relationship to the lower border of the mandible discussed in Chapter 8. Damage to this particular branch results in a disfiguring deformity of the lower lip. Communication between the mandibular branch and the remaining branches is uncommon, accounting for the frequency of lower lip weakness (usually temporary) following parotid surgery. The cervical branch innervates the platysma.

The primary separation into temporozygomatic and cervicofacial divisions is constant however the pattern of branching and anastomoses between the branches is particularly variable. The presence of these communicating rami explains the occasional absence of paresis with division of a small nerve branch (Figure 7.4).

In parotid surgery the two methods of identifying the main trunk of the facial nerve and its branches are either:

- Identification of the main trunk of the nerve as it exits the stylomastoid foramen with subsequent anterior dissection of the peripheral branches; termed 'antegrade' or 'centrifugal' dissection.
- Initial identification of peripheral branches with dissection in a posterior direction towards the main trunk; termed 'retrograde' or 'centripetal' dissection.

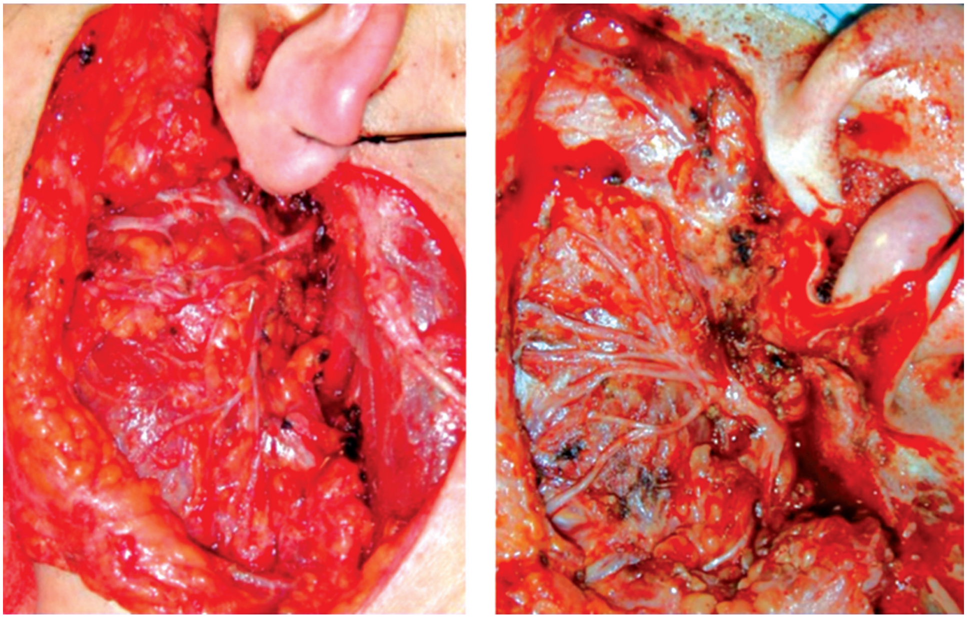

Figure 7.4 Separation into temporozygamatic and cervicofacial divisions. The relative abundance of zygomatic branches is evident.

Whilst different anatomical landmarks are used for these approaches, surgeons should be aware of the available landmarks of both approaches as it may be necessary to alter the original surgical plan at the time of surgery. A combination of approaches may also be adopted in selected cases.

During nerve identification it is useful to check that anaesthetic-induced paralysis has worn off. A nerve stimulator can be helpful in identifying both the main trunk of the facial nerve. Overzealous use of the nerve stimulator should be avoided and the associated branches.

In the anterograde approach the most common anatomical landmarks for identifying the main trunk of the facial nerve are the tragal 'pointer', the posterior belly of digastric, the inferior aspect of the bony external auditory meatus, the mastoid tip, and the tympanomastoid suture. More than one, or all can be used. Adequate exposure of these structures prior to attempting to locate the main trunk is advisable.

The tragal 'pointer' is the bluntly pointed tip of the cartilage of the external meatus and arguably the most commonly used landmark. It is located by opening the avascular preauricular plane immediately anterior to the cartilaginous meatus. CT & MRI studies have confirmed the main trunk is located about 1.0 – 1.5 cms deep to the pointer and slightly inferior to it. This landmark has been criticised in view of the variation in its size and shape and at times, absence. Dissection beyond this landmark is with fine mosquito forceps with the knowledge of the approximate position of the main trunk.

The posterior belly of the digastric as a landmark can be considered an adjunct to the tragal pointer. On average, the main trunk of the facial nerve is approximately 1cm deep to the upper border of the muscle and 4-5 mm anterior to its attachment at the skull base (digastric groove of the mastoid). The value of the digastric as a 'stand-alone' landmark for the main trunk of the nerve is questionable particularly if the effects of soft tissue retraction during surgery and changes in surgical positioning are also considered.

An aide-memoir often used is that the main trunk runs forward along a line midway between the tip of the mastoid process and the inferior aspect of the bony external meatus. The tip of an index finger will identify the both these bony landmarks – the depth of the nerve judged from both the tragal pointer and the posterior belly of the digastric i.e. approximately 1 cm deep to this line (Figure 7.5).

The most reliable landmark for the main trunk of the nerve is considered to be the tympanomastoid fissure – a bony landmark – located between the mastoid and the tympanic plate. The main trunk of the nerve was found on average to be 2.7 mms deep the medial limit of the fissure.

The styloid process has been suggested as a landmark – this is a deep structure, absent in about

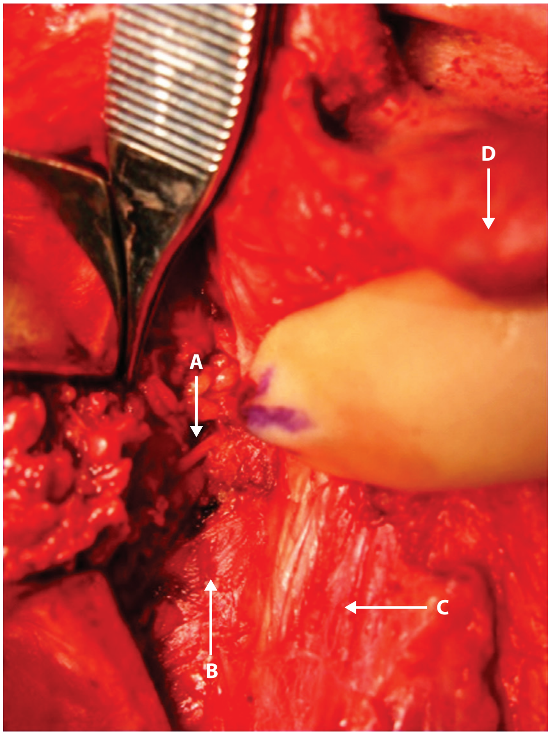

Figure 7.5 Finger placed on mastoid immediately below the inferior aspect of the bony external auditory meatus. Arrow on tip of finger pointing to the main trunk. A – main trunk of facial nerve. B – posterior belly of digastric. C – sternocleidomastoid. D – lobe of ear elevated. Image courtesy of Mr I P Downie, Consultant Oral and Maxillofacial Surgeon, Salisbury District Hospital.

1/3 of the population. It is unreliable and it has been demonstrated that its use increases the likelihood of injury to the main trunk.

Whilst removal of the mastoid tip as a further adjunct has been suggested, it is of questionable value if grafting of the main trunk is not required.

Tumours may either displace or overly the main trunk of the facial nerve making its identification difficult. In such cases resort to the landmarks used in the retrograde approach – see below – can be helpful.

The posterior auricular artery or one of its branches, most commonly the stylomastoid branch with its accompanying vein, run in close proximity to the main facial nerve trunk and should not be ligated until identification of the facial nerve is confirmed. Care with bipolar diathermy is mandatory.

When nerve branches disappear into the tumour, malignancy should be suspected. Nerve resection is indicated when the nerves are clinically involved. The greater auricular nerve can be used as a nerve graft.

During dissection, the individual nerve branches are dissected with a fine mosquito clamp. The overlying parotid mass is divided with adequate haemostasis. The superficial lobe is therefore swung back like a door on a hinge to demonstrate the facial nerve under it. Resection is then completed with the facial nerve and all branches in full view. Lesions deep to the facial nerve necessitate removal of the superficial parotid tissue first. The remaining tissue can then be carefully dissected out between nerve branches.

In the retrograde approach the buccal branch is frequently the initial branch identified – using the parotid duct as a landmark; the relationship between these structures is discussed above. The marginal mandibular branch may be identified by first locating the retromandibular vein as it enters the gland inferiorly, and identifying this branch as it crosses superficial to the vein. The zygomatic branches are identified by blunt dissection inferior to the lower border of the zygomatic arch. The dissection progresses proximally to the bifurcation of the main trunk by creating a tunnel superficial to the nerve branches using fine mosquito forceps. The extent of the remaining dissection tailored to the requirements of the pathology.

Frey's (auriculotemporal) syndrome

Frey's syndrome is localized sweating and flushing during the mastication of food. It is a common disorder that occurs in 35 per cent to 60 per cent of patients after parotidectomy with facial nerve dissection. Presentation is usually several months after surgery with variable severity. It results from aberrant regeneration of nerve fibres from postganglionic secretomotor parasympathetic innervation to the parotid gland occurring through the severed axon sheaths of the postganglionic sympathetic fibres that supply the sweat glands of the skin.

Sialocele

Sialocele is a discrete subcutaneous salivary collection that accumulates after parotidectomy or trauma of the parotid gland. Sialocele typically starts within the first week of the surgery and often resolves within a month. Clinically it presents as a nontender fluctuance at the angle of the mandible. The incidence after parotidectomy varies from 6 per cent to 40 per cent.

FURTHER READING

De Ru JA, van Bentham PP, Bleys RL, Lubsen H, Hordijk GJ. Landmarks for parotid gland surgery. *Journal of Laryngology and Otology*. 2001; 115(2): 122–5.

Langdon J, Patel M, Ord R, Brennan PA. (Eds.). *Operative Oral and Maxillofacial Surgery, 2nd ed*. London: Hodder Arnold, 2010.

McGurk M, Combes J. *Controversies in the Management of Salivary Gland Disease*. Oxford: Oxford University Press, 2012.

O'Regan B, Bharadwaj G, Bhopal S, Cook V. Facial nerve morbidity after retrograde nerve dissection for benign disease: a 10 year prospective study observational study of 136 cases. *British Journal of Oral and Maxillofacial Surgery*. 2007; 45:101-107.

Standring S. (Ed.). *Gray's Anatomy: The Anatomical Basis of Clinical Practice, 40th ed*. Edinburgh: Elsevier/Churchill Livingstone, 2008.

Zhao K, Qi DY, Wang LM. Functional superficial parotidectomy. *Journal of Oral and Maxillofacial Surgery*. 1994; 52: 1038–1041.

8

Submandibular triangle

DARYL GODDEN AND BARRIE T. EVANS

Introduction 69
Basic anatomy 69
The superficial plane of the submandibular triangle 69
The submandibular space 70
The floor of the submandibular triangle 72
Clinical relevance 73
Submandibular gland excision 73
Soft tissue space infection 74
Submandibular mass 75
Further reading 75

INTRODUCTION

The submandibular triangle forms only a small part of the anterior triangle of the neck, yet its anatomic significance should not be overlooked since many disease processes which may require surgical treatment can occur in this region. It is routinely encountered as part of a neck dissection in which the lymph nodes of the neck and submandibular gland are excised during cancer surgery. In addition, dissection of the triangle is a necessary part of submandibular gland excision which may be for malignant or benign pathology. Knowledge of the anatomy is necessary for diagnostic purposes such as occurs with lymph node biopsy, and the submandibular space may be involved in cervico facial infections; how the anatomy and disease processes interlink is crucial in their management. Finally, dissection through the submandibular triangle provides access to the lower border of the mandible, e.g. in the fixation of mandibular fractures or during mandibular resection, and it provides access to the facial artery and facial veins which may be required during microvascular anastomosis.

The submandibular triangle contains the submandibular gland and lymph nodes, the facial vessels and lingual artery, and three significant nerves – the mandibular branch of the facial nerve, the hypoglossal nerve and the lingual nerve. Surgery must navigate a safe way around these structures if they are to be preserved. The following description will cover the basic anatomy of the submandibular triangle and will then focus on the surgical significance of its anatomy.

BASIC ANATOMY

The submandibular triangle lies between the inferior border of the mandible superiorly, the posterior belly of the digastric and stylohyoid muscles posteriorly and the anterior belly of the digastric muscle anteriorly (Figure 8.1). The submandibular triangle must be distinguished from the submandibular 'space'. It can be divided into three surgical planes from superficial to deep.

The superficial plane of the submandibular triangle

The superficial plane consists of skin, subcutaneous fat and superficial fascia investing the platysma.

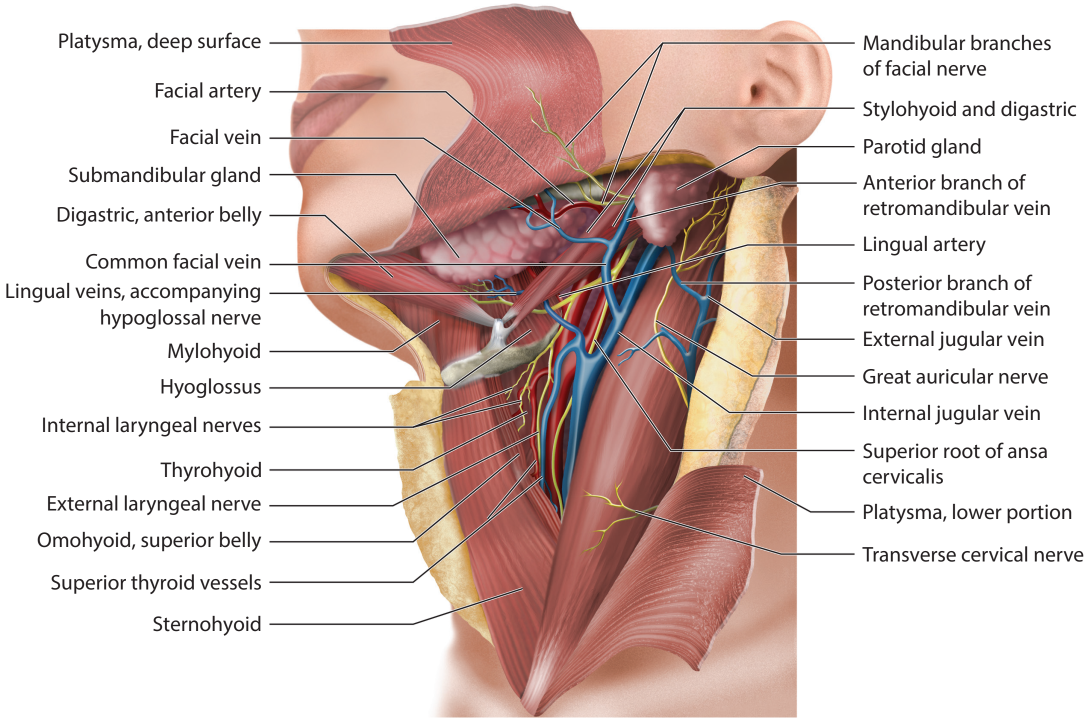
Platysma, deep surface
Facial artery
Facial vein
Submandibular gland
Digastric, anterior belly
Common facial vein
Lingual veins, accompanying hypoglossal nerve
Mylohyoid
Hyoglossus
Internal laryngeal nerves
Thyrohyoid
External laryngeal nerve
Omohyoid, superior belly
Superior thyroid vessels
Sternohyoid
Mandibular branches of facial nerve
Stylohyoid and digastric
Parotid gland
Anterior branch of retromandibular vein
Lingual artery
Posterior branch of retromandibular vein
External jugular vein
Great auricular nerve
Internal jugular vein
Superior root of ansa cervicalis
Platysma, lower portion
Transverse cervical nerve

Figure 8.1 The submandibular triangle is bounded superiorly by the lower border of the mandible, anteriorly by the anterior belly of the digastric muscle and posteriorly by the posterior belly of the digastric muscle. (Adapted from *Last's Anatomy: Regional and Applied*, by Chummy S. Sinnatamby.)

This fascial layer is thin and of no clinical significance. The mandibular and cervical branches of the facial nerve are deep to platysma (Figure 8.2).

The mandibular branch, sometimes referred to as the *marginal* mandibular branch, is one of the five main branches of the facial nerve. It has the longest course across the face. The facial nerve forms a rich anastomotic network between the various divisions; however, only 12 per cent of mandibular branches receive communication from the buccal branch. This explains why neural damage to the mandibular branch is so profound. The nerve supplies the lip depressors and damage to it results in an inability to evert the lower lip as in whistling and gives an asymmetric smile.

The mandibular branch exits the lower anterior border of the parotid gland and in approximately 80 per cent of cases it traverses the face along or above the lower border of the mandible.[1] In the remainder the nerve drops down below the lower border before ascending again to cross it superficial to the facial artery and vein. Anterior to the facial artery the facial nerve is always above the lower border of the mandible.

The submandibular space

The second surgical plane, and of the most clinical significance, is formed by the investing layer of deep cervical fascia. This fascial layer forms the roof of the submandibular space. The contents of the submandibular space are contained between its roof and floor, and consist of the submandibular salivary gland and lymph nodes, facial artery and common facial vein.

The common facial vein is formed by the merging of (anterior) facial vein and the anterior branch of the retromandibular vein; it drains into the internal jugular. The common facial vein should be secured with a transfixion suture when divided as loss of a ligature may result in significant and life-threatening haemorrhage. The facial artery has a

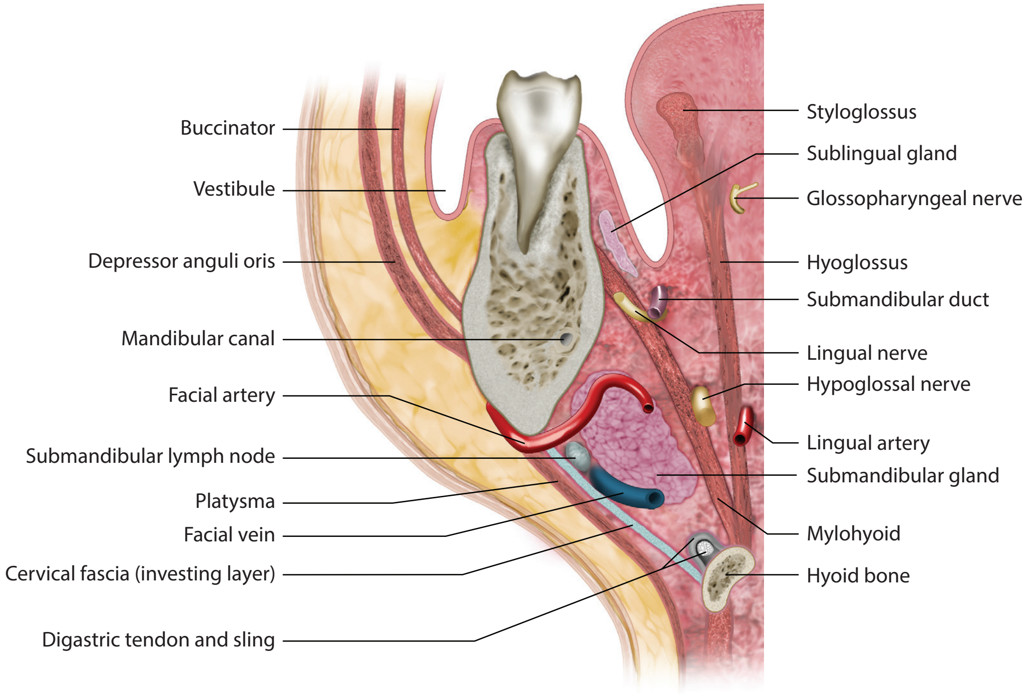
Buccinator
Vestibule
Depressor anguli oris
Mandibular canal
Facial artery
Submandibular lymph node
Platysma
Facial vein
Cervical fascia (investing layer)
Digastric tendon and sling
Styloglossus
Sublingual gland
Glossopharyngeal nerve
Hyoglossus
Submandibular duct
Lingual nerve
Hypoglossal nerve
Lingual artery
Submandibular gland
Mylohyoid
Hyoid bone

Figure 8.2 Coronal section of the left side of the mandible demonstrating the superficial and deep boundaries and contents of the submandibular space. (Adapted from *Last's Anatomy: Regional and Applied,* by Chummy S. Sinnatamby.)

different course and enters the triangle beneath the posterior belly of digastric and through the stylohyoid muscle and runs up and forwards grooving the deep aspect of the superficial lobe of the submandibular gland before crossing the lower border of the mandible anterior to the origin of the masseter. It can be palpated as it crosses the lower border.

The submandibular gland has a superficial lobe invested by a condensation of the deep cervical fascia forming the submandibular capsule, and it has a deep lobe which extends around the posterior border of the mylohyoid. The deep cervical fascia which splits to form the submandibular capsule runs from the greater cornu of the hyoid bone. The superficial layer of this split fascia forming the capsule on the lateral aspect of the gland, inserts into the lower border of the mandible. The deep layer forming the medial capsule is inserted into the mylohyoid line of the mandible. The deep lobe in the floor of the mouth, does not have a capsule. Approximately half the gland lies below the mandible and the remainder above the lower border, in the submandibular fossa on the lingual aspect of the mandible.

The superficial lobe of the submandibular gland extends anteriorly from the anterior belly of digastric back to the stylomandibular ligament which separates it from the tail of the parotid. Inferiorly it extends to the intermediate tendon of digastric.

Anteriorly the medial surface is related to the mylohyoid muscle, nerve and vessels. Posteriorly, it is related to the hyoglossus and is separated from it, in part, by the submandibular ganglion, lingual and hypoglossal nerves. Further posteriorly it is related to the styloglossus and stylohyoid ligament.

Above the lower border of the mandible the lateral surface lies next to the submandibular fossa of the mandible superiorly. The gland is grooved by the facial artery which emerges from its deep aspect at the anterior edge of the mandibular attachment of the masseter. Below the lower mandibular border the gland is related laterally to the platysma, (marginal) mandibular branch of the facial nerve and the facial vein – separated from these structures by the investing layer of deep cervical fascia

The deep lobe of the gland, functionally an oral structure, extends forwards between the mylohyoid laterally and styloglossus and hyoglossus medially. It curves around the posterior border of the mylohyoid. The deep surface lies adjacent to the lingual nerve above and the hypoglossal nerve and deep lingual vein below. Numerous venae commitantes (small calibre veins) are frequently present superficial to the hypoglossal nerve – injudicious diathermy of these vessels can result in damage to the nerve (Figure 8.2). Anteriorly it merges with the sublingual gland and posteriorly is bounded by the stylohyoid, posterior belly of digastric and the parotid gland. Its superior edge is submucosal in the floor of the mouth.

The submandibular duct (Wharton's duct) drains forwards within the deep lobe, and as it bends around the posterior border of the mylohyoid (the 'hilum' of the gland) it can be a site at which salivary stones impact (Figure 8.3). This can cause obstruction of the submandibular gland and obstructive sialadenitis. The relationship between the lingual nerve and the submandibular duct in the floor of the mouth is relevant surgically. The lingual nerve runs in a plane deeper than the duct in the anterior floor of the mouth, running from the lateral border of the tongue towards the third molar region. In the region of the hilum – where the duct enters the gland - the nerve passes under to the duct, ascending between the duct and the medial aspect of the mandible (Figure 8.4).

Beside the submandibular gland the space contains several lymph nodes which may be adjacent to the gland or within its substance. Diagnostic confusion can occur with submandibular masses since it is difficult to tell whether a mass is an enlarged lymph node or an enlarged submandibular gland. Because the submandibular gland passes around the posterior border of the mylohyoid, a mass arising within the gland can be palpated bimanually whereas an enlarged lymph node cannot.

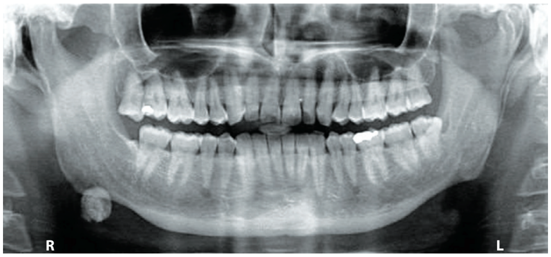

Figure 8.3 Panoral radiograph showing submandibular duct stone impacted at posterior border of the right mylohyoid muscle.

The submandibular gland receives parasympathetic secretomotor fibres from the superior salivary nucleus of the facial nerve; these pass to the gland via the chorda tympani, a branch of the facial nerve, and lingual nerve to the submandibular ganglion. Post-ganglionic sympathetic fibres run from the superior sympathetic ganglion and reach the gland along the facial artery.

The floor of the submandibular triangle

The floor of both the submandibular triangle and submandibular space is formed by the mylohyoid muscle and nerve, the hyoglossus and middle constrictor of the pharynx. This is the third surgical plane of the submandibular triangle.

LYMPHATIC DRAINAGE

The submandibular triangle receives lymph from the face, submental lymph nodes and oral cavity. Lymph drains to the jugulodigastric and jugulo-omohyoid lymph nodes of the deep cervical chain.

EMBRYOLOGY

The embryology of the submandibular triangle is complex and fascinating, and it explains why the muscular boundaries have different neural innovation. The posterior belly of the digastric, stylohyoid and platysma muscles are derived from the second branchial arch and in consequence innervated by the facial nerve, whereas the anterior belly and mylohyoid muscle are derived from the first branchial arch and are innervated by the mandibular branch of the trigeminal nerve. The cartilage of the second branchial arch forms the lesser horn of the hyoid and the stylohyoid ligament. The greater horn is derived from the third branchial arch.

The submandibular gland develops from the mucosa of the stomodeum (primitive oral cavity) in the sixth week of life. The evolving submandibular gland or primordium proliferates as cords in which lumens develop. This process is repeated until terminal bulbs form the terminal ducts and acini.

Submandibular gland aplasia is unusual and may occur in rare ectodermal syndromes and is also reported in a small percentage of Treacher-Collins patients. One of the commonest embryological abnormalities encountered in the submandibular triangle are branchial cleft cysts. These are believed to be congenital epithelial cysts which arise on the lateral part of the neck due to failure of obliteration of the second branchial cleft in early embryonic development (Figure 8.4). They typically occur anterior to the sternomastoid, and although they arise in the carotid triangle, they may overlap the submandibular triangle. They pass between the internal and external carotid arteries to the tonsillar fossa. They typically present in young adulthood, and whilst presentation may occur in later years, such a mass should be treated as a cystic metastatic lymph node until the definitive histopathology has been obtained. A less frequent congenital abnormality is the first branchial cleft cyst which runs from the angle of the mandible to the external auditory canal.

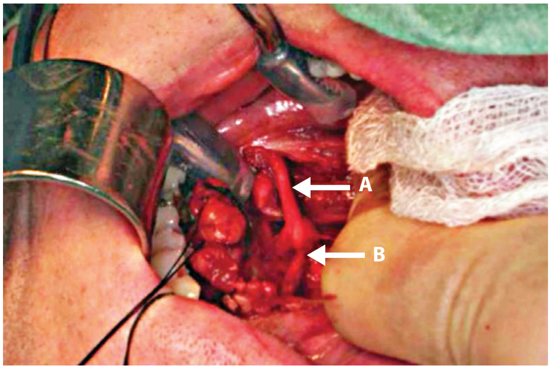

Figure 8.4 In the third molar region the lingual nerve passes beneath the duct where the duct enters the gland (hilum), and ascends lateral to the duct towards the base of the skull. A - lingual nerve. B - submandibular duct. From McGurk M. Surgical release of a stone from the hilum of the submandibular gland: a technique note. *International Journal of Oral and Maxillofacial Surgery* 2005; 34: 208–210. With permission.

CLINICAL RELEVANCE

Submandibular gland excision

The surgical approach to the submandibular gland is via an incision placed in a suitable skin crease traditionally two finger breadths or 3 cm below and parallel with the lower border of the mandible. The incision is extended for 5 cm through the subcutaneous fat to the platysma. Flaps are developed immediately beneath the platysma layer to the lower border of the mandible. Care is taken to locate the mandibular branch of the facial nerve, if necessary with a nerve stimulator. The facial vessels are tied at the superior aspect of the gland and the tie is retracted upwards on a clip; this is known as the Hayes-Martin manoeuvre. This manoeuvre lifts the mandibular branch of the facial nerve, which lies superficial to the vein, out of the operative field. Whilst many surgeons will formally identify the mandibular branch with a nerve stimulator, some will simply incise the submandibular capsule at the level of the hyoid and stay within the capsule during submandibular gland excision knowing that the facial nerve is well above and superficial. This technique is inappropriate in an oncological excision.

The superficial lobe of the submandibular gland is then mobilized to access the deep lobe which too is mobilized by retracting the mylohyoid muscle anteriorly to expose the lingual nerve, submandibular ganglion and submandibular duct. The submandibular duct is transected as forward as possible to avoid the post-operative complication of residual stone disease arising from the duct, and finally the facial artery is double tied as it emerges from the deep aspect of posterior belly of digastric to deliver the gland. Failure to ligate the artery here can result in significant haemorrhage from a retracted facial artery. At completion, the wound is checked for bleeding vessels and closed in layers

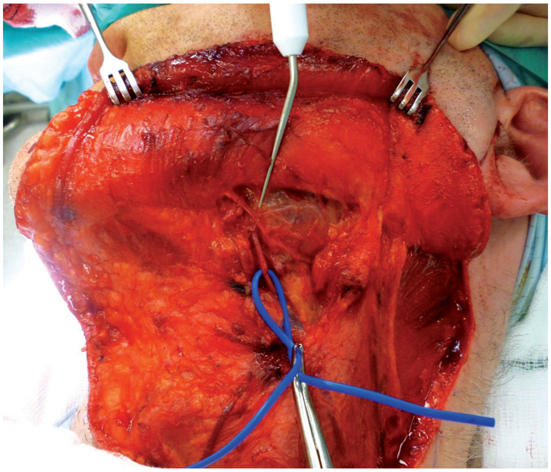

Figure 8.5 The mandibular branch of the facial nerve (pointer) runs along the lower border of the mandible superficial to the facial vein (demonstrated by the vascular sling) where it can be protected by traction superiorly during dissection.

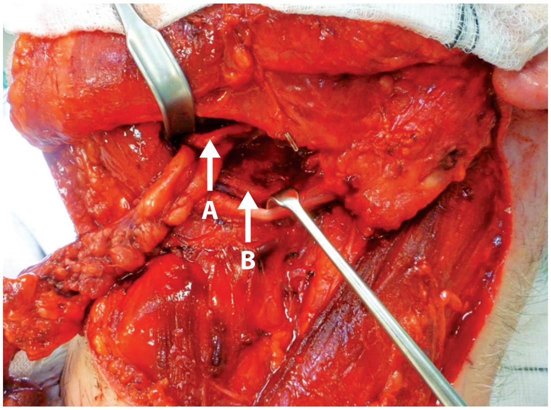

Figure 8.6 Following excision of the submandibular contents during a neck dissection, the lingual nerve (A) is seen superiorly and the hypoglossal nerve (B) inferiorly, just superior to the tendon of digastric. Note that the facial nerve is lifted upwards by the traction sutures on the facial vein.

with a resorbable suture to the platysma and a subcuticular suture for skin.

One of the commonest risks during submandibular gland excision is inadvertent damage to one of the three nerves: the mandibular branch of the facial nerve, the hypoglossal nerve and the lingual nerve (Figures 8.5 and 8.6).The anatomy of the submandibular triangle is fairly consistent, though the position of the mandibular branch of the facial nerve is variable. In 1962 Dingman and Grabb described the mandibular branch in cadaveric sections and reported its course across the face. They noted that the nerve crossed the anterior surface of the facial vein in all cases and passed superficially or deep to the facial artery. In 81 per cent of cases the nerve ran above the lower border of the mandible, and in 19 per cent of cases it ran 1 cm or less below the inferior border. These results have been questioned, and the position of the nerve is affected by neck extension. In some studies the nerve has been described passing 3–4 cm beneath the lower border; Nason et al. describe the nerve being >1 cm below the mandible in 54 per cent of cases and >2 cm in 10 per cent of cases.

Neural damage occurs temporarily in about 30 per cent of cases. The mandibular branch of the facial nerve can be permanently damaged in up to 10 per cent of cases whilst the hypoglossal and lingual nerves are much less frequently affected with rates of up to 1 per cent and 5 per cent, respectively. Neural damage occurs most frequently following chronic infection, previous surgery or radiotherapy. It should be routine to warn patients during consent of these risks and consequences.

Soft tissue space infection

The submandibular space is the potential space which communicates deep to the mylohyoid with the sublingual space and superficial to the mylohyoid with the submental space. The submandibular space can become infected either by pus tracking into it from the submental or sublingual space or directly from the mandible following periapical infections from the root apices of the lower molars which lie beneath the mylohyoid line. The investing layer of deep cervical fascia effectively converts the neck into a closed space (compartment). This fascial arrangement encourages the opening up of the contiguous tissue spaces deep to the fascia. As a result in most instances spontaneous external (through the skin) drainage is a late event. Airway compromise is a common occurence – the deep cervical fascia offering greater resistance than the sublingual, submandibular and parapharyngeal spaces. Synchronous bilateral submandibular and sublingual cellulitis is a surgical emergency and acute airway obstruction may occur. Treatment depends on opening and draining all spaces.

Submandibular mass

The most frequent causes for a submandibular mass are either infective or neoplastic; submandibular sialadenitis, submandibular lymphadenopathy and less commonly tumour of the submandibular gland are the most common.

Sialadenitis needs to be differentiated from submandibular tumours which may be benign or malignant in roughly equal proportions, and submandibular lymphadenopathy. The submandibular lymph nodes drain lymph from the oral cavity, face and submental nodes, and any examination of a submandibular lymph node is not complete without examining these areas. It is possible for the submandibular space to contain nonsalivary tumours; of these the lipoma is one of the most frequent, but cysts such as a dermoid cyst or salivary ranula can also occur.

FURTHER READING

Dingman RO, Grabb WC. Surgical anatomy of the mandibular ramus of the facial nerve based on the dissection of 100 facial halves. *Plastic and Reconstructive Surgery and the Transplant Bulletin.* 1962; 29: 266–72.

McGurk M. Surgical release of a stone from the hilum of the submandibular gland: a technique note. *International Journal of Oral and Maxillofacial Surgery* 2005; 34: 208–210.

Nason RW, Binahmed A, Torchia MG, Thliversis J. Clinical observations of the anatomy and function of the marginal mandibular nerve. *International Journal of Oral and Maxillofacial Surgery.* 2007; 36: 712–5.

Preuss SF, Klussmann JP, Wittekindt C, Drebber U, Beutner D, Guntinas-Lichius O. Submandibular gland excision: 15 years of experience. *Journal of Oral and Maxillofacial Surgery.* 2007; 65(5): 953–7.

Sinnatamby CS. *Last's Anatomy: Regional and Applied, 12th ed.* Oxford: Churchill Livingstone Elsevier, 2011.

Standring S. (Ed.). *Gray's Anatomy: The Anatomical Basis of Clinical Practice, 40th ed.* Edinburgh: Elsevier/Churchill Livingstone, 2008.

9

Oral cavity

MADAN G. ETHUNANDAN

Lip and vestibule 78
Tongue 80
Floor of mouth 83
Hard palate 84
Tissue space infections 85
Buccal space 85
Submandibular space 86
Submental space 86
Sublingual space 86
Ludwig's angina 86
Further reading 87

The oral cavity is the entry point to the alimentary tract and has an important role to play in the preparation of food, swallowing, speech, breathing and structural support to the face and aesthetics. The shape and size changes with age and is influenced by the eruption and loss of teeth and age-related changes of the surrounding skin, muscles, ligaments and bone. Lined by mucous membrane of differing characters, it is lubricated by major and minor salivary glands. A detailed appreciation of its anatomy is mandatory for safe surgical practice.

The oral cavity can be divided into two parts: the oral cavity proper and the oral vestibule. The vestibule is a narrow slit-like space between the lips and cheek on one side and the teeth and gingivae on the other. It communicates with the exterior through the oral fissure and the oral cavity proper through the retro-molar region and interdental spaces. The oral cavity proper is the area limited by the dental arches and the oropharyngeal isthmus, i.e. the junction of the oral cavity with the oropharynx. It is principally occupied by the tongue and is a 'potential space' that only exists when the mouth is open. The oropharyngeal isthmus is defined by the junction of the hard and soft palate superiorly, palatoglossal folds laterally and sulcus terminalis delineating the oral from the pharyngeal tongue, inferiorly. This transition from the oral cavity to the oropharynx is a watershed in terms of function and innervation. Functionally, the transition is from the voluntary to the reflex (involuntary) phase of swallowing.

The motor supply to the musculature of the oral cavity, i.e. orbicularis oris and buccinator (buccal and marginal mandibular branches of the facial), tongue (hypoglossal) and mylohyoid (motor root of trigeminal) is under voluntary control. The only muscle of the tongue not innervated by the hypoglossal is the palatoglossus (pharyngeal plexus), which is functionally a pharyngeal structure. Conversely, notwithstanding the reflex nature of pharyngeal function, the tensor palatini (motor root of the trigeminal) remains under voluntary control despite being a pharyngeal structure.

The innervation of the soft palate and pharynx is discussed in Chapter 18.

LIP AND VESTIBULE

The lip is a dynamic sphincter made up of a principal circular muscle – orbicularis oris – and 10 radially arranged dilator muscles. The decussation of the orbicularis oris and the radial muscle fibres occurs about 1 cm lateral to the corner of the mouth and is termed the modiolus.

The lip is covered by skin externally and lined by mucous membrane internally. The mucocutaneous junction is well defined by the vermilion border, and a further less distinct junction can be appreciated between the wet and relatively dry labial mucosa, the wet line. The corner of the mouth formed by the junction of the upper and lower lip is termed the commissure. The contour of the vermilion border of the upper lip, said to resemble an archer's bow, is termed the Cupid's bow. The philtrum is the vertical groove in the midline of the upper lip bordered by the lateral – philtral - ridges. Accurate approximation of the vermilion border is critical with any lip repair (Figure 9.1).

The position of the commissure changes with age, secondary to decreased vertical dimension associated with tooth wear/loss and loss of elasticity of the facial skin. This can lead to angular chelitis as a result of salivary pooling and candida/staphylococcal infection. The lips are a common site for squamous cell carcinoma, which is often related to smoking and sun exposure. The prognosis of these tumours is generally better than those arising in other parts of the oral cavity, but worse than those from other parts of the facial skin.

The lip also contains minor salivary glands, which are mucinous, and receives its blood supply from the labial arteries, sensory innervation from the mental and infra-orbital nerves and motor supply from the branches of the facial nerve. The mental nerve (terminal branch of the inferior alveolar nerve) emerges from the mental foramen, deep to the depressor anguli oris, and divides into three to four (angular, medial inferior labial, lateral inferior labial, mental) branches that supply the lips, chin and gingiva. The morphology of the transition zone between the inferior dental and mental nerve at the mental foramen can be categorized into loop (61.5 per cent), straight (23.1 per cent) and vertical (15.4 per cent) with the mean distance between the anterior margin of the mental foramen and anterior loop being 1.74 mm (range 0.73–2.63 mm)

The terminal lip branches are often visible just under the mucosa when the lip is everted. The lower labial branches run in an oblique direction on the orbicularis oris and the mean angulation between the nerve and muscle is 36°. It is suggested that mucosal incisions are therefore made approximately 36° to the long axis of the lip when performing small soft tissue procedures and a slightly *U*-shaped incision with lateral limbs parallel to the branches is preferred for symphyseal bony access (Figure 9.2).

The position of the mental foramina changes with age, tooth loss and alveolar resorption. In a

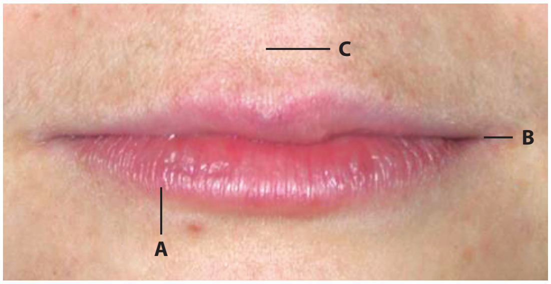

Figure 9.1 A – vermilion border. B – commissure. C – philtrum.

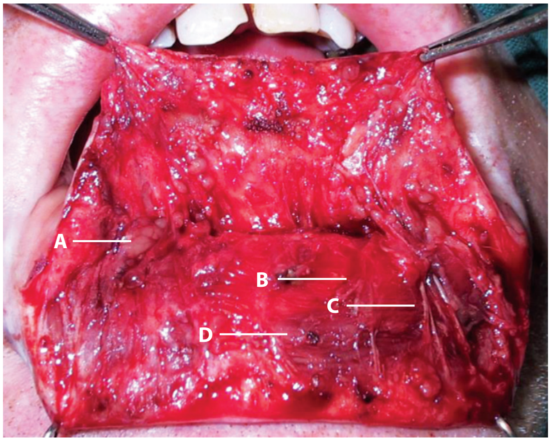

Figure 9.2 Mucosa of lower lip lifted off underlying minor salivary glands, branches of the mental nerve and the orbicularis oris. A – Mucinous minor salivary glands. B, C – terminal branches of the mental nerve – note varying angulation with respect to the radial fibres of orbicularis oris, D.

http://e-surg.com

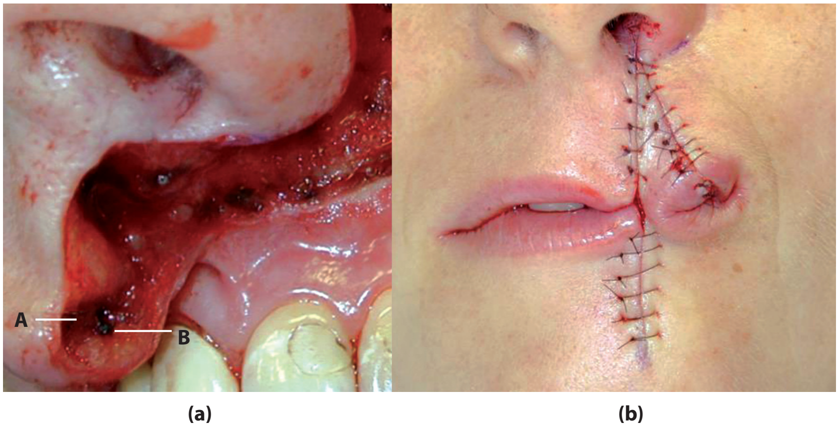

Figure 9.3 **(a)** A – fibres of orbicularis oris. B – labial artery on mucosal aspect of muscle. **(b)** lip switch procedure; vascular supply of transposed segment from labial artery.

long-standing edentulous mandible, the mental foramina may be on the crest of the alveolus, relevant in siting incisions.

The minor salivary glands lie immediately beneath the oral mucosa and are closely related to the fine mental nerve filaments — the latter at risk during labial salivary gland biopsy. Mucoceles (mucous extravasation/retention cysts) are more common in the lower lip and occur infrequently in the upper lip, where a mass is more likely to be a minor salivary gland tumour.

The superior and inferior labial arteries are branches of the facial artery. The superior labial artery, about 45 mm in length (range 29–85 mm), originates at or above the level of the commissure at a mean distance of about 12 mm from the commissure. It may be unilateral in up to 29 per cent of individuals. The labial arteries run along the free border of the lip on the posterior surface of the orbicularis oris, closer to the mucosal aspect than the skin; their position is relevant in various lip flaps (Figure 9.3).

The upper and lower labial frena (singular frenum) are midline folds of mucosa that cross the vestibule from the upper and lower lip and attach to the underlying alveolar mucosa and periosteum of the maxilla and mandible (Figure 9.4). Aberrant attachment of the frenum may result in a gap between the upper incisors (diastema) or interfere with denture stability and require removal, called ‘frenectomy’. A torn frenum in a young child can be a sign of abuse.

The mucosa lining the vestibule is nonkeratinized and adherent to the underlying buccinator and lip muscles. The buccinator, the deepest muscle of facial expression, is often considered an accessory muscle of mastication. It is a thin, flat muscle, originating from the maxilla and

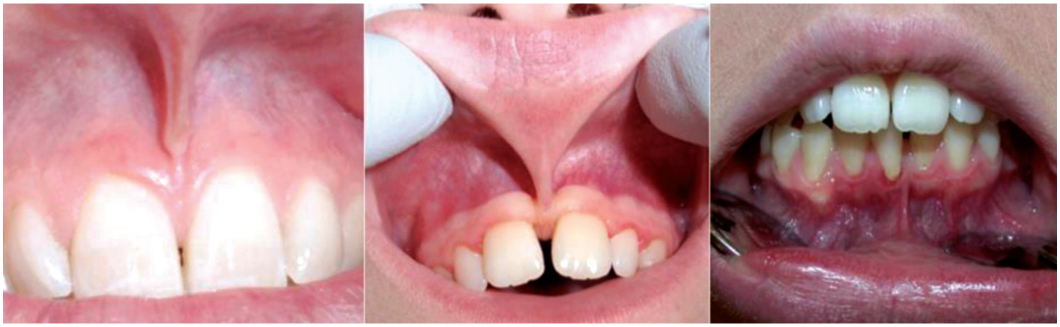

Figure 9.4 Labial frena.

http://e-surg.com

mandible adjacent to the molar teeth and from the pterygomaxillary ligament and pterygomandibular raphae posteriorly. Anteriorly at the modiolus, it forms a chiasma, with the fibres arising from the maxilla and mandible passing into the respective upper and lower lips. The central fibres originating from the pterygomandibular raphae, however, decusate, with the upper fibres passing into the lower lip and lower fibres into the upper lip.

The motor supply of the buccinator muscle is from the buccal branches of the facial nerve. The adjacent buccal mucosa receives its sensory supply from the (long) buccal branch(es) of the mandibular nerve. The long buccal nerve leaves the infratemporal fossa, crossing the anterior border of the ramus at the level of the occlusal plane and pierces the buccinator to supply the buccal mucosa, gingiva and vestibular mucosa. The other fibres continue anteriorly to supply the skin of the cheek.

The parotid (Stensen's) duct emerges from the anterior border of the parotid gland and runs forward on the surface of the masseter muscle, before turning sharply at its anterior border. It passes through the buccal fat pad, pierces the buccinator muscle and runs further forward obliquely between the muscle and the mucosa, before terminating at the parotid papilla, adjacent to the second maxillary molar teeth. The distal part of the duct, between the buccinator and the oral mucosa, is compressed when the intraoral pressure is increased and prevents air entry into the ductal system (pneumoparotid). The parotid papilla can be flush with the surrounding mucosa or pendulous, which can influence the ease with which one is able to cannulate the duct.

TONGUE

The tongue is a muscular structure covered by mucosa and consists of a tip, dorsum, ventral surface and root. The anterior two-thirds forms part of the oral cavity and the posterior one-third part of the oropharynx. The V-shaped sulcus terminalis defines the junction between the anterior two-thirds and the posterior one-third. The foramen caecum is situated at the apex of the V and denotes the remnants of the upper end of the vestigial thyroglossal duct.

The mucosa of the dorsal anterior two-thirds is roughened by the presence of the filiform, fungiform and circumvallate papillae. The filiform papillae are conical shaped and most numerous. Fungiform papillae are pink, discrete, mushroom-shaped projections, which are mainly situated in the tip and lateral borders of the tongue. Circumvallate papillae are dome-shaped and are situated just anterior to the sulcus terminalis and about 8–12 in number. Foliate papillae form part of the posterior one-third of the tongue and are identified as a series of mucosal folds at the lateral extremity and also contain taste buds. Numerous taste buds are present on the fungiform, circumvallate and foliate papillae, which are termed gustatory papillae, but not on the filiform papillae. The filiform papillae are elongated in the condition of 'black hairy tongue' (Figure 9.5). (Ducts of lingual salivary glands, known as Von Ebner's glands, open into the circular depression, around the base of the circumvallate papillae.)

The roughened mucosa covering the dorsum and tip is replaced by thin, smooth mucous membrane covering the ventral tongue. The junction between the ventral tongue and floor of the mouth is imprecise. The mucous membrane covering the posterior one-third has a nodular appearance due to the presence of the underlying lymphoid follicles (lingual tonsil), serous and mucous glands.

The muscles of the tongue insert into the mucosa and are separated by a midline fibrous septum and include four pairs of intrinsic (wholly within the tongue) and four pairs of extrinsic muscles, which have bony attachments. The intrinsic muscles comprise superior longitudinal, inferior longitudinal, vertical and transverse muscles. They have no bony attachments and alter the shape of the muscle. The extrinsic muscles comprise the genioglossus, hyoglossus, palatoglossus and styloglossus. These are principally concerned with the position of the tongue in addition to changes in shape.

The genioglossus is a fan-shaped muscle and accounts for most of the substance of the tongue. It is attached to the superior genial tubercle (mental spine) and the fibres radiate to insert into the tongue mucosa, with the most inferior fibres inserting into the hyoid. The hyoglossus is a thin, flat muscle, originating from the body and greater cornu of the hyoid bone and passing upward to insert into the

http://e-surg.com

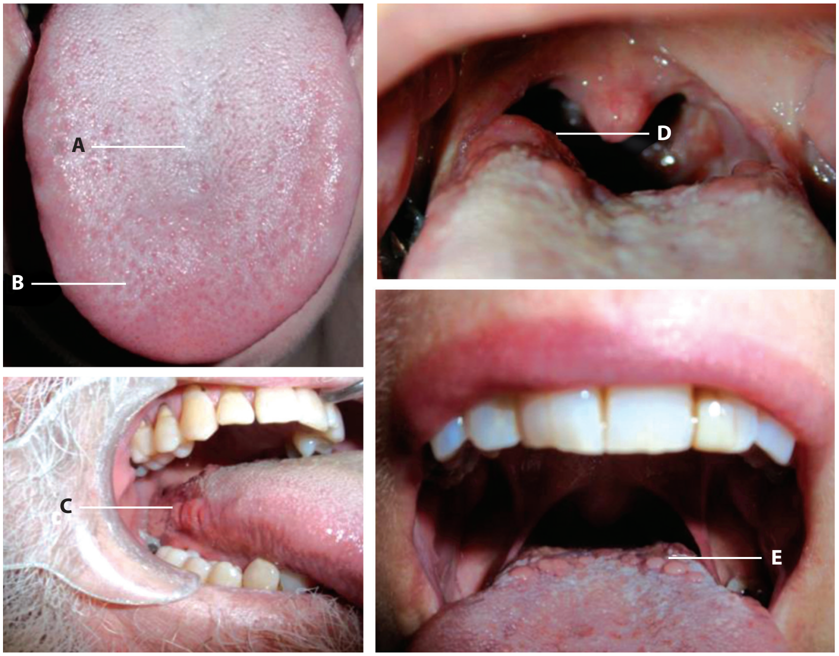

Figure 9.5 A – Filiform papillae. B – fungiform papillae. C – foliate papillae. D – enlarged lingual tonsillar tissue. E – circumvallate papillae.

inferior lateral substance of the tongue, intermingling with the fibres of the styloglossus and inferior longitudinal muscles. The styloglossus is a triangular muscle which originates from the anterolateral surface of the styloid process and passes forward to the postero-lateral surface of the tongue. The palatoglossus originates from the inferior surface of the palatine aponeurosis and passes downward to insert into the postero-lateral tongue and contributes to the palatoglossal fold, marking the lateral junction of the oral cavity and oropharynx.

The lymphatic drainage of the tongue is complex. It consists of superficial and deep networks. The superficial network extends from the tip to the circumvallate papilla and drains into the deeper muscular system. The deep system is further subdivided into three groups: (1) apical (anterior), which drains the tip of the tongue to level I and III lymph nodes; (2) marginal (lateral), draining the lateral one-third of the tongue from the tip to the circumvallate papillae to level I, II and III nodes; and (3) central, which drains the middle two-thirds of the dorsum into level I and III nodes. The posterior tongue drains into levels II and III. Bilateral drainage is common from the central segments and 'skip metastasis' to level IV, without involvement of the intervening levels, is sometimes detected from tongue malignancies. Refer to chapter 24 for more on the anatomical boundaries of the neck levels.

There is increasing awareness of an 'intrinsic' lingual lymphatic system consisting of a median node within the septum, a lateral lingual node medial to the sublingual gland and a further node related to the lingual artery deep to the hyoglossus. It is suggested that occult tumour metastases to these nodes may be difficult to detect due to their proximity to the primary tumour. Failure to resect these nodes is suggested as a possible contributory cause of local tumour recurrence.

The principal arterial supply to the tongue is from the lingual artery, with smaller contributions from branches of the facial and ascending pharyngeal arteries (Figure 9.6). The lingual artery arises from the external carotid artery at the level of the greater cornu of the hyoid bone, either as a separate branch or as a common linguofacial/thyrolingual trunk. It is divided into three parts by the hyoglossus muscle; the first part runs obliquely up to the posterior border; the second part is horizontal, deep to the muscle; and the third part runs vertically along the anterior

http://e-surg.com

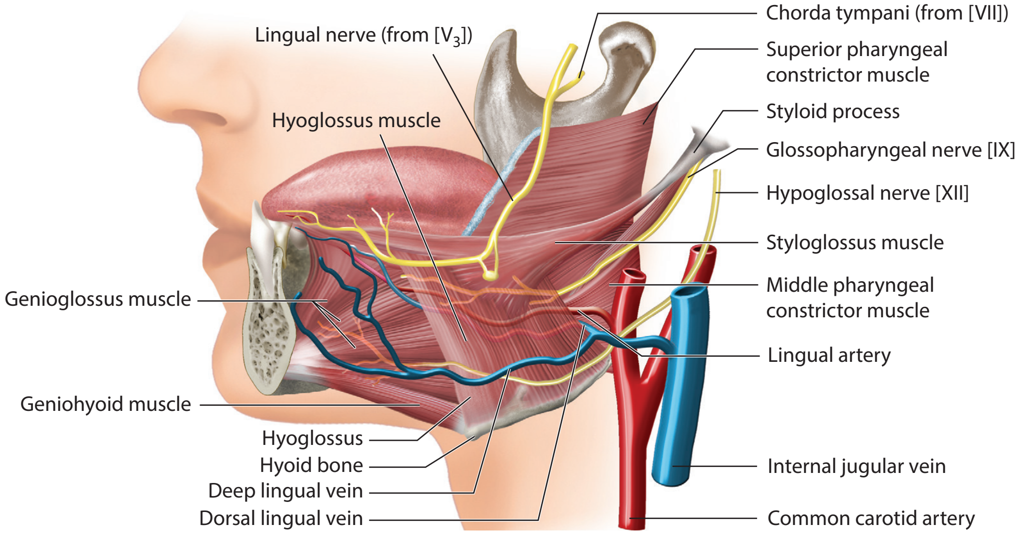
Lingual nerve (from [V3])
Hyoglossus muscle
Chorda tympani (from [VII])
Superior pharyngeal constrictor muscle
Styloid process
Glossopharyngeal nerve [IX]
Hypoglossal nerve [XII]
Styloglossus muscle
Middle pharyngeal constrictor muscle
Lingual artery
Genioglossus muscle
Geniohyoid muscle
Hyoglossus
Hyoid bone
Deep lingual vein
Dorsal lingual vein
Internal jugular vein
Common carotid artery

Figure 9.6 Adapted from student *Gray's Anatomy*.

border of the muscle, before coursing anteriorly to the tip of the tongue. Pirogov's (Pirogoff's) triangle, which is less well-known these days, is the space defined by the tendon of the digastric, posterior border of the mylohyoid and hypoglossal nerve, where the lingual artery can be found and is one of the suggested sites for ligation of the artery. The artery divides into suprahyoid, sublingual, dorsal lingual and deep lingual branches. There is very little cross anastomosis with its counterpart across the midline of the tongue, and therefore the lingual arteries are often considered end arteries. Resections of the posterior tongue involving the proximal lingual artery and giant cell arteritis can lead to avascular necrosis of the ipsilateral tongue. In contrast to the tongue, there are abundant vascular anastomoses across the midline in the anterior floor of the mouth.

The venous drainage of the tongue accompanies the arterial branches (Figure 9.6). Deep lingual veins drain the tip of the tongue and course submucosally on the ventral surface on either side of the midline. The veins are visible on the ventral surface of the tongue and can develop varicosities in later life (Figure 9.7). They are joined by the sublingual vein at the anterior border of the hyoglossus and form the vena comitanes of the hypoglossal nerve, which empties into the facial, lingual or internal jugular veins. The dorsal lingual veins drain the dorsum and sides of the tongue and join the lingual vein and empty into the internal jugular vein.

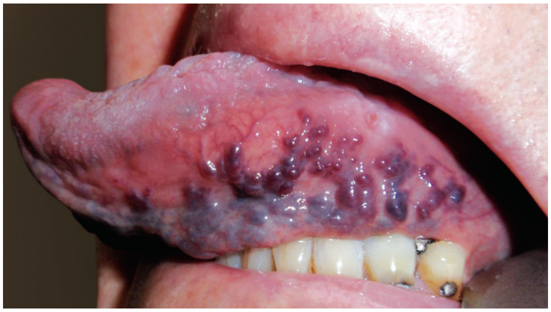

Figure 9.7 Lingual varicosities.

The motor supply to all the tongue muscles is from the hypoglossal nerve, except the palatoglossus, which is supplied by the pharyngeal plexus. It exits the skull through the hypoglossal canal, runs forward between the carotid artery and internal jugular vein, onto the surface of the hyoglossus to supply the tongue musculature. Damage to the hypoglossal nerve can lead to atrophy of the ipsilateral tongue, with deviation 'towards' the affected side (Figure 9.8).

The sensory supply to the anterior two-thirds of the tongue is from the lingual nerve and the posterior one-third from the glossopharyngeal nerve, with a small contribution from the internal laryngeal nerve, itself a branch of the vagus nerve. The

http://e-surg.com

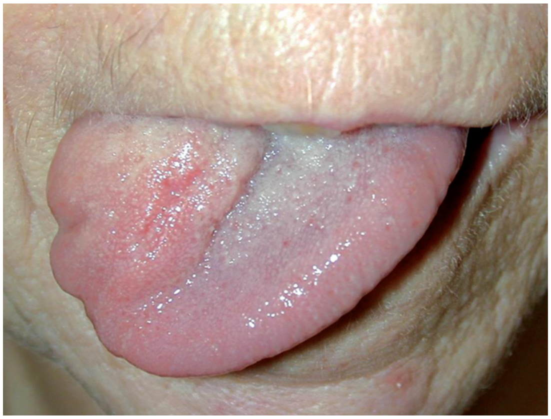

Figure 9.8 Deviation and wasting of the right tongue with right hypoglossal nerve paresis.

chorda tympani nerve mediates taste sensation and carries secretomotor fibres to the submandibular and sublingual glands (Figure 9.6). Some anatomists regard the chorda tympani as forming part of a 13th cranial nerve.

FLOOR OF MOUTH

The floor of the mouth is *U*-shaped, lying beneath the tongue and limited anteriorly and laterally by the lingual surface of the mandible. It contains the sublingual gland, submandibular duct and lingual nerves. The lingual frenum extends as a fold of mucosa from the ventral/inferior surface of the tongue to the floor of the mouth, in the midline. Its thickness and extent of attachment varies considerably and can lead to restriction of tongue movement (tongue tie/ankyloglossia), which can be corrected by a lingual frenectomy.

The submandibular papillae, representing the openings of the submandibular ducts, lie on either side of the lingual frenum. The sublingual plica/fold overlies the sublingual gland (Figure 9.9). The mylohyoid muscle is attached to the mylohyoid line on the lingual surface of the mandible, and the anterior/central fibres extend medially to decussate with their counterpart to form the midline raphae. The raphae extends from the inferior symphysis menti to the body of the hyoid bone. The posterior fibres are attached to the body of the hyoid bone. The diaphragm is reinforced by the geniohyoid on the deep aspect and the anterior belly of the digastric muscle in the superficial aspect. The mylohyoid diaphragm separates the oral cavity from the neck. Dehiscences are relatively common in the diaphragm and can lead to herniation of the sublingual gland.

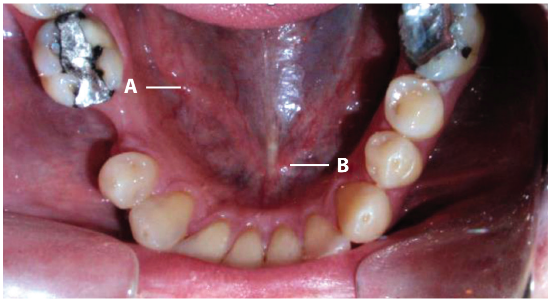

Figure 9.9 A – sublingual plica. B – submandibular papilla.

The almond-shaped sublingual glands are the smallest of the major salivary glands. They lie on the surface of the mylohyoid muscle and are covered by the mucous membrane of the floor of the mouth. Their saliva is drained by multiple ducts (ducts of Rivinus) that open directly into the oral mucosa in the region of the sublingual fold and a major duct which opens into the distal submandibular duct or separately at the sublingual caruncle. The posterior edge of the gland often merges into the anterior portion of the deep lobe of the

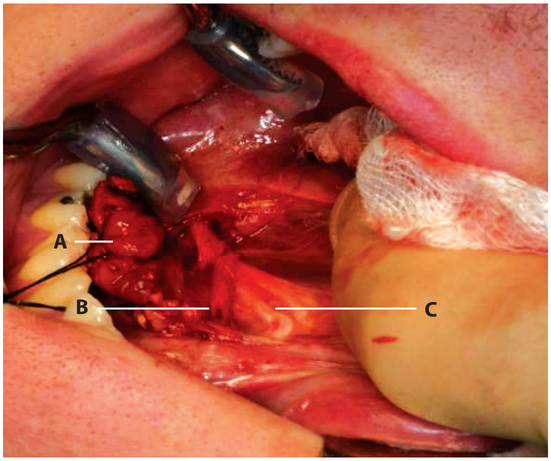

Figure 9.10 Relationship of lingual nerve, submandibular duct and sublingual gland in the right floor of mouth. A – Retracted sublingual gland. B – submandibular duct. C – lingual nerve. (Photograph courtesy Professor M. McGurk.)

http://e-surg.com

submandibular gland. Mucous extravasation cysts arising from the sublingual gland are termed ranula, as they resemble a frog's belly and present as a mass in the floor of the mouth. Dehiscence in the mylohyoid can lead to them presenting as a neck lump and is termed a 'plunging' ranula.

The submandibular gland straddles the free posterior border of the mylohyoid muscle, which divides it into a superficial and deep lobe. The main submandibular duct (Wharton's duct) emerges from the deep lobe of the gland, is 4–6 cm in length and runs forward on the surface of the hyoglossus and genioglossus muscles, before opening at the submandibular papilla. The portion of the deep lobe from which the duct emerges is termed the hilum. Salivary stones (calculi) presenting in the submandibular duct, up to the hilum, can be accessed through an intra-oral incision. The lingual nerve is at risk during intra-oral surgical removal of a submandibular duct stone, particularly in the region of the hilum.

The lingual nerve, a branch of the mandibular division of the trigeminal nerve, leaves the infratemporal fossa and emerges from the anterior border of the pterygomandibular fossa and enters the oral cavity passing under the inferior attachment of the pterygomandibular raphe above the mylohyoid and lateral to hyoglossus.

It is closely related to the lingual aspect of the mandible in the third molar region and it may be in contact with the mandibular periosteum. In about 15 per cent of cases (one in seven) the nerve may run above the crest of the alveolar bone. It is acknowledged that this nerve is at risk with lower third molar surgery and mandibular osteotomies. Significantly, the nerve may remain in close proximity to the mandible for >2.5 cm before moving in a medial direction into the floor of the mouth, suggesting that it is at risk with second and possibly first molar surgery if the lingual cortical plate is violated. The vertical and horizontal relationship to the mandible is variable between individuals and between the right and left sides in the same patient. The average diameter of the nerve in the third molar region assessed by magnetic resonance imaging (MRI) is of the order of 2.5 mm. The lingual nerve continues anteriorly and medially, crossing beneath the submandibular duct in the floor of the mouth from a postero-lateral to anteromedial direction, before dividing into multiple branches to supply the mucosa of the tongue, floor of mouth and lingual gingiva (Figure 9.10).

In the floor of the mouth, the submandibular duct lies on the lateral surface of the hyoglossus with the lingual nerve superiorly and the hypoglossal nerve inferiorly. On the medial surface of the muscle lie the glossopharyngeal nerve, stylohyoid ligament and lingual artery in a superior to inferior orientation (Figure 9.6).

HARD PALATE

The hard palate forms the superior boundary of the oral cavity. It separates the oral from the nasal cavity and is formed by the palatine processes of the paired maxillae and the horizontal plates of the palatine bones. Its anterior and lateral boundaries are the tooth-bearing alveolar processes. The nasopalatine, greater and lesser palatine neurovascular bundles perforate the hard palate: the nasopalatine via the incisive fossa, the greater and lesser palatine through the foramina of the same name.

The premaxilla (Goethe's bone) is that part of the maxilla containing the incisor teeth. A transverse suture – the incisive suture – marks the junction between the palatal portion of the premaxilla and the palatal process of the maxilla; in some instances this may persist into adult life.

General sensation and taste are provided by the palatine nerves; fibres conveying taste travel centrally to the pterygopalatine ganglion, through which they pass without synapsing, exiting via the greater petrosal nerve. Their cell bodies are in the facial ganglion. The nasopalatine nerves supply sensation to the anterior hard palate to the canine/first premolar region. The greater palatine nerves supply sensation from the posterior border of the hard palate overlapping anteriorly with the area of nasopalatine innervation. The lesser palatine nerves supply the soft palate uvula and tonsil.

The vascular supply to the hard palate is from the nasopalatine and greater palatine vessels, all branches of the maxillary artery. Considerable anastomoses occur between these vessels – branches of the greater palatine artery anastomosing with the nasopalatine via the incisive fossa. Less well appreciated are the anastomoses between the greater palatine vessels themselves; indirect

http://e-surg.com

evidence for this is the fact the mucosa of the entire hard palate may be pedicled on a single greater palatine vessel. The vascular supply of the hard palate mucosa derived from the greater palatine vessels running in an postero-anterior direction is fortuitous as it permits safe elevation of large axial pattern palatal mucosal flaps. The denuded bone donor defect will epithelialize within about six weeks.

The thick keratinized mucosa of the hard palate is firmly bound down to the underlying periosteum. A narrow midline ridge (the palatal raphe) runs anteroposteriorly, devoid of submucosa. An oval prominence – the incisive papilla – overlies the incisive fossa at the anterior limit of the raphe (Figure 9.11). Palatal rugae – transverse ridges of mucosa – in the anterior half of the hard palate radiate outwards from the palatal raphe. The rugae may aid articulation and mastication. Lateral to the raphe submucosa is present containing the neurovascular bundle. In the posterior half of the hard palate behind the rugae, minor salivary glands are present in within the submucosa – a not uncommon site of neoplasms. The periphery of the hard palate consists of the palatal gingivae of the maxillary dentition.

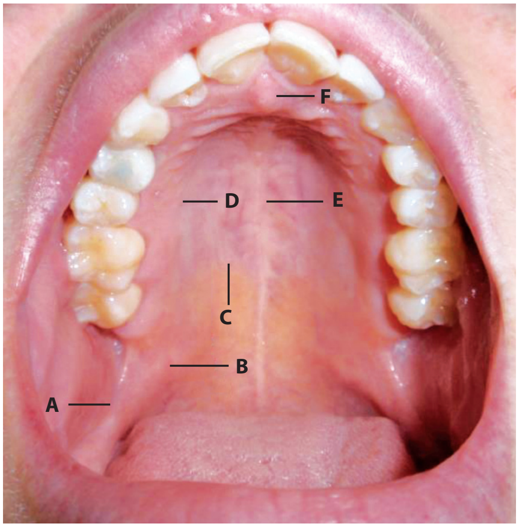

Figure 9.11 A – pterygomandibular raphe. B – site of pterygoid hamulus immediately beneath mucosa. C – sharp demarcation between hard and soft palate. D – palatal gingival. E – midline palatal raphe. F – incisive papilla.

A bony prominence – torus palatinus – may be present in the midline. This requires no treatment unless interfering with a denture. Diagnosis is clinical; if biopsied, healing is prolonged unless protected by a dental plate.

Immediately posterior to the hard palate, the pterygoid hamulus may be palpable beneath the mucosa of the soft palate just medial to the maxillary tuberosity. This is occasionally a cause of concern to patients.

TISSUE SPACE INFECTIONS

Oro-facial infections can accumulate and spread along tissue spaces, which are ‘potential spaces’ defined by bones, muscles and fascial layers. These spaces are ‘compartments’ in name only – they are in free communication with each other offering little resistance to the spread of infection.

Buccal space

This is a potential space, limited laterally by the skin, medially by the buccinator, anteriorly by the oral commissure and extending posteriorly to the pterygomandibular raphae. It is continuous with the pterygomandibular, parapharyngeal and masseteric spaces. Periapical dental infections, perforating the buccal cortex above and below the buccinator attachment in the maxilla and mandible, respectively, involve the buccal space. The teeth most often responsible are the premolars and

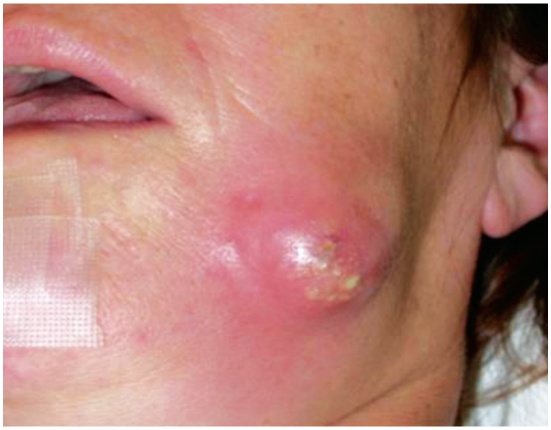

Figure 9.12 Buccal space infection.

http://e-surg.com

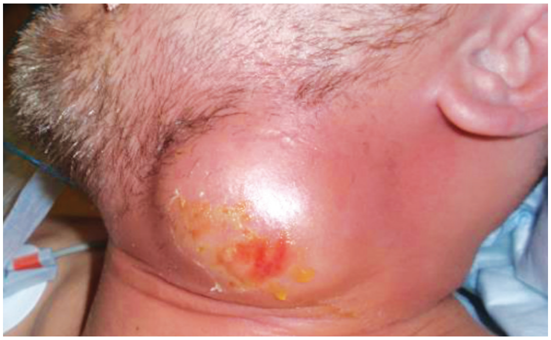

Figure 9.13 Extensive submandibular space infection/collection. It has penetrated the investing layer of deep cervical fascia.

molars. Periapical infection perforating the buccal cortex below and above the attachment of the buccinator in the maxilla and mandible, respectively, will present as an intra-oral swelling in the vestibule. Buccal space infections present as a cheek swelling (Figure 9.12).

Submandibular space

This is a potential space limited by the mylohyoid muscle superiorly, platysma and the investing fascia inferiorly, laterally by the body of the mandible and anteriorly and posteriorly by the anterior and posterior bellies of the digastric. It contains the submandibular gland and lymph nodes. Periapical infections that perforate the lingual cortex, below the attachment of the mylohyoid, and infections arising from the submandibular gland and lymph nodes involve the submandibular space. The principal teeth responsible are the lower molars.

Submandibular space infections present as a swelling in this site (Figure 9.13).

Submental space

The boundaries of this space are those of the submental triangle: The base is the body of the hyoid bone, the apex the lower border of the mandibular symphysis and bounded laterally by the anterior bellies of the digastric (Figure 9.14). The floor is the mylohyoid and the roof is the investing layer of deep cervical fascia. A small number of lymph nodes (one to six) are present and drain the lower incisor teeth, lower lip, chin, anterior floor of mouth and tongue tip. Infection, limited by the mylohyoid and deep cervical fascia, spreads readily to the adjacent submandibular space. There are no critical structures in this space.

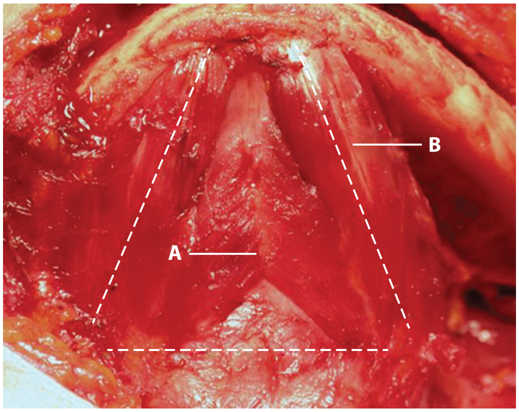

Figure 9.14 Submental triangle. Dotted line – submental triangle. A – midline raphe mylohyoid. B – anterior belly digastric.

Sublingual space

This is a potential space bounded by the mylohyoid muscle inferiorly, oral mucosa superiorly, mandible anterolaterally and the genioglossus muscle and tongue medially. Periapical infections perforating the lingual mandibular cortex above the mylohyoid attachment, and infections resulting from obstruction to the submandibular duct may result in infection in this space. The principal teeth responsible are the incisors, canines and premolars.

The swelling in the floor of the mouth can displace the tongue upward and backward. The tissues offer little resistance to spread to the opposite side.

The so-called mylohyoid-hyoglossal cleft between the mylohyoid and the hygolossal muscles connects the sublingual and submandibular spaces.

Ludwig's angina

This is a spreading inflammatory oedema affecting the submandibular, sublingual and submental spaces bilaterally. It presents as a brawny, erythematous swelling on both sides of the mylohyoid diaphragm bilaterally. The tongue is pushed

http://e-surg.com

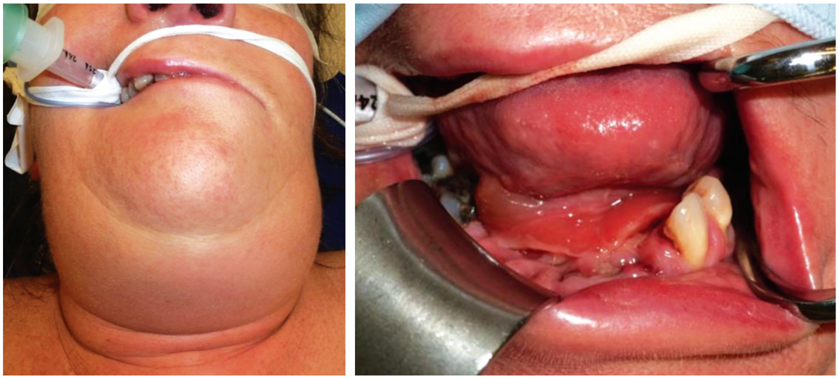

Figure 9.15 Ludwig's angina. Note tongue elevation.

upward and backwards. The patient often has difficulty swallowing, drooling of saliva and difficulty breathing. Spread to the lateral pharyngeal space is common. It is a surgical emergency, with a potential for catastrophic airway compromise (Figure 9.15).

FURTHER READING

Alantar, Roche Y, Maman L, Carpentier P. The lower labial branches of the mental nerve: Anatomic variations and surgical relevance. *Journal of Oral and Maxillofacial Surgery*. 2000; 58: 415–8.

Ettinger RL, Manderson RD. A clinical study of sublingual varices. *Oral Surgery, Oral Medicine, Oral Pathology*. 1974; 38: 540–5.

Hennekam, RC, Cormier-Daire V, Hall J, Méhes K, Patton M, Stevenson R. Elements of morphology: Standard terminology for the nose and philtrum. *American Journal of Medical Genetics Part A*. 2009; 149A: 61–76.

Hu KS, Yun HS, Hur MS, Kwon HJ, Abe S, Kim HJ. Branching patterns and intraosseous course of the mental nerve. *Journal of Oral and Maxillofacial Surgery*. 2007; 65: 2288–94.

Lang J. *Clinical Anatomy of the Masticatory Apparatus and Peripharyngeal Spaces.* New York: Thieme Publishers, 1995.

Magden O, Edizer M, Atabey A, Tayfur V, Ergur I. Cadaveric study of the arterial anatomy of the upper lip. *Plastic and Reconstructive Surgery*. 2004; 114: 355–9.

Miloro M, Halkias LE, Slone HW, Chakeres DW. Assessment of the lingual nerve in the third molar region. *Journal of Oral and Maxillofacial Surgery*. 1997; 58: 134–7.

Mukherji SK, Armao D, Joshi VM. Cervical nodal metastasis in squamous cell carcinoma of the head and neck: What to expect. *Head and Neck*. 2001; 23: 995–1005.

Ong HS, Ji T, Zhang CP. Resection for oral tongue squamous cell carcinoma: A paradigm shift from conventional wide resection towards compartment resection. *International Journal of Oral and Maxillofacial Surgery*. 2014; 43: 784–6.

Pogrel MA, Renaut A, Schmidt B, Ammar A. The relationship of the lingual nerve to the mandible third molar region: An anatomic study. *Journal of Oral and Maxillofacial Surgery*. 1995; 53: 1178–81.

Zhang L, Cai ZG, Wang Y, Zhu ZH. Clinical and anatomic study on the ducts of the submandibular and sublingual glands. *Journal of Oral and Maxillofacial Surgery*. 2010; 68: 606–10.

http://e-surg.com

http://e-surg.com

10

Alveolar process

NIALL McLEOD

Embryology of the alveolus 89
Growth and remodelling of the alveolus 90
Anatomy of the alveolus 91
Osteology *91*
Mucosa *91*
Periodontium *92*
Blood supply *92*
Lymphatic drainage *92*
Nerve supply *92*
Physiological changes of the alveolus 93
Growth and eruption of teeth *93*
Adaptation after tooth loss *93*
Topographical relationship of the alveolus 95
The maxillary sinus *95*
The lingual nerve *95*
Anatomical relevance in surgery of the alveolar process 95
Local anaesthesia *95*
Nonsurgical extraction of teeth *96*
Implant placement *96*
Nerve injury and dento-alveolar surgery *96*
Development abnormalities 97
Further reading 97

The alveolar process may be defined as that part of the maxilla and mandible which forms and supports the sockets of the teeth and therefore strictly only develops during their eruption.

EMBRYOLOGY OF THE ALVEOLUS

Fusion of the medial nasal and maxillary prominences forms the upper jaw and lip and separates the nasal cavity from the oral cavity. The lower jaw and lip are formed from the merging of the lateral mandibular processes. The mandible itself forms from intra-membranous bone lateral to Meckel's cartilage, from one ossification centre on each side arising in the sixth week in the region of the bifurcation of the inferior alveolar nerve and artery into mental and incisive branches (Figures 10.1 and 10.2).

At this stage the tooth germs still lie above the developing mandible, but near the end of the second month of fetal life the alveolar processes develop as a trough in response to the tooth buds and become superimposed on the basal bone of the maxillary and mandibular bodies (Figure 10.3). In a later stage the tooth germs are contained in this groove which also includes the dental nerves and vessels. Gradually, bony plates develop between the adjacent tooth germs and much later separate them from the mandibular canal.

The mesenchyme surrounding the dental follicle ossifies to form the dental crypt that the teeth form in, with an investing layer of mesenchyme differentiating into the periodontal ligament.

http://e-surg.com

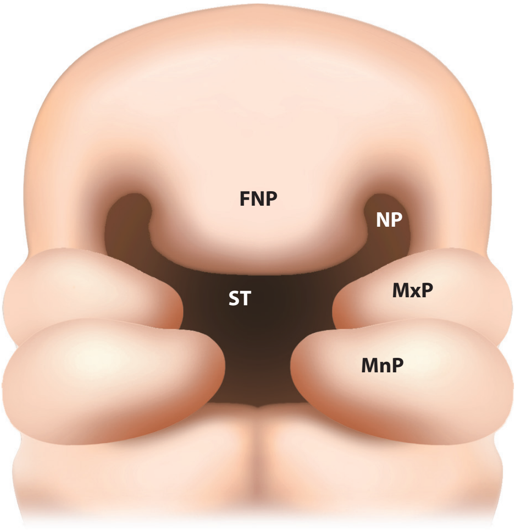
FNP
NP
ST
MxP
MnP

Figure 10.1 Embryology of the face at approximately five weeks in utero. Simplified to show the five major prominences that form the face. FNP – fronto-nasal prominence. NP – nasal pit. MxP – maxillary process. MnP – mandibular process. ST – stomadeum.

GROWTH AND REMODELLING OF THE ALVEOLUS

The position of the alveolar processes of the maxilla and mandible relative to the skull base and each other is largely determined by growth of the facial skeleton.

Bone deposition on the posterior surface of the maxillary tuberosity induces corresponding anterior displacement of the entire maxilla relative to the skull base, and growth at the midline palatal suture creates widening of the maxilla. The result is that the anterior and lateral surface of the maxillary alveolus displays resorption during growth whilst the palatal and posterior surface show depositional growth (Figure 10.4).

In the mandible, bone deposition occurs on the posterior border of the ramus while concomitant

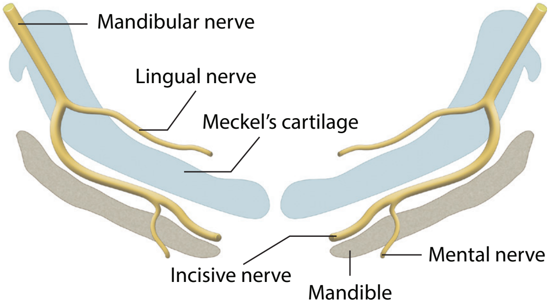
Mandibular nerve
Lingual nerve
Meckel's cartilage
Incisive nerve
Mandible
Mental nerve

Figure 10.2 Development of the mandible.

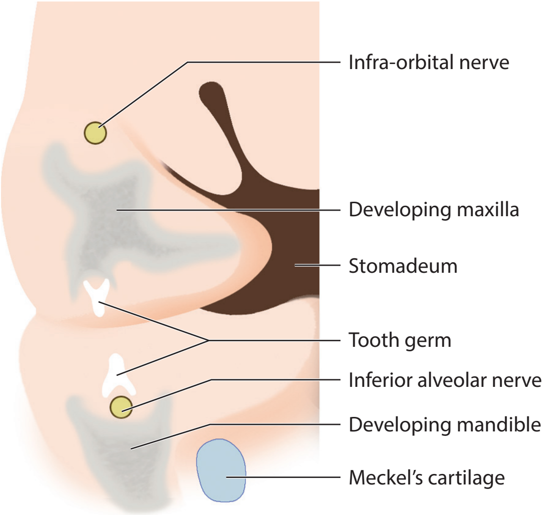
Infra-orbital nerve
Developing maxilla
Stomadeum
Tooth germ
Inferior alveolar nerve
Developing mandible
Meckel's cartilage

Figure 10.3 Development of the dento-alveolar complex.

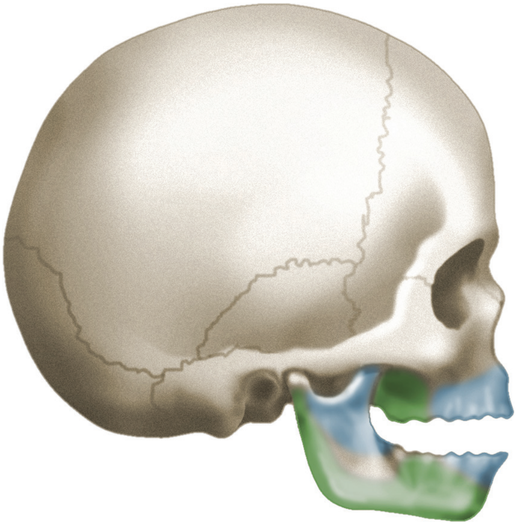

Figure 10.4 Growth of the mandible and maxilla. Areas of resorption during growth are shaded blue; areas of deposition are shaded green.

http://e-surg.com

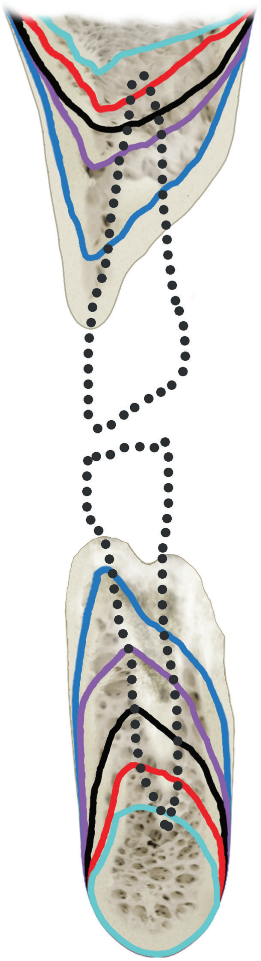

Figure 10.5 Resorption of the maxilla and mandible after the extraction of teeth. See Table 10.1 for description.

resorption of the anterior border of the ramus moves it backwards in relation to the body of the mandible, converting bone at the anterior edge of the ramus into the posterior mandibular body, and in this manner the body of the mandible lengthens. There is resorptive growth at the labial surface of the anterior mandibular alveolus, which results in increasing prominence of the mental process, but the remainder of the alveolus displays depositional growth (Figure 10.4).

The growth pattern of the alveolar arch itself differs from that of the facial skeleton, being related to the sequence of tooth development. The growth of the alveolar processes adds significantly to the vertical height of the maxilla and mandible. In the maxilla this creates depth to the palate and allows expansion of the maxillary sinus.

In the mandible it adds to the height and thickness of the body of the mandible and manifests as a ledge extending lingually to the ramus to accommodate the third molars.

ANATOMY OF THE ALVEOLUS

Osteology

The alveolus consists of cortical and cancellous bone, covered by mucoperiosteum, breached at its oral surface by erupted teeth. Anatomically, no distinct boundary exists between the body of the maxilla or mandible and their respective alveolar processes.

As a result of its adaptation to function, two parts of the alveolar process can be distinguished. The first consists of a thin lamella of bone which surrounds the root of the tooth and gives attachment to the principal fibres of the periodontal membrane. This is the alveolar bone proper. The second part is the supporting bone which consists of two parts: the compact cortical plate forming the vestibular and oral plates of the alveolar processes, and the spongy cancellous bone between these plates and the alveolar bone proper.

The cortical plates are continuous with those of the mandibular and maxillary bodies and are generally much thinner in the maxilla than the mandible. They are thickest in the premolar and molar regions of the mandible, particularly on the buccal side, and thinnest around the anterior teeth where the lamina dura may effectively be fused with the outer cortical plate.

Mucosa

The maxillary and mandibular alveolus are predominantly covered by a tightly bound mucoperiosteum which makes up the gingiva. This is in continuity with the mucosa of the palate, which is also mucoperiosteum, but also the alveolar mucosa laterally in the buccal vestibule and medial to the mandible in the floor of mouth. The demarcation of the alveolar mucosa and gingiva can be seen due to the different colouration, with the former a deep

http://e-surg.com

red and the latter more pink. The alveolar mucosa itself is thin, nonkeratinized stratified squamous epithelium.

Periodontium

The periodontal ligament is a specialized connective tissue which surrounds the roots of the teeth, attaching to the cementum on the surface of the roots and the alveolar bone. It supports the teeth within their sockets and allows them to withstand masticatory forces. It is composed of tight bundles of type 1 collagen formed into systematic bundles.

Blood supply

The blood supply of the maxillary alveolus comes from the third part of the maxillary artery.

The posterior superior alveolar artery is the first branch given off, and multiple branches enter the posterior maxilla with the corresponding nerves. The greater palatine artery enters the foramen of the same name and passes around the palate to enter the incisive canal. The infraorbital artery, the last branch of the maxillary artery, passes through the inferior orbital fissure and along the floor of the orbit, exiting through the infraorbital foramen. The first and last of these provide an intrabony supply to the maxillary alveolus, whilst the greater palatine artery and infraorbital artery provide supply to the periosteum of the alveolus.

The blood supply to the mandibular alveolus is from the inferior alveolar artery, a branch of the first part of the maxillary artery, which passes forward between the neck of the mandible and the sphenomandibular ligament, onto the medial surface of the mandibular ramus, where it meets the nerve of the same name and enters the mandibular foramen, passing forward and supplying the teeth, mandibular body and alveolus. Its mental branch then emerges through the mental foramen to supply the nearby muscle and skin.

The periosteal blood supply of the mandibular alveolus has a more complicated origin with contribution from the lingual artery to the lingual gingiva and alveolar mucosa, and the buccal artery to the buccal gingiva and alveolar mucosa in the molar region.

The primacy of the inferior alveolar artery in supplying the mandible in the elderly, particularly edentulous mandibles, has been questioned by a number of studies which demonstrated an absence of this vessel in elderly patients using angiographic imaging; however, a Doppler study of the mental artery showed that whilst blood flow was reduced it was still present in all patients, and histological studies have shown no increase in stenosis or occlusion with advancing age.

Lymphatic drainage

Lymphatic drainage of the dentoalveolar processes of the mandible and maxilla follows two routes, in keeping with the vascular drainage. Most lymphatic drainage is thought to follow the principal venous drainage of the bone, whilst a lesser route of drainage follows the periosteal venous drainage. All of it ultimately drains into the regional lymph nodes and onto the deep cervical nodes along the internal jugular vein.

Maxillary lymphatic channels accompany the blood supply to drain into the retropharyngeal and deep cervical lymph nodes.

The lower incisors and gingiva drain into the submental lymph nodes, which themselves drain to the submandibular nodes.

The remainder of the mandibular alveolus and most of the maxillary alveolus drain into buccal and mandibular lymph nodes and into the submandibular lymph nodes. These then drain to the deep cervical nodes.

Some of the posterior alveolus drains into the retropharyngeal nodes, and on to the deep cervical nodes.

Nerve supply

The maxillary division of the trigeminal nerve provides sensory innervation of the maxillary alveolus and teeth.

As the maxillary nerve enters the pterygopalatine fossa, the posterior superior alveolar nerve branches are given off and enter the posterior maxilla to supply usually the second and third molars and the palatal and distobuccal roots of the first molar and the surrounding alveolus. Within the infraorbital canal, the middle superior alveolar nerve branches are

http://e-surg.com

given off to the mesiobuccal root of the first molar and the first and second premolars and surrounding alveolus. The infra-orbital nerve then gives off branches to the remaining teeth before exiting the infra-orbital foramen where it gives branches to the gingiva of the anterior aspect of the maxillary alveolus. The buccal gingiva is innervated by a gingival branch of the posterior superior alveolar nerve which does not penetrate the posterior maxilla. The palatal gingiva is innervated by the greater palatine nerve and a terminal branch of the nasopalatine nerve which passes through the incisive canal to innervate the palatal gingiva of the incisor teeth.

The mandibular division of the trigeminal nerve provides sensory innervation of the mandibular alveolus and teeth. The inferior alveolar nerve (sometimes called inferior dental nerve) is a branch of its posterior division and emerges below the lateral pterygoid to cross the lateral surface of the medial pterygoid between the sphenomandibular ligament and the ramus of the mandible and enter the mandibular canal. It divides at the mental foramen into its terminal incisive and mental branches. The former innervates the anterior mandible and teeth beyond the premolars whilst the latter innervates the labial gingiva and the lower lip and chin. The lingual nerve is also a branch of the posterior division of the mandibular nerve, and whilst its principal innervation is given in its name, it also supplies the mucosa of the lingual aspect of the mandible.

The buccal nerve is a branch of the anterior division of the mandibular nerve which is wholly sensory and provides innervation of the buccal gingiva up to the mental foramen.

PHYSIOLOGICAL CHANGES OF THE ALVEOLUS

The internal structure of the bone is adapted to mechanical stresses. It changes continuously during growth and as a result of alteration of functional stresses.

In the alveolus this change takes place according to the growth, eruption, wear and loss of teeth.

Growth and eruption of teeth

The mechanism by which teeth erupt has not been fully elucidated. The elongation of the developing root, the deposition of cementum once root formation is complete, guidance from the Gubernacular cords (remnants of the attachment of the dental follicle to the oral epithelium), tissue pressure around the root, changes in vascularity of the periodontal tissues and contraction of the periodontal ligament fibres have all been postulated to play a role, and it is likely that several factors are involved.

The teeth are normally unerupted at birth, although the deciduous teeth will have commenced root formation at this stage, and some of the permanent dentition will have commenced calcification (Table 10.1).

The pattern of eruption of teeth is fairly predictable, although there can be quite significant variation in ages of eruption. Failure of development of tooth germs will have an impact on the development of the alveolus in that region as does the ectopic development of teeth.

The height of the alveolus is greatly controlled by the height of eruption of teeth, which in turn is controlled by several factors including the development of an occlusion with opposing teeth. The basic position of the erupting teeth is largely genetically determined, but as they erupt the teeth are subject to a number of forces, including those from the lips, cheeks and tongue and adaptive forces to habits such as tongue thrusting or digit sucking. The size of the teeth relative to the size of the dental alveolus and the relationship between the dental arches, due to relative growth of the mandibular and maxillary basal bone, form the final components of the developing occlusion. When there is no opposing tooth to occlude against, the teeth may over-erupt with consequent excessive alveolar growth. This can occur during eruption of the teeth or be a consequence of extraction of the opposing teeth in later life.

Adaptation after tooth loss

As the primary role of the alveolus is to support the teeth, if these are lost, the absence of functional forces results in the gradual resorption of the alveolar process and potentially some of the basal bone of the mandible and maxilla. This adaptive resorption occurs most quickly in the first six months after tooth loss and gradually slows but continues throughout life. Osteoporosis, renal impairment

http://e-surg.com

Table 10.1 Times of development and eruption of deciduous and permanent dentition

Tooth	Tooth germ completed	Calcification begins	Crown complete	Eruption in mouth	Root completed
Deciduous teeth					
Incisors	12–16 weeks iu	3–4 months iu	2–4 months	6–8 months	18–24 months
Canines		4–5 months iu	9 months	18–20 months	30–36 months
1st Molars		4–5 months iu	6 months	12–15 months	24–30 months
2nd Molars		5–7 months iu	11–12 months	24–30 months	3 years
Permanent teeth					
Central incisors	30 weeks iu	3–4 months	4–5 years	Maxilla 7–8 years Mandible 6–7 years	9–10 years
Lateral incisors	32 weeks iu	Maxilla 10–12 months Mandible 3–4 months	4–5 years	Maxilla 8–9 years Mandible 6–7 years	10–11 years
Canines	30 weeks iu	4–5 months	6–7 years	Maxilla 11–12 years Mandible 9–10 years	12–15 years
1st Premolars	30 weeks iu	18–24 months	5–6 years	10–12 years	12–14 years
2nd Premolars	31 weeks iu	24–30 months	6–7 years	10–12 years	12–14 years
1st Molars	24 weeks iu	Birth	3–5 years	5–7 years	9–10 years
2nd Molars	6 months	30–36 months	7–8 years	12–13 years	14–16 years
3rd Molars	6 years	7–10 years	12–16 years	17–21 years	18–25 years

iu = time in utero

and nutritional deficiencies are amongst many systemic factors which can play a role in the rate and degree of bone resorption.

Cawood and Howell (1988) demonstrated that this resorption does not occur in a symmetrical fashion, but there is angular loss of bone from the crest towards the labial surface of the maxillary alveolus and from the crest towards the lingual surface of the mandibular alveolus (Figure 10.5). They classified the shape of the alveolus from dentate to

Table 10.2 Cawood classification of the edentulous jaws

Class I	Dentate
Class II	Postextraction
Class III	Convex ridge form, with adequate height and width of alveolar process
Class IV	Knife-edge form with adequate height but inadequate width of alveolar process
Class V	Flat-ridge form with loss of alveolar process
Class VI	Loss of basal bone that may be extensive but follows no predictable pattern

http://e-surg.com

the extreme where there is loss of basal bone (Table 10.2). This asymmetric loss, together with the counterclockwise rotation of the mandible which occurs due to a loss of vertical dimension, from either tooth surface loss or absence of occluding teeth in the partially dentate or edentulous patient, produces an adverse skeletal relationship in all three dimensions, with typically a reverse relationship of the alveolar crest remnant and posterior cross bite. When restoring missing teeth, particularly when they have been absent for some time, it is therefore important to consider the three-dimensional relationship of the jaws, as failure to correctly restore the dental relationship in any of these can result in functional and cosmetic difficulties.

Resorption of the mandibular alveolus also changes the relationship of the mental nerve as it emerges from the mental canal between the position of the lower first and second premolar teeth. Whilst in the dentate patient the nerve emerges approximately halfway up the height of the mandible, in the edentulous patient, as the alveolar crest reduces in height, the position of the nerve is relatively raised, such that it may eventually present on the crest of the residual mandible. This may pose difficulties in prosthetic rehabilitation as the denture flange presses on the emerging nerve causing pain.

TOPOGRAPHICAL RELATIONSHIP OF THE ALVEOLUS

The maxillary sinus

The maxillary sinus forms during the sixteenth week in utero as a shallow groove on the nasal aspect of the maxilla and is rudimentary at birth (about 3–4 mm in diameter, 0.5 cm depression). It continues to enlarge throughout life in a nonlinear fashion with spurts of growth around 7–8 years and 12–14 years (Figure 10.6). From birth to adult life, growth is due to enlargement of the bone that encloses it; in old age 'growth' is due to resorption of surrounding cancellous bone.

With this resorption of the inferior maxillary bone, the sinus extends around the roots of the posterior teeth of the maxilla, and the bone between the roots and mucosal lining of the sinus can be very thin or even absent

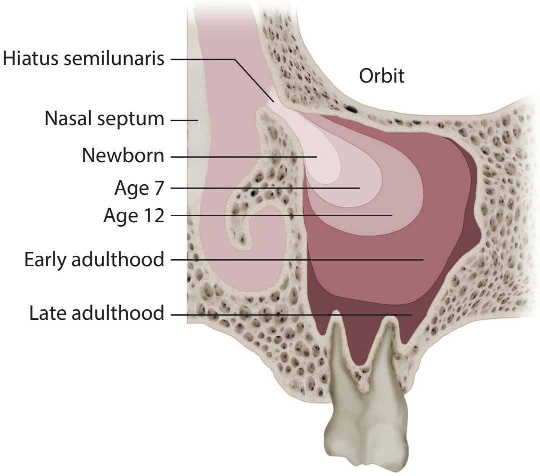

Figure 10.6 Development of the maxillary sinus and relationship with the teeth.

The lingual nerve

The lingual nerve arises from the posterior division of the mandibular nerve just beneath the lateral pterygoid, passing between the mandibular ramus and the medial pterygoid, and coming to lie against the lingual surface of the mandibular alveolus between the pterygomandibular raphe and the posterior edge of the mylohyoid, opposite the third molar. There it gives off its gingival branch before running downwards, forwards and medially to reach the anterior tongue.

ANATOMICAL RELEVANCE IN SURGERY OF THE ALVEOLAR PROCESS

Surgery of the alveolar process is predominantly related to the removal and replacement of teeth.

Local anaesthesia

Much exodontia and other surgical procedures on the dentoalveolar process are undertaken under local anaesthesia, and a clear understanding of the anatomy of the sensory innervation of the alveolus is clearly important in undertaking this successfully.

Local anaesthesia may be administered as local infiltration, nerve blocks or periodontal ligament

http://e-surg.com

injection. Local infiltration implies the supraperiosteal deposition of local anaesthetic solution which then requires infiltration of the periosteum and bone surrounding the relevant tooth. Factors which will determine the success of this technique include the biochemical properties of the chosen local anaesthetic solution and the thickness of the bone surrounding the teeth. Most infiltration is administered buccally/labially to the teeth, which will effectively anaesthetize the teeth for dental restorations but will not anaesthetize the palatal/lingual mucosa, and therefore exodontia requires further infiltration of the tissues palatally or lingually, or the use of a nerve block.

A nerve block of the inferior alveolar nerve by infiltration of local anaesthetic solution close to the lingula of the mandible is the most commonly used block in the dental context and effectively anaesthetizes the mandibular teeth, and by virtue of the very close proximity of the lingual nerve to the lingula normally anaesthetizes the lingual tissue at the same time. A posterior superior alveolar nerve block may also be useful to anaesthetize the posterior maxillary alveolar teeth, particularly the palatal roots of the teeth.

Periodontal ligament anaesthesia can be very effective but requires specific equipment with a fine needle and the ability to infiltrate the anaesthetic solution under pressure.

Devices have also been described which penetrate the buccal bone and permit intra-bony infiltration of local anaesthetic solution.

Nonsurgical extraction of teeth

Extraction of teeth requires disruption of the periodontal ligament around the teeth, and often expansion of the socket to allow removal of the root.

It is important to understand the shape of roots and the relative thickness of bone around them to minimize surgical trauma during exodontia.

In the maxilla the alveolar supporting bone is thickest palatally and increases in thickness towards the apex of the teeth, whilst in the mandible there is a gradual shift from the buccal bone being thickest in the molar region to the lingual bone being thickest in the incisor region. The extraction technique should apply force along the long axis of the roots and seek to expand the bone of the socket towards the thinnest plate of bone.

Implant placement

The placement of dental implants requires sufficient height and width of bone to permit osseointegration and support the implant-based restoration.

Whilst the alveolus surrounding erupted teeth is sufficient to allow implant insertion, it may be reduced in size or bone quality due to periodontal disease, normal bone resorption after extraction, or the presence of intra-bony pathology such as cysts and abscesses. Further anatomic considerations include the position of the maxillary sinus and the inferior dental canal in the posterior segments of the maxilla and mandible, respectively.

Where there is insufficient bone height or width to support implant placement, a number of techniques exist to augment the existing bone, including onlay and interpositional bone grafts and alveolar distraction. Alveolar distraction, unlike the other techniques, seeks to expand both the existing bone and soft tissue to restore near normal bone volume for implantation. It is important that once a graft is placed, dental implant placement occurs as soon as adequate healing has occurred, otherwise the bone will simply resorb again.

Nerve injury and dento-alveolar surgery

The position of the inferior alveolar canal at the inferior margin of the mandibular alveolus, close to the proximity of the roots of the teeth, puts it at risk of injury during dental extractions, particularly of mandibular third molars. Methodological flaws in most studies (mostly poor standardization of position of teeth, surgical technique, experience of surgeon and patient factors) make reliable data on temporary or permanent inferior alveolar nerve injury difficult to quantify. Figures from 1.3 to 7.8 per cent risk of temporary injury and 0.02 to 2 per cent risk of permanent injury have been published.

http://e-surg.com

Patient age, tooth angulation, relationship of apices to inferior dental canal and experience of operator have all been associated with increased risk. In terms of position of the canal radiographically, Rood and Shehab (1990) identified five features that were related to inferior alveolar nerve injury: radiolucency across the roots of the third molar, deviation of the mandibular canal, interruption of the white line of the canal, deflection of the third molar roots by the canal and narrowing of the third molar roots. The relationship of the inferior dental canal and the third molar roots can be assessed even more accurately with cross-sectional imaging such as with cone beam computerized tomography (CT).

The inferior alveolar nerve may be at risk during the surgical extraction of other teeth, particularly where these are ectopic and positioned more inferiorly in the mandible. It is also at risk during the placement of dental implants in the posterior mandible, when after post-extraction alveolar bone resorption, it will be relatively more superiorly positioned in the remaining mandible. It is imperative when placing dental implants in the posterior mandible to carefully assess the position of the nerve radiographically, ideally with cross-sectional imaging.

It is also worthwhile remembering that the mental nerve itself often passes anteriorly in the mandible (anterior to the mental foramen) before turning upwards and backwards to exit the foramen. This can sometimes be seen and appreciated on plain radiographs.

It is therefore possible to damage the nerve anterior to the mental foramen during bone surgical exodontia or implant placement as the nerve does not usually follow the direct route out of the foramen as one might expect.

The lingual nerve may also be at risk during the extraction of mandibular teeth, as it lies on the lingual alveolus opposite the third molar. The risk associated with third molar removal has been quoted as between 0.2 and 22 per cent temporary disturbance and between 0 and 2 per cent permanent disturbance. The raising of a lingual periosteal flap and perforating the lingual bone with a surgical instrument are associated with an increased risk.

DEVELOPMENT ABNORMALITIES

Many congenital abnormalities originate in maldevelopment of neural crest tissue that gives rise to much of the skeletal and connective tissue primordia of the face. Neural crest cells may be deficient in number, may not complete their migration to their destination or may fail in their inductive capacity or cytodifferentiation.

Failure of development of the alveolus is mostly otherwise related to failure of development of the underlying basal bone of the maxilla or mandible, which prevents migration of the processes which form the alveolus.

The principal developmental abnormality of the alveolar process occurs in association with cleft lip, which is described elsewhere in this text.

In hemifacial microsomia the relationship between the development of the maxillary and mandibular alveolus is clearly demonstrated. Mandibular hypoplasia results in a failure of normal downward development of the posterior maxilla and alveolus, resulting in an occlusal cant. A similar pattern of abnormal growth is seen with acquired abnormalities such as ankylosis of the temporomandibular joint.

With correction of mandibular abnormality, for example with the placement of a costochondral graft, the maxillary growth can be demonstrated to catch up with the contra-lateral side to a large degree.

FURTHER READING

Cawood JL, Howell RA. A classification of the edentulous jaws. *International Journal of Oral and Maxillofacial Surgery.* 1988; 17: 232–6.

Ethunandan M, Birch A, Evans BT, Goddard JR. Doppler sonography for the assessment of central mandibular blood flow. *British Journal of Oral and Maxillofacial Surgery.* 2000; 38(4): 294–8.

Loescher AR, Smith KG, Robinson PP. Nerve damage and third molar removal. *Dental Update.* 2003; 30: 375–82.

Proffit WR, Fields HW, Sarver DM. *Contemporary Orthodontics.* London: Mosby, 2012.

http://e-surg.com

Rood JP, Sheheb BAAN. The radiological prediction of inferior alveolar nerve injury during third molar surgery. *British Journal of Oral and Maxillofacial Surgery.* 1990; 28: 20–5.

Sinnatamby CS. *Last's Anatomy, Regional and Applied.* London: Churchill Livingstone, 2011.

Tobias PV, Sperber GH. *Craniofacial Embryology.* London: Butterworth-Heinemann Ltd., 1989.

http://e-surg.com

11

Anatomy of cleft lip and palate

SERRYTH COLBERT AND CHRIS PENFOLD

Introduction 99
Embryology of cleft lip and palate 99
Lip anatomy 100
Lip *100*
Philtrum *100*
Vermilion *100*
White roll *100*
Frenum *100*
Muscle anatomy 101
Unilateral cleft lip *102*
Bilateral cleft lip *102*
Hard palate anatomy 103
Soft palate anatomy 103
Cleft palate anatomy 105
Hard palate repair 106
Soft palate repair 107
Further reading 108

INTRODUCTION

Clefts of the lip and palate (CLP) are the most common craniofacial birth defects and are among the most common of all birth defects, with birth prevalence ranging from 1 in 500 to 1 in 2000 depending on the population. CLP represents a significant public health problem due to the significant lifelong morbidity and complex aetiology of these disorders. An understanding of embryology and anatomy of the cleft deformity is essential in order to optimize surgical treatment of CLP.

EMBRYOLOGY OF CLEFT LIP AND PALATE

At approximately 30–37 days' gestational age, the primary palate forms by the growth and fusion of the medial nasal, lateral nasal and maxillary processes (Figure 11.1). The maxillary process, derived from the proximal half of the first arch, grows to meet and fuse with the nasal processes that have grown and moved in association with the olfactory placode. The secondary palate arises from the two palatal shelves, which are positioned vertically on either side of the tongue. At 7 weeks gestational age, the head extends and together with mandibular growth allows the tongue to drop below the palatal shelves, which then rotate upwards and extend medially to meet in the midline. A cleft palate results from failure of the palatal shelves to meet or to fuse in the midline.

A cleft is caused by one or a combination of the following: hypoplasia, abnormal directional growth of mesenchymal processes, failure of fusion, or breakdown of fusion of mesenchymal processes. Disruption of matrix metalloprotinease (MMP) enzyme activity and its effect on the medial edge epithelium is an example of a possible common pathway for the range of genetic and environmental influences that result in cleft palate. The

http://e-surg.com

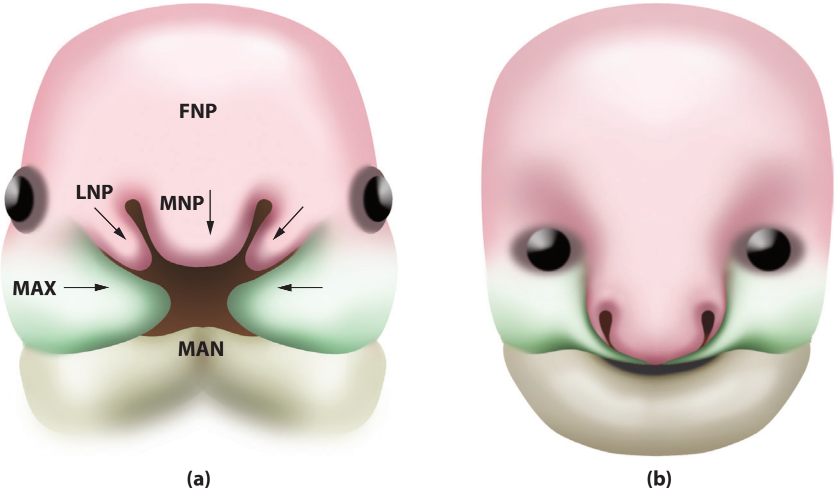

Figure 11.1 Development of the facial processes. **(a)** Representation of a 30- to 32-day-old human embryo showing the development of the facial processes. FNP – frontal nasal process. MAX – maxillary process. MAN – mandibular process. MNP – medial nasal process. LNP – lateral nasal process. **(b)** Representation of an 8½-week-old embryo showing the fate of the facial process.

severity of the deformity is related to the amount, timing and location of the embryonic interruption.

LIP ANATOMY

Lip

The lip is of variable thickness and presents two surfaces, superficial and deep. The superficial (or outer) surface is itself subdivided into two parts: the cutaneous lip and the mucous membrane or vermilion. The transition between these two zones is represented by the mucocutaneous ridge, or white roll, which extends from one corner of the mouth to the other. It is characterized by the *V*- or *U*-shaped indentation it forms in the midline, which is called the Cupid's bow.

Philtrum

Directly above the Cupid's bow, the upper lip forms a vertical groove-shaped depression called the philtrum. This is bordered by two rounded vertical elevations of variable prominence, known as the philtral ridges, which converge towards the midpoint of the transverse columellar groove if it exists or, if not, towards the centre of the base of the columella.

Vermilion

The visible portion of the vermilion is subdivided into two transverse zones, which are not clearly delimited. The outer zone is a pinkish red and, since it is not generally moist, it appears matt. The inner zone is a richer, translucent red. Its moist aspect resembles that of the mucosa with which it is continuous. The entire visible portion of the vermilion presents tiny vertical striations.

White roll

The junction between the skin and vermilion forms a pale and raised to a variable degree. It is most prominent in the upper lip and forms an important landmark in cleft lip repair.

Frenum

In the midline, the upper lip is attached to the gum by a fold of mucous membrane called a frenum. Key features of the anatomy of the normal lip are illustrated in Figure 11.2.

1. Sub-alar furrow.
2. Nasal sill.
3. Columellar base lifted by mesial crura.

http://e-surg.com

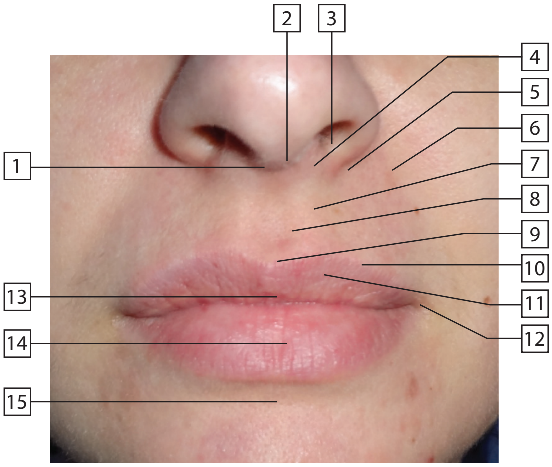

Figure 11.2 Anatomy of the lip.

4. Transverse groove of the columella.
5. Alar base.
6. Nasolabial triangle.
7. Philtral ridges.
8. Philtrum.
9. Nasolabial fold.
10. Cupid's bow.
11. Tubercle of the upper lip.
12. White roll/mucocutaneous ridge.
13. Vertical creases of the vermilion.
14. Matt zone of the vermilion.

MUSCLE ANATOMY

There are a series of three interconnected muscle rings extending from the infraorbital rim and nose down to the chin. These rings form part of the fascial envelope in continuity with the superficial musculoaponeurotic system (SMAS) (Figure 11.3).

Some general observations from the perspective of cleft lip repair are apparent:

- The convergence of the transverse nasalis towards the anterior nasal spine and the nasal septum.
- The transverse nasalis muscle intermingles with the levator labii superioris and levator labii superioris aleque nasi to form a modiolus that fans out to insert into the nasal sill. It influences the shape and position of the ala cartilage and the height of the nasal sill.
- The significance of the almost vertical orientation of the external or superficial part of the orbicularis oris and its connections with the muscles of the upper ring and with the lower ring through the modiolus.

In the unilateral cleft lip and palate, the upper and middle muscle rings are incomplete. All the muscle groups on the cleft side, which normally

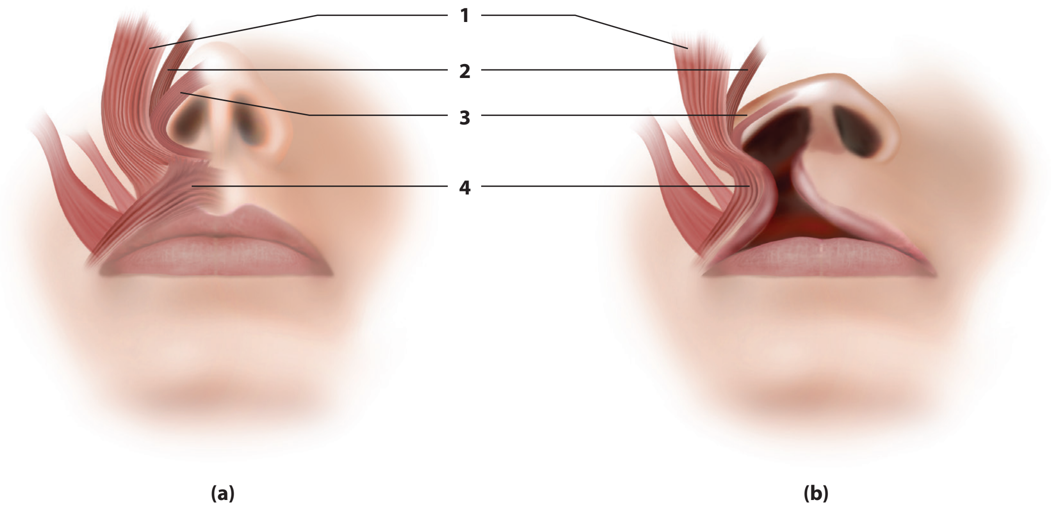

Figure 11.3 Nasolabial muscle anatomy in complete unilateral cleft lip. **(a)** Normal. **(b)** One side of a bilateral cleft lip. The abnormal muscle arrangements on the other side is usually identical. Muscles: 1 – levator labii superioris. 2 – levator labii superioris alaeque nasi. 3 – transverse nasalis. 4 – external bands of orbicularis labii superioris in unilateral cleft lip.

http://e-surg.com

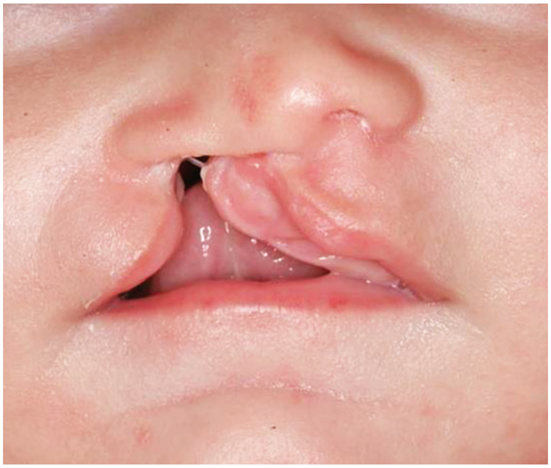

Figure 11.4 Surface anatomy of the unilateral cleft lip.

insert onto the ANS, septum and anterior surface of the premaxilla, become bunched up at the border of the cleft. The abnormal muscle function produces characteristic nasal and mucocutaneous abnormalities which have to be addressed at the time of primary lip repair.

Unilateral cleft lip

The skin around the cleft lip deformity shows that it is both retracted and displaced (Figure 11.4). The skin of the nasal floor is thin and hairless, and quite different from lip skin. It is pulled down into the upper part of the lip.

The cleft side muscle deprived of insertion to the anterior nasal spine and septum pulls the lateral lip element and alar base of the nose laterally. The alar cartilage is deformed but is not hypoplastic. Its lateral crus is pulled laterally and lengthened at the expense of the medial crus, thereby flattening the dome. Its inferior border is also rotated inferiorly forming a web inside the nostril. The anterior nasal septum and columella are deviated to the noncleft side.

Growth of the minor segment of the maxillofacial complex seems to be reduced as a probable consequence of absence of stimulation from the nasolabial muscles.

Bilateral cleft lip

The nasolabial muscle rings are disrupted in complete bilateral cleft lips, and their abnormal insertions result in unrestrained lateral displacement of the lateral nasolabial elements (Figure 11.5).

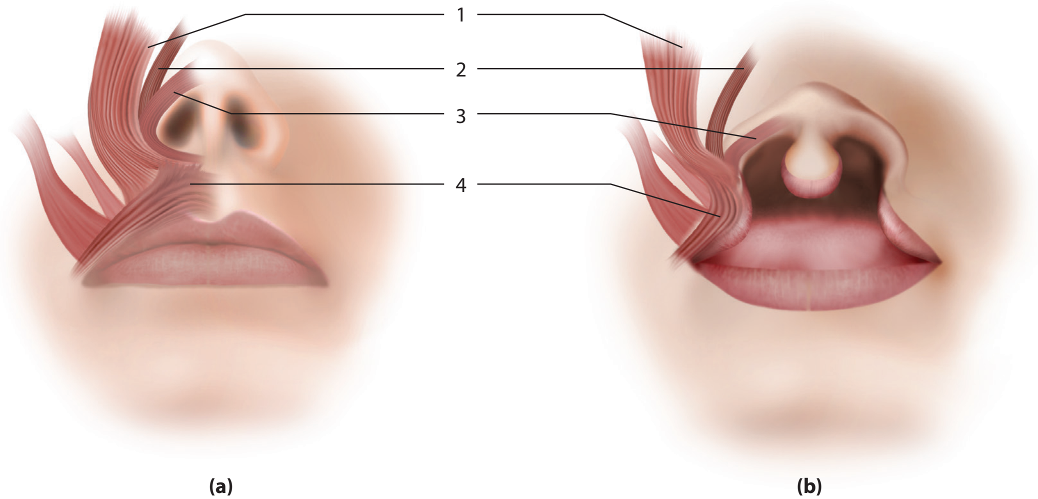

Figure 11.5 Nasolabial muscle anatomy in complete bilateral cleft lip. **(a)** Normal. **(b)** One side of a bilateral cleft lip. The abnormal muscle arrangements on the other side is usually identical. Muscles: 1 – levator labii superioris. 2 – levator labii superioris alaeque nasi. 3 – transverse nasalis. 4 – external bands of orbicularis labii superioris.

http://e-surg.com

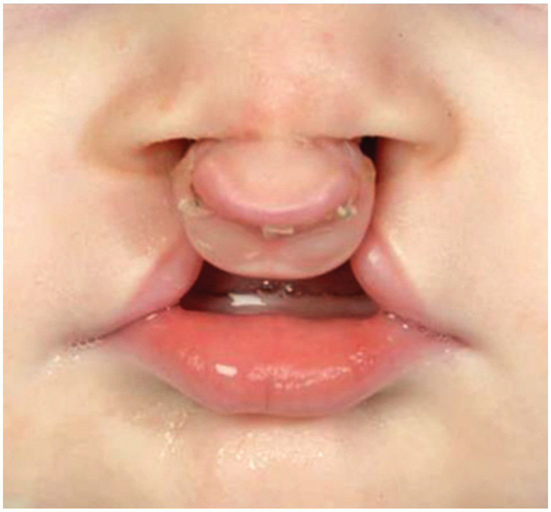

Figure 11.6 Surface anatomy of the bilateral cleft lip.

The isolated prolabium, which is deprived of muscle and normal vermilion, protrudes anteriorly and is rotated upwards (Figure 11.6). Its dimensions are reduced by secondary hypoplasia and the frequent absence of lateral incisors. A detailed analysis of the skin around the cleft lip shows that it is retracted and displaced, secondary to the absence of normal muscle function (Figure 11.7).

The most important feature of the bilateral cleft is the short columella that is produced by an unopposed muscular pull on elements of the lateral cleft in the early stages of fetal development. The bilateral nasal cleft is seldom corrected by functional surgery alone, and the appearance of a repaired bilateral cleft lip is often dominated by the short, tethered appearance of the columella, and a broad nasal tip.

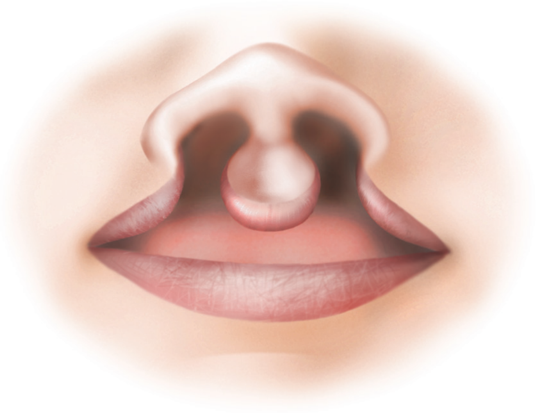

Figure 11.7 Skin distortion and secondary hypoplasia in bilateral cleft lip.

HARD PALATE ANATOMY

The hard palate is made up of premaxilla, maxilla and palatine bones. The incisive foramen runs obliquely backwards into the nose from just behind the incisor teeth in the midline. The greater palatine foramen emerges between the palatine bone and the maxilla.

The main vascular supply to the hard palate is by way of the descending branch of the greater palatine artery, which runs anteriorly from the greater palatine foramen and finally anastomoses with the terminal branch of the sphenopalatine artery as it emerges from the incisive foramen. The greater palatine artery also sends branches posteriorly into the velum, but the main vascular supply to the soft palate is from branches of the ascending palatine artery and, to a lesser extent, branches from the ascending pharyngeal artery that enter the velum with the levator palatini and palatopharyngeus muscles.

The oral surface of the hard palate is covered by mucoperiosteum that forms tranverse ridges or rugae anteriorly. It is firmly attached to the underlying bone by Sharpey's fibres. In the coronal plane the mucoperiosteum of the hard palate can be divided into three zones (Figure 11.8). The intermediate zone is thickened with connective tissue that transmits the neuromuscular bundle from the greater palatine foramen. Posteriorly, the mucosa overlying the palatine bones is separated from the underlying periosteum by mucous glands.

SOFT PALATE ANATOMY

An understanding of normal velar anatomy is fundamental to achieving a satisfactory cleft palate repair. The velar muscles include:

- tensor veli palatini (TVP).
- levator palatini (LP).
- palatopharyngeus (PP).
- palatoglossus (PG).
- muscularis uvulae (MU).

A fibrous aponeurosis occupies the anterior third of the velum (Figure 11.9). It is attached to the

http://e-surg.com

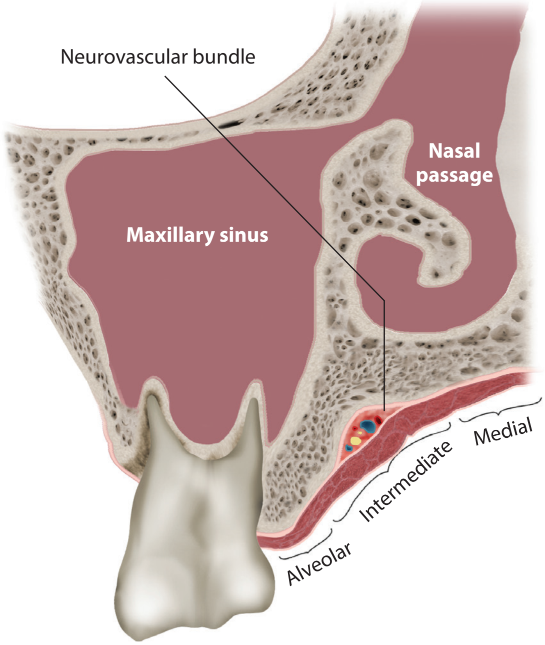

Figure 11.8 Coronal section through middle of hard palate.

posterior edge of the hard palate and is continuous with the tendon of tensor veli palatini (TP). The TP tendon exits the soft palate laterally and winds around the hamulus to which it is partly attached, before ascending to its origin in the scaphoid fossa, spine of the sphenoid bone and membranous portion of the tympanic tube. This latter attachment hints at the two TVPs' primary function, which is to help maintain patency of the Eustachian tube. The other primary function of the TVP is to tense the soft palate and by doing so assists the levator veli palatini in elevating the palate to occlude and prevent entry of food into the nasopharynx during swallowing.

The main velar muscles are the LP, PP and palatoglossus (PG). The PP arises from the upper surface of the palatine aponeurosis and the PP arises from the inferior surface of the aponeurosis. They course postero-laterally in the soft palate splitting at the posterior margin to form the fauces on either side of the tonsil. The PG is a thin sheet of muscle that extends inferiorly to form the anterior pillar of fauces. The PP is a much more substantial muscle. In the velum it is split into two heads by the insertion of the LP (Figure 11.10). From the velum

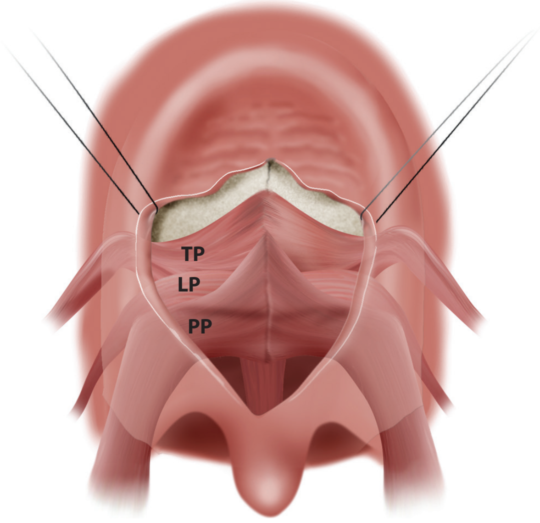

Figure 11.9 Inferior view of velar muscles. LP – levator palatini. PP – palatopharyngeus. TP – tensor palatine.

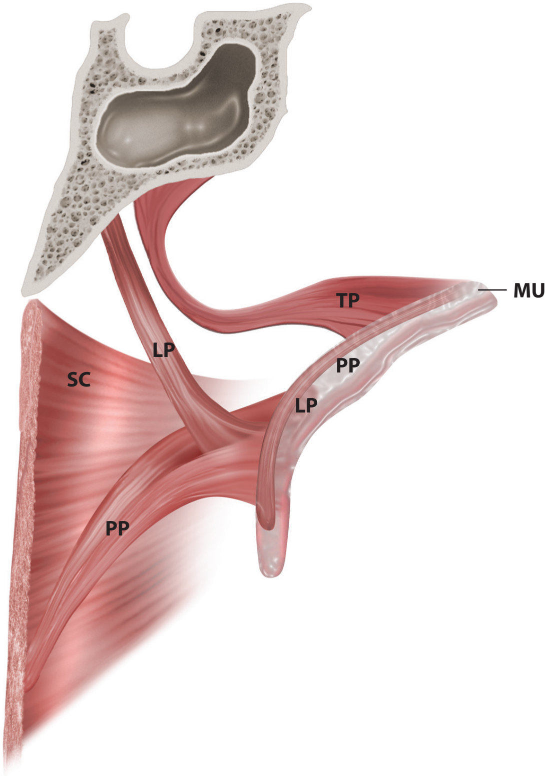

Figure 11.10 Medial view of velar muscles. LP – levator palatini. PP – palatopharyngeus. TP – tensor palatini. SC – superior constrictor. MU – muscularis uvulae.

http://e-surg.com

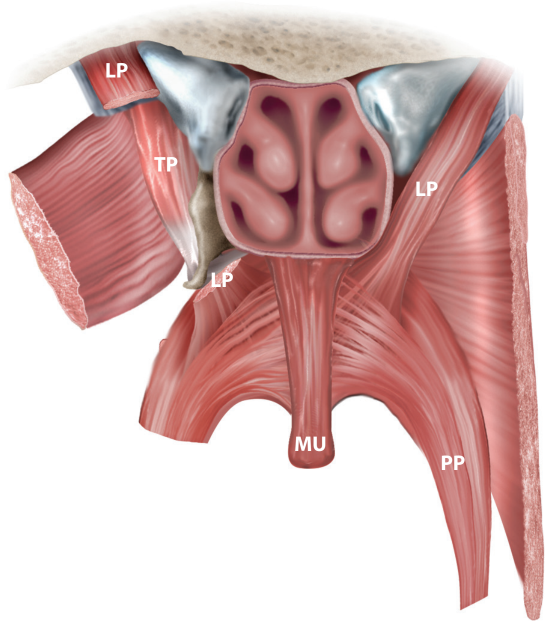

Figure 11.11 Posterior view of velar muscles. LP – levator palatini. PP – palatopharyngeus. TP – tensor palatine. MU – muscularis uvulae.

it runs down to form the posterior pillar of fauces and inserts into the thyroid cartilage and pharyngeal aponeurosis. Passavant's ridge is a prominence on the posterior wall of the nasopharynx formed by the contraction of the superior constrictor muscle of the pharynx during swallowing.

The LP muscle originates from the medial part of the Eustachian tube and from the petrous temporal bone. It runs down anteriorly and medially to enter the middle one-third of the velum between the two heads of the PP to join with its partner from the opposite side and form a "levator sling" (Figure 11.11).

The last muscle to consider is the MU, which runs anteroposteriorly from the posterior nasal spine to the uvula beneath the nasal mucosa.

The LP is the prime elevator of the velum. The PP and PG act as depressors, and all three muscles act to lengthen the velum. The function of the MU remains unknown.

Movement of both the velum and pharyngeal walls contributes to normal velopharyngeal closure. The pattern of closure differs among individuals and among different speech sounds. Closure during swallowing is much slower and occurs at a lower level in the pharynx than that which occurs during speech.

The size of the velum in relation to the depth and width of the oropharynx and the slope of the posterior pharyngeal wall determines the potential area of contact during velopharyngeal closure. This contact area includes adenoid tissue, which can make an important contribution to velopharyngeal closure. The extensibility of the velum and the capacity of the velar muscles to lift and pull the velum posteriorly creates a levator knee that presses against the pharyngeal wall and forms an airtight seal during speech and swallowing.

CLEFT PALATE ANATOMY

The isolated cleft palate extends in the midline anteriorly from the uvula up to the incisive foramen. Its extent varies from the mildest form of bifid uvula and a submucous cleft palate to a complete cleft of the hard palate and velum (soft palate) extending up to the incisive foramen. The most common presentation is a complete cleft of the velum extending into the posterior one-third of the hard palate (Figure 11.12).

The width of the cleft varies from a few millimeters up to 2 cm at the posterior margin of the hard palate (Figure 11.13). In complete clefts of the lip and palate the midline palatal cleft extends through the alveolus at the line of fusion between the premaxilla and maxilla (Figure 11.14). In complete unilateral

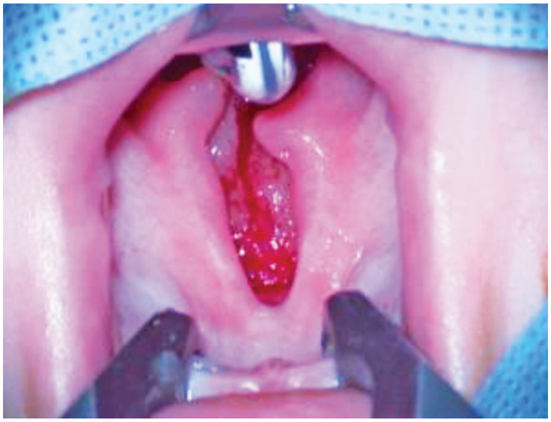

Figure 11.12 Cleft palate – complete cleft of soft and partial hard palate.

http://e-surg.com

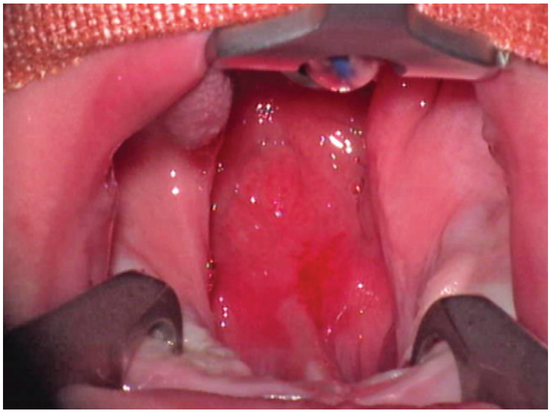

Figure 11.13 Cleft palate – *U*-shaped complete cleft of hard and soft palate.

cleft lip and palate the alveolar cleft is on one side only and divides the maxilla into lesser and greater segments. In complete bilateral clefts of the lip and palate the nasolabial muscle ring is completely disrupted and is unable to exert any control over premaxillary growth. The premaxilla protrudes anteriorly and rotates superiorly often to a dramatic degree (Figure 11.15).

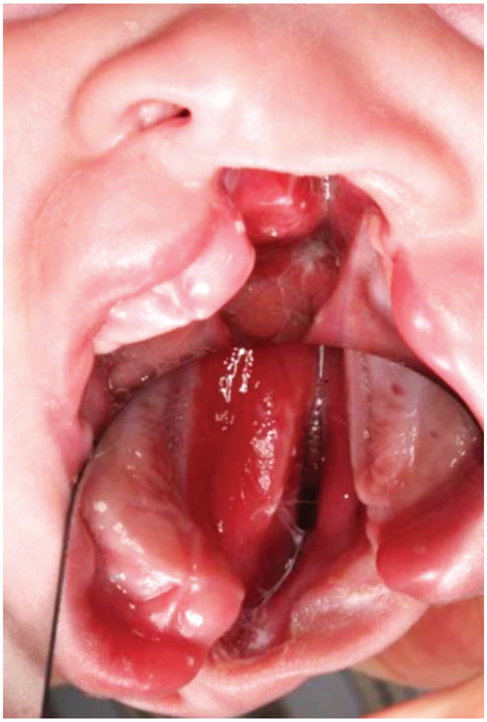

Figure 11.14 Complete unilateral cleft lip and palate.

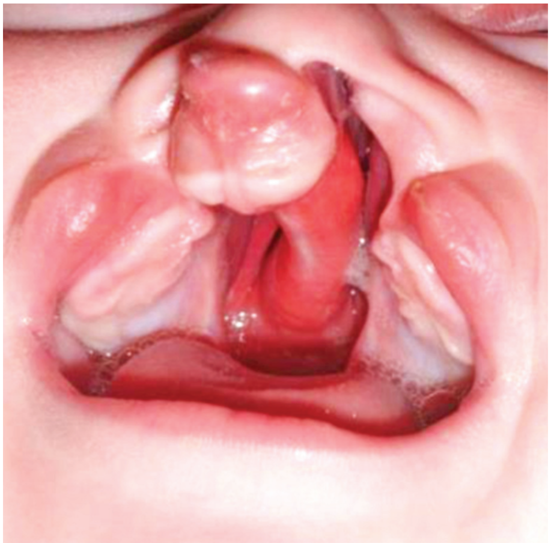

Figure 11.15 Complete bilateral cleft lip and palate.

The velar cleft muscle deformity was first described by Veau and has since been elaborated on by several authors. In cleft palate the tensor aponeurosis is thickened into a fan shape that inserts into the lateral part of the posterior edge of the hard palate. The LP and PP are unable to meet in the midline and run forward to insert into the medial part of the posterior edge of the hard palate as well as into the edge of the contracted aponeurosis (Figure 11.16).

A submucous cleft palate is characterized by a midline diastasis of the muscle sling in the presence of intact palatal mucosa. It is associated with a bifid uvula and absence of the posterior nasal spine. Varying degrees of muscle abnormality can occur, ranging from a mild diastasis to a complete midline dehiscence with absence of the muscularis uvulae.

HARD PALATE REPAIR

Traditional methods of closure involve transposition of either bipedicled flaps (Langenbeck) or axial flaps based on the greater palatine vessels (Veau flap). It is now recognized that scars formed by leaving areas of exposed bone in the hard palate,

http://e-surg.com

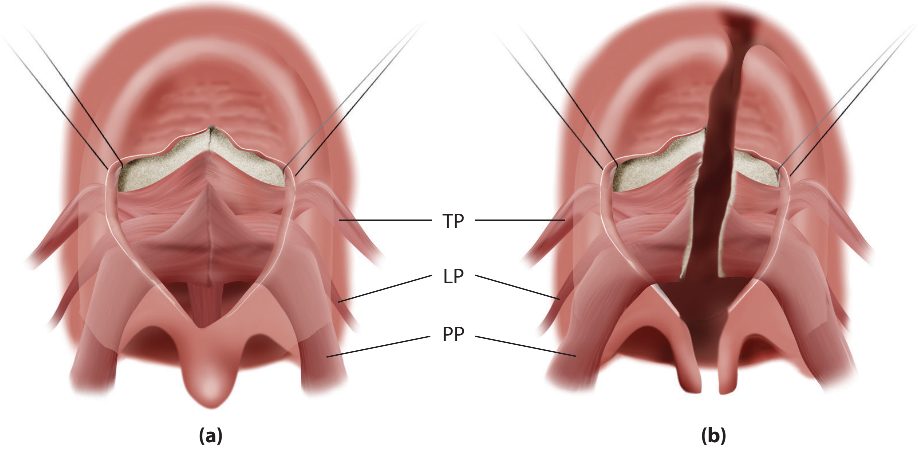

Figure 11.16 Cleft palate muscles. **(a)** Normal anatomy. **(b)** Cleft muscle anatomy. LP – levator palatini. PP – palatopharyngeus. TP – tensor palatine.

especially the anterior and lateral margins of the palate, have the potential to inhibit both anterior and transverse growth of the maxilla.

The use of a vomer flap to repair the hard palate cleft was first described by Pichler in 1926 and has now become a well-established method of palate repair. It can be used as a single-layer closure for the cleft alveolus and hard palate. The periosteal surface of the flap is transposed to the palatal side where it becomes epithelialized, leaving a large part of the vomer exposed to heal by secondary intention. Alternatively, it can be used as part of a two-layer closure. In bilateral clefts, vomer flap repair is usually performed one side at a time with an interval of 6-8 weeks to avoid compromising the vascular supply to the isolated premaxilla. Current evidence shows that use of the vomer flap causes only minimal growth disturbance.

SOFT PALATE REPAIR

The first step in muscle repair of the cleft velum is to separate the abnormal attachment of the aponeurosis and muscles from the posterior edge of

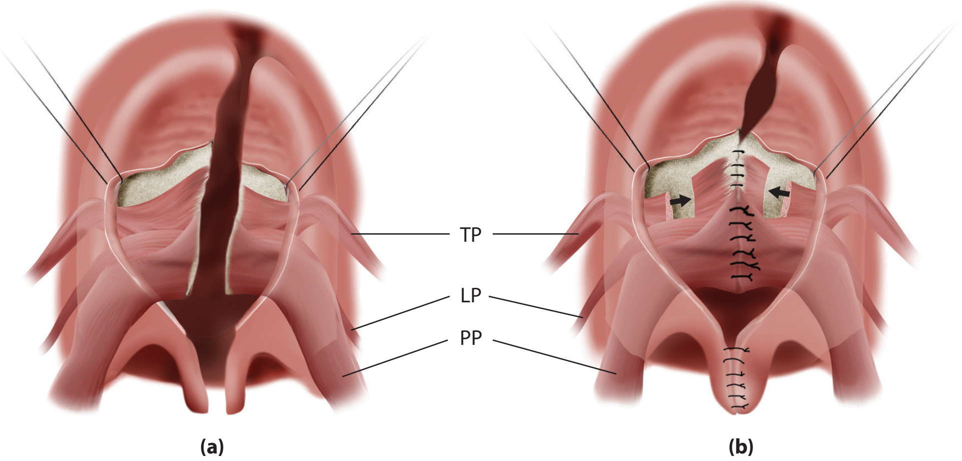

Figure 11.17 Cleft palate muscles repaired. **(a)** Cleft palate muscle anatomy. **(b)** Repaired cleft palate muscles. LP – levator palatini. PP – palatopharyngeus. TP – tensor palatine.

http://e-surg.com

the hard palate. The muscles are then dissected from their attachment to the nasal and oral mucosa and reorientated to a varying degree. In the most radical approach, the LP muscles are dissected off the nasal mucosa and united in the midline just in front of the base of the uvula (Figure 11.17). There is now evidence to support the view that more radical muscle dissection using the operating microscope improves velar function.

FURTHER READING

Birch M. Sommerlad BC, Bhatt A. Image analysis of lateral velopharyngeal closure in repaired cleft palates and normal palates [erratum appears in *British Journal of Plastic Surgery*. 1995 Apr; 48(3): 178]. *British Journal of Plastic Surgery*. 1994; 47(6): 400–5.

Boorman JG, Freelander E. Surgical anatomy of the velum and pharynx. In: *Recent Advances in Plastic Surgery 4*. Edinburgh: Churchill Livingstone, 1992; Ch. 2:17–28.

Carinci F, Pezzetti F, Scapoli L, Martinelli M, Avantaggiato A, et al. Recent developments in orofacial cleft genetics. *Journal of Craniofacial Surgery*. 2003; 14: 130–43.

Ferguson MWJ. Developmental mechanisms in normal and abnormal palate formation with particular reference to the artiology, pathogenesis and prevention of cleft palate. *British Journal of Orthodontics*. 1987; 8: 115–37.

Finkelstein Y, Berger G, Nachmani A, Ophir D. The functional role of the adenoids in speech. *International Journal of Pediatric Otorhinolaryngology*. 1996; 34(1–2): 61–74.

Gorlin RJ, Cohen MM Jr, Hennekam RCM. *Syndromes of the Head and Neck*. 4th ed. New York: Oxford University Press, 2003.

Kerrigan JJ, Mansell JP, Sengupta N. Palatogenesis and potential mechanisms for clefting. *Journal of the Royal College of Surgeons of Edinburgh*. 2000: 45: 351–8.

Kriens O. Anatomical approach to veloplasty. *Plastic and Reconstructive Surgery*. 1969; 43: 29.

Marazita ML, Mooney MP. Current concepts in the embryology and genetics of cleft lip and cleft palate. *Clinics in Plastic Surgery*. 2004; 31: 125–40.

Malek R, Psaume J. Nouvelle conception de la chronologie et de la technique du traitement des fentes labio-palatines. *Annals de Chirurgie Plastique Esthétique*. 1983; 28: 237.

Marsh JL, Grames LM, Holtman B. Intravelarveloplasty: A prospective study. *Cleft Palate Journal*. 1989; 26: 46–50.

Oneida A, Arosarena, MD. Cleft lip and palate. *Otolaryngologic Clinics of North America*. 2007; 40: 27–60.

Pichler H. Zur operation der doppelten lippengaumenspalten. *Deutsche Zeitschrift für Chirurgie*. 1926; 195: 104.

Ross B. Treatment variables affecting facial growth in complete unilateral cleft lip and palate. Part 7: An overview of treatment and facial growth. *Cleft Palate Journal*. 1987; 24: 71–7.

Semb G, Borchgrevink H, Saelher IL, Ramsted T. *Multidisciplinary Management of Cleft Lip and Palate in Oslo, Norway*. In: *Multidisciplinary Management of Cleft Palate*. Eds. Bardach J, Morris HL. Philadelphia: WB Saunders, 1990: 27–37.

Stanier P, Moore GE. Genetics of cleft lip and palate: Syndromic genes contribute to the incidence of non-syndromic clefts. *Human Molecular Genetics*. 2004; 13: 73–81.

Sommerlad BC. A technique for cleft palate repair. *Plastic and Reconstructive Surgery*. 2003; 112(6): 1542–8.

Sykes JM, Senders CW. *Facial Plastic Surgery: Cleft Lip and Palate, Volume 9*. New York: Thieme Medical Publishers, 1993.

Sykes JM, Tollefson TT. Management of the cleft lip deformity. *Facial Plastic Surgery Clinics of North America*. 2005; 13: 157–67.

Veau V. *Division Palatine*. Paris: Masson, 1931.

http://e-surg.com

PART 4

12 Orbital skeleton 111
Barrie T. Evans and Simon Holmes
13 Orbital contents and periorbita 119
Antony Tyers
14 Mandible 133
Barrie T. Evans, Darryl Coombes, Peter A. Brennan and Vishy Mahadevan
15 Maxilla and zygoma 141
Barrie T. Evans, Darryl Coombes, Vishy Mahadevan and Peter A. Brennan
16 Infratemporal fossa, pterygopalatine fossa and muscles of mastication 151
Barrie T. Evans
17 Temporomandibular joint 167
Andrew J. Sidebottom

http://e-surg.com

http://e-surg.com

12

Orbital skeleton

BARRIE T. EVANS AND SIMON HOLMES

Introduction 111
Average orbital measurements 111
Globe position 112
Orbital position 112
Orbital margin/rim 114
Orbital roof 114
Medial wall 115
Orbital floor 116
Lateral wall 117
Superior orbital fissure 117
Further reading 118

INTRODUCTION

The orbit contains and protects the globe and the visual apparatus. It is described as a quadrilateral pyramid with the base projecting forwards and laterally with the apex postero-medial between the optic foramen and the medial end of the superior orbital fissure. The periorbita adheres loosely to the bones of the orbit except at the orbital rim, the sutures, fissures and foramina and is readily lifted by both tumours and infection, offering little resistance to either. The medial orbital walls are parallel to each other whilst the lateral walls are at an angle of 45 degrees to the medial walls. If the lateral orbital walls are traced posteriorly they intersect at an angle of 90 degrees in the middle fossa.

AVERAGE ORBITAL MEASUREMENTS

The average measurements of the orbit in adults are as follows:

- Vertical height at the orbital rim is 35 mm.
- Width at the orbital rim is 40 mm.
- Depth measured from the rim to the optic strut (the bone between the optic foramen and the superior orbital fissure) is 45–55 mm.
- Length of the superior orbital fissure is 22 mm.
- Inferior orbital foramen is 4 mm in diameter and 7–10 mm below the inferior rim.
- Orbital volume is 30 cm^3.
- Globe volume is 7 cm^3.

These measurements vary considerably. Therefore, absolute measurements in orbital surgery cannot be relied on, particularly in relation to the location of the superior orbital fissure and optic canal (Figure 12.1).

The orbit develops around the eye and is further ‘bulged out’ by the lacrimal gland – analogous to the stimulus to the growth of the calvarium by the developing brain. An orbit in which the globe fails to develop – anophthalmia/microphthalmia – is significantly reduced in size (Figure 12.2).

The growth of the eye, complete by about the age of seven, is reflected in the tendency of the internal orbit towards a spherical shape with the maximum concavity, i.e. the widest part, being about 1.5 cm posterior to the orbital rim, corresponding to the coronal equator of the globe.

http://e-surg.com

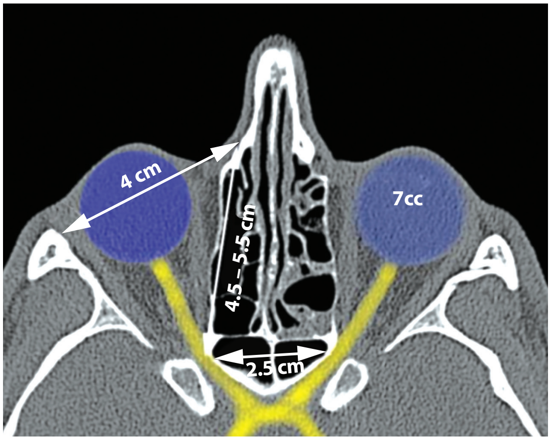

Figure 12.1 Axial view of orbit.

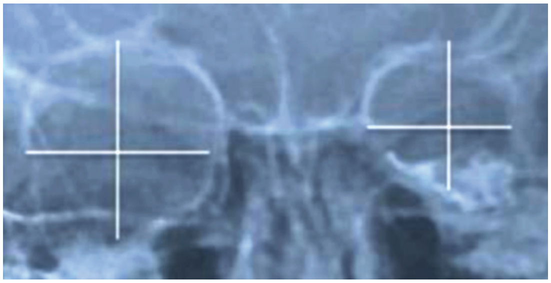

Figure 12.2 Microphthalmic left orbit.

GLOBE POSITION

The globe is placed anteriorly in the orbit to ensure the optimum field of vision, which has the disadvantage of reducing the protection afforded by the orbital walls. The globe is particularly vulnerable laterally. The lateral rim is approximately 20 mm posterior to the medial rim, and the plane between them has about half of the eye anterior to it.

The superior and medial orbital rims are anterior to the inferior and lateral rims. The adult corneal apex is 8–10 mm posterior to the superior rim and 2–3 mm anterior to the inferior rim and just reaches the plane between the two (Figure 12.3).

The shape of the visual fields reflects the influence of the orbital rims on vision, with vision being greatest laterally and inferiorly and reduced superiorly and in the nasal field.

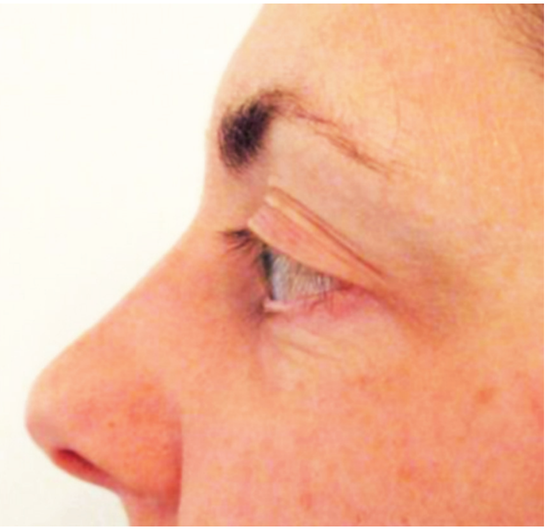

Figure 12.3 Globe protection laterally is reduced to improve the visual field. Approximately 50 per cent of the globe is anterior to the lateral orbital rim.

A compromise is made between optimal vision and globe protection (Figure 12.4).

ORBITAL POSITION

The position of the orbits determines the spatial relationship between the eyes. The distance between the orbits, usually measured from the anterior lacrimal crests, is approximately 25 mm in adults, essential for both binocular vision and conjugate eye movements. Increased separation between the orbits — malposition in the horizontal plane — is described as orbital hypertelorism or teleorbitism. Found mainly in congenital deformities, it can prevent the development of binocular single vision. Likewise, orbital dystopia, a term describing orbital malposition in the vertical plane, can interfere with conjugate gaze. Tumours, trauma or conditions such as fibrous dysplasia can also alter the position of the orbit three-dimensionally, beyond the tolerance of the neural mechanisms to achieve conjugate gaze (Figure 12.5).

http://e-surg.com

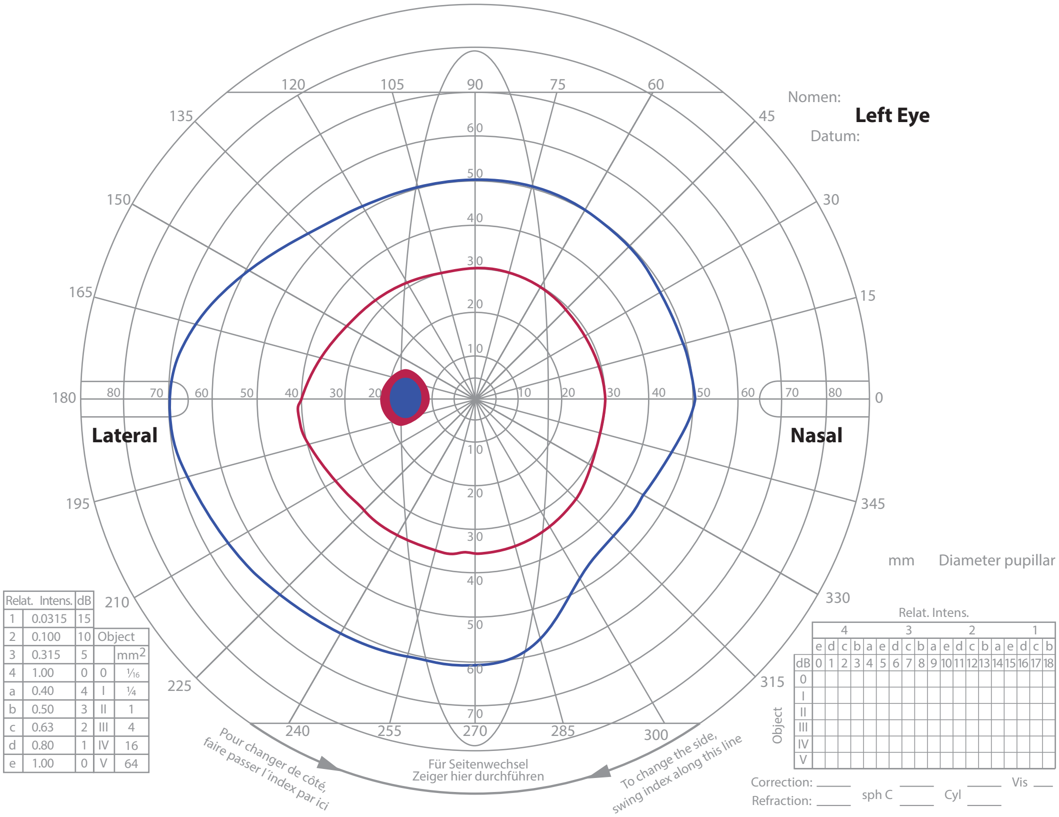

Figure 12.4 Normal visual field of the left eye.

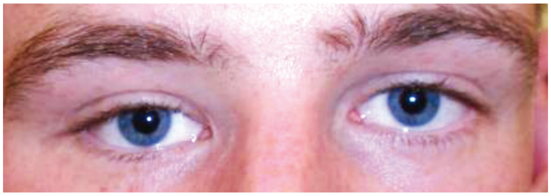

Figure 12.5 Orbital dystopia.

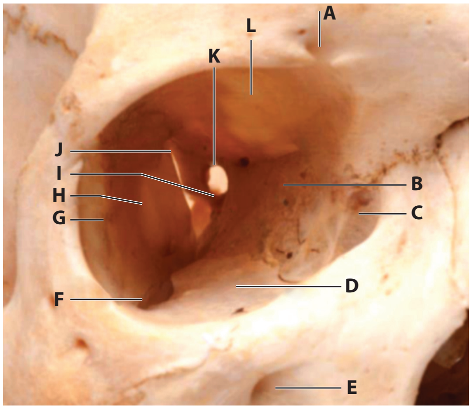

Figure 12.6 Orbital skeleton. A – supraorbital notch. B – orbital plate of ethmoid. C – lacrimal bone. D – orbital plate of maxilla (orbital floor). E – infraorbital foramen. F – inferior orbital fissure. G – sphenozygomatic suture. H – greater wing of sphenoid. I – optic strut. J – superior orbital fissure. K – optic foramen. L – orbital plate of frontal bone (orbital roof. The orbital plate of the palatine bone is shown to advantage in Figure 12.10).

The orbit is made up of seven bones (Figure 12.6):

- Maxilla.
- Lacrimal bone.
- Ethmoid.
- Sphenoid.
- Frontal bone.
- Zygoma.
- Palatine bone.

http://e-surg.com

ORBITAL MARGIN/RIM

The margin is rectangular in shape with rounded corners. The bone of the orbital rim is thicker than that of the internal bony walls and better able to resist impact.

The **superior margin** formed from the frontal bone is rounded in the medial half due to the underlying frontal sinus; the degree of pneumatization of the frontal sinus varies considerably. Laterally it has a well-defined margin strengthened by the angular process immediately superior to the suture with the frontal process of the zygoma. With anteriorly directed forces the frontal sinus absorbs the impact by fracturing, reducing energy transmission to the underlying brain. The lateral aspect of the superior rim, less likely to fracture, offers little brain protection. The supraorbital notch/foramen which transmits the supraorbital neurovascular bundle is sited 25–30 mm from the midline.

The superior rim merges imperceptibly with the medial rim. The trochlear fossa is a small depression 4–5 mm posterior to the superomedial aspect of the rim – the site of the cartilaginous pulley of the superior oblique muscle. This is frequently detached with the periorbita in approaches to the orbital roof. The supratrochlear and infratrochlear neurovascular bundles and the dorsal nasal artery emerge here above the medial canthal tendon, and may be damaged with a frontoethmoid incision.

The **medial margin** is well defined at the anterior lacrimal crest, part of the frontal process of the maxilla. The strong anterior limb of the medial canthal ligament, which inserts onto the anterior crest, offers little resistance to detachment when dissecting in the subperiosteal plane. The posterior lacrimal crest, formed from the lacrimal bone, is less well defined and is the site of insertion of the deep component of the medial canthal tendon. Initial identification of the posterior crest is a useful manoeuvre to avoid inadvertent detachment of the medial canthal tendon when extending a coronal flap. The lacrimal sac fossa is between the anterior and posterior lacrimal crests.

The **inferior margin** derived from the maxilla medially and the zygoma laterally also has a well-defined margin. The inferior oblique muscle has its origin from a small, roughened area anteromedially, immediately behind the rim, just lateral to the lacrimal fossa. This muscle is frequently detached with the periorbita in approaches to the orbital floor.

The **lateral margin** is derived from the frontal process of the maxilla and the zygomatic process of the frontal bone. The fronto-zygomatic (f-z) suture is a weak articulation and fractures preferentially in zygomatic injuries. Located 10–11 mm below the f-z suture and 4–5 mm inside the lateral rim is a rounded bony elevation – Whitnall's tubercle – frequently more easily felt than seen. Several structures are attached to this tubercle:

- The lateral canthal tendon.
- Lockwood's suspensory ligament.
- The lateral horn of the levator aponeurosis.
- The check ligament of the lateral rectus muscle.

Their reattachment following lateral orbital surgery is necessary to preserve optimum aesthetics and function.

ORBITAL ROOF

Formed from the orbital plate of the frontal bone with a small contribution from the lesser wing of the sphenoid posteriorly, the orbital roof is triangular in shape and markedly concave anteriorly and flatter posteriorly. This shape must be reproduced in reconstruction of the roof.

The bone is thin and natural dehiscence can exist, necessitating care with dissection deep to the periorbita to avoid damage to the basal dura. The lacrimal fossa in the anterolateral part of the roof contains the lacrimal gland. The frontal sinus, in the superomedial orbit, can extend laterally into the lacrimal fossa and posteriorly as far as the optic canal.

The optic canal opens into the superomedial orbital apex at the junction of the roof and medial wall, and passes upwards and medially to the middle fossa medial to the anterior clinoid. It is formed from the body of the sphenoid medially, the lesser wing of the sphenoid superiorly and the optic strut from the sphenoid laterally and inferiorly. The canal is oval in shape.

http://e-surg.com

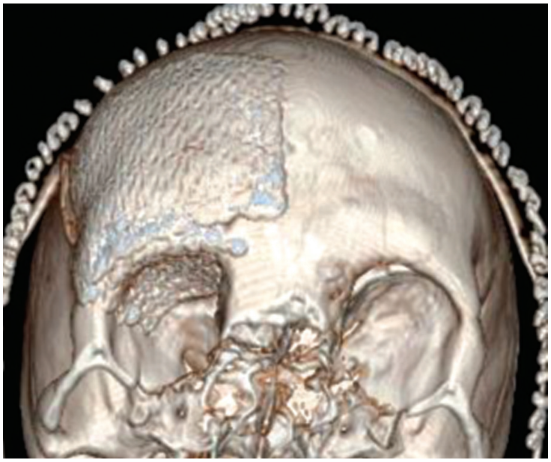

Figure 12.7 3-D CT of orbital roof reconstruction following resection of localized cranio-orbital fibrous dysplasia – convexity in lateral and A-P dimensions reproduced.

Unlike the medial wall, lateral wall and floor, vessels perforating the orbital roof are rarely encountered (Figure 12.7).

MEDIAL WALL

The medial walls, anterior to posterior, are formed from the frontal process of the maxilla, the lacrimal bone, the orbital plate of the ethmoid (lamina papyracea) and the sphenoid posteriorly. The lamina papyracea forms the majority of the medial wall. It is 'paper-thin' (0.2–0.4 mm in thickness) and although buttressed by the bony lamellae of the ethmoid sinuses, is fragile. It offers little resistance to deformation in trauma and to the spread of infection or tumours.

The fronto-ethmoid (f-e) suture line marks the junction of the medial wall and the roof. This is the level of the roof (fovea) of the ethmoid sinuses and the floor of the anterior cranial fossa. The fovea slopes down and medial to the cribriform plate. The cribriform plate can be 5–10 mm below the level of the f-e suture. Care must be exercised with bone removal and exploration medial to the f-e suture to avoid damage to the basal dura (Figure 12.8).

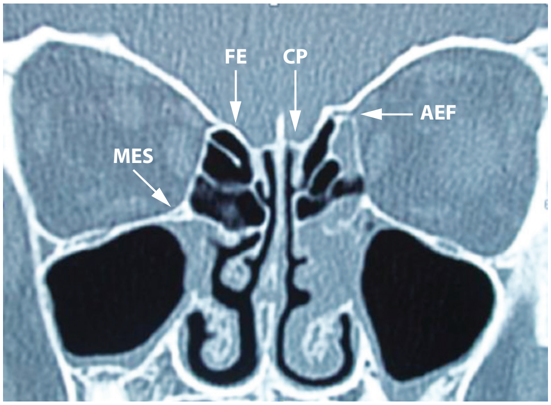

Figure 12.8 Recessed cribriform plate – inferior to the f-e suture/roof of ethmoid sinus. FE – fovea ethmoidalis. CP – cribriform plate. AEF – anterior ethmoidal foramen. MES – maxilloethmoid strut.

The inferior border of the medial wall is the suture between the ethmoid and maxillary sinuses. There is a relatively thick strut of bone – the maxilloethmoid strut – which frequently remains intact in less severe orbital trauma.

The ethmoid foramina are situated either in the f-e suture or above it and provide a guide to the height of medial orbital dissection.

The position and number of the ethmoidal foramina have been suggested as landmarks for the depth of dissection in the medial orbit and in particular the proximity of the optic canal. The aide-memoir '24-12-6 in mm' has been suggested as the distance from:

- The anterior lacrimal crest to the anterior ethmoid foramen.
- The distance between the anterior and posterior ethmoid foramina.
- The posterior ethmoid foramen to the optic canal.

These are average values at best. The distance from the posterior ethmoid foramen to the optic canal may be only 2 mm. A middle ethmoid foramen is present in between 28–33 per cent and a single ethmoid foramen may be present in 4 per cent of orbits. *The ethmoid foramina are unreliable guides of the depth of dissection* in the orbit. There are no reliable guides to the depth of dissection in the medial orbit.

By contrast, *the ethmoidal foramina and the f-e suture are valuable guides to the height of dissection*

http://e-surg.com

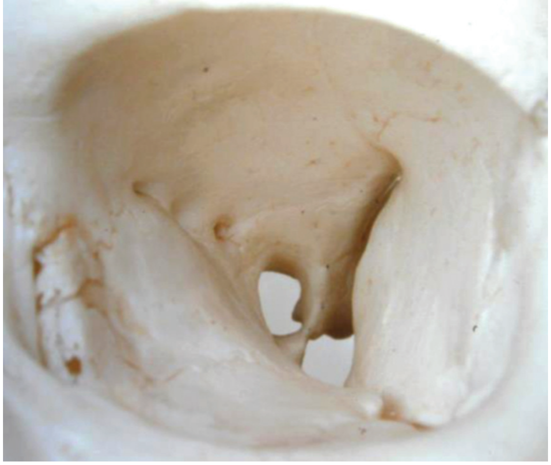

Figure 12.9 Anterior/middle/posteriorethmoid foramina at the level of the f-e suture. Note the line of the ethmoid foramina and the f-e suture leading to the upper edge of the optic canal. The bulge in the postero-medial orbital floor produced by the maxillary sinus is evident.

in the medial orbit; if traced posteriorly they lead to the upper edge of the optic canal at the junction of the roof and medial wall (Figure 12.9).

ORBITAL FLOOR

The floor of the orbit is triangular in shape and derived from three bones:

- The orbital plate of the maxilla.
- The orbital plate of the zygoma.
- The small triangular orbital plate of the palatine bone.

The major contribution to the floor is from the maxilla, which also forms the roof of the maxillary sinus. The small contribution from the zygoma is that area just anterior to the inferior orbital fissure. The orbital plate of the palatine bone also contributes little in terms of area to the floor – at the anterior margin of the inferior orbital fissure just medial to the infraorbital nerve. Its significance surgically, however, is twofold:

- It is rarely fractured with blunt trauma and therefore almost available as a surgical landmark and a 'ledge' on which to rest the material used to reconstruct the floor.
- It marks the postero-medial limit of the floor of the orbit, and reconstruction of the orbital floor cannot be taken beyond this point (Figure 12.10).

Whilst the floor merges in a gentle curve with the medial wall, there is an abrupt demarcation between the floor and lateral wall at the inferior orbital fissure which separates the floor from the lateral wall.

The inferior orbital fissure runs postero-medially and is bisected by the infraorbital neurovascular bundle running parallel to the medial wall. Lateral to the infraorbital nerve the fissure communicates with the infratemporal fossa and medial to the nerve, with the pterygopalatine fossa. The contents of the inferior orbital fissure can be safely divided as there are no critical structures that pass from either the infratemporal or pterygopalatine fossae through the fissure. The use of bipolar diathermy prior to division is helpful as branches of the inferior ophthalmic vein pass through the fissure to the pterygoid venous plexus. The infraorbital nerve must be identified and dissection medially must be superior to the nerve. Medial dissection along the inferior orbital fissure should not be taken further than the orbital plate of the palatine

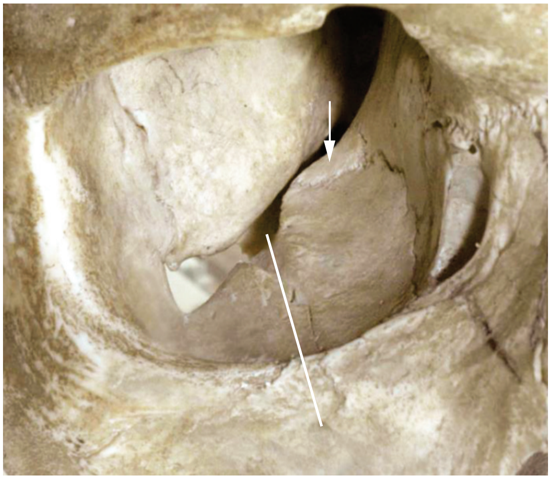

Figure 12.10 Orbital plate of the palatine bone – the posteromedial limit of the orbital floor (arrow). Course of the infraorbital nerve initially in the infraorbital groove, later the canal, parallel to the medial wall (line).

http://e-surg.com

bone in view of the proximity of the Annulus of Zinn and the inferior aspect of the superior orbital fissure.

In the anterior half of the orbital floor, the infraorbital neurovascular bundle runs in a canal from the infraorbital foramen. Further posteriorly in the orbit, the nerve runs more superficially in a sulcus immediately deep to the periorbita, to the inferior orbital fissure. In the adult the nerve is about 4.5 mm in diameter and provides a valuable soft tissue surgical landmark. Unnamed vessels arising from the infraorbital artery perforate the orbital floor in over 80 per cent of orbits – if inadvertently divided, it can cause brisk haemorrhage.

The bone of the floor is thin – 0.5–1 mm – particularly medial to the infraorbital nerve, and offers little resistance to deformation. This is the most common site for orbital blowout fractures.

The floor has a complex shape, likened to an elongated *S*. It is initially convex downwards to the point of maximum convexity about 1.5 cm from the rim and then takes a gentle upward curve to the inferior orbital fissure, medial to the infraorbital nerve. The downward convexity is produced by the growth of the eye whilst the upward and medial convexity is the result of pneumatization of the maxillary sinus. Reconstruction of this shape in three dimensions is essential if the globe position is to be restored in its original position following trauma or tumour surgery (Figure 12.11).

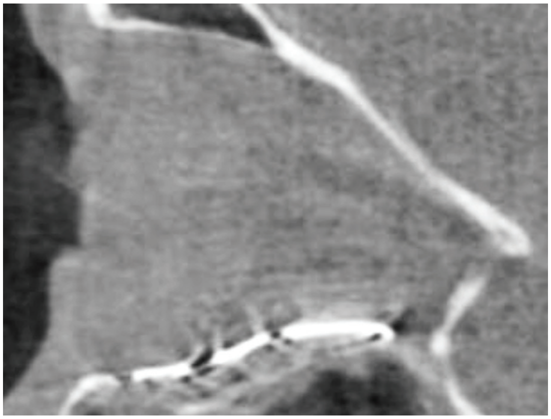

Figure 12.11 Reconstructed floor reproducing its curvilinear shape – the elongated S. The plate rests on the orbital plate of the palatine bone.

The orbital floor does not reach the orbital apex; it ends at the pterygopalatine fossa. Functionally, it ends at the posterior wall of the maxilla, marked at its most medial extent by the orbital plate of the palatine bone. The medial wall continues to the optic canal. It is questionable whether reconstruction of the medial wall needs to extend beyond the depth of the orbital plate of the palatine bone.

LATERAL WALL

The lateral is the strongest wall of the orbit. It is derived from the orbital plate of the zygoma and the greater wing of the sphenoid and bordered posteriorly by the superior and inferior orbital fissures. The greater wing of the sphenoid separates the orbit from the middle fossa and articulates superiorly with the frontal bone at the sphenofrontal suture.

The thickness of the greater wing in the lateral wall varies and is thinnest at its articulation with the zygoma anteriorly – the sphenozygomatic (s-z) suture. The zygoma fractures preferentially through this suture and the adjacent f-z suture. The central triangular 'trigone', very evident in axial computerized tomography (CT) images, is the strong central buttress; displaced fractures of the trigone are uncommon. The greater wing then thins out again at the inferior margin of the superior orbital fissure (Figure 12.12).

The zygomatico-facial and temporal neurovascular bundles exit the orbit separately through the orbital plate of the zygoma to supply the skin over the zygomatic (cheek) prominence and the temple. Both are readily identified in lateral orbital dissection deep to the periosteum; they should be coagulated prior to division. An inconstant vessel – present in about 40 per cent of orbits – is the recurrent meningeal branch of the ophthalmic artery and exits from the lacrimal foramen (foramen meningo-orbitale) immediately anterior to the superior orbital fissure.

SUPERIOR ORBITAL FISSURE

Approximately 22 mm in length, the superior orbital fissure's (SOF) superior margin is derived from the lesser wing of the sphenoid, the anterior

http://e-surg.com

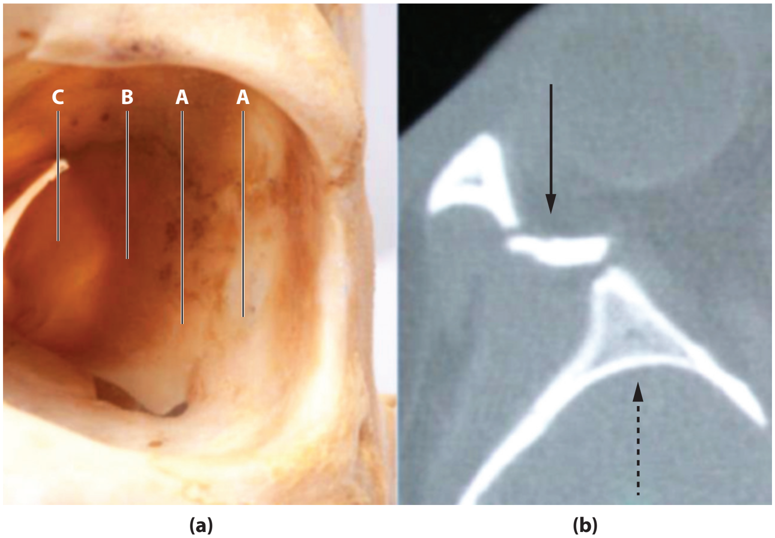

Figure 12.12 **(a)** A – thinner bone at the sphenozygomatic suture. B – thicker bone at the central buttress ('trigone'). C – orbital plate of the sphenoid thinner at the superior orbital fissure. **(b)** Fracture of the thinner bone in the region of the sphenozygomatic suture (solid arrow). The trigone remains intact (dashed arrow).

clinoid process and the optic strut medially. The annulus of Zinn (annular tendon/common tendinous origin) from which the rectus muscles arise divides the SOF into medial and lateral compartments. The lateral compartment transmits the lacrimal, frontal and trochlear nerves, which pass outside the annulus to the extraconal space of the orbit. The superior and inferior division of the oculomotor nerve, the naso-ciliary nerve, the sympathetic nerves to the orbit, the abducens nerve and the superior ophthalmic vein pass through the annulus and therefore the intraconal space.

FURTHER READING

Downie IP, Evans BT, Mitchell BS. Perforating vessel(s) of the orbital floor: A cadaveric study. *British Journal of Oral and Maxillofacial Surgery*. 1993; 31(2): 87–8.

Downie IP, Evans BT, Mitchell BS. The third (middle) ethmoidal foramen and its contents: An anatomical study. *Clinical Anatomy*. 1995; 8: 149.

Dutton J. *Atlas of Clinical and Surgical Orbital Anatomy*. London: Elsevier, 2011.

Evans BT, Webb AA. Post traumatic orbital reconstruction: Anatomical landmarks and the concept of the 'deep orbit.' *British Journal of Oral and Maxillofacial Surgery*. 2007; 45(3): 183–9.

Janfanza P, Nadol JB, Galla RJ, Fabian RL, Montgomery WW. *Surgical Anatomy of the Head and Neck*. Philadelphia: Lippincott Williams & Wilkins, 2001.

Rootman J, Stewart B, Goldberg RA. *Orbital Surgery – A Conceptual Approach*. Philadelphia: Lippincott-Raven Publishers, 1995.

Wagner A, Schneider C, Lagogiannis G, Hollman K. Pulsatile expansion therapy for orbital enlargement. *International Journal of Oral and Maxillofacial Surgery*. 2000; 29: 91–5.

http://e-surg.com

13

Orbital contents and periorbita

ANTONY TYERS

Surface anatomy of the eyelids 119
Orbicularis oculi muscle 119
Tarsal plates 120
Medial and lateral canthal tendons 121
Orbital septum 122
Eyelid lamellae 122
The eye 122
Rectus muscles and the muscle cone 123
Oblique muscles 124
Actions of the rectus and oblique muscles 124
Orbital connective tissue 125
Orbital fat 125
Levator palpebrae superioris muscle 125
Müller's muscle 125
Whitnall's ligament and the superior suspensory ligament of the fornix 125
Lower lid anatomy and Lockwood's ligament 126
Nerves of the orbit 126
The optic (second cranial) nerve 126
The oculomotor (third cranial) nerve 127
The trochlear (fourth cranial) nerve 127
The abducens (sixth cranial) nerve 127
Ophthalmic division of trigeminal (fifth cranial, V^1) nerve 127
Maxillary division of trigeminal (fifth cranial, V^2) nerve 128
The facial (seventh cranial) nerve 128
Blood supply to the orbit and lids 128
Arteries 128
Veins 130
Lacrimal system 130

SURFACE ANATOMY OF THE EYELIDS

The upper and lower eyelids enclose the palpebral aperture and join at the medial and lateral canthi. The palpebral aperture is about 30 mm horizontally in an adult and 10 mm vertically. The lateral canthus is acute, and the medial canthus is rounded and separated from the eye by a small bay, the tear lake (lacus lacrimalis), in which are a rounded elevation, the caruncle, and a vertical fold, the plica semilunaris. The caruncle contains sweat and sebaceous glands. The plica is the remnant of the third eyelid of lower animals.

The delicate skin of the upper lid has a crease 6–10 mm from the lid margin formed by the aponeurosis of the levator palpebrae superioris inserting into the orbicularis muscle at this level. This crease is usually not visible due to the redundant skin overlapping it. The upper lid may be approached through an incision in the skin crease, healing with minimal scarring. A similar crease exists in the lower lid about 5 mm from the lid margin.

Orbicularis oculi muscle

Deep to the skin and extending peripherally beyond the orbital rims is the orbicularis oculi muscle

http://e-surg.com

(Figure 13.1). This muscle is the main protractor of the eyelids. It is a thin sheet of concentric fibres surrounding the palpebral aperture and is divided into a *palpebral part*, which is subdivided into fibres lying anterior to the tarsal plates (pretarsal part) and fibres anterior to the septum (preseptal part), and an *orbital part*, lying over the orbital rims.

Innervated by the temporal and zygomatic branches of the facial nerve, which enter on their deep aspect, the palpebral and orbital components have separate antagonist muscles. Gentle lid closure is produced by the palpebral part, opposed by the levator palpebrae superioris. Forcible lid closure is produced by the orbital part, partly opposed by the frontalis muscle, which also draws down the eyebrow.

Deep to the orbicularis muscle are the tarsal plates and canthal tendons, within the lids, and the orbital septum peripheral to this, extending to the orbital rims.

Tarsal plates

The tarsal plates (Figure 13.2) maintain the shape of the lids. They are dense fibrous tissue structures about 29 mm long and 1 mm thick. The height of the superior tarsal plate is 11 mm and the inferior is 5 mm. The tarsal plates are suspended from the rims of the orbit by the medial and lateral canthal tendons (palpebral ligaments). Each tarsus contains 20–25 Meibomian glands, long sebaceous glands which empty onto the tarsal borders. Posteriorly, densely adherent conjunctiva lines the tarsal plates. It is reflected at the conjunctival fornices and reaches the globe to be inserted around the cornea at the limbus.

http://e-surg.com

Medial and lateral canthal tendons

The *lateral canthal tendon* (Figure 13.3) has fibrous and muscular components. The fibrous component forms as a *Y*-shaped thickening in the orbital septum. It joins the lateral ends of the tarsal plates to Whitnall's tubercle, a bony prominence 5 mm posterior to the lateral orbital rim. The muscular component is formed by the palpebral parts of the orbicularis muscle from the upper and lower lids. These arise from a raphe attached to the fibrous component. Lateral cantholysis, i.e. detachment of the lateral canthal tendon from the lateral orbital rim, can be used to reduce intraorbital pressure when retrobulbar haemorrhage or retroseptal infections place vision at risk. Detachment of the inferior limb of the tendon can form part of the transconjunctival approach to the orbital floor.

The medial canthal tendon (Figure 13.4) is a more complex structure. It also has muscular and fibrous components but, unlike the lateral canthal tendon, it has distinct superficial and deep insertions. The superficial fibrous and muscular part of the tendon inserts onto the anterior lacrimal crest; it has a well-defined inferior border, but the superior border blends with the periosteum. The deep fibrous and muscular part of the tendon originates from the deep surface of the anterior tendon just lateral to the anterior lacrimal crest and passes posteriorly, lateral to the lacrimal sac, to be inserted onto the posterior lacrimal crest. Contraction of the orbicularis muscle during blinking aids tear drainage.

The medial canthal tendon can be displaced in both blunt and penetrating injuries – 'traumatic telecanthus'. Its correct repositioning in three dimensions is essential for both cosmesis and function. Lateral displacement of the medial canthal tendon can result in epiphora – 'tearing' – due to malposition of the lacrimal puncta of the lower and upper lids. The intercanthal distance, about 32 mm in Caucasian adults, is about half the interpupillary distance. It varies with age, sex and race. For cosmesis, symmetry of the canthal position is perhaps more significant than the absolute distance. In the restoration of normal medial canthal

http://e-surg.com

position when the ligament has been detached from the bone of the medial orbit, it is essential to reattach it to the posterior lacrimal crest. Failure to do so can result in the lower lid being drawn away from contact with the globe, creating a hollow behind the medial end of the lower lid.

Orbital septum

The orbital septum is attached to the rim of the orbit at a thickened band of periosteum, the arcus marginalie. It follows the orbital rim below, laterally and above, bridges the supraorbital notch and follows the posterior lacrimal crest medially, and then passes forward in contact with the lacrimal sac fascia to the anterior lacrimal crest to regain the inferior orbital rim.

From its peripheral attachments it extends centrally into the lids immediately behind the orbicularis muscle. In the lower lid it inserts into the inferior border of the tarsal plate, but in the upper lid it inserts into the levator aponeurosis as it approaches the skin crease (see Figures 13.5 and 13.6). This prevents the septum from reaching the upper tarsal plate. The septum prevents infection spreading from the skin to the orbit and vice versa. Infection posterior to the septum is termed orbital cellulitis.

The intact orbital septum effectively converts the orbit into a closed space. Increase in the retroseptal orbital contents either acutely in infection or haemorrhage, or chronically with tumours or thyroid eye disease, will result in forward displacement of the globe and stretching or compression of the optic nerve, potentially compromising its circulation and threatening vision.

Eyelid lamellae

Eyelid anatomy is conveniently divided into two anatomical lamellae: the anterior lamella is the skin and the orbicularis muscle; the posterior lamella is the tarsal plate and the conjunctiva. The lamellae join at the grey line, visible along the border of each lid. Lashes arise from follicles within the margin of the anterior lamellae. The concept of eyelid lamellae is fundamental to understanding lid anatomy and reconstruction.

The eye

The adult eye, fully developed by about the age of 7 years, is a 7 cc sphere about 23–24 mm in diameter, suspended by the periocular soft tissues in the anterior orbit. The anterior one-sixth of the eye is

http://e-surg.com

the transparent cornea; the remainder is the tough, opaque sclera.

The visual axis of each eye is directed forward, parallel to the opposite eye and to the medial orbital walls. The eyes are kept straight by neural mechanisms that analyse the images from each eye and fuse them to eliminate double vision. The visual axis deviates from the orbital axis – the plane midway between the medial and lateral orbital walls – by an angle of approximately 23 degrees. Disruption of the visual axis by trauma or tumour can result in double vision – diplopia. Loss of vision in one eye results in the eye drifting laterally towards the orbital axis.

The anterior one-sixth of the eye, the cornea is termed the anterior segment. The remainder, the sclera, is the posterior segment. The cornea and the sclera meet at the limbus. The anterior segment is subdivided into an anterior chamber, anterior to the iris, and a posterior chamber, posterior to the iris.

The eye has three layers: the outer coat is the cornea and sclera; the middle layer is the uveal tract which includes the iris anteriorly, the ciliary body behind the iris and the choroid posteriorly; the inner layer is the retina which lines the eye behind the ciliary body.

The ciliary body contains the circumferential ciliary muscle, from which the lens is suspended 360 degrees by fine zonular fibres to allow focussing, and the ciliary processes, responsible for making aqueous humour. The main volume of the eye, between the retina and the lens, is filled with a fine gel, the vitreous humour. The normal intraocular pressure is 10–20 mm Hg and is firm to the touch. A ruptured eye offers no resistance and may be partly collapsed.

Nerve fibres from the rods and cones of the retina stream centrally to the optic disc, 3.5 mm medial to the posterior pole of the eye. The optic nerve passes back and medially for about 25 mm to the optic foramen at the apex of the orbit. As the nerve enters the optic canal it passes through a circular fibrous ring, the Annulus of Zinn, or common tendinous ring, which encircles the foramen, bridging the medial end of the superior orbital fissure and giving origin to the four rectus muscles.

Rectus muscles and the muscle cone

The four rectus muscles (Figure 13.7) are about 40 mm long. From their origin from the annulus they pass forward close to the four walls of the orbit to insert into the sclera of the eye behind the cornea at a distance of 5.5 mm (medial), 6.5 mm (inferior), 6.9 mm (lateral) and 7.6 mm (superior). They form a cone of muscles, creating an anatomical space, the intraconal space, with the eye anterior and the

http://e-surg.com

tendinous ring posterior. This space contains fat, the intraconal fat, which separates the optic nerve from the rectus muscles. It also transmits nerves and blood vessels to the eye. Outside the muscle cone extraconal fat separates the rectus muscles from the walls of the orbit.

Fascial sheets between adjacent rectus muscles strengthen the walls of the muscle cone, especially anteriorly. Fascia also encloses the rectus muscles and extends anteriorly around the eye as far as the cornea. This fascia is known collectively as Tenon's capsule.

Oblique muscles

Two additional muscles contribute to movement of the eyes. These are the obliques (Figure 13.8).

The *superior oblique muscle* arises from the bone just above the optic foramen, passes forward along the junction of the medial wall and roof of the orbit to become a rounded tendon at the trochlea, a U-shaped pulley of fibrocartilage attached to the frontal bone just within the orbital rim. The tendon passes through the trochlea and is directed back and laterally, between the superior rectus muscle and the eye, to insert into the superior postero-lateral quadrant of the eye.

The *inferior oblique muscle* arises from the anterior medial floor of the orbit – the only extraocular muscle to arise from the anterior orbit – just lateral to the nasolacrimal duct. It passes back and laterally, at a similar angle to the superior oblique tendon, passes inferior to the inferior rectus muscle and inserts into the inferior postero-lateral quadrant of the eye.

Actions of the rectus and oblique muscles

The medial and lateral rectus muscles attach symmetrically to the eye, producing pure medial movement, *adduction,* and lateral movement, *abduction*, respectively.

The superior and inferior rectus muscles do not simply elevate and depress the eye. They approach the eye from the orbital apex at an angle of 23 degrees to the optical axis and have more complex actions on eye movement, which depend on the position of gaze of the eye. In *abduction* the pull of the superior and inferior rectus muscles is along the axis of the eye, and they act as a simple elevator or depressor, respectively. In *adduction* the pull of the muscles is across the axis of the eye so that the action to elevate or depress is weaker but a rotation of the eye is introduced: the superior rectus rotates the eye inwards (intorsion), and the inferior rectus rotates the eye outwards (extorsion). In the primary position the superior and inferior rectus muscles have a composite action to elevate or depress as well as intort or extort the eye.

The pull of the oblique muscles is directed anteriorly and medially towards the front of the orbit medially so their actions also depend on the position of gaze of the eye. In *adduction* the superior oblique action is along the axis of the eye so it acts as a simple depressor of the eye. Similarly, the inferior oblique acts as a simple elevator. In *abduction* the pull of the obliques is across the axis of the eye; the superior oblique acts to intort the eye and the

http://e-surg.com

inferior oblique acts to extort. In the primary position each muscle has a composite of both actions.

Pure elevation of the eye from the primary position is produced by the superior rectus acting jointly with the inferior oblique. Pure depression from the primary position is produced by the inferior rectus acting with the superior oblique.

In practice none of the muscle actions work independently. Movement and coordination of the eyes is collaboration between all six muscles acting on each eye and the muscles moving the opposite eye.

Orbital connective tissue

The structures of the orbit are supported by a complex meshwork of delicate connective tissue septa elaborated by Koorneef. This system of interlocking septa, which effectively link the various orbital components, is well formed in the anterior orbit but is weaker posteriorly. As a result, although the moving structures within the orbit appear to act independently, the septa communicate the effect of each muscle, and the structures it moves, to all adjacent structures. Excessive movement is limited by the extensive septal attachments to the orbital walls.

Orbital floor fractures illustrate this complex arrangement. The inferior rectus and oblique muscles are not often themselves trapped within the fracture, but the septa joining the muscles with the prolapsed floor periosteum limit their action.

Orbital fat

The boundaries of the muscle cone divide the orbital fat into two parts: the intraconal fat and the extraconal fat. The intraconal fat is exposed by surgery in the intraconal space. The extraconal fat is frequently seen in lid surgery such as blepharoplasty. The orbital fat helps maintain the position of the globe.

In the upper lid there are two fat pads: a smaller medial fat pad and a larger central or preaponeurotic fat pad. These fat pads are separated by a fascial septum in the region of the trochlea. The lacrimal gland lies lateral to the preaponeurotic fat pad.

In the lower lid there are also two fat pads. The larger medial fat pad is often subdivided into two smaller collections by a septum in the region of the inferior oblique muscle origin. Care must be taken not to damage the inferior oblique muscle during reduction of this fat pad at blepharoplasty. The smaller lateral fat pad is separated from the medial fat pad by a fascial septum.

Levator palpebrae superioris muscle

The levator palpebrae muscle arises just above the optic foramen and passes forward between the superior rectus muscle and the roof of the orbit (see Figure 13.5). About 10 mm behind the orbital septum, it ends in an aponeurosis which descends into the lid. It spreads out to form medial and lateral ‘horns’, which attach close to the canthal tendons (see Figure 13.2). The lateral horn indents the anterior surface of the lacrimal gland which winds around its posterior border. The aponeurosis then descends further to insert into the lower anterior part of the tarsal plate. It slips forward into the orbicularis muscle at about the level of the top of the tarsal plate; these form the skin crease. The orbital septum inserts into the aponeurosis about 4 mm superior to the tarsus.

The levator is innervated by the superior division of the oculomotor nerve which enters the muscle at the junction of its middle and posterior thirds.

Müller’s muscle

Müller’s muscle arises from the inferior surface of the levator muscle close to the origin of the aponeurosis. It descends beneath the aponeurosis to insert into the superior border of the tarsal plate. It is a smooth muscle, innervated by sympathetic fibres, which travel with local arteries.

Whitnall’s ligament and the superior suspensory ligament of the fornix

On its upper surface the sheath of the levator is thickened close to the origin of the aponeurosis to form Whitnall’s ligament, a white transverse band that inserts medially into the trochlea and laterally into the fascia over the lacrimal gland and the adjacent orbital wall. It can be considered analogous to Lockwood’s ligament in the lower lid. Whitnall’s ligament acts as a fulcrum to redirect the levator muscle as it descends into the lid.

http://e-surg.com

On its lower surface the sheath of the levator muscle blends with the sheath of the underlying superior rectus muscle to form a common sheath which extends forwards to support the superior conjunctival fornix.

Lower lid anatomy and Lockwood's ligament

Lower lid anatomy is similar to that of the upper lid, but the muscles are fibrous with minimal muscle – the capsulopalpebral head (see Figure 13.6). They arise from the sheath of the inferior rectus muscle and extend forward to insert into the inferior border of the lower tarsal plate. They split to enclose the inferior oblique muscle and contribute to Lockwood's suspensory ligament just anterior to it. This transverse ligament is a thickening of the fascia around the eye which helps to support the globe. It attaches to the lacrimal and zygomatic bones. The orbital septum in the lower lid inserts into the tarsal plate with the lower lid retractors.

NERVES OF THE ORBIT

The optic (second cranial) nerve

The adult optic nerve (Figure 13.9) measures about 50 mm from the optic disc to the chiasm. It is 3 mm in diameter and surrounded by arachnoid and pia mater and bathed in circulating cerebrospinal fluid as far as the eye. It is protected by an outer coat of dura mater which is continuous with the sclera anteriorly and the intracranial dura posteriorly.

Functionally there are four segments: intraocular, intraorbital, intracanalicular and intracranial. The intraocular segment measures about 1 mm in length and leaves the globe 3.5 mm medial to the macula.

The intraorbital segment, 7–8 mm longer than the distance between the optic canal and the globe, is about 25–30 mm in length with a sinuous course to the optic canal. This laxity avoids stretching with ocular movement and permits considerable proptosis without visual compromise.

http://e-surg.com

The intracanalicular segment measures about 5–6 mm, and here the nerve is most vulnerable from trauma and compression. Within the optic canal the optic nerve is accompanied, within its dural sheath, by the ophthalmic artery inferiorly. The canal passes posteriorly and medially at an angle of about 36 degrees to the sagittal plane, towards the optic chiasm with the sphenoid sinus medially. Depending on the degree of pneumatization of the sinuses, part or all of the optic canal may project into the sphenoid sinus and also into the ethmoid. The bone covering the optic nerve in the sinuses may be thin (0.5 mm) or absent – the nerve is at risk in endoscopic sinus procedures.

The intracranial segment measures about 1 cm from the optic canal to the chiasm. The chiasm is related above to the floor of the third ventricle and below to the body of the sphenoid, just in front of the pituitary fossa and gland. The internal carotid arteries are lateral.

The nasal fibres of the optic nerve decussate in the chiasm and pass back, accompanied by the temporal fibres on each side, as the optic tracts to the lateral geniculate bodies and optic radiations to end in the visual cortex within the occipital lobes. Lesions of the optic nerve affect the vision of that eye alone. Lesions posterior to the optic chiasm always affect the homonymous field of both eyes.

The oculomotor (third cranial) nerve

From its nucleus in the floor of the aqueduct in the midbrain, it passes forward in the middle fossa, lateral to the posterior clinoid, and pierces the dura to lie in the lateral wall of the cavernous sinus above the trochlear nerve (IV) and ophthalmic division of the trigeminal nerve (V^1). It divides into superior and inferior branches; both enter the orbit through the annulus lateral to the optic nerve. The superior branch supplies the superior rectus and levator muscles. The inferior branch supplies the medial and inferior rectus muscles and the inferior oblique. They enter the muscles at the junction of the middle and posterior thirds.

The trochlear (fourth cranial) nerve

The nucleus is in the floor of the aqueduct. The nerve winds around the aqueduct and decussates dorsally, then passes forward into the lateral wall of the cavernous sinus below the oculomotor nerve. It enters the orbit through the superior orbital fissure, *outside* the annulus, and passes medially above the superior rectus and levator muscle to reach the superior oblique muscle at the junction of the middle and posterior thirds.

The abducens (sixth cranial) nerve

The nucleus is in the floor of the fourth ventricle. The nerve passes forward in the floor of the middle cranial fossa, across the apex of the petrous temporal bone, and enters the cavity of the cavernous sinus, lateral to the internal carotid artery. It enters the orbit within the annulus and enters the lateral rectus muscle at the junction of the middle and posterior thirds.

Ophthalmic division of trigeminal (fifth cranial, V^1) nerve

This division (Figure 13.10) divides in the wall of the cavernous sinus into three branches, the lacrimal, frontal and nasociliary nerves, which supply all sensation to the eye, upper lid, tip of the nose, forehead and anterior scalp.

http://e-surg.com

The *lacrimal nerve* enters the orbit outside the annulus and is the most laterally placed nerve in the superior orbital fissure. It travels along the lateral wall of the orbit above the lateral rectus muscle, with the lacrimal artery to reach the lacrimal gland. It passes on to supply sensation to the lateral part of the upper lid.

The *frontal nerve* enters the orbit outside the annulus between the lacrimal and trochlear nerves. Passing forwards beneath the periosteum in the roof of the orbit, it divides into the *supraorbital* and *supratrochlear* nerves. The supraorbital nerve travels with the supraorbital artery and passes through the supraorbital notch, or foramen, at the junction of the middle and medial thirds of the superior orbital rim. It supplies the central upper lid, forehead and scalp as far as the vertex. The supratrochlear nerve travels with the supratrochlear artery above the pulley of the trochlea, and ascends over the orbital rim medial to the supraorbital nerve supplying the medial upper lid and adjacent forehead.

The supraorbital and supratrochlear vessels, critical for axial forehead and scalp flaps, are best identified by Doppler.

The *nasociliary nerve* enters the orbit through the annulus and runs medially above the optic nerve with the ophthalmic artery. Near the anterior ethmoidal foramen it divides into two terminal branches, the *anterior ethmoidal* and *infratrochlear* nerves. The anterior ethmoidal nerve enters the anterior ethmoidal foramen with the anterior ethmoidal artery, enters the anterior cranial fossa, finally terminating as the external nasal nerve, supplying the tip of the nose. The infratrochlear nerve supplies the skin of the medial angle, the root of the nose, the lacrimal sac, canaliculi and caruncle.

In its course through the orbit, the nasociliary nerve gives off two long ciliary nerves, which run forward either side of the optic nerve to pierce the posterior sclera and supply sensation to the cornea and iris.

Maxillary division of trigeminal (fifth cranial, V^2) nerve

The infraorbital nerve (ION), a terminal branch of this division, enters the orbit at the midpoint of the inferior orbital fissure. It runs forward parallel to the medial orbital wall initially in the infraorbital groove and further forward in the canal, exiting onto the face through the infraorbital foramen. It supplies sensation to the lower lid, the side of the nose and the upper lip. The ION is a valuable landmark in surgery of the orbital floor.

Within the pterygopalatine fossa, zygomatic branches from the maxillary nerve enter the orbit through the inferior orbital fissure, travel up the lateral wall and send zygomaticotemporal and zygomaticofacial branches through small foramina in the zygomatic bone to supply the anterior temple and adjacent cheek.

The facial (seventh cranial) nerve

Both the orbital and the palpebral parts of orbicularis oculi and the frontalis muscle are supplied by the facial nerve. Due to the considerable branching and intercommunications between the branches of the nerve, the temporal, zygomatic and buccal branches of the nerve all contribute to this innervation.

Paresis of the frontalis muscle results in brow ptosis. Paresis of the eyelids results in incomplete lid closure, paralytic ectropion and epiphora, placing the eye at risk of exposure.

Autonomic innervation of the orbit and the periocular ganglia – ciliary and sphenopalatine – are discussed in Chapter 16.

BLOOD SUPPLY TO THE ORBIT AND LIDS

Arteries

OPHTHALMIC ARTERY

The ophthalmic artery arising from the internal carotid artery medial to the anterior clinoid passes through the optic canal below the optic nerve and within its dural sheath (Figure 13.11). It winds laterally over the optic nerve (or under it in 15 per cent), accompanying the nasociliary nerve. It divides into the dorsal nasal and supratrochlear arteries, which supply the lateral wall of the nose and adjacent forehead. The dorsal nasal artery terminates as two or three medial palpebral arteries which form arcades

http://e-surg.com

with the lateral palpebral arteries anterior to the upper and lower tarsal plates.

The ophthalmic artery gives origin to several branches within the orbit.

CENTRAL RETINAL ARTERY

The central retinal artery arises from the ophthalmic artery close to the optic foramen, then passes forward and pierces the dura of the optic nerve about 10–15 mm behind the eye. It runs in the centre of the optic nerve, emerges within the optic disc and divides to supply the retina.

CILIARY ARTERIES

Long posterior ciliary arteries

The two long posterior ciliary arteries arise from the ophthalmic artery while it is below the optic nerve. They pierce the sclera and travel forward in the suprachoroidal space to supply the iris and ciliary body.

Short posterior ciliary arteries

These also arise from the ophthalmic artery below the optic nerve. Several branches pierce the sclera and supply the optic nerve head; others supply the choroid. Occasionally, the anastomoses around the optic nerve head (disc) give rise to a cilioretinal artery, which passes laterally from the disc as a second supply to the macula, together with the central retinal artery. When present, macular function is preserved despite occlusion of the central retinal artery.

Occlusion of the short posterior ciliary arteries causes optic disc ischaemia and oedema with severe and permanent visual loss. Giant cell arteritis is a common cause in middle age and beyond.

Anterior ciliary arteries

The anterior ciliary arteries do not arise from the ophthalmic artery but are derived from the arteries to the four rectus muscles. The branches pass along the muscle tendons to the eye and supply the anterior segment, anastomosing with the long posterior ciliaries. Occlusion of more than two anterior ciliary arteries may lead to anterior segment ischaemia with anterior uveitis and opacification of the cornea. The most common cause is strabismus surgery on more than two rectus muscles.

LACRIMAL ARTERY

The lacrimal artery arises from the ophthalmic artery lateral to the optic nerve and passes forward along the upper border of the lateral rectus muscle to the lacrimal gland. It terminates as lateral palpebral arteries which anastomose with the medial palpebral arteries (Figure 13.12).

SUPRAORBITAL ARTERY

The supraorbital artery arises above the optic nerve and winds medially around the superior rectus and levator muscles to reach the roof of the orbit. It passes forward to join the supraorbital nerve and exits through the supraorbital notch or foramen. It contributes to the blood supply of the upper lid and then passes deep to frontalis to supply the scalp.

ETHMOIDAL ARTERIES

Anterior and posterior ethmoidal vessels enter their foramina and supply the ethmoid sinuses, adjacent meninges and the anterior part of the nasal mucosa and skin.

FACIAL ARTERY

The facial artery, a branch of the external carotid artery, winds around the border of the mandible and passes upwards and forwards to end near the inner corner of the eye 8 mm medial to the inner canthus as the angular artery.

Veins

The veins in this region communicate extensively and have no valves. They can be a channel for the spread of infection.

OPHTHALMIC VEINS

The superior and inferior ophthalmic veins communicate with the veins of the face, the cavernous sinus and the pterygoid venous plexus.

The *superior ophthalmic vein* enters the orbit above the medial canthal tendon and passes through the superior orbital fissure where it enters the cavernous sinus with the *inferior ophthalmic vein*.

The *angular vein* runs with the angular artery 8 mm medial to the inner canthus, superficial to the medial canthal tendon.

LYMPHATICS

The medial ends of the upper lids and most of the lower lids drain to the submandibular nodes. The lateral ends of the lower lids and most of the upper lids drain to the preauricular nodes. The orbit has no lymphatic drainage.

Lacrimal system

LACRIMAL GLAND

The lacrimal gland is situated in the lacrimal fossa (see Figure 13.2), posterior to the orbital septum. It consists of two lobes separated by the lateral horn of the levator aponeurosis but continuous behind it. The orbital lobe occupies the lacrimal fossa in the anterior lateral roof of the orbit. The palpebral lobe, one-third the size of the orbital lobe, occupies the lateral part of the superior conjunctival fornix.

Fine ductules empty into the superior fornix, mainly from the palpebral part. Parasympathetic fibres from the sphenopalatine ganglion stimulate tear production. Blinking sweeps the tear film medially to the lacus lacrimalis.

TEAR DRAINAGE SYSTEM

The tear drainage system consists of the lacrimal puncta, canaliculi and sac, and the nasolacrimal duct.

The *puncta* are small round or oval openings, one in each medial lid margin, on a slightly elevated papilla.

The *canaliculi* pass vertically from the puncta at right angles from the lid margins for 2 mm then turn parallel to the margins and pass medially for 8–10 mm to join as a common canaliculus which is 0–5 mm long and enters the lacrimal sac on its lateral aspect, about 2.5 mm from its apex. The entry into the sac has a flap of mucosa, the valve of Rosenmuller, which can make entry of a probe difficult. Stretching the lid laterally straightens the canaliculus and reduces the effect of this valve. The canaliculi are surrounded by fibres of the orbicularis muscle which promote tear drainage with blinking.

The *lacrimal sac* is within the lacrimal sac fossa between the anterior and posterior lacrimal crests. The sac is 12–15 mm in length. It opens below into the nasolacrimal duct, which is 15–18 mm long, and drains into the inferior meatus of the nose with a fold of mucosa, the valve of Hasner. The valves at either end of the drainage system prevent air and mucus from passing up into the eye. The sac and duct slope backwards by about 15–20 degrees along a line joining the inner canthus with the first upper molar.

14

Mandible

BARRIE T. EVANS, DARRYL COOMBES, PETER A. BRENNAN
AND VISHY MAHADEVAN

The body 133
The ramus 135
The mandibular canal 137
Blood supply of the mandible 137
Growth and senescence in the mandible 137
Mandibular fractures 138
Further reading 139

The mandible is the largest and strongest bone in the face. It has a horizontally curved body with two broad rami posteriorly. The body supports the mandibular teeth within the alveolar process. The rami bear the coronoid and condylar processes with each condyle articulating with the temporal bone at the temporomandibular joint. The masticatory muscles insert into the rami and their coronoid and condylar processes.

THE BODY

The body is *U*-shaped. The two halves of the developing mandible meet in the midline at the mandibular symphysis, the site of an inconstant faint median ridge starting at about the level of the apices of the central incisor teeth. Lateral to the ridge there may exist a depression on each side – the mental fovea. Inferiorly this ridge divides to enclose a triangular mental protuberance (mental trigone) with a depressed base centrally and a raised mental tubercle on each side. The mental protuberance and mental tubercles constitute the chin (Figure 14.1).

The terminology of the mandible can be confusing with clinical terms vying with anatomical terms. The 'surgical' chin is described as extending from one mental foramen to the other. The terms *symphysis* and *parasymphysis*, whilst in common parlance in trauma literature, are not anatomical terms. The symphsis can be considered the midline, running between the mental tubercles inferiorly to between the roots of the lower central incisor teeth superiorly (Figures 14.1 and 14.4). The parasymphysis, usually referred to in the singular whilst paradoxically given a side (Figure 14.6), is the area bounded by a vertical line distal (posterior) to the canine teeth.

The anterior belly of the digastric is inserted into a rough area near the midline at the lower border of the mandible – the digastric fossa.

The mental foramen, from which the mental neurovascular bundle emerges, is below the premolar teeth. Placed midway between the upper and lower borders of the body, it opens posterolaterally in adults. Its position is variable. The (external) oblique line (ridge) commencing imperceptibly on the lateral aspect of the body posterior to the mental foramen extends to the anterior border of the ramus. This is better developed in males.

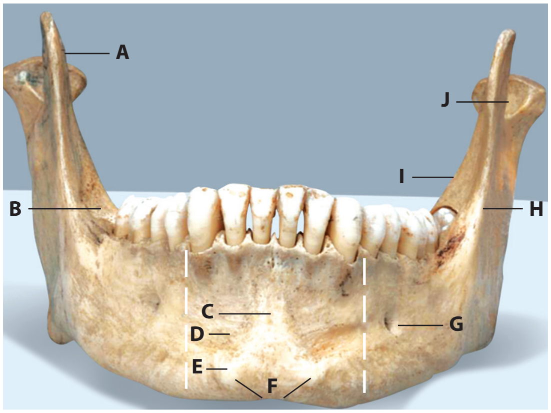

Figure 14.1 A – coronoid process. B – retromolar trigone. C – midline ridge mandibular symphysis. D – mental fovea. E – mental tubercle. F – mental protuberance. G – mental foramen. H – (external) oblique line. I – temporal crest. J – pterygoid fovea. The 'parasymphysis' is the region between the white dotted lines – the region between the distal (posterior) aspects of the canine teeth. The 'symphysis' is the midline, between the mental tubercles and the roots of the lower central incisor teeth.

As in the maxilla, there is an alveolar process, which contains the teeth and forms the dental arch. The term *basal bone* is used in dental literature to describe the mandible beneath the alveolar process – relevant in denture construction and dental implant surgery in particular. There is no demarcation between the alveolar process and the underlying basal bone of the mandible.

The mylohyoid arises from the oblique mylohyoid line on the inner aspect of the mandible. This extends from about 1 cm below the upper border behind the third molar, to the midline. It may be sharp in the molar region and cause discomfort beneath a lower denture. The relationship of mandibular dental roots above or below the mylohyoid muscle will influence the initial spread of dental infection into either the sublingual space (if above) or submandibular space (if below). The root apices of the lower molar teeth are usually below the mylohyoid. The pterygomandibular raphe arising from the pterygoid hamulus inserts into the mandible at the posterior end of the mylohyoid line. This tendinous band from which the buccinator arises anteriorly and the superior constrictor posteriorly, is visible and palpable as a vertical ridge beneath the mucosa with the mouth open, providing a landmark for the inferior alveolar nerve local anaesthetic block injection. The mylohyoid groove runs down and forward from beneath the mandibular foramen below the posterior end of the mylohyoid line and contains the mylohyoid neurovascular bundle.

The submandibular fossa, a concavity related to the deep lobe of the submandibular gland, is beneath the mylohyoid line. Incorporation of an ectopic segment of the submandibular gland into the mandible produces a characteristic well-defined lucency below the inferior alveolar canal – Stafne's bone 'cyst'/cavity. Above the line anteriorly is the sublingual fossa related to the sublingual gland. Much less frequently there may be incorporation of a portion of the sublingual gland into the lingual aspect of the mandible (Figure 14.2).

On the posterior aspect of the symphysis above the mylohyoid lines are the mental spines (genial tubercles). The upper is the attachment of the genioglossus and the lower the geniohyoid. They may be absent or simply a single small elevation when fused. Comminuted fractures of the symphysis may compromise tongue control in obtunded patients, placing the airway at risk (Figure 14.3).

Midline lingual (genial) foramina, above and/or below the genial tubercles, and lateral lingual

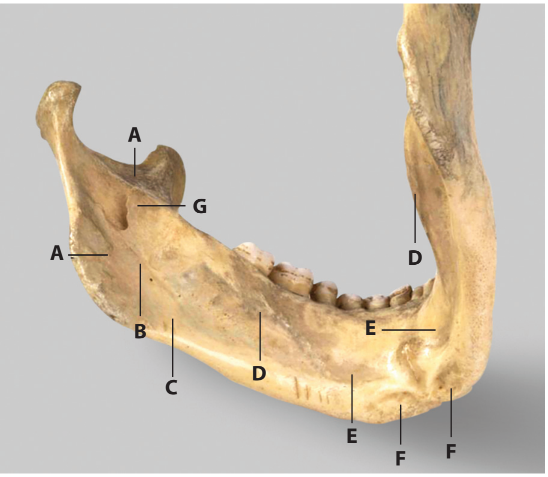

Figure 14.2 Inner (medial) aspect of mandible. A – fusion of outer and inner cortical plates above and posterior to the lingula (relevant in mandibular osteotomies). B – groove for nerve to mylohyoid. C – submandibular fossa. D – mylohyoid line. E – sublingual fossa. F – digastric fossa. G – lingula.

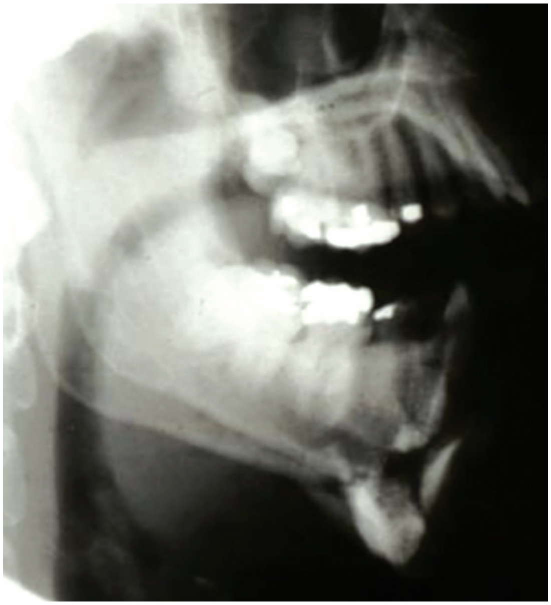

Figure 14.3 Comminuted fracture of the symphyseal region resulting in loss of tongue support with potential airway compromise in obtunded patient.

foramina in the premolar region, are present in most mandibles and are the sites of entry for vessels supplying the symphysis (see below, *Blood supply of the mandible*). A rounded elevation of compact bone, the torus mandibularis, sometimes develops above the mylohyoid line. It is most prominent in the premolar region, usually bilateral and only of clinical significance if repeatedly traumatized (Figure 14.4).

THE RAMUS

The ramus may be termed the *ascending ramus* by clinicians, notwithstanding the absence of a descending ramus.

The (external) oblique ridge is visible on its lateral aspect. The mandibular foramen, the site of entry of the inferior alveolar neurovascular canal, is midway between the anterior and posterior borders of the ramus at about the level of the occlusal surfaces of the teeth. It is overlapped anteriorly to a variable extent by spur of bone, the lingula, to which the sphenomandibular ligament is attached. The lingula is a landmark for the inferior alveolar local anaesthetic block injection. Below and behind the foramen, the mylohyoid groove runs obliquely downward and forward.

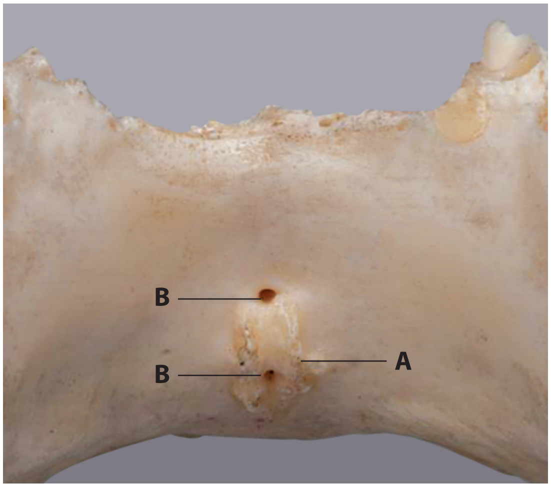

Figure 14.4 Mandibular symphysis, posterior view. A – fused genial tubercles. B – midline lingual (genial) foramina.

The term *antilingula* is used to describe an inconstant bony prominence on the lateral ramus, a supposed landmark for the mandibular foramen on the medial ramus, and has been used as such in mandibular osteotomies. There is poor correlation between the antilingula and the mandibular foramen; it is an unreliable point of reference.

The junction of the lower and posterior borders of the mandible forms the mandibular (gonial) angle. This *anatomical* angle differs from what may be termed the *surgical* angle, which is the junction between the body and the ramus at the external oblique line. The surgical angle is the angle surgeons refer to when considering mandibular angle fractures. The gonial angle is relevant in orthodontics and orthognathic surgery where the terms *high angle* and *low angle* are used. Variation exists in the gonial angle in relation to age, gender and ethnicity, and with loss of teeth. No 'angle' in terms of measurement exists in the 'surgical' angle, as this relates purely to a region (Figure 14.5).

The mandibular (sigmoid) notch (mandibular incisure) at the superior border is the depression between the coronoid process anteriorly and the condylar process posteriorly. The flat, triangular coronoid process is variable in height and its tip may be above or below the upper border of the

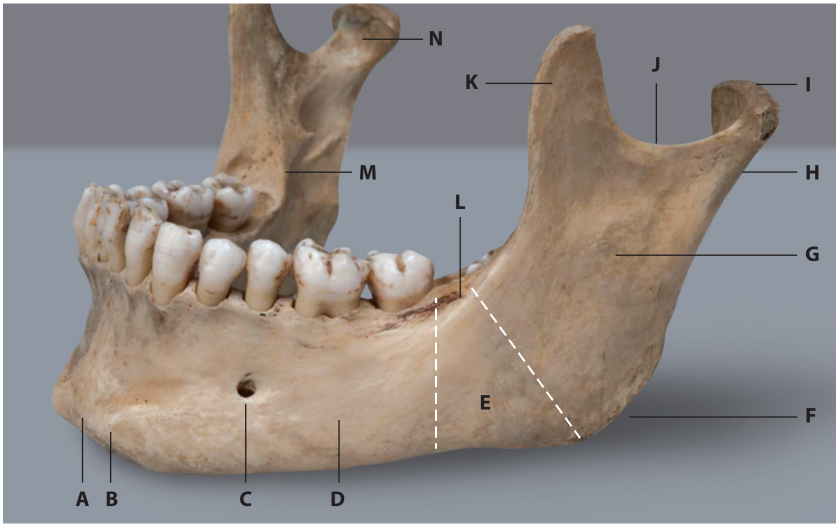

Figure 14.5 A – mental protuberance. B – mental tubercle. C – mental foramen. D – body of mandible. E – 'surgical' mandibular angle between dotted lines. F – mandibular (gonial) angle. G – ramus. H – condylar neck. I – condylar head. J – mandibular notch. K – coronoid process. L – (external) oblique line. M – temporal crest. N – pterygoid fovea.

condyle. Its anterior border is continuous inferiorly with the oblique line. The condylar process consists of the condylar neck and the head of the condyle. The pterygoid fovea is a small depression in the front of the condylar neck into which fibres of the lateral pterygoid insert (Figures 14.1 and 14.6).

Mirroring the oblique line laterally is the temporal crest. This ridge of bone descends on the medial aspect of the coronoid from its tip to the bone on the medial aspect of the third molar. Portions of the temporalis tendon are attached to it. The retromolar fossa (trigone) is a small triangular depression behind the third molar tooth formed by the temporal crest medially and the anterior border of the ramus. The insertion of the terminal fibres of the temporalis into the temporal crest and retromolar trigone can hinder the elevation of mucoperiosteal soft tissue flaps when accessing this area. The thickness of the ramus decreases significantly posterior to the temporal crest medially and above the lingula, where fusion of the outer and inner cortical plates of bone can occur. This is relevant in mandibular ramus osteotomies.

Elongation of the coronoid process can occur bilaterally or unilaterally, resulting in progressive, painless restriction of mandibular opening, due to the impingement of the coronoid process on the medial aspect of the zygomatic arches. Rarely,

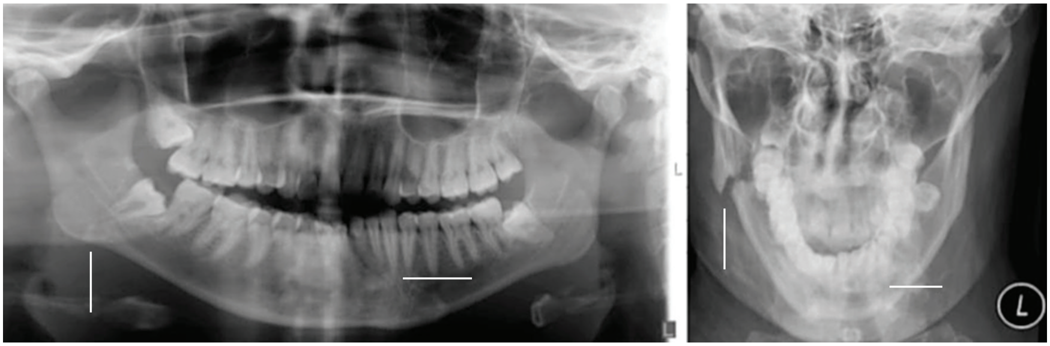

Figure 14.6 Fracture through right 'surgical' angle of the mandible and the left parasymphysis.

hyperplasia of the mandibular condyle can occur resulting in facial asymmetry and an altered bite.

THE MANDIBULAR CANAL

Commencing at the mandibular foramen, the mandibular canal runs downward and forward within the ramus, beneath the roots of the molar teeth with which it communicates by small openings, ascending in the premolar region to the mental foramen. The canal is not always easy to define on plain X-rays in part due to its walls being formed either by a thin layer of cortical bone or, more frequently, by trabecular bone. There is considerable variation in its position between mandibles both in the vertical and transverse plane; however, in general, the mandibular canal is situated nearer the lingual cortical plate in the posterior two-thirds of the bone, and closer to the labial cortical plate in the anterior third. Near the mental foramen the inferior alveolar nerve branches into the mental nerve, which ultimately leaves the mandible via the mental foramen, and the incisive nerve, which remains within the bone and supplies the anterior teeth. The mental nerve may extend anteriorly for 2–3 mm within the mandible before curving back to the mental foramen (the 'anterior loop' of the mental nerve). The availability of cone-beam computerized tomography (CBCT) allows surgeons to accurately assess the course of the mandibular canal throughout its length prior to any surgical procedure that could place the inferior alveolar and/or the mental nerve at risk, such as third molar removal, dental implant placement and mandibular osteotomies.

BLOOD SUPPLY OF THE MANDIBLE

The blood supply to the body of the mandible is derived from its principal nutrient artery, the inferior alveolar artery, and from the vessels supplying genioglossus, geniohyoid and anterior belly of digastric, which are all attached to its lingual aspect between the mental foramina. The blood supply to these muscles is from the sublingual branch of the lingual artery and the submental branch of the facial artery. Branches of these vessels may perforate the lingual cortical plate (Figure 14.4). Anastomoses between these perforating vessels and the inferior alveolar artery are common. A branch of the submental artery may anastomose with the mental artery, permitting retrograde vascular supply to the body and symphysis, which is relevant in mandibular fractures.

The blood supply to the interforaminal region of the body is of relevance in dental implant surgery and mandibular osteotomies at this site. Brisk, potentially life-threatening haemorrhage has been reported with dental implant placement in the mandibular symphysis, usually associated with perforation of the lingual cortical plate of the mandible. Death has resulted following genioplasty secondary to haemorrhage in the anterior floor of mouth (personal communication).

The inferior alveolar artery, supplemented by vessels supplying masseter and medial pterygoid, supplies the ramus, including the mandibular angle. The vascular supply to the coronoid process is derived from vessels supplying temporalis. The vascular supply to the temporomandibular joint is discussed in Chapter 4.17.

GROWTH AND SENESCENCE IN THE MANDIBLE

The unique feature of the maxilla and the mandible is the presence of the dentition. Both bones undergo greater remodelling during life than any other bone in the skeleton as a result of the eruption of the primary and secondary dentition and later tooth loss.

As with the maxilla the clinical implications of both growth and senescence are best appreciated if we consider the mandible as three separate bones:

1. **The developing – paediatric – mandible:** From birth to about the age of 10–12. The body of the mandible is occupied by developing tooth buds, and this, coupled with the condylar neck being shorter and thicker, influences both the pattern and treatment of mandibular fractures compared to adults. Intracapsular fractures of the condyle are more common particularly in children under 6 years of age, with increased risk of growth disturbance and ankylosis. Osteotomies of the mandibular body at any site carry an increased risk of damaging developing tooth germs (see Chapter 15, Figure 15.11).

2. **The adult dentate mandible:** From about the age of 12–16, with the eruption of the second molar teeth. The pattern of fractures involving the mandible and their treatment is similar to that of an adult. Developing tooth buds will not affect mandibular osteotomy design (see Chapter 15, Figure 15.11).
3. **The edentulous/atrophic mandible:** This is the result of tooth loss and variable resorption of both alveolar and basal bone. Whilst the direction of resorption of the alveolar and the basal bone is predictable, i.e. anteriorly and inferiorly – centrifugally – in the sagittal plane, the extent of resorption is variable.

   With tooth loss both alveolar and basal bone are resorbed to a variable extent, and both the mental foramen and the mandibular canal come to lie closer to the superior border. The mental foramen is placed higher than the mandibular canal posterior to it, and so resorption of the alveolus in edentulous patients exposes the nerve at the foramen prior to the nerve in the mandibular canal.

   There can be a profound ageing effect on facial appearance resulting from these changes, and clinical implications for pre-prosthetic and implant surgery and in the treatment of mandibular fractures (Figure 14.7).

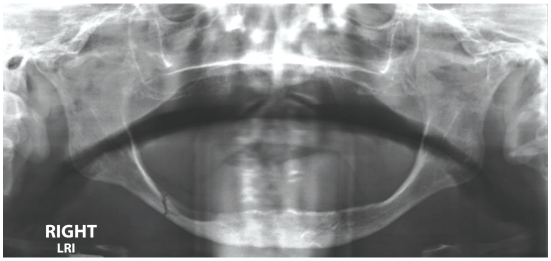

Figure 14.7 Asymmetric atrophy of the mandible with fracture of the right body. **Note:** The mental foramen and inferior alveolar canal are on the crest of the mandibular ridge; the mental foramen is not identifiable as it is no longer a 'foramen' as a result of the loss of its superior margin due to bone resorption.

MANDIBULAR FRACTURES

The mandible fractures preferentially at certain sites as indicated in Figure 14.8. These sites represent inherent areas of weakness. The pattern of the fractures sustained is the result of a number of factors, such as the degree and direction of the impact force and the age of the individual. The *U* shape

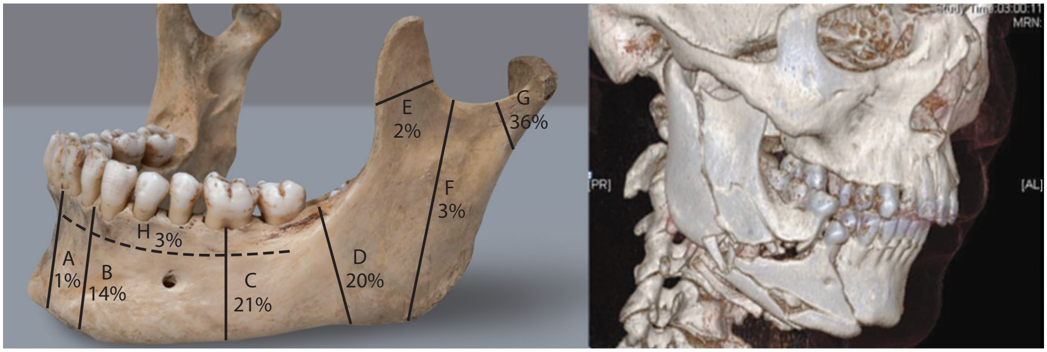

(a) **(b)**

Figure 14.8 **(a)** Incidence of mandibular fractures at various sites. A – symphysis. B – parasymphysis. C – body of mandible. D – mandibular angle. E – coronoid process. F – ramus. G – mandibular condyle; H – alveolar process. **(b)** 'High-energy' impact to the right mandible producing severe comminution and displacement of the fragments.

of the bone frequently results in bilateral fractures, with contra-lateral body/angle, parasymphysis/angle and parasymphysis/condylar fractures being perhaps the most common (Figure 14.3). The degree of displacement of the fracture(s) is the result once again of the degree of impact force. The direction of displacement is determined by the pull of the attached musculature. Predictably, displaced fractures in the tooth-bearing area, i.e. the alveolus, result in alteration of the occlusion, and if the inferior alveolar canal is involved, altered sensation (typically a neuropraxia) in the mental nerve dermatome will occur.

These predictable patterns of fractures, however, do not occur with high-energy impacts. The overwhelming impact force results in marked displacement of the fragments and significant comminution – hallmarks of high-energy injuries. Any inherent lines of weakness in the bone – in the skeleton in general and not simply the mandible – cease to play a role in the way the bone is disrupted.

FURTHER READING

Haskell R. *Applied Surgical Anatomy.* In: Williams JL. (Ed.). *Rowe and Williams Maxillofacial Injuries*. Edinburgh: Churchill Livingstone, 1994; 9–10.

Hogan G, Ellis E. The 'antilingula' – fact or fiction. *Journal of Oral and Maxillofacial Surgery*. 2006; 64: 1248–54.

Janfaza P, Nadol Jr JB, Galla RJ, Fabian RL, Montgomery WW, eds. *Surgical Anatomy of the Head and Neck*. Philadelphia: Lippincott Williams & Wilkins, 2001.

Lang J. *Clinical Anatomy of the Masticatory Apparatus and Peripharygeal Spaces.* Stuttgart: George Thieme Verlag, 1995; 19–41.

Loukota RA, Abdel-Ghalil K. *Condylar Fractures.* In: Ward-Booth P, Eppley BL, Schmelzeisen R. (Eds.). *Maxillofacial Trauma and Facial Reconstruction.* London: Elsevier, 2012; 270–87.

Obwegeser HL. *Mandibular Growth Anomalies – Terminology, Aetiology, Diagnosis, Treatment*. New York: Springer-Verlag, 2001: 19.

Perry M. *Mandible Fractures.* In: Langdon J, Patel M, Ord R, Brennan P. (Eds.). *Operative Oral and Maxillofacial Surgery*, 2nd ed. London: Hodder Arnold, 2010; 479–86.

Reynolds PA. *Infratemporal and Pterygopalatine Fossae and the Temporomandibular Joint*. In: Standring S. (Ed.). *Gray's Anatomy: The Anatomical Basis of Clinical Practice*. 40th ed. Edinburgh: Elsevier/Churchill Livingstone, 2008: 527–46.

15

Maxilla and zygoma

BARRIE T. EVANS, DARRYL COOMBES, VISHY MAHADEVAN
AND PETER A. BRENNAN

Maxilla 141
Posterior (infratemporal) surface *142*
Nasal surface *142*
Zygomatic bone 145
Growth and senescence in the maxilla 146
The midfacial pillars/buttresses 148
Further reading 149

A transverse line through the frontozygomatic, frontomaxillary and frontonasal sutures is the superior boundary of the middle third of the face. The occlusal plane of the maxillary teeth marks its inferior extent.

The paired maxillae and the zygomatic bones form the majority of the midfacial skeleton and will be considered in this chapter. An appreciation of their anatomy is relevant in the management of both congenital and neoplastic disease, as well as trauma of the midface.

MAXILLA

The paired maxillae form the upper jaw and the anterior walls of the infratemporal and pterygopalatine fossae and the majority of the floor of the orbit and lateral nasal wall. The term *maxilla* is frequently used in a clinical context to describe the paired maxillary bones.

Each maxilla has a body and four processes (Figure 15.1): zygomatic, frontal, alveolar and palatine processes.

The body is roughly pyramidal, with anterior, posterior (infratemporal) and nasal surfaces with the orbital surface forming the 'base'. The maxillary sinus is contained within.

The anterior surface faces anterolaterally and extends from the midline to the zygomatic buttress ('jugal crest') in the first molar region. This buttress – a vertical ridge of bone – is at the junction of the anterior and posterior surfaces. In the midline the anterior nasal spine projects forward at the level of the floor of the anterior bony nasal aperture – the piriform fossa. The anterior nasal spine is absent in nasomaxillary hypoplasia, known as Binder's syndrome. The posterior nasal spine arises from the horizontal plate of the palatine bone.

The prominent canine eminence overlying the root of the canine tooth demarcates the canine fossa laterally and the incisive fossa above the incisor roots, medially. The depressor septi muscle arises from the bone above the upper incisors and from the anterior nasal spine; it may be intentionally detached in nasal surgery. The anterior nasal spine may be reduced in nasal surgery and maxillary advancement osteotomies. The nasalis muscle and a slip of the orbicularis oris also arise from the incisive fossa below the inferior rim of the piriform fossa.

The maxilla forms the inferior and the majority of the lateral rim of the piriform fossa, completed superiorly by the nasal bones. The nasal bones vary in size, and therefore osteotomies in nasal surgery usually involve both the nasal bones and part of the frontal process of the maxilla.

The roots of the upper incisor teeth are below the piriform fossa and the nasal floor, and the tip of the canine roots are below and lateral to the piriform aperture. The margins of the piriform fossa are sharp. The floor of the nasal cavity may be below the rim, which is relevant in maxillary osteotomies.

The infraorbital foramen, below the infraorbital rim, is above the canine fossa. The levator labii superioris muscle arises from the anterior surface of the maxilla above the foramen and the levator anguli oris from below the foramen.

The zygomatic-maxillary suture at the inferior orbital rim is closely related to the foramen with the result that numbness in the infraorbital nerve distribution is common with zygomatic fractures.

The canine fossa is considered the 'danger area' of the face in view of the risk of infection spreading from this site via the angular vein to the orbit and then to the cavernous sinus via the ophthalmic veins (Figure 15.1).

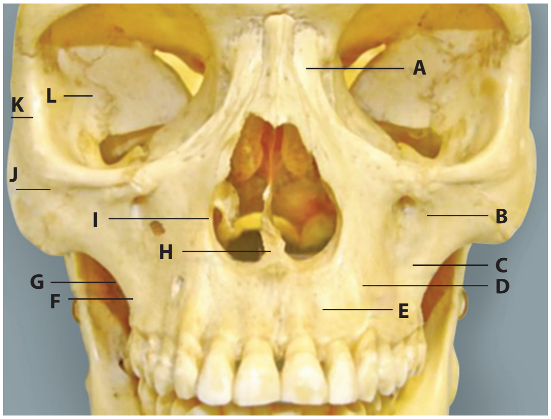

Figure 15.1 Anterior surface of the maxilla and zygoma. A – frontal process of maxilla between nasal and lacrimal bones. B – infraorbital foramen. C – canine fossa. D – canine eminence. E – incisive fossa. F – alveolar process with teeth. G – zygomatic buttress. H – groove for vomer from nasal crests of palatine process. I – margin of piriform aperture. J – body of zygoma. K – frontal process of zygoma. L – spheno-zygomatic suture in lateral orbit.

Posterior (infratemporal) surface

This surface faces posterolaterally. Two or three small foramina may be present transmitting the posterior superior alveolar neurovascular bundles. The maxillary tuberosity is its inferior limit. The tuberosity may fracture during molar extractions, particularly isolated upper molar teeth. If the tuberosity fragment is removed, this can create a large oro-antral communication. The absence of the tuberosity may cause difficulty in later denture construction.

A branch of the posterior superior alveolar (PSA) artery may be adherent to the tuberosity – a possible cause of brisk haemorrhage with PSA local anaesthetic injections (Figure 15.2).

Nasal surface

This forms the anteroinferior aspect of the lateral nasal wall. The maxillary hiatus (defect), situated posteriorly and superiorly, opens into the maxillary sinus. This hiatus is partially closed with contributions from the perpendicular plate of the palatine bone, the uncinate process of the ethmoid,

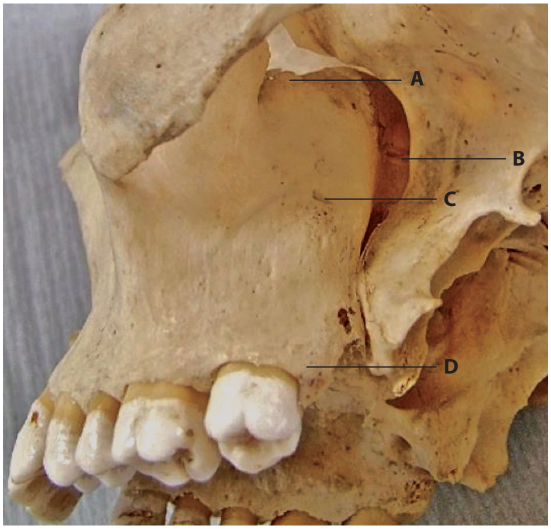

Figure 15.2 Posterior (infratemporal) surface of the maxilla forming the anterior walls of the infratemporal and pterygopalatine fossae. A – inferior orbital fissure. B – pterygomaxillary fissure. C – foramina for passage of posterior superior neurovascular bundles. D – maxillary tuberosity.

the inferior nasal concha and with a small contribution from the lacrimal bone. Anteriorly, the lacrimal groove is converted into a duct – the nasolacrimal duct – by the descending part of the lacrimal bone and the lacrimal process of the inferior concha; the nasolacrimal duct opens into the inferior meatus. Further anteriorly, the inferior nasal concha articulates with the oblique conchal crest. Posteriorly, the nasal surface articulates with the perpendicular plate of the palatine bone.

Below its articulation with the inferior nasal concha, the nasal surface of the maxilla forms part of the inferior meatus (Figure 15.3).

The orbital surface is triangular and forms the majority of the orbital floor and also forms the roof of the maxillary sinus.

Anteriorly, the medial border is grooved where it articulates with the lacrimal bone, together forming the lacrimal groove, which contains the lacrimal sac. Posterior to the lacrimal bone it articulates with the orbital plate of the ethmoid, and, further posterior, the orbital plate of the palatine bone.

The rounded posterior margin forms the major part of the anterior edge of inferior orbital fissure – completed medially with the small contribution from the orbital plate of the palatine bone.

The inferior orbital fissure is effectively bisected by the infraorbital groove where the infraorbital neurovascular bundle enters the orbit. Running parallel to the medial orbital wall, the groove becomes a canal, which opens onto the anterior surface of the maxilla, approximately 7–10 mm below the infraorbital rim. The anterior edge forms part of the orbital rim and is continuous with the anterior lacrimal crest of the frontal process (Figure 15.4).

The zygomatic process is formed by the convergence of the anterior, posterior and orbital surfaces. Triangular in cross-section, it is roughened superiorly where it articulates with the zygoma.

The frontal process is a strong projection inserted between the nasal and lacrimal bones forming the medial orbital rim and articulating superiorly with the frontal bone. Its lateral margin forms the anterior lacrimal crest from which the anterior limb of the medial canthal ligament arises. Its medial surface forms part of the lateral nasal wall.

The ethmoidal crest on its nasal surface articulates with the middle nasal concha of the ethmoid and forms the upper limit of the middle meatus.

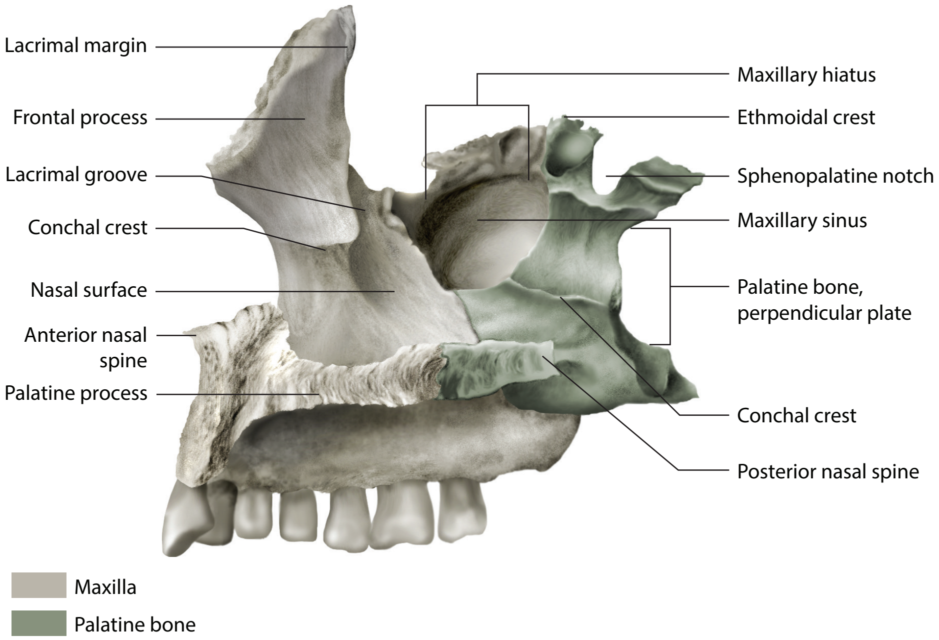
Lacrimal margin
Frontal process
Lacrimal groove
Conchal crest
Nasal surface
Anterior nasal spine
Palatine process
Maxillary hiatus
Ethmoidal crest
Sphenopalatine notch
Maxillary sinus
Palatine bone, perpendicular plate
Conchal crest
Posterior nasal spine
Maxilla
Palatine bone

Figure 15.3 The nasal surface of the maxilla and the palatine process (redrawn from *Gray's Anatomy*).

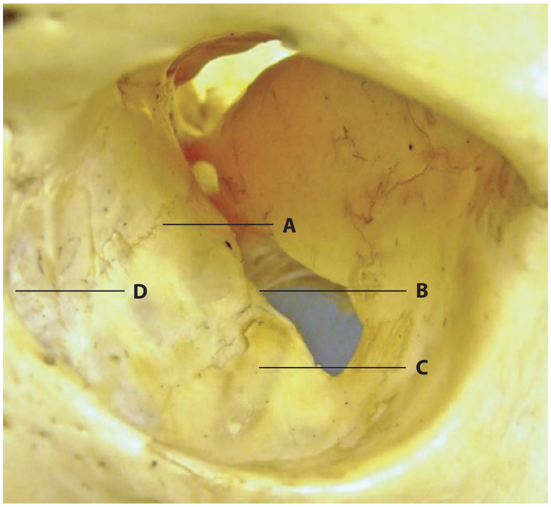

Figure 15.4 Orbital surface of the maxilla. A – suture between orbital plate of the ethmoid and orbital surface of the maxilla. B – orbital plate of the palatine bone. C – infraorbital groove. D – lacrimal fossa.

The alveolar process contains the teeth and forms the dental arch. Loss of teeth results in the variable resorption of the alveolar process in three dimensions. The term *basal* bone is used in the dental literature to describe the maxilla above the alveolar process, which is relevant in denture construction and dental implant surgery (Figure 15.5).

The palatine processes on each side projecting medially and meeting in the midline palatal suture form about three-quarters of the hard palate. The remainder is derived from the horizontal plate of the palatine bone; the suture between them lies between the first and second molars (Figure 15.6). The oral surface is concave and roughened with the indentations of the palatal minor salivary glands. The nasal surface is likewise concave transversely, is smooth and forms the majority of the nasal floor. The palatine processes are thicker anteriorly.

The medial aspects of the palatine processes form a crest – the nasal crest – which combine to make a groove which accommodates the vomer. The bone is thicker in the midline than immediately either side, which is relevant in maxillary osteotomies. The palatal surface is occasionally raised into a midline palatal torus.

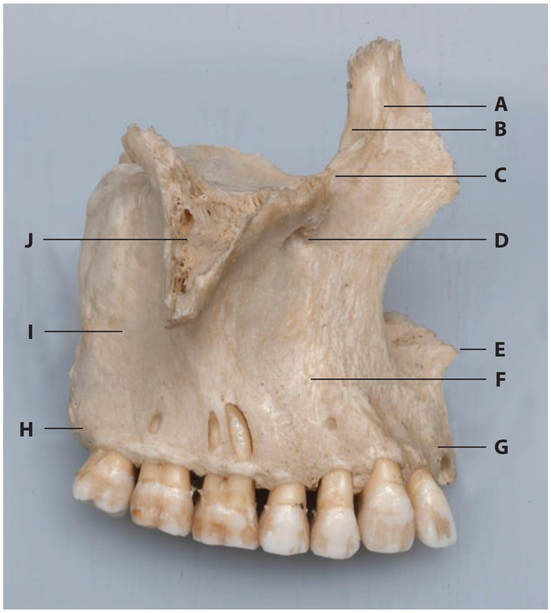

Figure 15.5 Lateral view of right maxilla. A – frontal process and anterior lacrimal crest. B – lacrimal notch. C – inferior orbital rim. D – infraorbital foramen. E – anterior nasal spine. F – canine fossa. G – alveolar process. H – maxillary tuberosity. I – posterior (infratemporal) surface. J – zygomatic process.

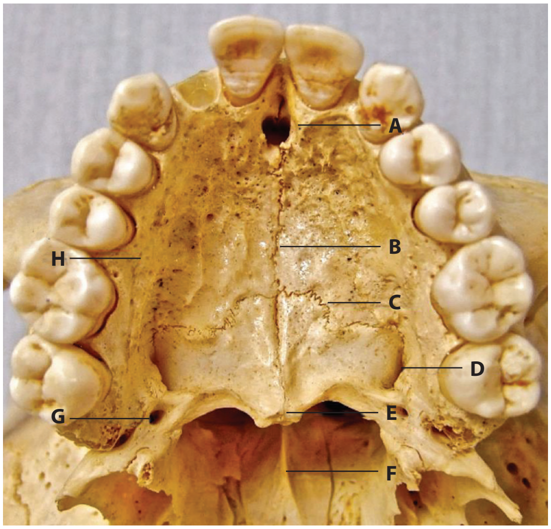

Figure 15.6 Palatine process of maxilla and horizontal plate of the palatine bone. A – incisive fossa. B – mid-palatal suture. C – suture between palatine process and horizontal plate of the palatine bone. D – greater palatine foramen. E – posterior nasal spine. F – vomer. G – lesser palatine foramen. H – alveolar process.

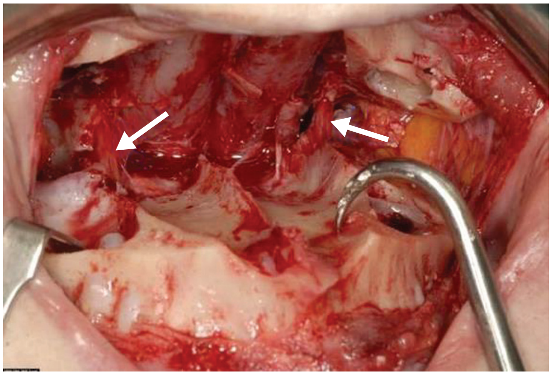

Figure 15.7 Le Fort 1 down-fracture. Arrows mark the greater palatine neurovascular bundles at the posterior aspect of the lateral nasal wall.

Posterolaterally, the oral surface is grooved by the greater palatine neurovascular bundles which enter the hard palate via the foramen of the same name, situated at the interface between the posterior surface of the maxilla and the vertical plate of the palatine bone. The greater palatine vessels and nerves are readily located in maxillary osteotomies by following the lateral nasal wall posteriorly (Figure 15.7).

The incisive canals transmitting the nasopalatine vessels and nerves terminate in the incisive fossa behind the upper central incisor teeth (Figure 15.6).

A bony prominence may develop in the midline – torus palatinus. Similarly, bony prominences may also develop bilaterally on the buccal (outer surface) of the alveolus. Their diagnosis is clinical. The torus mandibularis is the mandibular equivalent.

ZYGOMATIC BONE

The zygomatic bone ('zygoma'/'malar') is the cornerstone of the facial skeleton articulating with the frontal bone superiorly, the maxilla inferiorly, the temporal bone posteriorly and with the greater wing of the sphenoid on its medial aspect. It has a body, two processes (frontal and temporal) and three surfaces (lateral, orbital and temporal). With the exception of the nasal bones, it is the most commonly fractured bone of the facial skeleton (see Figure 15.1).

The body of the zygoma, approximately quadrilateral in shape with a convex lateral surface, forms the cheek prominence. The frontal process articulates with the zygomatic process of the frontal bone, which together form the lateral orbital margin. The temporal process of the zygoma and the zygomatic process of the temporal bone form the 'arch of the zygoma'. This is not an arch in the strict sense as it runs back from the body of the zygoma as almost a 'straight edge', curving medially at the level of the articular eminence of the temporomandibular joint. It is necessary to reconstruct this shape precisely following trauma (Figure 15.8).

The orbital surface articulates with the greater wing of the sphenoid at the sphenozygomatic suture, to form the lateral orbital wall. The concave temporal surface forms the anterior border of

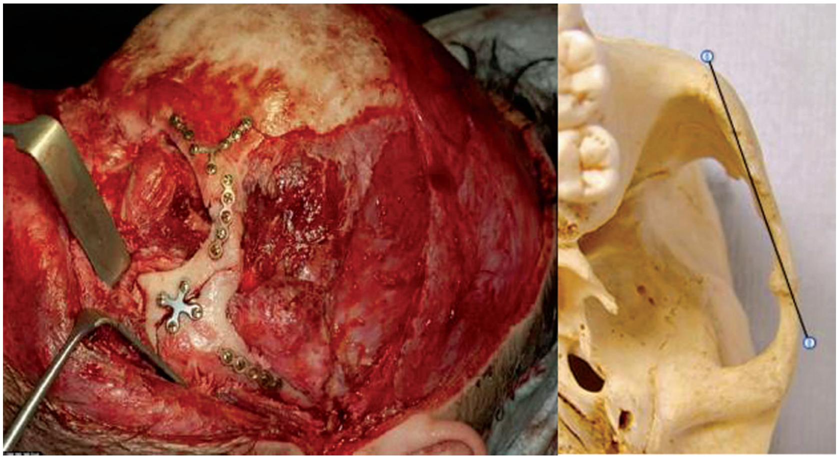

Figure 15.8 The arch of the zygoma restored to its correct 'straight-edge' configuration.

the temporal fossa. The orbital and lateral surfaces articulate with the maxilla to form the anterolateral orbital floor and the inferolateral orbital rim.

The zygomatic-orbital foramina within the lateral orbit are the site of exit of the zygomatico-temporal and zygomatico-facial sensory nerves, which traverse the body to open on its lateral aspect.

The frontozygomatic and sphenozygomatic sutures are lines of natural weakness in the lateral orbit and a common site of fracture.

The term *tripod* fracture remains in common parlance when referring to zygomatic fractures. This is inappropriate as there are a minimum of four fracture sites to consider with reduction and fixation:

1. The frontozygomatic (FZ) suture.
2. The infraorbital rim at the zygomaticomaxillary suture.
3. The zygomaticomaxillary suture in the region of the zygomatic buttress.
4. The zygomaticotemporal suture in the arch.

The articulation of the orbital surface with the greater wing of the sphenoid may also be considered (Figures 15.9 and 15.10).

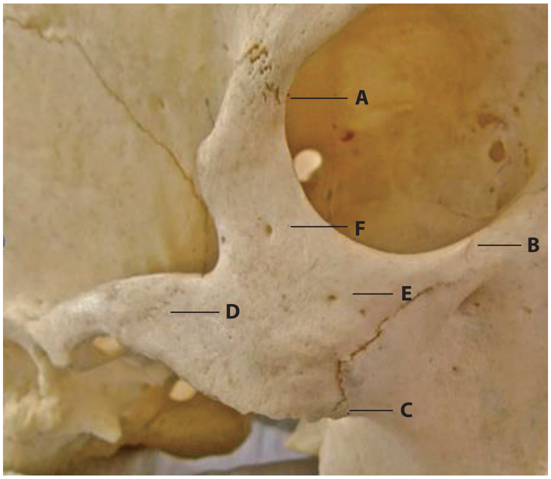

Figure 15.9 Right zygoma. A – zygomatic-frontal suture. B – zygomatic-maxillary suture at infra-orbital rim. C – zygomatic-maxillary suture at zygomatic buttress. D – zygomatic-temporal suture: the junction of the temporal process of the zygoma and the zygomatic process of the temporal bone – zygomatic arch. E – zygomatico-facial foramen. F – zygomatic-temporal foramen.

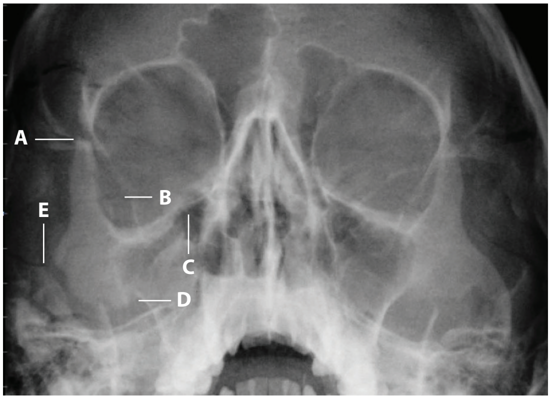

Figure 15.10 Fracture right zygoma, multiple sites of articulation. A – frontozygomatic suture. B – sphenozygomatic suture in lateral wall. C – zygomatic maxillary suture infraorbital rim. D – zygomatic maxillary suture at buttress. E – zygomaticotemporal suture at arch (arch fracture comminuted).

The zygoma in relation to the orbital skeleton is considered further in Chapter 12.

GROWTH AND SENESCENCE IN THE MAXILLA

The unique feature of the maxilla and the mandible is the presence of the dentition. Both bones undergo greater remodelling during life than any other bone in the skeleton as a result of the eruption of the primary and secondary dentition and later tooth loss.

Any description of the maxilla and the zygoma is incomplete without consideration of the maxillary sinus. The growth of the maxillary sinus is closely linked to the eruption of the permanent dentition. A significant increase in size of the sinus commences with the eruption of the first permanent molars and continues with the remainder of the permanent maxillary teeth. When the second permanent molar teeth erupt, the level of the sinus floor is at about the floor of the nose. Maxillary sinus growth is complete by about the age of 16. Conversely, the loss of posterior maxillary teeth, in particular, may result not only in loss of the supporting alveolar bone but also remodelling of the maxillary sinus.

These changes have clinical implications. They influence fracture patterns involving the midface, the design and timing of midface osteotomies and later pre-prosthetic and dental implant surgery.

The clinical implications are best appreciated if we consider the maxilla (and the mandible) as three separate bones:

1. **The developing – paediatric – maxilla:** From birth to about the age of 10–12. During this period, particularly in the younger child, the maxillary sinus is virtually absent with the midface occupied by the developing tooth buds. Le Fort 1 and zygomatic fractures are uncommon, as the bone structure of the midface must be weakened by the growth of the maxillary sinus for the typical fracture patterns that we see in adults to occur. Osteotomies at the Le Fort 1 level are precluded for similar reasons (Figure 15.11).
2. **The adult dentate maxilla:** This exists from about the age of 12–16 with the eruption of the second molar teeth and completion of maxillary sinus development. The pattern of fractures involving the maxilla, zygoma and the remaining midface will be those of the adult. Developing tooth buds will not affect midface osteotomy design (Figure 15.12).
3. **The edentulous/atrophic maxilla:** This is the result of tooth loss, variable resorption of

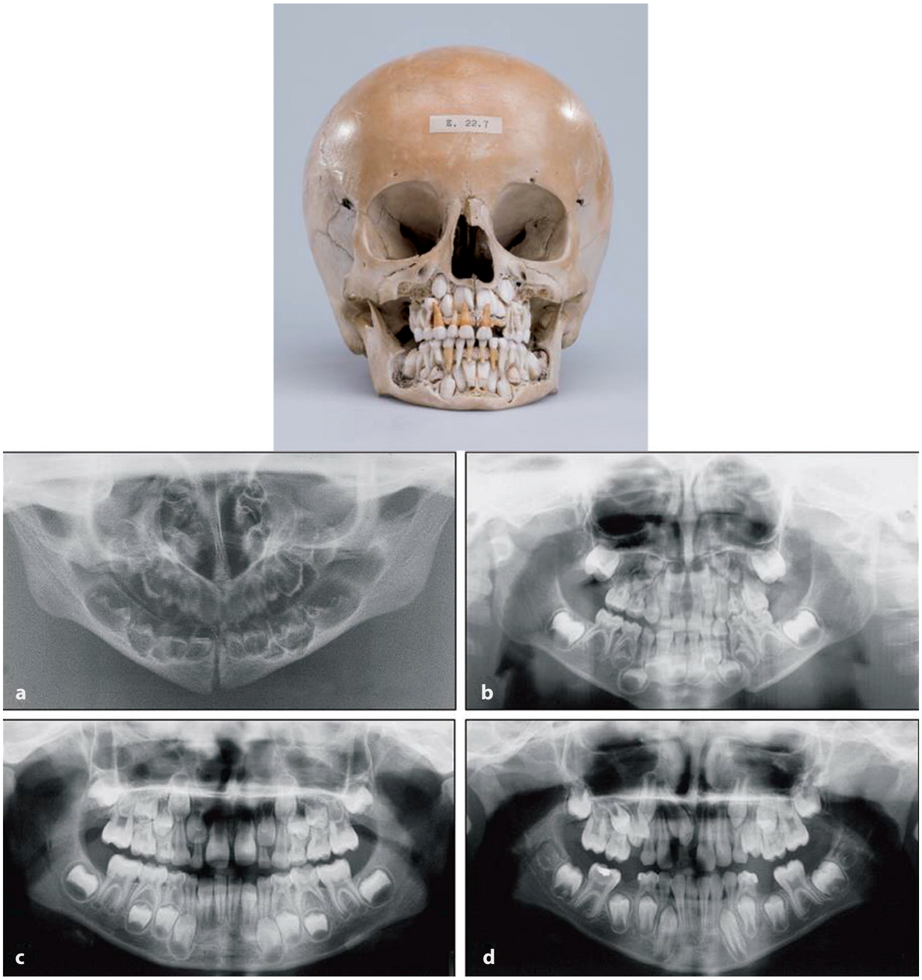

Figure 15.11 The paediatric maxilla and mandible. OPG radiographs of the developing dentition. At birth **(a)**; 2½ years **(b)**; 6½ years **(c)**; and 10 years **(d)**. X-rays from *Gray's Anatomy* used with permission.

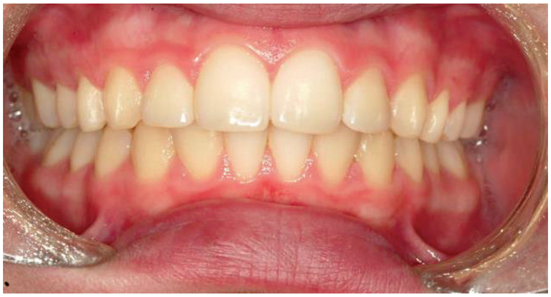

Figure 15.12 Adult maxilla.

both alveolar and basal bone and the change in the shape and size (pneumatization) of the maxillary sinus, as a result of both factors. The sinus may extend in both an anterior and inferior direction. Whilst the direction of resorption of the alveolar and the basal bone is predictable, i.e. posteriorly and superiorly, the extent of resorption is variable. Also variable and unpredictable are the changes in the maxillary sinus. There can be a profound ageing effect on facial appearance resulting from these changes and clinical implications for pre-prosthetic and implant surgery (Figure 15.13).

THE MIDFACIAL PILLARS/ BUTTRESSES

The skeleton of the middle third of the face, weakened by the presence of the maxillary sinus, must withstand the powerful vertical occlusal forces transmitted via the teeth to the base of the skull. Three pillars or buttresses of bone develop on either side in response to these forces of mastication (Figure 15.14):

1. The *medial* (nasomaxillary) buttress runs up through the canine eminence, the lateral rim of the piriform fossa and the frontal process of the maxilla to the frontonasal suture.
2. The *lateral* (zygomatic-maxillary) buttress runs up through the zygomatic buttress of the maxilla, and body and frontal process of the zygoma to the zygomatic process of the frontal bone.
3. The *posterior* (pterygoid) buttress – the pterygoid plates. Sometimes referred to as the 'pterygomaxillary buttress', the posterior maxilla provides no vertical buttressing role.

Additional strength is imparted to the midface by the cross-bracing provided by strong horizontal

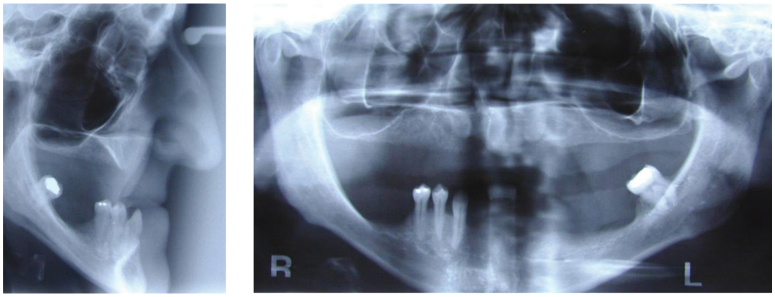

Figure 15.13 Edentulous maxilla. Posterior and superior resorption of the alveolar and basal bone demonstrated in the lateral view. Extension of the pneumatization of the maxillary sinus anteriorly and inferiorly demonstrated in the panoral view.

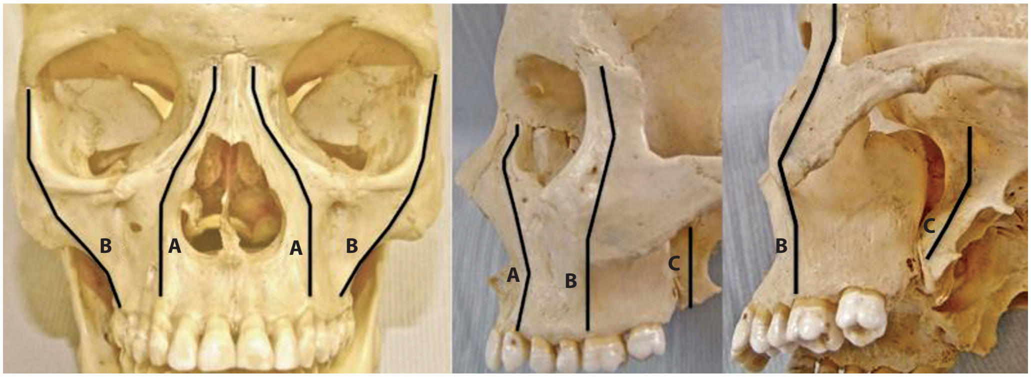

Figure 15.14 Midfacial buttresses. A – nasomaxillary. B – zygomatic. C – pterygoid.

buttresses at the level of the hard palate, infraorbital and supraorbital rims. All, with the exception of the pterygoid plates, may be used as sites of osteosynthesis, i.e. bone plates and screw can be inserted across fractures or elective osteotomy sites.

FURTHER READING

Janfaza P, Nadol Jr JB, Galla RJ, Fabian R L, Montgomery WW. (Eds.). *Surgical Anatomy of the Head and Neck*. Philadelphia: Lippincott Williams & Wilkins, 2001.

Manson PN. Skull and midface injuries. In: Mustarde JC, Jackson IT. (Eds.). *Plastic Surgery in Infancy and Childhood.* Edinburgh: Churchill Livingstone, 1988.

Standring S. (Ed.). *Gray's Anatomy: The Anatomical Basis of Clinical Practice, 40th ed.* Edinburgh: Elsevier/Churchill Livingstone, 2008.

16

Infratemporal fossa, pterygopalatine fossa and muscles of mastication

BARRIE T. EVANS

Infratemporal fossa 151
Masticatory space and the stylohamular plane *153*
Muscles of mastication 154
Temporal fossa, temporalis fascia and muscle *154*
Masseter *156*
Medial pterygoid *156*
Lateral pterygoid *157*
Mandibular nerve 158
Otic ganglion *160*
Vascular supply 160
Maxillary artery *160*
Pterygoid venous plexus *161*
The pterygopalatine (pterygomaxillary) fossa 161
Spatial arrangement of the neurovascular contents of the pterygopalatine fossa *162*
Pterygoid plates *162*
Pterygopalatine ganglion *162*
Maxillary nerve *162*
Maxillary artery *163*
Veins of the pterygopalatine fossa *164*
Surgical approaches 164
Further reading 165

The infratemporal fossa was an anatomical region for which Barrie T. Evans was renowned. Despite his expertise, Mr. Evans admitted to reviewing the anatomy every time before operating in this region. This is a longer chapter than some others in this book; it explains this complex region in considerable detail.

The infratemporal fossa (ITF) and pterygopalatine fossa (PPF) are compact, well-defined spaces behind the maxilla and below the skull base. Although adjacent, they are functionally distinct. The infratemporal fossa is the province of the masticatory muscles – the 'masticatory space'. The pterygopalatine fossa functionally is related to the nasal cavity and paranasal sinuses. Both contain a division of the trigeminal nerve and an autonomic ganglion and are supplied by the maxillary artery.

Improved imaging and surgical access – open and endoscopic – have made surgery in this region commonplace. Nonetheless, the abundant vascularity and proximity of critical structures make knowledge of the surgical anatomy a prerequisite for safe surgery.

Whilst the ITF and the PPF will be considered as discrete spaces anatomically, disease does not respect anatomical boundaries. Consideration of their proximity to, and communication with, adjacent areas is essential when planning treatment.

INFRATEMPORAL FOSSA

The infratemporal fossa is the space deep to the ramus of the mandible, beneath the middle fossa of the skull. It has a roof, and anterior, lateral and medial walls with no floor. It is open to the neck posteriorly. Although termed the *infratemporal* fossa, the majority of the roof is formed by the sphenoid. It contains the:

- medial and lateral pterygoid muscles.
- mandibular division of the trigeminal nerve (*the mandibular nerve*).
- chorda tympani branch of the facial nerve.
- otic parasympathetic ganglion.
- maxillary artery.
- pterygoid venous plexus.
- sphenomandibular ligament.

The styloid 'apparatus', i.e. the styloid process with its three muscles (stylopharyngeus/stylohyoid/styloglossus) and two ligaments (stylomandibular/stylohyoid), is immediately posterior and medial to the fossa. Whilst not within the infratemporal fossa it provides a surgical landmark – discussed later in this chapter – for its medial limit. The styloid apparatus also provides a safe landmark for the internal carotid artery and internal jugular vein as these vessels always ascend to the skull base deep to it.

The lateral pterygoid muscle in the roof of the infratemporal fossa provides the key to understanding the relationships of the structures contained within. The muscle runs horizontally backwards from its origin to the mandibular condyle. The medial pterygoid and the mandibular nerve and its branches at the skull base are deep to the muscle, and the maxillary artery is usually superficial. The buccal branch of the mandibular nerve emerges between the two heads of the lateral pterygoid, and the lingual and inferior alveolar nerves pass beneath its lower border. The pterygoid venous plexus is widely distributed around and within the lateral pterygoid. The deep temporal nerves and vessels emerge from above the upper border of the lateral pterygoid (Figure 16.1).

The roof is formed by the infratemporal crest and surface of the greater wing of the sphenoid completed posteriorly by the infratemporal surface of the temporal bone and ending at the articular eminence of the temporomandibular joint and the spine of the sphenoid on the deep medial aspect. Two and sometimes three foramina – all within the sphenoid – are within the roof: f.ovale, f.spinosum and, inconstantly, the sphenoidal emissary foramen (of Vesalius) medial to f.ovale.

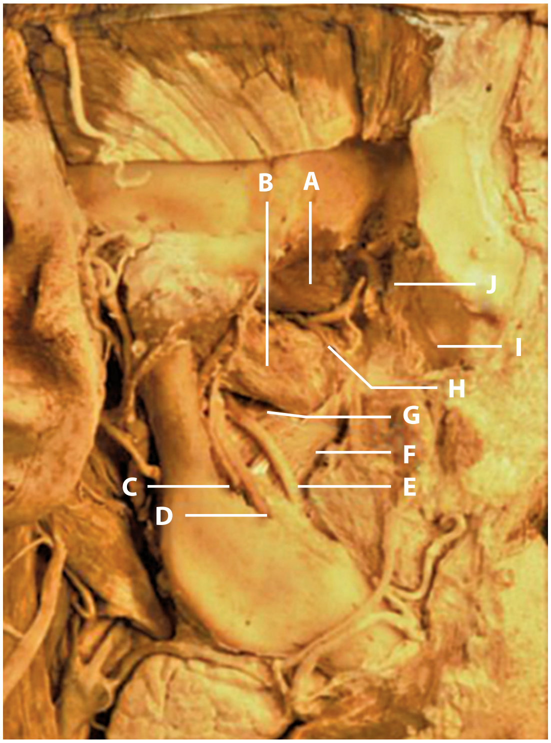

Figure 16.1 Relationship of the lateral pterygoid muscle to contents of the infratemporal fossa. A – upper head lateral pterygoid. B – inferior head lateral pterygoid. C – nerve to mylohyoid. D – inferior alveolar nerve. E – lingual nerve. F – superficial head medial pterygoid. G – deep head medial pterygoid. H – (long) buccal nerve emerging from between the upper and lower heads lateral pterygoid. I – posterior superior alveolar artery. J – maxillary artery entering pterygomaxillary fissure.

Foramen ovale is immediately behind the posterior edge of the lateral pterygoid plate at the skull base with foramen spinosum immediately posterior to ovale.

Foramen ovale transmits the mandibular nerve, the accessory meningeal artery, the lesser superficial petrosal nerve and an emissary vein linking the pterygoid venous plexus with the cavernous sinus. Foramen spinosum transmits the middle meningeal artery and the meningeal branch of the mandibular nerve. The foramen of Vesalius – medial to ovale – transmits an emissary vein.

Foramen ovale is a useful surgical landmark, located either by following a branch(es) of the mandibular nerve to the skull base or by following

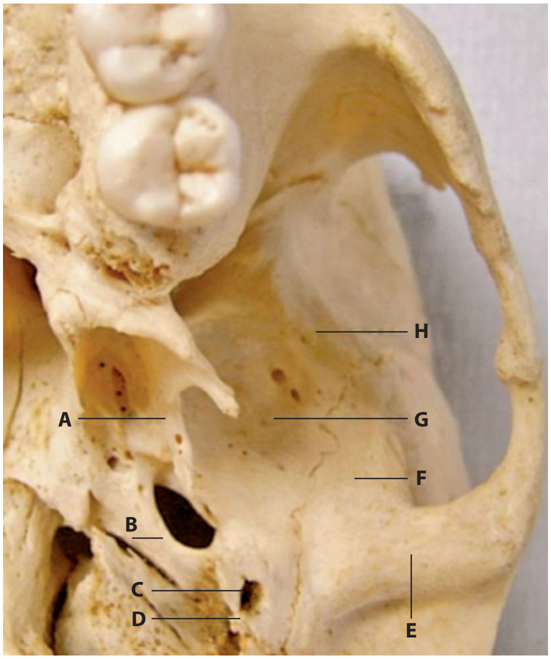

Figure 16.2 Roof of the left infratemporal fossa and in-line relation of the lateral pterygoid plate/foramen ovale/foramen spinosum/spine of sphenoid. A – posterior edge lateral pterygoid plate. B – f.ovale. C – f.spinosum. D – spine of sphenoid. E – articular eminence TM joint. F – infratemporal surface temporal bone. G – infratemporal surface greater wing of the sphenoid. H – infratemporal crest greater wing.

the lateral pterygoid plate to its posterior edge. Identification of this foramen orientates the surgeon both subcranially and intracranially (see Figures 16.2 and 16.10).

The chorda tympani exits the skull base from the medial aspect of the petrotympanic fissure. Entering the fossa posteriorly, it grooves the spine of the sphenoid medially, joining the lingual nerve at a variable distance below the skull base. It has two types of fibres: sensory fibres associated with taste to the anterior two-thirds of the tongue and the preganglionic parasympathetic secretomotor fibres to the submandibular ganglion.

The spine of the sphenoid provides the origin of the sphenomandibular ligament, which attaches inferiorly to the lingula of the mandibular foramen. This ligament, together with the pterygomasseteric sling (see later discussion), control the arc of rotation of the mandible.

The medial wall consists of the pterygomaxillary fissure anteriorly and the lateral pterygoid plate posterior to this, with a small contribution from the pyramidal process of the palatine bone. The medial wall is completed posteriorly by the sidewall of the pharynx. At this level the pharynx consists of: the pharyngobasilar fascia superiorly with the tensor veli palatini and levator veli palatini immediately lateral to the fascia, and the superior constrictor muscle continuing below the pharyngobasilar fascia (Figure 16.3).

The anterior wall is the posterior surface of the maxilla ending inferiorly at the maxillary tuberosity. The inferior orbital fissure forms the upper limit of the anterior wall meeting the pterygomaxillary fissure at right angles (Figure 15.2).

The lateral wall is the ramus and coronoid process of the mandible.

The infratemporal fossa communicates with the:

- temporal fossa deep to the zygomatic arch superiorly.
- orbit via the inferior orbital fissure.
- pterygopalatine fossa via the pterygomaxillary fissure.

Masticatory space and the stylohamular plane

The contents of the infratemporal fossa are contained within a well-defined space bounded by and incorporating the masticatory muscles, termed the *masticatory space*. The masseter and temporalis muscles are lateral, and the medial boundary is the medial aspect of the medial pterygoid muscle, which abuts the sidewall of the pharynx. A plane exists between the pharyngeal sidewall and the masticatory space/infratemporal fossa. This plane is readily identified by palpating the tip of the styloid process and with gentle blunt finger dissection passing anteriorly and medially to the pterygoid hamulus at the lower border of the medial pterygoid plate. This may be termed the *stylohamular plane*. It is the surgical plane defining the medial and superior boundary of the infratemporal fossa and is the medial boundary for tumours confined to the infratemporal fossa.

Resections using the stylohamular plane as a guide are safe as the internal carotid, internal

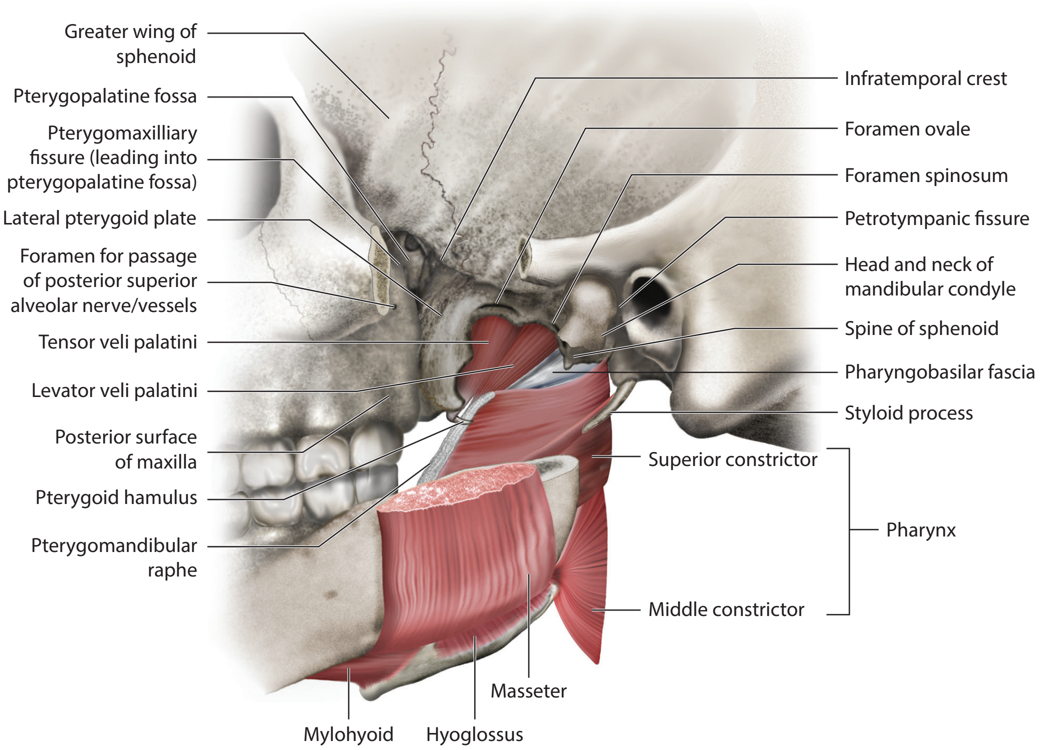
Greater wing of sphenoid
Pterygopalatine fossa
Pterygomaxilliary fissure (leading into pterygopalatine fossa)
Lateral pterygoid plate
Foramen for passage of posterior superior alveolar nerve/vessels
Tensor veli palatini
Levator veli palatini
Posterior surface of maxilla
Pterygoid hamulus
Pterygomandibular raphe
Infratemporal crest
Foramen ovale
Foramen spinosum
Petrotympanic fissure
Head and neck of mandibular condyle
Spine of sphenoid
Pharyngobasilar fascia
Styloid process
Superior constrictor
Pharynx
Middle constrictor
Masseter
Mylohyoid
Hyoglossus

Figure 16.3 Medial wall of the infratemporal fossa and the stylohamular plane.

jugular vein and the vagus nerve are deep to the styloid apparatus (Figures 16.3 and 16.4).

MUSCLES OF MASTICATION

The masticatory muscles define the infratemporal fossa and the masticatory space. Their innervation and vascular supply originate from within the infratemporal fossa. They are derived from the first branchial arch and are innervated by the nerve of that arch – the trigeminal nerve. The four additional muscles derived from the first arch – tensor veli palatini, tensor tympani, mylohyoid and anterior belly of the digastric – are also supplied by the trigeminal nerve.

The primary function of the muscles of mastication is the prehension, cutting and grinding of food. They have additional roles in speech articulation and mimetic facial movement.

Temporal fossa, temporalis fascia and muscle

The temporal fossa is a depression on the lateral aspect of the skull extending from the superior temporal line to the infratemporal crest of the greater wing of the sphenoid, containing the temporalis fascia and the temporalis muscle. Its limits are precise. The floor is formed by contributions from the parietal bone, squamous temporal bone, greater wing of the sphenoid and the frontal bone. The pterion – the *H*-shaped pattern of sutures between the frontal, parietal, squamous temporal and greater wing of the sphenoid, and the weakest area of the skull – marks the approximate position of the anterior branch of the middle meningeal artery, an unfortunate juxtaposition with acknowledged implications for extradural haematomas.

The temporalis fascia (deep temporal fascia) is a tough, fibrous structure arising from the entire superior temporal line and lateral aspect of the frontal process of the zygoma. A small tubercle – the marginal process – may be present on the posterior border of the frontal process, the result of ossification of the fascia.

The fascia divides into two layers at a variable distance, usually about 2 cm, above the zygomatic

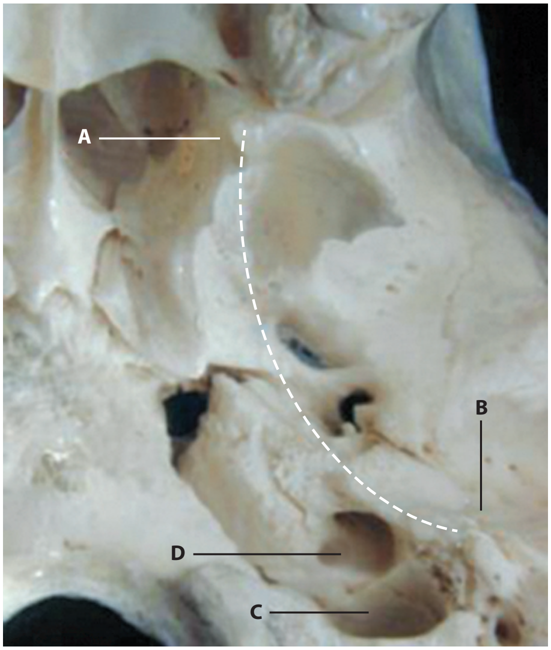

Figure 16.4 The stylohamular plane. The internal carotid artery and internal jugular vein are deep to this surgical plane. A – pterygoid hamulus. B – styloid process. C – jugular foramen. D – carotid canal.

arch inserting into the lateral and medial aspects of the arch. The zygomatic branch of superficial temporal artery, a small fat pad and branch of the maxillary nerve are contained within the two fascial leaves, not of significance surgically. The fascia is inextensible; its edges are difficult to approximate following incision.

The fan-shaped temporalis muscle arises from the temporal fossa, superiorly as far as the inferior temporal line and inferiorly to the infratemporal crest of the greater wing of the sphenoid. A plane exists between the fascia and muscle that is relevant surgically. The fascia may be lifted as a layer separate from the muscle when elevating a coronal scalp flap. This subfascial plane and the attachment of the temporalis fascia to the arch and frontal process of the zygoma is the basis for the temporal (Gillie's) approach for elevating fractures of the zygoma; the zygomatic fracture is elevated after an instrument is passed deep to both the fascia and the zygomatic arch.

The anterior fibres are orientated vertically, the most posterior horizontally – the latter the only muscle to retrude the mandible. The temporalis inserts into the crest, anterior and posterior borders and the medial aspect of the coronoid process. A tendinous extension runs down the anterior border of the ramus as far as the retromolar trigone. Myofascial pain in the muscle/tendon can be misdiagnosed as pain arising from the mandibular third molar tooth (Figure 16.5).

The blood supply is from the anterior and posterior deep temporal arteries – branches of the maxillary – and middle temporal artery from the superficial temporal artery. The arterial supply is

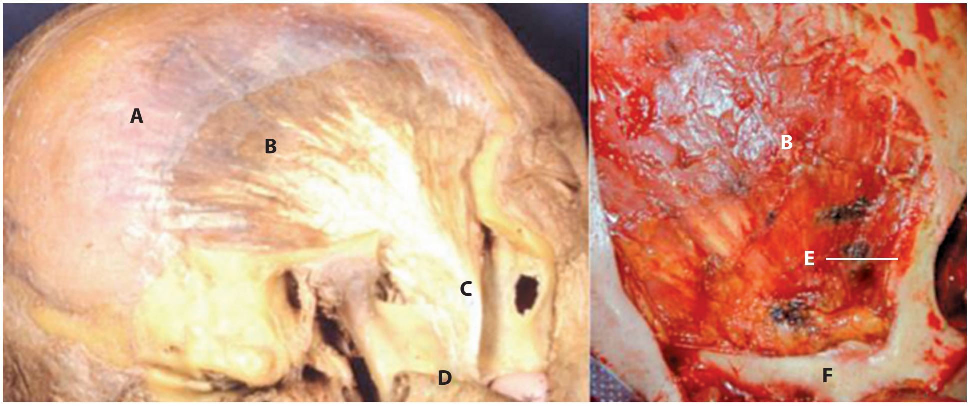

Figure 16.5 Temporalis muscle following reflection of the zygomatic arch on left and with arch in situ on right. A – temporalis fascia. B – temporalis muscle in temporal fossa, its multipennate (multidirectional) nature evident. C – temporalis tendon insertion into the coronoid process. D – masseter reflected. E – marginal process of zygoma. F – zygomatic arch/body.

axial, i.e. the vessels run the entire length of the muscle. This vascular arrangement permits the temporalis muscle to be used as an inferiorly based pedicled flap, either dynamic or static – increased length being obtained with division of the coronoid process – for reconstruction of a variety of local defects and in the treatment of facial paralysis. The temporalis fascia can be incorporated with the flap. The muscle may be split longitudinally (along its long axis), retaining its axial supply from individual arteries; the vessels are identified at operation, if necessary, with a Doppler.

A further vascular advantage is that the arterial supply is placed medial (*deep temporal*) and lateral (*middle temporal*) with few vessels in the mid-sagittal plane. Careful splitting of the flap in the sagittal plane is possible.

The nerve supply to the muscle is from the anterior deep temporal (ADT), middle deep temporal (MDT) and posterior deep temporal (PDT) nerves. – branches of the anterior division of the mandibular nerve – with additional motor supply from the masseteric and buccal nerves. Discrete neuromuscular subunits have been identified within the muscle based on the ADT, MDT PDT nerves, providing the possibility of individual dynamic muscle flaps, each with a different vector, in the treatment of facial palsy.

The temporalis is the most versatile masticatory muscle for local reconstruction.

Masseter

This muscle is quadrilateral in shape with three layers blending anteriorly. The superficial layers angle forwards at approximately 10 degrees from the vertical; the muscle is visible in lean individuals.

The masseter arises from the body and arch of the zygoma and the zygomatic process of the maxilla (*zygomatic buttress*). The deep fibres run vertically, evident just anterior to the temporomandibular joint where they are not covered by the superficial layers (Figure 16.6).

The muscle inserts onto the ramus laterally from the lower border to the lateral aspect of the coronoid process, blending with the fibres of the temporalis. Although fusion between the deep fibres of masseter and the temporalis has been described, a distinct plane exists between these two muscles anteriorly and is readily identifiable at operation.

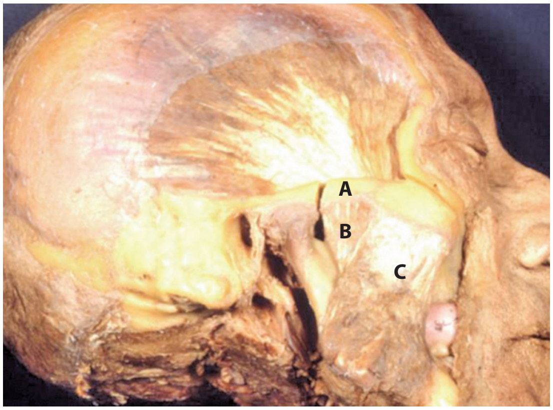

Figure 16.6 Masseter muscle. A – zygomatic arch. B – superficial fibres. C – deep fibres. Note the 10° anterior forward inclination of the superficial fibres.

The principal blood supply is from the masseteric arteries, branches of the maxillary artery. They enter the deep aspect of the muscle after passing through the sigmoid notch. Additional supply is derived from the transverse facial and superficial temporal arteries.

The masseter has been used as a muscle-only flap for local reconstruction; however, the arrangement of its blood supply limits its versatility.

The masseteric nerves, branches of the anterior division of the mandibular nerve, accompany the masseteric arteries through the sigmoid notch.

Medial pterygoid

The deepest of the masticatory muscles, the medial pterygoid has two heads of origin:

1. The deep – *pterygoid* – head provides the bulk of muscle. It arises from the medial aspect of the lateral pterygoid plate and the pterygoid fossa, deep to the lower head of the lateral pterygoid.
2. The superficial head arises from the maxillary tuberosity.

As with the masseter, it is quadrate in shape, mirroring the masseter on the medial aspect of the mandible. The muscle passes down and back at an angle of about 10 degrees – the same orientation of the superficial fibres of the masseter – and is inserted onto a roughened area on the medial aspect of the mandible below the mandibular foramen. Its angulation in the coronal plane – best seen in magnetic resonance imaging (MRI) images – is about 30 degrees to the long axis of the mandible, hence its role in lateral mandibular movement to the opposite side. The blood supply is from the pterygoid branches of the maxillary artery and is innervated by the medial pterygoid branch of the mandibular nerve (Figure 16.7).

The masseter and medial pterygoid form the so-called *pterygomasseteric sling* suspending the mandibular angle; inferior displacement of the mandible is also limited by the insertion of the sphenomandibular ligament onto the lingula medially. The pterygomasseteric sling and the sphenomandibular ligament together control the arc of rotation of the mandible.

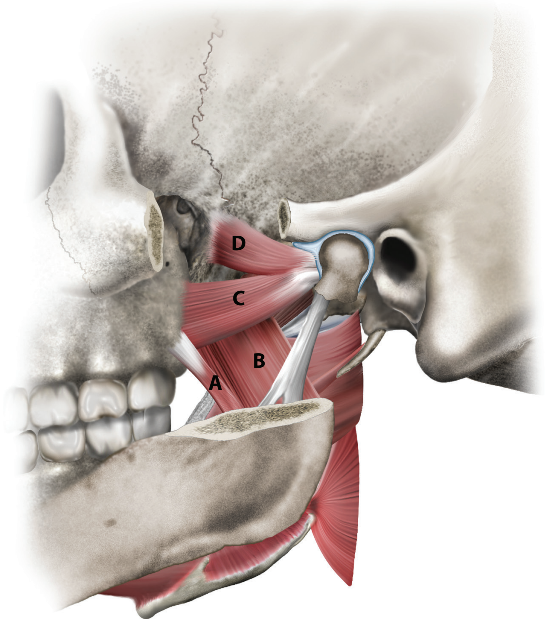

Figure 16.7 Medial and lateral pterygoid muscles. A – superficial head. B – deep head of medial pterygoid. Note the 10° anterior forward inclination mirroring the superficial masseter fibres. As demonstrated in Figure 16.1, the two heads of the medial pterygoid embrace the lower head of the lateral pterygoid. C – lower head. D – upper head of lateral pterygoid.

Lateral pterygoid

This muscle has assumed a specialized role in mandibular opening, reflected by the horizontal orientation of its fibres. There are two heads of origin:

1. The smaller superior head arises from the infratemporal surface and crest of the greater wing of the sphenoid.
2. The inferior head arises from the lateral aspect of the lateral pterygoid plate.

The fibres from both heads converge, run in a posterior and lateral direction, and insert into the capsule of the temporomandibular joint, the anterior and medial aspect of articular disc and the localized depression on the front of the neck of the mandibular condyle – the pterygoid fovea.

The blood supply is derived from the pterygoid branches of the maxillary artery with additional input from the ascending palatine artery.

The two heads are innervated individually – lateral pterygoid nerves – from the anterior division of the mandibular nerve. Electromyography (EMG) studies confirm that the two heads also function independently. The upper head is only active during closure/clenching, stabilizing the condyle and disc against the articular eminence. The lower head is active during mandibular opening and is a synergist of the suprahyoid muscles.

The orientation of the individual masticatory muscles is the direction in which they move the jaw. As with the extraocular muscles, the masticatory muscles function as a group, and it is only when pathology intervenes that their individual actions – or lack of action – become evident.

The individual lateral pterygoid muscles move the jaw to the opposite side, rotating around an axis of the opposite condyle. A useful aide memoir is that this is similar to the action of the sternocleidomastoid moving the head to the opposite side. Fractures of the mandibular condyle result in mandibular deviation to the affected side due to the unopposed action of the muscle on the opposite (normal) side.

With tumours affecting the motor root of the mandibular division, wasting of the masticatory muscles occurs, most obvious in the temporal fossa. The mandible deviates to the side of the pathology due to the unopposed action of the opposite lateral and medial pterygoid muscles.

MANDIBULAR NERVE

Located in the lateral wall of the cavernous sinus. the mandibular nerve exits the skull base at f.ovale lateral to the tensor veli palatini in the sidewall of the pharynx deep to lateral pterygoid. It is at a depth of about 4 cm just anterior to the condylar neck in the lateral view (Figure 16.8).

Before dividing into its anterior and posterior divisions , the main trunk gives of four branches:

- *Meningeal branch (nervus spinosus):* Enters the skull base via f.spinosum.
- *Nerve to medial pterygoid:* Passes through otic ganglion unchanged to enter the muscle.
- *Nerve to tensor tympani and tensor veli palatini*: Both pass through the otic ganglion without synapse to the respective muscles.

Anterior division: The smaller anterior division is motor except for the buccal nerve:

- *(Long) buccal nerve:* Passes between the upper and lower heads of the lateral pterygoid, sends a motor branch to the temporalis and then continues over the superficial surface of the buccinator supplying sensation to the buccal mucosa.
- *Motor branches to the lateral pterygoid, masseter and the temporalis* (anterior and posterior deep temporal nerves).

Posterior division: This division is sensory apart from the motor fibres distributed through the nerve to the mylohyoid.

- *Auriculotemporal nerve:* Its two roots encircle the middle meningeal artery deep to the lateral pterygoid and then run superiorly around the condylar neck deep to the sphenomandibular ligament. It is closely related to the main trunk of the superficial temporal artery in the temple, where it is most easily identified surgically. It supplies general sensation to the temple, superolateral aspect of the pinna, part of the external meatus and the tympanic membrane, and to the capsule of the temporomandibular joint. The nerve contains the postganglionic fibres from the otic ganglion to the parotid.
- *Inferior alveolar nerve:* The largest branch of the posterior division behind and lateral to the lingual nerve. It supplies sensation to the dentition and the mandible, exiting the mental foramen as the mental nerve(s) supplying sensation to the labial gingiva, mucosa and lower lip/chin. Prior to entering the inferior alveolar canal, it gives of the nerve to the mylohyoid, grooving the ramus medially. It contains the motor fibres for the anterior belly of the digastric. Sensory fibres in the nerve to the mylohyoid contribute to chin sensation.
- *Lingual nerve:* Emerging below the lateral pterygoid it is closely related to the lingual aspect of the mandible and at risk in lower third molar surgery. In 5 per cent of individuals it runs above the mandibular alveolus. The nerve contains the taste sensory fibres from the anterior two-thirds of the tongue (to chorda tympani) and the preganglionic parasympathetic fibres destined for the submandibular ganglion.

The proximity of the inferior alveolar and lingual nerves in the pterygomandibular space is utilized in the inferior alveolar nerve block dental (Figure 16.9).

Due to their size and location, both nerves provide landmarks in surgery of the ITF and can be followed to f.ovale. The internal carotid artery and internal jugular vein are deep and not at risk (Figure 16.10).

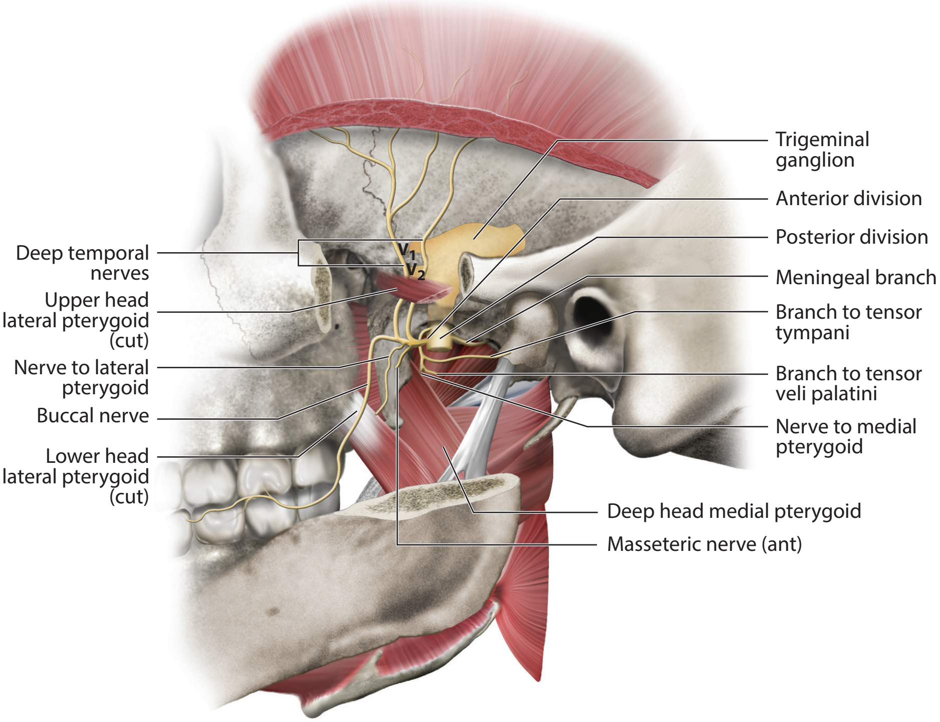
Deep temporal nerves
Upper head lateral pterygoid (cut)
Nerve to lateral pterygoid
Buccal nerve
Lower head lateral pterygoid (cut)
V_1
V_2
Trigeminal ganglion
Anterior division
Posterior division
Meningeal branch
Branch to tensor tympani
Branch to tensor veli palatini
Nerve to medial pterygoid
Deep head medial pterygoid
Masseteric nerve (ant)

Main trunk and anterior division

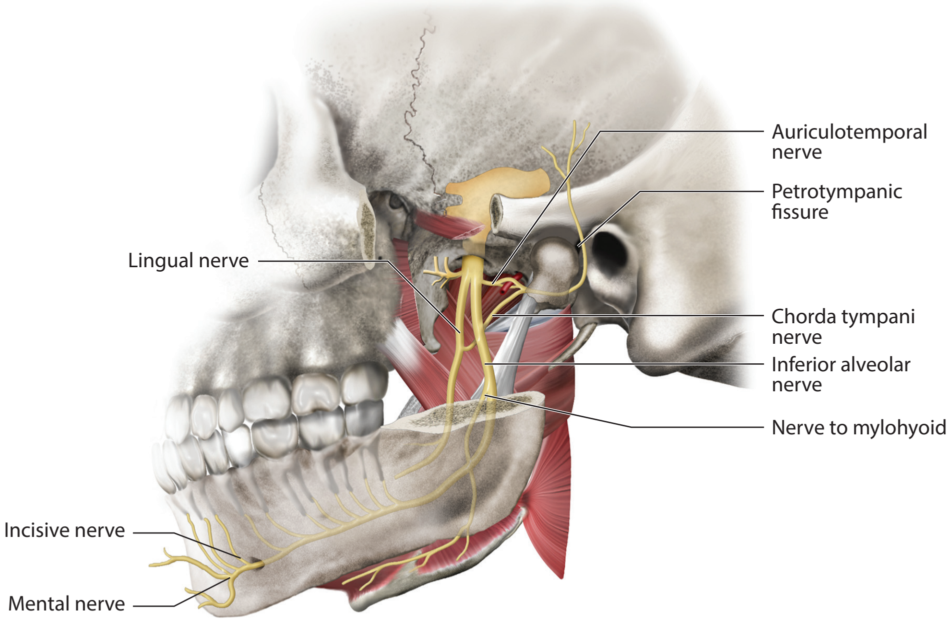
Lingual nerve
Incisive nerve
Mental nerve
Auriculotemporal nerve
Petrotympanic fissure
Chorda tympani nerve
Inferior alveolar nerve
Nerve to mylohyoid

Posterior division

Figure 16.8 Mandibular nerve.

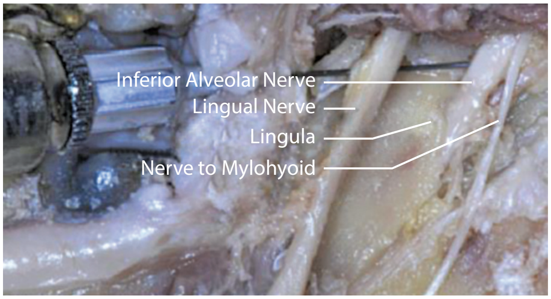

Figure 16.9 Spatial arrangement of nerves with inferior alveolar dental anaesthesia. Morris CD, Rasmussen J, Throckmorton GS, Finn S. The anatomic basis of lingual nerve trauma associated with inferior alveolar blocks. *Journal of Oral and Maxillofacial Surgery*. 2010; 68: 2833-36 – with permission.

Otic ganglion

This parasympathetic ganglion immediately below the foramen ovale on the medial side of the main trunk of the mandibular nerve is well protected. Its principal role is the provision of parasympathetic secretomotor fibres for the parotid gland. Only the parasympathetic fibres – derived from the lesser petrosal nerve exiting through f.ovale – synapse in the ganglion. The sensory root is derived from the auriculotemporal nerve. The postganglionic fibres with the sensory and sympathetic fibres reach the parotid gland with the auriculotemporal nerve.

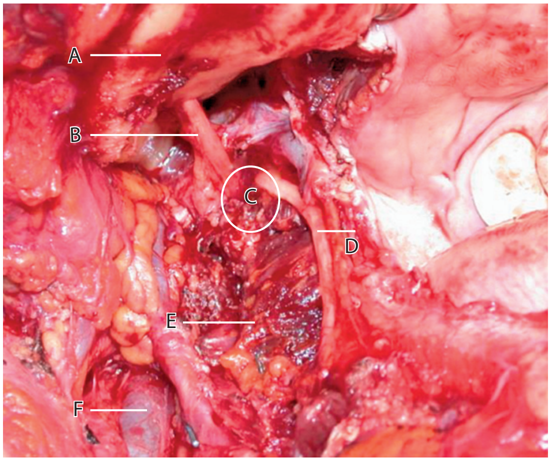

Figure 16.10 Lingual and inferior alveolar nerves traced to the skull base – foramen ovale – 'mandibular swing' osteotomy used for access. Pterygoid plates/pterygopalatine fossa contents resected. A – medial aspect mandible. B – inferior alveolar nerve. C – nerves converging at foramen ovale. D – lingual nerve. E – medial pterygoid. F – internal jugular vein

VASCULAR SUPPLY

The abundant arterial and venous capacity of the ITF is understandable as the vessels supply the high-energy demands of the masticatory muscles.

Maxillary artery

A terminal branch of the external carotid artery, the maxillary artery's diameter – from 2 to 6 mm – is larger than that of the other terminal branch of the external carotid artery, the superficial temporal artery. Its branches are distributed widely to the mandible, maxillary, teeth, masticatory muscles, palate, nose and dura.

Arising deep to the neck of the mandibular condyle within the parotid gland, it is described in three parts: mandibular, pterygoid and pterygopalatine (see Figures 16.1 and 16.12).

The *mandibular segment* runs horizontally immediately deep to the neck of the mandibular condyle and may be adherent to the joint capsule; therefore, it is at risk in temporomandibular joint surgery. The five branches of this segment all enter bone:

1. Inferior alveolar artery enters the inferior alveolar canal.
2. Middle meningeal artery enters f.spinosum.
3. Accessory meningeal artery enters f.ovale.
4. Deep auricular artery pierces the bony or cartilaginous external auditory meatus.
5. Anterior tympanic artery enters the petrotympanic fissure to the middle ear.

Surgically, the principal branches of the first part of the artery are the middle meningeal and the inferior alveolar arteries

The second part, the pterygoid segment, runs up and forwards medial to the temporalis either superficial or deep to the lower head of the lateral pterygoid and intimately associated with both the inferior alveolar and lingual nerves. Although described as having five branches to the masticatory muscles (described earlier with the individual muscles), the considerable anastomosis between individual branches and the variation in the vascular patterns make this description of little practical value to the surgeon. If the relationship of the artery to the lateral pterygoid is clinically relevant, this may be assessed with computerized tomography (CT) or MRI.

A branch of this segment, or the posterior superior alveolar artery from the third part of the vessel (see the following discussion), may be adherent to the maxillary tuberosity – a possible cause of brisk haemorrhage with tuberosity fractures and posterior superior local anaesthetic nerve injections.

Branches of the maxillary artery in the infratemporal fossa historically were accessed by a classical 'open' Caldwell-Luc approach. Current practice favours an endoscopic approach, usually either transnasal or Caldwell-Luc transmaxillary.

The artery terminates in the pterygopalatine fossa as the *pterygopalatine (third) segment*, described later in this chapter.

Pterygoid venous plexus

The plexus consists of copious large-calibre veins surrounding the pterygoid segment of the maxillary artery. The branches of the plexus, allowing for variation, correspond to the branches of the maxillary artery. Mandibular movement changing both the volume and position of the pterygoid muscles aids venous drainage; the venous plexus acts with the pterygoids as a 'venous pump'. There is considerable variation in the extent of this venous plexus between individuals. Haemorrhage from the plexus can be troublesome, and diathermy may prove ineffective in achieving control.

The pterygoid plexus communicates with:

- the middle fossa and cavernous sinus via emissary veins traversing f.ovale, f.vesalius and f.lacerum.
- the orbit via the inferior ophthalmic veins traversing the inferior orbital fissure.
- the facial vein via the deep facial vein.

The potential for infection to spread from the ITF to these sites or vice versa is evident.

The plexus drains into the maxillary vein, corresponding with the mandibular segment of the maxillary artery. The maxillary vein merges with the superficial temporal vein to form the retromandibular vein.

THE PTERYGOPALATINE (PTERYGOMAXILLARY) FOSSA

The pterygopalatine fossa (PTF) is a small, inverted pyramidal space immediately beneath the orbital apex. It measures approximately 2 cm vertically and 1 cm at its base. Effectively a 'side compartment' of the infratemporal fossa, wedged as it is between the infratemporal fossa laterally and the nasopharynx medially, it functions as a neurovascular conduit.

The body of the sphenoid forms the roof. The posterior boundary is the root of the pterygoid process of the sphenoid (containing the pterygoid (Vidian) canal and the greater wing of the sphenoid (containing foramen rotundum). The posterior wall of the maxilla forms the anterior boundary. Viewed anteriorly, foramen rotundum is above and lateral to the pterygoid canal (Figure 16.11).

Medially, the pterygopalatine fossa is separated from the nasal cavity by the perpendicular plate of

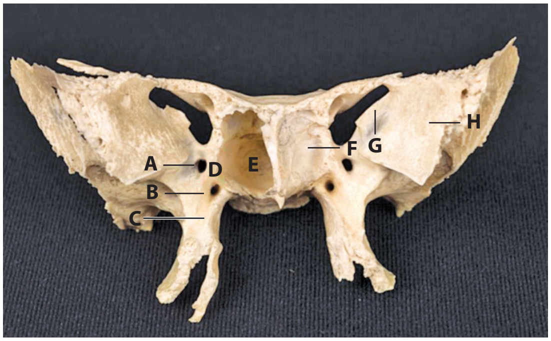

Figure 16.11 Anterior view of the sphenoid. A – foramen rotundum. B – pterygoid (Vidian) canal. C – pterygoid process (A–C forming the posterior boundary of the PT). D – surgical corridor between f.rotundum and Vidian canal to lateral wall sphenoid sinus, cavernous sinus and internal carotid. E – sphenoid sinus. F – anterior wall sphenoid sinus. G – superior orbital fissure. H – greater wing of sphenoid in lateral orbit.

the palatine bone (part of the lateral wall of the nose), with the sphenopaltine foramen linking both. The perpendicular plate divides superiorly into an anterior orbital process, forming part of the orbital floor, and a posterior sphenoid process which together with the roof form the sphenopalatine foramen. The perpendicular plate articulates with the medial surface of the medial pterygoid plate posteriorly and the medial wall of the maxillary sinus anteriorly.

The pterygopalatine fossa contains:

- the pterygopalatine ganglion
- the maxillary nerve
- the third (pterygopalatine) part of the maxillary artery and its accompanying veins

It communicates with the:

- *orbit* via the medial end of the inferior orbital fissure.
- *nasal cavity* through the sphenopalatine foramen.
- *nasopharynx* via the palatovaginal cana.
- *infratemporal fossa* through the pterygomaxillary fissure.
- *middle fossa/cavernous sinus* via foramen rotundum and the pterygoid canal.
- *oral cavity* via the greater palatine canal.

The close proximity to these adjacent areas permits ready spread of both tumours and infection from the pterygopalatine fossa and vice versa; this is particularly relevant when considering the possibility of complete resection of malignant neoplasm.

Spatial arrangement of the neurovascular contents of the pterygopalatine fossa

The maxillary artery and its branches are located in a plane anterior to the pterygopalatine ganglion, maxillary and Vidian nerves. Some consider this arrangement conceptually creates two compartments in the fossa: the anterior compartment containing the third part of the maxillary artery and its branches, and the posterior containing the pterygopalatine ganglion, maxillary and Vidian nerves and their branches. The veins accompanying the third (pterygoplatine) part of the maxillary artery, in common with those accompanying the second (pterygoid) part, are in the form of a venous plexus. Profuse haemorrhage may be encountered from this venous plexus. All structures in the pterygopalatine fossa are surrounded by fat which, taken together with the variable and tortuous course of the maxillary artery and its venous plexus, necessitates meticulous dissection.

This spatial arrangement is particularly relevant in endoscopic approaches to the pterygopalatine and infratemporal fossae.

Pterygoid plates

The infratemporal and pterygopalatine fossae demonstrate the role of the individual pterygoid plates. The lateral pterygoid plate and the adjacent pterygoid fossa (situated between the lateral and medial pterygoid plates) 'belong' to the infratemporal fossa/masticator space by providing origin to the lateral and medial pterygoid muscles. The medial pterygoid plate is the province of the pharynx – as the origin of the pharyngo-basilar fascia/superior constrictor and the pterygomandibular raphe. The significantly larger lateral pterygoid plates compared to the medial reflects their function.

Pterygopalatine ganglion

The largest of the peripheral parasympathetic ganglia is well protected deep in the pterygopalatine fossa. Immediately in front of the pterygoid canal, the nerve of that canal (Vidian n.) runs straight into the ganglion. The ganglion is below and medial to foramen rotundum and the maxillary nerve, and lateral to the sphenopalatine foramen. It is connected to the maxillary nerve by two ganglionic branches. The pterygopalatine ganglion's primary function is the parasympathetic secretomotor supply to the nasal cavity and paranasal sinuses – the 'ganglion of hay fever'. Intranasal local anaesthetic blockade of the ganglion has been used for the treatment of a variety of pain conditions.

Maxillary nerve

The second division of the trigeminal nerve is purely sensory. It exits the skull base at foramen rotundum and enters the upper part of the pterygopalatine fossa from which all its extracranial branches are derived. The meningeal branch is given off in the middle fossa and accompanies the middle meningeal artery.

The branches are classified into those coming directly off the nerve and those associated with the pterygopalatine ganglion. Branches from the main trunk include:

- *Ganglionic branches;* see earlier discussion.
- *Zygomatic nerve:* Enters the orbit via the inferior orbital fissure dividing into the zygomatico-temporal and zygomatico-facial nerves supplying the skin over the cheek prominence. The role of the zygomatico-temporal nerve carrying post-ganglionic fibres from the sphenopalatine ganglion thence to the lacrimal branch of the ophthalmic nerve to supply the lacrimal gland is questioned.
- *Posterior superior alveolar nerve(s).*
- *Infraorbital nerve:* The terminal branch of the maxillary nerve runs laterally in the pterygopalatine fossa for about 1 cm before entering the orbit entering the orbit via the inferior orbital fissure. Running parallel to the medial orbital wall, it provides a useful landmark in orbital exploration (see Chapter 12). The infraorbital nerve is a constant landmark in the superior aspect of the pterygopalatine fossa as it delineates the boundary between the infratemporal fossa laterally and the pterygopalatine fossa medially.

Branches from the ganglion include:

- *Orbital nerve:* Enters the orbit via the inferior orbital fissure to supply the orbital periosteum.
- *Nasopalatine nerve:* Enters the nasal cavity via the sphenopalatine foramen, crosses to the back of the nasal septum and then runs down and forwards to exit via the incisive canal to supply sensation to the anterior hard palate.
- *Posterior superior nasal nerves (lateral and medial):* Also enter the nasal cavity via the sphenopalatine foramen to supply sensation to the nasal side wall and a limited area of the nasal roof and septum.
- *Greater and lesser palatine nerves:* The greater palatine nerves pass down from the ganglion through the greater palatine canal onto the hard palate. Whilst in the canal they give off the *posterior inferior nasal nerve*. Taste from the palate is transmitted via the palatine nerves to the greater petrosal nerves; the cell bodies are in the facial (geniculate) ganglion. The lesser palatine nerves (two in number) pass behind the greater palatine nerves exiting the lesser palatine foramina to supply the soft palate.
- *Pharyngeal branch:* Supply sensation to the nasopharynx.

Maxillary artery

The maxillary artery terminates in the pterygopalatine fossa and gives off branches that accompany the branches of the maxillary nerve. The artery has a tortuous and variable root. Significantly, it is always anterior to the nerves in the pterygopalatine fossa; this relationship is relevant in endoscopic and open approaches to the PPF (Figure 16.12).

It terminates as the sphenopalatine and the greater (descending) palatine arteries, both of which have surgical significance.

The sphenopalatine artery, the largest distal branch of the maxillary, enters the nasal cavity via the sphenopalatine foramen and provides the major blood supply to the nasal cavity. Ligation of this vessel may be needed in the management of refactory epistaxis; it is located endoscopically at the sphenopalatine foramen at the posterior end of the middle turbinate.

This vessel also provides the axial blood supply to the nasoseptal flap, middle turbinate flap and the posteriorly based inferior turbinate flap used in endoscopic skull base repair, reflecting the contribution of this vessel to the nasal blood supply.

The greater palatine artery gives off two or three lesser palatine arteries within the greater palatine canal to supply the soft palate and enters the roof of the hard palate at the greater palatine foramen running forwards to supply the hard palate. It provides the axial blood supply to posteriorly based palatal mucosal flaps used in local reconstruction. The entire mucosa of the hard palate can be pedicled on a single greater palatine artery.

The posterior superior alveolar artery exits the pterygomaxillary fissure (as noted earlier), and a branch of this vessel may be adherent to the maxillary tuberosity. The remaining branches are the

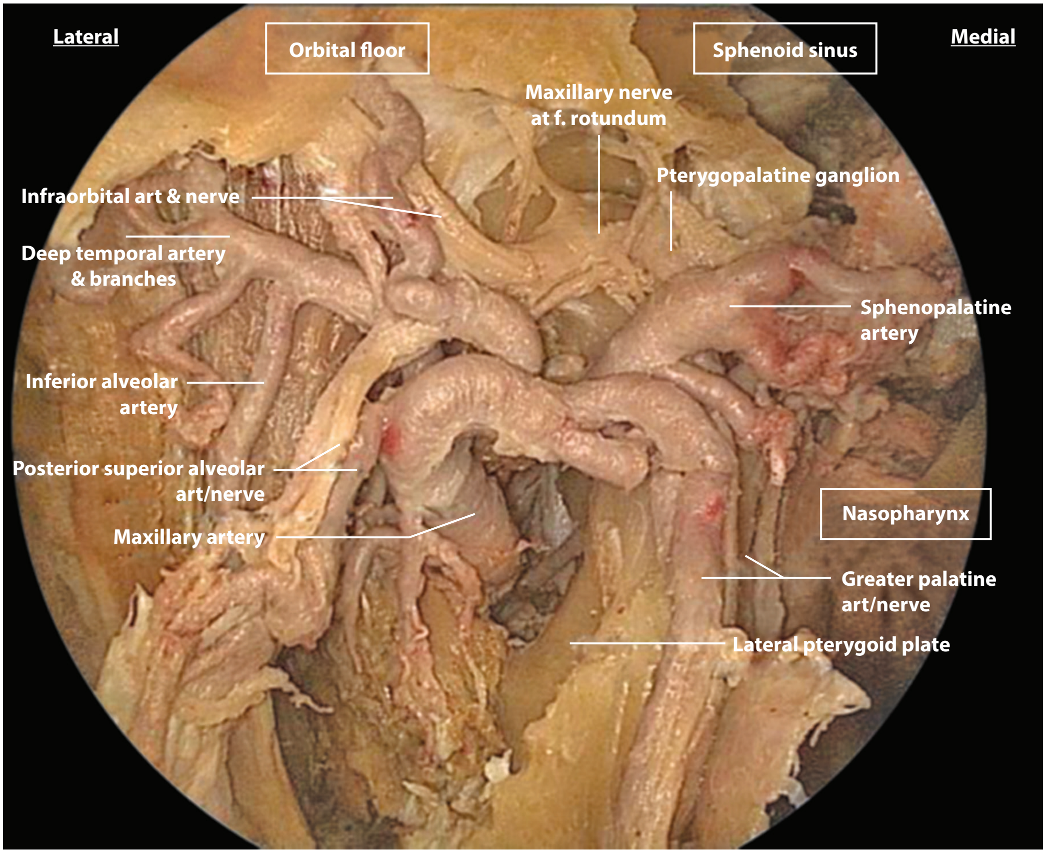
Lateral
Orbital floor
Sphenoid sinus
Medial
Maxillary nerve at f. rotundum
Pterygopalatine ganglion
Infraorbital art & nerve
Deep temporal artery & branches
Sphenopalatine artery
Inferior alveolar artery
Posterior superior alveolar art/nerve
Maxillary artery
Nasopharynx
Greater palatine art/nerve
Lateral pterygoid plate

Figure 16.12 Endoscopic dissection of the right pterygopalatine fossa viewed from an anterior direction through a 00 endoscope. The anterior relationship of the maxillary artery and its branches in the fossa to the maxillary nerve and its branches is evident. The anterior aspect of the sphenopalatine foramen has been removed to expose the artery as it enters the nasal cavity. Dissection performed by Professor Carl Snyderman, University of Pittsburgh Medical Center. Image reproduced from *Gray's Anatomy*, 41st ed., with permission.

infraorbital artery, the artery of the pterygoid canal (Vidian artery) and the pharyngeal artery.

Veins of the pterygopalatine fossa

As noted, a rich venous plexus drains the second and third parts of the artery. Only the first part of the maxillary artery has an accompanying vein – the maxillary vein.

SURGICAL APPROACHES

Surgical interest in the ITF/PTF dates back to the 1850s when exposure was needed to treat sphenopalatine neuralgia. As a result of their deep location behind the face and beneath the middle cranial fossa, a variety of surgical approaches have been used to provide access. The increased use of endoscopic endonasal and endoscopic transantral approaches has resulted in the less frequent use of the open transfacial/transmandibular/transzygomatic/transcranial approaches and the microscopic transmaxillary and transantral approaches. Image guidance has improved both accuracy and safety.

Whilst the various surgical approaches are beyond the remit of this chapter, following is a summary of some of the available anatomical landmarks.

1. The in-line arrangement of the posterior edge of the lateral pterygoid plate and f.ovale, f.spinosum and spine of the sphenoid (Figure 16.2).
2. Stylohamular plane (Figures 16.3 and 16.4).
3. Lingual and/or inferior alveolar nerves traced to f.ovale (Figure 16.10).
4. The infraorbital nerve delineates the infratemporal fossa laterally and the pterygopalatine fossa medially – best appreciated by considering the intracranial relationship of the anterior margin of f.ovale and posterior margin f.rotundum. Both are in-line and in the same plane as the lateral pterygoid plate, i.e. the lateral limit of the PTF.
5. The posterior edge of the medial pterygoid plate is immediately anterior to f.lacerum and the anterior genu (*terminal portion*) of the petrous internal carotid artery immediately superior and within f.lacerum.
6. The Vidian nerve runs from f.lacerum to the pterygopalatine fossa medial to the mandibular nerve and provides a landmark for both the anterior genu of the petrous internal carotid and f.lacerum.
7. Endoscopic/microscopic proximal dissection of the maxillary and the Vidian nerves in the PPF defines a surgical corridor between them that can be traced back to the lateral wall of the sphenoid sinus (Figure 16.11) and to the cavernous sinus and internal carotid.
8. The spatial arrangement ('topography') of the vessels and nerves in the PTF: The third part of the maxillary artery and its branches are anterior to the sphenopalatine ganglion, maxillary and Vidian nerves (Figure 16.12).

These landmarks are valuable adjuncts whether surgery is endoscopic or microscopic (Figure 16.12) or open (Figure 16.13).

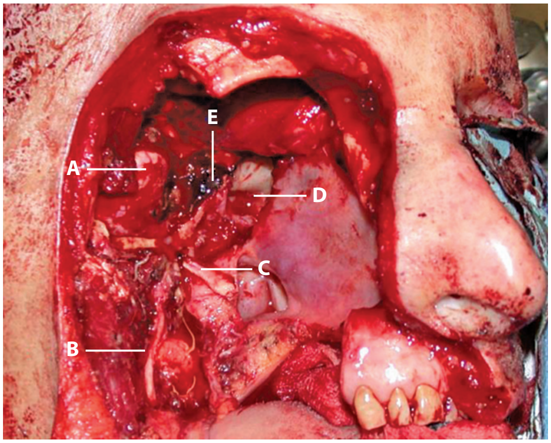

Figure 16.13 Composite resection of the floor of the anterior/middle fossae, right orbit and maxilla, infratemporal/pterygopalatine fossae. A – temporal lobe dura. B – lingual nerve traced to foramen ovale. C – remnant of infraorbital nerve traced to f.rotundum (later resected). D – right sphenoid sinus. E – right cavernous sinus.

FURTHER READING

Alfieri A et al. Endoscopic endonasal approach to the pterygopalatine fossa: Anatomic study. *Neurosurgery*. 2003; 52: 372–4.

Chang Y, Cantelmi D, Wisco JJ, Fattah A, Hannam AG, Agur AM. Evidence for the functional compartmentalization of the temporalis muscle: A 3-dimensional study of innervation. *Journal of Oral and Maxillofacial Surgery*. 2013; 71: 1170–7.

Cheung LK. The vascular anatomy of the human temporalis muscle. *International Journal of Oral and Maxillofacial Surgery*. 1996; 25: 414–21.

Cavallo LM et al. Extended endoscopic endonasal approach to the pterygopalatine fossa: Anatomical study and clinical considerations. *Neurosurgical Focus*. 2005; 19(1) E5; 1–7.

Friedman WH, Katsantonis GP, Copper MH et al. Stylo-hamular dissection: A new method for en-bloc resection of malignancies of the infratemporal fossa. *Laryngoscope*. 1981; 91: 1869–79.

Janfaza P, Nadol Jr JB, Galla RJ, Fabian RL, Montgomery WW. (Eds.). *Surgical Anatomy of the Head and Neck*. Philadelphia: Lippincott Williams & Wilkins, 2001.

Lang J. *Clinical Anatomy of the Masticatory Apparatus and Peripharyngeal Spaces*. Stuttgart: George Thieme Verlag. 1995.

McMahon JD, Wong LS, Crowther J, Taylor WM, McManners J, Devine JC, Wales C, MacIver C. Patterns of local recurrence after primary resection of cancers that arise in the sinonasal region and the maxillary alveolus. *British Journal of Oral and Maxillofacial Surgery*. 2013; 51: 389–93.

Standring S. (Ed.). *Gray's Anatomy: The Anatomical Basis of Clinical Practice*. 40th ed. Edinburgh: Elsevier/Churchill Livingstone, 2008.

Theodosopolous PV. Anatomical approach to the infratemporal fossa: An anatomical study. *Neurosurgery*. 2010; 66: 196–203.

17

Temporomandibular joint

ANDREW J. SIDEBOTTOM

Basic structures of the temporomandibular joint 167
Function of the TMJ 168
Development of the TMJ 168
The capsule 168
Articular disc 168
Synovial membrane 169
Ligaments associated with the TMJ 169
Lateral ligament *169*
Sphenomandibular ligament *169*
Stylomandibular ligament *169*
Otomandibular ligaments *170*
Sensory nerve supply 170
Blood supply 170
Muscles of mastication 172
Other neural structures in close association with the TMJ 172
Facial nerve *172*
Articular fossa and eminence 173
Condyle of the mandible 174
The coronoid process 174
Arthroscopy 174
Main surgical approaches to the TMJ 175
Superior approach *175*
Inferior approach *176*
Wound closure *177*
Summary 177
Further reading 177

BASIC STRUCTURES OF THE TEMPOROMANDIBULAR JOINT

The temporomandibular joint (TMJ) is a bilateral diarthrodial, ginglymoid synovial joint, which is independently freely mobile. Diarthrodial means there are two articulating bone components, and ginglymoid means hinge-like. The TMJ is also unique in that between the two joints lie the articulating surfaces of the teeth, such that minor changes in joint structure can lead to changes which are reflected in changes of occlusion; however, there is no conclusive evidence that the reverse is true.

The joint is synovial, which consists of the following:

- Capsule.
- Bones – condyle and glenoid fossa – providing smooth articular surfaces.
- Articular disc.
- Synovial membrane.
- Ligaments – lateral, stylomandibular, sphenomandibular, malleolomandibular and discomalleolar.
- Innervation – trigeminal nerve branches; auriculotemporal nerve, masseteric branch.
- Blood supply – terminal branches of the external carotid – maxillary and superficial temporal.
- Muscles of mastication – lateral pterygoid, medial pterygoid, temporalis, masseter.

FUNCTION OF THE TMJ

The function of the joint is to permit mastication of food, assist swallowing and aid in articulation during speech. The muscles of mastication provide the movements required to allow a hinge-like opening (lower joint space) for incision and glide to permit sideways movements and protrusion (upper joint space) during chewing. The hinge component permits around 26 mm opening whilst the glide permits the remainder of movement with 97 per cent of the population achieving 35 mm or more of opening. Loss of function of the upper joint space due to lubricant or disc related problems is the commonest cause of restricted opening and leads to reduced movement to the contralateral side. Opening remains more than 26 mm due to maintained lower joint space rotation. More marked restriction will be due to both intra- and extra-articular causes.

DEVELOPMENT OF THE TMJ

The joint starts to develop from the 10th week IU as two separate mesenchymal origins, the upper in the temporal bone and the lower in the condyle. The disc develops from a separate superior area. The temporal and condylar elements differentiate, leading to formation of a recognizable joint at 12 weeks IU. The condylar head provides the secondary growth centre which may be active until the third decade. Prolonged growth or excessive activity may be responsible for the development of condylar hyperplasia and associated growth disturbances in teenage life. Failure to grow will lead to clinically obvious issues in the first decade (e.g. hemifacial microsomia). This growth centre lies within the proximal condylar cartilage and is disrupted when the cartilage is damaged either following trauma (where growth may also be affected by loss of blood supply) or due to the induced growth arrest of high condylar shave.

The disc (not meniscus) is initially cellular and vascular and is continuous anteriorly with the lateral pterygoid muscle. The immature disc is rich in elastic fibres, and all three zones (anterior, intermediate and posterior) are recognizable by the 14th IU week. This gradually becomes avascular and therefore incapable of repair.

THE CAPSULE

The TMJ capsule attaches into the glenoid fossa superiorly and the eminence anteriorly. It is attached inferiorly to the condylar neck up to 1 cm from the condylar head. A thickening of the lateral portion has been called the lateral ligament. The intra-articular disc divides the capsule into upper and lower joint compartments. The capsule is fibroelastic, vascular and innervated mainly from the auriculotemporal nerve.

ARTICULAR DISC

The articular disc (which is not a meniscus) forms an oval shape between condyle and articular fossa of the temporal bone. It is biconcave, thicker at the rim and thinner in the centre. The disc is avascular and consists of type 1 collagen which is multidirectional. The main components of the connective tissue comprise proteoglycans (keratan sulphate, chondroitin sulphate and hyaluronic acid). The negative charges of the glycosaminoglycans (GAGs) attract water and permit the deformation which occurs during function, with return of disc shape at rest. Loss of these GAGs has been shown experimentally to lead to degenerative changes.

Anteriorly, the disc is continuous with the lateral pterygoid muscle and also with the capsule. Medially and laterally, it is inserted into the condyle which provides lower joint compartment movement and subsequent glide of the disc-condyle complex over the articular eminence on wider opening.

The smooth surface of the disc permits free movement of the two joint compartments, and loss of disc mobility or surface damage reduces movement. Surface lubrication is provided by the phospholipids and hyaluronic acid of the articular fluid. Synovial fluid provides the oxygen and metabolic needs of the surface cells and aids joint function. The theoretical attributes consist of boundary lubrication which reduces surface tension and permits free function whilst the fluid film keeps the joint surfaces apart. Loss of lubrication leads to the acute reduction in joint mobility seen in anchored disc phenomenon.

The repeated compression and release of clenching is felt to contribute to the extrusion of fluid and adhesion of the joint surfaces. This can be seen during arthroscopy with evidence of areas of fibrillation where the joint surfaces have been drawn apart by the hydrodissection of fluid infusion. Relubrication can be achieved by arthrocentesis which by hydrodissection separates the joint surfaces allowing the lubricant producing cells to recover and relubricate the joint naturally. Hyaluronic acid injections have additionally been used to facilitate improved outcome; however, there is little convincing evidence that they provide any advantage.

SYNOVIAL MEMBRANE

The synovial membrane surrounds the inner surface of the capsule of the joint and is the source of the synovial fluid. It contains free nerve endings, which is why inflammatory changes – synovitis – are painful. This pain responds to anti-inflammatory drugs (nonsteroidal anti-inflammatory drugs [NSAIDs] and steroids). The synovial cavity is around 2.2 mL (1.2 mL in the upper joint space) and contains the synovial fluid which provides a negative pressure within the joint and aids surface coating and therefore lubrication.

LIGAMENTS ASSOCIATED WITH THE TMJ

Lateral ligament

This ligament consists of a thickening of the lateral portion of the capsule of the joint (Figure 17.1). Whilst this is often described as consisting of a superficial and medial portion, clinically these are often difficult to define. Some authors feel repair of this is essential in closing the joint as it constrains anterior subluxation.

Sphenomandibular ligament

This ligament runs from the spine of the sphenoid to the lingula of the mandible and limits lateral movement of the mandible. It may also limit opening if it becomes calcified secondary to trauma.

Stylomandibular ligament

This 'ligament' is a thickening of the deep cervical fascia and runs from the tip of the styloid process to the angle of the mandible and limits protrusion of the mandible.

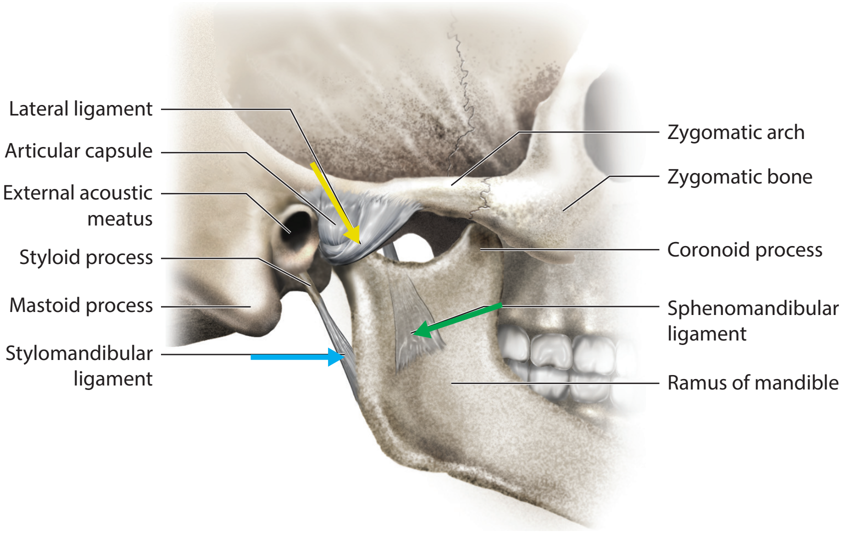

Figure 17.1 Ligaments of the TMJ: lateral ligament (yellow arrow), sphenomandibular ligament (green arrow), stylomandibular ligament (blue arrow).

Otomandibular ligaments

The otomandibular ligaments have become of interest due to their putative role in the relationship between the TMJ and tinnitus as they connect the malleus with the TMJ (discomalleolar present in 30 per cent dissections) and the malleus with the region of the lingula of the mandible (malleolar-mandibular). Whilst these have been dissected in cadaveric studies, there remains little conclusive evidence of any clinical significance.

SENSORY NERVE SUPPLY

Joint innervation is mainly from the auriculotemporal and also the masseteric branch of mandibular division of the trigeminal nerve (Figure 17.4). The disc and the cartilage are not innervated. Hilton's law suggests that a joint is innervated by the nerve which supplies the muscles moving it, hence the trigeminal nerve (mandibular division) is the motor supply to the muscles of mastication and the sensory supply to the joint. This can cause 'confusion' in locating the origin of pain from either the joint or muscles of mastication. Changes in innervation tend to occur with disease and increased sensitivity with inflammation. The auriculotemporal nerve arises as the mandibular division emerges from foramen ovale and travels along the posterior border of lateral pterygoid. It gives off many of its sensory branches on the medial side of the joint, traverses the posterior aspect of the joint and emerges posterolaterally, crossing the posterior capsule approximately one-third of the size. (Hence cryoanalgesia laterally will only control one-third of the sensory supply.) It progresses superiorly to supply sensation to the temple and superior half of the pinna.

BLOOD SUPPLY

The terminal branches of the external carotid artery lie in close proximity to the joint and provide its blood supply (Figures 17.2, 17.3 and 17.4). The external carotid artery divides around 2 cm proximal to the condylar head deep to the posterior ramus of the mandible and forms the superficial temporal and maxillary arteries. The superficial temporal artery continues superolaterally to run over the posterolateral capsule of the TMJ and continues just anterior to the tragal groove to divide at the top of the tragus to supply the forehead and temple, giving branches to the joint, external ear and zygomatic skin along the way. The maxillary artery heads medially into the infratemporal fossa with its three parts lying before and on the lateral pterygoid and the final part extending to within the inferior orbital fissure.

For superficial dissections down to the joint, the superficial temporal artery and vein are at risk and will be encountered at the superior part of the external ear if a temporal extension is continued from the pre-auricular incision. The vessels lie on the temporalis fascia and requires ligation or diathermy. Inferior to this they should be retracted anteriorly with the dissection proceeding just anterior to the auricular cartilage in a relatively avascular plane.

For deeper dissections the pterygoid venous plexus lying within the lateral pterygoid muscle provides the next source for bleeding on the deep surface of the disc and capsule. This may be encountered during discectomy.

Deeper dissections associated with condylectomy or dissection along the medial side of the sigmoid notch may encounter the maxillary artery branches – masseteric branch traversing the sigmoid notch, maxillary artery itself lying on lateral pterygoid in the base of the wound a few millimetres deep to periosteum and the middle meningeal artery somewhat deeper and at risk during dissection at the medial side of the disc deep to lateral pterygoid. The middle meningeal artery lies deep between lateral pterygoid and the sphenomandibular ligament and enters the cranium through foramen spinosum. The maxillary artery may traverse a medially growing ankylotic mass. Where this is suspected, vascular imaging and consideration for preoperative embolization may be necessary. Otherwise, intra-operative arterial haemorrhage which cannot be controlled locally requires ligation of the terminal external carotid artery either in the neck (Figure 17.3), where the hypoglossal nerve traverses the bifurcation, or higher up in the retromandibular groove deep to posterior belly of digastric. The prudent surgeon will have opened the posterior mandibular approach prior to resecting the ankylotic mass in case urgent access to the terminal carotid is required. More distal ligation is preferable as external carotid ligation below the

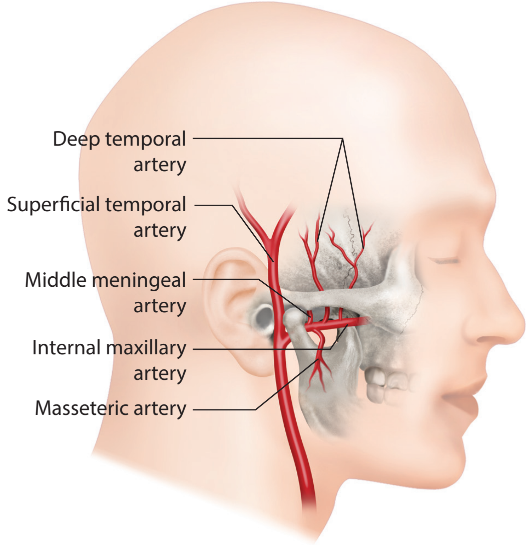
Deep temporal artery
Superficial temporal artery
Middle meningeal artery
Internal maxillary artery
Masseteric artery

Figure 17.2 Branches of the terminal carotid and maxillary artery in relation to the TMJ.

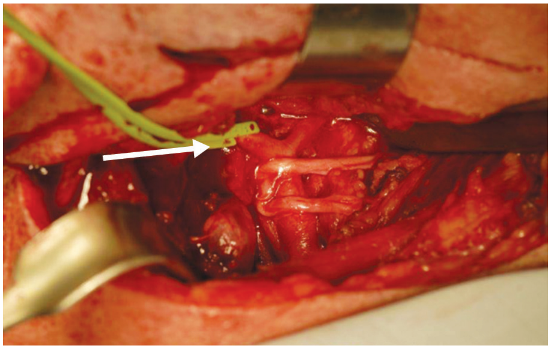

Figure 17.3 Position of the terminal external carotid in relation to the retromandibular wound and hypoglossal nerve, deep to digastric retracted.

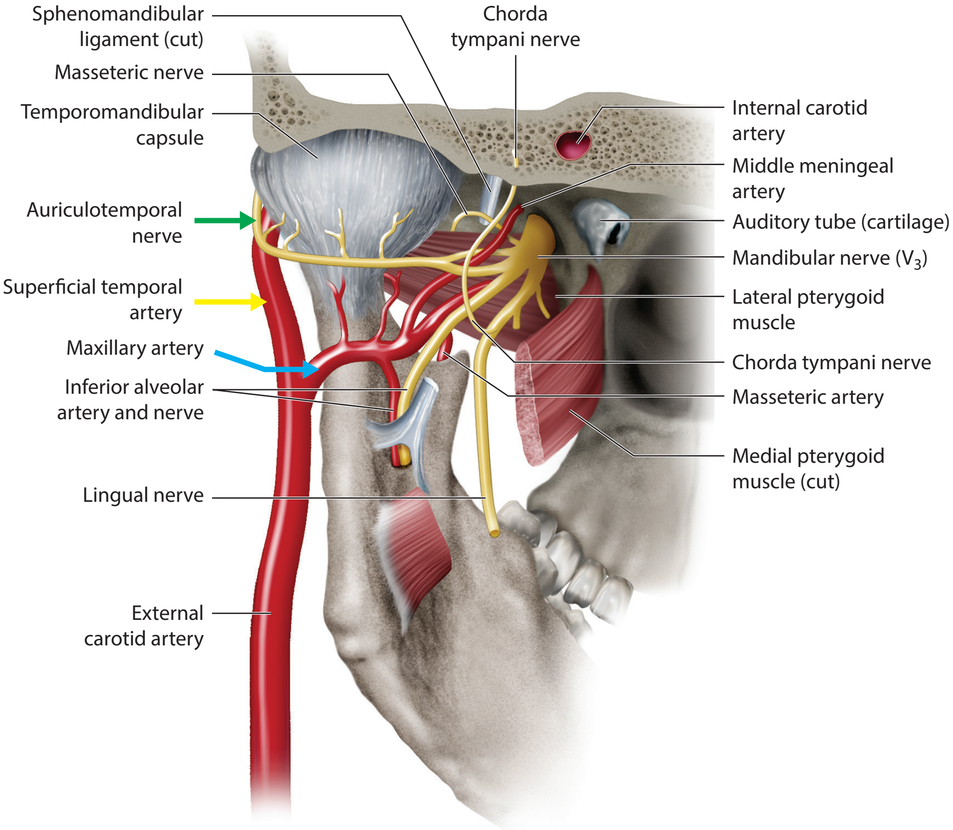
Sphenomandibular ligament (cut)
Masseteric nerve
Temporomandibular capsule
Auriculotemporal nerve
Superficial temporal artery
Maxillary artery
Inferior alveolar artery and nerve
Lingual nerve
External carotid artery
Chorda tympani nerve
Internal carotid artery
Middle meningeal artery
Auditory tube (cartilage)
Mandibular nerve (V_3)
Lateral pterygoid muscle
Chorda tympani nerve
Masseteric artery
Medial pterygoid muscle (cut)

Figure 17.4 Infratemporal fossa from behind. Auriculotemporal nerve (green arrow), superficial temporal artery (yellow arrow), maxillary artery (blue arrow).

linguofacial trunk only reduces flow by 40 per cent, above this level by 73 per cent, whereas above this origin and the origin of the posterior auricular-occipital it trunk reduces flow by 99.2 per cent.

Superficial to the terminal external carotid and lying within the substance of the parotid gland is the retromandibular vein. This may cause troublesome haemorrhage from the bottom end of a superior preauricular approach or if the retromandibular approach extends deeply. It can be controlled in the retromandibular groove from below.

MUSCLES OF MASTICATION

The major muscles of mastication are the masseter and temporalis, which are jaw closers, and the medial and lateral pterygoid, which cause jaw deviation. The digastric and hyoid muscles are the weaker jaw openers. The nerve supply is the motor division of the trigeminal nerve which exits with the mandibular division through foramen ovale.

The masseter is a multipennate muscle which runs from the zygomatic arch to the angle of the mandible in an inferior and slightly posterior direction. Its main nerve and blood supply come through the sigmoid notch and supply the deep surface, although vascularity is also achieved through periosteal branches.

The temporalis arises from below the superior temporal groove of the temporal fossa in an arcuate shape and forms a narrower tendon which passes below the zygomatic arch and inserts onto the coronoid process of the mandible and along the anterior margin of the ramus. Its blood supply is from the deep surface branches of the maxillary artery, and the nerve supply runs with these vessels. It is covered by the temporalis fascia which attaches above to the superior temporal line and below to the zygomatic arch where it becomes continuous with the parotid and deep cervical fascia. Just above the zygomatic arch, this divides into two layers to surround the tendon as it passes below the arch. Division of the superficial layer at the base of the arch allows the surgeon to carry out subperiosteal dissection along the arch, lifting the temporal branch of the facial nerve on top of the fascia and thus protecting it from direct injury – though not stretching.

The medial pterygoid runs from the medial surface of the lateral pterygoid plate to the medial surface of the lower ramus of the mandible, and its contraction causes deviation towards the contralateral side. Nerve and blood supply enter the muscle directly.

The lateral pterygoid runs from the lateral surface of the lateral pterygoid plate to the fovea and head of the condyle and to the anterior portion of the disc as two seemingly separate parts, with the upper head largely attaching to the disc to cause its forward motion during mouth opening. The lower head brings the condyle forward with it and causes the mandible to deviate to the opposite side. Detachment of this muscle during condylar resection will cause mouth opening to deviate towards the side of resection. Spasm of this muscle may cause the articular disc to be held forward and cause ‘locking’ and restriction of opening.

OTHER NEURAL STRUCTURES IN CLOSE ASSOCIATION WITH THE TMJ

The inferior alveolar and lingual sensory nerves lie deep to the lateral pterygoid and may be stretched during surgery into the infratemporal fossa, particularly during ankylosis surgery.

Facial nerve

Whilst the facial nerve (Figure 17.5) is not related to joint function its close relationship to the joint makes it an important anatomical structure to avoid during TMJ surgery. The two branches most at risk are the temporal branch during superior approaches and the marginal mandibular branch during inferior approaches. Bramley and Al Kayat describe the position of the temporal branch as lying between 8 and 22 mm anterior to the tragus of the ear lying on the superficial temporalis fascia. Subperiosteal dissection from the base of the zygomatic arch will protect the nerve, and release of the fascia in a line from 5 mm anterior to the tragus to above 2 cm superior and lateral to the lateral canthus (the ‘safe zone’) will prevent direct nerve injury (see Figure 17.5).

The marginal mandibular nerve comes around the posterior border of the mandible above the angle and within the substance of the parotid gland. Blunt dissection through the gland is essential to prevent injury, although it is often found to lie on the masseteric fascia. Twenty per cent

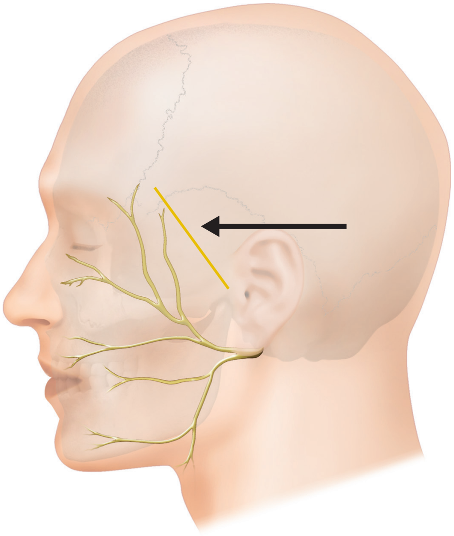

Figure 17.5 Facial nerve branches and "safe zone" (black arrow) above yellow line.

extends below the lower border, so a submandibular dissection should stay close to the undersurface of platysma (to which the nerve is just deep) until the nerve is located and retracted out of the wound.

ARTICULAR FOSSA AND EMINENCE

The upper bony part of the joint is formed from the articular fossa below the zygomatic arch extending in a sigmoid shape anteriorly to form the articular eminence. Behind the fossa lies the retro-articular protuberance which is continuous with the bony meatus of the ear canal. The disc-condyle complex initially rotates within the fossa and subsequently descends down the articular eminence. In hypermobile joints this may continue beyond the height of the eminence and come to lie superior and anterior to the eminence. Persistence in this position is anterior dislocation.

The fossa may be thin and in places may even be absent. Perforation is hence a risk during arthroscopy. In addition the foramen of Hushke (tympanic foramen present in around 4 per cent of cadaveric dissections) may communicate directly with the middle cranial fossa or middle ear. Both of these may cause issues particularly during arthroscopy of the joint, creating a risk of intracranial perforation.

The articular eminence is that portion of the zygomatic arch which lies just anterior to the articular fossa. Release of the zygomatic periosteum and subperiosteal forward dissection will expose it as it descends below the level of the arch. If eminectomy is considered then the position of the joint (feel the joint move, then go in front of this) will guide, as it is relatively easy for the novice to consider the retroarticular protrusion to be the eminence and reduction of this can lead to perforation of the external bony meatus of the auricular canal. The eminence itself contains mastoid air cells in 2–5 per cent of cases (Figure 17.6). A recent cone beam computed tomography (CBCT) study suggests that this number may be as high as 21 per cent in the eminence and 38 per cent in the fossa, requiring careful assessment prior to resection. Exposure of these can permit mastoid infection to spread into the joint or exposure of the cranial cavity to the joint. These should be excluded prior to eminence reduction.

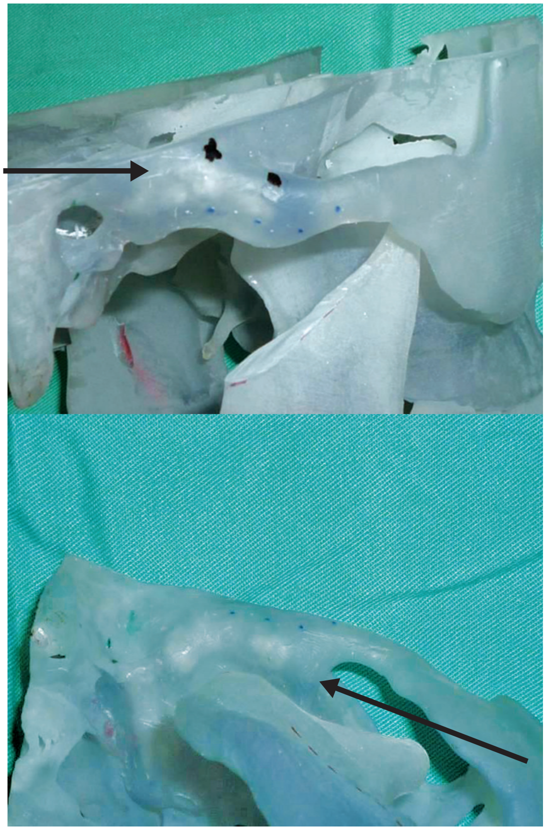

Figure 17.6 Air cells in the articular eminence (black arrows).

CONDYLE OF THE MANDIBLE

The condyle forms the lower part of the bony articulation of the joint. It is the proximal portion of the mandible and the first centimetre is contained within the capsule. Above it forms the lower joint compartment which rotates over the articular disc. The so-called disc-condyle complex then glides down the articular eminence. The condylar surface is covered with fibrocartilage due to its embryological origin , the only other fibrocartilagenous joint is the sternoclavicular joint hence its occasional use in joint reconstruction. The articular cartilage provides the secondary growth of the mandible up until the third decade. Removal of this layer or its damage will reduce or halt growth, and this may be used in benefit in the management of condylar hyperplasia by removing the cartilage cap. Degenerative changes are often more noticeable in the condylar head than the fossa with the classic formation of osteophytes, subchondral cysts, loss of joint space and localized bone sclerosis.

The fovea on the anterior surface is the point of attachment of the lower head of the lateral pterygoid muscle which pulls the joint forward during the glide movement and rotates the mandible to the contralateral side. The blood supply largely comes from branches of the inferior alveolar artery from below, although the muscle attachment also provides a supplemental periosteal supply. Fractures within the capsule carry the risk of avascular necrosis.

THE CORONOID PROCESS

The coronoid process forms the attachment of the temporalis muscle. It can be accessed through the mouth where the lower fibres of temporalis can be seen to extend down the anterior ramus well beyond the coronoid. The superior tip can extend deep to the zygomatic arch, making access to this difficult, and in certain cases this may impinge on the back of the maxilla causing restriction of movement – coronoid hyperplasia. The blood supply is from the mandible below and also from the periosteum via the muscle.

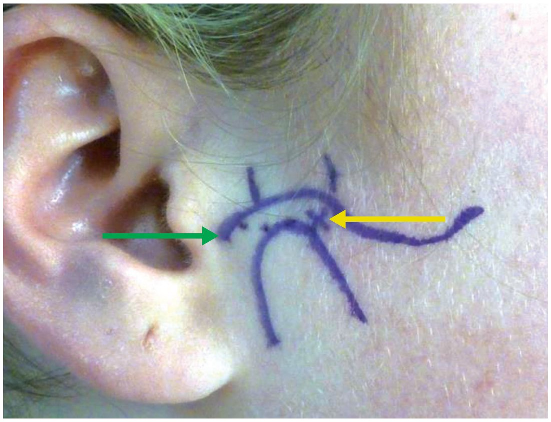

Figure 17.7 Access points for TMJ arthroscopy. Dots for traditional 30-degree angled scope (green arrow) and cross for 0-degree scope (yellow arrow).

ARTHROSCOPY

TMJ arthroscopists need to consider both the position of the facial nerve branches and the superficial temporal vessels in access to the joint (Figure 17.7). The cartilaginous meatus may also be penetrated posteriorly, and rarely the floor of the fossa may be thin and could be penetrated leading into the middle cranial fossa. Too deep introduction can damage the medial structures, and fluid leakage into the medial tissues can cause swelling in the lateral pharyngeal wall and supraglottic airway obstruction. Description of the access for arthroscopy can be found in standard textbooks and the diagram above serves as illustration (Figure 17.7).

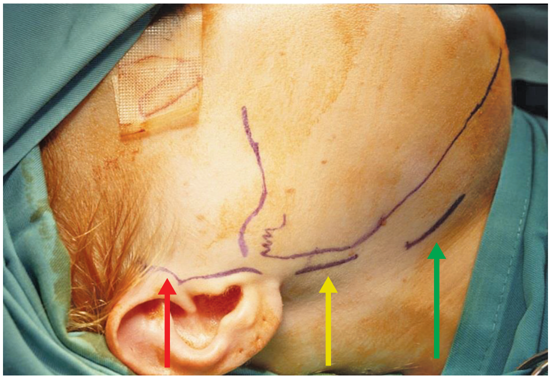

Figure 17.8 The three main approaches to the TMJ. Preauricular (red arrow), retromandibular (yellow arrow) and submandibular or Risden (green arrow).

MAIN SURGICAL APPROACHES TO THE TMJ

Superior approach

A preauricular incision is made in the skin crease anterior to the auricle from the lobule to the tip of the pinna. Alternative approaches such as endaural are described in standard textbooks. This is continued at the superior end in the immediate precartilaginous plane until the temporalis fascia is located (Figure 17.9). Scissors are inserted closed below this plane and opened to spread the wound towards the inferior end. The scissors can then be placed with one blade deep and the other superficial to the commenced wound and the tissues between the blades divided in the precartilaginous 'avascular' plane (see Figure 17.9). The temporalis fascia can then be freed from the overlying tissues, and the base of the zygomatic arch is located. If a relieving incision is continued into the hairline, then the superficial temporal vessels will need to be controlled with either diathermy or ligation.

The temporalis fascia is then divided at the base of the zygomatic arch, and a 45-degree relieving incision through the superficial temporalis fascia in a superoanterior direction aiming 2 cm above and lateral to the lateral canthus will permit subperiosteal dissection along the zygomatic arch and exposure of the articular eminence whilst protecting the temporal branch of the facial nerve (Figure 17.10). The capsule of the joint can then be exposed by sweeping the tissues in the plane of the subperiosteal dissection inferiorly and anteriorly. This will give about a 2 cm triangle of tissue of the capsule, and an occasional superficial vessel may need diathermy. The joint is identified by ensuring that you can feel it moving before continuing. The joint can be opened with a vertical incision along the posterior border of the condyle to the level of the disc and the capsule is opened with a horizontal incision to expose the upper and lower joint spaces and permit inspection of the disc and joint surfaces (Figure 17.11).

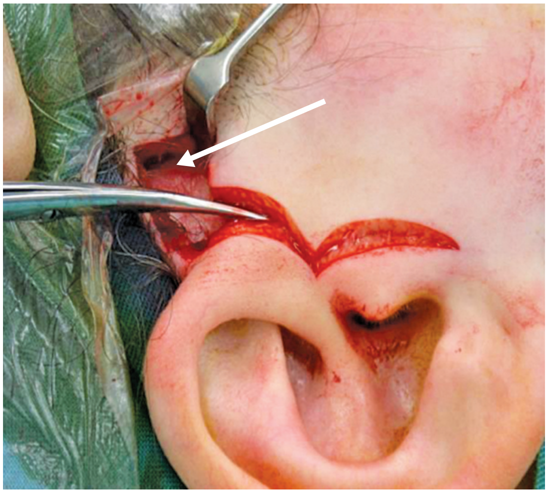

Figure 17.9 Preauricular incision with exposure of temporalis fascia (white arrow) and division of preauricular skin.

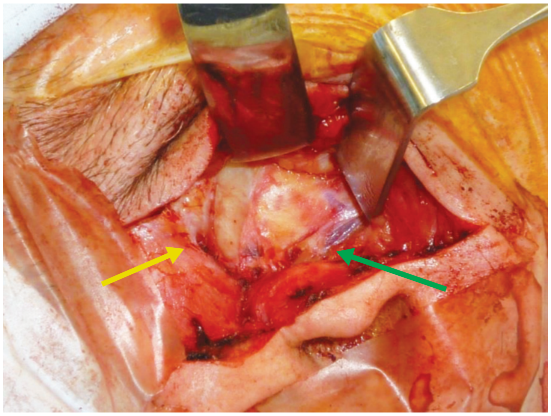

Figure 17.10 Division of temporalis fascia (yellow arrow) and subperiosteal exposure of arch with exposure of capsule (green arrow).

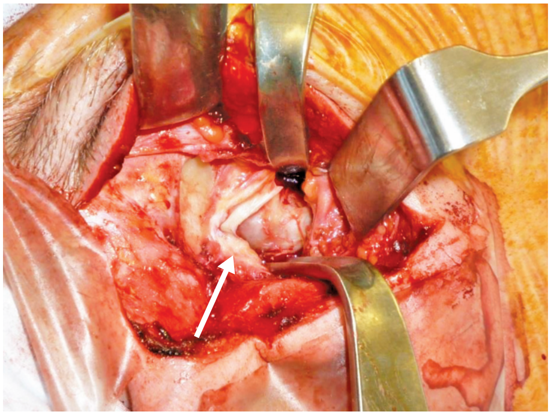

Figure 17.11 Exposure of condylar head (white arrow) with retraction of anterior and posterior tissues using Dautrey retractors (osteochondroma).

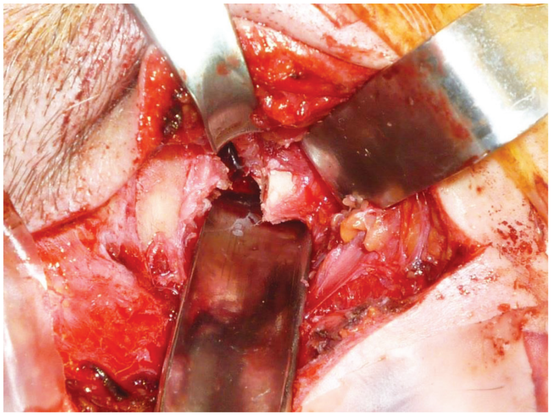

Figure 17.12 Condylectomy with disc preservation.

Condylar shave will not generate many issues other than bone end bleeding. Condylectomy (Figure 17.12), however, requires very careful preservation of the medial periosteum as the maxillary artery lies a few millimetres deep to this. Likewise the masseteric artery runs through the sigmoid notch, and the middle meningeal runs superiorly deep to the pterygoid.

Eminoplasty or eminectomy (Figure 17.13) may cause exposure of the mastoid air cells which extend into the arch and eminence. Careful preoperative planning will have warned the surgeon of this possibility. Other than this, there is little vascular risk from this procedure.

Disc plication involves division of the retrodiscal tissues which may be quite vascular, and there is the possibility of damage to the retromandibular vein during this division or subsequent suturing. Discectomy inevitably involves division of the disc from the pterygoid muscle and oozing from the venous plexus contained within this muscle. Deeper dissection may, however, damage the middle meningeal vessel which is difficult to control, and care should be taken in how deep diathermy is performed to control this as just deep to this lies the foramen ovale and the mandibular division of trigeminal nerve.

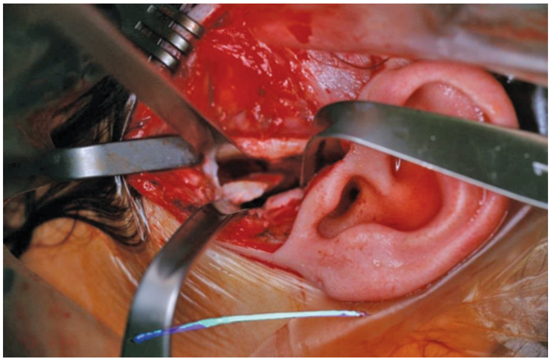

Figure 17.13 Eminectomy.

Inferior approach

The author's preferred method for access to the superior ramus and condyle is a variant of the retromandibular approach. The skin incision is made in a line which lies ½ to 1 cm behind the ascending ramus of the mandible. The parotid fascia is exposed with wide subcutaneous dissection and then divided in line of the skin incision. Gentle, broad fronted, blunt dissection through the parotid with meticulous haemostasis is continued, looking for the marginal mandibular branch traversing the wound from posterosuperior to anteroinferior. It is often found lying on the masseteric fascia and is carefully retracted. The masseter can then be divided along the posterior border of the mandible extending along the inferior border if required to divide the pterygomasseteric sling which forms the attachment of the masseter and medial pterygoid along the lower border of the mandible. Subperiosteal dissection along the posterior border superiorly permits access to the whole ramus, lower condyle, sigmoid notch and coronoid process (Figure 17.14). The only vessel at risk

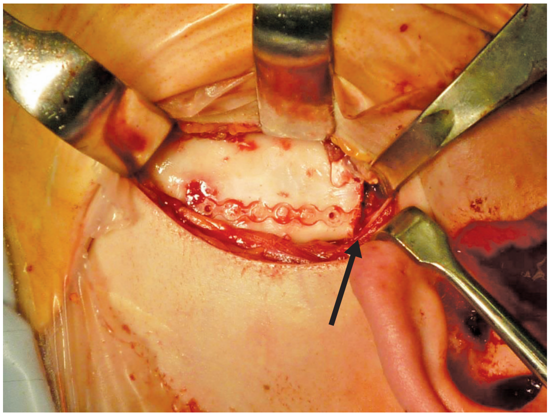

Figure 17.14 Retromandibular exposure of ramus, condylectomy defect and facial nerve buccal branch (black arrow) retracted superiorly.

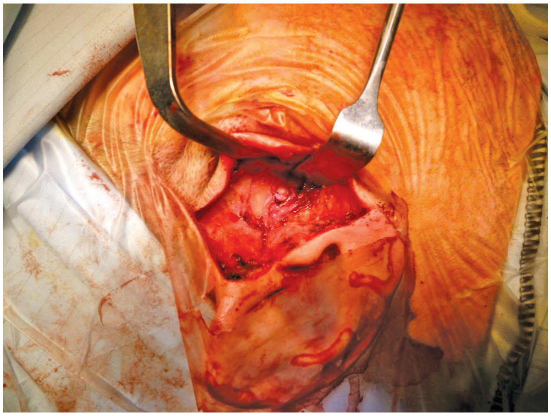

Figure 17.15 Closure of capsule.

during this dissection is the retromandibular vein. At this point access to the terminal external carotid is behind the posterior border of the mandible down to the digastric and just deep to this. Access may be required to ligate this portion of the vessel should arterial haemorrhage not be controlled in the superior wound.

Coronoidectomy can be carried out via either the superior or inferior extraoral route or by direct access to the base of the coronoid through an intraoral vertical ramus incision. Bleeding may occur from the masseteric vessel passing through the sigmoid notch, and strict subperiosteal dissection will help to prevent this occurrence.

Wound closure

Closure of the upper wound should include closure of the capsule (if not excised) and temporalis fascia (Figure 17.5). Closure of the lower wound should close the parotid fascia with a watertight seal to help to prevent sialocoele.

SUMMARY

TMJ surgery when performed with anatomical understanding should carry minimal risk to both vascular and motor nerve function. Carefully following recognized surgical planes will help to maintain a safe and bloodless field which will not require drainage.

FURTHER READING

Bouloux GF, Perciaccante VJ. Massive hemorrhage during oral and maxillofacial surgery: Ligation of the external carotid artery or embolization. *Journal of Oral and Maxillofacial Surgery*. 2009; 67: 1547–51.

Cillo JE Jr, Sinn D, Truelson JM. Management of middle meningeal and superficial temporal artery hemorrhage from total temporomandibular joint replacement surgery with a gelatin-based hemostatic agent. *Journal of Craniofacial Surgery*. 2005; 16(2): 309–12.

Lacout A, Marsot-Dupuch K, Smoker WR, Lasjaunias P. Foramen tympanicum, or foramen of Huschke: Pathologic cases and anatomic CT study. *American Journal of Neuroradiology*. 2005; 26(6): 1317–23.

Ladeira DBS, Barbosa GLR, Nascimento MCC, Cruz AD, Freitas DQ, Alemida SM. Prevalence and characteristics of pneumatisation of the temporal bone evaluated by cone beam computed tomography. *International Journal of Oral and Maxillofacial Surgery*. 2013; 42: 771–5.

Rosenberg I, Austin JC, Wright PG, King RE. The effect of experimental ligation of the external carotid artery and its major branches on haemorrhage from the maxillary artery. *International Journal of Oral Surgery*. 1982; 11(4): 251–9.

Sidebottom AJ, Carey EC, Madahar AK. Cryoanalgesia in the management of intractable pain in the temporomandibular joint: A five-year retrospective review. *British Journal of Oral and Maxillofacial Surgery*. 2011; 49: 653–6.

Smith TP. Embolization in the external carotid artery. *Journal of Vascular and Interventional Radiology*. 2006; 17(12): 1897–912.

Talebzadeh N, Rosenstein TP, Pogrel MA. Anatomy of the structures medial to the temporomandibular joint. *Oral Surgery, Oral Medicine, Oral Pathology, Oral Radiology and Endodontology*. 1999; 88(6): 674–8.

PART 5

18 Pharynx 181
Anthony D. Cheesman
19 Superior and posterior mediastinum 195
Vishy Mahadevan
20 Tissue spaces of the head and neck 201
Daren Gibson and Curtis Offiah
21 Larynx, trachea and tracheobronchial tree 209
Emma V. King and Vishy Mahadevan
22 Thyroid gland 221
Vishy Mahadevan and James N. Crinnion
23 Parathyroid glands 233
James N. Crinnion and Tom Wiggins

18

Pharynx

ANTHONY D. CHEESMAN

Embryology 181
Pharynx anatomy 181
Muscular coat of pharynx *182*
Soft palate *185*
Laryngopharyngeal elevators *187*
Nerve supply *188*
Blood supply *189*
Lymph drainage *189*
Lining mucosa *190*
Lumen of the pharynx *190*
Further reading 193

EMBRYOLOGY

The primitive gut extends cephalically and meets the stomadeum at the bucco-pharyngeal membrane. The membrane breaks down at the fourth week and the cephalic part of the primitive gut forms the pharynx.

Condensations of mesoderm in the side wall of the pharynx form the six pharyngeal arches. Deep grooves develop between the arches giving externally the branchial clefts and internally the pharyngeal pouches.

The tongue develops from the first third and fourth arches and the occipital myotomes migrate anteriorly to form the musculature of the tongue. The derivatives of the pharyngeal arches are listed in Table 18.1 and are discussed in the other chapters.

PHARYNX ANATOMY

The pharynx is a fibromuscular tube which extends from the base of the skull to the level of the cricoid cartilage anterior to the C6 vertebra. It communicates anteriorly with the nose, oral cavity and the larynx. This results in the lumen of the pharynx being subdivided into:

- the nasopharynx.
- the oropharynx.
- the laryngopharynx.

It is traversed by the upper air and food passages. The main function of the pharynx is to mediate in swallowing. Apart from the maintenance of balance, swallowing is probably the body's most important neuromuscular activity, transferring the food bolus from the oral cavity to the oesophagus, whilst closing off the larynx to protect the airway.

It also forms a major part of the upper vocal tract, and its discrete movements are vital for the normal articulation and resonance of speech. Consequently, with pharyngeal surgery it is important to preserve these fine muscular structures. When tonsillectomy is performed in a singer, the tonsillar capsule should be defined by sharp dissection in the supratonsillar fossa at the upper pole and along faucial pillars.

Table 18.1 Derivatives of pharyngeal arches

Pharyngeal arch	Muscle components	Skeletal components	Nerve	Artery
1st Mandibular	Muscles of mastication, anterior belly of digastric, mylohyoid, tensor tympani, tensor palati	Maxilla, model for mandible, malleus and incus. Meckel's cartilage	Trigeminal V2 and V3	Maxillary artery External carotid artery
2nd Hyoid	Muscles of facial expression, buccinator, platysma, stapedius, stylohyoid, posterior belly of digastric	Stapes, styloid process, hyoid (lesser horn and superior body), Reichert's cartilage	Facial nerve	Stapedial artery, hyoid artery
3rd	Stylopharyngeus	Hyoid (greater horn and inferior body)	Glossopharyngeal nerve	Common carotid and internal carotid arteries
4th	Cricothyroid, levator palati	Thyroid and epiglottic cartilages	Vagus nerve. Superior laryngeal branch	Right subclavian artery aortic arch
6th	Intrinsic muscles of larynx except cricothyroid	Cricoid and arytenoid cartilages	Vagus nerve. Recurrent laryngeal branch	Right pulmonary artery. Left pulmonary artery and ductus arteriosus

Muscular coat of pharynx

All the muscles of the pharynx, apart from cricopharyngeus, are paired structures laterally.

The major part of the pharynx muscular wall is composed of three muscles: the superior, middle and inferior constrictors (Figure 18.1). Each of the constrictors sequentially overlaps the constrictor above it. There are also three laryngopharyngeal elevator muscles: the salpingopharyngeus, stylopharyngeus and palatopharyngeus.

The superior constrictor does not extend to the skull base being absent from the wall of the nasopharynx. It is suspended from the skull base by a fibrous membrane, the pharyngobasilar fascia. This fascia is a thickening of the submucosa that lines the pharynx. In the posterior midline it is thickened to form the pharyngeal raphe. The pharyngeal raphe continues inferiorly in the posterior midline to end in another fibrous area with a deficient muscular coat; this is known as Killian's dehiscence.

The upper end of the pharyngeal raphe is attached to the pharyngeal tubercle just anterior to the foramen magnum. The pharyngobasilar fascia passes laterally from the tubercle anterior to the

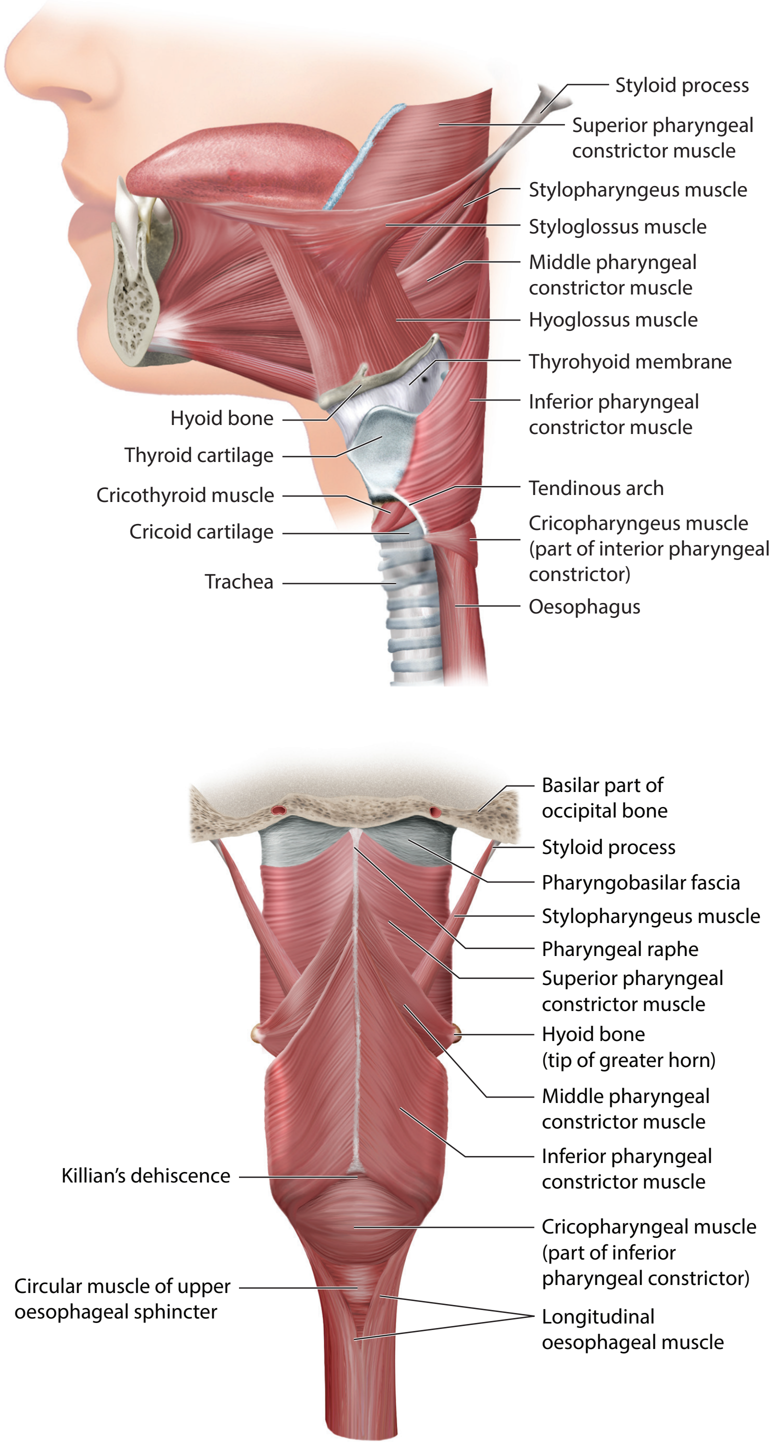
Styloid process
Superior pharyngeal constrictor muscle
Stylopharyngeus muscle
Styloglossus muscle
Middle pharyngeal constrictor muscle
Hyoglossus muscle
Thyrohyoid membrane
Inferior pharyngeal constrictor muscle
Hyoid bone
Thyroid cartilage
Cricothyroid muscle
Cricoid cartilage
Trachea
Tendinous arch
Cricopharyngeus muscle (part of interior pharyngeal constrictor)
Oesophagus
Basilar part of occipital bone
Styloid process
Pharyngobasilar fascia
Stylopharyngeus muscle
Pharyngeal raphe
Superior pharyngeal constrictor muscle
Hyoid bone (tip of greater horn)
Middle pharyngeal constrictor muscle
Inferior pharyngeal constrictor muscle
Killian's dehiscence
Cricopharyngeal muscle (part of inferior pharyngeal constrictor)
Circular muscle of upper oesophageal sphincter
Longitudinal oesophageal muscle

Figure 18.1 External posterolateral view of constrictors. Combining the lateral and posterior views shows the relationship of the cricopharyngeus to the upper oesophageal sphincter plus Killian's dehiscence.

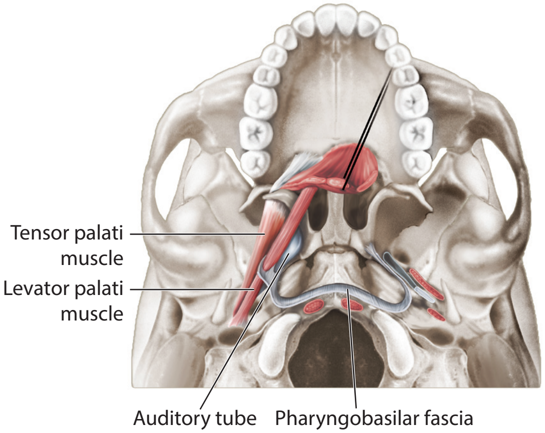

Figure 18.2 Relationship of the pharyngobasilar fascia to the auditory tube and elevator palati at the skull base. The soft palate musculature has been retracted with the black sling.

longus capitis muscle to be attached to the temporal bone just anterior to the carotid canal. It continues along the skull base below the cartilaginous auditory tube to attach to the posterior edge of the medial pterygoid plate. This rigid circumferential attachment of the pharyngobasilar fascia ensures that the lumen of the nasopharynx is held open permanently to facilitate the upper airway. The fascia is penetrated by both the auditory tube and the levator palati; this weakened area in the fascia is known as the sinus of Morgagni.

Inferiorly, the pharyngobasilar fascia is overlapped by the upper border of the superior constrictor muscle (Figure 18.2).

SUPERIOR CONSTRICTOR MUSCLE

Anteriorly, the muscle fibres of the superior constrictor are attached to the posterior border of the medial pterygoid plate down to the tip of the hamulus. It continues inferiorly attached to the posterior aspect of the pterygomandibular raphe.

The muscle fibres fan out posteriorly, terminating in the pharyngeal raphe where it meets its pair. Superiorly, the muscle fibres reach the pharyngeal tubercle and inferiorly extend to the level of the vocal folds. The lower edge of the superior constrictors is overlapped by the middle constrictors.

MIDDLE CONSTRICTOR MUSCLE

Anteriorly, the middle constrictor muscle arises from the lower portion of the stylohyoid ligament, the lesser horn of the hyoid bone and its adjacent greater horn, where it is overlapped by the hyoglossus muscle. Posteriorly, the muscle fibres again fan out to the pharyngeal raphe. The lower fibres extend inferiorly to the level of the vocal folds and are overlapped by the upper border of the inferior constrictors.

INFERIOR CONSTRICTOR MUSCLE

The inferior constrictor muscle is composed of two parts, the thyropharyngeus and the cricopharyngeus, so named from their anterior attachments.

The thyropharyngeus arises from the oblique line of the thyroid cartilage and from a fibrous arch over the cricoid thyroid muscle. Its fibres pass superiorly to the midline raphe covering the lower portion of the middle constrictor.

The cricopharyngeus has traditionally been considered the lowermost extent of the pharyngeal constrictors. However, it has a different morphology, being a more rounded muscle in distinction to the flattened muscles of the superior and middle constrictors. It is a single circumferential muscle and does not insert into the posterior pharyngeal raphe. There is a gap between its upper edge and the lower border of the thyropharyngeus where it is inserted into the pharyngeal raphe. This localized gap in the circumferential muscular tube is known as Killian's dehiscence.

The cricopharyngeus is perhaps better considered as an integral part of the upper oesophageal sphincter with which it is continuous inferiorly, although its upper most fibres are attached anteriorly to the lateral aspect of the cricoid cartilage.

The upper oesophageal sphincter is a circular coat of striated muscle present in the upper 4 cm of the oesophageal wall. On video fluoroscopy the cricopharyngeus and upper oesophageal sphincter are seen as one muscle, which normally closes off the oesophageal lumen during respiration, and opens in the final part of the pharyngeal phase of swallowing. The cricopharyngeus and upper oesophageal sphincter must be divided during laryngectomy to ensure tonic voice restoration (Figure 18.3).

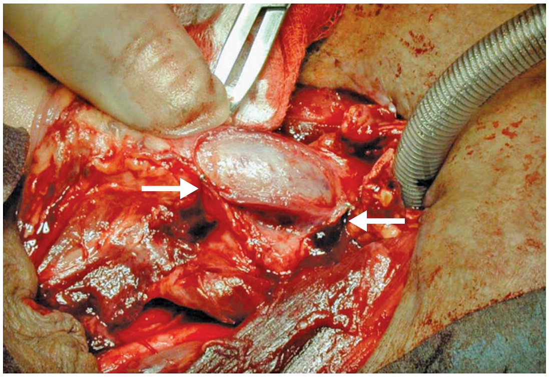

(a)

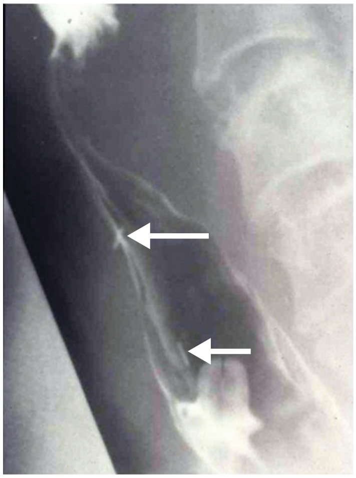

(b)

Figure 18.3 **(a)** Upper oesophageal sphincter myotomy during laryngectomy. Extent marked with ligaclips. **(b)** Videofluoroscopic image showing smooth entry into the neoglottis above the ligaclips.

Soft palate

The soft palate is a complex structure, whose primary function is to close off the nasopharyngeal isthmus during swallowing (Figure 18.4). It also plays an important role in articulation. Its main constituent is an aponeurosis attached to the inferior surface of the posterior edge of the hard palate, and it laterally merges with the interior of the pharyngeal wall. It has a free posterior edge with the uvula in the midline.

The main bulk of the soft palate is made up of a large number of secretory glands and, in the elderly, fat deposition. Its upper surface has a respiratory epithelium, and its oral surface and posterior edge have the usual squamous stratified epithelium.

Five paired muscles are attached to the aponeurosis and mediate its different movements. It is easier to understand the anatomy if one looks at it from the functional point of view.

CREATING A RIGID SOFT PALATE

The aponeurosis itself is considered by many to be the flattened terminal tendons of the tensor palati muscles. The muscle arises from the lateral surface of the cartilaginous pharyngo-tympanic tube and adjacent scaphoid fossa at the upper end of the medial pterygoid plate. It passes inferiorly, and as it hooks around the pterygoid hamulus to enter the pharynx it flattens to form the aponeurosis.

At rest the soft palate is arched, but with the contraction of the tensor palati muscles it becomes flattened, slightly depressed, and importantly more rigid. This rigidity of the soft palate enables the other paired muscles to work more efficiently.

The origin of the tensor palati muscles from the cartilaginous wall of the auditory tube means that when it contracts it also opens the tube to equalize the middle ear pressure with the atmosphere. This action occurs spontaneously with both swallowing and yawning. In young children the auditory tube is shorter and more horizontal, which is thought to be an aetiological factor in middle ear infections.

With a congenital cleft palate, discussed in Chapter 11, the aponeurosis is divided between the paired tensor muscles; consequently, on their contraction the tensor muscles fail to open the auditory tubes and this leads to problems with secretory otitis media.

Similarly, one of the techniques for the surgical correction of the cleft palate entails fracturing the hamulus to allow approximation of the two sides of the cleft. This technique again interferes with the normal function of the tensors, and the disturbed Eustachian tube function may result in various types of chronic suppurative otitis media.

ELEVATION OF THE SOFT PALATE

With a rigid soft palate it is elevated by the contraction of the levator palati muscles. This muscle arises

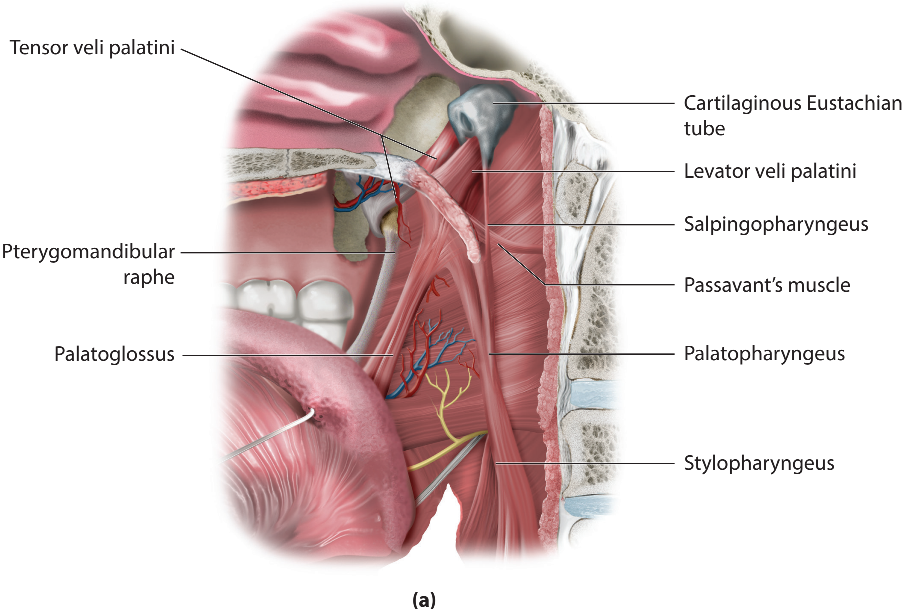
Tensor veli palatini
Cartilaginous Eustachian tube
Levator veli palatini
Salpingopharyngeus
Pterygomandibular raphe
Passavant's muscle
Palatoglossus
Palatopharyngeus
Stylopharyngeus
(a)

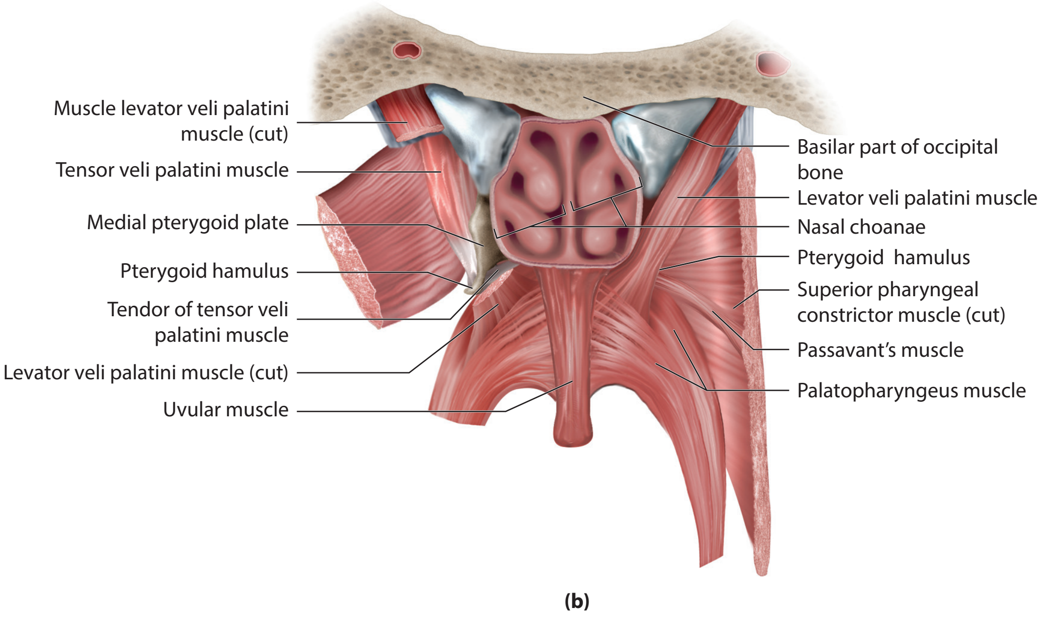
Muscle levator veli palatini muscle (cut)
Tensor veli palatini muscle
Medial pterygoid plate
Pterygoid hamulus
Tendor of tensor veli palatini muscle
Levator veli palatini muscle (cut)
Uvular muscle
Basilar part of occipital bone
Levator veli palatini muscle
Nasal choanae
Pterygoid hamulus
Superior pharyngeal constrictor muscle (cut)
Passavant's muscle
Palatopharyngeus muscle
(b)

Figure 18.4 Muscles of soft palate.

from the medial side of the cartilaginous auditory tube and from the adjacent bone of the petrous apex, anterior to the carotid canal. The paired levator muscles pass inferiorly and anteriorly to insert into palatal aponeurosis between the two origins of the palatopharyngeus muscles. Consequently, its contraction pulls the soft palate both superiorly and posteriorly, restoring its arch and opposing it against the posterior pharyngeal wall.

Also involved are the small musculus uvulae fibres which run along the upper surface of the aponeurosis from the posterior nasal spine to the uvula. They aid closure of the nasopharyngeal isthmus.

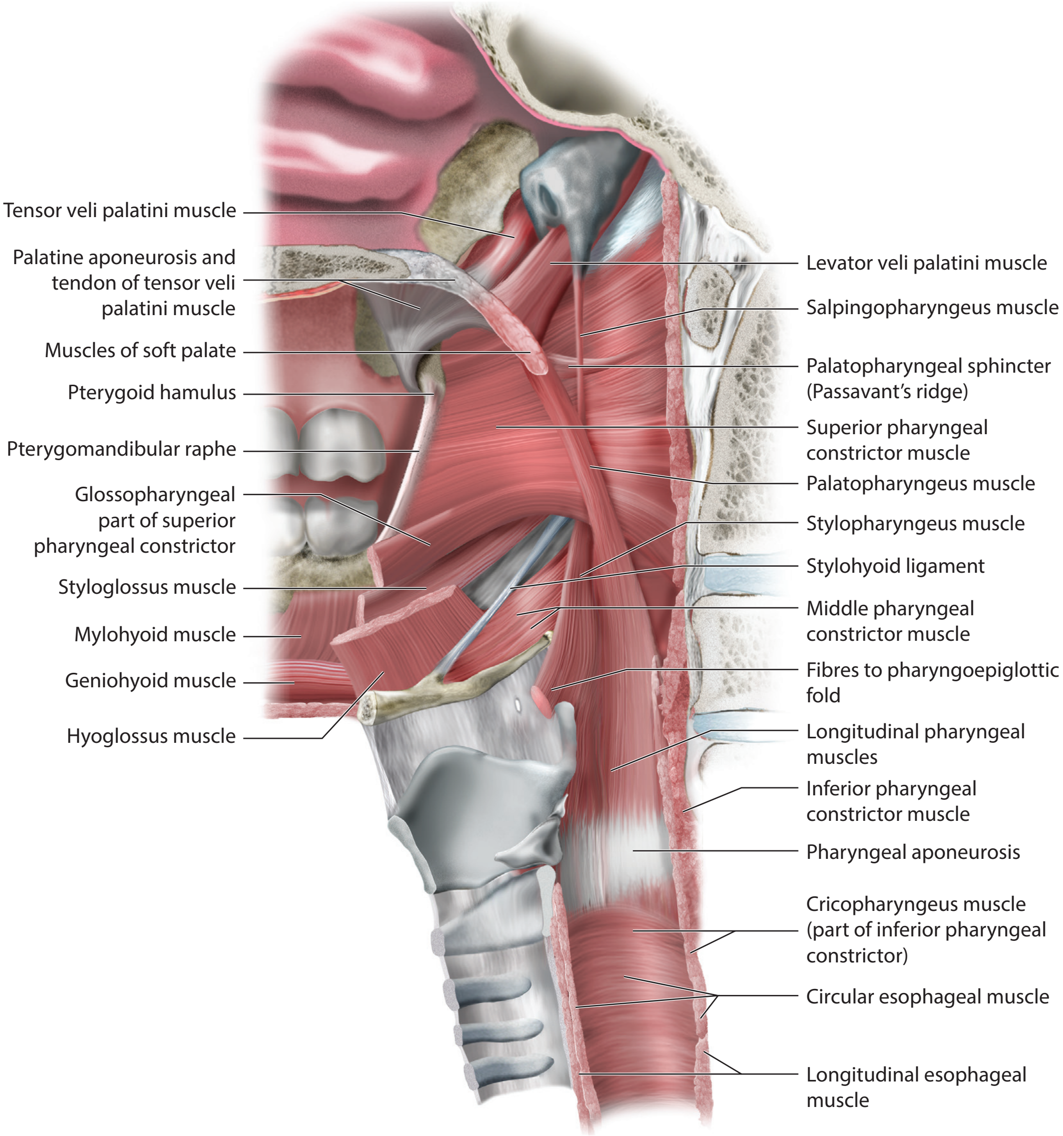
Tensor veli palatini muscle
Palatine aponeurosis and tendon of tensor veli palatini muscle
Muscles of soft palate
Pterygoid hamulus
Pterygomandibular raphe
Glossopharyngeal part of superior pharyngeal constrictor
Styloglossus muscle
Mylohyoid muscle
Geniohyoid muscle
Hyoglossus muscle
Levator veli palatini muscle
Salpingopharyngeus muscle
Palatopharyngeal sphincter (Passavant's ridge)
Superior pharyngeal constrictor muscle
Palatopharyngeus muscle
Stylopharyngeus muscle
Stylohyoid ligament
Middle pharyngeal constrictor muscle
Fibres to pharyngoepiglottic fold
Longitudinal pharyngeal muscles
Inferior pharyngeal constrictor muscle
Pharyngeal aponeurosis
Cricopharyngeus muscle (part of inferior pharyngeal constrictor)
Circular esophageal muscle
Longitudinal esophageal muscle

Figure 18.5 Pharyngolaryngeal elevators.

Laryngopharyngeal elevators

The laryngopharyngeal elevators (Figure 18.5) are three paired muscles inserted into the thyroid cartilage and adjacent pharyngeal wall:

- palatopharyngeus.
- stylopharyngeus.
- salpingopharyngeus.

They lie within the constrictor tube and one, palatopharyngeus, arises from the palatine aponeurosis. The other two arise from the skull base outside of the pharynx and enter it between the constrictors.

Palatoglossus, an elevator of the posterior tongue, should also be considered in this functional group of muscles.

Two pairs of muscles arise from the soft palate and pass inferiorly: the palatoglossus muscles and the palatopharyngeus muscles. Their function is not to depress the soft palate but rather to synchronously elevate the tongue, larynx and pharynx to close the oropharyngeal isthmus during swallowing.

The palatoglossus muscle arises from the undersurface of the aponeurosis passing inferiorly to merge with the styloglossus muscle and insert into the posterolateral border of the tongue. As it passes anterior to the tonsillar fossa, it raises a mucosal fold, the palatoglossus fold or the anterior pillar of the fauces. This is the anatomic division between the oral cavity and pharynx.

The palatopharyngeus muscle is more complex and arises from two heads. The anterior head arises from the posterior border of the hard palate and adjacent upper surface of the aponeurosis. A posterior head arises farther back on the aponeurosis. The two heads merge as they arch over the lateral edge of the aponeurosis to form a flat muscle just posterior to the tonsillar fossa. It raises another mucosal fold, the palatopharyngeal fold or posterior pillar of the fauces. As the muscle passes inferiorly, it merges with the stylopharyngeus and salpingopharyngeus muscles and is finally inserted into the posterior border of the thyroid lamina and its adjacent cornu.

The upper fibres of the palatopharyngeus, particularly those arising from its anterior head, run horizontally around the interior of the pharynx deep to the constrictor muscle (Passavant's muscle). When these fibres contract they create a ridge in the posterior pharyngeal wall, Passavant's ridge. It is against this ridge that the elevated soft palate becomes opposed to seal off the nasopharyngeal isthmus. In children with a cleft palate, this part of palatopharyngeus is often hypertrophied to compensate for the deficient soft palate elevation.

Stylopharyngeus arises from the deeper aspect of the upper part of the styloid process; it passes medially, anterior to the internal carotid artery, and enters the gap between the superior and middle constrictors. It passes inferiorly within the pharynx, merging with the palatopharyngeus into the posterior border of the thyroid cartilage.

Salpingopharyngeus is a small muscle which also arises from the auditory tube and passes inferiorly to blend with the palatopharyngeus.

Nerve supply

The majority of the nerve supply comes via the pharyngeal plexus (Figure 18.6). This is formed by the pharyngeal branches of the vagus and the glossopharyngeal nerves. It also receives sympathetic innervation from the cervical sympathetic nerves. The sensory component of the plexus is derived

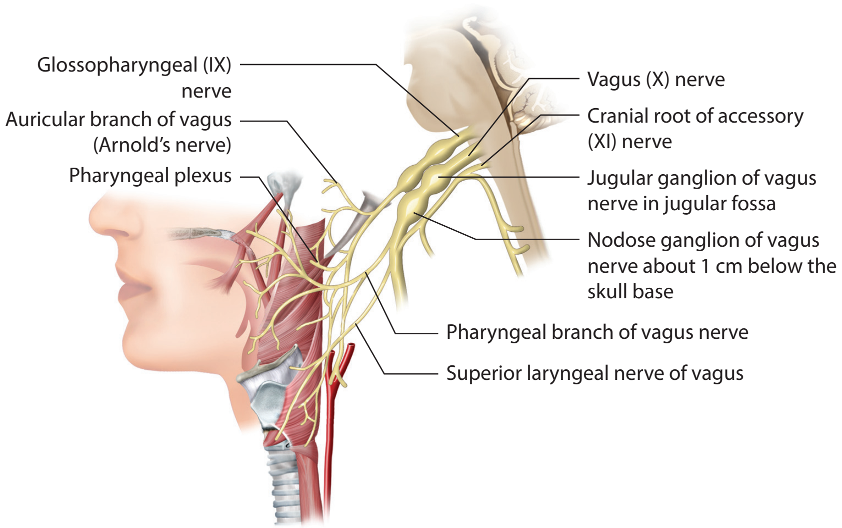
Glossopharyngeal (IX) nerve
Auricular branch of vagus (Arnold's nerve)
Pharyngeal plexus
Vagus (X) nerve
Cranial root of accessory (XI) nerve
Jugular ganglion of vagus nerve in jugular fossa
Nodose ganglion of vagus nerve about 1 cm below the skull base
Pharyngeal branch of vagus nerve
Superior laryngeal nerve of vagus

Figure 18.6 Constituents of the pharyngeal plexus with upper connections.

from the glossopharyngeal nerve, and the motor fibres are supplied from the vagus nerve.

The pharyngeal plexus lies on the external posterolateral wall of the pharynx mainly over the middle constrictor.

MOTOR NERVE SUPPLY TO THE PHARYNX AND SOFT PALATE

Tensor palati is a first arch derivative and is consequently supplied by the motor branch of the mandibular nerve via the nerve to the medial pterygoid.

All the other muscles of the soft palate and pharynx, apart from stylopharyngeus, receive their motor supply from the pharyngeal plexus. The motor nuclei are found in the nucleus ambiguus, and the motor fibres pass via the cranial root of the accessory to the vagus and enter the pharyngeal plexus. The cricopharyngeus is supplied by the vagus, but its motor fibres pass by the recurrent and external laryngeal nerves, which also innervates the upper oesophageal sphincter.

Stylopharyngeus is innervated by the motor branch of the glossopharyngeal nerve as it curves around the muscle.

The glossopharyngeal vagus and accessory nerves leave the skull by the jugular foramen. Pathology involving this area may cause compression of the nerves as they pass through the foramen. The resulting paralysis presents with:

- Loss of sensation to the posterior third of tongue and pharynx
- Dysphagia, and
- Weakness and wasting of the sternomastoid and accessory muscles.

This combination of symptoms is known as the jugular foramen syndrome (or Vermet's syndrome), the commonest cause being a jugular paraganglioma.

The dysphagia is due to the unilateral paralysis and wasting of the pharyngeal muscles. It is called **bulbar palsy** because of the lower motor neurone involvement.

Dysphagia is also a feature of **pseudo-bulbar palsy;** here the problem is incoordination of the pharyngeal musculature and there is no muscle wasting. This results from pathology of the upper motor neurones supplying the nucleus ambiguus.

Blood supply

The pharynx has a rich blood supply from the external carotid artery. There are pharyngeal branches from the ascending palatine branch of the facial artery and superiorly from the maxillary and lingual arteries. The inferior constrictor is supplied by branches from the superior and inferior laryngeal arteries.

There is a rich venous plexus which drains primarily into the internal jugular vein but also has connections with the pterygoid plexus.

Lymph drainage

Lymphatic drainage of the pharynx is into the retro-pharyngeal lymph nodes and thence into the upper and lower deep cervical lymph nodes.

The malignant spread from the nasopharynx into a high retro-pharyngeal node is often missed clinically; consequently, nasopharyngeal tumours often present late with cervical node involvement.

Table 18.2 Anatomic sites and subsites for TNM classification of pharyngeal carcinomas

Oropharynx

1. Anterior wall
   a. Posterior third of tongue
   b. Vallecula
2. Lateral wall
   a. Tonsil
   b. Tonsillar pillars and fossa
   c. Glossotonsillar sulcus
3. Posterior wall
4. Superior wall
   a. Inferior surface of soft palate
   b. Uvula

Nasopharynx

1. Postero-superior wall
2. Lateral wall
3. Inferior wall, upper surface of soft palate

Hypopharynx

1. Pharyngo-oesophageal junction (postcricoid area)
2. Pyriform fossa
3. Posterior pharyngeal wall

Lining mucosa

Apart from the nasopharynx, which is lined with a ciliated respiratory epithelium, the pharynx is lined with a stratified squamous cell epithelium. It has large numbers of mucous glands and frequent small deposits of lymphoid tissue. There are also many scattered minor salivary glands.

PHARYNGEAL TUMOURS

The commonest tumour is the squamous cell carcinoma. Several of the pharyngeal tumour sites are so-called silent sites because of their lack of primary presenting symptoms. The pyriform fossa, posterior third of tongue, supraglottis and tonsil are all so-called silent areas, in which the primary tumour is frequently missed and the patient tends to present with cervical lymphadenopathy. The minor salivary glands also produce salivary tumours and they are commonly of the more malignant type.

Nasopharyngeal tumours are commonly keratinized squamous cell carcinomas and the non-keratinized lymphoepithelioma. This is frequently related to the presence of the Epstein-Barr virus.

Lumen of the pharynx

The pharyngeal lumen (Figure 18.7) is divided into three areas related to its anterior openings.

- Nasopharynx.
- Oropharynx.
- Laryngopharynx.

NASOPHARYNX

The nasopharynx extends from the base of the skull to the upper surface of the soft palate and Passavant's ridge on the posterior pharyngeal wall. It is an integral part of the respiratory system and is hence lined with a ciliated columnar respiratory

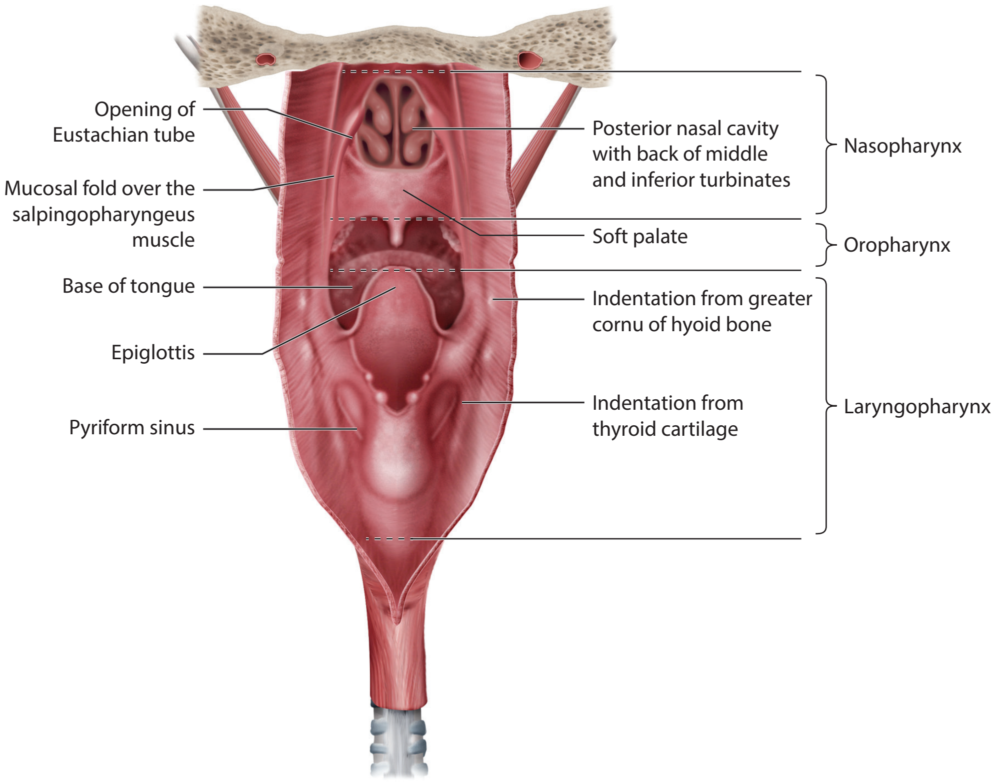
Opening of Eustachian tube
Mucosal fold over the salpingopharyngeus muscle
Base of tongue
Epiglottis
Pyriform sinus
Posterior nasal cavity with back of middle and inferior turbinates
Soft palate
Indentation from greater cornu of hyoid bone
Indentation from thyroid cartilage
Nasopharynx
Oropharynx
Laryngopharynx

Figure 18.7 Lumen of pharynx.

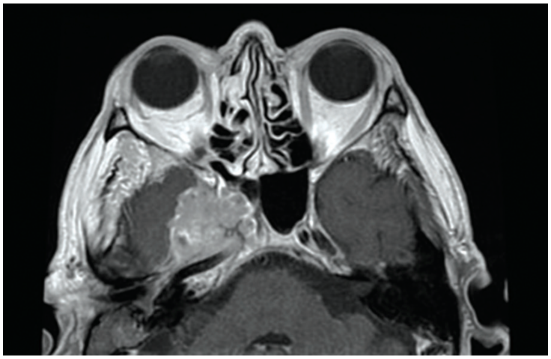

Figure 18.8 Nasopharyngeal carcinoma spreading via sinus of Morgagni.

epithelium. Its sensory nerve supply is from the first arch nerve, the mandibular nerve. The sensory fibres pass directly through the sphenopalatine ganglion.

The anterior wall consists of the posterior choana of the nasal cavity. Anteriorly, in the lateral wall just above the soft palate is the tubal eminence. This is the nasal end of the cartilaginous auditory tube. The end of the tube is surrounded by an inverted *J*-shaped cartilaginous swelling, with the long arm posteriorly and the opening inferiorly. In the child, the tubal eminence may be enlarged with lymphoid tissue, the tubal tonsil. Behind the tubal eminence is a lateral depression known as the fossa of Rosenmueller. Immediately deep to this mucosa is the sinus of Morgagni, the deficient part of the pharyngo-basilar fascia. This weakened area and the absence of the muscular coat is thought to facilitate the spread of nasopharyngeal tumours (see Figure 18.8) and infection through to involve adjacent structures of the skull base. Trotter's syndrome describes such pathology with one or more of the following symptoms:

- Unilateral conductive deafness from blockage of the auditory tube.
- Trigeminal pain from involvement of the mandibular nerve at the foramen ovale.
- Palatal paralysis from involvement of the tensor or elevator palati muscles.
- Trismus from infiltration of the pterygoid muscles.

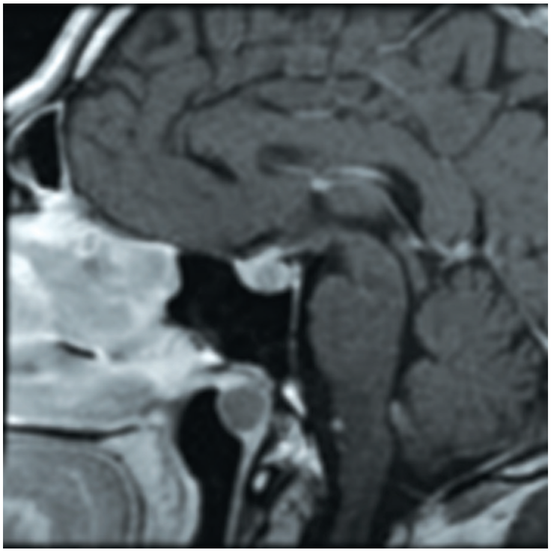

Figure 18.9 Thornwaldt's cyst.

In the posterior midline in children there is a collection of submucosal lymphoid tissue, the adenoid. It commonly has four to five grooves. Occasionally in the roof there is a small depression which is the nasal remnant of the embryonic Rathke's pouch.

Thornwaldt's cyst (Figure 18.9) is a cystic swelling in the roof of the nasopharynx. It is thought to be a notochordal remnant and magnetic resonance imaging is necessary to confirm the diagnosis and exclude a meningocoele.

The resting gap between the posterior soft palate and the posterior pharyngeal wall is known clinically as the nasopharyngeal isthmus. If this is narrowed by excessive fat deposition in the soft palate, obstruction of the nasal airway occurs. Clinically, this gives the condition known as obstructive sleep apnoea.

OROPHARYNX

The oropharynx extends from the lower surface of the soft palate to the level of the hyoid bone. Its anterior boundary is the palatoglossus fold, and it contains the palatine and lingual tonsils, the posterior third of tongue behind the vallate papillae and the valleculae (Figure 18.10).

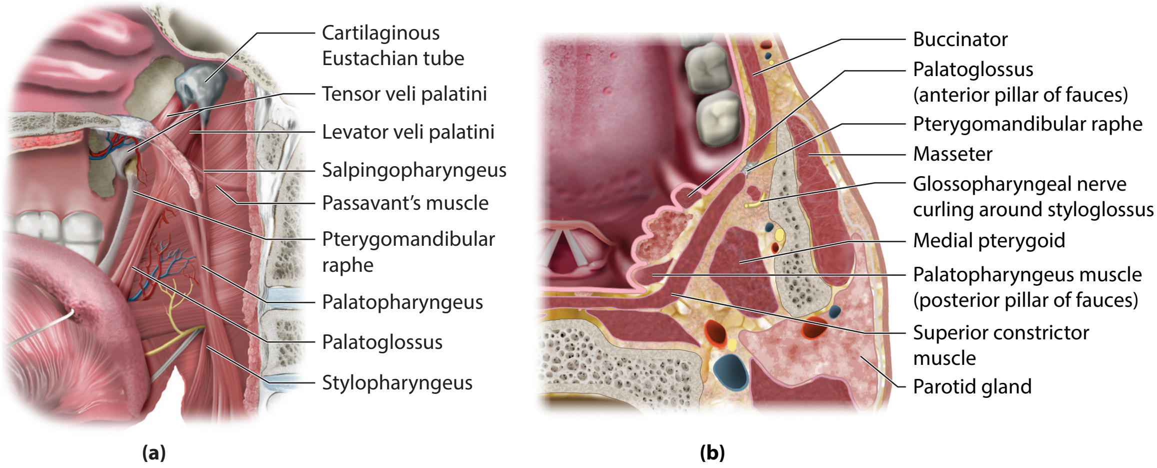
Cartilaginous Eustachian tube
Tensor veli palatini
Levator veli palatini
Salpingopharyngeus
Passavant's muscle
Pterygomandibular raphe
Palatopharyngeus
Palatoglossus
Stylopharyngeus
(a)
Buccinator
Palatoglossus (anterior pillar of fauces)
Pterygomandibular raphe
Masseter
Glossopharyngeal nerve curling around styloglossus
Medial pterygoid
Palatopharyngeus muscle (posterior pillar of fauces)
Superior constrictor muscle
Parotid gland
(b)

Figure 18.10 Relations of tonsil. **(a)** Sagittal view. **(b)** Axial view.

The pharyngo-epiglottic folds are considered parts of the laryngopharynx, and the epiglottis is part of the larynx.

The palatine tonsil is a large collection of lymphoid tissue between palato-glossal and palato-pharyngeal folds. It is lined with the pharyngeal mucosa composed of a stratified squamous epithelium. This epithelium is invaginated into the lymphoid tissue forming the tonsillar crypts. These crypts are often full of white squamous debris which is commonly misinterpreted as pus. Its deep surface has a thin fibrous capsule which separates it from the constrictor tube. The glossopharyngeal nerve is an immediate lateral relation in the parapharyngeal space. It gains its blood supply by perforating vessels from the ascending palatine branch of the facial artery. Its venous drainage is into the pharyngeal plexus. Its lymphatic drainage is to the jugulo-digastric node.

The lingual tonsil is a collection of lymphoid tissue on the upper surface of the posterior third of the tongue. Laterally, it is continuous with the palatine tonsil. Clinically, it is not normally enlarged.

WALDEYER'S RING

This is a ring of lymphoid tissue surrounding the upper air and food passages. It includes the adenoid and tubal tonsils of the nasopharynx, and both the lingual and palatine tonsils. There are also lymphoid deposits scattered in the pharyngeal mucosa.

This lymphoid tissue is thought to be essential for the normal development of the immune system and consequently is normally enlarged during childhood. There is often a similar enlargement of the cervical lymph nodes. This normal lymphoid enlargement tends to reduce around the eighth year of life.

Sensation from the oropharynx is conveyed by the glossopharyngeal branches of the pharyngeal plexus.

LARYNGOPHARYNX (HYPOPHARYNX)

It extends inferiorly from the level of the hyoid bone to the lower border of the cricoid cartilage. The area behind the cricoid and arytenoid cartilages is known as the pharyngo-oesophageal junction (or clinically as the postcricoid area).

Laterally on both sides are found the pyriform fossae (sinuses). These extend from the level of the pharyngoepiglottic fold to the upper end of the oesophagus. The lateral wall of the pyriform fossa is the mucous membrane lining the inner surface of the thyroid cartilage and thyrohyoid membrane above.

The rest of the laryngopharyngeal cavity is referred to as the posterior pharyngeal wall. Its upper portion above the level of the cricoid lies beneath the overlapping pharyngeal constrictors. At the level of the pharyngo-oesophageal junction the pharynx is surrounded by the inferior constrictor. Consequently, Killian's dehiscence is at the level of the upper border of the cricoid cartilage. This potentially weak area with an absent muscular covering is the site of a pharyngeal pouch (Figure 18.11). This mucosal pouch extends through the weakened fibrous area to pass inferiorly in the parapharyngeal space generally on the left side. It is usually managed by endoscopic division of the wall between the pouch and oesophageal lumen which also divides the cricopharyngeus and upper oesophageal sphincter muscles.

Sensation from the laryngopharynx is conveyed via the pharyngeal plexus.

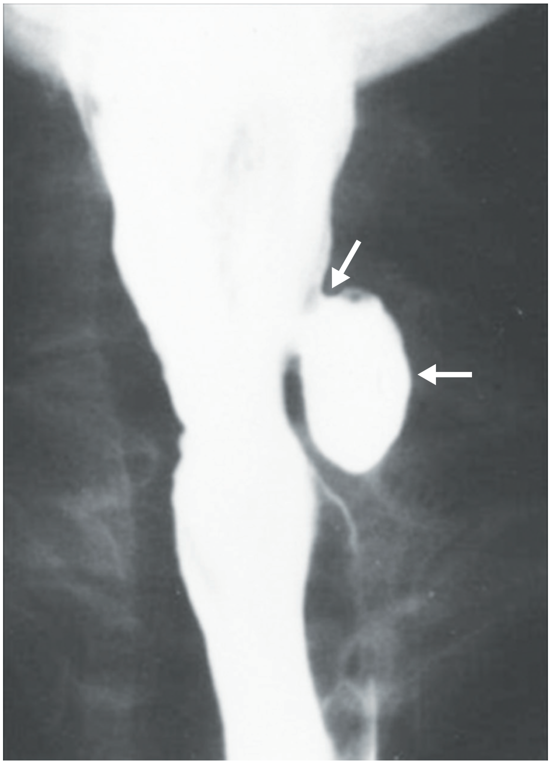

Figure 18.11 Barium swallow of pharyngeal pouch.

FURTHER READING

Blom E, Singer M, Hamaker R. *Tracheoesophageal Voice Restoration Following Total Laryngectomy*. San Diego: Singular Publishing Group, 1998.

Chan M, Sahgal A, Fatterpekar G, Yu E. Imaging of nasopharyngeal carcinoma. *Journal of Nasopharyngeal Carcinoma*. 2014; 11: 11.

Logemann JA, Rademaker AW, Pauloski BR, Ohmae Y, Kahrilas PJ. Normal swallowing physiology as viewed by videofluoroscopy and videoendoscopy. *Folia Phoniatrica et Logopaedica*. 1998 Nov-Dec; 50(6): 311–9.

McIvor J, Evans PF, Perry A, Cheesman AD. Radiological assessment of post laryngectomy speech. *Clinical Radiology*. 1990 May; 41(5): 312–6.

Tubbs RS, Jones VL, Loukas M, Shoja MM, Cohen-Gadol AA. Quantification and anatomy of the Sinus of Morgagni at the skull base. *Biomedicine International*. 2010; 1: 16–18.

Yoon KJ, Park JH, Park JH, Jung IS. Videofluoroscopic and manometric evaluation of pharyngeal and upper esophageal sphincter function during swallowing. *Journal of Neurogastroenterology and Motility*. 2014; 20(3): 352–61.

19

Superior and posterior mediastinum

VISHY MAHADEVAN

Boundaries of the mediastinum and subdivisions of mediastinum 196
Boundaries and principal contents of the superior and posterior mediastina 196
Superior mediastinum 196
The posterior mediastinum 199
Further reading 200

A comprehensive account of the clinical anatomy of the head and neck would be incomplete without a consideration of the anatomy of the mediastinum. The contiguity of the root of the neck and the superior mediastinum allows the easy propagation of inflammatory and neoplastic conditions from one region to the other. Furthermore, abnormal embryological development may result in structures normally situated in the neck being aberrantly located in the mediastinum. Thus clinicians specializing in the management of diseases of the head and neck must possess more than a superficial knowledge of mediastinal anatomy.

The mediastinum (Latin for *middle partition*) is the central part of the thoracic cavity situated between the right and left pleural sacs. The upper limit of the mediastinum is at the cervico-thoracic junction (root of the neck). Several structures in the neck enter the mediastinum through this junction, and numerous intrathoracic structures cross the junction to enter the neck.

It is conventional to describe the mediastinum as consisting of two parts, *superior mediastinum* and *inferior mediastinum*, demarcated from each other by an imaginary horizontal plane at the level of the manubriosternal junction.

Situated in its entirety within the inferior mediastinum and enclosing the heart is the fibrous pericardium. The fibrous pericardium allows the descriptive subdivision of the inferior mediastinum into three parts: anterior mediastinum (in front of the fibrous pericardium), posterior mediastinum (behind the fibrous pericardium) and the middle mediastinum, which refers to the fibrous pericardium and its contents.

Thus the mediastinum may be pictured as being made up of four regions (subdivisions), all of which are in communication with each other. Knowledge of the normal contents of each of the mediastinal subdivisions is of much usefulness to the clinician in making a clinical differential diagnosis of a mediastinal lesion. Knowledge of mediastinal anatomy is also of importance to the radiologist in the interpretation of mediastinal pathology. Widening of the mediastinum, as observed on a plain radiograph of the chest, is a feature of practically all mediastinal masses, neoplastic and non-neoplastic. The advent of computed tomography (CT) scanning and magnetic resonance imaging (MRI) has greatly added to the accuracy and specificity with which the clinician is now able to make a pre-operative diagnosis.

This chapter will describe the surgically relevant anatomy of the superior and posterior divisions of the mediastinum, as these two regions are of greater and more direct pertinence to the study of the clinical anatomy of the head and neck than are the middle and anterior divisions of the mediastinum.

BOUNDARIES OF THE MEDIASTINUM AND SUBDIVISIONS OF MEDIASTINUM

The mediastinum is a wide, median area within the thoracic cavity. Its posterior boundary is the entire length of the thoracic part of the vertebral column. The inferior boundary of the mediastinum is the upper surface of the diaphragm. The superior limit of the mediastinum is the plane of the superior aperture of the thoracic cage, while anteriorly, the mediastinum is bounded by the posterior surface of the sternum. The mediastinum is limited on each side by the medial aspect of the corresponding pleural sac. The mediastinum, thus defined, is customarily divided into two principal regions: superior mediastinum and inferior mediastinum. These two regions are 'demarcated' from each other by means of an imaginary horizontal plane at the level of the manubriosternal junction. This plane is known in radiological terminology as the transverse thoracic plane. When projected to the vertebral column, it meets the latter at the level of the lower border of the 4th thoracic vertebra (Figure 19.1).

Situated entirely within the inferior mediastinum is the fibrous pericardium containing the heart. The location of the fibrous pericardium in the inferior mediastinum allows the convenient subdivision of the inferior mediastinum into three parts or areas: anterior mediastinum (anterior to the fibrous pericardium); posterior mediastinum (posterior to the fibrous pericardium); and middle mediastinum (the fibrous pericardium itself). The boundary between the superior and inferior divisions of the mediastinum being purely imaginary, it follows that the posterior, middle and anterior mediastina are directly continuous with the superior mediastinum.

While the subdivision of the mediastinum into compartments may, at first sight, seem somewhat artificial and arbitrary, it is nevertheless a considerable aid to the topographical classification of mediastinal lesions.

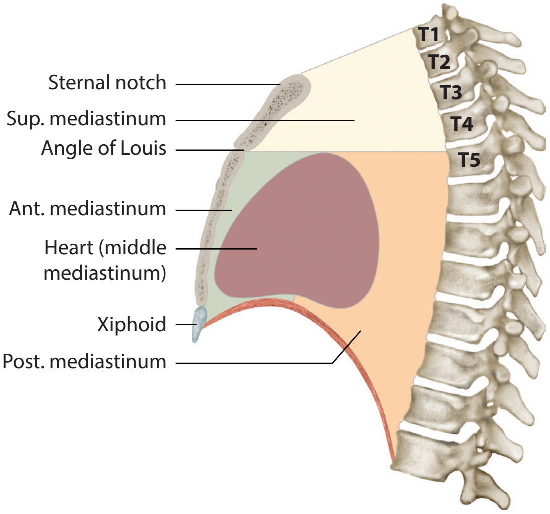

Figure 19.1 Schematic illustration of the subdivisions of the mediastinum (left lateral view).

Several of the contents and some of the boundaries of the mediastinum display considerable mobility. The heart, lungs, thoracic aorta, trachea, oesophagus and diaphragm are dynamic structures. For this reason only a small amount of loose connective tissue and fat are found in the mediastinum, and these are spread thinly and diffusely between the mediastinal structures so as not to inhibit the mobility of the mediastinal viscera. On the other hand, the absence of any substantial connective tissue septa allows the accumulation and easy spread of inflammatory fluid within the mediastinum, and allows distension of the mediastinum by inflammatory and neoplastic masses.

BOUNDARIES AND PRINCIPAL CONTENTS OF THE SUPERIOR AND POSTERIOR MEDIASTINA

Superior mediastinum

BOUNDARIES

The superior mediastinum is limited anteriorly by the manubrium sterni and posteriorly by the upper third of the thoracic vertebral column (i.e. 1st to 4th thoracic vertebrae and intervening intervertebral discs). The lateral boundary of the superior mediastinum on either side is the medial surface of the corresponding pleural sac. The inferior and superior boundaries of the superior mediastinum are both imaginary planes. The former is the transverse thoracic plane while the latter is the plane of the superior aperture of the thoracic cage (i.e. plane of the thoracic outlet). The thoracic outlet is made up of the sternal notch anteriorly, and the upper border of the body of the first thoracic vertebra posteriorly. Consequently, the plane of the thoracic outlet is oblique, being directed downwards and forward. The prevertebral and pretracheal layers of deep cervical fascia extend into the superior mediastinum (Figure 19.2). The prevertebral fascia drapes the front of the cervical prevertebral muscles including the scalene muscles. The inferior attachment of the prevertebral fascia is to the body of the 4th thoracic vertebra. The prevertebral space lies between the prevertebral fascia and the cervical vertebral column and contains the prevertebral muscles. Owing to the attachment of the prevertebral fascia to the 4th thoracic vertebra, the prevertebral space may be said to extend into the posterior part of the superior mediastinum. The pretracheal fascia extends into the superior mediastinum as a thin layer, lying behind the manubrium. It blends with the anterior surface of the fibrous pericardium just below the level of the manubriosternal junction. Thus an infection in the neck that is in front of the pretracheal fascia may potentially be directed into the anterior part of the superior mediastinum and thereby into the anterior mediastinum. A cervical infection in the prevertebral space may spread into the superior mediastinum but cannot extend below the level of the 4th thoracic vertebra (Figure 19.2). Elsewhere in the neck, infections can extend into the superior mediastinum and through the latter, into the posterior mediastinum.

CONTENTS OF THE SUPERIOR MEDIASTINUM

A striking feature of the arrangement of structures in the superior mediastinum is the lack of symmetry (Figures 19.3 and 19.4).

By far the most important structure situated in the superior mediastinum is the arch of the aorta (which lies in its entirety within the superior mediastinum). Other important structures in the superior mediastinum include the oesophagus and trachea (both on their way from the neck to the inferior mediastinum), the right and left phrenic nerves, the right and left vagus nerves, lymph nodes, remnants of the thymus, the right and left brachiocephalic veins and their confluence to form the superior vena cava, the upper end of the thoracic duct and various autonomic nerve fibres. Immediately in front of the prevertebral fascia lies the oesophagus. Anterior to the oesophagus is the trachea. In front of the trachea is the aortic arch. The trachea bifurcates in the inferior mediastinum, below the aortic arch and behind the ascending aorta. The latter is, of course, contained within the fibrous pericardium. Crossing obliquely in front of the aortic arch, from left to right, is the left brachiocephalic vein. In front of the brachiocephalic vein is the extension of pretracheal fascia from the neck into the superior mediastinum. Attached to the posterior surface of this extension of pretracheal fascia are thymic remnants.

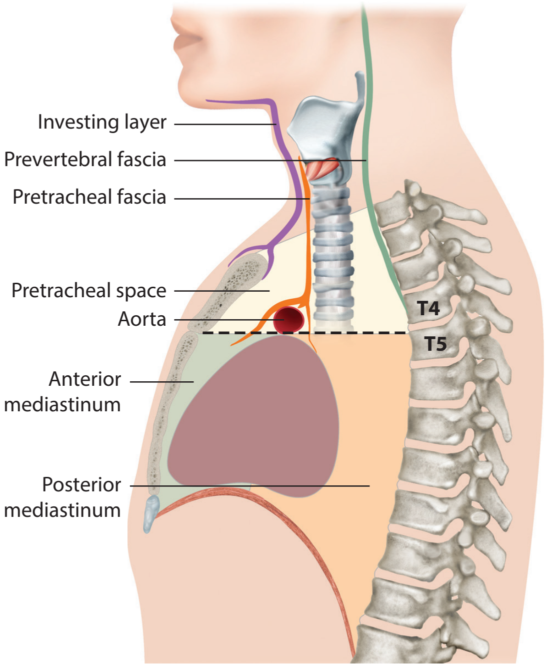

Figure 19.2 Schematic depiction of the fascial layers and fascial spaces in the neck, and their relationship to the subdivisions of the mediastinum (left lateral view).

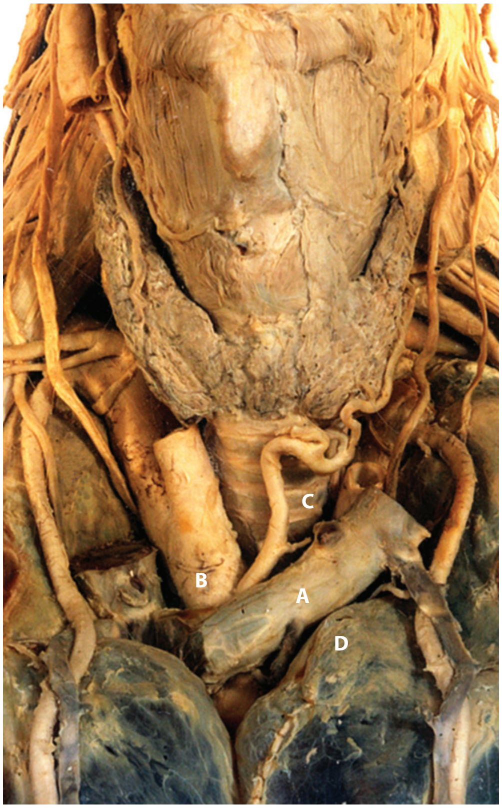

Figure 19.3 Dissection showing contents of the superior mediastinum viewed from the front, after removal of manubrium sterni. A – left brachiocephalic vein. B – brachiocephalic artery. C – trachea. D – apex of left lung.

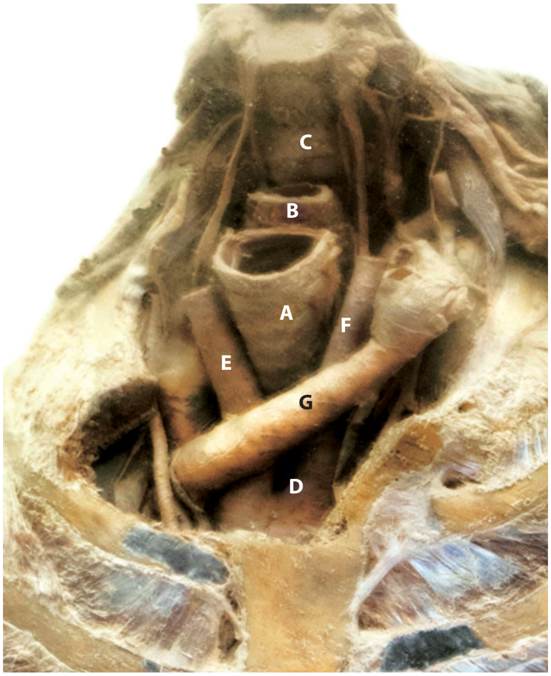

Figure 19.4 Oblique view (antero-inferior) of dissection of superior mediastinum and thoracic outlet. A – trachea. B – oesophagus. C – thoracic vertebral column. D – aortic arch. E – brachiocephalic artery. F – left common carotid artery. G – left brachiocephalic vein.

Arising from the convexity of the aortic arch, in succession, are the brachiocephalic (innominate) artery, the left common carotid artery and the left subclavian artery. The brachiocephalic artery runs upwards and to the right in front of the trachea before reaching its right lateral surface. Here, level with the upper border of the right sternoclavicular joint, it divides into the right common carotid and right subclavian arteries. The left common carotid and subclavian arteries run upwards on the left side of the trachea and intervene between the trachea and the left pulmonary apex. By contrast, the right pulmonary apex is practically in contact with the trachea (Figure 19.4).

The left brachiocephalic vein crosses over to the right and joins its much shorter right-sided counterpart, the right brachiocephalic vein, to form the superior vena cava. The latter (with the right phrenic nerve adhering to its lateral surface) runs inferiorly to enter the roof of the right atrium. The right vagus runs posteriorly behind the hilum of the right lung to reach the oesophagus in the posterior mediastinum. The left phrenic nerve and left vagus nerves run on the left side of the aortic arch before they pass inferiorly, respectively anterior and posterior to the left pulmonary hilum. The left vagus then courses posteromedially to reach the oesophagus. Before crossing the aortic arch, the left vagus gives off the left recurrent laryngeal nerve. The latter runs below the aortic arch and then medial to it before ascending in the left trachea-oesophageal groove.

As an embryological anomaly resulting from excessive downward migration of the thyroglossal duct, the thyroid isthmus and inferior poles of the thyroid lobes may, on occasion, be situated in the upper part of the superior mediastinum. Rarely, the entire thyroid gland may be situated within the superior mediastinum. Aberrant location of the parathyroid glands (especially the inferior parathyroids) in the superior or anterior mediastinum may also be explained on the basis of abnormal embryological development.

Surgical access to the superior mediastinum may be gained through a median sternotomy, partial or complete. In the former, only the manubrium sterni is divided, leaving the body of the sternum intact. Alternatively, the superior mediastinum may be approached through a transverse or slightly curved, low, cervical incision placed just above the level of the sternal notch. Surgical access may also be gained through a high intercostal thoracotomy. Of these surgical approaches, the one that provides the best exposure is median sternotomy. It is ideal for surgery on the aortic arch and the major vessels in the superior mediastinum. It is also the optimal approach for the excision of thymic, thyroid or parathyroid masses in the superior mediastinum.

The superior mediastinum may also be inspected endoscopically and lymph nodes sampled for histology. The procedure, termed *mediastinoscopy*, involves the introduction of a rigid endoscope through a short transverse incision placed just above the sternal notch. The endoscope traverses the suprasternal space obliquely before entering the area immediately behind the manubrium sterni.

The posterior mediastinum

BOUNDARIES

The posterior mediastinum is situated immediately behind the fibrous pericardium (Figure 19.1). The latter thus forms the anterior boundary of the posterior mediastinum. Within the fibrous pericardium the most posteriorly situated cardiac chamber is, of course, the left atrium.

The posterior boundary of the posterior mediastinum is the lower two-thirds of the thoracic vertebral column (i.e. 5th to 12th thoracic vertebrae and intervening intervertebral discs). The inferior limit of the posterior mediastinum is the upper surface of the diaphragm, postero-inferior to the fibrous pericardium. The superior limit of the posterior mediastinum is the transverse thoracic plane through which the posterior mediastinum communicates directly with the posterior part of the superior mediastinum, anterior to the prevertebral fascia. The lateral boundary of the posterior mediastinum on either side is the medial surface of the corresponding pleural sac.

CONTENTS OF THE POSTERIOR MEDIASTINUM

The contents of the posterior mediastinum (Figure 19.5) include the descending thoracic aorta and its branches, the oesophagus with the oesophageal nerve plexus on its wall, vena azygos on the right side, and the hemiazygos and accessory hemiazygos veins on the left. These large veins lie directly on the anterolateral aspect of the vertebral column. They drain the thoracic walls and thoracic viscera, and offer a collateral channel between the inferior and superior vena cava. Other significant structures in the posterior mediastinum are the ganglionated right and left thoracic sympathetic trunks and their splanchnic branches, lymph nodes and the thoracic duct. The latter is the largest lymphatic vessel in the body (Figure 19.5).

The descending thoracic aorta is the direct continuation of the aortic arch. It commences at the level of the upper part of the 5th thoracic vertebral body. Throughout its course the descending thoracic aorta is intimately related medially to the left lateral aspect of the thoracic vertebral column, and laterally to the mediastinal pleura of the left lung. At the lower end of the posterior mediastinum, the aorta gradually approaches the midline as it enters the abdomen between the two crura of the diaphragm. The descending thoracic aorta gives rise to nine pairs of posterior intercostal arteries, a pair of subcostal arteries, a variable number of small oesophageal branches, and bronchial arteries.

The oesophagus enters the posterior mediastinum more or less in the midline and remains so until it reaches the lower end of the posterior mediastinum where it deviates slightly to the left of the midline before crossing the oesophageal hiatus of the diaphragm. The oesophagus is closely related to the mediastinal pleura of the right lung, except at the lower end of the posterior mediastinum where it is related to the left-sided pleura. Inadvertent

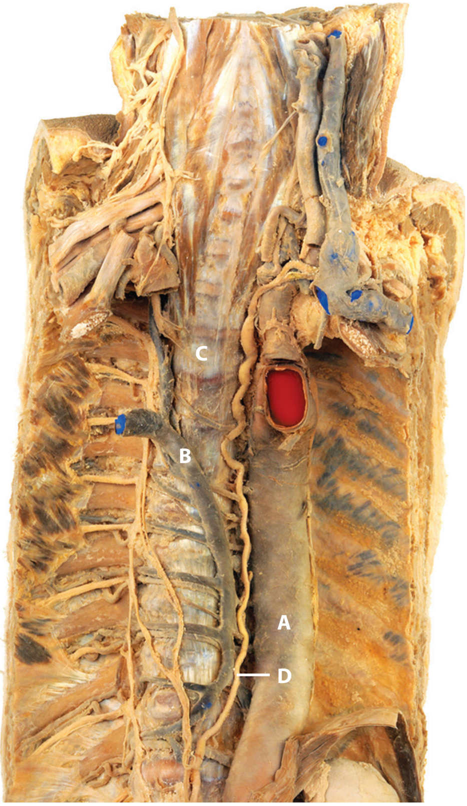

Figure 19.5 Posterior mediastinum and contents viewed from the front, after removal of oesophagus (dissection). A – descending thoracic aorta. B – vena azygos. C – thoracic vertebral column. D – thoracic duct.

perforation of the oesophagus is thus more likely to present as a right-sided pneumothorax.

Surgical access to the posterior mediastinum may be gained through a generous posterolateral thoracotomy, the side being determined by the nature and location of the lesion to be operated upon. For example, aneurysms of the descending thoracic aorta are approached through a left posterolateral thoracotomy, while a two-stage oesophagectomy for a cancer of the mid-oesophagus would require a right posterolateral thoracotomy.

Access to the posterior mediastinum may also be gained transabdominally through the oesophageal hiatus of the diaphragm. Transhiatal oesophagectomy and certain operations employed for the repair of hiatus hernia are examples of procedures in which the lower part of the posterior mediastinum is entered transabdominally.

The posterior mediastinum may also be approached endoscopically (thoracoscopy). Video-assisted thoracoscopic surgery (VATS) is now the preferred approach for thoracic sympathectomy, splanchnic nerve resection and the excision of various benign mediastinal masses.

FURTHER READING

Armstrong P, Wastie M, Rockall A. *Diagnostic Imaging*. 6th ed. Oxford: Wiley-Blackwell, 2009.

McMinn RMH. *Last's Anatomy: Regional and Applied*. 9th ed. Edinburgh: Churchill-Livingstone, 1994.

Moore KL, Dalley AF. *Clinically Oriented Anatomy*. 5th ed. Philadelphia: Lippincott Williams & Wilkins, 2006.

Riquet M, Manach D, Dupont P. Anatomic basis of lymphatic spread of lung carcinoma in the mediastinum: Anatomo-clinical correlations. *Surgical and Radiologic Anatomy*. 1994; 16: 229.

Sellke FW, del Nido PJ, Swanson SJ. *Sabiston and Spencer's Surgery of the Chest*. 8th ed. Philadelphia: Saunders Elsevier, 2010.

Shields TW. *The mediastinum, its compartments and the mediastinal lymph nodes*. In: *General Thoracic Surgery*. 5th ed. Philadelphia: Lippincott Williams & Wilkins, 2000.

20

Tissue spaces of the head and neck

DAREN GIBSON AND CURTIS OFFIAH

Superficial cervical fascia 201
Deep cervical fascia 201
Superficial layer of the deep cervical fascia 202
Middle layer of the deep cervical fascia 206
Deep layer of the deep cervical fascia 207
Further reading 207

To facilitate an effective surgical approach to disease, a sensible diagnostic interpretation of head and neck pathology is determined by a good working knowledge of normal anatomy and common variants as well as by a useful compartmentalization technique based upon applied cross-sectional anatomy. In order to know what something is, one first has to appreciate where it is. With the numerous and complex neurovascular structures present in the neck, a comprehensive understanding of the important anatomical relationships of any abnormality is fundamental. Imaging including ultrasound, CT, MRI and interventional radiology techniques are often used to help the surgeon pre-operatively.

SUPERFICIAL CERVICAL FASCIA

The superficial cervical fascia (SCF), also known as panniculus adiposus, is situated between the overlying dermis, which contains fibrofatty tissue, and the deep cervical fascia (DCF). The superficial musculo-aponeurotic system (SMAS) is an extension of this fascial layer over the face, scalp and temporal regions with the associated musculature arranged into four separate layers.

The platysma muscle originates from the deep fascia that overlies the superior aspects of the pectoralis major and anterior deltoid muscles and extends up into the neck; it is surrounded by the superficial fascia. The platysma muscle mainly inserts along the mandible with residual fibres passing more superiorly onto the face to reach the peripheral margin of the lips, the lateral aspect of the parotid gland and risorius muscles.

DEEP CERVICAL FASCIA

For ease of approach, the neck can be divided into the suprahyoid (skull base to hyoid) and infrahyoid (hyoid to clavicle) regions. These two compartments may be further subdivided and defined by the three layers of the DCF: (1) investing/superficial layer of the DCF, (2) middle/visceral layer and (3) the perivertebral/deep layer.

The SCF and the superficial (or investing) layer of the DCF should not be confused.

Cranially, the DCF is attached to the superior nuchal line of the occipital bone, the mastoid

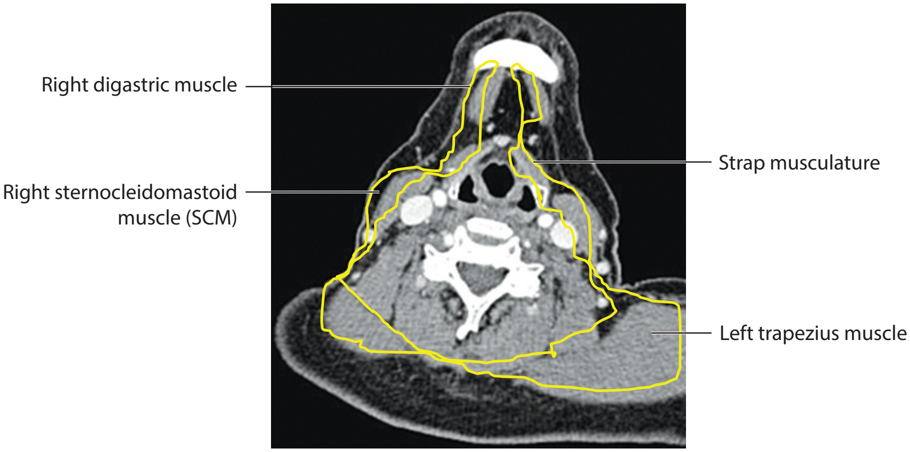

Figure 20.1 Contrast enhanced axial computed tomography (CT) scan demonstrating the superficial layer of the deep cervical fascia.

process of the temporal bone and the inferior border of the entire mandible. Caudally, the fascia is attached to the clavicles, manubrium sterni, scapulae and the acromion. The DCF is largely absent over the face.

Superficial layer of the deep cervical fascia

The investing layer of the DCF splits and surrounds the sternocleidomastoid, trapezius, digastric and strap musculature (Figure 20.1). Anteriorly, it attaches to the hyoid bone. In the suprahyoid region, it envelops the parotid and submandibular salivary glands and surrounds all muscles of mastication to define the encapsulated parotid space (PS) and the masticator space.

PAROTID SPACE

The deeper surface of the parotid capsule is separated from the pterygoid muscles by the fascial condensation known as the stylomandibular ligament. The styloid process separates the deeper lobe from the carotid sheath.

The terminating external carotid artery traverses the parotid capsule inferiorly to enter the gland substance.

The main parotid duct forms at the anterior surface of the gland and is barely perceptible at ultrasound when normal in calibre. Not uncommonly, it may receive minor ducts draining from accessory parotid tissue. The duct passes superficial to the masseter muscle before piercing the buccinator muscle and the oral mucosa to emerge at its ostium opposite the second maxillary molar tooth.

In health, the superficial lobe of the parotid gland accounts for around two-thirds of the total glandular volume.

On cross-sectional imaging, the position of the facial nerve within the parotid gland parenchyma can be inferred from the adjacent medially located retromandibular vein (Figure 20.2); however, the nerve is still not routinely identifiable with routine conventional magnetic resonance sequences.

Lymph nodes are often seen within the parotid parenchyma due to late glandular encapsulation at embryogenesis.

MASTICATOR SPACE

The complex infratemporal region lies immediately below the skull base, subjacent to the undersurface of the greater wing of the sphenoid and the squamous part of the temporal bone.

Its medial and lateral boundaries are the pharyngeal mucosa and the medial aspect of the mandibular ramus, respectively. Its posteromedial border includes the lateral pterygoid plate, the superior constrictor and the tensor and levator palatine muscles. Anteromedially, the medially tapering pterygomaxillary fissure communicates with the

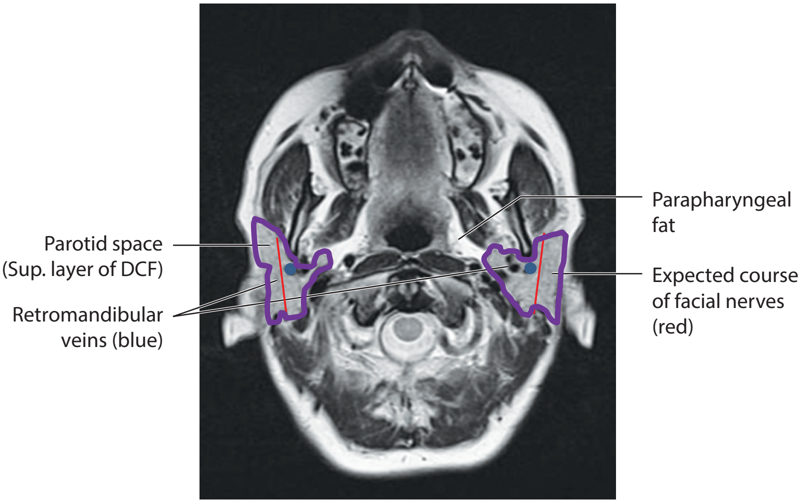
Parotid space
(Sup. layer of DCF)
Retromandibular
veins (blue)
Parapharyngeal
fat
Expected course
of facial nerves
(red)

Figure 20.2 T2W axial magnetic resonance image (MRI) at the level of the parotid glands demonstrates the projected course of the extra-temporal facial nerve.

pterygopalatine fossa and this can act as a conduit for contiguous disease spread (Figure 20.3).

The contents of the infratemporal fossa include the pterygoid muscles, the temporalis muscle tendon as it inserts on to the coronoid process, the maxillary artery and the pterygoid venous plexus. On postcontrast imaging, the latter enhancing venous plexus studies may appear asymmetric bilaterally and can be overreported, thought to represent a significant lesion. Neural structures include the mandibular branch of the trigeminal nerve and its branches, the chorda tympani nerve and the superior alveolar branches of the maxillary nerve.

The investing layer of the DCF splits around the masticator muscles. Its lateral slip covers the external surface of the masseter muscle and attaches to the zygomatic arch. Thereafter, it continues

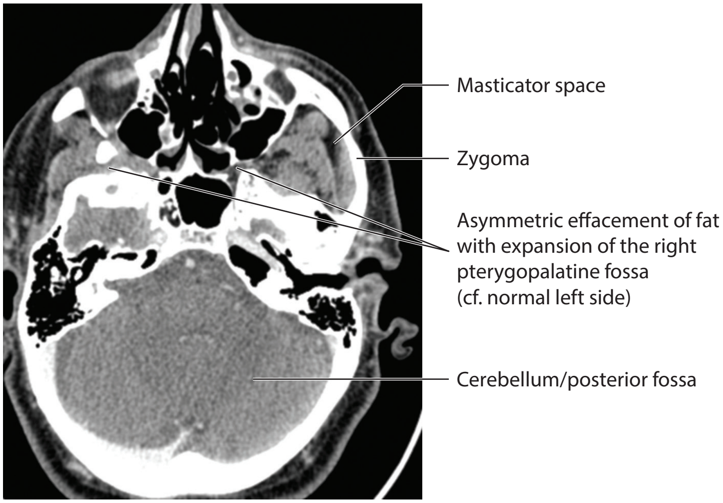
Masticator space
Zygoma
Asymmetric effacement of fat
with expansion of the right
pterygopalatine fossa
(cf. normal left side)
Cerebellum/posterior fossa

Figure 20.3 Middle-aged male with progressive right-sided trigeminal, abducens and facial nerve palsies. Biopsy proven occult SCC skin. Contrast enhanced CT showing effacement of the right pterygopalatine fossa space due to biopsy proven perineural spread from an occult skin squamous cell carcinoma.

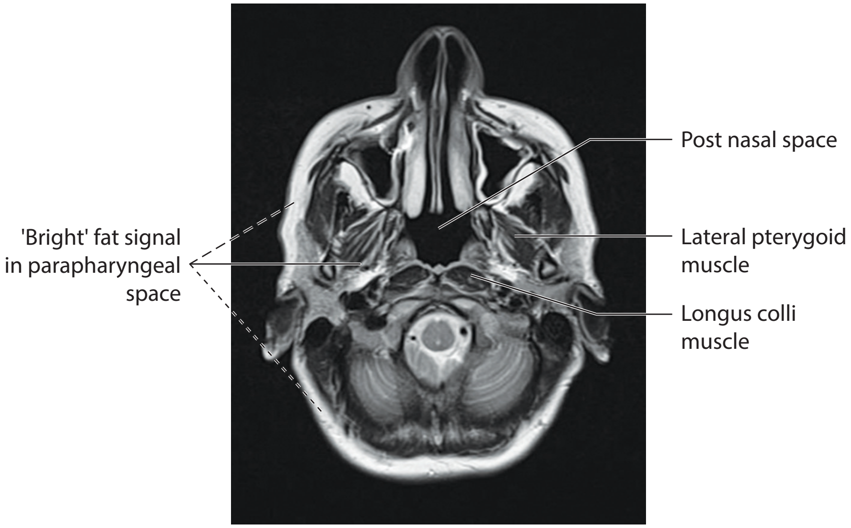
'Bright' fat signal in parapharyngeal space
Post nasal space
Lateral pterygoid muscle
Longus colli muscle

Figure 20.4 MRI of characteristic areolar fat within the parapharyngeal space.

superiorly over the surface of temporalis muscle to generate a 'suprazygomatic' component to the masticator space. The medial slip of the investing layer is anatomically sparser and less clearly defined.

PARAPHARYNGEAL SPACE

Between the defined neck spaces there are 'potential' unbounded spaces which are poor barriers to disease. The parapharyngeal space has the shape of an inverted pyramid with its floor at the skull base. Radiologically, it is readily identified axially and coronally because its bulk consists of distinctive fatty areolar tissue (Figure 20.4). The contents include: the mandibular division of the trigeminal nerve, branches of the internal maxillary artery and the ascending pharyngeal artery and veins. Minor salivary gland rests may also be present.

On cross-sectional imaging, the displacement of this fat-containing space assists in localizing the origin of a soft tissue mass: a mass arising from the deep lobe of the parotid gland lesion will displace the fat of the parapharyngeal space medially; a masticator space lesion will displace the fat within the parapharyngeal space posteromedially; a carotid space mass will displace the posterior surface of the parapharyngeal space; a retropharyngeal and the perivertebral space lesion will displace the parapharyngeal fat laterally (Figure 20.5).

SUBMANDIBULAR AND SUBLINGUAL SPACES

The paired parotid, submandibular and sublingual glands constitute the 'major' salivary glands.

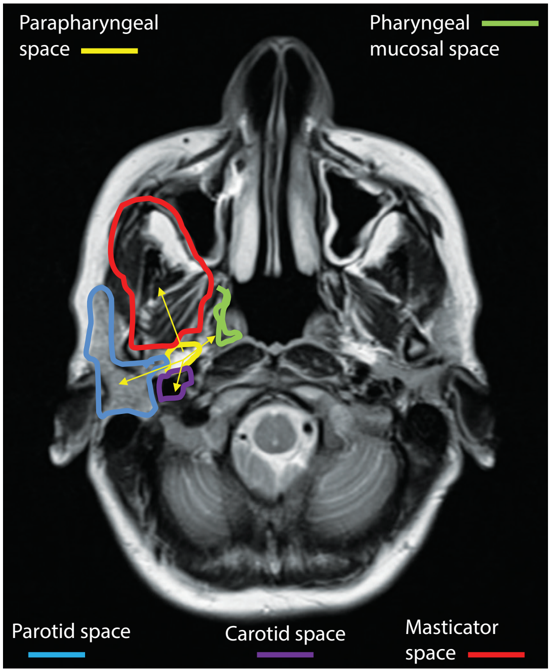
Parapharyngeal space
Pharyngeal mucosal space
Parotid space
Carotid space
Masticator space

Figure 20.5 Lesion origin as defined by schematic directional displacement of the parapharyngeal space.

Innumerable minor salivary glands are also present throughout the entire upper aerodigestive tract including the hard and soft palate, sinuses and trachea.

The mylohyoid muscle originates from the mylohyoid line of the hemimandible and inserts into an anterior median fibrous raphe that extends from the mandibular symphysis to the hyoid. This sheetlike muscle thereby forms a muscular sling inferior to the tongue and separates the submandibular space and the sublingual space (Figure 20.6). Posteriorly, the mylohyoid muscle has a free margin through which the submandibular and sublingual spaces will directly communicate.

Variably sized developmental dehiscences in the integrity of the mylohyoid muscle with potential herniation of salivary tissue (boutonniere defects) commonly exist and are often bilateral.

The submandibular gland has superficial and deep lobes as defined by the relationship to the posterior free margin of the mylohyoid muscle.

Calculi may impact at this transition due to the acute ductal angulation at this site. The main proximal submandibular duct courses anterosuperiorly between the mylohyoid and hyoglossus muscles. It then passes between the ipsilateral sublingual gland and the geniohyoid muscle to terminate at the tongue frenulum.

The contents of the SMS include lymph nodes medial to the mandibular body and the facial vessels. The cervical branch of the facial nerve and the hypoglossal nerve are also traversing this space.

The lingual vessels pass medially, lying deep to the submandibular gland.

The ceiling of the sublingual space simply consists of the floor of mouth squamous mucosa. The midline genioglossus-geniohyoid muscle complex lies medial to the sublingual space. The contents of the sublingual space include the sublingual glands and their draining ducts, the medially placed distal submandibular duct, the lingual nerve, artery and vein, and also the hypoglossal and glossopharyngeal nerves.

Anatomical Hazard: The mylohyoid muscle attaches obliquely onto the lingual surface mandibular body, inferiorly sloping towards the anterior midline. The relevance of this lies in the fact that odontogenic infection involving the incisors, canine, premolars or first mandibular molar, with medial cortical loss, will result in inflammation and abscess formation first in the sublingual and then into the submandibular space bilaterally with a ‘Ludwig’s angina’ that can cause an acute airway embarrassment.

CAROTID SPACE

Extending from the skull base to the aortic arch and sited posterior to the parapharyngeal space,

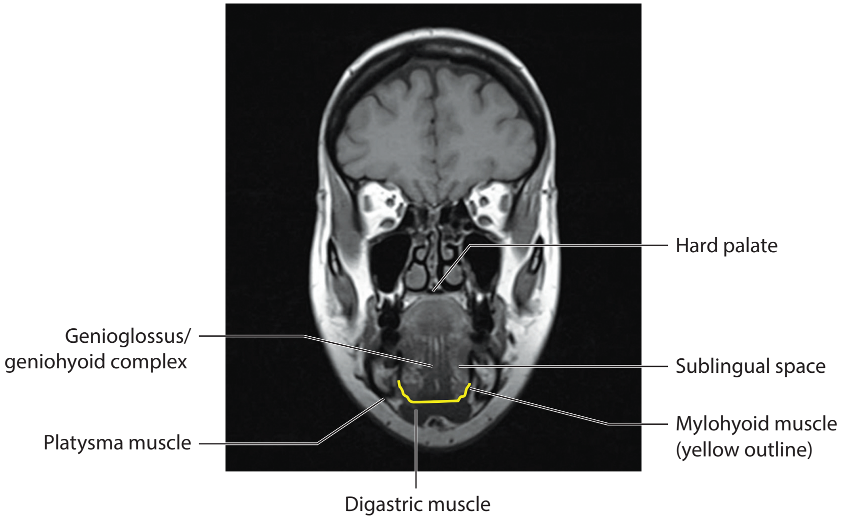

Figure 20.6 Coronal T1W MRI illustrates the mylohyoid muscle separating the inferolateral submandibular and superomedial sublingual spaces.

the carotid sheath receives contributions from all three layers of the DCF. These fascial contributions are discontinuous and incomplete superiorly but more densely consolidated inferiorly.

The carotid space contents include the carotid arteries, cervical lymph nodes, the internal jugular vein and the traversing lower four cranial nerves. After exiting the skull base foramina, the glossopharyngeal, spinal accessory and hypoglossal nerves typically exit the carotid space at the level of the soft palate whilst the vagus nerve remains within the sheath to the level of the aortic arch.

Anatomical Hazard: At surgery, the position of the carotid sheath can be altered and made less predictable in the presence of an abscess, infection or tumour.

Middle layer of the deep cervical fascia

The pretracheal or middle layer of the DCF defines the lateral border of the pharyngeal mucosal space (PMS) in the suprahyoid neck.

From the upper aerodigestive mucosa outwards, the middle layer will also encompass the lymphoid tissue of Waldeyer's ring (adenoidal, palatine and lingual tonsils) and the superior and middle constrictor muscles. All of these structures lie within the PMS. An infectious or neoplastic process spreading laterally from the pharynx can easily extend into both the submandibular and sublingual spaces.

VISCERAL SPACE

Spanning the anterior midline of the infrahyoid neck, the cylindrical visceral space is surrounded entirely by the middle layer of the DCF. Posterolaterally, its immediate relation is the carotid space (Figure 20.7). Directly posterior to the visceral space lies the retropharyngeal space (RS).

The normal contents of the visceral space include the thyroid and parathyroid glands, the larynx, the cervical trachea and oesophagus, the recurrent laryngeal nerves and the pre- and paratracheal lymph nodes.

Although there can be variability in the number of parathyroid glands, over 80 per cent of the population will characteristically have two superior and two inferior glands.

RETROPHARYNGEAL SPACE

Like the parapharyngeal space, the retropharyngeal space is a potential space situated between the anteriorly placed pharyngeal constrictors and pharyngeal mucosa and the posteriorly positioned deep perivertebral layer of the DCF.

Initially described by Grodinsky and Holyoke in 1938, anatomists have further divided the space coronally by the slender alar fascia made up of fibroareolar tissue. This layer splits the retropharyngeal space into the anterior retropharyngeal space 'proper' (extending down to the 4th thoracic vertebral body) and the posteriorly placed 'danger' space (reaching the diaphragm via the posterior mediastinum).

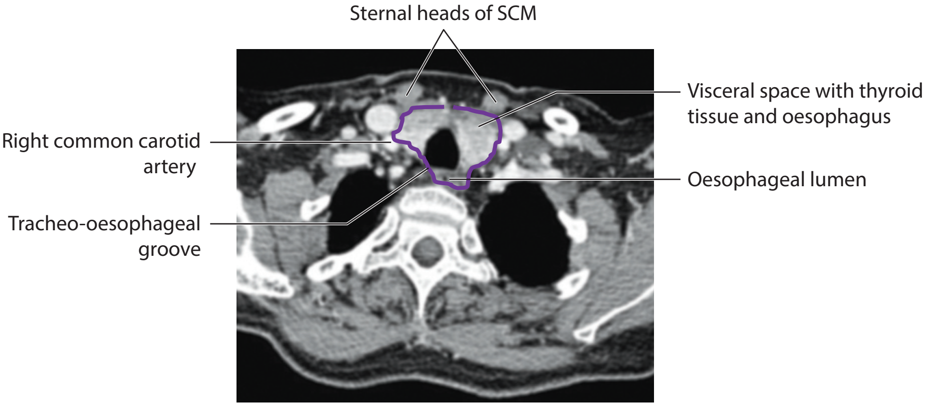
Sternal heads of SCM
Visceral space with thyroid tissue and oesophagus
Right common carotid artery
Oesophageal lumen
Tracheo-oesophageal groove

Figure 20.7 Axial CT: The visceral space and its immediate relations.

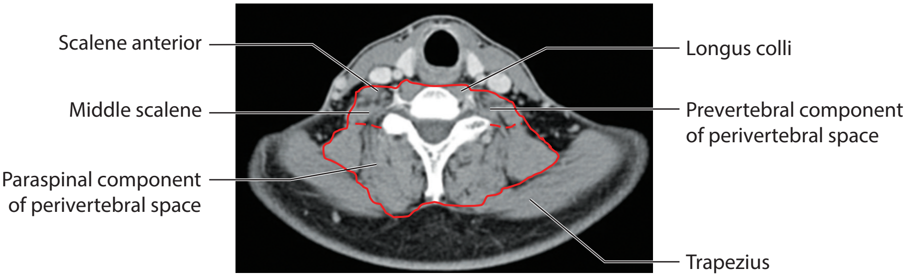
Scalene anterior
Middle scalene
Paraspinal component of perivertebral space
Longus colli
Prevertebral component of perivertebral space
Trapezius

Figure 20.8 Axial CT: Prevertebral and paraspinal components of the prevertebral space.

The retropharyngeal space proper contains areolar fat, connective tissue and the laterally and inconsistently identified medially placed regional lymph nodes. The transverse process of the atlas, the posterolateral sympathetic trunk and the superior sympathetic ganglion are important surgical landmarks to allow nodal clearances anterior to the alar fascia.

Deep layer of the DCF

PERIVERTEBRAL SPACE

The tough prevertebral/deep layer of the DCF circumscribes the perivertebral space. It attaches to the skull base and terminates inferiorly at approximately the 3rd thoracic vertebra. It has fascial slips attaching to the transverse processes of the cervical spine that further subdivide the perivertebral space into separate prevertebral and paraspinal components (Figure 20.8). The fibrous deep layer of the DCF is a resilient barrier to the spread of disease.

The perivertebral space contains the scalene, longus colli and longus capitis muscles, the brachial plexus trunks, the phrenic nerve (C3, 4 and 5 foramina), the vertebral bodies and the vertebral artery and vein as they traverse the foramen transversarium.

The paraspinal space contains the more distal divisions and cords of the brachial plexus, the paraspinal musculature and the posterior bony elements of the cervical spine.

FURTHER READING

Chong V. Retropharyngeal space. *Clinical Radiology*. 2000; 55: 740.

Harnsberger HR. Suprahyoid neck. *American Journal of Radiology*. 1991; 157: 147.

Harnsberger HR, Glastonbury CM, Michel MA et al. *Diagnostic Imaging: Head and Neck*. 2nd ed. Philadelphia: Lippincott Williams & Wilkins, 2011.

White DK et al. Accessory salivary tissue in the mylohyoid boutonniere. *American Journal of Radiology*. 2001; 22: 406.

21

Larynx, trachea and tracheobronchial tree

EMMA V. KING AND VISHY MAHADEVAN

Introduction 209
Embryology of the larynx and trachea 210
Anatomy of the larynx and trachea 210
Extrinsic laryngeal ligaments 211
Intrinsic laryngeal ligaments 211
Laryngeal subdivisions 212
Internal laryngeal muscles 213
External laryngeal muscles 213
Blood supply, venous drainage and lymphatic drainage of the larynx 214
Nerve supply of the larynx 214
Anatomical hazards in laryngeal and tracheal surgery 214
Arytenoid dislocation/subluxation following intubation 215
Developmental aberrations of the larynx and trachea 216
The trachea and tracheobronchial tree 216
Topographical relations of the trachea 217
Arterial supply, venous and lymphatic drainage and sensory innervation of the trachea 218
The bronchial tree 218
Further reading 220

INTRODUCTION

The larynx, trachea and the bronchial apparatus collectively constitute the lower respiratory tract.

The primary function of the larynx is to act as a protective sphincter for the lower airway. A secondary and important role of the larynx, and one that has evolved to the peak of its functional sophistication in the human, is to act as an organ of phonation.

The larynx is clinically divided into three areas, the supraglottis (cranial to the vocal cords), glottis (the vocal cords) and subglottis (caudal to the vocal cords). The subglottis becomes continuous with the trachea at the lower border of the cricoid cartilage.

The tracheobronchial tree is a bidirectional air conduit that possesses a specialized internal lining of respiratory epithelium.

The larynx can be approached surgically through a neck incision (open approach), or via the oral cavity and pharynx (endoscopic approach). Significant technological developments in the design of surgical equipment (including lasers and robots) allow radical endoscopic procedures to be undertaken with safety. Irrespective of approach, a thorough and complete three-dimensional understanding of laryngeal anatomy is required for safe and effective surgery.

In this chapter a general review of the essential embryology of the larynx and trachea will be followed by a detailed description of the surgically relevant anatomy of the larynx and tracheobronchial tree.

EMBRYOLOGY OF THE LARYNX AND TRACHEA

The tracheobronchial groove or ridge is a respiratory primordium including the larynx, trachea, bronchi and lungs. It develops from a ventromedian diverticulum of the foregut, caudal to the pharyngeal pouches. Lateral furrows develop on either side of the respiratory diverticulum, which progressively deepen and finally unite to form the laryngotracheal tube. The cranial end of this tube (which is just behind the hypobranchial eminence and between the 4th and 6th branchial arches) develops into the primitive laryngeal aditus or slit.

The margins of the laryngotracheal groove unite in a caudocranial direction to form the tracheo-oesophageal septum (separating the oesophagus from the laryngotracheal groove). By the fifth week of intrauterine development, the larynx consists of three primary tissue masses: anteriorly, the primordium of the epiglottis, which is derived from the hypobranchial eminence (2nd and 4th arches), and lateral to the laryngeal aditus, two swellings of mesenchymal tissue forming the arytenoid cartilages (ventral ends of the 6th arch). By 6 weeks, the three primary masses of tissue grow, approximate, and move towards the tongue base, resulting in a *T*-shaped laryngeal aditus.

At 11–12 weeks the major topography of the larynx is formed and chondrification begins. By the end of the second trimester (and continuing to the end of the first year of life), the anterior hyoid bone overlaps the superior border of the thyroid cartilage. In addition, the fetal larynx is (1) at an obtuse angle to the jaw, and (2) positioned higher in the neck (C1–C2) compared with an adult larynx (C3–C6). At birth, this relatively cranial position allows concurrent breathing or vocalization and deglutition. By 6 years, the larynx has descended into an adult position, allowing the individual a greater range of phonation (due to a wider supra-glottic pharynx) but at the expense of the ability to swallow and breathe simultaneously.

The laryngeal muscles are derived from mesenchyme of the 4th and 6th pharyngeal arches. Therefore, all laryngeal muscles are innervated by branches of the vagus nerve: The superior laryngeal nerve innervates derivatives of the 4th pharyngeal arch, and the recurrent laryngeal nerve innervates derivatives of the 6th pharyngeal arch (see discussion that follows).

The embryology of the thyroglossal duct is described in Chapter 22.

ANATOMY OF THE LARYNX AND TRACHEA

The larynx is a composite organ, containing a mucosal surface, cartilage, ligaments, muscles and joints. There are three unpaired pieces of cartilage, the thyroid, the cricoid and the epiglottis; and three paired pieces of cartilage, the arytenoid, the corniculate and the cuneiform (Figure 21.1). The ligaments are subdivided into extrinsic (the thyrohyoid membrane, the cricotracheal, the hyoepiglottic and the thyroepiglottic ligaments) and intrinsic (the quadrangular membrane) and conus elasticus (cricovocal membrane). It is the cranial part of this latter ligament that forms the vocal cord.

Cranial to the larynx is the hyoid bone, suspended by both suprahyoid and tongue muscles.

The *thyroid cartilage* includes two conjoined laminae, with free posterior borders projected cranially and caudally as superior and inferior horns, respectively. Each inferior horn articulates with the cricoid cartilage (the cricothyroid joint). This joint is important surgically as it can be palpated to identify the position of the recurrent laryngeal nerve as it enters the larynx. Anteriorly, the fusion of the laminae produces the laryngeal prominence (Adam's apple) and cranial to this, a deep midline notch, the thyroid notch.

The *cricoid cartilage* is signet ring–shaped, and both the thyroid and arytenoid cartilages articulate with the cricoid cartilage by means of synovial joints. The cricoid is the only complete cartilage ring in the respiratory tract.

The *epiglottic cartilage* is shaped as a curved leaf; caudally, the slender process (petiole) attaches to the inner surface of the thyroid cartilage (below the thyroid notch), by the thyroepiglottic ligament. From this insertion, the epiglottic cartilage overhangs the vestibule of the larynx. It is anchored to the posterior surface of the hyoid bone and thyroid cartilage by the hyoepiglottic and thyroepiglottic ligaments, respectively. The aryepiglottic folds of mucous membrane connect the epiglottis to the arytenoid cartilages laterally. The median glossoepiglottic fold attaches the epiglottis to the base of the tongue, and the lateral glossoepiglottic folds attach the epiglottis to the pharynx.

The *arytenoid cartilages* articulate with the upper border of the cricoid cartilage and provide attachment for the vocal folds and various laryngeal muscles. They are pyramid shaped but at their base have an anterior projection (vocal process) attached to the vocal cord and a lateral projection (muscular process) for the cricoarytenoid muscles. The superior process of the arytenoid articulates with the corniculate cartilage, which is attached to the aryepiglottic fold. Further forward, within the aryepiglottic fold lies the cuneiform cartilage.

Extrinsic laryngeal ligaments

The thyrohyoid membrane extends between the hyoid bone and the thyroid cartilage. Within it are thickenings, one in the midline, the median thyrohyoid ligament (Figure 21.1), and dorsally, the lateral thyrohyoid ligaments. Both of these latter ligaments contain a small triticeal cartilage. The thyrohyoid membrane forms the lateral border of the piriform recess and is perforated by the internal branch of the superior laryngeal nerve and the superior laryngeal vessels. The pre-epiglottic space lies behind the thyrohyoid membrane.

The cricothyroid ligament connects the cricoid to the thyroid cartilage: Its deep aspect is the cricovocal membrane (conus elasticus) and is discussed in the next section.

Intrinsic laryngeal ligaments

The quadrangular membrane extends from the arytenoid cartilages to the epiglottis (Figures 21.1 and 21.2). The ventral border is attached to the side of

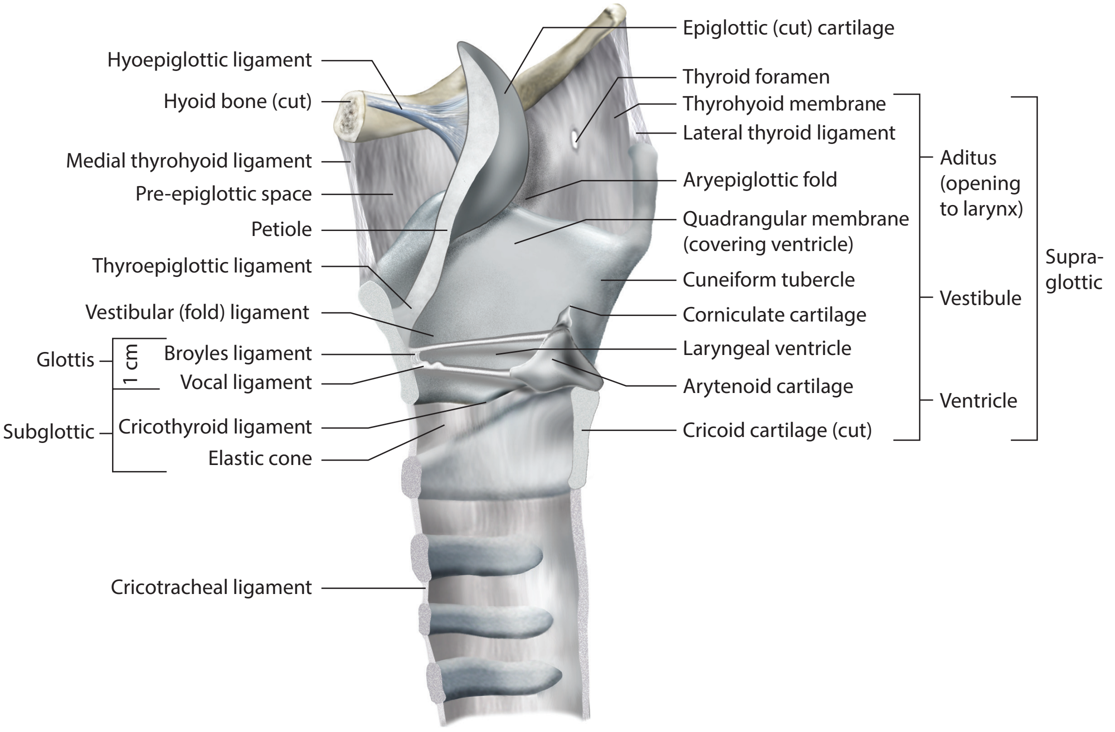
Hyoepiglottic ligament
Hyoid bone (cut)
Medial thyrohyoid ligament
Pre-epiglottic space
Petiole
Thyroepiglottic ligament
Vestibular (fold) ligament
Glottis
1 cm
Broyles ligament
Vocal ligament
Subglottic
Cricothyroid ligament
Elastic cone
Cricotracheal ligament
Epiglottic (cut) cartilage
Thyroid foramen
Thyrohyoid membrane
Lateral thyroid ligament
Aryepiglottic fold
Quadrangular membrane (covering ventricle)
Cuneiform tubercle
Corniculate cartilage
Laryngeal ventricle
Arytenoid cartilage
Cricoid cartilage (cut)
Aditus (opening to larynx)
Vestibule
Ventricle
Supra-glottic

Figure 21.1 Line illustration to show laryngeal ligaments, membranes and spaces, sagittal view.

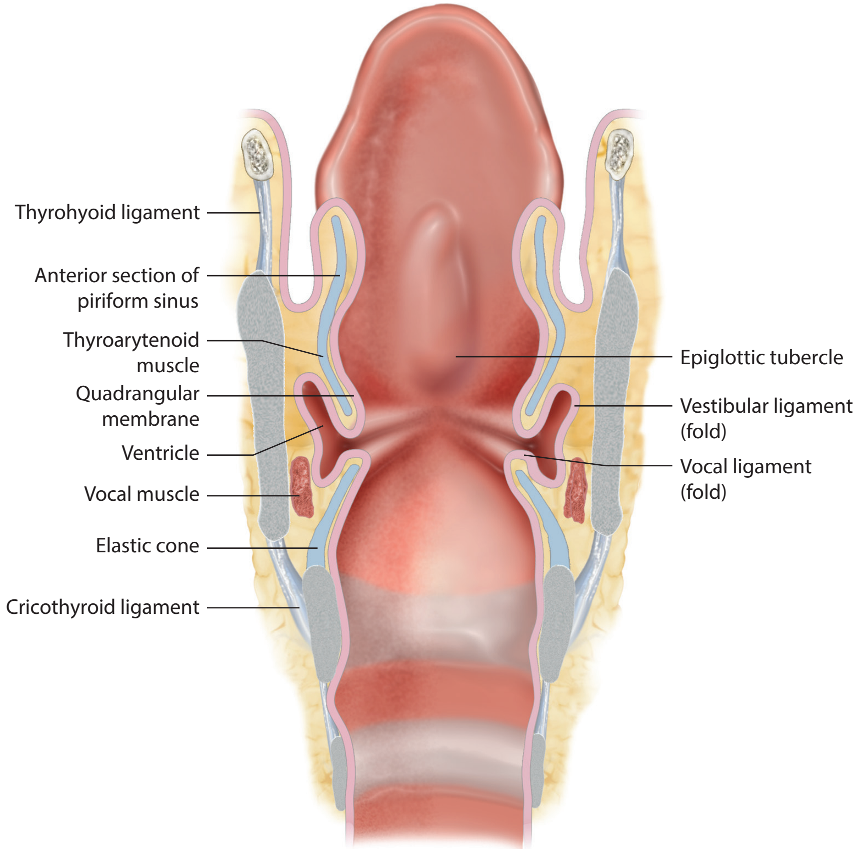
Thyrohyoid ligament
Anterior section of piriform sinus
Thyroarytenoid muscle
Quadrangular membrane
Ventricle
Vocal muscle
Elastic cone
Cricothyroid ligament
Epiglottic tubercle
Vestibular ligament (fold)
Vocal ligament (fold)

Figure 21.2 Line illustration to show posterior aspect of larynx.

the lower half of the epiglottis. The dorsal border is from the arytenoid to the corniculate cartilage. The cranial border, at the inlet of the larynx, forms the aryepiglottic fold, and the caudal border is free, forming the false vocal cord (Figures 21.3 and 21.4).

The cricothyroid ligament is thickened in the midline to form the median cricothyroid ligament, alternatively known as the conus elasticus. The more important lateral part contains an abundance of elastic fibres and is called the lateral cricothyroid membrane, the triangular membrane or the cricovocal membrane. It projects cranially from the arch of the cricoid cartilage to the junction of the laminae of the thyroid cartilage, midway between the notch and the caudal border, where it is adjacent with its fellow. Dorsally, it is attached to the vocal process of the arytenoid cartilage. The cranial border is free, thickened and covered by mucous membrane. This is the cricovocal ligament or vocal fold (vocal cord).

Laryngeal subdivisions

The inlet of the larynx faces both cranially and dorsally and is bounded by the epiglottis, aryepiglottic folds and interarytenoid fissure. The

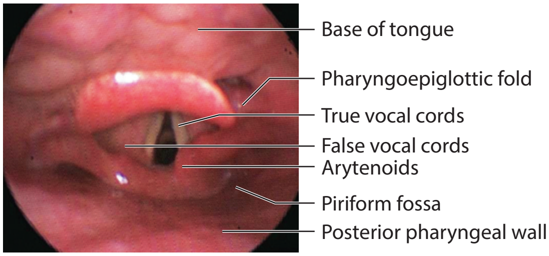
Base of tongue
Pharyngoepiglottic fold
True vocal cords
False vocal cords
Arytenoids
Piriform fossa
Posterior pharyngeal wall

Figure 21.3 Clinical photograph to show an endoscopic view of the larynx (picture courtesy of Kate Heathcote).

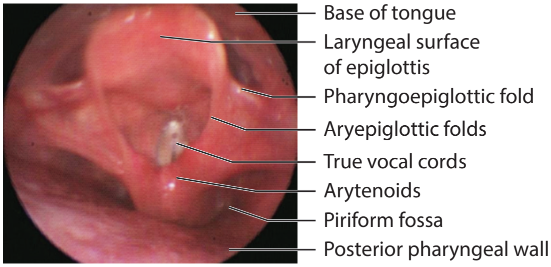

Figure 21.4 Clinical photograph to show an endoscopic view of the larynx, during valsalva manoeuvre (picture courtesy of Kate Heathcote).

space below the inlet as far as the vestibular folds (false vocal cords) is the vestibule (Figure 21.1). The space between the vestibular and true vocal folds is the ventricle of the larynx, also called the laryngeal sinus. Opening from the ventral end of the laryngeal sinus is the laryngeal saccule: This is a pouch of mucous membrane, extending cranially for a few millimetres between the vestibular fold and the thyroid lamina. The ventrodorsal slit through which air passes is the rima of the glottis. The anterior 60 per cent (intermembranous part) is bounded on each side by the vocal fold. The posterior 40 per cent (intercartilaginous part) is formed by the vocal process of the arytenoid cartilages.

Laryngeal spaces are important clinically for staging neoplastic disease:

1. The *pre-epiglottic space* contains fat and areolar tissue. It is bound anteriorly by the thyroid cartilage and thyrohyoid membrane, superiorly by the median thyroepiglottic ligament and vallecula, posteriorly by the anterior surface of the epiglottic cartilage and the petiole, and laterally it is continuous with the periglottic space.
2. The *paraglottic space* is bound anterolaterally by the inner perichondrium of the thyroid cartilage, elastic cone and quadrangular membrane, medially by the laryngeal ventricle and posteriorly by a reflection of the piriform sinus mucosa.
3. The *subglottic space* is bound superiorly by the vocal cord and superolaterally by the elastic cone.

Internal laryngeal muscles

The internal muscles of the larynx are subgrouped into those muscles altering the size and shape of the inlet and those moving the vocal cords. The former group consists of the aryepiglottic muscles, the oblique arytenoid and the thyroepiglottic muscles. The muscles responsible for vocal cord movement are subdivided into abductor and adductor and muscles that lengthen and shorten the vocal cord. The muscle responsible for abduction is the posterior cricoarytenoid. This is opposed by the two adductors, the lateral cricoarytenoid and the transverse arytenoid. The muscle responsible for lengthening the vocal cord is the cricothyroid, the opponent of which is the thyroarytenoid. The changes in length and tension control the pitch of the voice and occur normally when the cords are in contact for phonation.

External laryngeal muscles

The external laryngeal muscles move the larynx either cranially or caudally. Those elevating muscles include thyrohyoid, stylopharyngeus, palatopharyngeus, salpingopharyngeus and the inferior constrictor. Muscles indirectly elevating the larynx via the hyoid include the mylohyoid, digastric, stylohyoid and geniohyoid. The sternothyroid acts directly on the larynx to move it downwards. The sternohyoid and omohyoid indirectly depress the larynx by pulling the hyoid caudally. The external muscles play an important role in swallowing and as accessory muscles of respiration.

Histologically, the upper vestibular folds are covered with a pseudostratified ciliated columnar epithelium with goblet cells. The underlying lamina propria contains an abundance of mixed serous and mucous glands, and the excretory ducts open onto the epithelial surface.

The ventricle is the site where the epithelium transitions from respiratory epithelium on the false cords to the stratified squamous epithelium on the vocal folds. The lamina propria within the laryngeal ventricles blends with the perichondrium of the hyaline thyroid cartilage. No distinct submucosa exists.

The vocal folds are lined with a thick stratified squamous epithelium, which functions to protect the mucosa from abrasion caused by the rapid movement of air during breathing and phonation. A thicker layer of connective tissue is located beneath the vocal fold epithelium and is subdivided into three layers: the superficial lamina propria, the intermediate lamina propria, and the deep lamina propria. The superficial lamina propria contains few elastic or collagenous fibres, resulting in increased pliability; the intermediate lamina propria is mainly composed of elastic and collagenous fibres, and it condenses in its anterior and posterior extension forming the bulk of the macule flavae; and the deep lamina propria is made up of more collagenous fibres. These elastic and collagenous fibres within the intermediate and deep layers form the vocal ligament. Beneath the deep lamina propria, the skeletal muscle fibres of the vocalis muscle form the innermost layer and body of the vocal folds. Understanding the histological structure is important for endoscopic resections.

BLOOD SUPPLY, VENOUS DRAINAGE AND LYMPHATIC DRAINAGE OF THE LARYNX

Both the superior laryngeal artery (a branch of the superior thyroid artery, from the external carotid artery) and the inferior laryngeal artery (a branch of the inferior thyroid artery) supply mucosa and muscles of the larynx and anastomose with each other. The inferior thyroid artery is a branch of the thyrocervical trunk, which in turn is a branch of the first part of the subclavian artery.

The superior laryngeal artery enters the piriform recess with the internal laryngeal nerve by piercing the thyrohyoid membrane and divides into ascending and descending branches.

The venous drainage of the larynx is into the superior and inferior laryngeal veins. The superior laryngeal veins accompany the artery and drain into the superior thyroid veins. Likewise, the inferior laryngeal veins drain into the inferior thyroid veins, which drain into the brachiocephalic veins.

Bleeding within from the supraglottic vessel can be a fatal complication following endoscopic laryngeal surgery. From an endoluminal perspective, these vessels can be identified within the superior third of a 'triangle' defined by the vocal process, the anterior commissure, and the epiglottic attachment of the aryepiglottic fold. Knowledge of their position allows both caution and meticulous haemostasis.

The lymphatic drainage of the larynx is as follows. From the upper and lower halves of the larynx the lymphatic vessels drain into the superior (cranial to the omohyoid muscle) and inferior cervical lymph nodes, respectively. Additionally, a few lymphatics drain into the laryngeal (Delphian) or pre-tracheal nodes. The vocal folds have minimal lymphatic drainage, and an early stage glottic tumour is very unlikely to develop regional metastatic disease. Supraglottic tumours are at risk of bilateral lymphatic disease, but the mechanism remains obscure: There does appear to be cross-drainage of the superficial mucosal lymphatics, but no consistent direct cross-drainage of the deep collecting ducts has been described.

NERVE SUPPLY OF THE LARYNX

All the intrinsic muscles of the larynx are supplied by the recurrent (or inferior) laryngeal nerve, except cricothyroid, which is supplied by the external branch of the superior laryngeal nerve. As described earlier, the recurrent laryngeal nerve enters the larynx behind the cricothyroid joint, often at this time divided into two branches, the anterior (adductor) branch and the posterior (abductor) branch.

The mucous membranes of the larynx are supplied by the internal branch of the superior laryngeal nerve above the vocal folds and the recurrent laryngeal nerve below the folds. The internal laryngeal nerve (already bi- or trifurcated) enters the larynx through the thyrohyoid membrane. The sympathetic (vasoconstrictor) supply tracks the arterial supply from the superior and middle cervical sympathetic ganglia.

ANATOMICAL HAZARDS IN LARYNGEAL AND TRACHEAL SURGERY

Both the superior and (inferior) recurrent laryngeal nerve must be identified and preserved in all laryngeal/tracheal and thyroid surgery. Bilateral injury to the superior laryngeal nerves makes it impossible to produce high tones, and paralysis of the internal branch results in a sensory deficit in the supraglottic larynx, resulting in aspiration and dysphagia. Unilateral recurrent laryngeal injury will produce dysphonia; bilateral injury may result in severe dyspnea, or the dyspnea may be slight with severe dysphonia, depending on the cord position.

The hypoglossal nerve (the 12th cranial nerve) must be identified and preserved during a laryngectomy. Its course is very close to the greater horn of the hyoid bone (Figure 21.5), and damaging it results in severe and lasting patient morbidity including impaired speech and swallow.

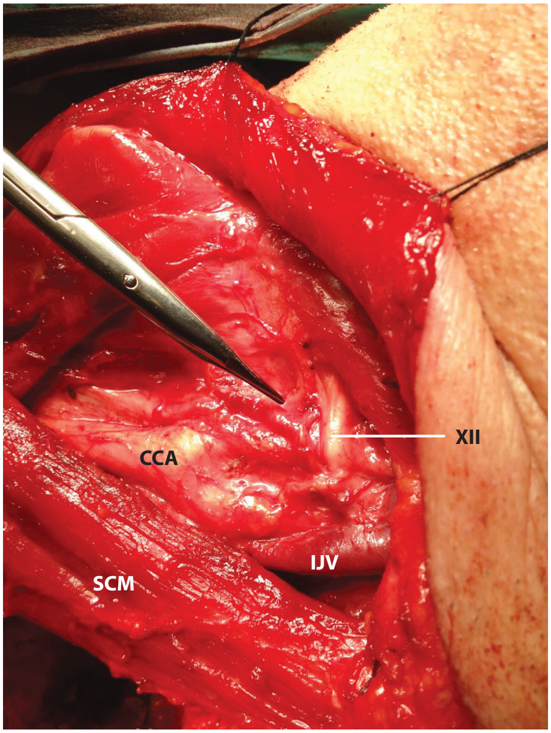

Figure 21.5 Clinical photograph of a left neck dissection to show the close relationship between the hypoglossal nerve (XII) and the greater horn of the hyoid bone (at the tip of the scissors). SCM – sternocleidomastoid muscle. CCA – common carotid artery. IJV – internal jugular vein.

Arytenoid dislocation/subluxation following intubation

Traumatic tracheal intubation can dislocate or subluxate the cricoarytenoid joint. Common presenting symptoms include hoarseness, breathy voice, and dysphagia. The incidence of arytenoid dislocation is unknown, but it is reported to occur in 0.1 per cent of tracheal intubations. Delay in reduction (either closed or open with stenting) is associated with an inferior outcome.

Subglottic stenosis (Figure 21.6) can result from a tracheostomy (surgical or percutaneous) or a fracture to the cricoid cartilage.

As outlined above, meticulous haemostasis of the superior laryngeal vessels is required in endoscopic surgery. These vessels are large, as demonstrated in Figure 21.7. If the patient is undergoing a neck dissection, ligating the superior laryngeal vessels during the dissection as well will ensure haemostasis. An alternative is introducing a cuffed tracheostomy tube, allowing the cuff to be inflated if there is a postoperative bleed, protecting the airway until the patient can be returned to theatre for haemostasis.

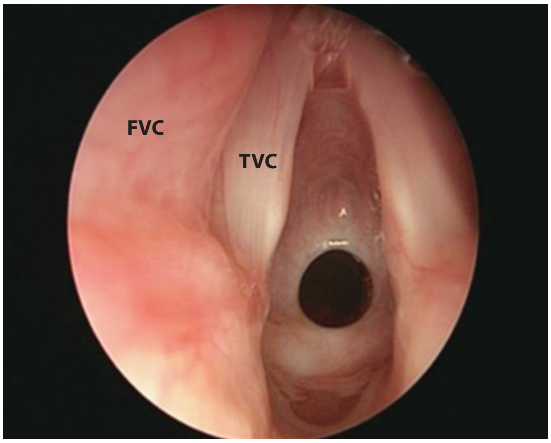

Figure 21.6 Clinical photograph of an endoscopic view of the larynx to show subglottic stenosis secondary to tracheostomy. TVC – true vocal cord. FVC – false vocal cord (courtesy of Roberto Puxeddu).

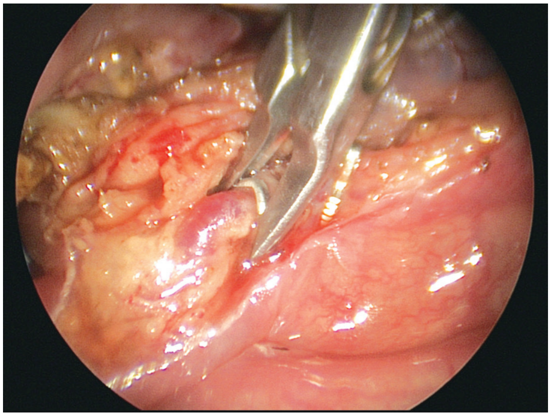

Figure 21.7 Clinical photograph of an endoscopic view of the left epiglottis during a laser endoscopic supraglottic laryngectomy demonstrating ligaclip haemostasis to the supraglottic laryngeal vessels (courtesy of Roberto Puxeddu).

DEVELOPMENTAL ABERRATIONS OF THE LARYNX AND TRACHEA

Developmental aberrations of the larynx and trachea are symptomatic from birth or shortly after and include laryngeal web, laryngo-tracheo-oesophageal web and trachea-oesophageal fistula (associated with oesophageal atresia). The latter occur in approximately 1 in 3000 births and can be part of the VACTERL association (**v**ertebral anomalies, **a**nal atresia, **c**ardiac defects, **t**rachea-oesophageal fistula/oesophageal atresia, **r**enal anomalies and **l**imb defects), a collection of defects of unknown aetiology but occurring more frequently than predicted by chance alone.

THE TRACHEA AND TRACHEOBRONCHIAL TREE

The trachea is the direct, distal continuation of the larynx and commences at the lower border of the cricoid cartilage (Figure 21.8). In a neck that is neither hyperflexed nor hyperextended, the commencement of the trachea corresponds to the level of the body of the 6th cervical vertebra, approximately 5 to 6 cm above the sternal notch. This also signifies the level at which the oesophagus commences as the direct continuation of the pharynx.

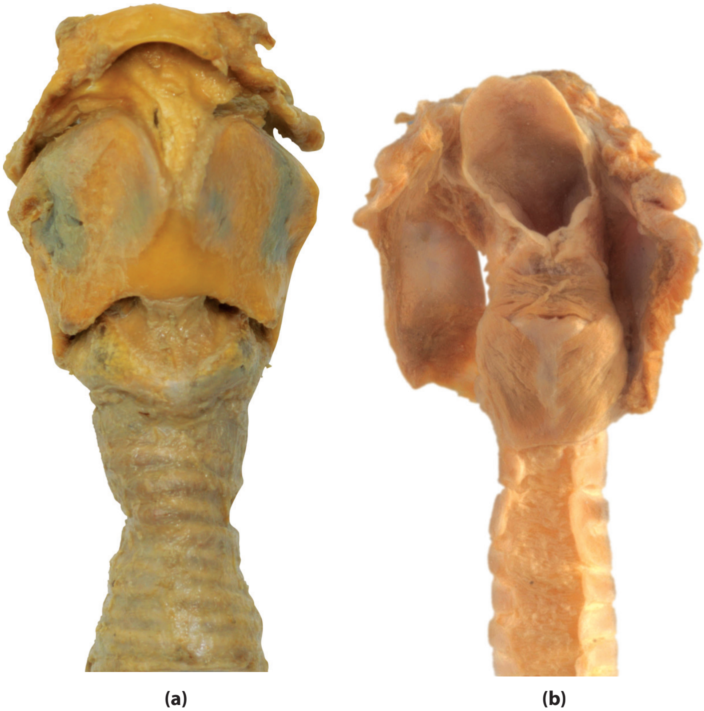

Figure 21.8 Dissection of larynx and trachea. **(a)** Anterior view. **(b)** Posterior view.

On average, the adult trachea measures 12 cm in length and 2.5 cm in internal diameter, these dimensions being somewhat smaller in women than in men.

The trachea is a wide and semirigid tube that is kept patent by a series of so-called tracheal rings, made of hyaline cartilage (Figure 21.8). These rings, numbering 15–20, are in fact incomplete circles and occupy the anterior three-quarters of the circumference of the tracheal wall. The gaps in these incomplete rings are situated posteriorly and in line with one another. The gaps are bridged by transverse strips of smooth muscle called trachealis. Unlike the convex anterior wall of the trachea, the posterior surface of the trachea is somewhat flat and is closely applied to the anterior surface of the oesophagus, to which it is attached by loose connective tissue. Of all the tracheal rings, the first is the thickest and broadest. It is a cardinal surgical principle that the first tracheal ring be left intact and undisturbed when performing a tracheostomy in order not to risk the delayed but serious complication of subglottic stenosis. The tracheal lumen has a lining of typical respiratory mucosa, characterized by ciliated, pseudo-stratified, columnar epithelium and mucus-secreting goblet cells overlying a submucosa containing mucous glands and lymphoid follicles.

The trachea leaves the neck in the midline to enter the superior mediastinum through the superior aperture of the thoracic cage. It descends through the superior mediastinum, and at a variable distance below the level of the manubriosternal junction, the trachea bifurcates into right and left main bronchi. Thus, for purposes of description, the trachea may be described as consisting of a cervical part and a thoracic part. The presence of elastin in the wall of the trachea gives it resilience and a considerable extensibility. Indeed, at the end of deep inspiration the tracheal bifurcation may descend 5 to 6 cm below the level of the manubriosternal junction.

TOPOGRAPHICAL RELATIONS OF THE TRACHEA

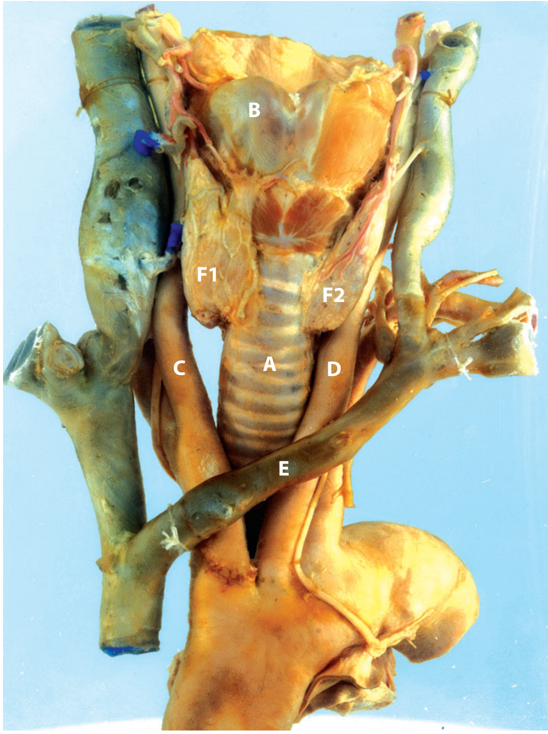

Figure 21.9 Dissection to show relationship of carotid vessels and thyroid gland to trachea and larynx. A – trachea. B – thyroid cartilage. C – right common carotid artery. D – left common carotid artery. E – left brachiocephalic vein. F1 – right thyroid lobe. F2 – left thyroid lobe. Thyroid isthmus has been removed.

The topographical relations of the cervical trachea that are of particular relevance in tracheal surgery include the isthmus of the thyroid which lies in front of the trachea (Figure 21.9) (typically overlapping the 2nd, 3rd and 4th tracheal rings), and the thyroid lobes which are related to the sides of the trachea and oesophagus and the tracheo-oesophageal groove. Running superiorly in the tracheo-oesophageal groove on each side is the corresponding recurrent laryngeal nerve. Overlapping the thyroid isthmus and lobes on either side of the midline are the strap muscles. On each side the strap muscles are arranged in two layers: sternothyroid (deep) and sternohyoid (superficial). (Figure 21.10). When performing a tracheostomy, the narrow, midline strip of connective tissues between the strap muscles of the two sides is identified and incised to allow the strap muscles on either side to be retracted away from the midline. This will bring into view the thyroid

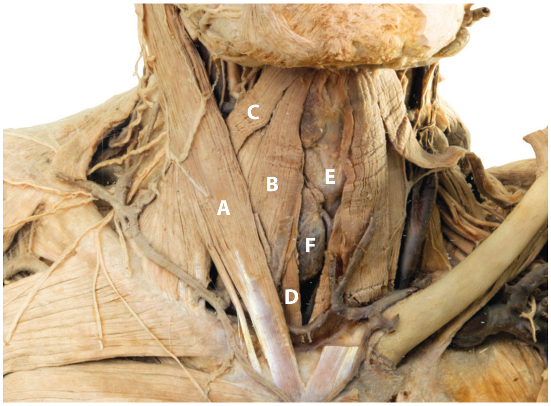

Figure 21.10 Dissection of anterior part of neck to show relationship of strap muscles to trachea and larynx. (A – sternocleidomastoid. B – sternohyoid. C – omohyoid. D – sternothyroid. E – thyroid notch. F – thyroid isthmus.)

isthmus and trachea. Immediately posterior to the trachea is the oesophagus.

The trachea in the superior mediastinum lies behind the aortic arch. The brachiocephalic artery runs obliquely to the right of the trachea while the left common carotid and left subclavian arteries run along the left side of the trachea.

ARTERIAL SUPPLY, VENOUS AND LYMPHATIC DRAINAGE AND SENSORY INNERVATION OF THE TRACHEA

The blood supply of the trachea is essentially from the right and left inferior thyroid arteries which together supply the full length of the cervical trachea and the proximal two-thirds of the thoracic trachea. The terminal 3 or 4 cm of the trachea is supplied by small ascending branches of the bronchial arteries. These anastomose with the tracheal branches of the inferior thyroid arteries. As observed during mobilization of the trachea, the pretracheal plane and the plane between the trachea and oesophagus are relatively avascular. Venous drainage of the trachea is principally into the inferior thyroid venous plexus and thereby into the left and right brachiocephalic veins. The lymphatic drainage of the trachea is into the pretracheal, paratracheal and subcarinal lymph nodes.

The sensory innervation of the tracheal mucosa is by sensory branches of the right and left recurrent laryngeal nerves. Additionally, the trachea receives sympathetic and parasympathetic fibres.

THE BRONCHIAL TREE

Viewed through a bronchoscope, the tracheal bifurcation shows on its inner aspect a prominent anteroposterior ridge, termed the carina, which lies between the openings of the right and left main bronchi (Figure 21.11). The main bronchi (also called primary or principal bronchi), like the trachea, have walls that are reinforced by incomplete rings of hyaline cartilage. From its origin, each main bronchus is directed inferolaterally towards the hilum of the corresponding lung (Figure 21.12). The right main bronchus is usually shorter than the left one. Its average length in the adult is 2.5 cm, contrasting with the length of the left main bronchus (5 cm). The lumen of the right main bronchus is significantly wider than that of the left, a feature that is readily apparent on bronchoscopy. Another significant feature is that the long axis of the right main bronchus subtends a much smaller angle with the axis of the trachea than does the left main bronchus. In other words the right main bronchus is more vertical than the left main bronchus. It is for these reasons that an inadvertently aspirated solid object that enters the trachea is more likely to drop into the right main bronchus than the left one.

Each main bronchus divides into the next generation of bronchi, termed lobar or secondary bronchi (Figure 21.12). The right main bronchus divides into three lobar bronchi corresponding to the three lobes of the right lung, while the left main bronchus divides into two lobar bronchi: one for the upper lobe and one for the lower lobe. Each lobar bronchus gives rise to the next generation of bronchi, termed segmental (or tertiary) bronchi (Figure 21.12). The number of segmental bronchi arising from each lobar bronchus is remarkably constant. Thus in the right lung the

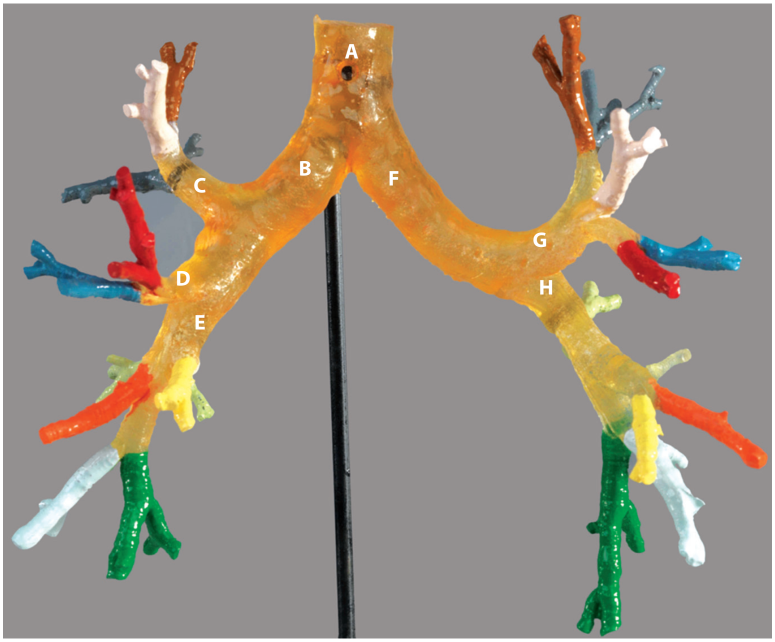

Figure 21.11 Resin corrosion cast of adult tracheo-bronchial tree showing lower trachea, tracheal bifurcation and primary, secondary and tertiary bronchi bilaterally. A – trachea. B – right main bronchus. C – right upper lobe bronchus. D – right middle lobe bronchus. E – right lower lobe bronchus. F – left main bronchus. G – left upper lobe bronchus. H – left lower lobe bronchus. The variously coloured bronchial branches are segmental bronchi.

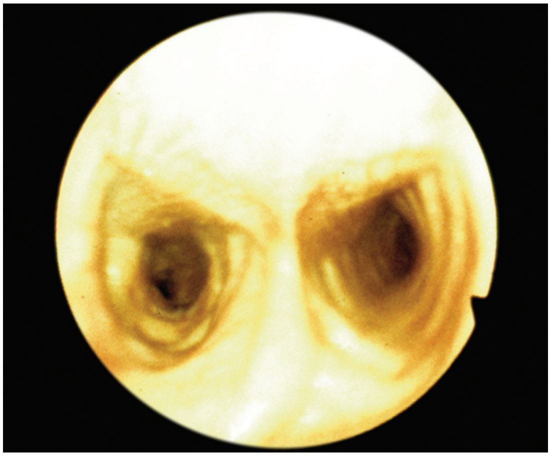

Figure 21.12 Bronchoscopic view of tracheal bifurcation showing carina and commencement of right and left main bronchi.

upper lobe bronchus gives rise to three segmental bronchi; the middle lobe bronchus gives rise to two segmental bronchi; and the lower lobe bronchus, five segmental bronchi. On the left side the two lobe bronchi give rise to five segmental bronchi each. Hyaline cartilage is present in the walls of the lobar and segmental bronchi, giving them a certain rigidity.

Each bronchus and its succeeding branches are accompanied by corresponding branches of the pulmonary artery (carrying deoxygenated blood to the pulmonary alveoli). A tertiary bronchus and its accompanying branch of the pulmonary artery ramify in a structurally separate and functionally independent wedge-shaped segment of pulmonary tissue within a lobe. This collective unit comprising a segmental bronchus, segmental branch of pulmonary artery and corresponding segment of lung is termed a bronchopulmonary segment. It is an anatomically definable (and resectable) entity. There are typically 10 bronchopulmonary segments in each lung. In the right lung, they are allocated to the lobes as follows: three in the upper lobe, two in the middle lobe and five in the lower lobe. In the left lung there are five segments in each lobe.

FURTHER READING

Agur AMR. *Grant's Atlas of Anatomy*. Philadelphia: Williams & Wilkins, 1991: 588–604.

Brock RC. *The Anatomy of the Bronchial Tree: With Special Reference to the Surgery of Lung Abscess*. 2nd ed. London: Oxford University Press, 1954.

Imanishi N, Kondoh T, Kishi K, Aiso S. Angiographic study of the superior laryngeal artery. *Okajimas Folia Anatomica Japonica*. 2009; 86(2): 61–5.

Janfaza P, Nadol JB, Galla RJ, Fabian RL, Montgomery WW. *Surgical Anatomy of the Head and Neck*. Philadelphia: Lippincott Williams & Wilkins, 2001: 639–73.

McMinn RMH. *Last's Anatomy: Regional and Applied*. 9th ed. Edinburgh: Churchill-Livingstone, 1994.

Moore KL, Dalley AF. *Clinically Oriented Anatomy*. 5th ed. Philadelphia: Lippincott Williams & Wilkins, 2006.

Mukherji SK, Armao D, Joshi VM. Cervical nodal metastases in squamous cell carcinoma of the head and neck: What to expect. *Head & Neck*. 2001; 23(11): 995–1005.

Norris BK, Schweinfurth JM. Arytenoid dislocation: An analysis of the contemporary literature. *Laryngoscope*. 2011; 121: 142–6.

Paraskevas GK, Raikos A, Ioannidis O, Brand-Saberi B. Topographic anatomy of the internal laryngeal nerve: Surgical considerations. *Head & Neck*. 2012; 34(4): 534–40.

Raghuraman G, Rajan S, Marzouk JK, Mullhi D, Smith FG. Is tracheal stenosis caused by percutaneous tracheostomy different from that by surgical tracheostomy? *Chest*. 2005; 127(3): 879–85.

Remacle M, Van Haverbeke C, Eckel H, Bradley P, Chevalier D, Djukic V, de Vicentiis M, Friedrich G, Olofsson J, Peretti G, Quer M, Werner J. Proposal for revision of the European Laryngological Society classification of endoscopic cordectomies. *European Archives of Otorhinolaryngology*. 2007; 264(5): 499–504.

Remacle M, Eckel HE, Antonelli A, Brasnu D, Chevalier D, Friedrich G, Olofsson J, Rudert HH, Thumfart W, de Vincentiis M, Wustrow TP. Endoscopic cordectomy. A proposal for a classification by the Working Committee, European Laryngological Society. *European Archives of Otorhinolaryngology*. 2000; 257(4): 227–31.

Sadler TW. *Langman's Medical Embryology*. 10th revised ed. Philadelphia: Lippincott Williams and Wilkins, 2006.

Salassa JR, Pearson BW, Payne WS. Gross and microscopical blood supply of the trachea. *Annals of Thoracic Surgery*. 1977; 24: 100–7.

Sellke FW, del Nido PJ, Swanson SJ. *Sabiston and Spencer's Surgery of the Chest*. 8th ed. Philadelphia: Saunders Elsevier, 2010.

Souvirón R, Maranillo E, Vázquez T, Patel N, McHanwell S, Cobeta I, Scola B, Sañudo J. Proposal of landmarks for clamping neurovascular elements during endoscopic surgery of the supraglottic region. *Head & Neck*. 2013; 35(1): 57–60.

Ted L, Tewfik TL. Congenital malformations of the larynx. Emedicine. 2013. Available from http://emedicine.medscape.com/article/837630-overview.

Williams PL. *Gray's Anatomy: The Anatomical Basis of Medicine and Surgery*. 38th ed. Edinburgh: Churchill Livingstone, 1995.

22

Thyroid gland

VISHY MAHADEVAN AND JAMES N. CRINNION

Introduction 221
Embryology 221
Anatomy 222
Topographical relations of the thyroid 225
Anterolateral relations 225
Posterior relations 226
Medial relations 227
Blood supply 227
Venous drainage 229
Lymphatic drainage 229
Anatomical hazards in thyroid surgery 229
Recurrent laryngeal nerve 230
External laryngeal nerve 230
Compromise of parathyroid blood supply and consequent hypocalcaemia 231
Developmental aberrations 231
Further reading 231

INTRODUCTION

A prerequisite to successful thyroid surgery is a detailed understanding of the regional anatomy. During surgical dissection there are important anatomical structures that must be identified and preserved. Excellent surgical results with negligible complications are achievable through a proper appreciation of the local topographical anatomy and by observing meticulous technique.

This chapter shall consider the embryology, topographical anatomy, blood supply and lymphatic drainage of the thyroid gland. The anatomy will be described with reference to the surgical steps performed during thyroidectomy, and will be illustrated with operative photographs.

The anatomical hazards of thyroidectomy will be defined and the clinically relevant developmental abnormalities will be described.

EMBRYOLOGY

Understanding the embryology of the thyroid and parathyroid glands is facilitated by a preliminary consideration of the development of the neck and pharynx. In all mammalian embryos the primitive mouth (stomodeum) is bounded cranially by the forebrain projection and caudally by the cardiac prominence. The intervening area – the primitive pharynx – is destined to give rise to the mandibular region, lower face and all of the neck. Embryological development of these parts is characterized and greatly influenced by the appearance of the pharyngeal (branchial) arches which appear during the fourth and fifth weeks of intrauterine development. The mesoderm of the primitive pharynx is reinforced by a large number of migratory neural crest cells, and the resultant mesenchyme gives rise to six curved (arched) cylindroid thickenings, termed the pharyngeal arches, in the pharyngeal wall on either side. Each pharyngeal arch commences lateral to the hindbrain and grows ventrally through the lateral wall of the pharynx to meet its contralateral fellow in the ventral midline. In all, six such arches appear in a cranio-caudal sequence. In the human embryo the fifth arch has an ephemeral existence and does not give rise to any definitive structures. Each arch comprises a core of mesenchyme covered externally by ectoderm, and internally by endoderm. Ventrally, successive arches are virtually contiguous one with another. However, laterally, on either side, adjacent pharyngeal arches are separated on the external aspect by ectodermal depressions termed pharyngeal clefts (branchial grooves). Correspondingly, on the internal aspect adjacent arches are separated by endodermal outpouchings termed pharyngeal pouches.

Embryologically, the thyroid gland is essentially an endodermal derivative, and appears initially as a midline cellular proliferation in the floor of the primitive pharynx between the first and second pharyngeal arches. The site of origin of this bud is marked in later life by the midline foramen caecum on the dorsum of the tongue. The thyroid bud descends in the ventral midline as the thyroglossal duct (thyroglossal tract) in front of the pharyngeal gut crossing, successively, the anterior aspect of the developing hyoid and larynx before reaching its definitive position in front of the trachea. In its descent, the thyroglossal duct, after crossing in front of the hyoid, loops upwards behind the body of the hyoid before recommencing its midline descent. The distal end of the thyroid bud bifurcates. Subsequent proliferation of this bifurcation gives rise to the thyroid isthmus and the bilateral lobes. A further contribution to the developing thyroid comes from the ultimobranchial body (a derivative of the fourth pharyngeal pouch) which gives rise to the parafollicular, C – cells which secrete calcitonin. The tubercle of Zuckerkandl, a small visible elevation on the posterolateral aspect of the thyroid lobe halfway between the upper and lower poles, is believed to be a remnant of the ultimobranchial body.

During its descent the thyroid remains initially connected to its site of pharyngeal origin by the thyroglossal duct. With further development this duct disintegrates completely.

ANATOMY

The normal thyroid gland is a firm, well-vascularized, reddish-brown organ located in the anterior aspect of the lower part of the neck, with an average weight of 17 g in the adult. Pathological changes within the gland may lead to massive increase in glandular size.

The thyroid comprises two lobes, right and left, which flank the larynx and trachea. Each lobe is approximately 5 cm in length and roughly pyramidal in shape, with a narrow upper pole and a broad lower pole. The thyroid lobe lies in a bed made up medially of the trachea, oesophagus and tracheo-oesophageal groove; posteriorly, the carotid sheath, and anterolaterally, the strap muscles overlain by the sternocleidomastoid (Figures 22.1, 22.2, and 22.3).

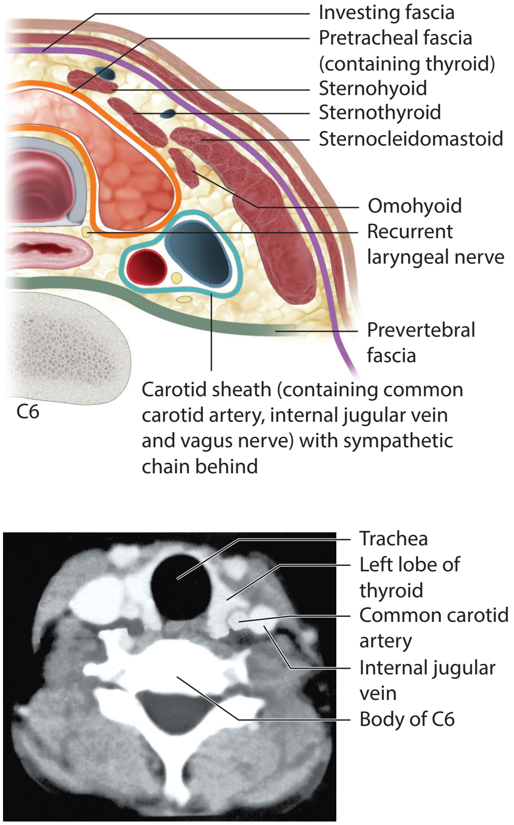
Investing fascia
Pretracheal fascia (containing thyroid)
Sternohyoid
Sternothyroid
Sternocleidomastoid
Omohyoid
Recurrent laryngeal nerve
Prevertebral fascia
Carotid sheath (containing common carotid artery, internal jugular vein and vagus nerve) with sympathetic chain behind
C6
Trachea
Left lobe of thyroid
Common carotid artery
Internal jugular vein
Body of C6

Figure 22.1 Transverse section of neck at level of C6 vertebra, showing the fascial and muscular planes in relation to the thyroid.

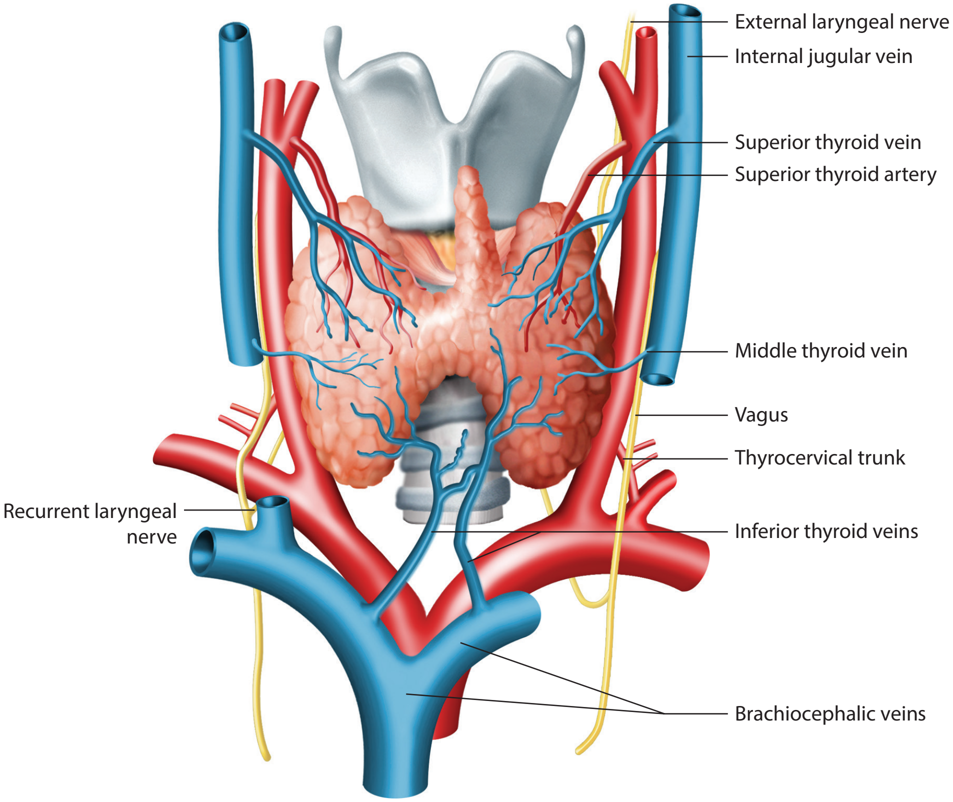
External laryngeal nerve
Internal jugular vein
Superior thyroid vein
Superior thyroid artery
Middle thyroid vein
Vagus
Thyrocervical trunk
Inferior thyroid veins
Brachiocephalic veins
Recurrent laryngeal nerve

Figure 22.2 Anterior view of thyroid and related structures. Arora A, Tolley NS, Tuttle RM. *A Practical Manual of Thyroid and Parathyroid Disease*, Fig. 7.3 (p. 68), chapter 7.

Thus in cross section, each lobe of the thyroid appears triangular, presenting a superficial or anterolateral surface (related to the strap muscles), a posterior surface (related to the carotid sheath) and a medial surface (related to the tracheo-oesophageal groove, trachea and oesophagus) (Figures 22.2 and 22.3). When the thyroid gland enlarges it often does so in a posterolateral direction, displacing the carotid sheath in such a way that the latter becomes a lateral rather than a posterior relation.

The anteromedial aspects of the lower parts of the thyroid lobes are joined to each other by a flattened bridge of thyroid tissue, the thyroid isthmus, which lies across the front of the trachea, usually overlying the 2nd and 3rd (and sometimes 4th) tracheal rings (Figure 22.1). The isthmus is approximately 1.5 cm in width and height. A superiorly directed, conical projection of thyroid tissue from the isthmus, somewhat to the left of the midline, is a frequent feature. Termed the pyramidal lobe, it is thought to occur in 40–50 per cent of individuals. The pyramidal lobe is an important consideration in surgery for thyrotoxicosis, as failure to remove it may result in recurrence of thyrotoxicosis. Occasionally, a fibromuscular band extends from the upper pole of the pyramidal lobe to the inferior margin of the hyoid body. It denotes the route of embryological migratory descent of the thyroid anlagen and is called levator glandulae thyroid.

The thyroid gland possesses a thin capsule, outside which it possesses a fascial covering, the pretracheal fascia. The pretracheal fascia is firmly attached to the anterior wall of the upper trachea behind the isthmus and on either side to the lateral aspects of the cricoid and thyroid cartilages. This attachment ensures that the thyroid moves

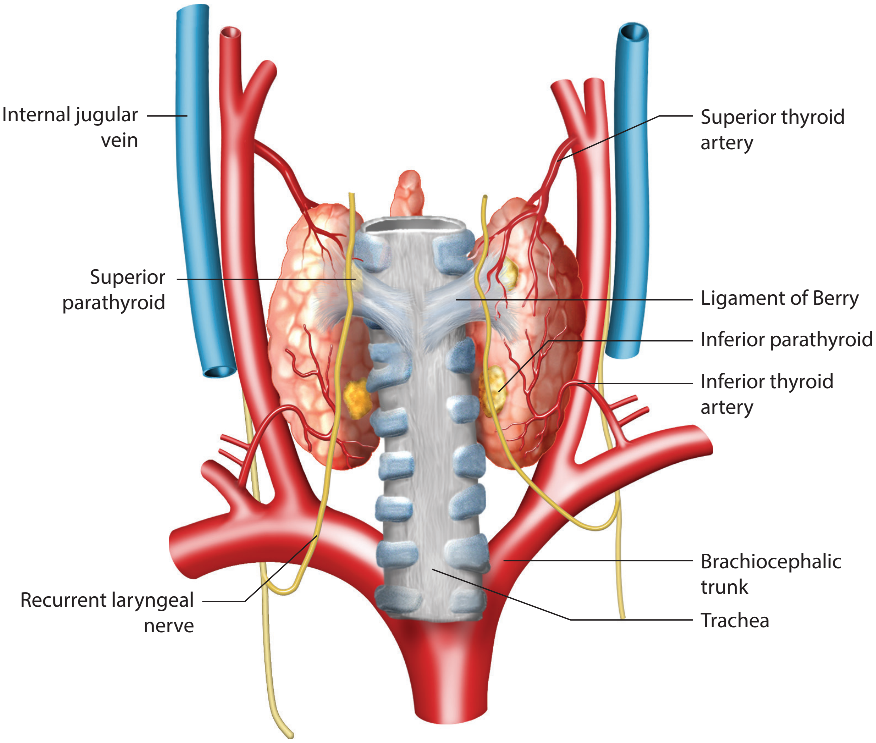
Internal jugular vein
Superior parathyroid
Recurrent laryngeal nerve
Superior thyroid artery
Ligament of Berry
Inferior parathyroid
Inferior thyroid artery
Brachiocephalic trunk
Trachea

Figure 22.3 Posterior view of thyroid and related structures. Arora A, Tolley NS, Tuttle RM. *A Practical Manual of Thyroid and Parathyroid Disease*, Fig. 7.4 (p. 69), chapter 7.

upwards during deglutition. A distinct band of thickening in the pretracheal fascia between the medial aspect of the lobe and the cricoid cartilage is termed the lateral ligament of the thyroid or the ligament of Berry (Figure 22.4).

The recurrent laryngeal nerve runs behind or with this ligament before entering the larynx and may be injured at this level unless identified and protected. The pretracheal fascia blends laterally with the fascia of the carotid sheath (Figure 22.5), and during mobilization of the thyroid lobe this fascial envelope must be divided to separate the thyroid safely from the common carotid artery (Figure 22.3).

When excising large goitres the gland is often seen to be densely adherent to the carotid sheath, and separation of the two must be done with extreme care. When the thyroid lobe has been mobilized anteriorly it remains attached along its posteromedial surface by the pretracheal fascia. This fascial attachment to the trachea and larynx

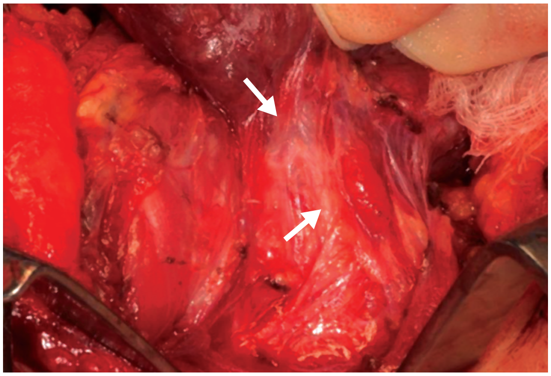

Figure 22.4 This illustrates the final stages of resection of the right thyroid lobe which is tethered by Berry's ligament (upper arrow). The thyroid is retracted medially and the recurrent laryngeal nerve (lower arrow) is seen to run beneath this ligament towards the lower edge of the inferior constrictor. To the right of the nerve (inferiorly) is a preserved parathyroid gland.

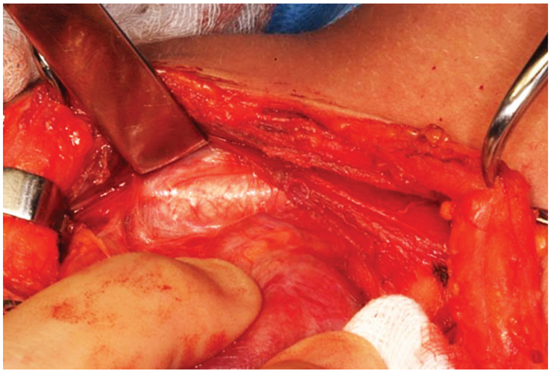

Figure 22.5 Division of the pretracheal fascia between the left thyroid lobe and carotid sheath which demonstrates the common carotid artery. This is a safe bloodless plane developed by firm retraction of the left thyroid lobe with counter-traction on the sternothyroid muscle.

must be carefully divided after visualization of the recurrent laryngeal nerve and the parathyroid glands. This step in the surgical dissection of the thyroid is perhaps the most crucial one in the safe excision of the thyroid. The surgeon must dissect in a plane immediately superficial to the true thyroid capsule, carefully separating the thyroid lobe from the recurrent laryngeal nerve and parathyroid glands (Figure 22.6).

At the microscopic level, the pretracheal fascial envelope is an important landmark in the histopathological staging of papillary and medullary neoplasms of the thyroid.

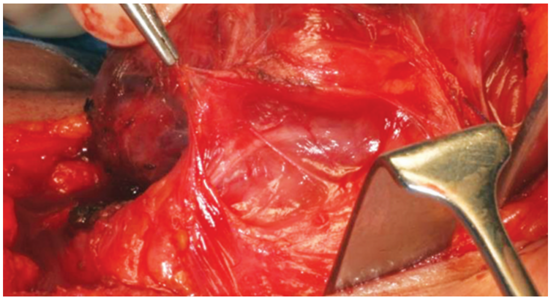

Figure 22.6 Mobilization of the left thyroid lobe by careful division of the pretracheal fascia to reveal the recurrent laryngeal nerve.

TOPOGRAPHICAL RELATIONS OF THE THYROID

Anterolateral relations

Each thyroid lobe is overlapped anterolaterally by the ipsilateral strap muscles, the sternothyroid being the immediate relation, with the sternohyoid and superior belly of omohyoid overlapping the sternothyroid. In the operation of thyroid lobectomy, each lobe is approached by separating the paired strap muscles in the midline through a natural plane of cleavage. The upper pole of each thyroid lobe is restricted by the upper attachment of the sternothyroid muscle to the oblique ridge (oblique line) on the lateral aspect of the thyroid lamina. To facilitate optimal exposure of the superior pole of the thyroid lobe, or when mobilizing a large goitre, it may at times be necessary for the surgeon to divide the strap muscles (sternohyoid and sternothyroid). In these circumstances it is advisable to divide the strap muscles transversely near their upper attachments and to coapt the divided muscles upon conclusion of the procedure. The rationale for the recommended high division of the strap muscles is that the nerves supplying the strap muscles (branches of the ansa cervicalis) enter the muscles near their lower ends and course upwards within the muscles.

When approaching a large goitre, one of the authors (JC) has found it helpful initially to dissect laterally through the avascular plane between the sternohyoid and the subjacent sternothyroid muscle (Figure 22.7). This plane is then developed until the carotid sheath is reached. This simple manoeuvre facilitates the mobilization of large glands and reduces the amount of bleeding. Following this procedure the underlying attenuated sternothyroid still requires division, but the sternohyoid muscle can almost always be left intact. In cases of recurrent thyroid goitre, dense scarring usually leads to marked adhesions between the strap muscles and the underlying thyroid lobe. To avoid a difficult and time-consuming dissection, the recurrent goitre is approached by initially reflecting the medial border of the sternocleidomastoid from the anterior surface of the sternohyoid/omohyoid muscles. The thyroid lobe is then dissected by developing a plane between the lateral border of the sternohyoid

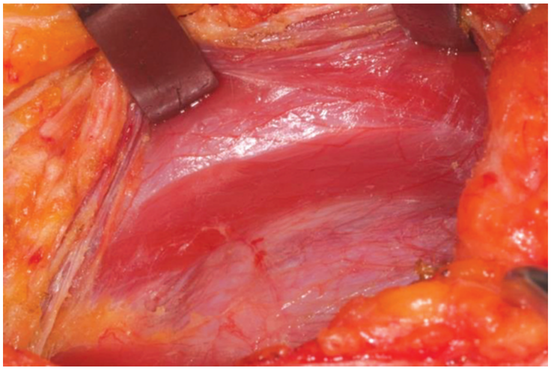

Figure 22.7 Lateral retraction of the sternohyoid muscle demonstrates the underlying sternothyroid and below this the thyroid gland covered by pretracheal fascia. This picture demonstrates the bloodless plane between these two muscles which may be developed to greatly facilitate the safe excision of large goitres.

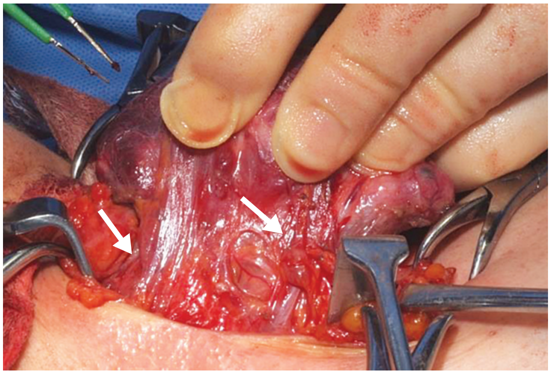

Figure 22.8 Pericapsular dissection of the right thyroid lobe reveals both parathyroid glands (arrows), the inferior thyroid artery and the recurrent laryngeal nerve. The inferior gland is directly on the anterior surface of the inferior thyroid artery and in its typical position anterior to the plane of the recurrent laryngeal nerve.

and the carotid sheath. Division of the inferior belly of the omohyoid may be necessary to provide adequate access. This manoeuvre is referred to as the posterior or back-door approach to the thyroid, and is the favoured approach in cases of recurrent multinodular goitre.

Posterior relations

Posterior to each thyroid lobe is the common carotid artery lying within the carotid sheath. As explained earlier, an enlarged thyroid can displace the carotid sheath to such an extent that the sheath becomes a lateral rather than posterior relation of the thyroid lobe. Lying lateral to the artery within the carotid sheath is the internal jugular vein, and interposed between the two in the sheath is the vagus nerve. Because of the somewhat posterior location of the vagus in the carotid sheath, it is unusual to encounter the vagus during a routine thyroid operation. Embedded in the anterior wall of the sheath is the ansa cervicalis, a looped motor nerve which supplies the ipsilateral strap muscles.

Even more closely related to the posterior aspect of each thyroid lobe are the two ipsilateral parathyroids (superior and inferior) (Figure 22.8). These are small ovoid structures which are normally about 5 mm in diameter. Their embryological development is quite distinct from that of the thyroid. The parathyroids may be located within the pretracheal fascial covering of the thyroid, or outside the fascia. At times they may be densely adherent to the capsule and can only be preserved with an intact blood supply by extremely meticulous dissection. Rarely one or other parathyroid may be embedded within the thyroid substance.

The superior parathyroid gland lies posterolateral to the middle of the thyroid lobe usually outside the pretracheal fascia. The gland lies superior to the inferior thyroid artery and posterior to the plane of the recurrent laryngeal nerve. During thyroidectomy the thyroid lobe is mobilized by careful division of the pretracheal fascia posterolaterally. It is at this stage that the superior parathyroid gland is visualized (Figure 22.9).

The inferior parathyroid is usually located behind the lower pole of the thyroid lobe. Typically, it lies caudal to the inferior thyroid artery, and anterior to the plane of both the recurrent laryngeal nerve and the superior parathyroid gland.

Preserving the parathyroids while performing thyroidectomy is extremely important (Figures 22.8 and 22.10). This can be achieved with meticulous haemostasis and by gentle and precise dissection in the pericapsular plane. Using this technique the parathyroids will be visualized and preserved. Inadvertent excision of parathyroid

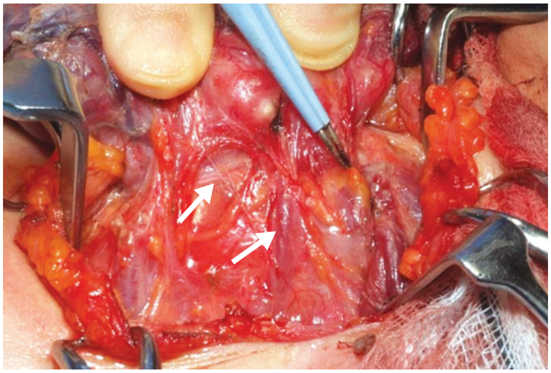

Figure 22.9 Dissection of the left lobe to reveal a typical superior parathyroid gland which is adjacent to the tip of the bipolar forceps. Arrows mark the recurrent laryngeal nerve and the inferior thyroid artery. The superior parathyroid is in its typical anatomical position superior to the inferior thyroid artery and posterior to the plane of the recurrent laryngeal nerve. With adequate retraction and careful haemostasis these important structures can be easily identified and protected.

tissue is uncommon in the hands of an experienced surgeon.

Medial relations

Medially, the thyroid lobe is related to the lateral aspects of the larynx and trachea, and to the tracheo-oesophageal groove. On either side running upwards in the tracheo-oesophageal groove before entering the larynx is the corresponding recurrent laryngeal nerve (Figures 22.4, 22.6, 22.8 and 22.9).

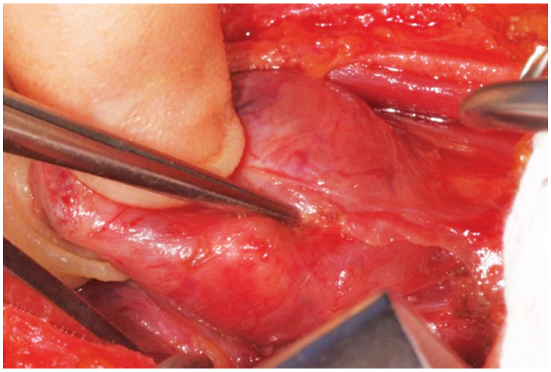

Figure 22.10 Dissection of a small inferior parathyroid gland which is adherent to the posterolateral surface of the right lower pole of the thyroid.

Thus depending on their direction of growth, expanding neoplasms of the thyroid may compress any of the related structures mentioned above.

Note: The term *inferior laryngeal nerve*, sometimes used in surgical literature, is synonymous with recurrent laryngeal nerve.

BLOOD SUPPLY

The thyroid possesses a rich arterial blood supply, which it derives from the right and left superior thyroid arteries, and the right and left inferior thyroid arteries. These four arteries anastomose freely with each other both within the gland and on its surface.

The superior thyroid artery is usually the first branch of the external carotid artery and typically arises from its anterior or anteromedial aspect at the level of the greater horn of the hyoid, a short distance above the level of the upper border of the thyroid cartilage. The superior thyroid artery descends obliquely in an anteromedial direction on the surface of the inferior pharyngeal constrictor and deep to the sternothyroid muscle to reach the superior pole of the thyroid lobe. The superior thyroid artery may occasionally arise directly from the common carotid artery.

On reaching the upper pole of the thyroid lobe, the superior thyroid artery typically divides into two branches: anterior and posterior. The posterior branch descends on the posterior surface of the thyroid lobe and anastomoses with a branch of the inferior thyroid artery. The anterior branch descends on the medial aspect of the lobe and then along the upper border of the isthmus to anastomose with its fellow from the other side. Accompanying the superior thyroid artery towards the upper pole of the thyroid is the external branch of the superior laryngeal nerve, known also as the external laryngeal nerve (a terminal branch of the superior laryngeal nerve; in turn a branch of the vagus) (Figures 22.11 and 22.12).

The artery is typically somewhat posterolateral to the nerve. An exclusively motor nerve, the external laryngeal nerve innervates the cricothyroid

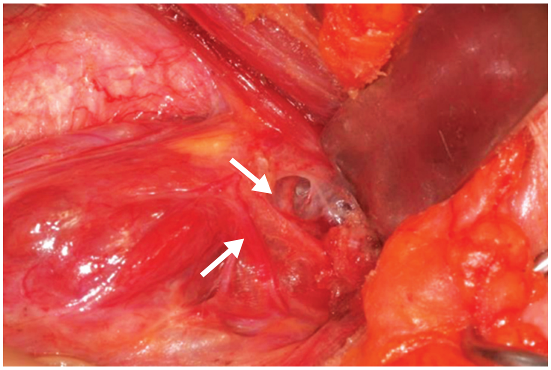

Figure 22.11 Dissection of the right upper pole. The retractor is placed under the sternothyroid muscle to demonstrate both the anterior branch of the superior thyroid artery (top arrow) and the important external laryngeal nerve (lower arrow), which must be protected.

muscle. The proximity of the recurrent and external laryngeal nerves to the thyroid vessels puts these nerves at risk of inadvertent injury during thyroid surgery. Injury to the external laryngeal nerve and consequent paralysis of the cricothyroid muscle results in laxity of the vocal fold causing impairment of voice projection and loss of high-pitched phonation.

The inferior thyroid artery typically arises from the thyrocervical artery (trunk), which in turn is a branch of the first part of the subclavian artery arising in the root of the neck.

From its origin, the inferior thyroid artery courses superomedially behind the carotid sheath, anterior to the scalenus anterior muscle and its covering of prevertebral fascia. At approximately the level of the lower border of the cricoid cartilage, it loops inferomedially towards the lower pole of the thyroid lobe, giving off at this level a branch called the ascending cervical artery. During thyroidectomy the inferior thyroid artery is visualized after division of the pretracheal fascia which is necessary for full mobilization of the thyroid lobe. It is a useful landmark for the surgeon because it intersects the recurrent laryngeal nerve adjacent to the midpolar level (Figure 22.13). The exact relationship, however, is variable, with the nerve running deep (50 per cent), superficial (25 per cent) or between the branches of the inferior thyroid artery (25 per cent). The inferior thyroid artery may be absent in 5 per cent of individuals. Rarely, a fifth artery, the thyroidea ima artery, may be present. It occurs in 1–3 per cent of individuals. Its origin, in descending order of frequency, is from the brachiocephalic artery, right common carotid artery and aortic arch. An aberrant artery arising from either subclavian artery and supplying the thyroid is usually regarded as an anomalous inferior thyroid artery rather than as a thyroidea ima artery.

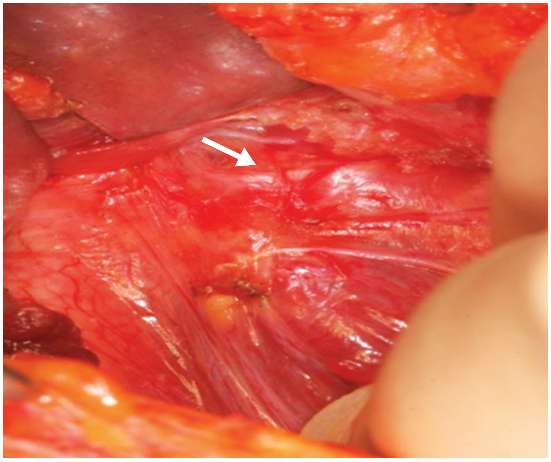

Figure 22.12 The superior pole has been mobilized to demonstrate the external laryngeal nerve (arrow) supplying the cricothyroid muscle.

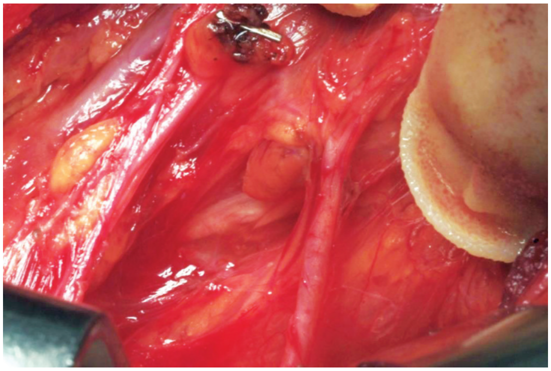

Figure 22.13 Retraction of the left thyroid lobe to reveal the inferior thyroid artery anterior to the recurrent laryngeal nerve and a typical parathyroid gland.

VENOUS DRAINAGE

The pattern of venous drainage of the thyroid gland is subject to greater variation than is the pattern of arterial supply. The venous drainage of the thyroid gland is initially into a venous plexus which surrounds the thyroid gland and is situated in the interval between the thyroid capsule and the pretracheal fascial envelope. The plexus is made up of intercommunicating venous channels. Three principal veins emerge from the plexus on either side of the midline. The superior thyroid vein emerges from the upper part of the thyroid lobe and accompanies the superior thyroid artery (usually running posterolateral to the artery) to drain directly into the ipsilateral internal jugular vein or indirectly by joining the facial vein; the facial vein in turn drains into the internal jugular vein. The middle thyroid vein emerges from the anterolateral aspect of the thyroid lobe, somewhat nearer the lower pole than the upper, and runs laterally, anterior to the common carotid artery, before draining into the internal jugular vein. During thyroidectomy, gentle lateral retraction of the carotid sheath facilitates identification (and thus ligation) of the middle thyroid vein. The middle thyroid vein is present in 50 per cent of individuals. Each inferior thyroid vein emerges from the lower part of the corresponding thyroid lobe. The right vein runs inferolaterally and, crossing anterior to the brachiocephalic artery, drains into the right brachiocephalic vein. The left inferior thyroid vein runs down in front of the trachea to drain into the left brachiocephalic vein. It is common for the right and left inferior thyroid veins to anastomose with each other in front of the trachea by multiple channels. The surgeon should be mindful of this feature when dissecting the pretracheal region during thyroidectomy, and also when performing a tracheostomy. Large retrosternal goitres can compress the brachiocephalic veins, and this venous obstruction may result in considerable engorgement of the inferior thyroid veins in the pretracheal region.

LYMPHATIC DRAINAGE

A sound understanding of the lymphatic drainage of the thyroid gland is essential to the rational and effective clinical management of thyroid malignancies, in particular those malignancies which have a tendency to metastasize to lymph nodes. Papillary adenocarcinomas of the thyroid have a particular propensity to spread to lymph nodes. Not uncommonly, medullary carcinomas of the thyroid also metastasize to regional lymph nodes.

The thyroid has a rich lymphatic drainage which may flow in multiple directions.

At the histological level, the intrathyroid lymphatic channels are numerous and surround the thyroid follicles. They form an extensive network within the gland and enable lymph flow from one lobe to the other. The lymphatic drainage of the thyroid gland is principally to the prelaryngeal and pretracheal lymph nodes which lie in front of the thyrohyoid membrane and the upper trachea, respectively, and to the tracheo-oesophageal lymph nodes which are situated alongside the tracheo-oesophageal grooves bilaterally. These sets of lymph nodes all belong to the anterior cervical group of deep cervical lymph nodes, and thus are situated deep to the investing layer of deep cervical fascia. Lymphatics from the thyroid also drain to the middle and lower jugular groups of lymph nodes which lie alongside the internal jugular vein.

ANATOMICAL HAZARDS IN THYROID SURGERY

Two important nerves are related to each thyroid lobe: the recurrent laryngeal nerve and the external laryngeal nerve. No account of the surgical anatomy of the thyroid gland would be complete without a detailed consideration of the proximity of these nerves to the thyroid, and their consequent susceptibility to inadvertent damage during surgery.

Both nerves are branches of the vagus. The recurrent laryngeal nerve is a direct branch, while the external laryngeal nerve is a branch of the superior laryngeal nerve, in turn a direct branch of the vagus.

A further anatomical hazard in relation to thyroid surgery is inadvertent devascularization of the parathyroids with resultant postoperative hypocalcaemia.

Recurrent laryngeal nerve

Most medicolegal claims relating to thyroid surgery involve the recurrent laryngeal nerve. A thorough understanding of the anatomy of the recurrent laryngeal nerve (including its anatomical variations) and meticulous surgical technique facilitated by optimal illumination and magnification are of paramount importance in avoiding iatrogenic trauma to the nerve.

The right recurrent laryngeal nerve arises from the right vagus in the root of the neck anterior to the first part of the right subclavian artery and winds around the subclavian artery, passing from front to back, and ascends in the neck behind the common carotid artery. It then curves medially to ascend in the right tracheo-oesophageal groove. The left recurrent laryngeal nerve, a branch of the left vagus, has a significantly longer course. It originates lateral to the aortic arch and winds around the aortic arch, passing from lateral to medial below the aortic arch before ascending in the left tracheo-oesophageal groove. Once in the vicinity of the tracheo-oesophageal groove, the right and left recurrent laryngeal nerves pursue a similar course on their respective sides. Each nerve runs behind the ipsilateral inferior cornu of the thyroid cartilage either behind or through the ligament of Berry, before running deep to the cricothyroid muscle to enter the larynx.

Awareness of the following anatomical points in relation to the recurrent laryngeal nerve is of great practical usefulness in reducing the incidence of operative nerve injury.

The right recurrent laryngeal nerve may have an aberrant (nonrecurrent) course in 0.5–0.7 per cent of individuals. In these individuals the nerve branches off from the vagus at the level of the cricoid cartilage or even higher, and runs medially behind the common carotid artery to reach the larynx. Very rarely the left recurrent laryngeal nerve may have a nonrecurrent course (incidence 0.04 per cent), this anomaly being associated with malformations of the aortic arch.

Another important, if subtle, anatomical feature of practical significance concerns the relative positions of the right and left recurrent laryngeal nerves in relation to the tracheo-oesophageal groove. The nerve on the left side is more predictably situated in the groove (approximately 80 per cent of individuals). The shorter right recurrent laryngeal nerve ascends more obliquely from lateral to medial often only following the tracheo-oesophageal groove for the last 1–2 cm before entering the larynx. In the remainder the nerve is situated somewhat more anteriorly, lying lateral to the trachea. Exceptionally, either nerve may be situated posterior to the tracheo-oesophageal groove, lying beside the oesophagus.

The recurrent laryngeal nerve and inferior thyroid artery are closely related to each other and this renders the artery a useful, though not consistent, landmark in identifying and locating the nerve. The inferior cornu of the thyroid cartilage, however, is a significantly more useful palpable landmark. The recurrent laryngeal nerve typically lies immediately behind the inferior cornu. With experience and gentle dissection the recurrent laryngeal nerve can be properly identified and protected. In most thyroid operations it is most easily located in the vicinity of the inferior thyroid artery and traced carefully to its laryngeal entry.

A further anatomical variation of the recurrent laryngeal nerve of practical significance, and therefore worthy of note, is the occasional tendency for the nerve, in its extralaryngeal ascent, to run as a duplicated structure. It should be noted that idiopathic, unilateral vocal cord paralysis, usually asymptomatic, is believed to occur in approximately 1 per cent of the population. For this reason, and as a defence against possible future litigation, several experts exercise the precaution of performing a laryngoscopic examination of cord function prior to thyroid surgery.

External laryngeal nerve

The external laryngeal nerve is vulnerable when ligating the superior thyroid vascular pedicle. The nerve is rather slender and runs in proximity to the superior thyroid artery, typically lying anteromedial to the artery. However, in a significant number of individuals (15–20 per cent), the nerve is intimately related to, or intertwined with, the artery at the level of the upper pole of the thyroid. Thus in order to avoid accidental injury to the nerve it is important to display the upper pole of the thyroid adequately. It is frequently necessary to divide the sternothyroid muscle near its insertion to the thyroid cartilage to facilitate this manoeuvre. During mobilization of the upper pole of the thyroid, the external laryngeal nerve should be sought and protected. In addition the superior thyroid vessels must be carefully isolated and ligated whilst avoiding any possible neural structure. It is important to note that in approximately 20 per cent of individuals the external laryngeal nerve runs deep to the fascia covering the inferior constrictor, and consequently does not appear in the operative field.

Compromise of parathyroid blood supply and consequent hypocalcaemia

A serious concern when performing a total thyroidectomy is the potential for accidentally devascularizing the parathyroids, thereby rendering the patient hypocalcaemic. In over 80 per cent of individuals the blood supply to the four parathyroids is derived largely, if not exclusively, from the two inferior thyroid arteries. To avoid the serious metabolic complication of postoperative hypocalcaemia, it is advised that the main trunk of the inferior thyroid artery should not be ligated. Instead, the technique of pericapsular dissection should be employed whereby the very terminal branches of the inferior thyroid artery are ligated on the thyroid capsule, thus preserving the blood supply to the parathyroid tissue. In this way the blood supply to the parathyroids may be preserved. In the case of parathyroid glands that are of doubtful viability following thyroidectomy, it is recommended that they be excised, diced into small fragments and reimplanted within the ipsilateral sternocleidomastoid muscle.

DEVELOPMENTAL ABERRATIONS

Aberrant location of the thyroid gland may be explained on the basis of incomplete descent or exaggerated descent of the developing thyroid bud.

Rarely (1 in 3500 individuals), there may be a total failure of thyroglossal duct (tract) descent, the condition presenting as a lingual thyroid located at the base of the tongue.

Incomplete embryological descent of the thyroglossal duct may result in the thyroid being situated superior to its normal position. Thus the thyroid gland may be found at the level of the hyoid bone or in an infrahyoid position.

Conversely, the thyroglossal duct may show excessive descent resulting in the thyroid being located at the level of the root of the neck, or even partially in the superior mediastinum (intrathoracic thyroid).

Another class of developmental abnormalities of the thyroid is attributable to persistence of part (or all) of the thyroglossal duct. The commonest example of this is the presence of the pyramidal lobe and levator glandulae thyroidea, which is due to failure of obliteration of the lower end of the thyroglossal duct. This feature is of such common occurrence as to be regarded as an anatomical variation rather than as an anomaly. Persistence of the thyroglossal duct also predisposes to thyroglossal cyst formation. Typically, thyroglossal cysts are found in the midline (or just off the midline) of the anterior neck, corresponding to the line of descent of the thyroglossal duct. The majority of thyroglossal cysts are found in the vicinity of the hyoid. Thyroglossal cysts are the commonest of all congenital, midline cystic lesions, accounting for nearly 70 per cent of such lesions. An almost invariable clinical sign of a thyroglossal cyst is the distinct 'tug' felt by the examiner's palpating fingers when he holds the cyst while the patient protrudes his tongue. As thyroglossal cysts are prone to infections and fistulation, it is advisable to excise these lesions. However, it is important when excising these lesions to define the cyst and thyroglossal duct and to remove them along with the body of the hyoid. This is the principle of the Sistrunk operation for thyroglossal cyst. Failure to remove the hyoid may result in the formation of cysts in remnants of the thyroglossal duct that are lodged behind the body of the hyoid.

Other developmental anomalies of the thyroid are the result of partial agenesis of the thyroid anlagen. Thus in 0.1–0.2 per cent of individuals the isthmus or one or other lobe may fail to develop.

FURTHER READING

Bailey BJ, Calhoun KH, Friedman NR. Thyroid and parathyroid. In: Bailey BJ, Calhoun KH. (Eds.). *Atlas of Head and Neck Surgery*

– *Otolaryngology*. 2nd ed. Philadelphia: Lippincott Williams & Wilkins, 2001: 228–34.

Bliss RD, Gauger PC, Delbridge LW. Surgeon's approach to the thyroid gland: Surgical anatomy and the importance of technique. *World Journal of Surgery*. 2000; 24(8): 891–7.

Gavilan J, Gavilan C. Recurrent laryngeal nerve: Identification during thyroid and parathyroid surgery. *Archives of Otolaryngology – Head & Neck Surgery*. 1986; 112: 1286–8.

Hansen JT. Embryology and surgical anatomy of the lower neck and superior mediastinum.In: Falk SA. (Ed.). *Thyroid Disease*. Philadelphia: Lippincott Raven, 1997.

Mahadevan V. *Clinical Anatomy and* developmental aberrations. In: Arora A, Tolley NS, Tuttle RM. (Eds.). *A Practical Manual of Thyroid and Parathyroid Disease*. Hoboken, NJ: Wiley-Blackwell, 2010.

Randolph GW. Surgical anatomy of the recurrent laryngeal nerve. In: Randolph GW. (Ed.). *Surgery of the Thyroid and Parathyroid Glands*. Philadelphia: Saunders, 2003.

23

Parathyroid glands

JAMES N. CRINNION AND TOM WIGGINS

Introduction 233
Embryology of parathyroid glands 233
Acquired migration 234
Anatomy of the parathyroid glands 234
Morphology *234*
Location of inferior glands *235*
Location of superior glands *235*
Gland symmetry *236*
Vascular supply of the parathyroid glands 236
Modern surgical treatment of primary hyperparathyroidism 237
Focused approach *237*
Bilateral neck exploration *237*
Mediastinal parathyroid glands *239*
Further reading 239

INTRODUCTION

Endocrine and thyroid surgeons must be familiar with the embryology, morphology and location of the parathyroid glands. Such knowledge will help to prevent inadvertent excision of normal glands during thyroidectomy and enable the surgeon to conduct a systematic search for enlarged hyperplastic glands during operations for hyperparathyroidism. The unique embryological development and the acquired migration of enlarged parathyroid glands explain why they are often found in various ectopic locations.

In recent years the operative treatment of primary hyperparathyroidism has become more focused, being directed by preoperative imaging. The specialist surgeon must be able to appreciate the appearance and visualize the location of parathyroid adenomas demonstrated with preoperative imaging techniques.

This chapter will describe the embryology and anatomy of the parathyroid glands with a particular emphasis on the knowledge required by the practicing surgeon.

EMBRYOLOGY OF PARATHYROID GLANDS

The parathyroid glands develop from the third and fourth pharyngeal pouches and first appear at 5 to 6 weeks of fetal development. The inferior parathyroid glands (parathyroid III) develop from the dorsal wing of the third pharyngeal pouch, while the ventral wing gives rise to the thymus gland. Both structures migrate together in a caudal and medial direction with the thymus coming to rest in the anterior mediastinum. The inferior parathyroid glands migrate for a variable distance but most commonly settle adjacent to the lower pole of the thyroid lobe. However, they may be found at any point in this path of migration from the angle of the jaw to the superior border of the pericardium.

The superior parathyroid glands (parathyroid IV) develop from the fourth pharyngeal pouch and attach to the posterior surface of the thyroid gland as it migrates caudally. They are usually found behind the upper two-thirds of the ipsilateral thyroid lobe. Their more predictable location may be attributed to their much shorter path of migration compared to the inferior glands.

ACQUIRED MIGRATION

The unique embryological development partially explains why the parathyroid glands may be found in ectopic sites. However, in addition, abnormally enlarged glands may migrate from their initial anatomical position. This is thought to occur as a result of the mass of the enlarged gland, negative intrathoracic pressure and the action of swallowing. Adenomatous superior glands frequently migrate in a posterior and inferior direction to lie in a para- or retro-oesophageal position on the anterior surface of the prevertebral fascia. They may migrate significantly and not infrequently may be found in the posterior superior mediastinum. Although inferior glands may also migrate into the anterior mediastinum, this is thought to be a less frequent event.

ANATOMY OF THE PARATHYROID GLANDS

Morphology

There are four parathyroid glands in most individuals, although additional glands can be found in 13 per cent of the population. These supernumerary glands are particularly prevalent in patients suffering with the multiple endocrine neoplasia (MEN) syndromes and uraemia induced secondary hyperparathyroidism. It has also been reported that 3 per cent of individuals have only three glands.

Macroscopically normal glands vary in colour from light brown to reddish tan and are frequently described as mahogany (Figure 23.1). In obese individuals the normal glands contain more fat and as a result assume a yellow-brown colour barely distinguishable from the surrounding fat. Abnormal hyperplastic or adenomatous glands are typically deep red-brown in colour (Figure 23.2). Normal glands are often described as flattened leaf-like or bean-shaped structures. They have a discrete, encapsulated surface which is smooth in comparison to the lobular surface of the thyroid or pitted surface of lymph nodes. Normal glands are usually located between the anterior and posterior layers of the pretracheal fascia. They are often surrounded by fat and demonstrate a unique gliding motion when the surrounding tissue is gently manipulated. They typically measure 4–6 mm in length and 2–4 mm in width. The combined glandular weight is typically 106–166 mg in men and 130–168 mg in women, with each gland weighing 30–40 mg. In contrast, parathyroid adenomas are usually much larger and occasionally weigh several

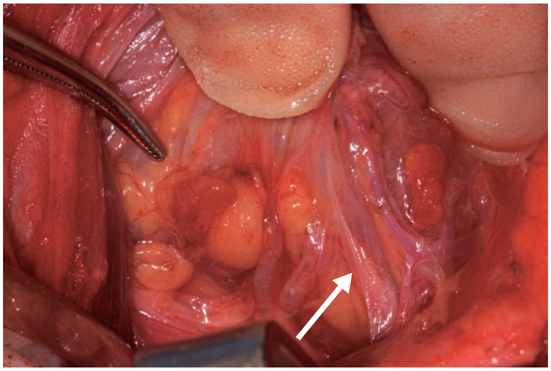

Figure 23.1 The right thyroid lobe has been retracted to reveal two normal parathyroid glands with the upper gland adjacent to the tip of the haemostat. They are separated by the inferior thyroid artery (arrow) which is a very helpful landmark during parathyroid exploration.

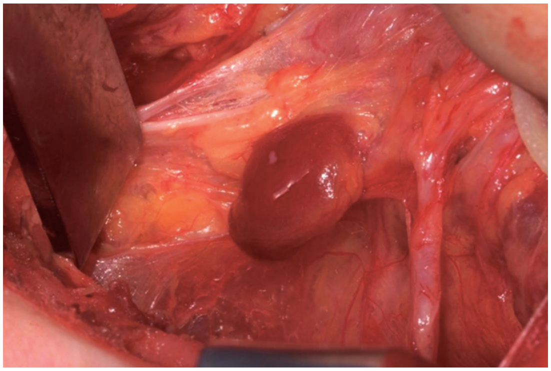

Figure 23.2 A typical brick red globular appearance of a small parathyroid adenoma. This was an inferior gland which is seen just caudal to the inferior thyroid artery.

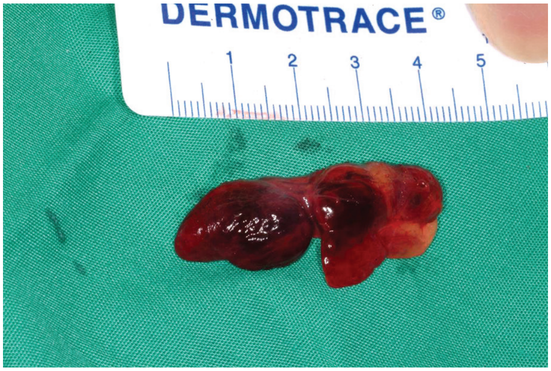

Figure 23.3 A large multi-nodular parathyroid adenoma. During excision the capsule of the gland must not be breached as this may spill abnormal tissue in the neck which can result in recurrent hyperparathyroidism.

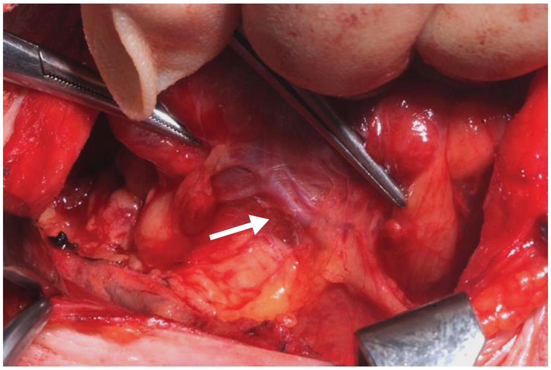

Figure 23.4 A right-sided inferior parathyroid adenoma (tip of forceps) adjacent to the lower pole of the right thyroid lobe and a normal superior gland. These are located in their most common sites and can be clearly seen in their typical relation to the inferior thyroid artery (arrow). Note how both glands are supplied by a distinct arterial pedicle and the blood supply to the superior gland can be seen to be arising directly from the inferior thyroid artery.

grams. The usual length is 1–1.5 cm with an average weight of around 400 mg. However, several patients have been cured with primary hyperparathyroidism who have had adenomatous glands that weigh just in excess of 100 mg. Although such glands were only marginally enlarged, they were easy to identify because of their globular structure and their deep reddish brown colour (Figures 23.2 and 23.3).

Location of inferior glands

The inferior glands (Figures 23.1, 23.2 and 23.4) are typically inferior to the inferior thyroid artery and anterior to the plane of the recurrent laryngeal nerve. In about 50 per cent of individuals the inferior glands are found within a 1 cm radius of the lower pole of the thyroid in an inferior, lateral or posterior position. They are often adherent to the capsule of the inferior aspect of the thyroid gland and in this position may be inadvertently excised during thyroidectomy. In a further 25 per cent of cases the inferior glands are found in the thyrothymic horn or ligament, which is a condensation of fibro fatty tissue between the lower lobe of the thyroid and the thymus gland. The inferior glands may be found medial to the inferior pole of the thyroid (around 8 per cent of cases) and in a discrete lateral position in about 12 per cent of patients.

The truly ectopic locations of inferior parathyroid glands occur as a result of either incomplete descent or excessive migration (Figure 23.8). During development around 3 per cent of glands will migrate with the thymus to eventually lie within the anterior mediastinum. Rarely, parathyroid tissue has also been found as far caudally as the pericardium within the aorto-pulmonary window. Rarely, the inferior gland fails to descend and is found 2–3 cm lateral to the superior thyroid pole adjacent to the carotid bifurcation. Undescended inferior parathyroid glands may even be found higher in the neck adjacent to the angle of the mandible, near the hyoid bone.

Location of superior glands

The superior glands (Figures 23.4, 23.5 and 23.6) are usually found in close proximity to the intersection of the recurrent laryngeal nerve and the inferior thyroid artery on the posterior aspect of the upper half of the thyroid lobe. They are found beneath the anterior layer of pretracheal fascia and are typically superior to the artery and posterior to the plane of the recurrent laryngeal nerve. However, as the position of these two structures may vary, another useful landmark for the superior gland is the cricothyroid junction (junction

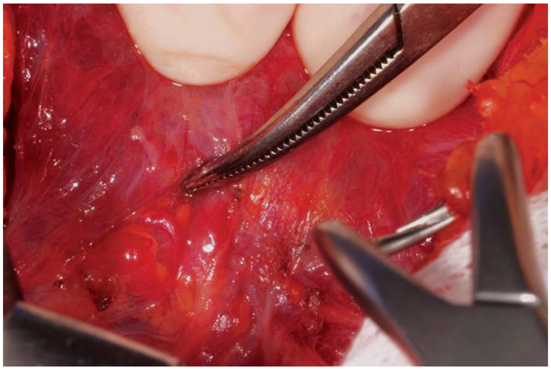

Figure 23.5 The thyroid lobe has been retracted to reveal a superior parathyroid gland beneath the thin layer of pretracheal fascia.

of the cricoid and thyroid cartilage). Although the site of the upper glands is more constant than that of the inferior glands, they may occasionally be found in ectopic positions that include the carotid sheath, para-oesophageal, retrooesophageal or retropharyngeal regions (Figure 23.7). Acquired migration is usually responsible for these ectopic positions. They may sometimes be found within the capsule of the posterior aspect of the thyroid gland or, rarely, they are truly intrathyroidal. This unusual site should always be considered when a thorough bilateral neck exploration to treat primary hyperparathyroidism has failed to identify an adenomatous gland.

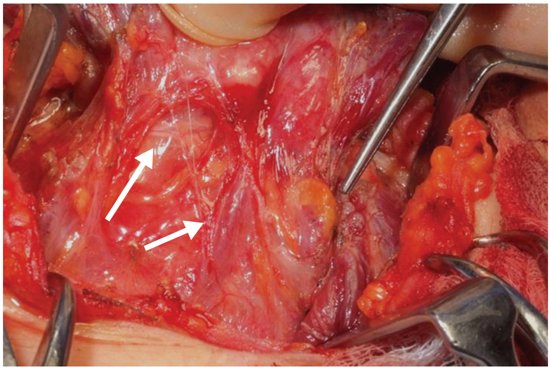

Figure 23.6 A superior parathyroid gland with a typical covering of adipose tissue. This lies in the classic site for a superior gland, superior to the inferior thyroid artery (right arrow) and posterior to the recurrent laryngeal (left arrow).

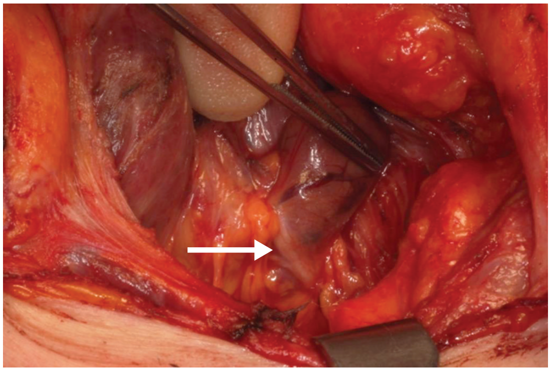

Figure 23.7 A large right superior parathyroid adenoma which had migrated posteriorly. The gland has been partially dissected and retracted medially to reveal the closely related recurrent laryngeal nerve (arrow). It is imperative that the recurrent laryngeal nerve is demonstrated and protected during parathyroid exploration.

Gland symmetry

In 80 per cent of cases the upper glands lie in a symmetrical position on either side of the neck. There is similar positional symmetry of the inferior parathyroid glands in 70 per cent of patients. This rule of symmetry assists the surgeon in locating missing glands during parathyroid exploration.

In some patients the upper and lower parathyroid glands can be very close to each other and differentiating between them may be difficult. Their position relative to the recurrent laryngeal nerve is often helpful in differentiating superior and inferior glands. If the path of the recurrent laryngeal is considered as a coronal plane, then the upper parathyroid will lie deep to this and the inferior gland superficial.

VASCULAR SUPPLY OF THE PARATHYROID GLANDS

The parathyroid glands have a distinct hilar vessel that helps to discriminate them from lymph nodes or thyroid nodules. The inferior thyroid artery, or an anastomosis between the inferior and superior thyroid artery, usually supplies the superior parathyroid gland. Following the branches of the inferior thyroid artery may occasionally identify an enlarged superior gland that has migrated.

The inferior thyroid artery usually supplies the inferior parathyroid gland, even if it is found in the anterior mediastinum. Rarely, a deep mediastinal gland may be supplied by a thymic branch of the internal mammary artery or via a direct branch from the aortic arch. The venous drainage of such glands is also via thymic veins which drain directly into the left innominate vein. With radiological expertise such veins can be cannulated, and high levels of parathyroid hormone suggest the presence of a mediastinal adenoma.

MODERN SURGICAL TREATMENT OF PRIMARY HYPERPARATHYROIDISM

Primary hyperparathyroidism is one of the most common surgical endocrine disorders, and the number of operations performed annually to treat this condition continues to rise. Most cases (>90 per cent) are due to a single enlarged parathyroid adenoma. The remaining cases are due to multigland disease (hyperplasia or double adenoma) with around 1 per cent of cases due to parathyroid carcinoma.

Focused approach

The current approach favoured by most surgeons is to attempt to localize the likely single adenoma preoperatively. A combination of ultrasound, technetium sestamibi scanning, magnetic resonance imaging and computed tomography will identify the culprit gland in about 70 per cent of cases, allowing a focused minimal incision approach. The senior author utilizes ultrasound immediately preoperatively to visualize the enlarged gland, which is then approached by gentle dissection in the bloodless plane between the carotid sheath and lateral border of the strap muscles. This technique avoids unnecessary dissection and produces very little postoperative scarring. In most cases the parathyroid adenoma is quickly identified and removed with a small (2–3 cm) incision and negligible morbidity. Such an approach has a 95 per cent to 97 per cent cure rate with the few failures occurring as a result of other small abnormal glands that were not revealed by the preoperative tests.

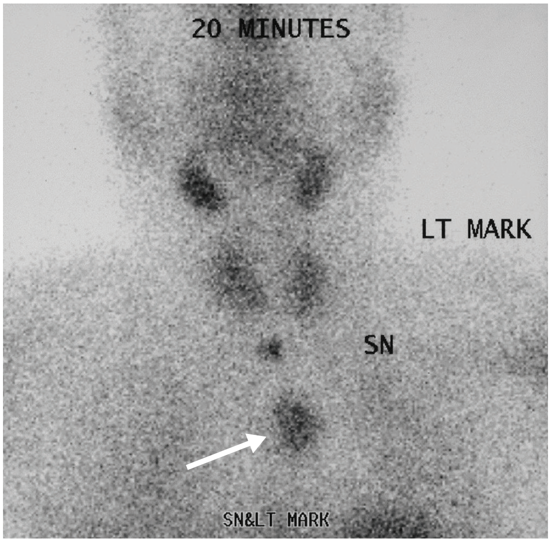

Figure 23.8 An early phase technetium sestamibi scan showing a large ectopic inferior parathyroid gland adenoma (arrow). This was excised via a mini-sternotomy.

The preoperative imaging will occasionally reveal a single ectopic adenoma within the mediastinum (Figure 23.8). If this is located in the superior aspect of the thymus, then it may be accessible from a cervical incision. However, glands within the inferior thymus can only be easily approached via a mini-sternotomy.

Bilateral neck exploration

In about 30 per cent of cases preoperative imaging fails to identify a parathyroid adenoma and a traditional four-gland parathyroid exploration is necessary to locate the enlarged glands. This operation requires a thorough knowledge of anatomy, and a gentle, meticulous and systematic approach to search for and identify the parathyroid glands. If possible all four glands should be visualized and then the abnormal gland or glands are excised.

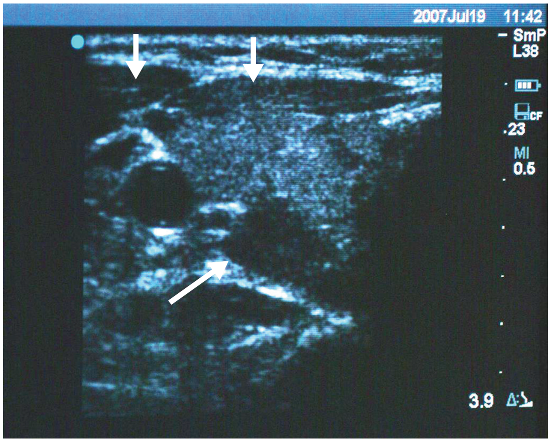

Figure 23.9 A transverse ultrasound image demonstrates a typical echolucent parathyroid gland (arrow) posterior to the thyroid lobe medial to the carotid artery. A common approach used to access and excise such a gland is by dissecting between the sternomastoid muscle (thick arrow) laterally and the strap muscles medially (thick arrow). Gentle retraction on the carotid artery and thyroid lobe will reveal the adenoma.

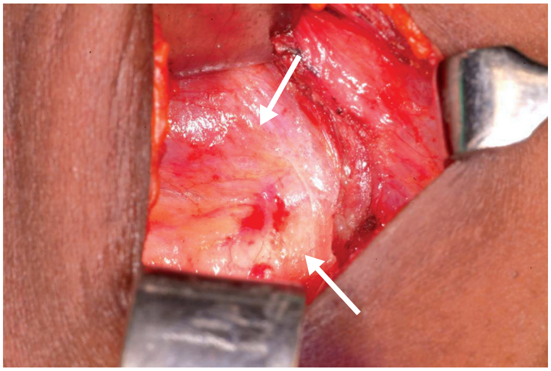

Figure 23.10 The strap muscles and sternomastoid have been retracted to demonstrate the right common carotid artery and the right thyroid lobe (arrows). Gentle retraction and dissection between these structures will provide direct access to the posteriorly placed parathyroid adenoma. To achieve this, it is necessary to divide the pretracheal fascia between these structures.

Several principles can guide the surgeon through this operation that requires significant concentration and patience:

- A bloodless field must be maintained during dissection as any bloodstaining will quickly distort the delicate tissue planes and render the identification of normal glands difficult.
- The recurrent laryngeal nerve (RLN) should be sought early in the dissection and protected. The plane of the nerve helps to differentiate inferior from superior glands with the former being anterior to and the latter posterior to this plane.
- The surgeon should make use of the positional symmetry of the glands that is often evident. When a gland is located confidently on one side of the neck, the surgeon will usually be rewarded by finding its counterpart in a similar position on the contralateral side.
- All glands must be visualized in their entirety to ensure that there is not an attached adenoma, and similarly the surgeon must be aware of the possibility of bi-lobed adenomas that must be completely excised if the patient is to be cured.
- Once a gland has confidently been identified, it is usually possible from its position to determine whether it is a superior or inferior parathyroid. The surgeon can then carefully dissect in the normal and ectopic sites to locate the missing ipsilateral gland.
- Normal glands must never be excised as this may lead to permanent hypoparathyroidism.

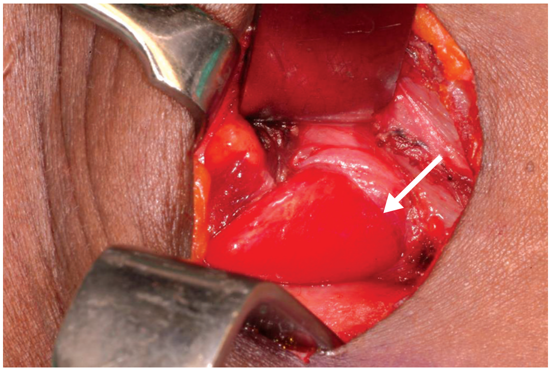

Figure 23.11 Division of the pretracheal fascia and retraction on the carotid sheath and strap muscles has revealed a large parathyroid adenoma (arrow).

When performing a bilateral neck exploration the surgeon must be alert to the possibility of multi-gland disease, and if possible, all four parathyroids must be identified. It is of paramount importance that a systematic approach is adopted. The author has found the algorithms described by Rothmund and Randolph to be very helpful.

Rothmund stated that the majority of parathyroid glands are located within a 1–2 cm circle around the intersection of the inferior thyroid artery and the recurrent laryngeal nerve with the superior gland cephalad to the artery and dorsal to the nerve, and the inferior gland caudal to the artery and ventral to the nerve. The procedure starts with a thorough exploration of this normal anatomical site on both sides of the neck and is usually rewarded by finding at least some of the glands. If the presumed adenoma has not been located, it is then necessary to extend the search for the missing gland in extended normal positions, in embryological sites of positional variation and also in the ectopic positions that result from acquired migration.

If the inferior gland is missing, then the regions ventral to the RLN should be explored. A thorough examination of the thyro-thymic ligament and upper thymus is performed with the latter achieved by slowly drawing the thymus into the neck. Other expanded normal sites for inferior glands include regions more than 1 cm medial or lateral to the inferior thyroid pole. If exploration of these positions is unrewarding, then an attempt should be made to perform a transcervical thymectomy to enable inspection of the middle and lower thymus. If the inferior gland is still elusive, then a search should be made for an undescended gland. These glands are usually found above the superior thyroid pole either medial to or within the carotid sheath and may be as high as the submandibular gland. If all these sites reveal no adenoma, then an intrathyroidal or subcapsular inferior parathyroid gland should be considered.

If a superior parathyroid gland is missing, then the surgeon should focus the dissection in the region dorsal and lateral to the RLN, initially exploring the regions posterolateral to the superior thyroid pole incorporating the adjacent retrolaryngeal and retrooesophageal areas. If these expanded normal locations prove negative, then caudal migration of an adenoma should be considered. The fascia between the carotid artery laterally and trachea and oesophagus medially should be opened to fully explore the retrolaryngeal and retro-oesophageal regions from the superior thyroid pole to posterior mediastinum. This in the authors' experience is the most common site for ectopic adenomas.

If all four glands are identified and appear normal, then the possibility of a fifth gland should be considered. These supernumerary glands have been identified in around 5 per cent of normal individuals. Fifth gland adenomas are almost always found in the mediastinal thymus and may be excised by transcervical thymectomy.

Mediastinal parathyroid glands

The incidence of mediastinal parathyroid adenomas has been reported as high as 20 per cent in patients with primary hyperparathyroidism. In many cases these can be removed via a cervical incision, but in around 2 per cent of cases a thoracic approach is required which can be in the form of a mini-sternotomy or with recent advances using thoracoscopic technique.

FURTHER READING

Akerstrom G, Malmaeous J, Bergstrom R. Surgical anatomy of human parathyroid glands. *Surgery.* 1984; 95: 14.

Alveryd A. Parathyroid glands in thyroid surgery, I. Anatomy of parathyroid glands. II. Postoperative hypoparathyroidism – Identification and autotransplantation of parathyroid glands. *Acta Chirurgica Scandinavica.* 1968; 389: 1–120.

Bruinin HA. Operative strategy and primary hyperparathyroidism. In: Kaplan EL. (Ed.). *Clinical Surgery International, Vol. 6: Surgery of the Thyroid and Parathyroid Glands*. Edinburgh: Churchill Livingstone, 1983.

DeLellis RA. Tumours of the parathyroid glands. In: *Atlas of Tumour Pathology, Third Series, Fascicle 6*. Washington, DC: Armed Forces Institute of Pathology, 1993.

DeLellis RA. Surgical pathology of the parathyroid glands. In: Randolph GW. (Ed.). *Surgery of the Thyroid and Parathyroid Glands.* Philadelphia: Saunders, 2003.

Fancy T, Gallagher D III, Hornig JD. Surgical anatomy of the thyroid and parathyroid glands. *Otolaryngologic Clinics of North America.* 2010; 43: 221–7, vii.

Mohebati A, Shaha AR. Anatomy of thyroid and parathyroid glands and neurovascular relations. *Clinical Anatomy*. 2012; 25: 19–31.

Prinz RA, Lonchyna V, Carnaille B, et al. Thorascopic excision of enlarged mediastinal parathyroid glands. *Surgery.* 1994; 116: 999–1004.

Randolph G, Urken M. Surgical management of primary hyperparathyroidism. In: Randolph GW. (Ed.). *Surgery of the Thyroid and Parathyroid Glands*. Philadelphia: Saunders, 2003.

Randone B, Costi R, Scatton O, et al. Thorascopic removal of mediastinal parathyroid glands: A critical appraisal of an emerging technique. *Annals of Surgery.* 2010; 251(4): 717–21.

Rothmund M. A parathyroid adenoma cannot be found during neck exploration of a patient with presumed primary hyperparathyroidism. *British Journal of Surgery*. 1999; 86: 72–6.

Sadler TW, Langman J. *Langman's Medical Embryology*. 10th ed. Philadelphia: Lippincott Williams & Wilkins, 2006.

Wang CA. Surgical management of primary hyperparathyroidism. *Current Problems in Surgery.* 1985; 12:1.

PART 6

24 The neck 243
Peter A. Brennan, Vishy Mahadevan and Barrie T. Evans
25 Posterior triangle and its contents 253
Rolfe Birch
26 Thoracic outlet 261
Vishy Mahadevan
27 Cervical spine 267
Hitesh Dabasia and Jason Harvey

24

The neck

PETER A. BRENNAN, VISHY MAHADEVAN AND BARRIE T. EVANS

Introduction 243
Surgically relevant surface anatomy 244
Muscles of the neck 245
Tissue planes and fascial layers in the anterior part of neck 246
Supra-hyoid area 247
Anatomy deep to the sternomastoid – upper neck level II and III 249
Inferior neck (level IV) 250
Further reading 251

INTRODUCTION

This chapter describes in a broad yet systematic manner the relevant surgical anatomy arrangement of the viscera, muscles, nerves and major blood vessels in the neck. It defines the anatomical relationships of these structures to each other and to the various fascial layers in the neck. Detailed anatomical descriptions of individual viscera fall outside the scope and purpose of this chapter, and detailed accounts of the course and distribution of individual nerves and vessels in the neck are provided where surgically relevant. The posterior triangle is covered separately in Chapter 25.

A clear and detailed understanding of the manner in which the various fascial layers of the neck are arranged, and an appreciation of the disposition of the muscular planes in the neck is of paramount importance in the surgery of the neck. Equally important is an awareness of how these structures relate to the cervical viscera and major vessels and nerves in the neck. These features constitute the very essence of the surgical anatomy of the neck. In addition mastery of such anatomical detail is an essential requisite to safety and precision in all neck operations, thereby minimizing damage to the many structures contained in such a small area.

From a surgical perspective, the neck is usually divided into two triangles – the anterior triangle and posterior triangle. The sternocleidomastoid muscle is the key to understanding both of these triangles (Figures 24.1).

Posterior to the trapezius muscle is the posterior cervical region which includes the cervical vertebral column (with the contained cervical portion of the spinal cord), the post-vertebral musculature and other post-vertebral soft tissues. The posterior cervical region may be said to extend from the level of the superior nuchal line above to the level of the vertebra prominens, which is usually the seventh cervical vertebra. The post-vertebral muscles are arranged in layers and function collectively as extensors and stabilizers of the cervical part of the vertebral column and/or as extensors of the head on the vertebral column. They are innervated segmentally by the dorsal rami of the cervical spinal nerves. This area is rarely operated on by head and neck surgeons.

For all practical purposes, the anterior region (which forms the remainder of this chapter) extends from the skull base (inferior surface of

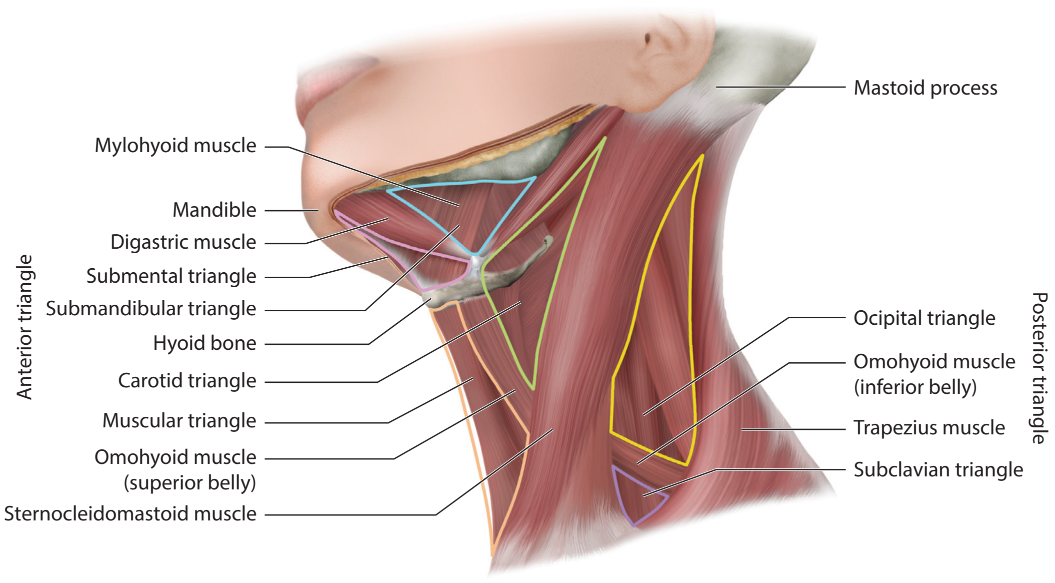
Mastoid process
Mylohyoid muscle
Mandible
Digastric muscle
Submental triangle
Submandibular triangle
Hyoid bone
Carotid triangle
Muscular triangle
Omohyoid muscle (superior belly)
Sternocleidomastoid muscle
Anterior triangle
Ocipital triangle
Omohyoid muscle (inferior belly)
Trapezius muscle
Subclavian triangle
Posterior triangle

Figure 24.1 The triangles of the neck.

the clivus) above to the root of the neck below. The root of the neck or cervico-thoracic junction is the area circumscribed by the shafts of the first ribs on either side, the sternal notch anteriorly and the upper border of the first thoracic vertebral body posteriorly.

SURGICALLY RELEVANT SURFACE ANATOMY

A number of superficial, palpable landmarks provide useful topographical clues to the precise location of deep structures that are not usually palpable or visualized. The thyroid notch is readily palpable and often visible. It lies in the midline at the level of the upper border of C4 vertebra (or disc between C3 and C4). The superior borders of the thyroid laminae can be felt on other side of the thyroid notch. The body of the hyoid bone lies 2 cm directly superior to the thyroid notch at the level of the body of C3.The angle of the mandible is easily felt and lies at the level of C2. The hard palate lies at the level of the anterior arch of the atlas (C1).

The anterior arch of the cricoid cartilage lies 1 cm directly below the lower border of the thyroid cartilage; the interval between the thyroid and cricoid being bridged by the tough median cricothyroid ligament (membrane). The arch of the cricoid lies at the level of C6.

At this level, on either side of the midline one can palpate the rather prominent transverse processes of C6. The sternal notch (i.e. the notched, thick upper border of the manubrium sterni) lies at the level of the upper part of T3 (3rd thoracic vertebra).

The surface anatomy gives an approximate idea of the surgical levels of the neck. These are summarized in Table 24.1. The course of the spinal accessory nerve can be approximated clinically by dividing the sternomastoid into thirds and drawing a line from the junction of the upper and middle thirds to a point on the anterior border of the trapezius approximately 5 cm above the clavicle. This is only an approximation of the course of the muscle as both points vary considerably. The great auricular nerve (GAN, C2,3) can also be drawn prior to raising a skin flap for neck dissection, facelift or parotidectomy by marking the midpoint of the sternomastoid 6.5 cm below the external auditory meatus. It also lies approximately 1 cm posterior to the external jugular vein. Erb's point (where the GAN comes round the posterior border

Table 24.1 Surgical levels of the neck

Level I: Submental and submandibular triangles. IA is the submental triangle bound by the anterior bellies of the digastric and the mylohyoid. IB is the triangle formed by the anterior and posterior bellies of the digastric and body of mandible.
Level IIA: Region anterior to the spinal accessory nerve bounded by the digastric muscle superiorly and the hyoid bone (clinical landmark), or the carotid bifurcation (surgical landmark) inferiorly down to the prevertebral fascia.
Level IIB: Posterior to the accessory nerve and extending to the skull base.
Level III: Extending from the carotid bifurcation superiorly to the cricothyroid notch (clinical landmark), to the omohyoid muscle (surgical landmark). Note that the omohyoid position moves with head position so the inferior extent of this level can be arbitrary.
Level IV: Lower jugular nodes extending from the omohyoid muscle superiorly to the clavicle inferiorly.
Level V: Posterior triangle. The posterior boundary is the anterior border of the trapezius muscle, and the anterior boundary is the posterior border of the sternocleidomastoid and inferiorly the clavicle. Divided into level Va above and Vb below the course of the accessory nerve as it crosses this triangle.
Level VI: Anterior neck compartment extending from the level of the hyoid bone superiorly to the suprasternal notch inferiorly. On each side, the lateral boundary is the medial border of the carotid sheath.

of sternomastoid) is also a useful point to find the accessory nerve, the latter being approximately 1 cm above this point.

MUSCLES OF THE NECK

The muscles of the anterior and posterior triangles of the neck may be classified into a superficial group comprising the right and left platysma muscles; an anterolateral group comprising the sternocleidomastoid and trapezius muscles; and an anterior group including mylohyoid, anterior and posterior bellies of digastric (useful guides at operation) and stylohyoid, and the infrahyoid strap muscles (omohyoid being relevant surgically). Finally, there is a vertebral group of muscles (made up of two subgroups). These are the anterior prevertebral muscles exemplified by the longus colli and longus capitis which run longitudinally anterior to the cervical vertebral bodies, and the lateral prevertebral muscles comprising scalenus anterior, medius and posterior, and levator scapulae. All of these arise from the transverse processes of cervical vertebrae and run inferolaterally to attach to the upper part of the rib cage or upper border of the scapula. These muscles are not usually encountered during head and neck surgery as they lie deep to the prevertebral fascia, a relatively dense layer of tissue which forms a useful barrier to deeper dissection. The loose fibro-fatty tissue can readily be dissected off this fascia using a damp swab in a sweeping motion thereby avoiding inadvertently going through it. Deep to the prevertebral fascia lies the phrenic nerve (C3,4,5) which crosses from lateral to medial on the scalenus anterior muscle (Figures 24.2a and 24.2b). and more laterally in the posterior triangle, the brachial plexus, which emerges between the scalenus anterior and medius muscles. All the nerves that penetrate and emerge from the prevertebral fascia arise from the cervical plexus and are mostly sensory (with the exception of the cervical root C2,3 of the ansa cervicalis, which is motor to the infra-hyoid musculature). These include the lesser occipital (C2), great auricular (C2,3), transverse cervical (C2,3) and supraclavicular nerves (C3,4).

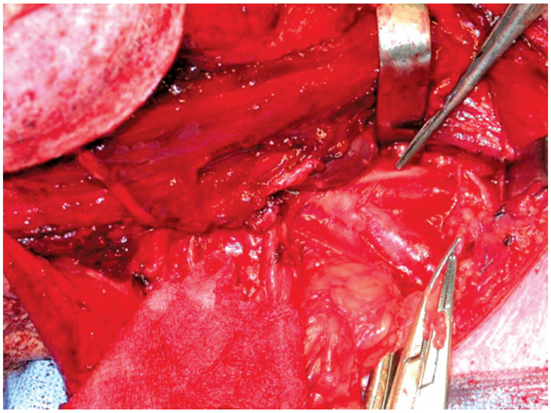

Figure 24.2a The course of the phrenic nerve under the prevertebral fascia passing from lateral to medial on scalenus anterior. The sternomastoid is retracted and the clips are on the transverse cervical vessels.

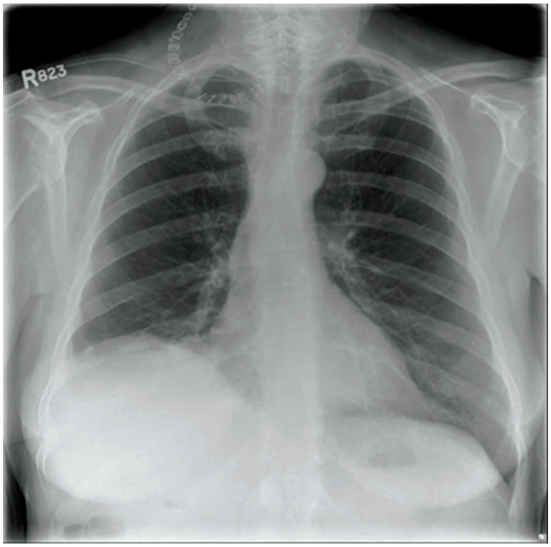

Figure 24.2b Chest radiograph after elective sacrifice of the phrenic nerve during a neck dissection for metastasis invading the prevertebral fascia. Note the raised hemi-diaphragm.

TISSUE PLANES AND FASCIAL LAYERS IN THE ANTERIOR PART OF NECK

The skin is thinner and generally more mobile over the anterior part of the neck than over the posterior part. Immediately deep to the skin of the neck is the superficial fascia, essentially a layer of subcutaneous fat arranged circumferentially around the neck, which is generally thinner in the anterior part of the neck than in the posterior region. Lying immediately deep to the subcutaneous fat, on either side of the anterior midline, is the platysma (Figure 24.3a), a relatively thin but wide sheet of muscle, which is confined to the anterior and anterolateral parts of the neck and usually is not present in the posterior triangle. This makes raising subplatysmal skin flaps in the posterior triangle more difficult, and care should be taken to avoid damage to the relatively superficial accessory nerve in this region. Superiorly, platysma is loosely attached to the lower border of the mandible before crossing superficial to the mandible to become continuous with the SMAS (superficial musculo-aponeurotic system) layer of the face. Inferiorly, platysma crosses superficial to the clavicle and blends with the fascia overlying pectoralis major, about 1–2 cm below the clavicle. Above the level of the hyoid, the platysma on both sides often merges or lies edge to edge. However, in some patients there is a dehiscence between the muscle resulting in more prominent jowls in later life.

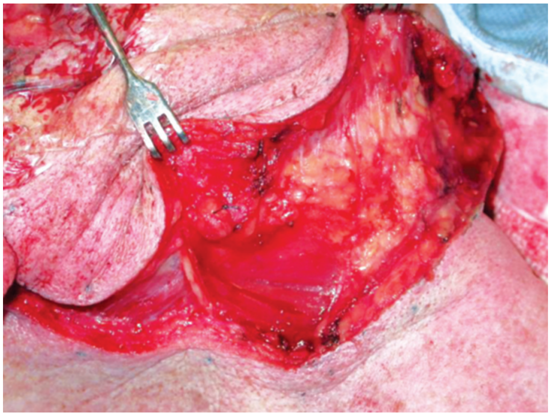

Figure 24.3a The platysma muscle. Note the great auricular nerve crossing the sternomastoid.

Deep to the platysma is the investing layer of deep cervical fascia which invests the neck like a collar. It is the most superficial of the various layers of the deep cervical fascia (the other layers being the prevertebral fascia, the carotid sheaths and the pretracheal fascia) (Figure 24.3b).

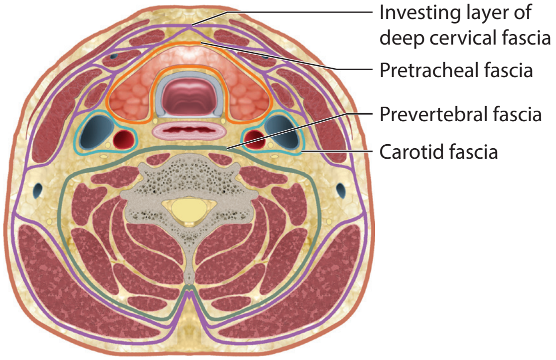

Figure 24.3b Schematic drawing of the fascia of the neck.

Lying within the fascia are the marginal mandibular and cervical branches of the facial nerve. While the latter is not so important and is routinely sacrificed during surgery, care should be taken to find the marginal mandibular nerve (often two branches) to preserve lip depressor function. It can readily be found crossing the facial vessels, but only descends into the neck proper in about 20 per cent of cases and is therefore sometimes not found.

Superiorly, the investing layer of deep cervical fascia is attached to the entire length of the lower border of the mandible, from midline to angle on either side. Traced posteriorly from the angle of the mandible, it is attached to the mastoid process and superior nuchal line on either side and to the external occipital protuberance in the posterior midline. In the interval between the angle of the mandible and the mastoid process (a distance of nearly 5 to 6 cm), the investing layer of deep cervical fascia splits to enclose the parotid salivary gland as the parotid fascia or parotid capsule.

Inferiorly, the deep cervical fascia attaches to the sternal notch anteriorly, the upper surface of the clavicle, acromion and spine of the scapula. The fascia splits to enclose the sternocleidomastoid and continues posterolaterally to form the fascial roof of the posterior triangle and splits to enclose the trapezius.

All the cervical viscera, major blood vessels and nerves of the neck, and all the cervical muscles (with the sole exception of the platysma) come to lie within the sweep of the investing layer of deep cervical fascia. The deepest layer of the deep cervical fascia is the prevertebral fascia, a relatively dense layer which runs across from one side to the other in front of the prevertebral musculature and the cervical vertebral column.

The surgical relevance of this fascia is that it protects the brachial plexus and phrenic nerve which lie immediately deep to it.

SUPRA-HYOID AREA

Above the hyoid bone are the paired mylohyoid muscles which interdigitate in the anterior midline at the mylohyoid raphe to form a mobile muscular sheet extending between the inner aspects of the right and left halves of the mandible. This mylohyoid 'sheet' is an important surgical landmark as it demarcates the neck below from the oral region above. It is innervated by the nerve to mylohyoid, the only motor branch of the anterior division of the third (mandibular) division of the trigeminal nerve (Figure 24.4). This pieces the sphenomandibular ligaments and runs superficial on the mylohyoid itself. It can sometimes be preserved during neck dissection and also supplies the anterior belly of digastric and is sensory to the inferior part of the chin.

Lying superficial to the mylohyoid (i.e. on the neck side of mylohyoid) are the stylohyoid and digastric muscles (the latter muscle comprising

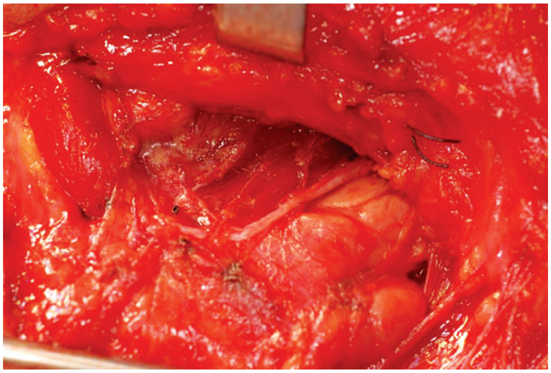

Figure 24.4 The anterior digastric is seen on the left with the nerve to the mylohyoid running across the darker mylohyoid muscle. The left submandibular gland is preserved below the muscle.

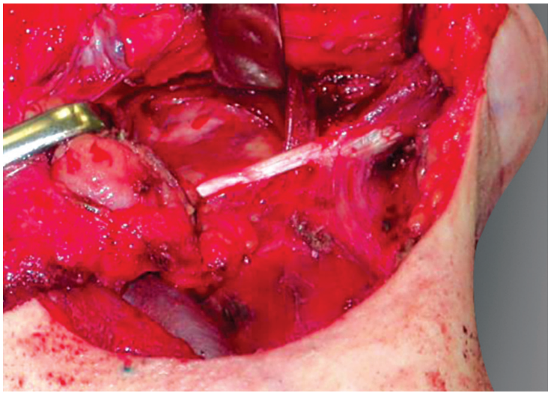

Figure 24.5a The right submandibular triangle. The anterior digastric is on the right with the mylohyoid retracted to show the lingual nerve. (The dissected submandibular gland is retracted to the left.)

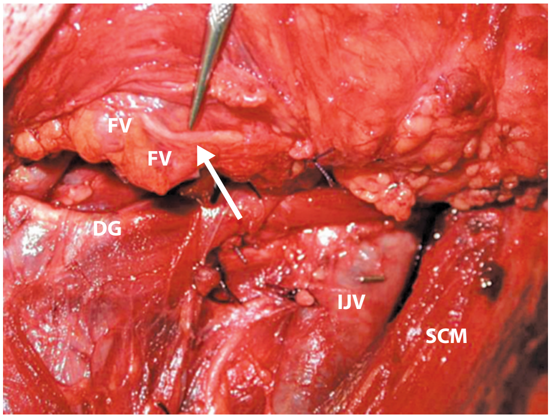

Figure 24.5b Left submandibular gland removed showing the marginal mandibular branch of the facial nerve (arrowed) crossing the facial vessels (FV).

anterior and posterior bellies). The two bellies of digastric and the lower border of the mandible together form an inverted triangular outline known as the digastric triangle or submandibular triangle. The floor (or deep limit) of this triangular area is the mylohyoid muscle (Figure 24.5a). Situated within the submandibular triangle are the submandibular salivary gland and level IB lymph nodes. The anterior digastric receives a blood supply from the submental artery, a branch of the submandibular artery which itself originates from the facial vessels and runs superficially on the mylohyoid muscle. These vessels can cause troublesome bleeding if not formally identified during neck dissection or submandibular gland excision but are used when lifting a submental island flap. The marginal mandibular branch of the facial nerve may be seen in the submandibular triangle (below the lower border of the mandible) in about 20 per cent of cases and lying in the fascia and superficial to the facial vessels (Figure 24.5b). Ligation and upward retraction of these vessels can be a useful method of protecting this nerve.

The digastric muscle is a useful anatomical guide when operating on the neck. It can be dissected along its course with relative ease and safety as no vital structures cross it.

However, there are many other structures that run either superior or inferior to the digastric. These include the lingual and hypoglossal nerves (superior and inferior respectively), branches of the external carotid anteriorly and internal carotid posteriorly, and internal jugular vein and accessory nerve. Finally, the main trunk of the facial nerve lies approximately 1 cm above and in the same plane as the posterior belly of the digastric near its origin on the mastoid process. The posterior belly is supplied by the facial nerve (Figure 24.6).

The digastric muscle is therefore useful for finding (or avoiding) vital structures. The facial artery passes over its superior border before

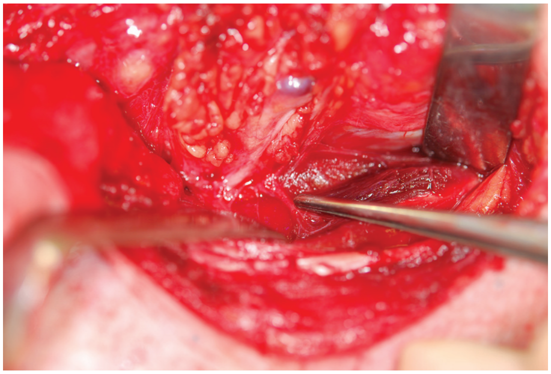

Figure 24.6 Main trunk of the left facial nerve about 1 cm above and in the same plane as the posterior digastric. In this case, the nerve to the posterior digastric is demonstrated at the end of the tissue forceps.

turning into the submandibular gland, and it is often found and isolated here during microvascular surgery.

When the facial artery is not suitable, the lingual artery can readily be found in the forgotten Pirogoff's triangle, formed by the intermediate tendon of digastric, the posterior border of the mylohyoid muscle and the hypoglossal nerve.

ANATOMY DEEP TO THE STERNOMASTOID – UPPER NECK LEVEL II AND III

The sternomastoid forms the key to an understanding of the deeper structures of the neck. The investing layer of deep cervical fascia can be incised and dissected anteriorly along the whole length of the muscle. The external jugular vein crosses the muscle from medial to lateral and can be a useful guide for finding the great auricular nerve which lies posterior to the vein. As the sternomastoid is retracted posteriorly on a broad front, the posterior digastric muscle will be found. Between these two muscles and deep to the digastric, the accessory nerve will be located (Figure 24.7). In about 70 per cent of cases, it lies superficial to the internal jugular vein (IJV), and less commonly is found deep to the vein. Rarely, the accessory nerve penetrates the vein. Superior to the accessory nerve and extending to the skull base is level IIB. Once the accessory and IJV have been found, level IIB can be dissected with confidence to its floor. The occipital artery which runs along the inferior aspect of the digastric can sometimes cause unexpected bleeding.

Further dissection along the sternomastoid inferiorly will find the omohyoid muscle which has crossed the posterior triangle en route to the hyoid bone. Deep to its intermediate tendon lies the internal jugular vein. As with the digastric muscle, the omohyoid can be used as a surgical guide with confidence as no vital structures cross it.

The carotid sheath, a condensation of connective tissue around the major vessels of the neck, lies lateral to the prevertebral fascia and is readily found by mobilization of the sternomastoid. It contains the laterally based IJV and common carotid artery, with the vagus nerve lying between them and often on the posterolateral aspect of the carotid (Figures 24.8a and 24.8b). Above the level of the common carotid bifurcation, the internal carotid artery runs within the carotid sheath. Situated posteromedial to the carotid sheath (outside the carotid sheath) and anterior to the prevertebral fascia is the ganglionated, cervical sympathetic chain (Figure 24.9). This can rarely be damaged during neck dissection surgery resulting in a unilateral Horner's syndrome.

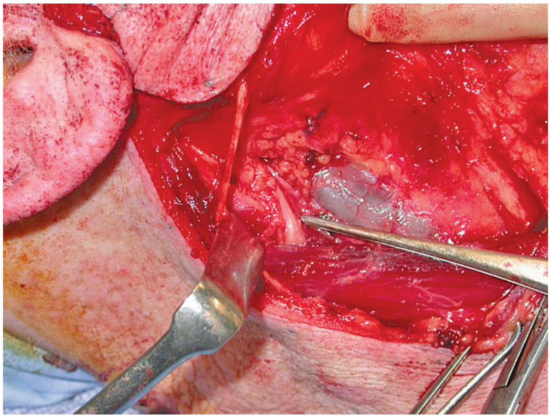

Figure 24.7 Identification of the right accessory nerve, crossing the internal jugular vein and entering the sternomastoid. The great auricular nerve can be seen superficially.

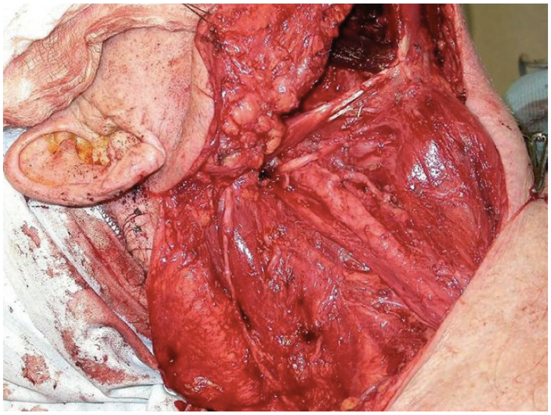

Figure 24.8a Right carotid tree. The sternomastoid and IJV have been removed. The vagus nerve is running behind the carotid. The hypoglossal nerve is seen crossing the carotids, and the accessory is running across the posterior triangle.

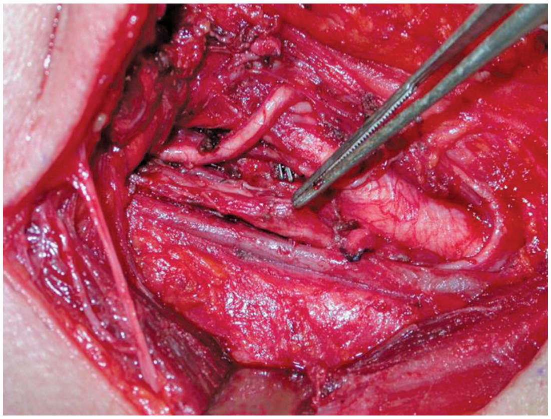

Figure 24.8b Right carotid tree anteriorly and IJV posteriorly with, in this case, a vagal nerve tumour lying between them. The hypoglossal nerve is seen crossing the carotid arteries.

The hypoglossal nerve crosses the internal and then external carotid artery, and is usually inferior to the posterior digastric muscle. It runs with a plexus of veins which are delicate and will bleed if provoked. It carries the only motor branch of C1, descendens hypoglossi, which runs inferiorly to join the C2,3 branch to form the ansa cervicalis (C1,2,3) (Figure 24.10).

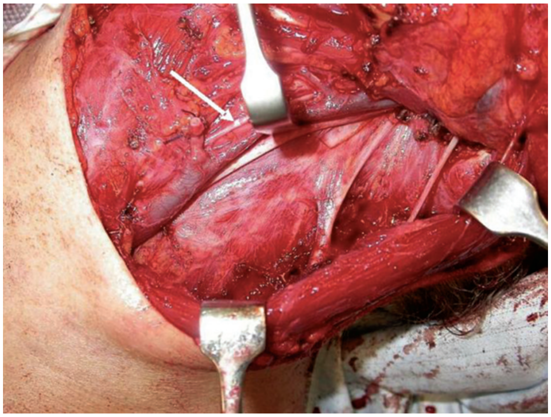

Figure 24.9 Left carotid sheath retracted anteriorly to show the vagus nerve and sympathetic chain posteriorly. The descending C1 branch of the ansa is arrowed, and branches of the cervical plexus can be seen passing under the sternomastoid.

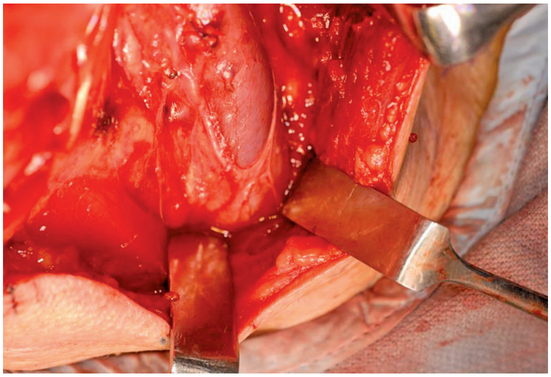

Figure 24.10 Lower part of the left neck showing the formation of the ansa cervicalis on the IJV.

The descending branch is anterior to the IJV but to the inexperienced eye can be confused with the vagus nerve. A nerve stimulator can be used to confirm the ansa.

The IJV receives several tributaries on its anterior surface including (from superior to inferior) the facial, lingual and thyroid veins. It is often written that there are no veins entering the posterior wall of the IJV, but in our experience this is not true and small veins can be encountered, often when least expected.

INFERIOR NECK (LEVEL IV)

At operation, this level is arbitrarily divided from level III superiorly by the omohyoid muscle, though the latter moves with head positioning and is not constant. From a surgical anatomy viewpoint, the great vessels and vagus nerve are essentially unchanged, though surgical access becomes more difficult the more inferiorly any dissection is taken. It is not usually advisable to dissect behind the sternum or clavicle. The thoracic duct lies on the left side of the neck in level IV and can easily be damaged during dissection. There is considerable anatomical variation of the thoracic duct, although it usually courses along the medial border of the scalenus medius muscle. The terminal arch of the duct can be between 0.5 and 4 cm above the clavicle before one or multiple ducts – which can be thin walled and delicate – join the venous system, most commonly the IJV. In one cadaveric study it was found that in all cases the thoracic duct approached the junction of the IJV and subclavian vein, posteriorly entering it within 1 cm of this landmark.

The centrally located cervical visceral compartment comprises, most posteriorly, the pharynx and its distal continuation the oesophagus. The pharyngo-oesophageal junction is typically at the level of the lower border of the cricoid cartilage (corresponding to the lower part of the body of C6). The pharynx is an elongated chamber that extends from the clivus superiorly to the pharyngo-oesophageal junction inferiorly. From above downwards it lies successively behind the nasal cavity (nasopharynx), the oral cavity (oropharynx) and the larynx (laryngopharynx). The larynx, which lies in front of the lower third of the pharynx, has a skeletal framework which is made up entirely of cartilages (including the thyroid and cricoid cartilages) and is continuous with the trachea at the level of the lower border of the cricoid cartilage (i.e. at the level of the lower part of C6). Thus the laryngo-tracheal junction is at the same horizontal level as the pharyngo-oesophageal junction. Lying astride the anterior aspect of the upper trachea is the thyroid isthmus, which on either side of the midline is coextensive with the corresponding thyroid lobe. All of these structures are considered elsewhere in this book, as is the posterior triangle of the neck.

FURTHER READING

Ammar K, Tubbs RS, Smyth MD, Wellons III JC, Blount JP, Salter G, Oakes WJ. Anatomic landmarks for the cervical portion of the thoracic duct. *Neurosurgery*. 2003; 53: 1385–7.

Langford RJ, Daudia AT, Malins TJ. A morphological study of the thoracic duct at the jugulo-subclavian junction. *Journal of Craniomaxillofacial Surgery*. 1999; 27: 100–4.

Mizen KD, Mitchell DA. Anatomical variability of omohyoid and its relevance in oropharyngeal cancer. *British Journal of Oral and Maxillofacial Surgery*. 2005 Aug; 43(4): 285–8.

Murphy R, Dziegielewski P, O'Connell D, Seikaly H, Ansari K. The great auricular nerve: An anatomic and surgical study. *Journal of Otolaryngology – Head and Neck Surgery*. 2012; 41: S75–7.

Salgarelli AC, Landini B, Bellini P, Multinu A, Consolo U, Collini M. A simple method of identifying the spinal accessory nerve in modified radical neck dissection: Anatomic study and clinical implications for resident training. *Journal of Oral and Maxillofacial Surgery*. 2009; 13: 69–72.

Tubbs RS, Rasmussen M, Loukas M, Shoja MM, Cohen-Gadol AA. Three nearly forgotten anatomical triangles of the neck: Triangles of Beclard, Lesser and Pirogoff and their potential applications in surgical dissection of the neck. *Surgical and Radiologic Anatomy*. 2011; 33: 53–7.

25

Posterior triangle and its contents

ROLFE BIRCH

Introduction 253
Skin, platysma and superficial fascia 253
Muscles forming the floor of the posterior triangle 255
The first rib 256
Blood vessels 256
Nerves in the posterior triangle 257
The brachial plexus: anterior primary rami, trunks and divisions 258
Exposure of the posterior triangle 258
Further reading 259
Acknowledgements 259

INTRODUCTION

The posterior triangle of the neck contains the spinal accessory nerve (SAN), phrenic nerve (C3, 4, 5) and branches of the cervical plexus and the supraclavicular brachial plexus with its proximal branches. The apical pleura and lung extend upwards behind the first rib, and the proximal subclavian artery and vein pass anterior to it. This concentration of vital structures is a common site for severe, even life-threatening, injuries from knife, missile or severe traction, and also for clinical mishaps during blocks, infusions or operations for benign lesions.

The triangle is bounded by the posterior edge of the sternocleidomastoid (SCM) muscle anteriorly, the anterior margin of the trapezius posterolaterally and the middle portion of the clavicle below. The omohyoid muscle is a valuable landmark crossing the triangle obliquely, subdividing it into the occipital triangle above and the supraclavicular triangle below. The triangle is often depicted as a space between the two flanking muscles. In fact the SCM sweeps across the trapezius (Figure 25.1), overlying the triangle as far down as the transverse process of C4 or even C5. The width of the insertion of the two muscles varies so that the triangle may be narrowed to a cleft. The obliquity of the first rib varies: in the long slender neck the subclavian artery can be seen two or even three fingers' breadth above the clavicle. In the short muscular neck the artery does not rise above the clavicle, and the pulse is only detectable deep to it. An accessory rib or band thrusts the subclavian artery and the rami and trunks of the brachial plexus upwards and forwards (Figure 25.2).

SKIN, PLATYSMA AND SUPERFICIAL FASCIA

The skin of the posterior triangle is very mobile. The platysma is the main constituent of the superficial fascia, forming a broad sheet extending between the lower border of mandible and lower lip and the deltopectoral fascia. The muscle fibres attach to the skin by fibrous septa, so inducing the tense oblique ridges and the pulling down of the lower lip in expressions of horror. The skin is

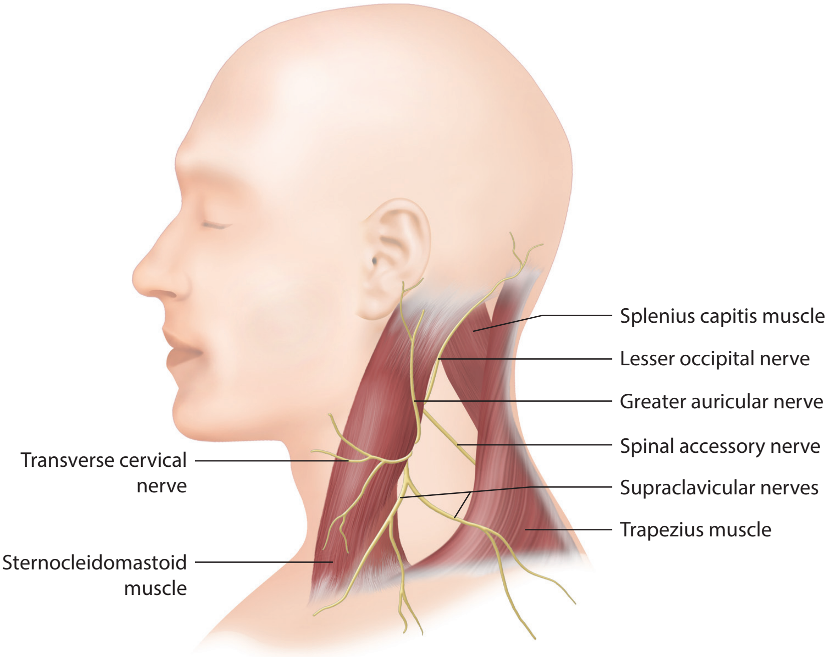

Figure 25.1 The cutaneous branches of the cervical plexus and the spinal accessory nerve which enters the posterior triangle about 5–10 mm above (cephalad) to the greater auricular nerve. The interval between the trapezius and SCM is not as extensive as shown.

innervated by the supraclavicular nerves (C3 and C4); the platysma by the cervical branch of the facial nerve. The blood supply to both is rich, from the suprascapular and transverse cervical arteries and, superiorly, by branches of the facial artery. Large flaps of skin, with platysma, can be elevated with ease from the underlying investing layer of the deep cervical fascia.

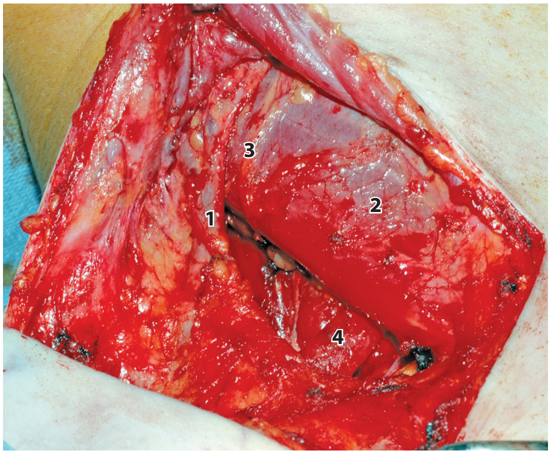

Figure 25.2 The external jugular vein (1) and supraclavicular nerves, with the anterior margin of the fat pad, have been separated from the SCM (2), which is crossed by the transverse cervical nerve (3). The inferior belly of the omohyoid (4) is visible.

The deep fascia forms two planes: the investing and the prevertebral. The investing layer envelops the SCM and trapezius muscles, and sweeps across the intervening fat pad as a thin but definite translucent membrane. The greater auricular and transverse cervical nerves pass deep to it as they cross the anterior face of the SCM; the spinal accessory n lies deep to it. The supraclavicular nerves enter the triangle deep to the investing fascia, perforating it at varying levels.

The external jugular vein (EJV) runs superficial to the investing layer, down the posterior margin of the SCM then piercing the fascia at the postero-inferior corner of the muscle before joining with the internal jugular and subclavian veins at the tri-radiate junction of the brachio cephalic vein. Air embolism is a real risk in wounds here. During operation, a rapid head down tilt may be required.

The fat pad is a glistening mass of blood and lymphatic vessels and areolar fatty tissue, which

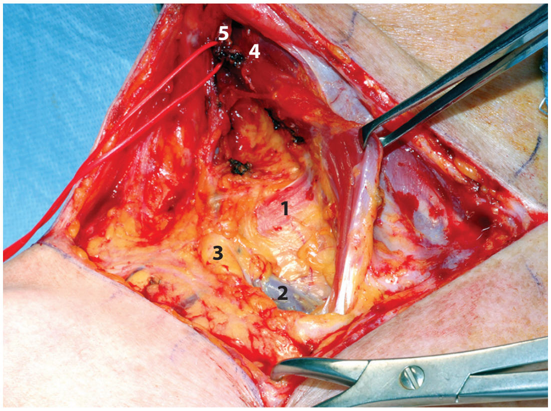

Figure 25.3 The level of omohyoid varies. Here, the inferior belly (1) is higher than in Figure 25.2. The transverse cervical vessels (2) are seen after reflection of the superficial leaf of the fat pad (3). The transverse cervical (4) and greater auricular (5) nerves are seen.

occupies most of the supraclavicular fossa. It is widest and deepest at its base. The prevertebral fascia lies deep to it. The pad acts as a buffer for the underlying brachial plexus, as a compressible space for the expansion of the subclavian vein and EJV, and as an important source of new blood vessels after repair of the brachial plexus. The pad commonly forms two distinct leaves, separated by the transverse cervical vessels (Figure 25.3).

The SAN crosses the apex of the anterior face of the fat pad in the narrow interval between the SCM and trapezius; the supraclavicular nerves emerge from deep to the SCM to pass down anteriorly and splay out across it. The intermediate tendon of the omohyoid lies deep to the posterior margin of the SCM. It is held down to the first rib below by a sling of the investing fascia, so that the inferior belly runs transversely through the fat pad towards the upper border of scapula; the superior belly runs near vertically to the hyoid.

The prevertebral fascia sweeps over the scalenus anterior and the muscles forming the floor of the posterior triangle. It extrudes to form a tapering cylinder around the rami and trunks of the brachial plexus, and the subclavian artery. The fascial tube is continuous with the axillary sheath below the clavicle. The phrenic, dorsal scapular, suprascapular, and the long thoracic nerves are deep to it (Figures 25.4 and 25.5).

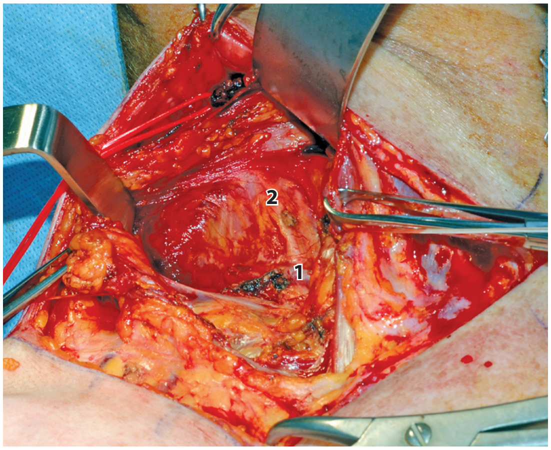

Figure 25.4 A case of severe traction lesion of the brachial plexus. The fat pad and omohyoid have been reflected, revealing the prevertebral fascia and phrenic nerve (2). The nerve is crossed by the transverse cervical artery (1).

MUSCLES FORMING THE FLOOR OF THE POSTERIOR TRIANGLE

The uppermost muscles, splenius capitis and levator scapulae, pass dorsally, whereas the three scaleni pass anteriorly to the upper two thoracic ribs. A deepening valley is formed with an increasingly prominent medial buttress of scaleni.

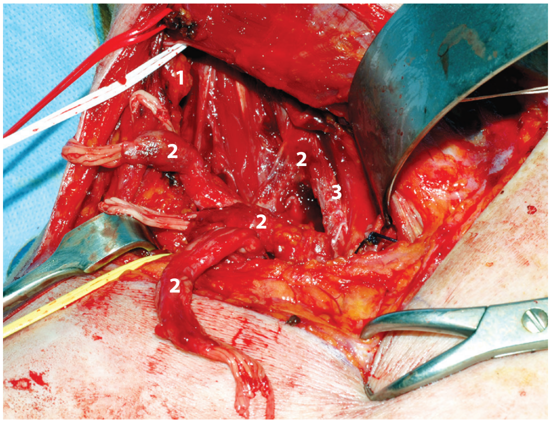

Figure 25.5 Division of the prevertebral fascia reveals the ruptured stumps of C5 and C6 (1), and the rootlets and dorsal root ganglia of avulsed C7, C8 and T1 (2). The deep cervical artery (3) passes between the upper trunk and C7; the relations here are distorted by the displaced avulsed nerves.

The splenius capitis (C2 and C3) arises from the mastoid and the adjacent occipital bone to pass down medially to the ligamentum nuchae and the tips of spinous processes C7 to T3.

The levator scapulae (dorsal scapular nerve, C5) arise from the transverse processes of the atlas and axis and the posterior tubercles of transverse processes C3–C4. The fibres pass down and laterally to the superomedial scapular border.

Scalenus posterior (C6–C8) arises from the posterior tubercles of transverse processes C4–C6 to insert on the outer surface of the second rib, behind the tubercle for serratus anterior.

Scalenus medius (C3–C8), the largest and longest of the scaleni, passes from the transverse process of the axis and the posterior tubercles of the transverse processes of C3–C7 to insert upon the upper surface of the first rib posterior to the groove of the SCA.

The scalenus anterior (C4–C6) is attached to the anterior tubercles of the transverse processes C3–C6 and inserts upon the first rib anterior to the groove for the subclavian artery. The subclavian vein, suprascapular and transverse cervical arteries pass anterior to it. The phrenic nerve runs almost vertically down its anterior face. The subclavian artery and the ventral rami of the brachial plexus run behind it. The suprapleural membrane and the spinal pleura (Figure 25.6) extend above its posterior medial surface. The vertebral artery and veins lie below and behind the muscle origin from C6, in their course to the foramen intertransversarium. The muscle may bifurcate to include the subclavian artery, it may be bulky and the tendon may curve posteriorly round the artery to form a kind of snare.

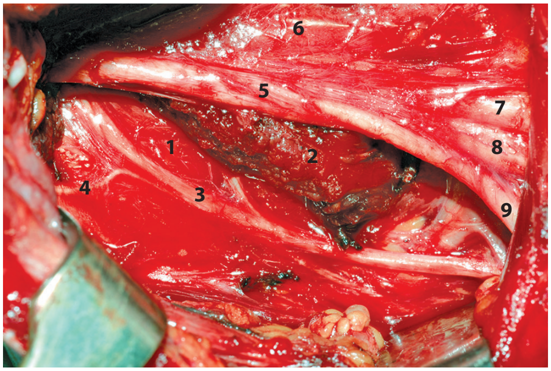

Figure 25.6 The LTN (3) seen running down the levator scapulae (1) after section of the scalenus medius (2). A communicating branch (4) from the dorsal scapular nerve is common. The upper trunk (5) passes between the scalenus anterior (6) and scalenus medius (2). The anterior (7) and the posterior (8) divisions and the suprascapular nerve (9) run anterior to the LTN.

THE FIRST RIB

The broad, flat first rib extends from the head at the vertebral body, the neck and the costotransverse articulation, over the apical pleura to curve round to the costo-chondral junction and then to the manubrium. The healthy apical pleura is easily separable from the head, neck and most of the underside of the first rib, but it is more adherent behind the costochondral junction. The scalenus medius is attached to the upper rib posteriorly. In front of the scalenus medius, the surface of the rib is grooved by the passage of the first thoracic nerve and lower trunk. There is a distinct tubercle at the attachment of the scalenus anterior, behind which is the groove for the subclavian artery. In front of the scalenus tubercle, the subclavian vein runs over the upper surface of the rib. The intercostal muscles are attached to the edge of the rib. The lower part of the cervicothoracic (stellate) ganglion lies on the head of the rib, deep to the proximal part of the vertebral artery (Figure 25.7).

BLOOD VESSELS

The subclavian artery arises from the brachiocephalic trunk on the right, but directly from the arch of the aorta on the left. The artery is considered in three parts: anterior to scalenus anterior, deep to it and then lateral to it. The second and third parts are virtually identical on both sides. They are in close relation to the primary ventral rami of C7, C8 and T1, and the lower and middle trunks. The subclavian artery becomes the axillary artery at the inferior margin of the first rib, and it is closely related to the divisions of the brachial plexus behind the clavicle (Figure 25.8). The third part of the subclavian artery is easily blocked by firm digital pressure against the first rib. The method was successfully used for high amputation during the Napoleonic wars and remains the best method of emergency control of bleeding from the deeply placed axillary artery.

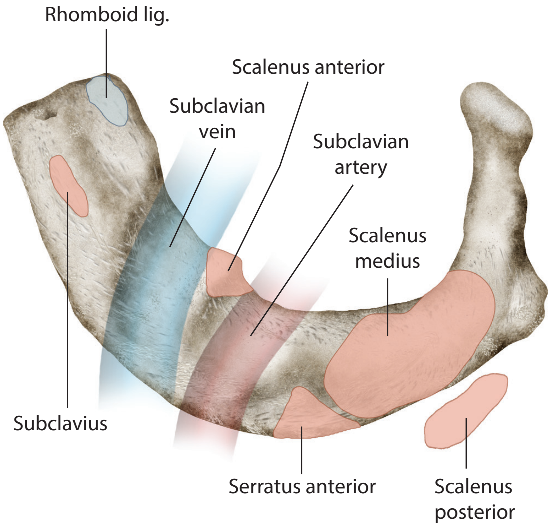

Figure 25.7 The upper surface of the first left rib, showing the sites of the arterial and venous crossings and the muscular attachments.

Important branches supply the contents of the posterior triangle and provide a vital collateral pathway in occlusion of the axillary artery.

The thyrocervical artery is a short, wide branch from the first part of the subclavian artery, close to the medial border of the scalenus anterior. It divides into the inferior thyroid, suprascapular and transverse cervical arteries. The transverse cervical divides into the superficial cervical and the dorsal scapular arteries. Branches pass through the fat pad anterior to the upper and middle trunks. The deep cervical artery springs from the costocervical branch, usually from the second part of the subclavian artery. It passes between the middle and lower trunks. The suprascapular artery runs anterior to the phrenic nerve and scalenus anterior, behind the IJV and subclavian vein to pass behind and parallel to the clavicle. This substantial vessel must be carefully ligated during emergency osteotomy of the bone.

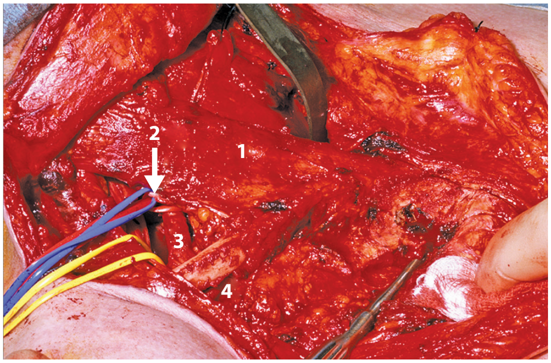

Figure 25.8 A stage during transclavicular exposure of tumour enveloping the right vertebral artery (see Further Reading). The SCM (1) has been defined. The phrenic nerve (2) and the subclavian artery (3) have been traced after division of the scalenus anterior. The subclavian vein (4) is visible below the clavicle.

Variations are common. These vessels are often ruptured in closed traction lesion; they are embedded in forbidding fibrosis after injury or operation and they become stenosed and fragile after radiotherapy.

The venous return from the triangle and its contents is by deep veins running with the arteries; superficial veins from the skin and platysma mostly terminate in the EJV. On the left the thoracic duct and on the right the right lymphatic duct enter the brachiocephalic vein at the tri-radiate junction.

NERVES IN THE POSTERIOR TRIANGLE

The lesser occipital nerve (C2), greater auricular (C2–C3) and transverse cervical nerves (C2–C3) are important signposts. Whilst deep to the SCM, they run in a plane posterior to the SAN. The lesser occipital moves anterior to the SAN at the posterior margin of the SCM before ascending. The great auricular and transverse cervical nerves encircle the SCM to traverse its anterior face. The supraclavicular nerves (C3–C4) enter the triangle as a common trunk, about 5 mm caudad to the transverse cervical, anterior to the fat pad, posterolateral to the EJV. Three main nerves are formed, the medial, intermediate and lateral supraclavicular nerves, which pierce the deep fascia, and innervate the skin of the triangle and a wide territory beyond. Intraoperative injury causes pain, which may be severe.

The phrenic nerve arises from the ventral rami of C4 with contributions from C3 and C5. The nerve is formed at the lateral margin of the scalenus anterior, and passes almost vertically down its anterior face. It inclines towards the lower medial border of the scalenus anterior running posterior to the thyrocervical and suprascapular arteries, the

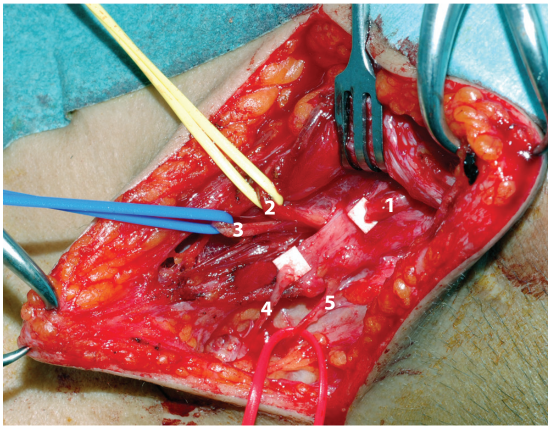

Figure 25.9 The SAN (1) emerges as one trunk from deep to the SCM about 5–10 mm cephalad to the greater auricular (2) and transverse cervical (3) nerves. The nerve had been transected 15 months earlier, during lymph node biopsy, and there is atrophy of the distal stump (4). The proximal branch (5) to the uppermost trapezius was also divided.

IJV and, on the left, the thoracic duct. The nerve may be deviated by fibrosis in ruptures of the upper trunk. Injury during operations in infancy causes life-threatening paralysis of the hemi diaphragm.

The spinal accessory nerve passes deep to, or through, the SCM. The greater auricular nerve (Figure 25.9) is the key to exposure of the SAN, which emerges usually as one trunk, about 5–10 mm cephalad to the point where the greater auricular winds around the SCM. The SAN traverses the apex of the fat pad, deep to the thin investing layer of the cervical fascia, in close relation to the superior superficial lymph nodes. One slender branch passes to the uppermost fibres of the trapezius either deep to the SCM or just beyond it. The nerve passes down deep to the inner face of the trapezius and the investing fascial layer in a characteristic sinuous fashion. It is joined by a sensory branch from the cervical plexus (C3–C4) just above the clavicle.

The brachial plexus: anterior primary rami, trunks and divisions

The anterior primary rami enter the posterior triangle through the cleft between the scalenus anterior and scalenus medius. C5 runs nearly vertically downwards, the other rami enter the triangle with increasing obliquity, and T1 passes upwards round the neck of the first rib, behind the pleura, the vertebral artery and the first part of the subclavian artery. C5 and C6 become the upper trunk, the middle trunk is the continuation of C7, and C8 and T1 form the lower trunk. The trunks lie in front of one another rather than side to side, with the subclavian artery passing anteromedially. The upper trunk divides at varying levels above the clavicle; the posterior is consistently larger than the anterior division. The divisions of the middle and lower trunks are deep to the clavicle. The upper trunk and its divisions are palpable posterolateral to the subclavian pulse.

Three important nerves arise from the supraclavicular brachial plexus.

1. The dorsal scapular nerve runs posteriorly from C5, through the scalenus medius and then behind the levator scapulae, which it partially supplies, before terminating in the rhomboids.
2. The long thoracic nerve is formed by rami from C5 and C6, and, usually, by rami from C4 and C7. These join, deep to the scalenus medius, and the nerve passes down posterolateral to the muscle, on the floor of the posterior triangle deep to the suprascapular nerve. The long thoracic nerve is at risk during operation upon the first rib.
3. The suprascapular usually springs from the upper trunk, and it passes down laterally deep to the fat pad, and trapezius, to the suprascapular notch. In the short, stout neck, the nerve is behind the clavicle; usually it is palpable and displays rather easily in the triangle.

EXPOSURE OF THE POSTERIOR TRIANGLE

Some simple rules enable safe, reliable exposure.

1. Position is supine, semisedentary, with head elevated to 30°, the neck extended in neutral rotation.
2. Skin preparation includes the earlobe, jawline, extending below the clavicle, beyond the midline and posterior to the fold of the trapezius. The whole of the clavicle, acromion, acromioclavicular and sternoclavicular joints are included (Figure 25.10).

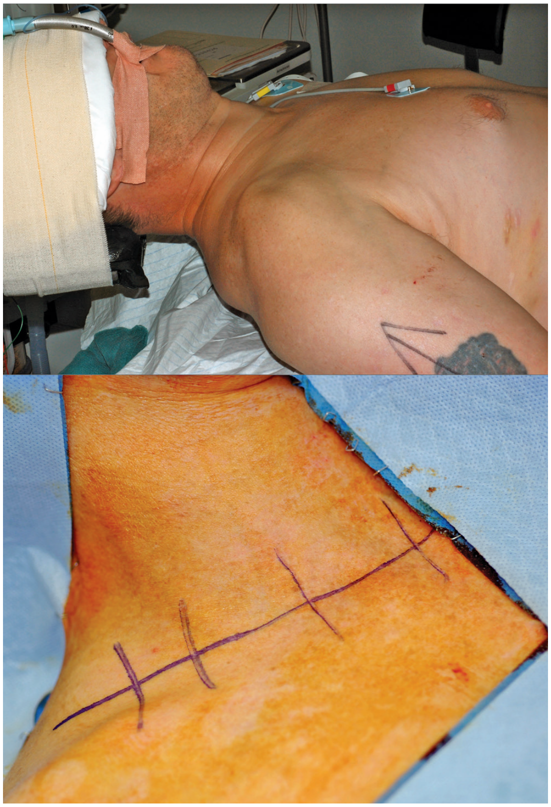

Figure 25.10 The transverse supraclavicular approach to the brachial plexus. Note the position of the patient and the line of the incision.

3. Instruments include bipolar diathermy and a nerve stimulator. Of retractors, Jolls thyroid, narrow malleable and narrow Deavers are useful; toothed self-retaining retractors are dangerous. Coloured plastic slings help to mark and retract nerves.
4. *Technique*. There is no place for 'blunt dissection'. This must be done by scalpel or sharp, blunt-ended scissors.
5. The incision is transverse supraclavicular, elevating platysma with the skin. In the urgent case it lies just above the clavicle, running from beyond the midline to the fold of the trapezius. For exposure of the upper trunk, the incision is shorter, about two fingers' breadth above the clavicle.
    - The anterior face of the SCM muscle is exposed, tracing the transverse cervical and greater auricular nerves. The spinal accessory is found 5–10 mm cephalad to the emergence of the greater auricular nerve.
    - The door to deeper structures is opened through the plane between the EJV (behind) and the posterior margin of the SCM muscle (in front). This protects the supraclavicular nerves which are displaced laterally.
    - The fat pad is divided or reflected. The transverse cervical vessels must be preserved if the subclavian or axillary artery has been occluded.
    - The omohyoid marks the depth. It is divided between stay sutures and reflected.
    - The glistening prevertebral fascia is revealed, enveloping the scalenus anterior, binding the vertically running phrenic nerve to its anterior face, and sweeping across the rami, trunks, and the subclavian artery in the valley between the scalenus anterior and medius.
    - Exposure of the subclavian artery requires careful division of the scalenus anterior close to its attachment to the first rib. Rarely, the subclavian artery runs anterior to the muscle; less rarely, it penetrates it. The phrenic nerve is gently mobilized, the margins of the muscle defined, and the plane between it and the underlying artery carefully developed. A narrow malleable retractor is useful.

FURTHER READING

Birch R. *Surgical Disorders of the Peripheral Nerves*. 2nd ed. London: Springer-Verlag, 2011: 231–302, 375–428.

Camp SJ, Birch R. Injuries to the spinal accessory nerve – a lesson to surgeons. *Journal of Bone and Joint Surgery*. 2011; 93B: 62–7.

ACKNOWLEDGEMENTS

Figure 25.1 is drawn by Amanda Williams.

Figures 25.2 to 25.10 are from the author's work, *Surgical Disorders of the Peripheral Nerves*, 2nd ed., 2011, by kind permission of the publishers Springer UK.

26

Thoracic outlet

VISHY MAHADEVAN

Introduction 261
Anatomy of the thoracic outlet 261
Structures crossing the thoracic outlet *262*
The first rib *264*
The scalene muscles 265
Further reading 265

INTRODUCTION

An appreciation of the anatomy pertaining to the superior aperture of the thoracic cage is integral to any comprehensive consideration of the anatomy of the head and neck. It is also a requisite to the proper understanding and rational clinical management of a group of disorders collectively termed *thoracic outlet syndrome*. The superior aperture of the thoracic cage defines the upper limit of the thoracic cavity. It lies at the junction between the neck and thoracic cavity. In clinical practice and clinical terminology it is referred to as the *thoracic outlet*. (It must be noted that in anatomical nomenclature, the same area is termed the *thoracic inlet*.) In this chapter the term *thoracic outlet* shall be used in its clinical connotation and thus synonymously with the superior aperture of the thoracic cage. The thoracic outlet is traversed by numerous structures descending from the neck into the thoracic cavity and other structures coursing from the thoracic cavity into the neck. In the context of thoracic outlet syndrome, the structures that merit particular consideration are the subclavian vessels and brachial plexus. Two structures which are key to the clinician's understanding of the anatomical basis to thoracic outlet syndrome are the scalenus anterior muscle and the first rib.

In this chapter a general description of the bony outline of the thoracic outlet shall be followed by a detailed consideration of the first rib, the scalene muscles and the neurovascular structures which cross above the first rib to enter the axilla. The various sites at which these neurovascular structures may be subjected to pathological compression shall be highlighted.

ANATOMY OF THE THORACIC OUTLET

The superior aperture of the thoracic cage, also known as the thoracic outlet, lies at the cervicothoracic junction. This junction and its immediate vicinity are referred to as the root of the neck. The thoracic outlet is traversed by numerous structures, some descending from the neck into the thoracic cavity and others ascending from the thoracic cavity into the neck (Figure 26.1). In the context of thoracic outlet syndrome, the important structures that cross this region are (i) the subclavian artery on its way from the neck to the axilla, (ii) the subclavian vein which is the proximal

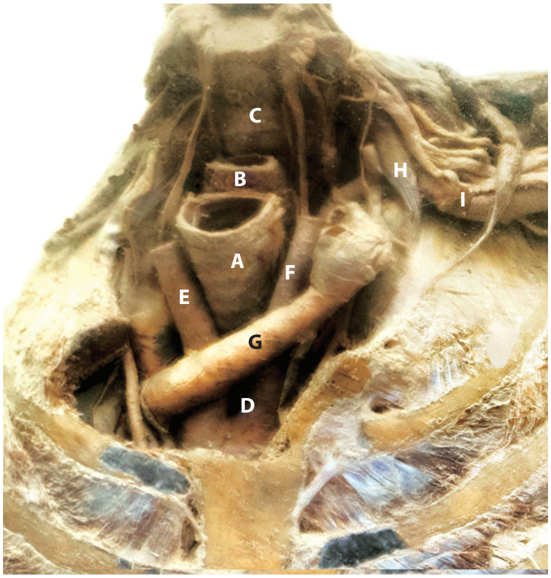

Figure 26.1 Dissection showing structures crossing the thoracic outlet (anterior view). The clavicles and manubrium have been removed. A – trachea. B – oesophagus. C – vertebral column. D – aortic arch. E – brachiocephalic artery. F – left common carotid artery. G – left brachiocephalic vein. H – left scalenus anterior. I – left subclavian artery crossing above the first rib.

continuation of the axillary vein and (iii) the brachial plexus, with the lower trunk of the brachial plexus being particularly susceptible. The thoracic outlet is kidney-shaped in outline (Figure 26.2) with a maximal transverse diameter of 10–12 cm and an anteroposterior dimension, in the median plane, of 5–6 cm. The boundaries of the thoracic outlet (Figure 26.2) are as follows. On either side, the thoracic outlet is bounded by the inner border of the shaft of the corresponding first rib and its costal cartilage. The posterior boundary of the thoracic outlet is the anterior margin of the upper surface of the body of the first thoracic vertebra, while the anterior boundary is the sternal notch. The latter is the thick, notched upper border of the manubrium sterni. Owing to the obliquity of the lie of the first rib, the plane of the thoracic outlet is not horizontal but slopes downwards and forwards. Stated in another way, the sternal notch lies at a lower level than the upper surface of the first thoracic vertebra.

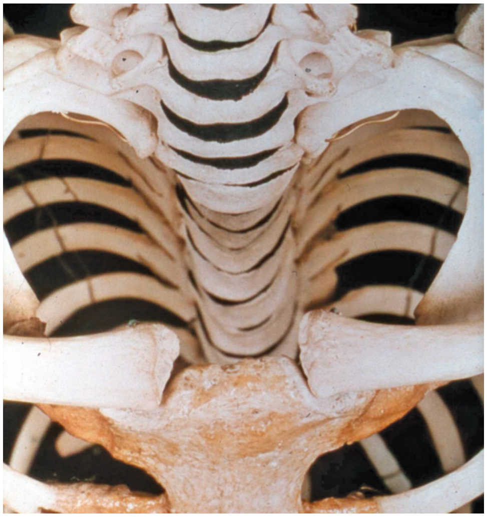

Figure 26.2 Skeletal boundaries of the thoracic outlet.

The terms *thoracic outlet* and *thoracic outlet syndrome* are of relatively recent coinage and were devised in 1958 by Rob and Standeven. Thoracic outlet syndrome denotes a group of disorders that are characterized by a pathological and sustained compression of neurovascular structures at, or in the vicinity of, the superior aperture of the thoracic cage. In a strictly anatomical sense, the term *thoracic outlet* refers to the area circumscribed by the right and left first ribs and sternal notch. However, in the context of thoracic outlet syndrome, the term *thoracic outlet* includes a good deal more regional anatomy than is implied by the strict and precise anatomical definition of the term.

Structures crossing the thoracic outlet

The central part of the thoracic outlet is occupied by the oesophagus and trachea, the latter lying in front of the oesophagus and immediately behind the sternal notch. The oesophagus at this level lies immediately in front of the vertebral column. Lateral to these two large tubes, on either side, are the corresponding vagus and phrenic nerves (Figure 26.1). Crossing the thoracic outlet from below upwards are: (i) the left common carotid and subclavian arteries which lie to the left of the trachea and oesophagus and (ii) the brachiocephalic artery lying to the right of the trachea and oesophagus. Crossing the thoracic outlet from above downwards are the right and left brachiocephalic veins. Each brachiocephalic vein is formed behind the corresponding sternoclavicular joint by the confluence of the ipsilateral internal jugular and subclavian veins. Having thus entered the superior mediastinum, the left brachiocephalic vein runs obliquely to the right where it joins the much shorter right brachiocephalic vein to form the superior vena cava (Figure 26.1). Crossing the posterolateral part of the thoracic outlet on either side, immediately in front of the neck of the corresponding first rib, are the ipsilateral ganglionated sympathetic chain and the ventral ramus of the first thoracic nerve. The latter helps to form the lower trunk of the brachial plexus (Figure 26.3).

Crossing the left side of the thoracic outlet from below upwards are the thoracic duct and left recurrent laryngeal nerve.

In the context of thoracic outlet syndrome, however, it is the neurovascular structures that are destined for the upper limb that are significant. These are the subclavian artery, subclavian vein and brachial plexus (Figure 26.4). The subclavian artery and brachial plexus emerge in the narrow interval between the scalenus anterior and scalenus medius, while the subclavian vein runs in front of the scalenus anterior before crossing above the first rib to enter the axilla. Any of these structures, either singly or in combination, may be subject to pathological compression, resulting in thoracic outlet syndrome. Thus thoracic outlet syndrome may be classified into neurogenic, arterial or venous types, or any combination thereof. Clinical examination complemented by the results of appropriate neurophysiological and vascular investigations will usually lead to an accurate diagnosis.

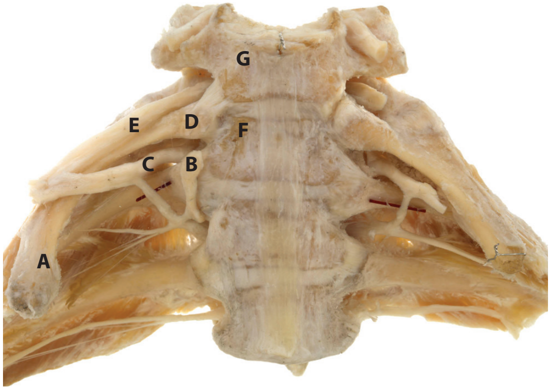

Figure 26.3 Structures crossing the posterolateral (right) aspect of the thoracic outlet. A – first rib. B – sympathetic chain. C – ventral ramus of T1. D – head of first rib. E – ventral ramus of C8. F – T1 vertebra. G – C7 vertebra.

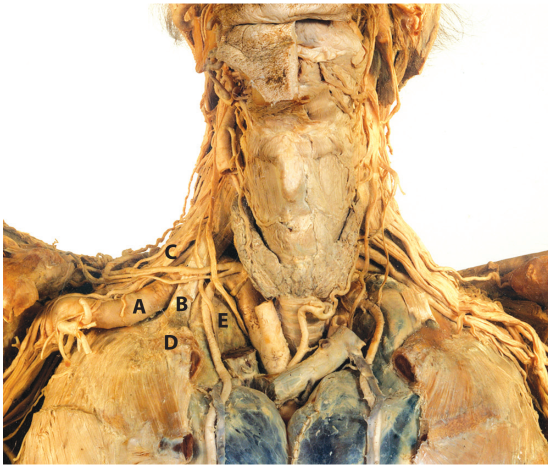

Figure 26.4 Dissection showing the scalene muscles of the right side and neurovascular structures crossing above the first rib. A – subclavian artery. B – scalenus anterior. C – brachial plexus. D – first rib. E – apex of right lung.

Conceptually speaking, thoracic outlet neurovascular compression may occur at one of four possible anatomical levels. Starting proximally these four levels are as follows:

1. Interscalene level (between scalenus anterior and medius).
2. Sternocostovertebral space (e.g. due to a congenital abnormality such as a cervical rib or cervical band).
3. Costoclavicular passage (the interval between the first rib and middle third of the clavicular shaft through which the neurovascular structures pass into the axilla).
4. Subcoracoid space (deep to pectoralis minor).

The first rib

Of all the ribs, the first rib is the most acutely curved and often the shortest (Figure 26.5). Its shaft is flat and wide, and presents upper and lower surfaces that are demarcated from each other by inner and outer borders. The posterior end of the rib is termed *the head of the rib* by which the rib articulates with the body of the first thoracic vertebra at a stable synovial joint. Extending posterolaterally from the head of the rib is a narrow neck which is continuous laterally with the shaft of the rib. The anterior end of the shaft is attached to the costal cartilage which in turn articulates with the manubrium sterni through a primary cartilaginous joint. This joint is practically immovable. On the outer aspect of the first rib, at the junction of the neck and shaft, is a prominent tubercle. This forms a very stable synovial articulation with the transverse process of the first thoracic vertebra.

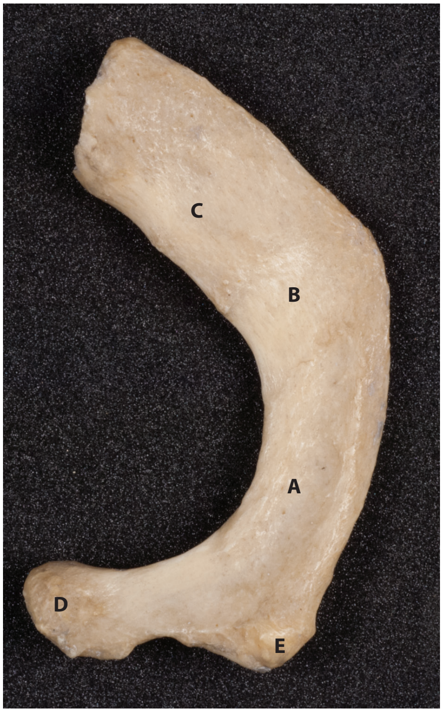

Figure 26.5 The right first rib (viewed from above). A – site of attachment of scalenus medius. B – groove for subclavian artery. C – site of attachment of scalenus anterior. D – head of rib. E – tubercle of rib.

The upper surface of the shaft of the first rib shows a shallow but significant groove running from the inner border of the rib to the outer border (Figure 26.5). The subclavian artery and the lower trunk of the brachial plexus lie over this groove as they cross the first rib to enter the axilla. Posterolateral to this groove, on the upper surface of the shaft, is a relatively large quadrilateral area to which is attached the scalenus medius muscle (Figures 26.4 and 26.5). Attached to the scalene tubercle and to an adjacent area on the upper surface of the rib is the scalenus anterior muscle. The scalene tubercle is a small, triangular inward projection of the inner border of the first rib, about two-thirds of the way from the posterior end of the rib. Lying above the first rib, anterior to the attachment of the scalenus anterior, is the subclavian vein. Attached to the inner border of the shaft of the first rib is a fibrous sheet, the suprapleural membrane (Sibson's fascia), which sits atop the apical pleura.

Should thoracic outlet syndrome occur in the absence of a cervical rib or cervical band, excision of the first rib may offer the best chance of providing satisfactory relief from thoracic outlet compression. The rationale for this procedure is that by excising the middle segment of the first rib, the costoclavicular interval is substantially widened. Also, any compressive effects caused by the scalene muscles (due to presumed scalene muscle hypertrophy) are eliminated when the scalene muscles are detached from their costal attachments. Excision of the first rib undertaken for thoracic outlet syndrome involves removal of the middle third of the rib. The posterior third of the rib (including the head, neck and tubercle) is left intact as are the anterior end of the rib and first costal cartilage. Prior to removal of the middle third of the rib, the scalenus anterior and medius muscles must be carefully detached from the upper surface of the rib, taking great care not to damage the subclavian vessels and brachial plexus. The intercostal muscles and the first digitation of the serratus anterior must be detached from their respective attachments to the outer border of the shaft of the first rib. The suprapleural membrane must be freed from its attachment to the inner border of the first rib, taking care not to damage the underlying apical pleura and lung. Yet another important structure which is at risk during first rib excision is the phrenic nerve. The latter runs immediately in front of the scalenus anterior.

THE SCALENE MUSCLES

As with all neck muscles, the scalene muscles are symmetrically arranged on either side of the vertical midline of the neck. The scalene muscles constitute the lateral prevertebral musculature and are covered by the prevertebral layer of deep cervical fascia. On each side of the neck there are three scalene muscles: scalenus anterior, scalenus medius and scalenus posterior (Figure 26.4). They are flat muscles which arise as narrow slips from the transverse processes of the cervical vertebrae, and run inferolaterally to attach to the upper part of the rib cage. Scalenus anterior and medius are attached to the upper surface of the shaft of the first rib, while scalenus posterior is attached to the upper and outer surface of the second rib. Scalenus anterior arises by tendinous slips from the anterior tubercles of the 3rd, 4th, 5th and 6th cervical vertebrae. The muscle runs inferolaterally to gain attachment to the scalene tubercle and adjacent upper surface of the first rib. Scalenus medius arises from the posterior tubercles of nearly all of the cervical vertebrae. The slips of origin of the muscle unite to form a single mass which is attached to the upper surface of the first rib over a fairly large area (Figures 26.4 and 26.5). Scalenus posterior arises from the posterior tubercles of the lower two or three cervical vertebrae. The slender muscle passes over the shaft of the first rib deep to the first digitation of serratus anterior, to gain attachment to the second rib.

Surgical decompression of the thoracic outlet may be achieved by either of two approaches: (i) supraclavicular approach or (ii) transaxillary approach. Anterior scalenotomy (division of scalenus anterior muscle) and excision of an aberrant cervical rib or cervical band are best done using a supraclavicular approach. However, should excision of the first rib be indicated, this is most safely and effectively undertaken through a transaxillary approach.

FURTHER READING

Dorazio RA, Ezzet F. Arterial complications of the thoracic outlet syndrome. *American Journal of Surgery*. 1979; 138: 246–50.

Janssen F, Niblett PG, Raji E, Thompson JF. The thoracic outlet syndromes. *Vascular Medicine Review*. 1995; 6: 215–25.

McMinn RMH. *Last's Anatomy: Regional and Applied*. 9th ed. Edinburgh: Churchill-Livingstone, 1994.

Pollak EW. Surgical anatomy of the thoracic outlet syndrome. *Surgery, Gynecology, and Obstetrics*. 1980; 97–102.

Rob CG, Standeven A. Arterial occlusion complicating thoracic outlet compression syndrome. *British Medical Journal*. 1958; 2: 709–12.

Roos DB. The place for scalenectomy and first rib resection in thoracic outlet syndrome. *Surgery*. 1982; 92: 1077–85.

Roos DB. Transaxillary first rib resection for thoracic outlet syndrome: Indications and techniques. *Contemporary Surgery*. 1985; 26: 55–62.

Sellke FW, del Nido PJ, Swanson SJ. *Sabiston and Spencer's Surgery of the Chest*. 8th ed. Philadelphia: Saunders Elsevier, 2010.

Urschel Jr HC, Kourlis Jr H. Thoracic Outlet Syndrome – A 50-year experience at Baylor University Medical Center. *Baylor University Medical Center Proceedings*. 2007; 20: 125–35.

27

Cervical spine

HITESH DABASIA AND JASON HARVEY

Introduction 267
Bony anatomy 267
Typical *267*
Atypical *269*
Neural anatomy 269
Anatomical considerations for cervical spine surgery 269
Anterior procedures *269*
Posterior procedures *272*
Anatomical hazards *273*
Vertebral artery: anatomy *273*
Anterior approaches *274*
Posterior approaches *274*
Anomalies *275*
Further reading 275

INTRODUCTION

The key to successful surgery on the cervical spine is detailed planning. This includes a thorough understanding of the relevant surgical anatomy, both of the bony cervical spine and its overlying structures and of their relationship to the chosen surgical approach.

This chapter will present key features of the bony anatomy and describe the relevant anatomy with respect to the anterior and posterior surgical approaches. The key anatomical hazards of cervical spine surgery will also be discussed.

BONY ANATOMY

The cervical spine comprises seven vertebrae, four typical and three atypical.

Typical

The typical vertebra, C3 to C6, comprises a body and a vertebral arch formed from posterolateral projections of the pedicles and lamina (Figure 27.1). At the superior border of each vertebra there is a posterolateral bony projection called the uncus or uncinate process. This articulates with the inferior aspect of the vertebra above, forming the 'uncovertebral joints' or 'joints of Luschka'. The superior and inferior facets, arising from the lateral mass, form a synovial joint that is surrounded by a fibrous capsule. They are inclined at 45 degrees from the horizontal plane. Lateral to the body are two contributing roots, anterior and posterior, forming the transverse process. This contains a foramen through which passes the vertebral artery. The spinous processes of C3 to C6 are usually bifid.

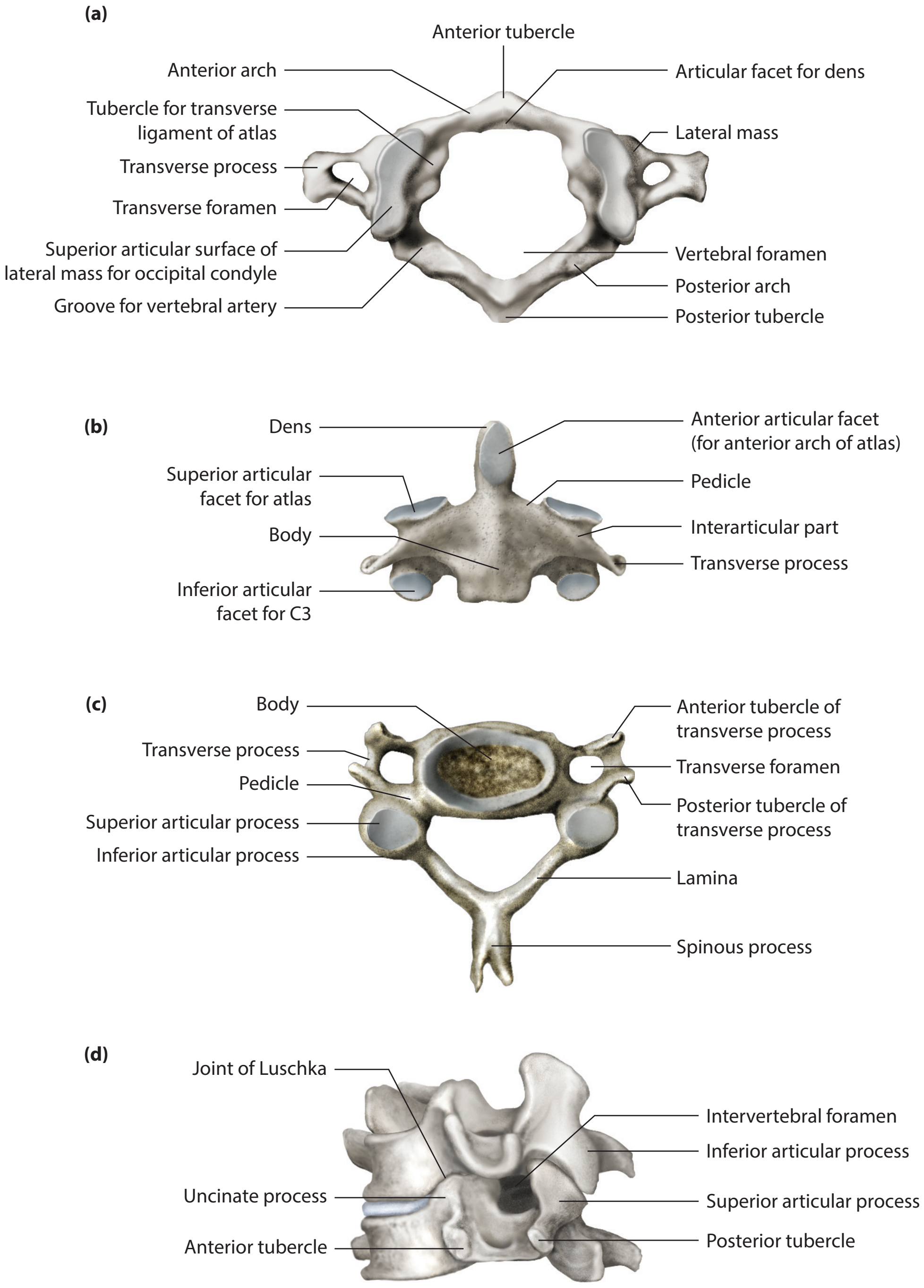
(a)
Anterior tubercle
Anterior arch
Articular facet for dens
Tubercle for transverse ligament of atlas
Lateral mass
Transverse process
Transverse foramen
Superior articular surface of lateral mass for occipital condyle
Vertebral foramen
Posterior arch
Groove for vertebral artery
Posterior tubercle
(b)
Dens
Anterior articular facet (for anterior arch of atlas)
Superior articular facet for atlas
Pedicle
Body
Interarticular part
Transverse process
Inferior articular facet for C3
(c)
Body
Anterior tubercle of transverse process
Transverse process
Transverse foramen
Pedicle
Posterior tubercle of transverse process
Superior articular process
Inferior articular process
Lamina
Spinous process
(d)
Joint of Luschka
Intervertebral foramen
Inferior articular process
Uncinate process
Superior articular process
Anterior tubercle
Posterior tubercle

Figure 27.1 Diagrammatic representation of **(a)** C1 vertebra [atlas]; **(b)** C2 vertebra [axis]; **(c)** typical cervical vertebra and **(d)** articulation of two typical cervical vertebrae demonstrating the intervertebral foramen and uncovertebral joint of Lushka.

Atypical

The C1, C2 and C7 vertebrae are considered to be atypical. The C7 vertebra, although similar to the typical cervical vertebra, has a longer, nonbifid spinous process and a transverse foramen that may be present but does not contain a vertebral artery.

The C1 vertebra (atlas) and C2 vertebra (axis) (Figure 27.1) are unique in their appearance. C1 lacks a body and spinous process. It comprises a ring-like structure formed by a short anterior arch, longer posterior arch and a set of lateral masses. The vertebral artery and C1 nerve root course a groove on its upper surface.

The C2 vertebra is characterized by a long spinous process and a superior bony projection from the body called the 'dens' or 'odontoid peg'. This articulates with the anterior arch of the atlas. The transverse foramen is directed upwards and outwards, thereby allowing the coursing vertebral artery to reach the more laterally placed C1 foramen. The dimensions of the spinal canal are greatest at this level.

NEURAL ANATOMY

There are eight cervical nerves, each exiting above the correspondingly numbered vertebra, with the exception of the 8th cervical nerve, which leaves through the foramen formed between C7 and T1. The foramen is bounded by the pedicles superiorly and inferiorly, posteriorly by the facet joints, and anteriorly by the uncovertebral joint and intervertebral disc (Figure 27.1). The exiting nerve passes above its correspondingly numbered pedicle. This differs from the thoracic and lumbar spine; the exiting nerve here passes below its correspondingly numbered pedicle.

ANATOMICAL CONSIDERATIONS FOR CERVICAL SPINE SURGERY

Anterior procedures

The structures anterior to the cervical spine are arranged into various compartments by the overlaying fascial layers. An awareness of these layers is fundamental to the understanding of anterior approaches to the cervical spine. The anatomical structures that are encountered will differ depending on the level of surgery. Superficial palpable landmarks in the midline can act as a useful marker for the underlying cervical level: hyoid bone (C3 vertebra), thyroid cartilage (C4/C5 level) and cricoid cartilage (C6 vertebra). We would nevertheless recommend the use of intraoperative imaging to help confirm the desired level.

The fascial layers can be divided into the superficial and deep cervical fascia. The deep cervical fascia has three principal layers: the investing fascia, pretracheal fascia and prevertebral fascia, with the addition of the carotid sheath. The 'workhorse' and commonly used surgical approach to the anterior cervical spine is that described by Robinson and Smith, and later modified by Southwick and Robinson. This involves surgical dissection through these fascial planes and usually provides adequate surgical exposure from C3 to T1 (Figure 27.2).

The superficial fascia is continuous around the neck and merges with the fascial layers over the clavicle and deltopectoral regions. It contains the platysma muscle, a thin, flat structure which extends from the inferior margin of the mandible down to the pectoralis major and deltoid muscle. It is usually split in line with its longitudinally orientated fibres. The external jugular vein is often encountered in this layer and can be either mobilized or ligated. This now exposes the investing fascia, a circumferentially orientated layer that splits around, and encompasses, the sternocleidomastoid and trapezius muscles.

The sternocleidomastoid muscle is a prominent and important palpable landmark. It courses obliquely from the mastoid process to its two heads of origin on the sternum and clavicle. It forms a boundary between the anterior and posterior triangles of the neck. It is supplied by the spinal part of the accessory nerve, which enters the muscle proximally, approximately 3 cm below the mastoid process. The fascia is dissected along the anterior border of the muscle, carefully releasing it inferiorly and superiorly and ensuring good haemostasis (Figure 27.3). If the surgical plane of dissection strays beyond the medial border of this muscle, the accessory nerve is at risk of potential injury when it re-emerges along the posterior border, about a third to halfway down the muscle. We would

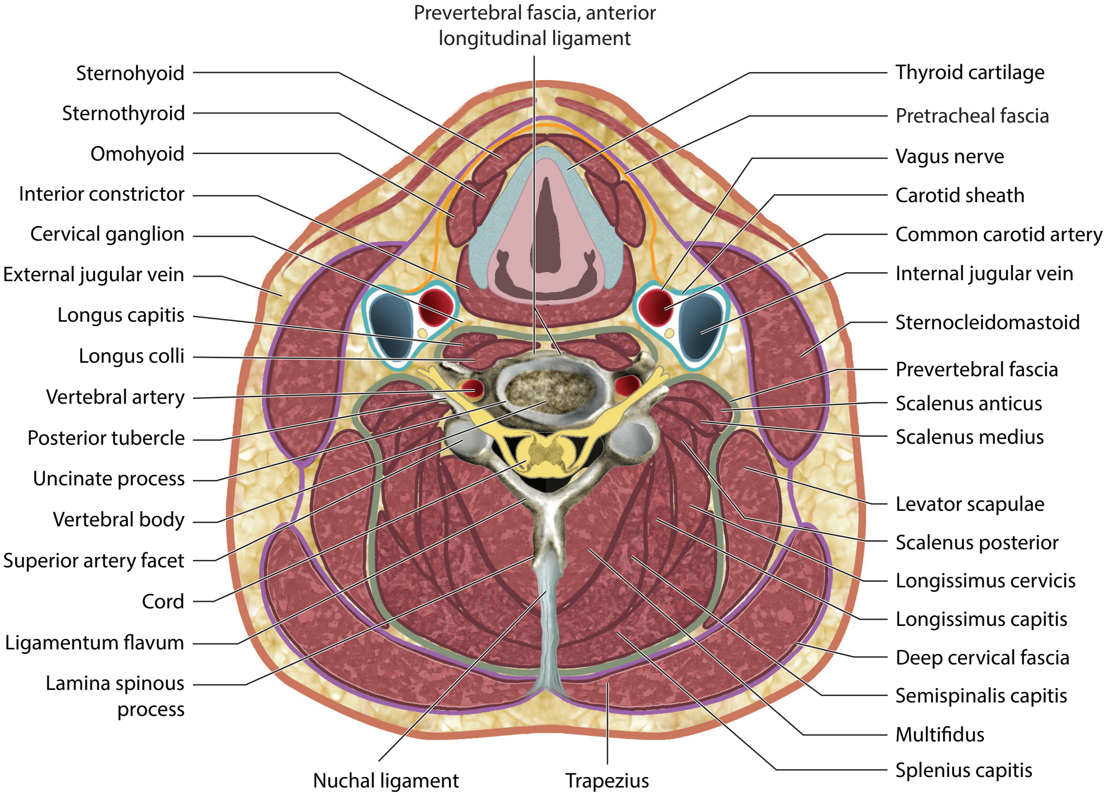
Prevertebral fascia, anterior longitudinal ligament
Sternohyoid
Sternothyroid
Omohyoid
Interior constrictor
Cervical ganglion
External jugular vein
Longus capitis
Longus colli
Vertebral artery
Posterior tubercle
Uncinate process
Vertebral body
Superior artery facet
Cord
Ligamentum flavum
Lamina spinous process
Nuchal ligament
Trapezius
Thyroid cartilage
Pretracheal fascia
Vagus nerve
Carotid sheath
Common carotid artery
Internal jugular vein
Sternocleidomastoid
Prevertebral fascia
Scalenus anticus
Scalenus medius
Levator scapulae
Scalenus posterior
Longissimus cervicis
Longissimus capitis
Deep cervical fascia
Semispinalis capitis
Multifidus
Splenius capitis

Figure 27.2 Cross section through the mid-cervical spine demonstrating the key fascial layers, as well as the adjacent structures lying anterior, posterior and lateral to it.

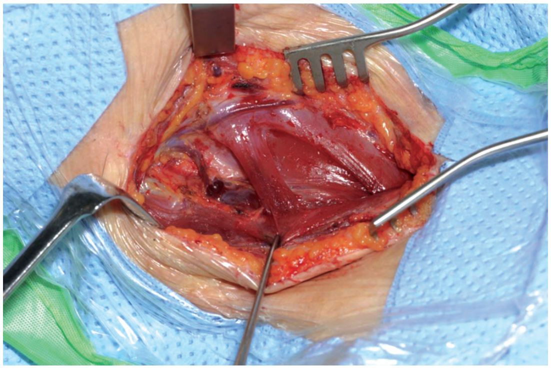

Figure 27.3 The investing fascia overlying the sternocleidomastoid has been released. The strap muscles are orientated closer to the midline, with the omohyoid crossing obliquely across the surgical field. The sternocleidomastoid is reflected laterally with the forceps (at the bottom of this image).

recommend using blunt finger dissection to help develop the plane deep to this.

The carotid artery within its sheath should now be palpable and visualized. The carotid sheath is intimately related to the fascial layers of the neck; anterolaterally it is fused with the investing fascia, anteromedially with the pretracheal fascia and posteriorly it has loose connections with the prevertebral fascia. Using blunt finger dissection the exposure is continued through the pretracheal fascia along the medial border of the carotid sheath (Figure 27.4).

After retraction of the sternocleidomastoid and carotid sheath laterally, and the oesphagus, trachea and strap muscles medially, the anterior surface of the cervical spine should be exposed (Figure 27.5). It is important to maintain gentle, controlled medial retraction to minimize inadvertent damage to the oesophagus. The prevertebral fascia covers the anterior longitudinal ligament and the longus

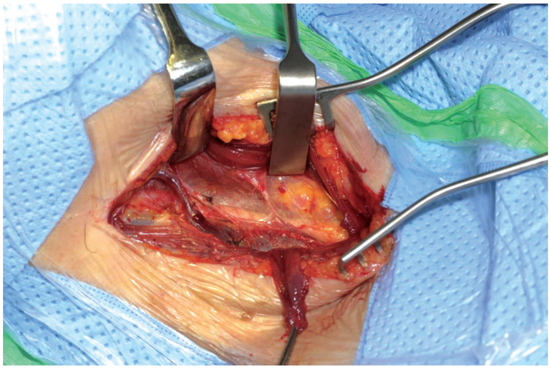

Figure 27.4 The carotid artery is identified below the medial border of the sternocleidomastoid. Further dissection is continued through the pretracheal fascia. (Note that the omohyoid has been divided and retracted laterally.)

colli muscles on either side of the vertebral body (Figure 27.6). This layer can be bluntly dissected off using peanut dissectors. Often at this point the surgeon will confirm that the correct surgical level has been exposed using intraoperative imaging. The longus colli muscles are elevated subperiosteally on either side to provide further exposure (Figure 27.7). They extend from the atlas to the third thoracic vertebra and are segmentally innervated by the anterior rami of the spinal nerves. It is vital not to stray too lateral, especially at the level of the disc, as this can injure the vertebral artery. It also helps in avoiding injury to the cervical sympathetic plexus that runs over the longus colli at the level of the transverse processes. Injury to this structure can lead to a postoperative Horner's syndrome.

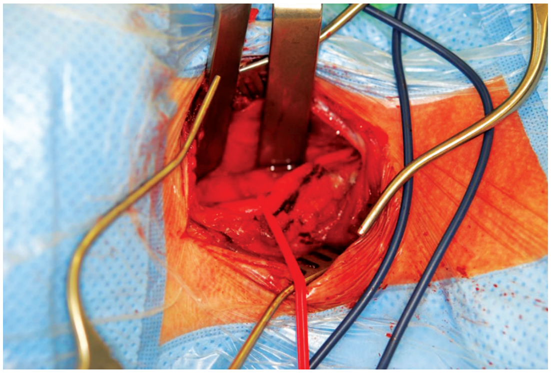

Figure 27.5 Dissection progressed onto the anterior cervical spine, with the carotid artery gently retracted laterally with a vascular sling in situ.

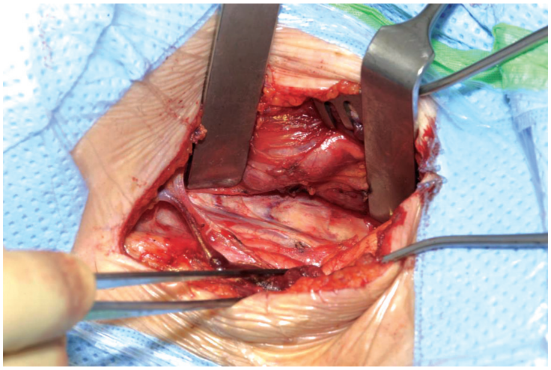

Figure 27.6 The anterior vertebral bodies and intervertebral discs are exposed after bluntly dissecting off the prevertebral fascia.

The recurrent laryngeal nerve is a structure that can potentially be injured during anterior cervical spine surgery. The differing anatomical course of the right and left recurrent laryngeal nerves is described in detail in Chapter 22. Some surgeons advocate a left-sided approach because the differing course, as well as possible anatomical variations on the right, can place it at greater risk of injury. However, this is not supported by evidence in the literature.

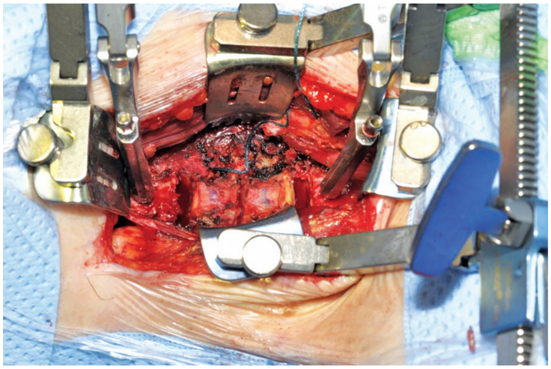

Figure 27.7 Using appropriate retraction systems, excellent exposure is achieved. The longus colli muscles have been elevated and reflected laterally. The intervertebral discs have been excised, prior to undertaking a two-level vertebrectomy.

Surgical exposure at the level of C3 may encounter the superior thyroid artery, the first branch of the external carotid artery. It is important to be aware that the superior laryngeal nerve often follows it closely. Exposure of the lower cervical spine may encounter the inferior thyroid artery. Approaches to the cervico-thoracic junction through a left-sided approach can injure the thoracic duct. This is the primary lymphatic structure into which smaller tributaries drain. It extends vertically in the chest, on the left of the oesophagus, curving posteriorly to the left carotid artery, internal jugular vein and vagus nerve to empty into the systemic circulation, either at the junction of the left internal jugular and subclavian vein, or into one of these structures solely.

Posterior procedures

The posterior cervical spine is covered, from superficial to deep, by longitudinally orientated musculature. Two important palpable surface landmarks are the external occipital protuberance and the spinous process of C7.

The ligamentum nuchae is a midline fibro-elastic structure that originates from external occipital protuberance and inserts on the tubercle of the C7 spinous process. It sends septae down to each of the cervical spinous processes and merges with the investing layer of the deep cervical fascia. It is the clinical equivalent of the supraspinous ligament in the cervical spine but is virtually a vestigial structure in humans.

The posterior cervical musculature is divided into three layers (Figure 27.2). The muscle of the superficial layer is the trapezius and covers the entire cervical spine. This muscle takes a largely broad origin from the external occipital protuberance and superior nuchal line, down through to the C7 to T12 spinous processes. It is supplied by the spinal accessory nerve and C3 to C4 cervical nerves. The intermediate layer is made up of the splenius capitis, a flat muscle that takes origin from the ligamentum nuchae and spinous processes of C7 to T3. It inserts laterally onto the occipital bone. Below this is the deeper layer of muscles (semispinalis capitis, semispinalis cervicis, multifidus muscles and short and long rotators).

The approach to the posterior cervical spine is through a midline incision. It is important to maintain sharp subcutaneous dissection onto the investing fascial layer over the trapezius. We recommend the use of diathermy to incise this fascia and to maintain dissection in the relatively avascular plane of the ligamentum nuchae, either side of the midline (Figure 27.8). The paraspinal muscles are elevated subperisoteally en masse from the spinous processes, and then off the lamina and the lateral mass to provide complete exposure (Figures 28.8 and 27.9). The ligamentum flavum, 'yellow ligament', is a paired structure that connects adjacent lamina, extending from the midline to the facet capsule laterally. Directly beneath this lies the spinal cord, and dissection of this ligament must therefore be done carefully.

The anatomy around the posterior C1 and C2 vertebra is important to be aware of because of its pertinent surgical relevance. Below the previously discussed layers of muscle, this region contains a deep group of four muscles (rectus capitis posterior major and minor, and oblique capitis superior and inferior). They form the boundaries of a region called the sub-occipital triangle. The most important structure to be aware of in this triangle is the vertebral artery. After exiting the C1 transverse foramen it courses medially along the posterior ring of C1 and pierces the posterior atlanto-occipital membrane approximately 1.5 cm from the midline. Two cutaneous nerves cross the surgical field laterally, the greater occipital nerve and third

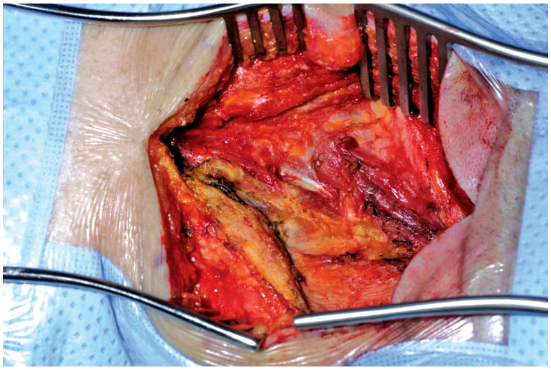

Figure 27.8 After superficial dissection the investing fascia overlying the paraspinal musculature is exposed. The ligamentum nuchae is identified in the midline.

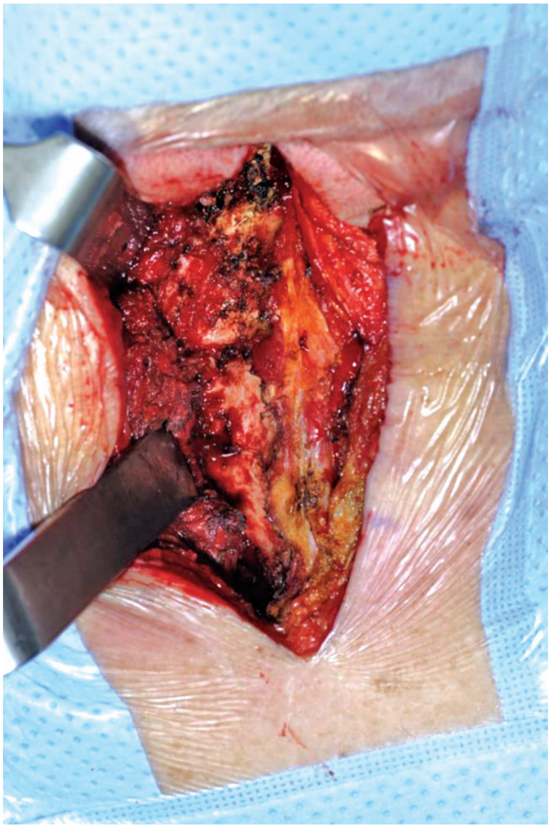

Figure 27.9 Subperiosteal dissection of the paraspinal musculature exposes the underlying spinous processes in the midline, the laminae and the interconnecting ligamentum flavum.

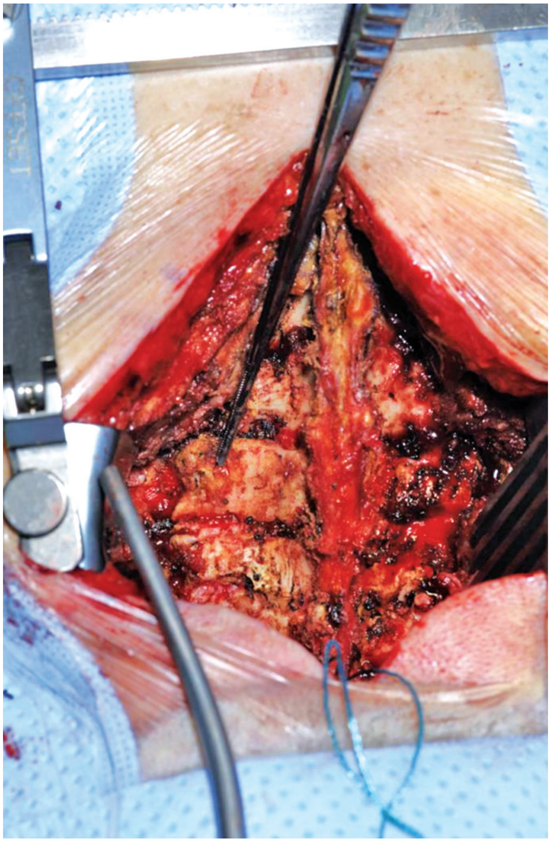

Figure 27.10 Exposure either side of the midline demonstrates the posterior cervical spine as far as the lateral mass.

occipital nerve, posterior primary rami of C2 and C3, respectively. Excessive lateral retraction places them at risk of injury.

Anatomical hazards

A thorough understanding of the anatomy around the cervical spine will help the surgeon identify and negotiate potential anatomical hazards. The importance of careful preoperative planning cannot be stressed enough. This includes evaluating the location of key anatomical structures on available imaging, selecting the most appropriate procedure and approach for a given patient and ensuring optimal patient positioning.

The main hazard for the anterior and posterior approach is the vertebral artery. Other potential hazards are the recurrent laryngeal nerve (discussed in Chapter 22) and the oesophagus.

Vertebral artery: anatomy

Injury to the vertebral artery during cervical spine surgery is rare, with reported rates of between 0.3 per cent and 0.5 per cent for anterior procedures. The consequences of injury are catastrophic and potentially fatal. It arises from the first part of the subclavian artery, coursing between longus colli and scalenus anterior. It can be considered in four anatomical segments. The first, V1, is the proximal segment running from its origin at the subclavian artery to its entry into the C6 transverse foramen. V2 is the segment that runs in the transverse foramen of C6 to C1. V3 is from the arch of the atlas to

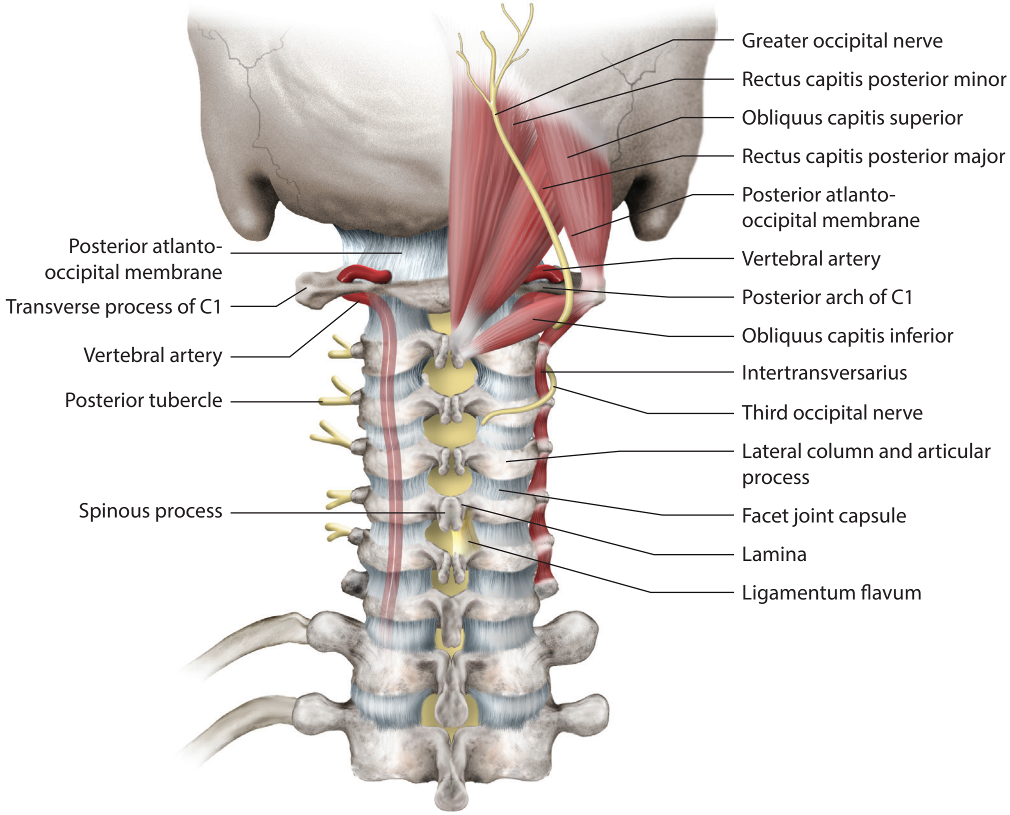
Greater occipital nerve
Rectus capitis posterior minor
Obliquus capitis superior
Rectus capitis posterior major
Posterior atlanto-occipital membrane
Vertebral artery
Posterior arch of C1
Obliquus capitis inferior
Intertransversarius
Third occipital nerve
Lateral column and articular process
Facet joint capsule
Lamina
Ligamentum flavum
Posterior atlanto-occipital membrane
Transverse process of C1
Vertebral artery
Posterior tubercle
Spinous process

Figure 27.11 Diagrammatic representation of the deep muscles of the posterior cervical spine and their relation to the vertebral artery as it ascends towards the atlanto-axial and atlanto-occipital level.

the foramen magnum, and V4 is the final segment that unites with the contralateral vertebral artery to terminate as the basilar artery.

Anterior approaches

The V2 segment is the most susceptible to injury during anterior procedures. The uncovertebral joints provide a reliable intraoperative landmark with the V2 segment taking a course lateral to them. The transverse foramen is less than 6 mm away from the medial margin of these joints, and therefore this should limit the extent of neuroforaminal decompression. It should also be appreciated that there is medialization of the V2 segment in the foramen from C6 to C3, as well as progression from a relatively anterior to posterior position between these levels.

The use of intervertebral disc space distraction causes the uncovertebral joints to open by 3 to 6 mm, and inadvertent instrumentation can injure the artery. It is important to remember that at the C6/C7 level the vertebral artery lies outside of the transverse foramen, and lateral dissection beyond the longus colli at this level places it at risk of injury.

Posterior approaches

During these approaches the artery is at greatest risk when undertaking a C1/C2 transarticular screw insertion. The vertebral artery may be injured by an inadvertent screw trajectory, a too low or too lateral one, as it courses its lateral bend at the level of the lateral mass of C2. The reported rates range from 4.1 per cent to 8.2 per cent. As previously highlighted, it is vulnerable during the posterior approach to the C1/C2 level. An alternative surgical fixation technique at this level, such as that popularized by Harms, involving a C1 lateral mass and C2 pedicle screw rod fixation construct, uses a more medial screw trajectory and may afford a potentially lower risk of injury. Nevertheless, care should be taken with C1 lateral mass screw fixation as the exiting artery from the C2 transverse foramen is in close proximity. It is important to note that at C1 the artery courses posteromedially along a groove on the posterior arch before piercing the atlanto-occipital membrane. It has been recommended that dissection should remain within 12 mm of the midline on the posterior aspect of the ring and within 8 mm of the midline on the superior aspect to avoid damaging it. The subaxial spine can be stabilized with lateral mass screws, which in terms of vertebral artery injury are considered a relatively safer procedure.

Anomalies

Despite adhering to well-described techniques, the presence of anatomical anomalies can predispose to iatrogenic injury. The rates described for anatomical variation range from 2.3 per cent in the subaxial spine to up to 20 per cent in the atlanto-axial spine. In the presence of a tortuous course, the normal landmarks used during anterior surgery, the uncovertebral joints of Luschka, may not be sufficiently reliable to prevent injury. An enlarged C2 vertebral groove has been reported in up to 20 per cent of patients and can erode the pedicle and lateral mass. The bending point of the VA can be anomalous such that it courses the posterior arch of C1 rather than passing through the C1 transverse foramen. Radiological studies have identified a high riding C2 transverse foramen, at least on one side, in 18 per cent of the population, and this potentially places the vertebral artery at risk of injury during C1/C2 transarticular fixation.

The risk of injuring the vertebral artery can be minimized by closely evaluating the preoperative computerized tomography and magnetic resonance imaging to identify the position of the vertebral artery and its relationship to bony landmarks and surrounding structures. Additional arterial imaging is useful where normal morphology no longer exists, such as when dealing with infection, tumours and rheumatoid arthritis.

FURTHER READING

Heller JG, Pedlow Jr FX, Gill SS. Anatomy of the cervical spine. In: Clark CR and The Cervical Spine Research Society. (Ed.). *The Cervical Spine*. 4th ed. Philadelphia: Lippincott Williams & Wilkins, 2005.

Hoppenfeld S, deBoer P, Buckley R. (Eds.). *Surgical Exposures in Orthopaedics: The Anatomic Approach*. 4th ed. Philadelphia: Lippincott Williams & Wilkins, 2009 ; 257–358.

Peng CW, Chou BT, Bendo JA, Spivak JM. Vertebral artery injury in cervical spine surgery: Anatomical considerations, management and preventative measures. *The Spine Journal*. 2009; 9: 70–6.

Silber JS, Albert TJ. Anterior and anterolateral, mid and lower cervical spine approaches: Transverse and longitudinal (C3 to C7). In: Herkowitz HN. (Ed.). *The Cervical Spine Surgery Atlas*. 2nd ed. Philadelphia: Lippincott Williams & Wilkins, 2004; 91–8.

PART 7

28 Neuroanatomy for the head and neck surgeon 279
Peter C. Whitfield
29 Skull base 287
Peter C. Whitfield
30 Osteology of the skull 295
Susan Standring
31 Overview of the cranial nerves 309
Susan Standring
32 Autonomic system in the head and neck 317
Susan Standring

28

Neuroanatomy for the head and neck surgeon

PETER C. WHITFIELD

Overview and embryology 279
The meninges 280
Topography of the brain 280
Blood supply 280
Surgical hazards 283
Venous sinuses, meningeal vessels and bridging veins *283*
Olfactory tract *284*
Optic nerve and chiasm *284*
Internal carotid artery *284*
Cavernous sinus *284*
Facial nerve *284*
Lower cranial nerves, the foramen magnum and clivus *285*
Summary 285
Further reading 285

OVERVIEW AND EMBRYOLOGY

An estimated 100 billion neurones are organized into the human brain. The 1400 g of tissue comprising the brain is arranged in a highly complex series of neural networks receiving 750mL/min^{-1} of blood. The brain develops from the cephalic end of the neural tube. Three primary vesicles form giving rise to the forebrain, midbrain and hindbrain. These give rise to the cerebral hemispheres, thalamus, hypothalamus, midbrain, pons, medulla and cerebellum. The brain communicates with the head and neck structures via the cranial nerves; most of these arise from the brainstem. Connections with the limbs and trunk are via the afferent and efferent spinal cord pathways. The calvarial part of the skull, or skull vault, is formed by membranous ossification of mesenchyme that invests the embryonic brain. The bones of the newborn skull are joined by sutures. The sagittal, coronal and lambdoid sutures are of major importance, with premature fusion leading to craniofacial deformity. The skull base is formed by endochondral ossification of cartilage leading to formation of the skull base components of the ethmoid, sphenoid, petrous and occipital bones. The bones of the face are mainly formed from cartilages of the first two pharyngeal arches with the associated musculature supplied by the mandibular and facial nerves, respectively.

Common disease processes include neoplastic, vascular and traumatic conditions. Surgical access to the brain is achieved directly through the calvarium, or via the skull base or a combination of approaches. No part of the skull, brain or surrounding tissues is immune to pathological processes, with many conditions requiring collaborative surgical teams encompassing neurosurgery, maxillofacial surgery, otolaryngology and plastic surgery.

THE MENINGES

The brain is invested in a layer of pia mater that is adherent to the gyri and sulci. The subarachnoid space lies between the pial layer and the arachnoid. The arachnoid layer is a transparent membrane that envelops the brain. Cerebrospinal fluid (CSF) cisterns are arachnoidal sacs of CSF that are found in close proximity to the cranial nerves at the skull base. They lie between the arachnoid membrane and the pial surface. Microsurgical opening of the CSF cisterns facilitates drainage of CSF and visualization of the vessels and nerves in the area under consideration. These cisterns are evident in life but are not well visualized in cadaveric specimens.

The dura mater is a thick, fibrous membrane that lines the inner surface of the skull. Folds of dura form structurally important partitions within the cranial cavity. The falx cerebri is a sickle-shaped dural membrane located in the midline sagittal plane, separating the cerebral hemispheres. Anteriorly, it is attached to the crista galli. It arches over the corpus callosum to a posterior attachment at the internal occipital protuberance. At this level it forms the tentorium cerebelli, dividing the cranial cavity into the supra and infratentorial compartments. The cerebellum lies beneath the tentorium cerebelli. The superior sagittal venous sinus lies within a dural enclosed fold along the superior aspect of the falx cerebri. The inferior sagittal sinus lies in the free inferior margin of the falx cerebri.

TOPOGRAPHY OF THE BRAIN

The brain comprises the cerebral hemispheres which lie in the supratentorial compartment (Figures 28.1 and 28.2). They are connected by the commissural fibres of the corpus callosum. The cerebellum and brainstem (midbrain, pons, medulla) are located in the infratentorial compartment. The midbrain lies at the level of the tentorial hiatus acting as a conduit for information between the hemispheres and the brainstem. Most of the cranial nerves originate from the brainstem. The hemispheres are subdivided into the frontal, temporal, parietal and occipital lobes. The different lobes undertake important functions; language functions are usually lateralized to the dominant hemisphere. Frontal lobe functions include motor, personality, executive functions and the expressive component of speech. Temporal lobe functions include memory and auditory processing including the receptive component of speech. The parietal lobe is involved in the perception of touch and the integration of sensory information, and the occipital lobe is responsible for visual processing. Deeper structures include the basal ganglia, thalamus and hypothalamus. The basal ganglia contribute to movement control. The thalamus is a key relay station in sensory and circuits and contributes to movement control. The nearby hypothalamus is a centre for autonomic nuclei that subserve sympathetic and parasympathetic functions and is directly connected to the posterior lobe of the pituitary gland. The adjacent anterior pituitary is crucial in orchestrating the body's hormonal milieu, secreting growth hormone, thyroid stimulating hormone, adrenocorticotrophic hormone, gonadotrophic hormones and prolactin. The cerebellum is concerned with the control of posture and muscle coordination.

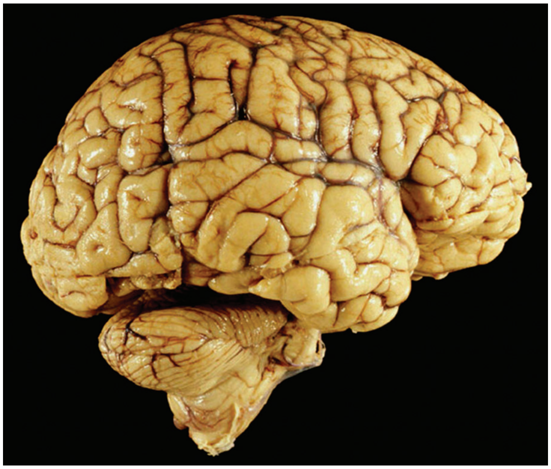

Figure 28.1 Lateral view of the right cerebral hemisphere. From this view note the Sylvian (frontotemporal) fissure lying between the frontal and temporal lobes. Note the cerebellar hemisphere inferiorly. (Supplied by Dr D. Hilton.)

BLOOD SUPPLY

The arterial blood to the brain is supplied by bilateral internal carotid and bilateral vertebral arteries. These supply the anterior and posterior

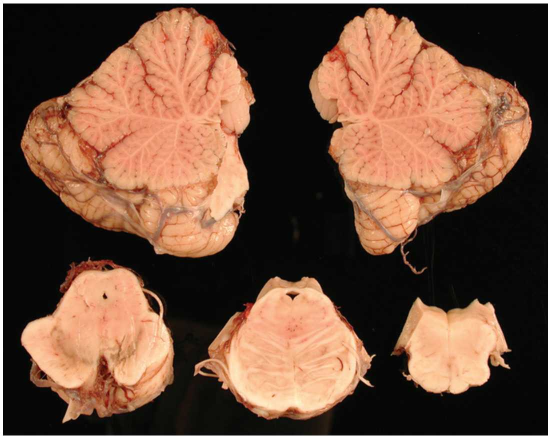

Figure 28.2 Topography of the brain – the cerebellum and brainstem. The cerebellum has been divided in the sagittal plane and splayed open like the pages of a book. This demonstrates the arboreal architecture of the cerebellum. Note the cerebellar tonsil projecting inferiorly. This impacts against the craniocervical junction if 'coning' occurs. The lower panel illustrates axial sections of the midbrain, pons and medulla (from left to right). In the midbrain note the small diameter of the Aqueduct of Sylvius, the pigmented substantia nigra and the cerebral peduncles projecting anteriorly. The pons is characterized by the prominent transverse pontine fibres – these are fibres connecting the motor cortex to the cerebellum allowing the cerebellum to modulate coordination. The medulla contains several cranial nerve nuclei subserving autonomic functions. Compression of these during coning ultimately causes brainstem death. (Supplied by Dr D. Hilton.)

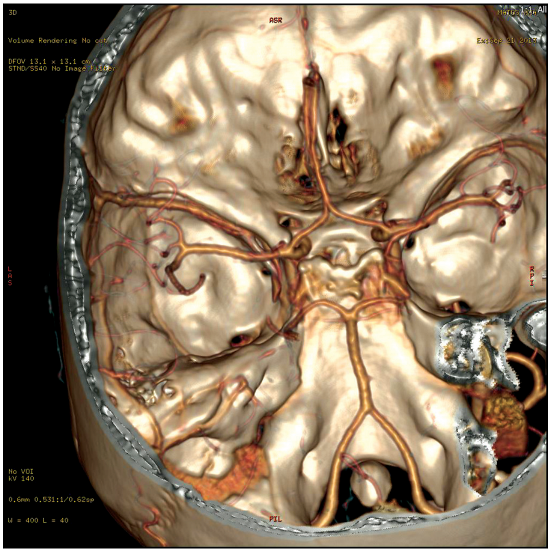

Figure 28.3 Circle of Willis. This is a 3D computerized tomography angiogram. In the posterior circulation, the vertebral arteries unite forming the basilar artery. Anteriorly, the bilateral internal carotid arteries bifurcate into the medially projecting anterior cerebral arteries and the laterally projecting middle cerebral arteries. The distal segments of the anterior cerebral arteries travel in the interhemispheric plane in close apposition to each other. In this case the posterior communicating arteries are not well visualized. (Supplied by Dr W. Mukonoweshuro.)

circulations, respectively. The posterior communicating arteries arise from the posterior aspect of the intracranial component of the internal carotid arteries and join the posterior cerebral arteries providing an anastomotic link (of variable degree) between the anterior and posterior circulations. This was eloquently described as the Circle of Willis in the seventeenth century (Figure 28.3). On entry into the skull, the internal carotid artery (Figure 28.4) traverses the cavernous sinus. The ophthalmic artery is a small branch that arises at the point of emergence into the subarachnoid space. The next branch is the posterior communicating artery followed by the anterior choroidal artery: a small branch that often supplies the descending motor fibres located within the confines of the internal capsule. The internal carotid artery then bifurcates into the medially directed anterior cerebral artery and the laterally directed middle cerebral artery. The anterior cerebral artery crosses the optic nerve and then abruptly turns in an anterosuperior direction to supply the frontomedial aspect of the cerebral hemispheres via the frontobasal, pericallosal and callosomarginal terminal branches. At the point of inflection, the anterior communicating artery, a short (2 mm) branch, provides a direct communication between the right and left anterior cerebral vessels. This is a key component of the Circle of Willis. The middle cerebral artery travels in the frontotemporal (Sylvian) fissure. After a few centimetres it bifurcates into end arteries supplying the bulk of the cerebral hemispheres.

Perforating branches arise from both the anterior and middle cerebral vessels supplying the deep structures including the basal ganglia, thalamus, hypothalamus, internal capsule and insula. The vertebral arteries enter the dura at the level of the foramen magnum (Figures 28.4 and 28.5). The first significant branch is the posterior inferior cerebellar artery which follows a tortuous course, supplying the lateral brainstem and the posterolateral aspect of the cerebellar hemispheres. The vertebral arteries unite on the ventral surface of the brainstem forming the basilar artery. This projects superiorly on the ventral surface of the pons, giving rise to the paired anterior inferior cerebellar arteries, labyrinthine arteries, superior cerebellar arteries and multiple pontine perforating branches. At the level of the midbrain the basilar artery bifurcates, forming the paired posterior cerebral arteries. These course around the midbrain, pass above the tentorium cerebelli and supply the medial aspect of the occipital lobes. They receive important anastomotic connections with the anterior circulation via the posterior communicating arteries.

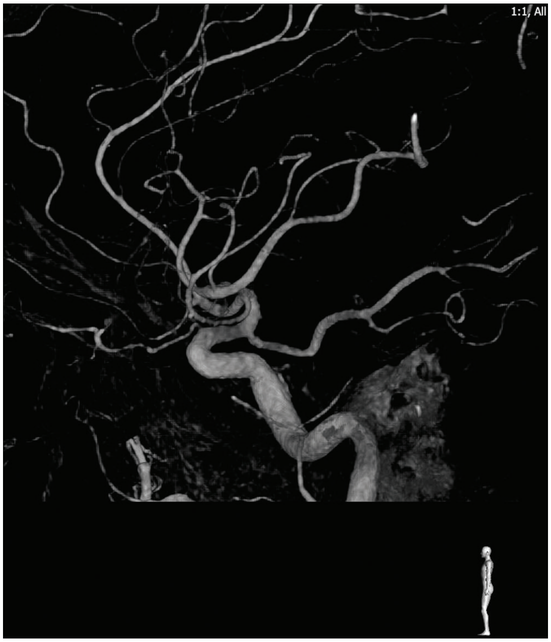

Figure 28.4 Internal carotid artery. This is a 3D angiogram of the left internal carotid artery. The tortuous course of the cervical, petrous and cavernous segments is evident. The first branch of the supraclinoid segment is the ophthalmic artery: a small vessel in this case. The posterior communicating artery is then seen to project posteriorly. In this case it is a large vessel and appears to supply the occipital lobes via the posterior cerebral vessels. This arrangement is an embryological variant called a 'fetal type' circulation and is present in approximately 20 per cent of cases. (Supplied by Dr W. Mukonoweshuro.)

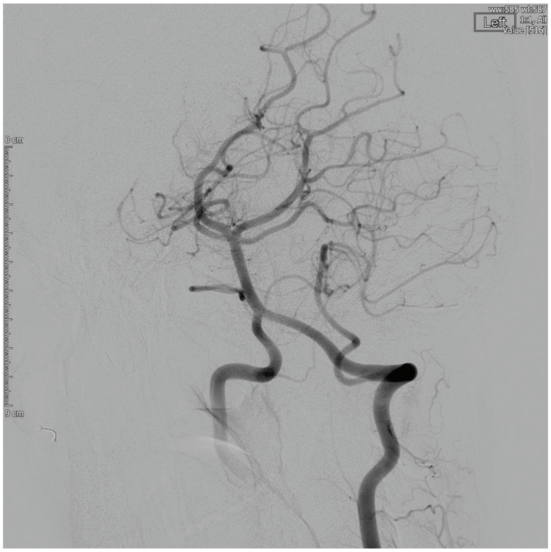

Figure 28.5 Oblique view digital subtraction angiogram of the left vertebral artery. In this case conventional posterior circulation anatomy is evident. The basilar artery can be traced to the basilar bifurcation where the posterior cerebral arteries are formed. The large branches just below the posterior cerebral vessels are superior cerebellar arteries and supply much of the upper part of the cerebellum and upper brainstem. (Supplied by Dr W. Mukonoweshuro.)

The venous drainage of the brain is via superficial and deep venous drainage networks (Figure 28.6). Deep structures (e.g. thalamus) drain via the paired basal and internal cerebral veins. These then unite with the superior cerebellar vein from the upper brainstem and the inferior sagittal sinus, forming the Great Cerebral Vein (of Galen) that drains into the straight sinus. The straight sinus lies in the midline 'ridge' of the tentorium cerebelli. At the internal occipital protuberance, deep venous blood is usually directed into the left transverse sinus and thence the sigmoid sinus before departing the cranium in the left internal jugular vein. The superficial components of the hemispheres drain into cerebral veins. The middle cerebral vein (or superior Sylvian vein) is located superficially in the Sylvian fissure and enters the cavernous sinus, which then drains posteriorly to the basilar-petrosal sinus confluence and jugular veins. Other superficial cerebral veins pass directly to the superior sagittal sinus and to the transverse/sigmoid junction. The larger of these have eponymous names despite the considerable variability in clinical practice: the inferior anastomotic vein of Labbé drains in an postero-inferior direction from the Sylvian fissure to the transverse sinus; the superficial anastomotic vein of Trolard passes superomedially from the Sylvian fissure to the superior sagittal sinus at the level of the precentral (motor) gyrus; the Rolandic vein drains the superficial cortex to the superior sagittal sinus anterior to the vein of Trolard. Venous blood in the superior sagittal sinus travels posteriorly to the confluence of sinuses at the internal occipital protuberance. It then usually enters the right transverse and thence the sigmoid sinus on its descent to the internal jugular vein.

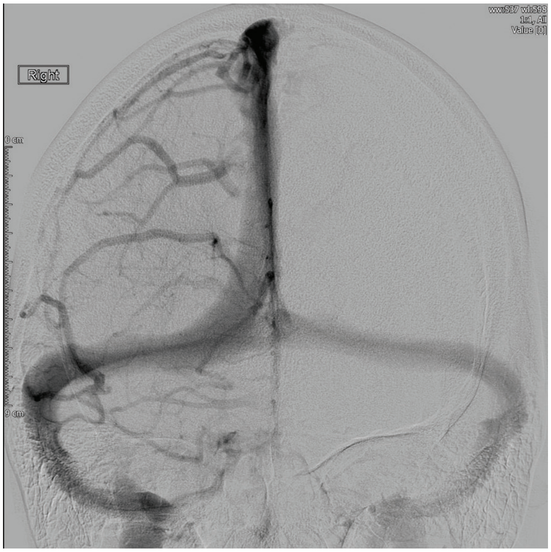

Figure 28.6 Venous drainage of the brain. This is an anteroposterior view of the venous phase of a cerebral angiogram. Cortical veins can be seen connecting to the midline superior sagittal sinus. Blood flows posteriorly towards the confluence of sinuses. In this case most of the blood drains from the confluence via the right transverse and sigmoid sinuses to the internal jugular vein. (Supplied by Dr W. Mukonoweshuro.)

SURGICAL HAZARDS

Surgical approaches to the brain can be undertaken from almost every trajectory. Even though intraoperative navigation can facilitate identification of anatomical landmarks, knowledge of key structures is necessary to minimize trauma and enhance operative safety. Some of the major anatomical hazards are discussed below.

Venous sinuses, meningeal vessels and bridging veins

A craniotomy can be safely elevated directly over a venous sinus, although if this can be avoided the risk of serious haemorrhage is minimized. The superior sagittal sinus lies in the midline as described above. The posterior extent is marked externally by the external occipital protuberance. The transverse sinus runs from the posterior occipital protuberance to the asterion, a junction of sutures where the temporal, parietal and occipital bones meet. This lies just posterosuperior to the mastoid process and is located at the same level as the zygomatic arch, an easily palpable surgical landmark.

The middle meningeal artery arises as a branch of the maxillary artery. It traverses the foramen spinosum, just posterolateral to the mandibular nerve within the larger foramen ovale. The vessel supplies the dura via several branches and can cause bleeding during a pterional craniotomy; it is safely sacrificed during a surgical approach where necessary. Anterior ethmoidal arteries supply much of the anterior fossa dura. These can be a source of profuse bleeding during surgery for invasive tumours of this region.

Once the intracranial compartment is opened, veins may be encountered traversing from the brain to the dural venous sinuses. These veins include bridging veins from the cerebral hemispheres to the superior sagittal sinus and polar veins from the tip of the temporal lobe to the spheno-parietal sinus. These can be divided to prevent inadvertent haemorrhage, though preservation is preferable in the region of the motor cortex.

Olfactory tract

The olfactory tract lies on the undersurface of the frontal lobe. It commences at the olfactory bulb immediately superior to the cribriform plate of the ethmoid bone and projects posteriorly to the proximal Sylvian fissure. The olfactory nerves are vulnerable to traumatic brain injury and is also at risk in anterior skull base surgery, particularly as a result of frontal lobe retraction during a bifrontal craniotomy or a pterional approach.

Optic nerve and chiasm

The optic nerve provides a well-recognized landmark during intracranial surgery that facilitates identification of the internal carotid artery. The optic nerve exits the orbit via the optic canal and emerges into the parasellar region travelling in a posteromedial direction towards the optic chiasm. The supraclinoidal segment of the internal carotid artery is located posterior to the optic nerve. The anterior cerebral artery crosses the posterior segment of the optic nerve. The pituitary stalk is located immediately posterior to the optic chiasm.

Internal carotid artery

The internal carotid artery can be subdivided into four segments. The *cervical* segment passes from the common carotid bifurcation to the skull base. This segment is usually exposed for the purposes of proximal vascular control when operating on pathology in this region of the skull base. The *petrous* segment is difficult to access and lies in close proximity to the cochlea and several cranial nerves (VII, IX, X, XII). The initial vertical component enters the carotid canal before turning at the genu into an anteromedially projecting horizontal segment. The sinusoidal course then continues as the *cavernous* segment. On emergence from the cavernous venous sinus, the internal carotid continues as the *supraclinoid* segment that terminates at the carotid bifurcation.

Cavernous sinus

The cavernous sinus comprises a series of interlinked venous channels and is located immediately lateral to the pituitary fossa. Surgical access to this area is achieved via trans-sphenoidal, pterional (greater wing of sphenoid) and orbitozygomatic approaches. The cavernous segment of the internal carotid is located within the sinus and usually lies several millimetres lateral to the midline. However, an abnormally tortuous vessel can approach the midline and impede trans-sphenoidal surgical access to the pituitary fossa. The lateral wall of the cavernous sinus contains the oculomotor (III) and trochlear (IV) nerves, and the ophthalmic (V1) and maxillary divisions (V2) of the trigeminal nerve. The abducent nerve takes a more medial route, traversing the cavernous sinus in a posterior-anterior direction. The oculomotor, trochlear, abducent and ophthalmic nerves enter the orbit via the superior orbital fissure whilst the maxillary nerve traverses the foramen rotundum.

Facial nerve

The facial nerve has a complex anatomical course and may be encountered in the extracranial, intrapetrous or intracranial segments. The facial nerve enters the deep facial structures at the stylomastoid foramen, passing superficial to the styloid process and entering the posteromedial aspect of the parotid gland where it divides into five principal branches. The temporalis branch innervates the frontalis muscle and is vulnerable during retraction of the temporalis muscle. This can be prevented by division of the temporalis immediately anterior to the tragus, extending inferiorly to the zygomatic arch.

The facial nerve is also vulnerable to injury during transtemporal approaches to the cerebellopontine angle (CP angle), the medial skull base and during otological surgery. The facial nerve traverses the CP angle with the superior and inferior vestibular nerves, the cochlear nerve and the nervus intermedius, which subserves taste and secretion of tears and saliva. The *intracanalicular* component of the facial nerve then traverses the internal auditory canal: this is exposed during retrosigmoid vestibular schwannoma excision. The nerve enters the bony facial canal with the initial *labyrinthine segment* coursing to a location just lateral to the cochlea. The nerve then angles sharply forwards to the geniculate ganglion. Traction on the emerging greater superficial petrosal branch (GPSN) can lead to facial nerve weakness during middle fossa surgery. At the genu, the nerve executes a hairpin bend and runs, as the *tympanic segment,* along the medial wall of the tympanic cavity, inferior to the labyrinth. At the second genu the nerve turns sharply inferior on the posterior wall of the tympanic cavity as the *mastoid segment,* passing directly to the stylomastoid foramen. Other intrapetrous branches include the nerve to stapedius and the chorda tympani.

Lower cranial nerves, the foramen magnum and clivus

Surgical procedures in the region of the jugular foramen, including far-lateral approaches to the foramen magnum, place the lower cranial nerves and the vertebral artery at risk. The vertebral artery usually hugs the posterior surface of the superior articular facet of the atlas. The levator scapulae muscle also provides a useful landmark since the vessel lies immediately medial to the upper attachments of the muscle (posterior tubercles of C1 to C4 transverse processes). The glossopharyngeal, vagus and spinal accessory nerves all exit the skull via the jugular foramen. Postoperative injury causes swallowing impairment and may necessitate tracheostomy. These nerves are soon joined by the hypoglossal nerve before each nerve pursues an individual route. The glossopharyngeal passes forward, superficial to the internal carotid artery, but deep to the external carotid artery supplying the pharynx and posterior one-third of the tongue. The vagus descends between the internal jugular vein and the internal carotid artery. The accessory nerve passes backwards to enter the anterior border of the sternomastoid muscle 3–6 cm below the mastoid tip, and the hypoglossal passes forwards, anterior to the internal and external carotid arteries to reach the tongue.

Extradural lesions in the region of the foramen magnum and clivus (the long bony incline between the posterior aspect of the pituitary fossa and the foramen magnum) are usually approached via an anterior midline corridor of access. This may constitute trans-sphenoidal, transmaxillary or trans-oral approaches. Occasionally, a mandibular osteotomy may be performed to improve access further. These anterior approaches minimize the risk of cranial nerve injury, providing a direct surgical route to the site of pathology. If dural opening is required, the vertebral arteries and basilar artery must be identified and protected. The main complication of such an approach is postoperative CSF leakage and infection.

SUMMARY

It is wise for the head and neck surgeon to be cognizant of basic neuroanatomy. The pattern of blood supply is based upon knowledge of the Circle of Willis and its tributaries. Venous anatomy is important when planning skull openings. Knowledge of cranial nerve regional anatomy is crucial for the avoidance of collateral damage when undertaking combined specialty approaches to the skull base. Such rudimentary knowledge will enhance patient safety and increase the surgical satisfaction achieved when operating on complex, challenging pathological conditions of the brain and surrounding structures.

FURTHER READING

Crossman AR, Neary D. *Neuroanatomy*. 4th ed. Edinburgh: Churchill Livingstone Elsevier, 2010.

Logan BM, Reynolds P, Hutchings RT. *McMinn's Colour Atlas of Head and Neck Anatomy*. 4th ed. Philadelphia: Mosby, 2009.

Rhoton Jr AL. *Cranial Anatomy and Surgical Approaches*. Philadelphia: Lippincott, Williams & Wilkins, 2003.

Sadler TW. *Langman's Medical Embryology*. 12th ed. Philadelphia: Lippincott, Williams & Wilkins, 2012.

29

Skull base

PETER C. WHITFIELD

Introduction 287
Anatomy of the skull base 287
Medial structures *287*
Lateral structures *288*
Specific considerations 288
Internal carotid artery *288*
Trigeminal nerve *288*
Facial nerve *290*
Foramen magnum *290*
Facial skeleton 291
Surgical approaches to the skull base 291
Further reading 294

INTRODUCTION

Surgery for intradural pathology lies within the expertise of the neurosurgeon. However, access to skull base lesions is difficult. A wide range of skull base approaches have evolved to facilitate exposure of skull base lesions, usually in combination with head and neck, ear, nose and throat (ENT), or maxillofacial surgeons. An understanding of anatomy enables surgical approaches along the major corridors of access to be undertaken. This chapter aims to aid understanding of this complex area by describing the regional anatomy and then referencing this to some of the key surgical approaches

ANATOMY OF THE SKULL BASE

Medial structures

The skull base comprises medial and lateral components. Descriptions of these structures can be considered from the inside of the skull (endocranial) or from outside the skull (exocranial). The endocranial midline structures in the anterior cranial fossa include the crista galli and cribiform plate, which are components of the ethmoid bone, and the planum sphenoidale (sometimes called the jugum of the sphenoid) towards the posterior aspect. The olfactory nerves pass through the cribiform plate. The central portion of the middle cranial fossa, located posterior to the planum sphenoidale, comprises the pituitary fossa, with the adjacent cavernous sinuses. The pituitary fossa overlies the sphenoid air sinus, enabling relatively straightforward access to be obtained via a trans-sphenoidal route. The cavernous sinus is a venous confluence that invests the cavernous component of the carotid artery in the parasellar region. The abducens nerve passes through the sinus. The oculomotor, trochlear, ophthalmic and maxillary nerves are all in close proximity to the lateral wall of the sinus. The clivus is the long slope of bone extending from the posterior aspect of the pituitary fossa (posterior clinoid processes) to the foramen magnum.

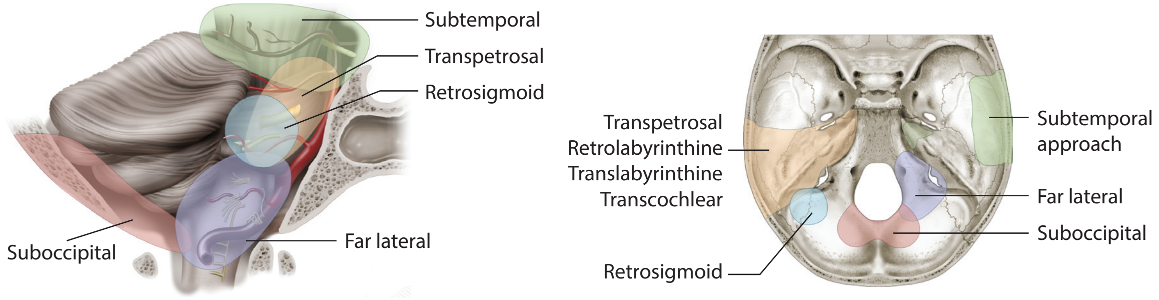

Figure 29.1 Neurosurg Focus@2005 American Association of Neurological Surgeons. Medscape.com

Lateral structures

The orbital part of the frontal bone and the lesser wing of the sphenoid bone form the lateral components of the anterior fossa floor. The lateral part of the middle fossa floor consists of the sphenoid and temporal bones. The superior orbital fissure is located between the greater and lesser wings of the sphenoid bone and provides passage for the oculomotor, trochlear, ophthalmic and abducens nerves. The optic canal (optic nerve) is located at the attachment of the lesser wing to the body of the sphenoid bone. The foramen rotundum (maxillary nerve) and foramen ovale (mandibular nerve) are located in the greater wing of the sphenoid bone. The foramen spinosum (middle meningeal artery) lies posterolateral to the foramen ovale within the greater wing. The remainder of the middle fossa floor consists of the squamous and petrous components of the temporal bone.

When the skull base is viewed from below, the central part comprises the body of the sphenoid and the clival part of the occipital bone, anterior to the foramen magnum. Anteriorly, the medial and lateral pterygoid plates project inferiorly from the sphenoid bone. These separate the medial and lateral components of the skull base. The lateral components of the exocranial aspect of the middle cranial fossa consist of the greater wing of the sphenoid bone and the squamous, styloid and petrous components of the temporal bone. Four spaces lie beneath the middle fossa floor. These are the infratemporal fossa, the pterygopalatine fossa, the parapharyngeal space and the infrapetrosal space. These are summarized in Table 29.1.

SPECIFIC CONSIDERATIONS

Internal carotid artery

The internal carotid artery (ICA) is described in four segments. The *cervical segment* of the ICA arises at the level of the thyroid cartilage (C4) and ascends, deep to the posterior belly of digastic, the styloid process and the parotid gland, to the carotid canal in the petrous temporal bone. The vessel is accompanied by sympathetic nerves from the superior cervical ganglion. The *petrous segment* ascends for a short distance in a vertical disposition. It then angulates, at the genu, travelling as the horizontal component, in an anteromedial direction. The vessel then crosses the foramen lacerum just before entering the cavernous sinus. The petrous segment is usually invested in bone. However, bone in the region of the tympanic cavity can be deficit (causing a bruit) and bone in the middle fossa floor can be deficient, placing the vessel in close apposition to the trigeminal ganglion. Within the sinus the *cavernous segment* grooves the body of the sphenoid bone as it passes forward. The abducens nerve is located laterally. The carotid then angulates superiorly as it leaves the cavernous sinus. The *supraclinoid segment* then gives rise to the intracranial branches.

Trigeminal nerve

The dominant sensory root of this nerve forms a ganglion on the floor of the middle cranial fossa. This is located in dural folds and gives rise to the ophthalmic, maxillary and mandibular divisions. The ophthalmic division supplies the cornea and

Table 29.1 Anatomical spaces that lie inferior to the middle cranial fossa

Space	Principal relations	Major contents
Infratemporal fossa	M – lateral pterygoid plate L – ramus of mandible A – posterior surface of maxilla P – styloid process S – greater wing of sphenoid I – opens into neck	Mandibular division of trigeminal nerve and its branches. Otic ganglion that supplies secretomotor fibres, derived from the IX cranial nerve (via the lesser petrosal nerve) to the parotid via the auriculotemporal nerve. The chorda tympani – This emerges from the facial nerve in the temporal bone and joins the lingual nerve carrying taste (anterior two-thirds tongue) and secretomotor fibres to the submandibular and sublingual glands. Medial and lateral pterygoid muscles. Maxillary artery (terminal branch of the external carotid artery) and branches including the middle meningeal artery that enters the foramen spinosum. Pterygoid venous plexus, maxillary vein and retromandibular vein.
Pterygopalatine fossa	M – palatine bone and nasal cavity L – infratemporal fossa via pterygomaxillary fissure A - maxilla P – pterygoid process of sphenoid S – body of sphenoid I – pterygoid plates	Maxillary nerve from foramen rotundum and branches, including those to the pterygopalatine ganglion, infraorbital nerve, zygomatic nerve and posterior superior alveolar nerve. Nerve of pterygoid canal (Vidian nerve) – Formed from the greater petrosal nerve (VII nerve – palatal taste and secretomotor to lacrimal gland) and deep petrosal nerve (sympathetic). Pterygopalatine ganglion and secretomotor fibres to lacrimal gland via zygomatic nerve. Maxillary artery and its terminal branches.
Parapharyngeal space (anterior to styloid process)	M – pharynx L – medial pterygoid and parotid fascia A – fascia covering medial pterygoid and tensor veli palatini P – styloid muscles and fascia S – sphenoid bone I – hyoid bone	Eustachian tube running from the temporal bone to the pharynx. Tensor and veli palatine muscles. Ascending pharyngeal and facial arteries. Branches of the glossopharyngeal nerve (to pharynx). Fat.

(*Continued*)

Table 29.1 Anatomical spaces that lie inferior to the middle cranial fossa (*Continued*)

Space	Principal relations	Major contents
Infrapetrosal space (posterior to styloid process)	M – posterior pharynx L – mastoid process A – styloid muscles and fascia P - jugular foramen and associated structures S – petrous bone I – posterior belly of digastric	Jugular bulb and lower end of inferior petrosal sinus forming jugular vein. Internal carotid artery en route towards the carotid canal. Ascending pharyngeal artery. Facial (VII) nerve at stylomastoid foramen. Glossopharyngeal (IX) nerve passing below styloglossus muscle. Vagus (X) nerve between the carotid artery and jugular vein. Spinal accessory (XI) nerve, lateral to the jugular vein. Inferiorly, the hypoglossal nerve (XII) crosses the anterior aspect of the carotid artery. Styloid muscles – styloglossus, stylopharyngeus and stylohyoid. Stylomandibular ligament. Posterior belly of digastric muscle.

Key – A = anterior; P = posterior; M = medial; L = lateral; S = superior; I = inferior.

forehead; the maxillary division supplies the skin overlying the maxilla and the teeth of the upper jaw. The mandibular nerve supplies the skin of the cheek, the skin overlying the mandible and the teeth of the lower jaw. The motor fibres all travel in the mandibular division to the muscles of mastication.

Facial nerve

This nerve pursues a tortuous route through the temporal bone. At the apex of the internal auditory meatus, the facial nerve enters the bony facial canal with the initial *labyrinthine segment* coursing to a location just lateral to the cochlea. The nerve then angles sharply forwards to the geniculate ganglion. Traction on the emerging greater superficial petrosal branch (GSPN) can lead to facial nerve weakness during middle fossa surgery. At the genu, the nerve executes a hairpin bend and runs, as the *tympanic segment*, along the medial wall of the tympanic cavity, inferior to the labyrinth. At the second genu the nerve turns sharply inferior on the posterior wall of the tympanic cavity, becoming the *mastoid segment* which passes directly to the stylomastoid foramen. Other intrapetrous branches include the nerve to stapedius and the chorda tympani.

Foramen magnum

The foramen magnum is surrounded by the occipital bone. The squamous part of the occipital bone forms the posterior part of the vault. The basilar part is also known as the clivus, lies anterior to the foramen magnum and is fused to the sphenoid bone at the spheno-occipital synchondrosis. The clivus is separated from the petrous temporal bone by the petroclival fissure, and more posterolaterally by the jugular foramen. The occipital condyles lie lateral to the foramen magnum and indeed encroach into the anterior part of the foramen. The condylar, or hypoglossal canal, through which the hypoglossal nerve passes is situated above the condyle. The jugular process of the occipital bone projects from the condylar region, lateral to the jugular bulb, and articulates with the temporal bone, thus forming the jugular foramen. The IX, X and XI cranial nerves traverse the jugular foramen. The craniocervical junction, the spinal accessory nerves, the vertebral arteries and the anterior and posterior spinal arteries all traverse the foramen magnum.

The atlanto-axial complex lies inferior to the foramen magnum. Articular capsules invest the atlanto-occipital joints. The anterior atlanto-occipital membrane is attached to the anterior border of the foramen magnum. Four ligamentous structures contribute to the stability of the atlanto-occipital joint. The apical ligament attaches the tip of the odontoid peg to the anterior margin of the foramen magnum. The bilateral alar ligaments extend laterally from the odontoid peg to the medial surfaces of the occipital condyles, and the tectorial membrane connects the body of the axis (C2) to the foramen magnum. The muscles of the sub-occipital triangle contribute to the stability of the cranio-cervical junction. These include the trapezius, sternocleidomastoid, splenius capitis, semispinalis capitis and longissimus capitis more superficially. The deeper muscles consist of the superior and inferior oblique muscles and the rectus capitis posterior major and minor muscles. The vertebral artery emerges from the transverse process of the atlas, and then passes behind the lateral mass of the atlas and the atlanto-axial joint. It then crosses the lateral part of the arch of the atlas and projects upwards to enter the dura in the lateral part of the foramen magnum.

FACIAL SKELETON

The facial skeleton is complex and discussed elsewhere (Chapters 12, 14 and 15). An understanding of anatomy is important when conducting transfacial approaches to the skull base. An anterior view of the skull enables identification of key components of the facial skeleton. Superiorly, the frontal bone forms the supraorbital ridge, containing foramina for the supraorbital nerves. The frontal bone contains an air sinus of variable size and configuration. At the nasion, the paired nasal bones form the root of the nasal skeleton. The solitary vomer lies in the midline of the **nasal cavity**, along with the midline, perpendicular plate of the ethmoid bone. The roof of the nasal cavity consists of the nasal spine of the frontal bone anteriorly, the cribiform plate of the ethmoid and more posteriorly of the body of the sphenoid bone. The palatine process of the maxilla and the horizontal plate of the palatine bone form the floor of the nasal cavity. The lateral wall of the nasal cavity consists mainly of the medial wall of the maxilla with contributions from the ethmoid, lacrimal and inferior nasal concha bones.

The orbital rim is formed by the frontal bone superiorly, the zygomatic bone inferolaterally and the maxilla inferomedially. Seven bones contribute to the walls of the **orbit**. The greater wing of the sphenoid bone and the zygomatic bone form the lateral wall of the orbit. Superiorly, the orbital roof is formed by the frontal bone. The medial wall is formed by the ethmoidal, nasal and lacrimal bones. The orbital floor is formed by the maxilla, the zygomatic bone and the palatine bone. The inferior orbital foramen provides a route for the inferior orbital nerve to access the facial soft tissue structures.

The **maxilla** and the **zygomatic** bones form the malar eminence. The maxilla contributes to formation of the orbit and the nasal cavity. It also is a major component of the bony palate (along with the palatine bone). Inferiorly, the alveolar process of the maxillary bone provides fixation for the upper dentition. The maxillary air sinus is contained within the maxillary bone and drains into the lateral wall of the nasal cavity. Laterally, the maxilla is attached to the zygoma. The temporal process of the zygoma projects posteriorly, forming the zygomatic arch with the zygomatic process of the temporal bone.

The **mandible** (Chapter 14) provides fixation for the lower teeth. The mandible comprises a body, an angle and a ramus. The latter has a posteriorly projecting neck that terminates in the head of the mandible: the neck and the head constitute the mandibular condyle. The head articulates with the temporal bone at the temporomandibular joint (TMJ) (please see Chapter 17). The mandibular ramus also has a more anterior projection called the coronoid process. This provides attachment for the temporal muscle.

SURGICAL APPROACHES TO THE SKULL BASE

Many approaches can be used to access skull base pathology. The approach should be tailored according to the specific pathology evident. A multidisciplinary approach often provides the best route of access. A summary of some of the key approaches is shown in Figure 29.1 and described in Table 29.2.

Table 29.2 Key surgical approaches to the skull base

Approach	Common pathology	Anatomical notes
Anterior craniofacial approach	Paranasal carcinoma, neurobastoma, midline anterior skull base tumours, craniofacial trauma	Bicoronal and paranasal facial incisions. Resection of medial orbital wall and nasal cavity structures. Intradural exposure of anterior cranial fossa floor (may require division of olfactory tracts). Resection of anterior fossa floor to provide clear tumour margins if possible. Frontal and sphenoid sinus may be opened. Vascularized dural flap used to achieve watertight closure.
Transoral and transfacial approaches	Midline tumours of the clival region	Transoral approach with retraction of the soft palate, incision of the posterior pharyngeal wall and removal of bone – clivus, C1 arch, odontoid peg, body of C2 – depending on level of the lesion. This approach can be extended for larger lesions with division of the hard and soft palate, mandibular osteotomy with splitting of the lip and/or chin. The transmaxillary approaches involve an osteotomy dividing the face horizontally. A sublabial incision is made, the osteotomy extends from the nasal cavity below the inferior orbital nerves but above the roots of the teeth, into the maxillary sinuses. The maxilla and hard palate are then retracted inferiorly or, with midline division of the hard and soft palate, are swung laterally providing access to the clivus. Variations on this technique include a unilateral maxillotomy approach.
Infratemporal middle fossa approach	Meningioma, chordoma, chondroma, chondrosarcoma, trigeminal schwannoma, parotid tumours, squamous cell carcinomas	Cranial pre-auricular 'question mark' incision. This is extended inferiorly below the earlobe to the anterior border of sternomastoid and extended into the neck. The anterior skin flap is retracted to expose the lateral border of the orbit down to the angle of the mandible. Access to the middle fossa is via an extended pterional craniotomy. Removal of the lateral margin of the orbit and the zygomatic arch allows access to the infratemporal fossa. Removal of the head of the mandible also improves access. Large resections may require a microvascular free flap. This approach is useful for large glomus tumours if combined with a transtemporal approach (see below).

Table 29.2 Key surgical approaches to the skull base (*Continued*)

Approach	Common pathology	Anatomical notes
Translabyrinthine and transtemporal approaches	Tumours of the cerebello-pontine angle, e.g. acoustic neuroma, meningioma, glomus jugulare tumours	Inverted postauricular hockey stick incision. The translabyrinthine approach involves temporal bone drilling with identification of the facial nerve within the facial nerve canal, removal of the semicircular canals, 270-degree removal of the internal auditory meatus and opening of the posterior fossa dura. Closure requires packing of the middle ear cavity to minimize risk of CSF leak via the Eustachian tube. For large tumours extending into the pre-pontine cistern, additional bone medial to the auditory canal and including the cochlear can be resected. Skeletonization and transposition of the facial nerve can improve access. If a total petrosectomy is required (e.g. cancer of the temporal bone), removing the petrous apex, the facial nerve may need to be sacrificed.
Pre-sigmoid, transtentorial retrolabyrinthine approach coupled with a middle fossa craniectomy	Tumours bridging the middle and posterior cranial fossae	In this approach a mastoidectomy is performed with preservation of the labyrinth. The sigmoid sinus is skeletonized. The superior petrosal sinus is divided with careful preservation of the vein of Labbe, enabling posterior retraction of the sigmoid sinus. If the approach is coupled with a middle fossa craniectomy, division of the tentorium cerebelli, with careful preservation of the trochlear nerve and posterior cerebral artery medially, provides space for tumour resection from the pre-pontine and mesencephalic cisterns anterior to the upper brainstem. If a wider exposure is required the labyrinth can also be resected as in the trans-labyrinthine approach.
Far lateral approach to the foramen magnum	Tumours in the region of the lower clivus	The oblique sub-occipital muscles are detached from the transverse process of C1 and the rectus capitis major is detached from the occipital bone. This enables identification of the vertebral artery. A lateral sub-occipital craniotomy is performed, often with a hemilaminectomy of the arch of C1. The posteromedial part of the condyle is removed – the hypoglossal canal is in close proximity. Additional room can be achieved by drilling the jugular tubercle, a bony prominence that lies above the hypoglossal canal. Caution must be exercised due to the close proximity of the IX, X and XI cranial nerves. The dural opening then enables access to the anterolateral aspect of the foramen magnum.

FURTHER READING

Logan BM, Reynolds P, Hutchings RT. *McMinn's Colour Atlas of Head and Neck Anatomy*. 4th ed. Philadelphia: Mosby, 2009.

Rhoton Jr AL. *Cranial Anatomy and Surgical Approaches*. Philadelphia: Lippincott Williams & Wilkins, 2003.

30

Osteology of the skull

SUSAN STANDRING

Introduction 295
Regions of the skull 295
Diploic bone 297
Sutures and synchondroses 297
Frontal (anterior) aspect of the skull 298
Facial skeleton 298
Lateral aspect of the skull 300
Posterior aspect of the skull 301
Base of skull: foramina and fissures 301
Sphenoid bone 302
Further reading 307

INTRODUCTION

This chapter provides an introduction to the bones of the skull in general and to the sphenoid bone in particular; other skull bones are described in detail in the relevant chapters.

The skull contains 28 separate bones. A working knowledge of their normal and variant anatomy is essential for the effective surgical treatment of disease and trauma in the head and neck. The relative proportions of the facial and cranial skeletons change over time, most particularly during the period from early childhood to the end of adolescence (Figure 30.1). To appreciate the impact of the rapid growth and expansion of the brain, the pneumatization of the paranasal and mastoid air sinuses and the eruption of occluding primary and secondary dentitions on these proportions, a chronological series of dried skulls and clinical images from infancy to the post-synostotic state should be examined. No site in the body provides a more eloquent demonstration of the way in which the normal processes of surface bone deposition and resorption influence growth and form.

REGIONS OF THE SKULL

The skull may be divided into neurocranium and viscerocranium, two regions which have evolved to perform very different functions.

The neurocranium houses the brain and the organs of special sense and is formed in adults by four single bones (frontal, ethmoid, sphenoid and occipital) and two bilateral pairs of bones (temporal and parietal). It consists of the cranial vault or calvaria (skull cap); cranial cavity, which houses the brain, meninges and cerebrospinal fluid, and the cranial portions of the cranial nerves and the cranial vasculature; cranial base (skull base, basicranium, chondrocranium); and the acoustic cavities, which house the bony and membranous labyrinths of the inner ear and the contents of

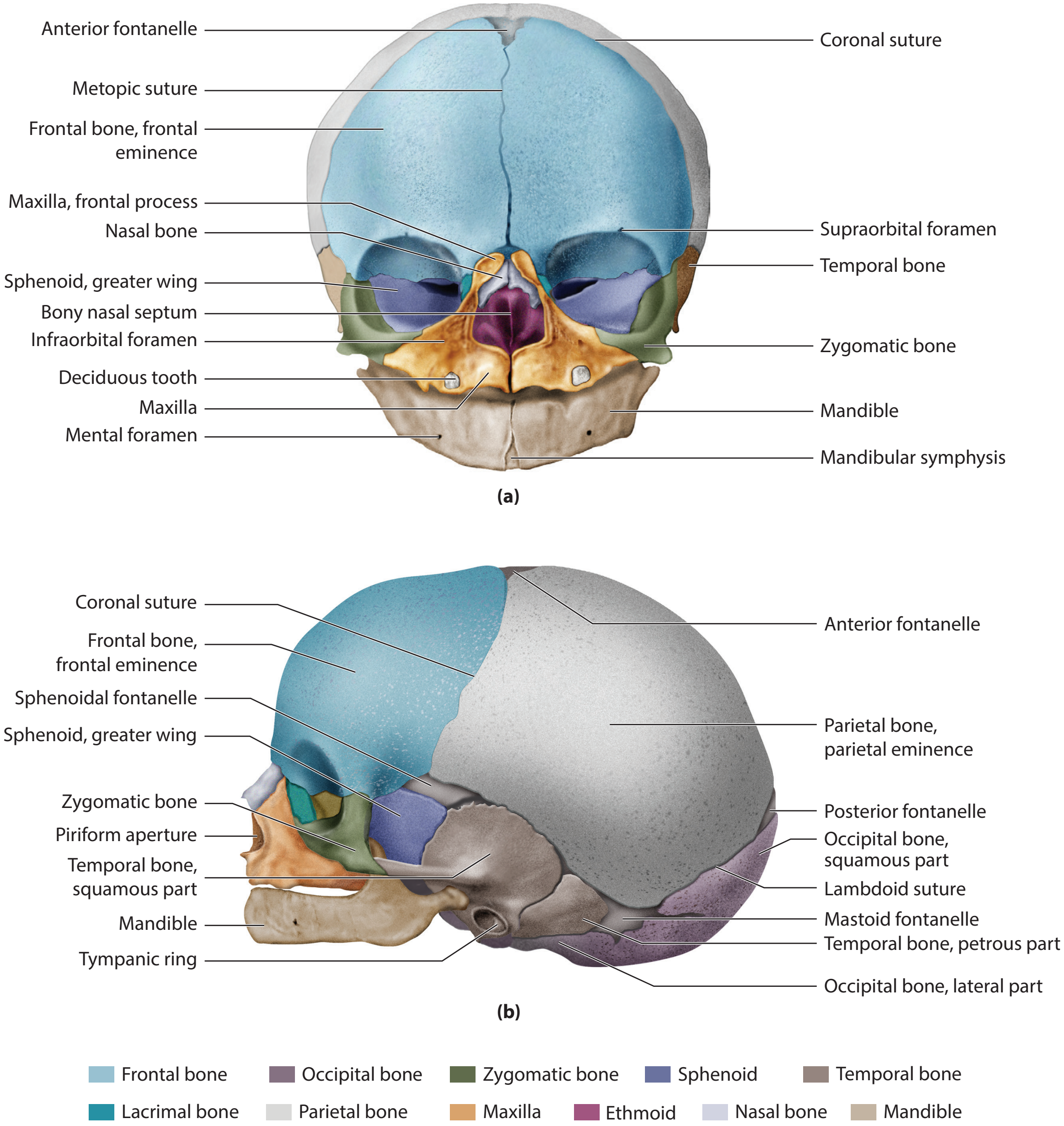
Anterior fontanelle
Metopic suture
Frontal bone, frontal eminence
Maxilla, frontal process
Nasal bone
Sphenoid, greater wing
Bony nasal septum
Infraorbital foramen
Deciduous tooth
Maxilla
Mental foramen
Coronal suture
Supraorbital foramen
Temporal bone
Zygomatic bone
Mandible
Mandibular symphysis
(a)
Coronal suture
Frontal bone, frontal eminence
Sphenoidal fontanelle
Sphenoid, greater wing
Zygomatic bone
Piriform aperture
Temporal bone, squamous part
Mandible
Tympanic ring
Anterior fontanelle
Parietal bone, parietal eminence
Posterior fontanelle
Occipital bone, squamous part
Lambdoid suture
Mastoid fontanelle
Temporal bone, petrous part
Occipital bone, lateral part
(b)
Frontal bone
Occipital bone
Zygomatic bone
Sphenoid
Temporal bone
Lacrimal bone
Parietal bone
Maxilla
Ethmoid
Nasal bone
Mandible

Figure 30.1 Neonatal skull. **(a)** Frontal aspect. **(b)** Lateral aspect. (This figure was published in Standring S. (Ed.). *Gray's Anatomy: The Anatomical Basis of Clinical Practice*, 40th ed., Chapter 26. Courtesy of Sobotta, copyright Elsevier 2008.)

the middle ear cleft, including the ossicular chain (malleus, incus and stapes).

The viscerocranium includes the bones which form most of the orbits and surround the nasal and oral cavities and so houses the cranial parts of the respiratory and digestive tracts; it is formed by three irregular bones centred on the midline (mandible, ethmoid, vomer) and six bilateral pairs of bones (maxilla, inferior concha/turbinate, palatine, zygomatic, lacrimal, nasal).

DIPLOIC BONE

The bones of the cranial vault consist of two thin plates of compact bone, the inner and outer tables, which enclose a narrow layer of cancellous bone, the diploic space or middle table, composed of an irregular network of bony trabeculae and vascular spaces. Diploic bone is a source for split-thickness calvarial bone grafts (Figure 30.2).

Cranial bone thickness and the presence of a diploic space are reliable predictors of age. As a general rule, the bones are thinner in women and children. Where the skull is thin, as in the temporal and occipital regions, the tables are close together; where the skull is thick, as in the parietal bone and around the external occipital protuberance, they are more widely separated. The inner tables may be normally eroded by gyral impressions, as typified by the cranial surface of the floor of the anterior cranial fossa, and also by vascular structures such as the branches of the middle meningeal artery as they travel across the intracranial surface of the sphenoid and parietal bones (see description later in this chapter). The inner table is thinner and more brittle than the outer table and is almost always more extensively splintered than the outer in skull fractures. It is thought that the differences in mechanical properties of the bony tables reflect their different functions: the outer table directly bears muscular loads, particularly those associated with mastication, while the inner table is subject only to intracerebral pressures transmitted via the dura mater. Moreover, blood within the diploic space may act as a fluid cushion to absorb traumatic forces. Diploic bone is haemopoeitic in the young: red marrow hyperplasia such as that seen in patients with thalassemia major produces expansion of the diploë, thinning of the outer table, destruction of some trabeculae and thickening of those that remain to produce characteristic ‘hair-on-end’ signs.

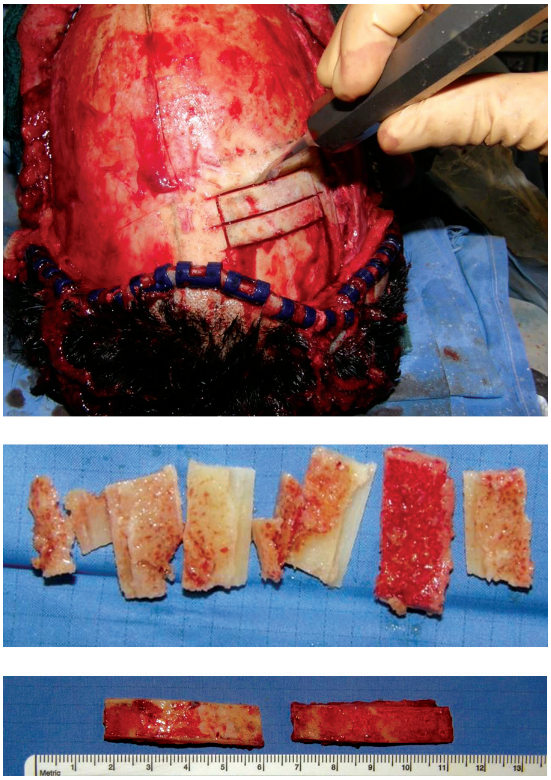

Figure 30.2 Harvesting split-thickness calvarial bone grafts from the parietal bone. See also Figure 30.4. (Courtesy of Professor Luigi Clauser, Unit of Cranio-Maxillo-Facial Surgery and Orbital Surgery, Ferrara, Italy.)

Very thin bones such as the vomer and the pterygoid plates of the sphenoid are typically unilamellar. The maxilla, ethmoid, frontal, sphenoid and temporal bones become pneumatized postnatally; the air spaces that develop in the maxilla, ethmoid, frontal and sphenoid are known collectively as the paranasal sinuses.

SUTURES AND SYNCHONDROSES

The articulations between individual skull bones reflect their development. Bones of the calvaria and some parts of the basicranium develop by intramembranous ossification in the mesenchyme of the embryonic pharyngeal arches without a cartilaginous phase: these bones are held together firmly by fibrous joints called sutures. Sutures may be classified morphologically as end-to-end, e.g. the midline metopic, sagittal and median palatine sutures, or overlapping, e.g. the lambdoid and coronal sutures.

The dura mater is an important regulator of sutural morphogenesis. With the exception of the metopic suture, which normally fuses during the first year of life, the sutures in the cranial vault normally remain patent until the third decade: sutural growth plays a significant role in the forward and downward transposition of the midface relative to the cranial base.

Six fibrous areas, fontanelles, occur at sites where two or more calvarial bones meet in the fetal and peri-natal skull. The anterior fontanelle is the largest and most important for clinical evaluation: the median time of its closure is 13.8 months. Wormian bones are accessory bones that may occur within cranial suture lines or fontanelles; they may be single or multiple and are diagnosed radiographically. They are rarely seen in the coronal or sagittal sutures.

The bones of most of the skull base develop by endochondral ossification (in which bone replaces preformed cartilaginous templates): the joints between these bones are primary cartilaginous joints called synchondroses. The cranial base synchondroses (fronto-ethmoidal, spheno-ethmoidal, intra-sphenoidal, petro-clival, spheno-petrosal, spheno-occipital, petro-occipital and intra-occipital) function as important growth centres and stabilizers for the entire craniofacial complex. The fronto-ethmoidal and intra-sphenoid synchondroses fuse and ossify by 3 years of age, whereas fusion of the spheno-occipital synchondrosis is usually complete by 17 years: the prolonged growth is consistent with the major role that the spheno-occipital synchondrosis plays in the postnatal growth of the cranial base, for example in facilitating the continued posterior expansion of the maxilla associated with the eruption of the posterior molar teeth. It is worth noting that the synchondroses are sites where skull base fractures seem preferentially to be propagated in young patients. Premature fusion of cranial sutures or synostosis of synchondroses during the early growth phase of the skull will result in various cranial abnormalities, for example, the characteristic midface deficiencies of achondroplasia produced by diminished growth of the skull base.

The articulations between the mandibular fossa of the temporal bone and the condyle of the mandible (temporomandibular joint, TMJ), the occipital condyle and the superior articular facet of the atlas (atlanto-occipital joint), and between the three auditory ossicles are all synovial. The two halves of the mandible articulate by a secondary cartilaginous joint (symphysis menti) which synostoses during the first postnatal year.

FRONTAL (ANTERIOR) ASPECT OF THE SKULL

From above downwards, the bones that form the anterior aspect of the adult skull are the frontal bone, usually unpaired, but occasionally still presenting as two bones separated by a midline metopic suture; paired maxillae, separated by the bones and spaces of the naso-ethmoidal complex; the body of the mandible and the mental protuberance. In the anatomical position, the lower margins of the orbits and the upper margins of the external acoustic meatuses are horizontal (in the orbito-meatal plane) (Figure 30.3).

FACIAL SKELETON

The facial skeleton is formed by all or part of the frontal, zygomatic, ethmoid, maxillary, nasal, vomer and lacrimal bones and mandible. It provides the framework on which the soft tissues of the face act during breathing, chewing, swallowing and communicating (both verbal and nonverbal). The maxillae lie on either side of the nasal cavity, between the cranial base superiorly and the dental occlusal plane inferiorly, and in this position they divide the facial skeleton and the associated soft tissues into thirds.

The upper third of the facial skeleton is occupied mainly by the frontal bone. The frontal bone also forms the major part of the roof of the orbit and the anterior cranial base. Each orbital opening is approximately quadrangular. The supraorbital margin is formed by the frontal bone; the lateral

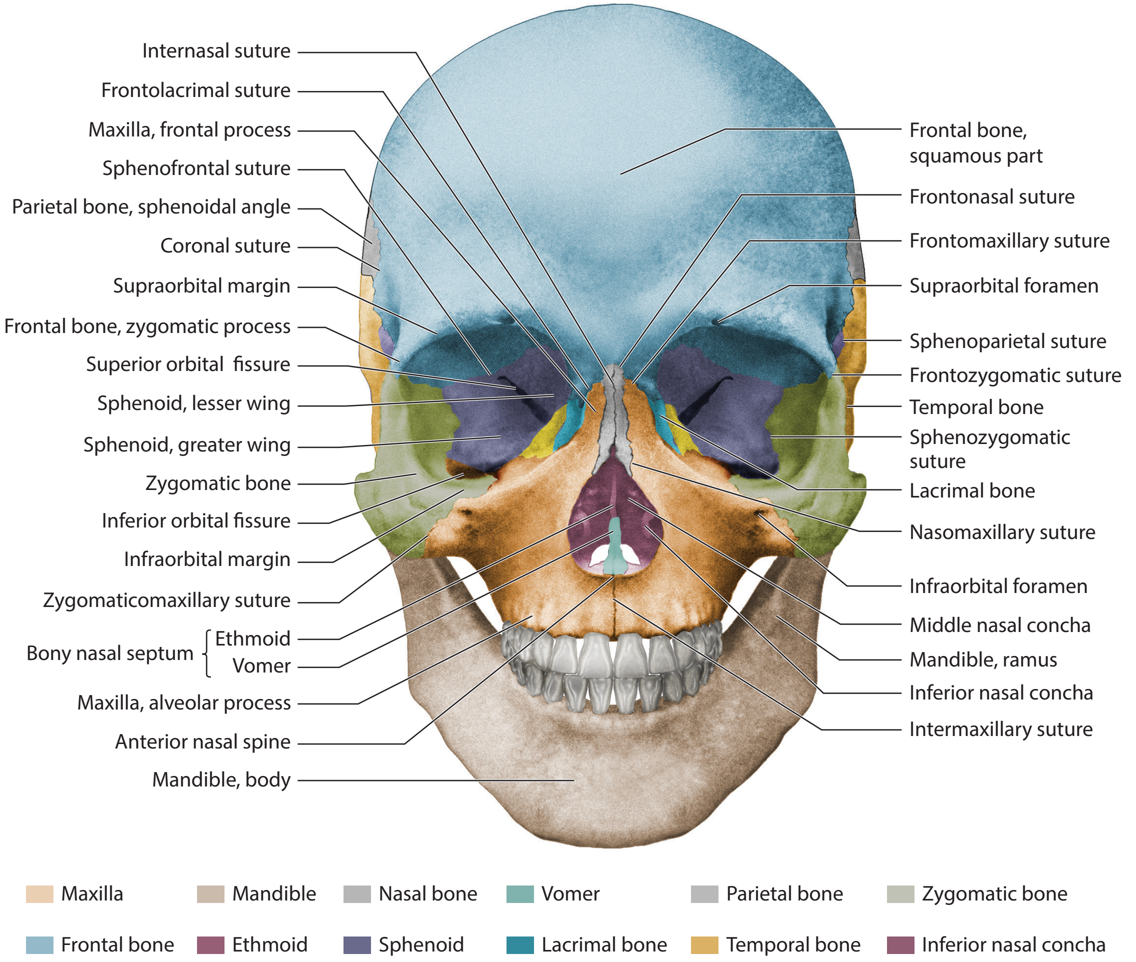
Internasal suture
Frontolacrimal suture
Maxilla, frontal process
Sphenofrontal suture
Parietal bone, sphenoidal angle
Coronal suture
Supraorbital margin
Frontal bone, zygomatic process
Superior orbital fissure
Sphenoid, lesser wing
Sphenoid, greater wing
Zygomatic bone
Inferior orbital fissure
Infraorbital margin
Zygomaticomaxillary suture
Bony nasal septum
Ethmoid
Vomer
Maxilla, alveolar process
Anterior nasal spine
Mandible, body
Frontal bone, squamous part
Frontonasal suture
Frontomaxillary suture
Supraorbital foramen
Sphenoparietal suture
Frontozygomatic suture
Temporal bone
Sphenozygomatic suture
Lacrimal bone
Nasomaxillary suture
Infraorbital foramen
Middle nasal concha
Mandible, ramus
Inferior nasal concha
Intermaxillary suture
Maxilla
Mandible
Nasal bone
Vomer
Parietal bone
Zygomatic bone
Frontal bone
Ethmoid
Sphenoid
Lacrimal bone
Temporal bone
Inferior nasal concha

Figure 30.3 Adult skull, frontal aspect. (This figure was published in Standring S. (Ed.). *Gray's Anatomy: The Anatomical Basis of Clinical Practice*, 40th ed., Chapter 26. Courtesy of Sobotta, copyright Elsevier 2008.)

margin by the frontal process of the zygomatic bone and the zygomatic process of the frontal bone; the infraorbital margin by the zygomatic bone laterally and maxilla medially; and the less distinct medial margin by the frontal bone above and the lacrimal crest of the frontal process of the maxilla below. The detailed anatomy of the bony orbit and orbito-nasal complex is described in Chapters 12 and 15.

The middle third of the face is formed by the two maxillae separated by the naso-ethmoidal complex and lies between the transverse line which connects the two zygomaticofrontal sutures (and passes through the frontomaxillary and frontonasal sutures) and the occlusal plane of the maxillary teeth. The posterior limit is the spheno-ethmoidal junction and includes the free margins of the pterygoid plates inferiorly. In life, but not in the macerated skull, lateral nasal and major and minor alar cartilages articulate with the bony margins of the anterior nasal aperture and define the profile of the external nose.

Unlike the robust bones that comprise much of the cranium, the bones of the mid-face are fragile, and in places may be little thicker than a sheet of paper. They are normally strengthened by shock-absorbing vertical or sagittal bony buttresses (paired nasomaxillary, zygomaticomaxillary and pterygomaxillary buttresses and unpaired

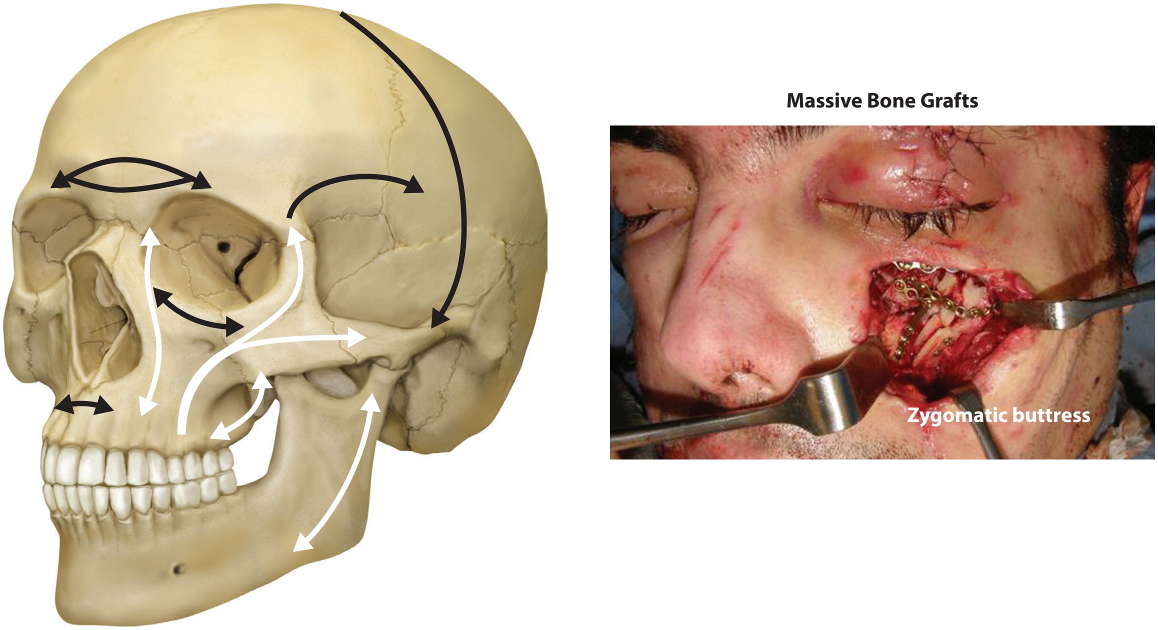

Figure 30.4 Facial buttresses (frontal oblique view). (Adapted from Linnau KF, Stanley RB Jr, Hallam DK, et al. Imaging of high-energy midfacial trauma: what the surgeon needs to know. *European Journal of Radiology*. 2003; 48: 17–32.) Photograph shows split calvarial bone grafts harvested in Figure 30.2 used to reconstruct the anterior maxilla and zygoma, the former via an existing laceration of the cheek and the latter accessed via the coronal flap used to access the zygoma and upper midface. (Courtesy of Professor Luigi Clauser, Unit of Cranio-Maxillo-Facial Surgery and Orbital Surgery, Ferrara, Italy.)

fronto-ethmoid-vomerine buttress) (Figure 30.4). Collectively, these seven buttresses act to diffuse the occlusal forces of mastication over the skull base; the greatest forces are absorbed by the zygomaticomaxillary buttress, where the cortical bone is thickest. The superior and inferior orbital rims and the alveolar ridge serve as horizontal buttresses but are less effective than their vertical counterparts in protecting the facial skeleton from impact.

Middle-third fractures may involve the orbit, maxilla, nasoethmoidal and zygomatic complexes and the body and greater and lesser wings of the sphenoid bone. They may be broadly divided into *central* fractures, which occur between the root of the nose and the alveolar processes of the maxillae, but do not involve the zygomatic bones, and *lateral* fractures, which involve the zygomatic bone as well as fractures of the floor of the orbit (blowout fractures). Where possible, surgical management of maxillary fractures aims to restore the integrity of the buttresses.

The lower third of the face is formed by the body of the mandible. The mental protruberance produces the characteristic prominence of the chin in the midline. Lower-third fractures correspond to fractures of the mandible; these are discussed in more detail in Chapter 14.

LATERAL ASPECT OF THE SKULL

Viewed from the side, the skull can be subdivided into three zones: face (anterior), temporal and infratemporal fossae and zygomatic arch (intermediate), occipital region (posterior) (Figure 30.5).

The temporal fossa is bounded anteriorly by the frontal process of the zygomatic bone, inferiorly by the zygomatic arch and superiorly and posteriorly by the temporal lines on the calvaria. The superior and inferior temporal lines are usually quite obvious anteriorly, but they fade as they arch across the parietal bone and the superior line often disappears. The inferior temporal line becomes more distinct over the squamous temporal bone and

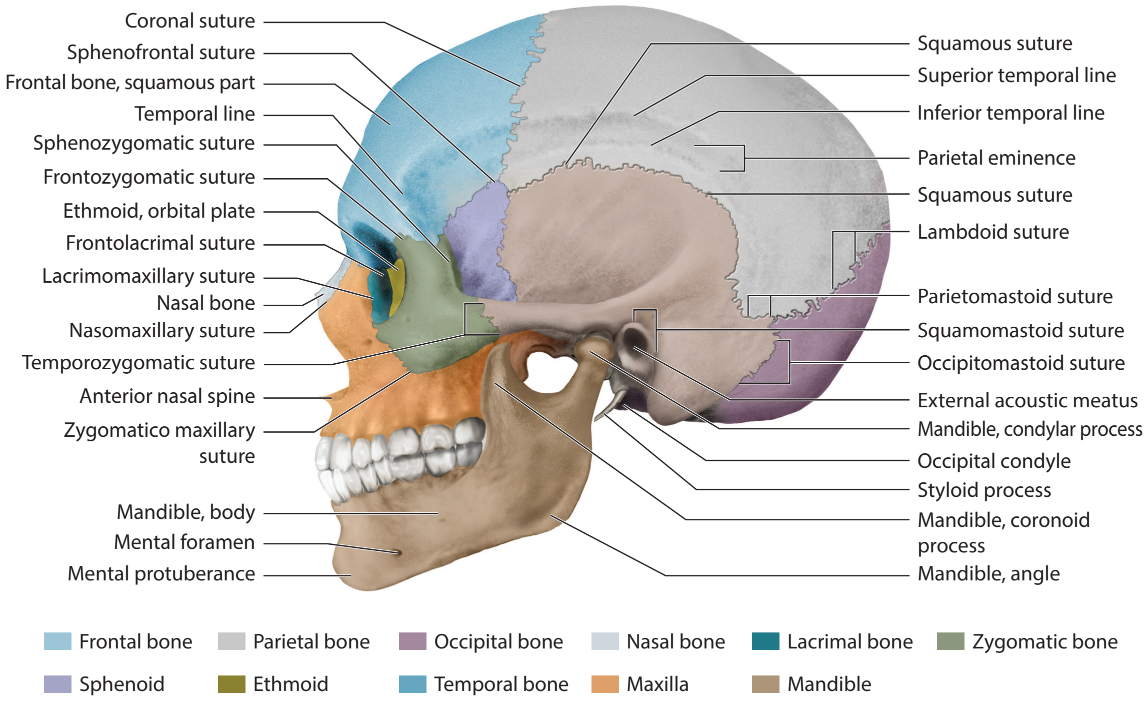
Coronal suture
Sphenofrontal suture
Frontal bone, squamous part
Temporal line
Sphenozygomatic suture
Frontozygomatic suture
Ethmoid, orbital plate
Frontolacrimal suture
Lacrimomaxillary suture
Nasal bone
Nasomaxillary suture
Temporozygomatic suture
Anterior nasal spine
Zygomatico maxillary suture
Mandible, body
Mental foramen
Mental protuberance
Squamous suture
Superior temporal line
Inferior temporal line
Parietal eminence
Squamous suture
Lambdoid suture
Parietomastoid suture
Squamomastoid suture
Occipitomastoid suture
External acoustic meatus
Mandible, condylar process
Occipital condyle
Styloid process
Mandible, coronoid process
Mandible, angle
Frontal bone
Parietal bone
Occipital bone
Nasal bone
Lacrimal bone
Zygomatic bone
Sphenoid
Ethmoid
Temporal bone
Maxilla
Mandible

Figure 30.5 Adult skull, lateral aspect. (This figure was published in Standring S. (Ed.). *Gray's Anatomy: The Anatomical Basis of Clinical Practice*, 40th ed., Chapter 26. Courtesy of Sobotta, copyright Elsevier 2008.)

terminates in the supramastoid crest at the base of the mastoid process.

The frontal, parietal, sphenoid and temporal bones articulate at the pterion, which was the site of the sphenoidal fontanelle (see following description). The temporal fossa continues beneath the zygomatic arch into the infratemporal fossa.

The temporal bone and the infratemporal fossa are described in Chapter 6, the lateral surface of the ramus of the mandible is described in Chapter 14.

POSTERIOR ASPECT OF THE SKULL

The posterior aspect of the skull consists of the parietal, temporal and occipital bones (Figure 30.6). The occipital bone articulates with the two parietal bones at the lambdoid suture, and the parietal bones articulate in the midline at the sagittal suture; the lambdoid and sagittal sutures meet at the lambda. The most notable features of the bones are the foramen magnum and occipital condyles, jugular foramen, mastoid and styloid processes of the temporal bone, stylomastoid foramen, mastoid notch and squamous part of the occipital bone up to the external occipital protuberance and the superior nuchal lines, hypoglossal (anterior condylar) and condylar (posterior condylar) canals.

BASE OF SKULL: FORAMINA AND FISSURES

The skull base has been likened to the keel of a ship, with a central, less-yielding foundation than the bones of the vault (Figure 30.7). It is oriented at approximately 45 degrees to the occlusal plane of the maxilla, is anatomically complex and surgically challenging. It forms the floor of the cranial cavity and therefore separates the brain and its coverings (which are intracranial and related to the cranial fossae) from the facial skeleton and associated soft tissues and the nasopharynx (which are extracranial but potentially able to communicate with the cranial cavity via foramina in the frontal, ethmoid, maxillae, sphenoid, temporal and occipital bones).

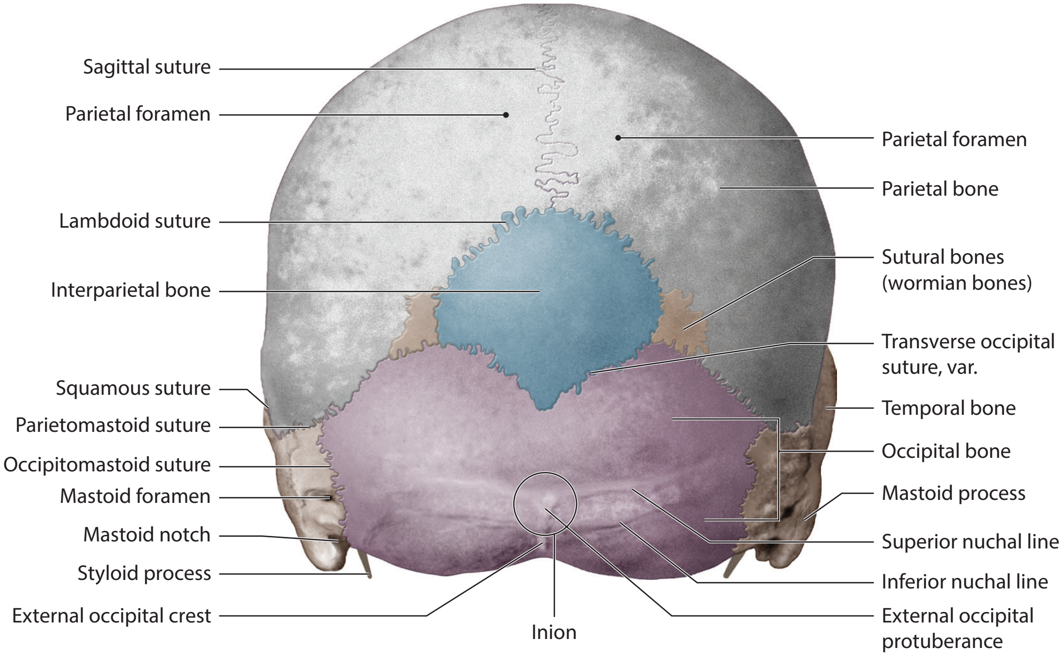
Sagittal suture
Parietal foramen
Lambdoid suture
Interparietal bone
Squamous suture
Parietomastoid suture
Occipitomastoid suture
Mastoid foramen
Mastoid notch
Styloid process
External occipital crest
Inion
Parietal foramen
Parietal bone
Sutural bones (wormian bones)
Transverse occipital suture, var.
Temporal bone
Occipital bone
Mastoid process
Superior nuchal line
Inferior nuchal line
External occipital protuberance

Figure 30.6 Adult skull, posterior aspect. (This figure was published in Standring S. (Ed.). *Gray's Anatomy: The Anatomical Basis of Clinical Practice*, 40th ed., Chapter 26. Courtesy of Sobotta, copyright Elsevier 2008.)

The extracranial skull base is subdivided into anterior, central (middle), and posterior regions which correspond to the three intracranial fossae. The anterior skull base is formed by the floor of the anterior cranial fossa and includes the roofs of the frontal and ethmoid sinuses, orbits and nasal cavity and the jugum sphenoidale; the middle skull base is formed mainly by the body and greater wings of the sphenoid, with a small contribution from the basiocciput; the posterior skull base is formed primarily by the occipital bone, with contributions from both sphenoid and temporal bones.

The cranial nerves, branches of the internal and external carotid arteries and the vertebral arteries, and the veins draining the brain all enter or leave the cranial cavity via foramina or fissures in the bones of the cranial base. These openings offer potential routes for the spread of infection and tumours in the head and neck, and they should be explored in an articulated skull using a fine wire. (In an earlier, less politically correct text, bristles from a housewife's broom were suggested.) With a little probing, it will be seen that the pterygopalatine fossa communicates with the cranial cavity via the foramen rotundum and the pterygoid canal, the orbit via the infraorbital fissure, the paranasal sinuses via the sphenopalatine foramen, the masticator space via the pterygomaxillary fissure and the hard palate via the greater and lesser palatine foramina. It will also be apparent that tumours within the dermatomal distribution of the trigeminal nerve may access the cranial cavity via any one of a number of foramina after extracranial perineural spread. Emissary foramina offer admittedly less constant routes by which veins draining the face and scalp communicate with intracranial veins. The extracranial margins of all of the openings in the skull base are bordered by soft tissues which contain a substantial amount of fat: progressive obliteration of a fat plane in the vicinity of a fissure or foramen facilitates evaluation of tumour spread on computerized tomography (CT) or magnetic resonance imaging (MRI).

SPHENOID BONE

The name is taken from the Greek *sphenon* meaning a 'wedge', but perhaps a more apt description is that the sphenoid forms a bridge between the

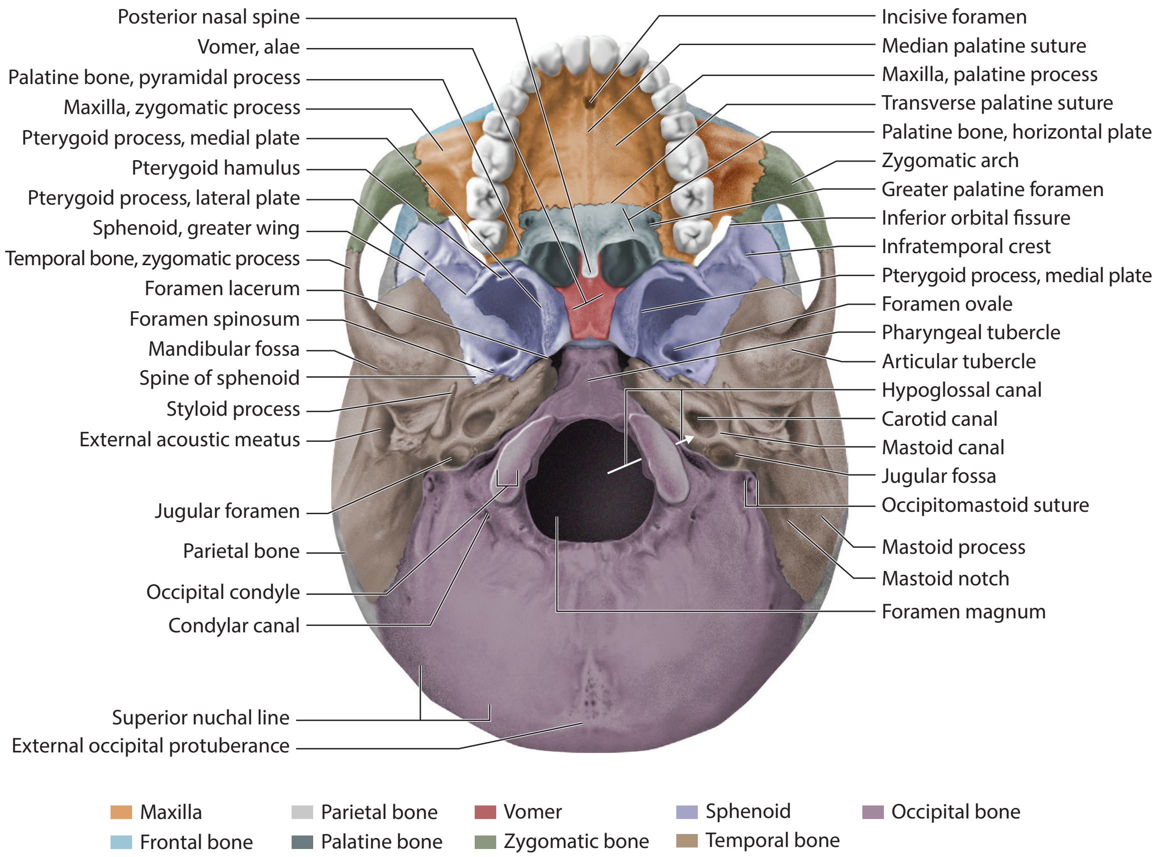
Posterior nasal spine
Vomer, alae
Palatine bone, pyramidal process
Maxilla, zygomatic process
Pterygoid process, medial plate
Pterygoid hamulus
Pterygoid process, lateral plate
Sphenoid, greater wing
Temporal bone, zygomatic process
Foramen lacerum
Foramen spinosum
Mandibular fossa
Spine of sphenoid
Styloid process
External acoustic meatus
Jugular foramen
Parietal bone
Occipital condyle
Condylar canal
Superior nuchal line
External occipital protuberance
Incisive foramen
Median palatine suture
Maxilla, palatine process
Transverse palatine suture
Palatine bone, horizontal plate
Zygomatic arch
Greater palatine foramen
Inferior orbital fissure
Infratemporal crest
Pterygoid process, medial plate
Foramen ovale
Pharyngeal tubercle
Articular tubercle
Hypoglossal canal
Carotid canal
Mastoid canal
Jugular fossa
Occipitomastoid suture
Mastoid process
Mastoid notch
Foramen magnum
Maxilla
Frontal bone
Parietal bone
Palatine bone
Vomer
Zygomatic bone
Sphenoid
Temporal bone
Occipital bone

Figure 30.7 Adult skull, external surface, base of skull. (This figure was published in Standring S. (Ed.). *Gray's Anatomy: The Anatomical Basis of Clinical Practice*, 40th ed., Chapter 26. Courtesy of Sobotta, copyright Elsevier 2008.)

Table 30.1 Foramina and fissures of the skull

Foramen or fissure	Content
Foramen caecum	Emissary vein to nasal cavity (inconstant)
Cribriform plate	Olfactory nerve, meninges, cerebrospinal fluid
Anterior and posterior ethmoidal foramina	Anterior and posterior ethmoidal vessels and nerves
Supraorbital foramen/notch	Supraorbital vessels and nerve
Frontal notch	Supratrochlear vessels and nerve
Infraorbital foramen	Infraorbital vessels and nerve
Inferior orbital fissure	Infraorbital and zygomatic branches of the maxillary nerve and accompanying vessels
Zygomaticofacial and zygomaticotemporal foramina	Zygomaticofacial and zygomaticotemporal branches of the maxillary nerve
Optic canal	Optic nerve, meninges, cerebrospinal fluid (CSF), ophthalmic artery

(*Continued*)

Table 30.1 Foramina and fissures of the skull (*Continued*)

Foramen or fissure	Content
Foramen rotundum	Maxillary branch of trigeminal nerve
Superior orbital fissure	Oculomotor, trochlear, abducens nerves (all oculogyric) and frontal, nasociliary and lacrimal branches of ophthalmic division of trigeminal nerve; ophthalmic veins
Foramen ovale	Mandibular division of trigeminal nerve; lesser petrosal branch of glossopharyngeal nerve; accessory meningeal branch of the maxillary artery, emissary vein linking cavernous venous sinus and pterygoid venous plexus
Foramen spinosum	Middle meningeal vessels; meningeal branch of the mandibular nerve
Vidian canal (pterygoid canal)	Deep petrosal nerve (postganglionic sympathetic) plus greater petrosal branch of facial nerve, together forming the nerve of the pterygoid canal; vidian vessels
Hiatus for greater petrosal nerve	Greater petrosal nerve and petrosal branch of middle meningeal artery
Sphenoidal emissary foramen (of Vesalius)	Emissary vein linking cavernous venous sinus and pterygoid venous plexus
Foramen lacerum	Internal carotid artery, carotid plexus of postganglionic sympathetic nerves, meningeal branches of the ascending pharyngeal artery, and emissary veins from the cavernous sinus
Sphenopalatine foramen	Nasopalatine branches of maxillary nerve; sphenopalatine vessels
Internal acoustic meatus (porus acousticus)	Facial nerve (plus nervus intermedius) and vestibulo-cochlear nerve; labyrinthine vessels
Jugular foramen	Inferior petrosal sinus (anterior); glossopharyngeal, vagus and accessory nerves (midway); internal jugular vein (posterior)
Carotid canal	Internal carotid artery; carotid plexus of postganglionic sympathetic nerves derived from superior cervical ganglion
Stylomastoid foramen	Facial nerve and stylomastoid artery
Petrotympanic fissure	Chorda tympani nerve
Mastoid foramen	Emissary vein from the superior sagittal sinus; branch of occipital artery to dura
Parietal foramen	Emissary vein from the superior sagittal sinus
Hypoglossal foramen (anterior condylar foramen)	Hypoglossal nerve, meningeal branch of the ascending pharyngeal artery, emissary vein from the basilar plexus
Foramen magnum	Brain stem, meninges and CSF; spinal accessory nerves, vertebral; arteries and vertebral plexus of postganglionic sympathetic nerves derived from superior cervical ganglion
Posterior condylar foramen (inconstant)	Emissary vein linking sigmoid sinus and vertebral veins
Greater and lesser palatine foramina	Palatine vessels and nerves
Incisive foramen	Nasopalatine nerve and the termination of the greater palatine vessels
Mental foramen	Mental vessels and nerves
Mandibular foramen	Inferior dental vessels and nerves

anterior and posterior skull bases (Figure 30.8). It articulates with the frontal, ethmoid, vomer, palatine, zygomatic, parietal, temporal and occipital bones and in so doing contributes to the bony anatomy of the calvaria, orbits, middle cranial base, nasopharynx and infratemporal fossae. The foramina and fissures in the sphenoid enable communication between the cranial cavity and the orbits, infratemporal and pterygopalatine fossae, nasal cavity and paranasal sinuses. Some features

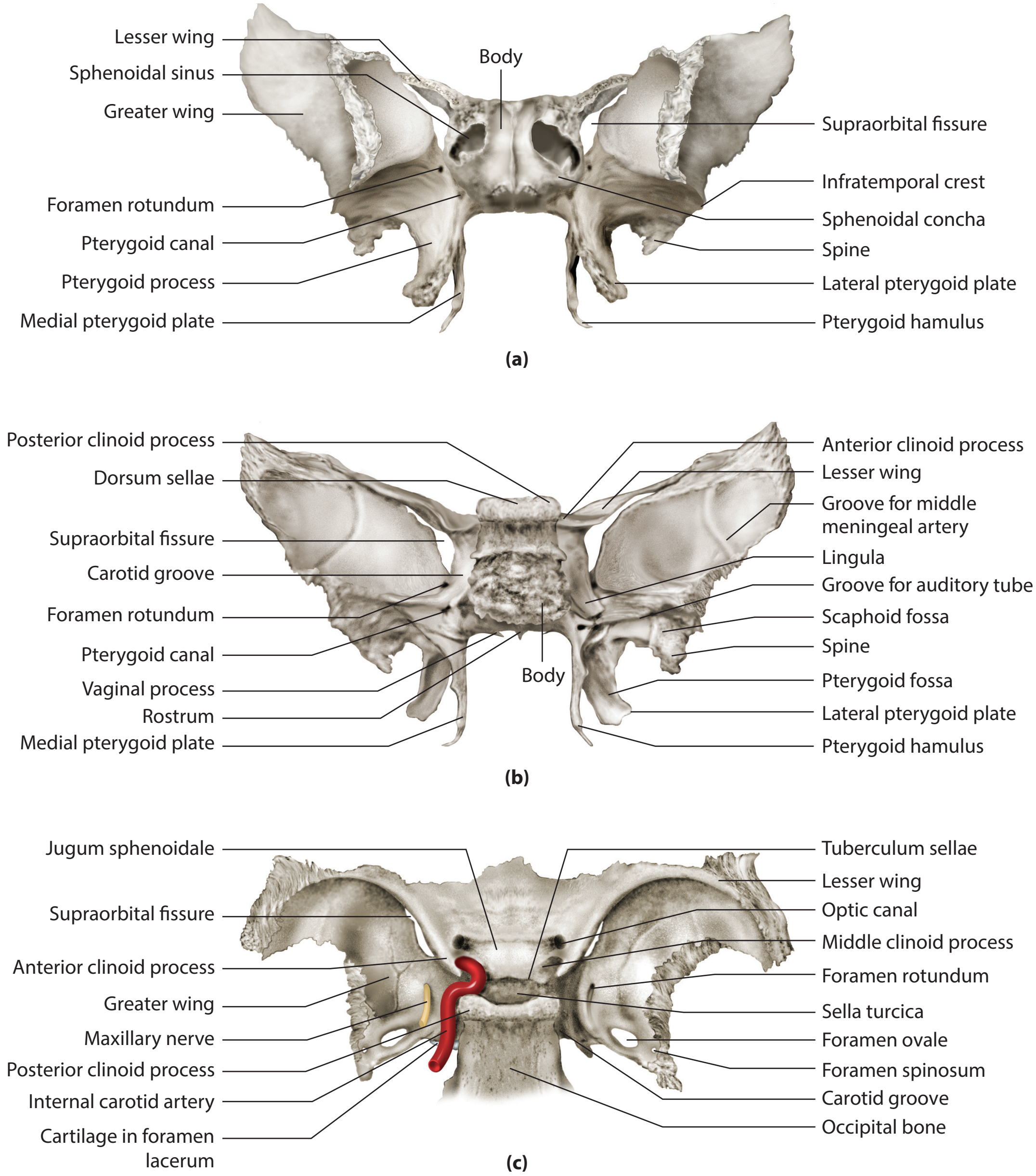
Lesser wing
Sphenoidal sinus
Greater wing
Foramen rotundum
Pterygoid canal
Pterygoid process
Medial pterygoid plate
Body
Supraorbital fissure
Infratemporal crest
Sphenoidal concha
Spine
Lateral pterygoid plate
Pterygoid hamulus
(a)
Posterior clinoid process
Dorsum sellae
Supraorbital fissure
Carotid groove
Foramen rotundum
Pterygoid canal
Vaginal process
Rostrum
Medial pterygoid plate
Body
Anterior clinoid process
Lesser wing
Groove for middle meningeal artery
Lingula
Groove for auditory tube
Scaphoid fossa
Spine
Pterygoid fossa
Lateral pterygoid plate
Pterygoid hamulus
(b)
Jugum sphenoidale
Supraorbital fissure
Anterior clinoid process
Greater wing
Maxillary nerve
Posterior clinoid process
Internal carotid artery
Cartilage in foramen lacerum
Tuberculum sellae
Lesser wing
Optic canal
Middle clinoid process
Foramen rotundum
Sella turcica
Foramen ovale
Foramen spinosum
Carotid groove
Occipital bone
(c)

Figure 30.8 Adult skull, sphenoid bone. **(a)** Anterior view. **(b)** Posterior view. **(c)** Superior view. (This figure was published in Standring S. (Ed.). *Gray's Anatomy: The Anatomical Basis of Clinical Practice*, 40th ed., Chapter 26. Courtesy of Sobotta, copyright Elsevier 2008.)

of the sphenoid are difficult, if not impossible, to see in an articulated skull and can only be appreciated on a disarticulated bone and/or in sagittal sections.

The sphenoid consists of a midline unpaired body and paired greater and lesser wings and pterygoid processes.

The body forms the bony roof of the nasopharynx: it articulates with the perpendicular plate of the ethmoid and the ala of the vomer via the ethmoidal crest and rostrum, respectively, i.e. it articulates with the bones which form the bony nasal septum. The body contains the sphenoidal air sinus, in reality two large, irregular cavities separated, usually unequally, by a bony septum and draining into the spheno-ethmoidal recess via orifices just lateral to the ethmoid crest. The sphenoid sinus may pneumatize bone beyond the body of the sphenoid, producing recesses which are named according to their location. The commonest are the opticocarotid recesses, between the optic nerve and the internal carotid artery; the medial opticocarotic recess is a key landmark in a trans-sphenoidal approach.

The external wall of the body is marked by the carotid sulcus, which houses the cavernous sinus and the internal carotid artery. The superior surface of the body has been likened to a Turkish saddle, hence its name, sella turcica. The base of the saddle is a depression of varying depth, the pituitary or hypophysial fossa, which houses the pituitary gland: the trans-sphenoid access to the pituitary gland is probably the most common approach for pituitary adenomas. The fossa is bounded anteriorly by a protruberance, the tuberculum sellae, on either side by anterior (middle) and posterior clinoid processes and posteriorly by an approximately rectangular sheet of bone, the dorsum sellae, which is continuous inferiorly with the clivus. A petrosal process on either side of the dorsum sellae articulates with the petrous portion of the temporal bone, forming the medial boundary of the foramen lacerum. At the level of the tuberculum sellae, where the mean bone thickness is 1 mm, the internal carotid artery is immobilized by the anterior clinoid process, optic strut, carotid sulcus, and distal dural ring and is therefore at increased risk during a trans-sphenoidal approach.

The lesser wings form the sharp posterior borders of the anterior cranial fossa, where they overhang the most anterior extent of the middle cranial fossa, and end medially as the anterior clinoid processes. They articulate with the frontal bone and are contiguous medially with the jugum sphenoidale (a flat region on the superior surface of the body of the sphenoid separating the cribriform plate anteriorly from the prechiasmatic sulcus posteriorly). The prechiasmatic sulcus ends on either side in the optic foramen. The optic strut lies between the upper side of the body and the lesser wing, separating the optic canal from the medial portion of the superior orbital fissure: it is a key landmark in CT angiographic scans to differentiate between intradural and extradural/intracavernous aneurysms involving the paraclinoid segment of the internal carotid artery (ICA).

The greater wings sweep laterally from the sides of the body and present orbital, lateral and superior surfaces. The orbital surface forms the posterior part of the lateral wall of the orbit and articulates with the orbital plate of the frontal bone and with the zygomatic bone. Inferiorly, it forms the posterolateral boundary of the inferior orbital fissure, and medially, it forms the lower boundary of the superior orbital fissure. The lateral surface contributes to the lateral wall of the calvaria just anterior to the squamous part of the temporal bones, articulating with the frontal, temporal and parietal bones at an approximately *H*-shaped suture called the pterion. The infratemporal surface of the greater wing forms the roof of the infratemporal fossa where it is divided by the infratemporal crest.

The superior surface forms the greater part of the floor of the middle cranial fossa and contains a crescent of foramina on either side of the base of the body of the sphenoid. From backwards, and from medial to lateral, these openings are the superior orbital fissure, foramen rotundum, foramen ovale and foramen spinosum. Collectively, they transmit cranial nerves III, IV, V and VI, the ophthalmic veins and middle meningeal vessels and parasympathetic fibres destined to synapse in the otic ganglion. The bone exhibits shallow but important grooves (sulci). The cartilaginous part of the auditory tube lies in the sulcus tubae, a groove medial to the foramen ovale and foramen spinosum. The superior and the lateral surfaces are usually marked by grooves which house the middle meningeal artery, which courses anterolaterally across the floor of the middle cranial fossa from the foramen spinosum before dividing into frontal and parietal branches. The frontal/anterior branch crosses the pterion, where it is vulnerable in trauma involving the temporal region, because the bone is relatively thin here and the artery is close to the inner table of the skull. The pterion is therefore an important landmark on the side of the skull because it overlies the anterior branch of the middle meningeal artery and the lateral (Sylvian) cerebral fissure intracranially. (It is also known as the Sylvian point.) The pterion corresponds to the site of the anterolateral (sphenoidal) fontanelle on the neonatal skull which disappears about three months after birth.

The pterygoid processes are named from the Greek *pteryx* meaning a 'wing'. They project downward from the inferior surface of the greater wings behind the maxillae. Each consists of a lateral and a medial plate, separated by a pterygoid fossa. The medial plate is prolonged by a delicate hook-like process, the pterygoid hamulus, and presents a longitudinal hollow, the scaphoid fossa (Cruveilhier's fossa) superiorly on its posterior surface. The pterygoid canal (Vidian canal) runs anteroposteriorly through the base of the medial pterygoid plate, its anterior opening flairs (Vidian's trumpet) into the pterygopalatine fossa at the level of the sphenopalatine foramen. Superiorly, the medial plate is prolonged onto the undersurface of the body as a thin lamina, the vaginal process, which articulates with both the sphenoidal process of the palatine bone and the ala of the vomer The lateral pterygoid plate is usually broader and longer than its medial counterpart.

FURTHER READING

Bashar A, Necmettin T, Bulent C, Ziya A, Nurperi G. Lateral sublabial endoscopic approach to foramen ovale: A novel endoscopic technique to access infratemporal fossa. *Journal of Craniofacial Surgery*. 2010; 21: 1241–45.

Bassed RB, Briggs C, Drummer OH. Analysis of time of closure of the spheno-occipital synchondrosis using computed tomography. *Forensic Science International*. 2010; 200: 161–4.

Berge JK, Bergman RA. Variations in size and in symmetry of foramina of the human skull. *Clinical Anatomy*. 2001; 14: 406–13.

Choudhri AF, Parmar HA, Morales RE, Gandhi D. Lesions of the skull base imaging for diagnosis and treatment. *Otolaryngologic Clinics of North America*. 2012; 45: 1385–1404.

Hosseini SMS, Razfar A, Carrau RL, Prevedello DM, Fernandez–Miranda J, Zanation A, Kassam AB. Endonasal transpterygoid approach to the infratemporal fossa: Correlation of endoscopic and multiplanar CT anatomy. *Head & Neck*. 2012; 34: 313–20.

Linnau KF, Stanley RB Jr, Hallam DK, et al. Imaging of high-energy midfacial trauma: What the surgeon needs to know. *European Journal of Radiology*. 2003; 48: 17–32.

Moonis G, Cunnane MB, Emerick K, Curtin H. Patterns of perineural tumor spread in head and neck cancer. *Magnetic Resonance Imaging Clinics of North America*. 2012; 20: 435–46.

Morriss-Kay GM, Wilkie AOM. Growth of the normal skull vault and its alteration in craniosynostosis: Insights from human genetics and experimental studies. *Journal of Anatomy*. 2005; 207: 637–53.

Nemzek WR, Brodie HA, Hecht ST, Chong BW, Babcook CJ, Seibert JA. MR, CT, and plain film imaging of the developing skull base in fetal specimens. *American Journal of Neuroradiology*. 2000; 21: 1699–1706.

Peterson J, Dechow PC. Material properties of the human cranial vault and zygoma. *Anatomical Record*. 2003; 274A: 785–97.

Reid RR. Facial skeletal growth and timing of surgical intervention. *Clinics in Plastic Surgery*. 2007; 34: 357–67.

Standring S. External skull. In: Standring S. (Ed.). *Gray's Anatomy: The Anatomical Basis of Clinical Practice*. 40th ed. Philadelphia: Elsevier, 2008; Chapter 26, 409–42.

Standring S. *Intracranial Region*. In: Standring S. (Ed.). *Gray's Anatomy – The Anatomical Basis of Clinical Practice*. 40th ed. Philadelphia: Elsevier, 2008; Chapter 27, 423–34.

31

Overview of the cranial nerves

SUSAN STANDRING

Introduction 309
Motor cell columns and nuclei 311
Sensory tracts and nuclei 312
Peripheral distribution of the cranial nerves 312
Further reading 314

INTRODUCTION

There are 12 pairs of cranial nerves, individually named and numbered (conventionally using Roman numerals) in a rostrocaudal sequence (Table 31.1). Collectively, they innervate all the striated and smooth muscle in the head; almost all of the facial skin and the scalp to the vertex; the lips; the conjunctivae, corneas and mucosae lining the nasal and oral cavities, paranasal sinuses and nasolacrimal ducts; the tooth pulps, periodontal ligaments and gingivae; the meninges; the temporomandibular and auditory ossicular joints; the major and minor salivary glands and the lacrimal glands. They are also the conduits for the special senses of olfaction, vision, taste, hearing and balance, carrying information from receptors in the olfactory epithelium, retina, taste buds, organ of Corti and vestibular apparatus respectively to second order neurons in the olfactory bulb or to an array of sensory nuclei in the thalamus or brainstem.

A cranial nerve can be damaged at any point along its course. Knowledge of the anatomy of each nerve beyond that of a textbook schematic is essential in localizing a site of pathology/traumatic injury and to avoid inflicting iatrogenous injury during any invasive procedure. In the brainstem, cranial nerve nuclei are adjacent to ascending and descending tracts (corticospinal, lemniscal and spinocerebellar pathways) and are likely to be involved in lesions affecting these tracts: patients with brainstem lesions commonly present with evidence of lower motor neuron disturbance at the level of the lesion and long tract signs below the lesion. In the periphery, cranial nerves have consistent anatomical relationships with other vessels and nerves and give off branches at predictable points along their course (enabling differentiation between proximal and distal lesions). They also pass through foramina in the skull base and may subsequently lie close to bone (where they may be compressed by expanding tumours or injured by spicules of fractured bone).

This chapter provides a brief overview of the locations of the motor and sensory nuclei of the cranial nerves together with a summary of their peripheral distribution. Detailed accounts of the peripheral course of each nerve will be found in the appropriate chapter.

Table 31.1 Distribution of the cranial nerves

No.	Name	Distribution/function
I	Olfactory	Olfaction
II	Optic	Vision
III	Oculomotor	Motor to medial rectus, superior rectus, inferior rectus, inferior oblique, levator palpebrae superioris Preganglionic parasympathetic drive to ciliary ganglion
IV	Trochlear	Motor to superior oblique
V	Trigeminal	
	Ophthalmic (Vi)	General sensation from forehead, scalp, eyelids, external nose, globe of the eye, conjunctiva, ethmoid sinuses
	Maxillary (Vii)	General sensation from mid-face, lower eyelid, nasal cavity, maxillary sinuses, palate, upper lip, maxillary teeth Postganglionic parasympathetic axons from pterygopalatine ganglion
	Mandibular (Viii)	General sensation from scalp, lower face including lower lip, tongue, floor of mouth, mandibular teeth, tympanic membrane, tragus and crus of helix of external ear Proprioception from muscles of mastication, temporomandibular joint, periodontal ligaments Motor to temporalis, masseter, medial and lateral pterygoids, tensor tympani, tensor veli palatini, anterior belly of digastric
VI	Abducens	Motor to lateral rectus
VII	Facial	General sensation from part of tympanic membrane, small inconstant areas of external acoustic meatus and skin behind pinna (fibres supplying pinna may travel with auricular branch of the vagus) Proprioception from facial muscles Taste from anterior two-thirds of tongue (but excluding vallate papillae) Motor to muscles of the face, stapedius, posterior belly of digastric, stylohyoid Preganglionic parasympathetic secretomotor and vasodilator drive to pterygopalatine and submandibular ganglia
VIII	Vestibulocochlear	Sensations of equilibrium and motion (vestibular division) Hearing (cochlear division)
IX	Glossopharyngeal	General sensation from posterior one-third of tongue, oropharynx, tympanic membrane and external acoustic meatus Sensation from carotid body (chemoreceptors) and carotid sinus (baroreceptors) Taste from posterior one-third of tongue (and from vallate papillae) Parasympathetic secretomotor and vasodilator drive to otic ganglion Motor to stylopharyngeus
X	Vagus	General sensation from pharynx, larynx, trachea, oesophagus, part of auricle and external auditory meatus Visceral sensation from thoracic and abdominal viscera Sensation from aortic bodies (chemoreceptors) and aortic arch (baroreceptors) Taste from scattered taste buds on the base of the tongue, valleculae and epiglottis Parasympathetic preganglionic drive to glands and smooth muscle in the pharynx, larynx, thoracic and abdominal viscera (ganglia are typically in walls of viscera) Motor to pharyngeal, external laryngeal and oesophageal striated muscles
XI	Accessory	
	'Cranial root'	Motor to muscles of soft palate (except tensor veli palatini) and intrinsic muscles of larynx (distributed via vagus in the pharyngeal plexus) NB: the existence of this root is disputed
	Spinal root	Motor to sternocleidomastoid and trapezius
XII	Hypoglossal	Motor to all intrinsic and extrinsic muscles of the tongue except palatoglossus

MOTOR CELL COLUMNS AND NUCLEI

Somatic motor and visceromotor axons travel in the oculomotor (III), trochlear (IV), trigeminal (V), abducens (VI), facial (VII), glossopharyngeal (IX), vagus (X), accessory (XI) and hypoglossal (XII) nerves. The lower motor neurons (LMNs) from which these axons are derived lie in discontinuous columns of motor nuclei within the brainstem (Figure 31.1). (This pattern is quite unlike the arrangement of LMNs in the spinal cord, where the motor columns are continuous throughout the ventral horns.) In terms of their supranuclear control, LMNs innervating the muscles of the lower part of the face (innervated by VII) are driven by the contralateral cortex, whereas LMNs innervating the muscles of the upper part of the face, tongue, palate, pharynx and larynx (via V, VII and IX–XII) are bilaterally innervated.

On either side, ascending the brainstem from the medulla oblongata to the pontine tegmentum, the motor nuclei lying closest to the midline innervate the muscles of the tongue (XII)

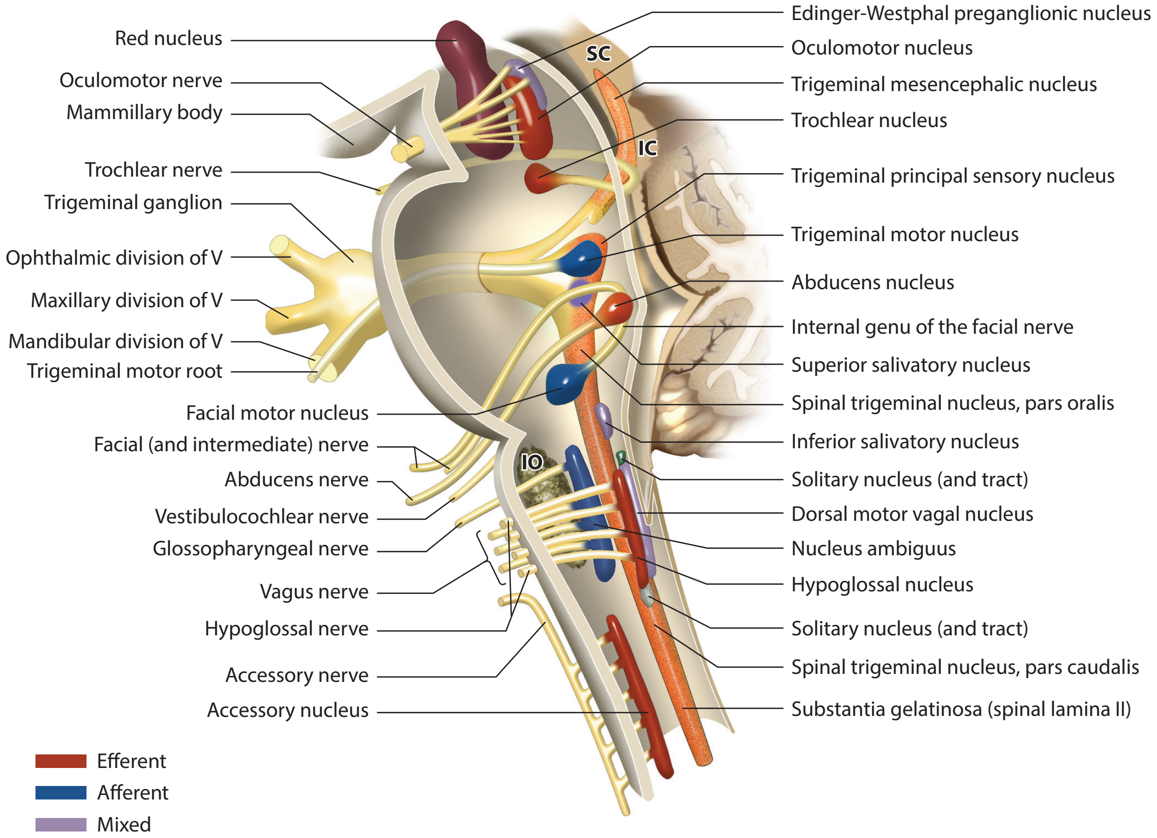
Red nucleus
Oculomotor nerve
Mammillary body
Trochlear nerve
Trigeminal ganglion
Ophthalmic division of V
Maxillary division of V
Mandibular division of V
Trigeminal motor root
Facial motor nucleus
Facial (and intermediate) nerve
Abducens nerve
Vestibulocochlear nerve
Glossopharyngeal nerve
Vagus nerve
Hypoglossal nerve
Accessory nerve
Accessory nucleus
SC
IC
IO
Edinger-Westphal preganglionic nucleus
Oculomotor nucleus
Trigeminal mesencephalic nucleus
Trochlear nucleus
Trigeminal principal sensory nucleus
Trigeminal motor nucleus
Abducens nucleus
Internal genu of the facial nerve
Superior salivatory nucleus
Spinal trigeminal nucleus, pars oralis
Inferior salivatory nucleus
Solitary nucleus (and tract)
Dorsal motor vagal nucleus
Nucleus ambiguus
Hypoglossal nucleus
Solitary nucleus (and tract)
Spinal trigeminal nucleus, pars caudalis
Substantia gelatinosa (spinal lamina II)
Efferent
Afferent
Mixed

Figure 31.1 The location of cranial nerve nuclei and the course of their axons within the brainstem. The functional components associated with each nucleus and with the axons to or from that nucleus are colour coded: dark red = motor to striated muscle not of branchial arch origin; dark blue = motor to striated muscle of branchial arch origin; light red = somatic afferent; light blue = visceromotor parasympathetic; dark green = special visceral afferent (taste); light green = visceral afferent; grey = special somatic afferent. IC – inferior colliculus. IO – inferior olive. SC – superior colliculus. (This figure was published in: Haines DE. *Fundamental Neuroscience for Basic and Clinical Applications. A Synopsis of Cranial Nerves of the Brainstem*. Chapter 14, 181–197. Copyright Elsevier 2012.)

and the oculogyric muscles (III, IV and VI), i.e. skeletal muscles that originate from paraxial mesenchyme not located in a pharyngeal arch. The motor nuclei lying most laterally are the nucleus ambiguus and the facial and trigeminal motor nuclei, which innervate the muscles of the larynx and pharynx (X, $\mathrm{XI}_{\mathrm{cranial}}$*, IX), the muscles of the face (VII) and the muscles of mastication ($\mathrm{V}_{\mathrm{iii}}$), i.e. skeletal muscle derived from the pharyngeal arches. Occupying an intermediate position between the two somatic efferent columns are the dorsal motor vagal nucleus, the salivatory nuclei (inferior and superior) and the accessory oculomotor or Edinger-Westphal nucleus: neurons in this visceral efferent column collectively constitute the cranial preganglionic parasympathetic system, and their axons travel to their target ganglia in X, IX, VII and III, respectively.

SENSORY TRACTS AND NUCLEI

The olfactory nerve (I) contains axons arising from olfactory receptor neurons in the olfactory epithelium which covers the superior conchae and superior part of the nasal septum. Bundles of axons ensheathed in a unique type of ensheathing glial cell pass through the openings in the cribriform plate of the ethmoid bone. They are surrounded by layers of meninges and cerebrospinal fluid and project exclusively to glomeruli in the olfactory bulb from where olfactory information is relayed to other regions of the brain via the axons of mitral and tufted cells in the glomeruli.

The optic nerve (II) is also surrounded by the meninges and cerebrospinal fluid and conveys retinotopically organized axons arising from retinal ganglion cells to four subcortical regions, namely the lateral geniculate nucleus (the major relay station to the primary visual cortex); superior colliculus (involved in the control of orienting eye movements); hypothalamus (regulation of circadian rhythms in response to light) and pretectum (regulation of visual reflexes).

With the exception of axons carrying proprioceptive information from the head, all of the sensory axons travelling in the trigeminal (V), facial (VII), glossopharyngeal (IX) and vagus (X) nerves are the peripheral processes of unipolar neurons located in sensory ganglia lying outside the skull. The central processes of these neurons project to somatic afferent or visceral afferent nuclear columns which run more or less continuously throughout the brainstem. The most medial column is the solitary tract and its nucleus, the latter lying in the dorsomedial medulla oblongata and extending from the level of the pyramidal decussation to the caudal part of the dorsal cochlear nucleus. Cardiovascular, visceral, respiratory, gustatory and oro-tactile information is relayed in anatomically and functionally discrete areas of the nucleus. Incoming axons terminate viscerotopically, those conveying the various types of taste relay in a rostral gustatory nucleus (via VII, IX and X), while visceral sensations from thoracic and abdominal viscera are relayed in a caudal cardiorespiratory nucleus (mainly via X) and are involved in the regulation of vital autonomic functions such as cardiovascular reflexes. (The vagus nerve wanders extensively beyond its distribution to structures in the head and neck, conveying preganglionic parasympathetic and visceral afferent axons to and from the viscera of the thorax and a significant part of the abdomen.)

Sensory axons travelling in the vestibulocochlear (VIII) nerve arise from bipolar neurons in either the vestibular (Scarpa's) or spiral (cochlear) ganglia in the inner ear. (The vestibular ganglion lies in the trunk of the vestibular nerve within the lateral end of the internal acoustic meatus, and the spiral ganglion lies in Rosenthal's canal in the modiolus.) The distal processes of the vestibular component innervate the semicircular canals and the otolith organs, while the central processes project to the vestibular nuclei (and also directly to the cerebellum). The distal processes of the auditory component innervate the organ of Corti, and the central processes project tonotopically to the cochlear nuclei.

---

* There is some dispute as to what to call the cranial portion of the accessory nerve. It has no functional connection with the spinal part of the accessory nerve, which arises from LMNs in the upper cervical cord and temporarily joins the vagus near the jugular foramen. The LMNs which give rise to the 'cranial part' of the accessory nerve lie in the nucleus ambiguus and functionally represent the caudal component of the vagus nerve.

The sensory nuclei of the trigeminal nerve are organized into an almost continuous, laterally sited column of cells that extends from the periaqueductal grey of the midbrain to the upper cervical spinal cord. In rostrocaudal sequence, these are the mesencephalic nucleus; the principal (chief or pontine) sensory nucleus, which lies at the midpontine level; and the spinal trigeminal nucleus. Axons entering the mesencephalic nucleus carry proprioceptive information from the muscles of mastication, periodontal ligaments and extraocular muscles; they have their cell bodies in the nucleus and not in the trigeminal ganglion. Axons carrying discriminative touch from the face and oral cavity terminate in the principal nucleus. The spinal tract nucleus is subdivided into the pars caudalis, pars interpolaris and pars oralis. Axons carrying pain, temperature or nondiscriminative touch in V, VII, IX or X all enter the spinal trigeminal tract and terminate somatotopically in the pars caudalis (pain and temperature), the pars interpolaris (pain and light touch) or the pars oralis (light and discriminative touch). Sensory axons carrying pain and temperature from the upper cervical nerves also terminate in the most caudal part of the pars caudalis.

PERIPHERAL DISTRIBUTION OF THE CRANIAL NERVES

All 12 pairs of nerves pass through foramina or fissures in the cranial base either individually (e.g. V_{ii} via the foramen rotundum) or in association with other nerves and vessels (e.g. V_i, III, IV, VI and the ophthalmic veins via the superior orbital fissure), and all are vulnerable to compression, traction, infection or laceration by expanding lesions or fractures involving these sites (see Chapter 30, Table 30.1).

Cranial nerves differ from spinal nerves in that not all are mixed: some are entirely sensory or entirely motor. Some also carry pre- or postganglionic parasympathetic axons (Table 31.2 and chapter 32) Functional components (somatic motor, visceromotor, somatic sensory or visceral afferent) and reflexes should be tested as appropriate during a neurological clinical examination (Tables 31.2 and 31.3). Brainstem reflex studies provide important information about both afferent and efferent pathways.

Table 31.2 Connections of the parasympathetic ganglia

Ganglion	Preganglionic fibres	Postganglionic fibres	Target
Otic	IX (lesser petrosal branch from tympanic plexus)	Auriculotemporal (V_{iii})	Parotid salivary gland
Ciliary	III (nerve to inferior oblique)	Short ciliary nerves	Ciliaris; sphincter pupillae
Submandibular	VII (chorda tympani)	Unnamed, travel along blood vessels or reenter lingual nerve	Submandibular, sublingual and anterior lingual salivary glands
Pterygopalatine	VII (greater petrosal nerve, becomes nerve of pterygoid canal when joined by deep petrosal nerve which is postganglionic sympathetic)	Zygomatico-temporal branches of V_{ii} and rami orbitales to lacrimal gland and choroid	Lacrimal gland, mucous glands in maxillary sinus, nasal cavity and oral cavity

Table 31.3 Reflexes mediated via cranial nerves

Reflex	Afferent limb	Efferent limb
Corneal	V_i (conjunctival innervation)	VII (orbicularis oculi)
Blink (somatosensory and trigeminal)	Median nerve or supra-orbital nerve used for testing	VII (orbicularis oculi)
Gag	IX	X
Swallowing	IX	IX, X
Pupillary light	II	III (sphincter pupillae); T1 (dilator pupillae)
Accommodation	II	III (sphincter pupillae, cilaris, medial rectus)
Glabellar	V_i	VII (orbicularis oculi)
Masseteric (jaw jerk)	V_{iii}	V_{iii}
Corneo-mandibular (von Sölder phenomenon)	V_i	V_{iii}
Sneeze	V_i, V_{ii}	V, VII, IX, X, phrenic nerve (C3,4,5) and motor innervation of intercostal muscles and abdominal muscles by segmental thoracic nerves
Vestibulo-ocular	VIII (vestibular component)	III, IV, VI (via medial longitudinal fasciculus)

FURTHER READING

Aramideh M, Ongerboer de Visser BW. Brainstem reflexes: Electrodiagnostic techniques, physiology, normative data, and clinical applications. *Muscle & Nerve*. 2002; 26: 14–30.

Bermúdez-Rattoni F. Molecular mechanisms of taste-recognition memory. *Nature Reviews Neuroscience*. 2004; 5: 209–17.

Flint PW, Haughey BH, Lund VJ, Niparko JK, Richardson MA, Robbins KT, Thomas JR. (Eds.). *Cummings Otolaryngology – Head & Neck Surgery*. 5th ed. Philadelphia: Mosby, 2010; Chapter 178, 2542–56.

Haines DE. (Ed.). *Fundamental Neuroscience for Basic and Clinical Applications*. 4th ed. Philadelphia: Saunders, 2013; Chapter 14, 181–97.

Kennelly KD. Electrodiagnostic approach to cranial neuropathies. *Neurologic Clinics*. 2012; 30: 661–84.

Lang IM. Brain stem control of the phases of swallowing. *Dysphagia*. 2009; 24: 333–48.

Lehn AC, Lettieri J, Grimley R. A case of bilateral lower cranial nerve palsies after base of skull trauma with complex management issues: Case report and review of the literature. *Neurologist*. 2012; 18: 152–4.

Müller F, O'Rahilly R. The initial appearance of the cranial nerves and related neuronal migration in staged human embryos. *Plant Cell Tissue and Organ Culture*. 2011; 193: 215–38.

Nattie E., Comroe Jr JH. Distinguished Lecture: Central chemoreception: then…and now. *Journal of Applied Physiology*. 2011; 110: 1–8.

Ramón-Cueto A, Muñoz-Quiles C. Clinical application of adult olfactory bulb ensheathing glia for nervous system repair. *Experimental Neurology*. 2011; 229: 181–94.

Ruggiero DA, Underwood MD, Mann JJ, Anwar M, Arango V. The human nucleus of the solitary tract: Visceral pathways revealed with an "in vitro" postmortem tracing method. *Journal of the Autonomic Nervous System*. 2000; 79: 181–90.

Valls-Solé J. The blink reflex and other cranial nerve reflexes. In: Aminoff M. (Ed.). *Aminoff's Electrodiagnosis in Clinical Neurology*. 6th ed. Philadelphia: Elsevier, 2012; Chapter 19, 421–35.

32

Autonomic system in the head and neck

SUSAN STANDRING

Introduction 317
Sympathetic system in the head and neck 317
Horner's syndrome 318
Parasympathetic system in the head and neck 319
Ciliary ganglion 319
Visual reflexes 319
Pterygopalatine ganglion 319
Submandibular ganglion 321
Otic ganglion 321
Gustatory sweating (Frey's syndrome or auriculotemporal syndrome) 322
Further reading 322

INTRODUCTION

The autonomic nervous system is subdivided into sympathetic and parasympathetic components. Both systems distribute their axons via autonomic ganglia* which act as peripheral relay stations. Preganglionic neurons are located in either visceral efferent nuclei in the brainstem or lateral grey columns of the spinal cord. The alternative names for the sympathetic and parasympathetic systems are the thoraco-lumbar and cranio-sacral outflows, respectively. Their axons pass to autonomic ganglia where they synapse on postganglionic neurons which are motor to smooth or cardiac muscle or the secretory ducts and acini of exocrine glands.

SYMPATHETIC SYSTEM IN THE HEAD AND NECK

Preganglionic sympathetic neurons are located within the lateral grey column of spinal cord segments T1–L1, 2. Most, but by no means all, postganglionic sympathetic neurons lie within either a ganglionated chain (sympathetic trunk) on either side of the vertebral column or within plexuses around the major branches of the abdominal aorta.

The cervical sympathetic trunks lie on the prevertebral fascia behind the carotid sheath. There are usually three interconnected ganglia on each side, superior, middle and inferior, receiving their preganglionic input from the upper three *thoracic* segments of the cord (Figure 32.1). Although there is no preganglionic input from the cervical segments of the spinal cord, the ganglia send postganglionic axons to the adjacent cervical spinal nerves.

---

* For the avoidance of doubt, and because the word seems to cause problems for many students, 'ganglion' (plural 'ganglia') here denotes a collection of neuronal cell bodies and their associated glia lying outside the brain or spinal cord. Sensory ganglia such as dorsal root ganglia and the trigeminal ganglion contain the cell bodies of unipolar sensory neurons and their glia but do *not* contain synapses. Autonomic ganglia contain the cell bodies of multipolar motor neurons and do contain synapses.

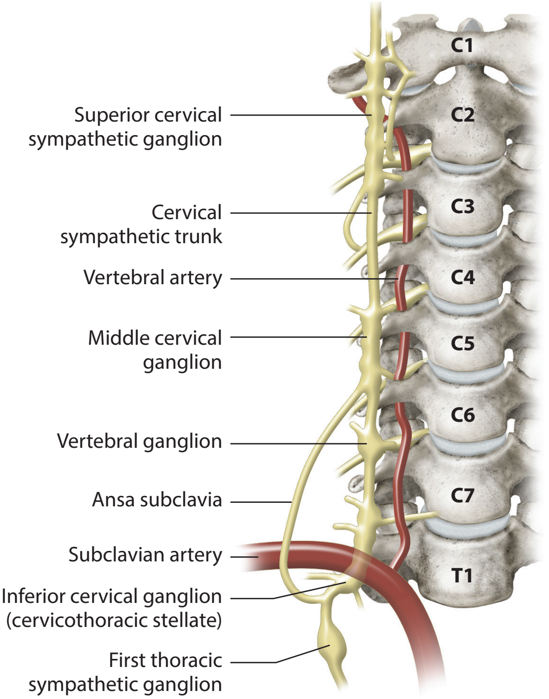
C1
C2
C3
C4
C5
C6
C7
T1
Superior cervical sympathetic ganglion
Cervical sympathetic trunk
Vertebral artery
Middle cervical ganglion
Vertebral ganglion
Ansa subclavia
Subclavian artery
Inferior cervical ganglion (cervicothoracic stellate)
First thoracic sympathetic ganglion

Figure 32.1 Cervical sympathetic chain and stellate ganglion. (This figure was published in: Huntoon, M et al. *Spinal Injections and Peripheral Nerve Blocks*, Chapter 8. Copyright Elsevier 2011.)

The *superior cervical ganglion* is the largest of the three ganglia. It lies on the transverse processes of the second and third cervical vertebrae behind the internal carotid artery and anterior to longus capitis. Postganglionic branches supply vasoconstrictor and sudomotor axons to the face and neck. The largest ganglionic branch accompanies the internal carotid artery into the cranial cavity as the internal carotid nerve and forms a plexus within the cavernous sinus. The postganglionic sympathetic supply to dilator pupillae and the smooth muscles of the eyelids is usually distributed via branches of the ophthalmic nerve via the sympathetic root of the ciliary ganglion (see discussion that follows).

Lateral branches travel in the upper four cervical nerves, and some may also travel with the glossopharyngeal, vagus and hypoglossal nerves. Medial branches are laryngo-pharyngeal or cardiac. The former supply the carotid body and contribute to the pharyngeal plexus. Cardiac branches descend along the posterior surface of the common carotid artery, where they are joined by branches from the middle and inferior ganglia, all ultimately entering the cardiac plexus in the thorax. Anterior branches form a plexus around the external carotid artery and its branches and are sudomotor and vasomotor to the face. Axons in the plexus around the facial artery pass through the submandibular ganglion. Axons in the plexus around the middle meningeal branch of the maxillary artery pass through the otic ganglion (see following discussion).

The *middle cervical ganglion*, the smallest of the three, is inconstant. When present, it is usually found at the level of the sixth cervical vertebra, anterior or just superior to the inferior thyroid artery. It gives off thyroid and recurrent cardiac branches.

The *inferior cervical ganglion* (cervico-thoracic/stellate) may be separate or may fuse with the first thoracic ganglion. It usually lies close to the lateral border of longus colli, between and anterior to the transverse process of the seventh cervical vertebra and the neck of the first rib, posterior to the vertebral vessels and separated from the cervical pleura inferiorly by the suprapleural membrane. It gives off postganglionic branches to the lower cervical spinal nerves and recurrent cardiac branches to the cardiac plexus in the thorax: the alternative name of the 'stellate' ganglion reflects the arrangement of these branches around the ganglion.

Vasomotor and sudomotor postganglionic sympathetic axons form plexuses on the subclavian artery and its branches and are distributed to targets within the watershed of these vessels. The vertebral plexus travels into the cranial cavity along the vertebral and basilar arteries, ultimately meeting a plexus from the internal carotid artery near the posterior cerebral artery.

Horner's syndrome

The sympathetic drive to the head and neck may be interrupted by destruction of axons either ascending from the thorax in the sympathetic trunk (e.g. when a bronchial carcinoma invades the trunk) or descending through the brainstem and damaged *en passant* by vascular occlusion or haemorrhage in the lateral medulla (presenting as part of

Wallenberg's syndrome). The outcome is Horner's syndrome, characterized by ptosis, enophthalmos, meiosis, vasodilatation and lack of thermal sweating (anhydrosis) on the affected side.

PARASYMPATHETIC SYSTEM IN THE HEAD AND NECK

There are four pairs of parasympathetic ganglia in the head, the ciliary, otic, submandibular and pterygopalatine ganglia, each connected by filaments to branches of the trigeminal nerve. In classical descriptions, every ganglion is said to receive three afferent roots (preganglionic parasympathetic, postganglionic sympathetic and somatic sensory). Recent cadaveric dissection studies have reported variations in this pattern and described additional connections. Preganglionic parasympathetic axons synapse on postganglionic neurons within each ganglion. All other axons enter via afferent roots and traverse the ganglia without synapsing; they exit the ganglia, together with postganglionic parasympathetic axons, in efferent roots.

Preganglionic parasympathetic axons arise from neurons in nuclei in the brainstem and travel to their designated ganglia in branches of the oculomotor, facial or glossopharyngeal nerves. Postganglionic axons are typically distributed either via branches of the trigeminal nerves or may pass directly from a ganglion to the target tissues. Collectively, the parasympathetic ganglia provide the secretomotor drive to the salivary and lacrimal glands and the mucous glands of the oral cavity and paranasal sinuses; vasodilator innervation to the arteries and arterioles of the head (both intracranial and extracranial) and neck; and motor innervation to sphincter pupillae, ciliaris and orbitalis.

Ciliary ganglion

The ciliary ganglion is a flat swelling connected to the nasociliary nerve near the apex of the orbit, where it lies posterolateral to the globe in loose areolar tissue between the optic nerve and lateral rectus muscle and close to the medial end of the superior orbital fissure (Figure 32.2). It can be injured during surgery for the repair of orbital fractures and laterally situated intraorbital mass lesions.

Preganglionic parasympathetic neurons lie in the accessory oculomotor or Edinger-Westphal nucleus in the rostral part of the midbrain; their axons travel to the ciliary ganglion via the nerve to the inferior oblique, a branch of the oculomotor nerve. Postganglionic axons leave the ganglion in short ciliary nerves, which pierce the sclera around the optic nerve and then run on the internal scleral surface to innervate the sphincter pupillae and ciliaris (mostly the latter). Vasomotor postganglionic sympathetic axons and somatic sensory axons which innervate the cornea, ciliary body and iris travel in both long and short ciliary nerves.

The parasympathetic root connecting the ganglion to the nasociliary nerve is sometimes absent, and the ganglion is then connected directly to the nerve to inferior oblique. It has been suggested that this close relationship might be a possible cause of postganglionic mydriasis following blowout orbital floor fracture or surgical repair of this type of fracture. The sympathetic root is also sometimes absent: sympathetic fibres may then access the orbit via a retro-orbital connection between the internal carotid plexus and the ophthalmic nerve within the cavernous sinus.

Visual reflexes

The accommodation and pupillary light reflexes are described in Chapter 13.

Pterygopalatine ganglion

As its name suggests, the pterygopalatine ganglion lies deep in the pterygopalatine fossa, just posterior to the sphenopalatine artery before it exits the sphenopalatine foramen and anterior to the pterygoid canal and foramen rotundum (see Chapter 12). The origin of some of the preganglionic neurons has been the subject of intense study in primates and other animals and remains controversial. Consensus has it that subpopulations of preganglionic neurons lie in or near the superior and inferior salivatory nuclear complex in the brainstem, close to the preganglionic neurons associated with the glossopharyngeal nerve. Their axons run initially in the greater petrosal branch of the facial nerve, which becomes the nerve of the pterygoid canal (Vidian nerve) after it is joined by

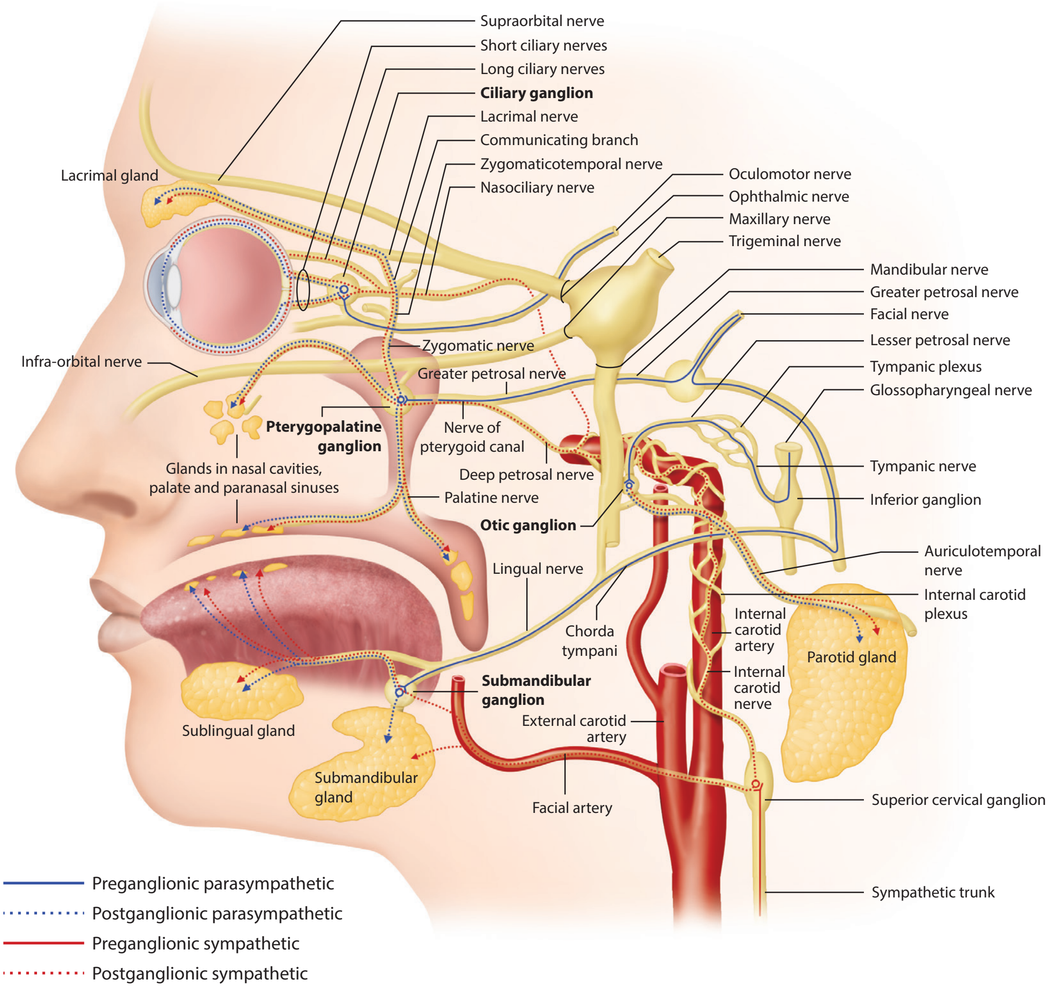
Supraorbital nerve
Short ciliary nerves
Long ciliary nerves
Ciliary ganglion
Lacrimal nerve
Communicating branch
Zygomaticotemporal nerve
Nasociliary nerve
Lacrimal gland
Oculomotor nerve
Ophthalmic nerve
Maxillary nerve
Trigeminal nerve
Mandibular nerve
Greater petrosal nerve
Facial nerve
Lesser petrosal nerve
Tympanic plexus
Glossopharyngeal nerve
Zygomatic nerve
Infra-orbital nerve
Greater petrosal nerve
Pterygopalatine ganglion
Nerve of pterygoid canal
Glands in nasal cavities, palate and paranasal sinuses
Deep petrosal nerve
Palatine nerve
Tympanic nerve
Inferior ganglion
Otic ganglion
Auriculotemporal nerve
Lingual nerve
Internal carotid plexus
Chorda tympani
Internal carotid artery
Parotid gland
Submandibular ganglion
Internal carotid nerve
Sublingual gland
External carotid artery
Submandibular gland
Facial artery
Superior cervical ganglion
Sympathetic trunk
Preganglionic parasympathetic
Postganglionic parasympathetic
Preganglionic sympathetic
Postganglionic sympathetic

Figure 32.2 Overview of the visceral efferent pathways in the head. (This figure was published in Standring S. (Ed.). *Gray's Anatomy – The Anatomical Basis of Clinical Practice*. 40th ed. Philadelphia: Elsevier, 2008; Chapter 25.)

the deep petrosal nerve. In endoscopic approaches to the lateral and posterior skull base, the Vidian canal and nerve lie lateral to the point at which the medial pterygoid plate joins the floor of the sphenoid; they are important landmarks for the anterior genu of the petrous part of the internal carotid artery, the anteromedial part of the cavernous sinus and the petrous apex.

The common, helpful name for the ganglion, the 'ganglion of hay fever', reflects the distribution of the postganglionic parasympathetic axons. They undoubtedly innervate secretory acini and blood vessels in the palatine, pharyngeal and nasal mucosa via the palatine and nasal nerves, but whether they also innervate the lacrimal gland via the zygomatic and zygomaticotemporal branches of the maxillary nerve, as was once thought, is less certain. It is likely that postganglionic orbital branches, carrying a mixture of postganglionic parasympathetic and somatic sensory axons, pass through the inferior orbital fissure and innervate the lacrimal gland and ophthalmic artery directly. Some axons pass into the cranial cavity via the ethmoidal vessels to innervate the choroid: the pterygopalatine ganglion is believed to be the main source of parasympathetic input to the choroid.

Postganglionic sympathetic axons from the superior cervical ganglion travel via the internal carotid plexus and deep petrosal nerve to enter the pterygopalatine ganglion within the nerve of the pterygoid canal. They pass through the ganglion without synapsing and ultimately supply blood vessels and orbitalis.

General sensory axons distributed via orbital, nasopalatine, superior alveolar, palatine and pharyngeal branches of the maxillary nerve also run through the ganglion without synapsing.

Experimental electrical stimulation of the pterygopalatine ganglion causes cerebral vasodilatation, prompting speculation that it plays a role in the pathogenesis of various pain syndromes including cluster headaches, trigeminal and sphenopalatine neuralgia, atypical facial pain and vasomotor rhinitis. Given the complexity of the connections of the pterygopalatine ganglion, it is perhaps not surprising that the detailed neuroanatomical pathways underlying these phenomena have yet to be elucidated. Anaesthesia or hypoaesthesia of the palate are complications that may follow ligation of the sphenopalatine artery or surgical procedures involving the pterygopalatine fossa.

Submandibular ganglion

The submandibular ganglion lies on the upper part of the hyoglossus, superior to the deep part of the submandibular gland and inferior to the lingual nerve, from which it is suspended by anterior and posterior filaments. These connections may render the lingual nerve susceptible to injury during level 1 lymph node dissection or other surgical procedures in the submandibular triangle because they tether the nerve inferiorly.

Preganglionic parasympathetic axons arise from neurons in the superior salivatory nucleus and travel in the facial, chorda tympani and lingual nerves to the ganglion. Postganglionic axons are secretomotor to the submandibular, sublingual and lingual salivary glands: some axons presumably re-enter the lingual nerve to access the lingual glands; others pass directly along blood vessels to enter the submandibular and sublingual glands.

Postganglionic sympathetic axons arise in the superior cervical ganglion and travel via the plexus on the facial artery. They traverse the ganglion without synapsing and are vasomotor to the blood vessels of the submandibular gland and its duct and to the sublingual and anterior lingual glands (the latter axons probably enter the tongue via plexuses around the lingual artery).

Somatic sensory axons pass through the ganglion without synapsing and are derived from the lingual nerve.

Otic ganglion

The otic ganglion is classically described as lying just below the foramen ovale, close to the origin of the nerve to the medial pterygoid, medial to the mandibular nerve, lateral to the tensor veli palatini (which separates the ganglion from the cartilaginous part of the pharyngotympanic tube) and anterior to the middle meningeal artery. However, it is worth noting that, in cadaveric dissections at least, the ganglion may be difficult to locate within the infratemporal fossa.

Almost all of the preganglionic axons arise from neurons in the inferior salivatory nucleus. They travel in the lesser petrosal branch of the glossopharyngeal nerve and access the ganglion by passing through the foramen ovale (see Chapter 29). Postganglionic axons pass by a communicating branch to the auriculotemporal nerve and are secretomotor and vasodilator to the parotid gland.

Vasomotor postganglionic sympathetic axons arise in the superior cervical ganglion and travel via the plexus on the middle meningeal artery. They pass through the otic ganglion without synapsing and travel with the postganglionic parasympathetic axons to join the auriculotemporal nerve. Branchial motor axons to the tensor veli palatini and tensor tympani usually pass through the ganglion without synapsing.

The otic ganglion is connected by fine branches to the chorda tympani and the nerve of the pterygoid canal. These branches may contain gustatory fibres from the presulcal portion of the tongue and preganglionic, parasympathetic secretomotor axons; only the latter group relay in the ganglion. Other somatic sensory axons that pass through the ganglion are thought to be derived from the auriculotemporal nerve.

Gustatory sweating (Frey's syndrome or auriculotemporal syndrome)

Frey's syndrome may be a complication after parotidectomy. Symptoms range from erythema related to the smell or taste of food to gustatory sweating and are thought to reflect aberrant innervation of sweat glands in the overlying flap of skin by regrowing cholinergic parasympathetic axons that previously innervated the parotid.

FURTHER READING

Boysen NC, Dragon DN, Talman WT. Parasympathetic tonic dilatory influences on cerebral vessels. *Autonomic Neuroscience*. 2009; 147: 101–4.

Haines DE. (Ed.). *Fundamental Neuroscience for Basic and Clinical Applications*. 4th ed. Philadelphia: Saunders, 2013; Chapter 29, 405–16.

Hamel O, Corre P, Ploteau S, Armstrong O, Rogez JM, Robert R, Hamel A. Ciliary ganglion afferents and efferents variations: A possible explanation of postganglionic mydriasis. *Surgical and Radiologic Anatomy*. 2012; 34: 897–902.

Izci Y, Gonul E. The microsurgical anatomy of the ciliary ganglion and its clinical importance in orbital traumas: An anatomic study. *Minimally Invasive Neurosurgery*. 2006; 49: 156–60.

Li J, Xu X, Wang J, Jing X, Guo Q, Qiu Y. Endoscopic study for the pterygopalatine fossa anatomy: via the middle nasal meatus-sphenopalatine foramen approach. *Journal of Craniofacial Surgery*. 2009; 20: 944–7.

Osawa S, Rhoton AL Jr, Seker S, Shimizu S, Fujii K, Kassam AB. Microsurgical and endoscopic anatomy of the vidian canal. *Neurosurgery*. 2009: 64 (5 suppl 2): 385–411.

Piagkou M, Demesticha T, Troupis T, Vlasis K, Skandalakis P, Makri A, Mazarakis A, Lappas D, Piagkos G, Johnson EO. The pterygopalatine ganglion and its role in various pain syndromes: from anatomy to clinical practice. *Pain Practice*. 2012; 12: 399–412.

Roitman R, Talmi YP, Finkelstein Y, Sadov R, Zohar Y. Anatomic study of the otic ganglion in humans. *Head and Neck*. 1990; 12: 503–6.

Ruskell GL. Distribution of pterygopalatine ganglion efferents to the lacrimal gland in man. *Experimental Eye Research*. 2004; 78: 329–35.

Siéssere S, Vitti M, Sousa LG, Semprini M, Iyomasa MM, Regalo SC. Anatomic variation of cranial parasympathetic ganglia. *Brazilian Oral Research*. 2008; 22: 101–5.

Surgery

Clinical Head and Neck Anatomy for Surgeons

Clinical Head and Neck Anatomy for Surgeons provides a refreshing new approach to the surgical anatomy of one of the most complex regions of the human body, the head and neck region. While similar books exist, few are written by surgeons for surgeons, detailing and illustrating the relevant surgical anatomy that needs to be mastered before operating in this fascinating area.

The book provides an expert overview of the relevant anatomy encountered during surgery along with anatomical relationships and valuable tips. Each chapter describes in detail the anatomy of a key area or structure, accompanied by high-quality medical illustrations to aid in understanding. The book also includes text with essential details of both common and rare anatomical variants as well as potential danger areas and pitfalls, thus enabling surgeons to be fully prepared for most eventualities.

Thoroughly illustrated with colour clinical photographs taken during surgery, the book displays the essential anatomy as encountered in the operating theatre. Line diagrams have been added where needed or when surgical photographs do not succinctly illustrate the point being made. A few radiological images have also been incorporated to complement the surgical anatomy. This book will provide you with trustworthy guidance to avoid hazards and assist with consistent outcomes for your patients.

WITH VITALSOURCE® EBOOK

- **download the ebook to your computer or access it anywhere with an internet browser**
- **search the full text and add your own notes and highlights**
- **link through from references to PubMed**

K18222

CRC Press
Taylor & Francis Group
an **informa** business
www.crcpress.com

6000 Broken Sound Parkway, NW
Suite 300, Boca Raton, FL 33487
711 Third Avenue
New York, NY 10017
2 Park Square, Milton Park
Abingdon, Oxon OX14 4RN, UK

ISBN: 978-1-4441-5737-6
90000
9 781444 157376